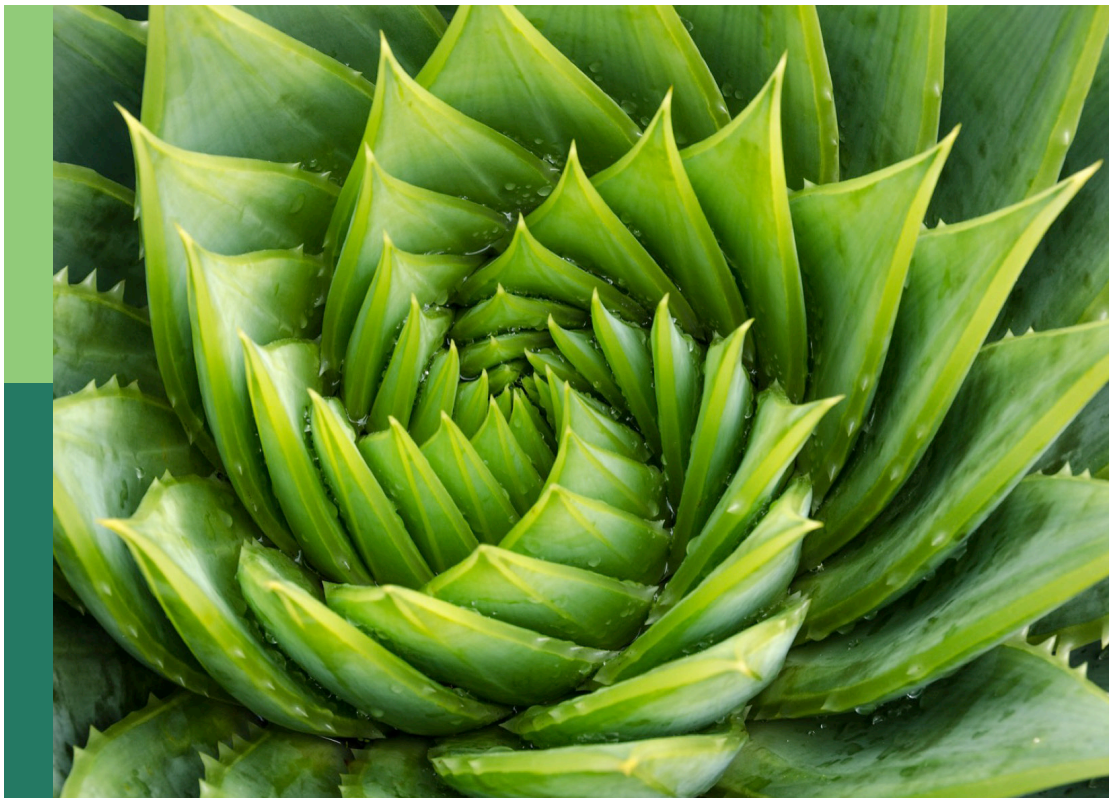
frontiers | Research Topics

Advanced breeding for abiotic stress tolerance in crops

Edited by
Meng Jiang, Xinyang Wu and Tianlun Zhao

Published in
Frontiers in Plant Science



FRONTIERS EBOOK COPYRIGHT STATEMENT

The copyright in the text of individual articles in this ebook is the property of their respective authors or their respective institutions or funders. The copyright in graphics and images within each article may be subject to copyright of other parties. In both cases this is subject to a license granted to Frontiers.

The compilation of articles constituting this ebook is the property of Frontiers.

Each article within this ebook, and the ebook itself, are published under the most recent version of the Creative Commons CC-BY licence. The version current at the date of publication of this ebook is CC-BY 4.0. If the CC-BY licence is updated, the licence granted by Frontiers is automatically updated to the new version.

When exercising any right under the CC-BY licence, Frontiers must be attributed as the original publisher of the article or ebook, as applicable.

Authors have the responsibility of ensuring that any graphics or other materials which are the property of others may be included in the CC-BY licence, but this should be checked before relying on the CC-BY licence to reproduce those materials. Any copyright notices relating to those materials must be complied with.

Copyright and source acknowledgement notices may not be removed and must be displayed in any copy, derivative work or partial copy which includes the elements in question.

All copyright, and all rights therein, are protected by national and international copyright laws. The above represents a summary only. For further information please read Frontiers' Conditions for Website Use and Copyright Statement, and the applicable CC-BY licence.

ISSN 1664-8714
ISBN 978-2-8325-3314-7
DOI 10.3389/978-2-8325-3314-7

About Frontiers

Frontiers is more than just an open access publisher of scholarly articles: it is a pioneering approach to the world of academia, radically improving the way scholarly research is managed. The grand vision of Frontiers is a world where all people have an equal opportunity to seek, share and generate knowledge. Frontiers provides immediate and permanent online open access to all its publications, but this alone is not enough to realize our grand goals.

Frontiers journal series

The Frontiers journal series is a multi-tier and interdisciplinary set of open-access, online journals, promising a paradigm shift from the current review, selection and dissemination processes in academic publishing. All Frontiers journals are driven by researchers for researchers; therefore, they constitute a service to the scholarly community. At the same time, the *Frontiers journal series* operates on a revolutionary invention, the tiered publishing system, initially addressing specific communities of scholars, and gradually climbing up to broader public understanding, thus serving the interests of the lay society, too.

Dedication to quality

Each Frontiers article is a landmark of the highest quality, thanks to genuinely collaborative interactions between authors and review editors, who include some of the world's best academicians. Research must be certified by peers before entering a stream of knowledge that may eventually reach the public - and shape society; therefore, Frontiers only applies the most rigorous and unbiased reviews. Frontiers revolutionizes research publishing by freely delivering the most outstanding research, evaluated with no bias from both the academic and social point of view. By applying the most advanced information technologies, Frontiers is catapulting scholarly publishing into a new generation.

What are Frontiers Research Topics?

Frontiers Research Topics are very popular trademarks of the *Frontiers journals series*: they are collections of at least ten articles, all centered on a particular subject. With their unique mix of varied contributions from Original Research to Review Articles, Frontiers Research Topics unify the most influential researchers, the latest key findings and historical advances in a hot research area.

Find out more on how to host your own Frontiers Research Topic or contribute to one as an author by contacting the Frontiers editorial office: frontiersin.org/about/contact

Advanced breeding for abiotic stress tolerance in crops

Topic editors

Meng Jiang — Zhejiang University, China

Xinyang Wu — China Jiliang University, China

Tianlun Zhao — Zhejiang University, China

Citation

Jiang, M., Wu, X., Zhao, T., eds. (2023). *Advanced breeding for abiotic stress tolerance in crops*. Lausanne: Frontiers Media SA. doi: 10.3389/978-2-8325-3314-7

Table of contents

06 Editorial: Advanced breeding for abiotic stress tolerance in crops
Tianlun Zhao, Xinyang Wu and Meng Jiang

09 Visible gland constantly traces virus-induced gene silencing in cotton
Zhanfeng Si, Huaitong Wu, Yue Tian, Zhiyuan Zhang, Tianzhen Zhang and Yan Hu

17 Unfolded protein response in balancing plant growth and stress tolerance
Yao Liu, Yonglun Lv, An Wei, Mujin Guo, Yanjie Li, Jiaojiao Wang, Xinhua Wang and Yan Bao

26 High temperature boosts resistant starch content by altering starch structure and lipid content in rice *ssIIIa* mutants
Yufeng Zhou, Zhenfeng Cheng, Shuo Jiang, Jinxi Cen, Dianxing Wu and Xiaoli Shu

40 Genome-wide association study reveals quantitative trait loci for waterlogging-triggered adventitious roots and aerenchyma formation in common wheat
Le Xu, Chenchen Zhao, Jiayin Pang, Yanan Niu, Huaqiong Liu, Wenying Zhang and Meixue Zhou

54 Functional physiological phenotyping and transcriptome analysis provide new insight into strawberry growth and water consumption
Lili Jiang, Ting Sun, Xiaofang Wang, Xiaojuan Zong and Chong Wu

67 Genome-wide characterization of NAC transcription factors in *Camellia sinensis* and the involvement of CsNAC28 in drought tolerance
Xueying Zhang, Linying Li, Zhuoliang Lang, Da Li, Yuqing He, Yao Zhao, Han Tao, Jiqian Wei, Qingsheng Li and Gaojie Hong

84 *De Novo* transcriptome combined with physiological analyses revealed key genes for cadmium accumulation in Zhe-Maidong (*Ophiopogon japonicus*)
Qian Zhao, Qing Li, Shuting Lin, Ruijun Hou, Jianying Liu, Yachen Tao, Ye Li, Yifeng Zhou, Zihong Ye, Xiaoping Yu and Jun Huang

97 Identification and expression pattern analysis of the *OsSnRK2* gene family in rice
Tongyuan Yu, Qiwen Cen, Lihua Kang, Wangshu Mou, Xiaoqin Zhang, Yunxia Fang, Xian Zhang, Quanxiang Tian and Dawei Xue

112 Current trends and insights on EMS mutagenesis application to studies on plant abiotic stress tolerance and development
Liuzhu Chen, Liu Duan, Minghui Sun, Zhuo Yang, Hongyu Li, Keming Hu, Hong Yang and Li Liu

125 Multi-omics approach reveals the contribution of *OsSEH1* to rice cold tolerance
Shuang Gu, Jia Zhuang, Zhe Zhang, Wanchun Chen, Hai Xu, Minghui Zhao and Dianrong Ma

142 Comparative transcriptomic analysis and functional characterization reveals that the class III peroxidase gene *TaPRX-2A* regulates drought stress tolerance in transgenic wheat
Peisen Su, Chao Sui, Yufei Niu, Jingyu Li, Shuhan Wang, Fanting Sun, Jun Yan and Shangjing Guo

155 Insight into the bZIP gene family in *Lagenaria siceraria*: Genome and transcriptome analysis to understand gene diversification in Cucurbitaceae and the roles of *LsbZIP* gene expression and function under cold stress
Jian Wang, Ying Wang, Xinyi Wu, Baogen Wang, Zhongfu Lu, Liping Zhong, Guojing Li and Xiaohua Wu

169 Targeted insertion of regulatory elements enables translational enhancement in rice
Rundong Shen, Qi Yao, Dating Zhong, Xuening Zhang, Xinbo Li, Xuesong Cao, Chao Dong, Yifu Tian, Jian-Kang Zhu and Yuming Lu

176 Integrated 16S and metabolomics revealed the mechanism of drought resistance and nitrogen uptake in rice at the heading stage under different nitrogen levels
Changhui Sun, Runnan Wang, Guoping Tang, Shuo Cai, Hong Shi, Fangping Liu, Hengwang Xie, Jinyan Zhu and Qiangqiang Xiong

189 OsWRKY76 positively regulates drought stress *via* OsbHLH148-mediated jasmonate signaling in rice
Mingxing Zhang, Ranran Zhao, Kai Huang, Zhiqi Wei, Boya Guo, Shuangzhan Huang, Zhao Li, Wenzhu Jiang, Tao Wu and Xinglin Du

202 Heterologous expression of *MirMAN* enhances root development and salt tolerance in *Arabidopsis*
Juanjuan Xu, Caiyu Yang, Shangyao Ji, Hui Ma, Jingwei Lin, Hui Li, Shuisen Chen, Hai Xu and Ming Zhong

215 Genome-wide characterization of ascorbate peroxidase gene family in pepper (*Capsicum annuum* L.) in response to multiple abiotic stresses
Xin Pang, Jun Chen, Yang Xu, Jia Liu, Yangmin Zhong, Linlin Wang, Jiaqiu Zheng and Hongjian Wan

225 Genome-wide investigation and expression profiling of *LOR* gene family in rapeseed under salinity and ABA stress
Su Yang, Jialuo Chen, Yonghe Ding, Qian Huang, Guangna Chen, Zaid Ulhassan, Ji'an Wei and Jian Wang

243 Achieving abiotic stress tolerance in plants through antioxidative defense mechanisms
Neelam Mishra, Chenkai Jiang, Lin Chen, Abhirup Paul, Archita Chatterjee and Guoxin Shen

261 A holistic and sustainable approach linked to drought tolerance of Mediterranean crops
Maurizio Trovato, Faiçal Brini, Khalil Mseddi, Sophia Rhizopoulou and Matthew Alan Jones

frontiers | Frontiers in Plant Science

TYPE Editorial
PUBLISHED 09 August 2023
DOI 10.3389/fpls.2023.1265339

Check for updates

OPEN ACCESS

EDITED AND REVIEWED BY
Junya Mizoi,
The University of Tokyo, Japan

*CORRESPONDENCE
Meng Jiang
mengjiang@zju.edu.cn

†These authors have contributed equally to this work

RECEIVED 22 July 2023
ACCEPTED 02 August 2023
PUBLISHED 09 August 2023

CITATION
Zhao T, Wu X and Jiang M (2023) Editorial: Advanced breeding for abiotic stress tolerance in crops. *Front. Plant Sci.* 14:1265339. doi: 10.3389/fpls.2023.1265339

COPYRIGHT
© 2023 Zhao, Wu and Jiang. This is an open-access article distributed under the terms of the Creative Commons Attribution License (CC BY). The use, distribution or reproduction in other forums is permitted, provided the original author(s) and the copyright owner(s) are credited and that the original publication in this journal is cited, in accordance with accepted academic practice. No use, distribution or reproduction is permitted which does not comply with these terms.

Editorial: Advanced breeding for abiotic stress tolerance in crops

Tianlun Zhao[1,2†], Xinyang Wu[3†] and Meng Jiang[1,2*]

[1]Hainan Institute, Zhejiang University, Sanya, China, [2]The Advanced Seed Institute, Zhejiang University, Hangzhou, China, [3]College of Life Sciences, China Jiliang University, Hangzhou, China

KEYWORDS

crops, breeding, abiotic stress, gene family, multiomics analysis, mechanism, advanced techniques

Editorial on the Research Topic
Advanced breeding for abiotic stress tolerance in crops

1 Introduction

Abiotic stress, including extreme temperature, salinity, drought, and other environmental pollution with excessive heavy metals, is regarded to be a global issue in agricultural systems that results in considerable yield and quality losses for crops (Waadt et al., 2022). With the continued rise of the world's population, it is crucial for sustainable agriculture and food security to develop advanced breeding strategies that effectively mitigate abiotic stress (Zhang et al., 2022). Additionally, a multifaceted strategy is required for crops to enhance their ability to adapt to abiotic stress, including hormone modulation, plant enzymatic system activation, and stress gene expression (Gong et al., 2020). Therefore, understanding how cereal crops react to abiotic stress is crucial (Mittler et al., 2022). Figure out the important characteristics of abiotic stress and their underlying physiological, biochemical, and molecular bases (e.g., genetic, epigenetic, transcriptomic, and metabolomic) will extend our knowledge in breeding efforts to create abiotic stress-resistant crops (Chang et al., 2020).

In this editorial, we set up a Research Topic of Advanced Breeding for Abiotic Stress Tolerance in Crops, which covers up-to-date scientific evidence and the potential for future research to improve our knowledge of the mechanisms that control the development of abiotic stress tolerance in the world's major crop species. The following themes are included in this Research Topic: (a) Advanced crop breeding applications for increasing abiotic stress resistance in crops; (b) Novel plant growth regulators for enhancing abiotic stress tolerance in plants; (c) Metabolomic and molecular strategies to improve abiotic stress-resistance in crops; (d) Genetic mechanisms related to abiotic stress tolerance in plants and their related traits in plants by quantitative trait loci (QTL) mapping, genome-wide association (GWAS) investigation, or QTL-sequencing; (e) Epigenetic bases of abiotic stress resistance and their applications in crop breeding.

Despite significant advances in understanding the underlying mechanism of abiotic stress, there remain knowledge gaps in these areas, and our Research Topic aims to address these gaps. In the end, we accepted and published 20 articles (16 Original Research, 3 Review, and 1 Perspective) written by 158 researchers from seven different countries, e.g. Australia, United Kingdom, Italy, Greece, Tunisia, India, and China. Unfolded protein

response in balancing plant growth and stress tolerance, current trends and insights on EMS mutagenesis application to studies on abiotic stress tolerance and plant development, and achieving abiotic stress tolerance in plants through antioxidative defense mechanisms were reviewed by Liu et al., Chen et al., and Mishra et al. A Perspective named 'A Holistic and Sustainable Approach Linked to Drought Tolerance of Mediterranean' was written by Trovato et al. The 16 Original Research articles will be divided into the following four parts for detailed interpretation.

2 Assay of gene family under abiotic stress

- Yang et al. included a thorough analysis of 56 *LOR* (*Lurp-One-Related*) genes in *Brassica napus*. Some reports found that *LOR* gene family members acted key functions in defense of *Hyaloperonospora parasitica* (Hpa) in *Arabidopsis*. This research improved our understanding of the *Brassica napus LOR* gene family and may help in the selection and identification of genes for stress-resistant breeding.

- Pang et al. discovered 9 members of the *APX* gene family in the pepper genome according to the conserved domain of the *APX* protein in *Arabidopsis thaliana*. The work discovered the activities of *APX* genes and provided information for further functional characterisation of *CaAPX* genes.

- Zhang et al. identified 104 *NAC* genes in *Camellia sinensis*. The thorough characterisation of *Camellia sinensis NAC* genes provided by the study may operate as a starting point for research into the molecular basis of *CsNACs*-mediated drought response.

- Wang et al. discovered the 65 potential *bZIP* genes in *Lagenaria siceraria* and described their gene structure, phylogenetic and orthologous connections, gene expression patterns in various tissues and cultivars. Through the use of RNA-Seq and RT-PCR, they have examined and confirmed the cold stress-responsive candidate *bZIP* genes in *Lagenaria siceraria*. This has resulted in the discovery of new information regarding the transcriptional control of bottle gourd *bZIP* family genes and their potential roles in the development of cold-tolerant varieties through breeding.

- Yu et al. found that ten *OsSnRK2* genes were discovered in the rice genome distributed across seven chromosomes and grouped into three subfamilies. The results offered valuable details for comprehending the *OsSnRK2* gene family and examining how it responds to drought, salt, and ABA treatment, particularly drought-salt joint stress.

3 Multiomics analysis under abiotic stress

- Xu L. et al. employed a genome-wide association study (GWAS) methodology using 90K single nucleotide polymorphisms (SNPs) in a panel of 329 wheat genotypes to identify the quantitative trait loci (QTL) for ARs and RCA. In breeding efforts, a number of genotypes that consistently performed well under various conditions can be utilized to create wheat varieties that can withstand waterlogging.

- Sun et al. discovered that during drought stress, rice plants' dry matter mass, N content, and N accumulation all grew to varying degrees even when the same amount of N was applied. The findings showed that pathways involved in energy metabolism, such as the phosphotransferase system (PTS) and D-alanine metabolism, were enriched. In general, the work offers a theoretical foundation for enhancing rice's drought tolerance and N use efficiency.

- Zhao et al. studied the distribution of Zhe-Maidong (*Ophiopogon japonicus*) roots reacting to Cd stress and the features of Cd transformation by growing Zhe-Maidong seedlings for 90 days in Cd-contaminated and uncontaminated soil. The findings may be useful in determining the features of Cd accumulation in Zhe-Maidong and may also serve as a bioinformatic starting point for research on gene functions and the screening of potential Cd-accumulation-related candidate genes.

- Gu et al. discovered that the rice gene *OsSEH1*, which codes for nucleoporins, is a positive regulator for cold stress. The findings showed that wild type plants and osseh1 lines had hypersensitive phenotypes, indicating that *OsSEH1* may influence cold tolerance *via* controlling ABA levels.

4 Exploration of underlying mechanism under abiotic stress

- Zhang et al. reported that OsWRKY76 positively controlled rice drought stress. Dehydration stress, exogenous MeJA, and PEG treatments can induce the expression of *OsWRKY76*. The findings provided a new lead in the quest to understand the processes behind drought tolerance by suggesting that OsWRKY76 provides drought tolerance through OsbHLH148-mediated jasmonate signaling in rice.

- Xu J. et al. discovered that the oil-tolerant plant *Mirabilis jalapa* contained a *mannanase* (*MAN*) gene called *MirMAN*, which was cloned and heterologously produced in *Arabidopsis*. The study showed that *MirMAN* is a potentially significant target gene that may be further used to enhance plant tolerance to abiotic stress.

- Zhou et al. investigated the effects of high temperature on rice (*Oryza sativa*) starch metabolite and the higher reductions in *BEI*, *BEIIa*, *BEIIb*, and *SSIVb* expression when exposed to high temperature. The study found that by generating more starch-lipid complexes under high temperatures, the increased long chains of amylopectin and lipids may be the main cause of the enhanced RS content in mutants.

- Su et al. measured physiological-biochemical parameters and assessed the drought tolerance of various wheat cultivars. While demonstrating the possibility of *TaPRX-2A* overexpression in boosting drought tolerance during crop development efforts, the study offered insights into the processes of tolerance.

- Jiang et al. found that during the progressive drought and water recovery phases, the midday transpiration rate Tr (Tr_m) and daily transpiration (E) as well as plant growth of water recovery at θcri (WR_θcri) was slightly lower or comparable to those of well irrigation (CK), but those of water recovery under severe drought (WR_SD) were significantly lower than those of CK during water stress and did not recover after rehydration. According to the findings, irrigation balances strawberry growth and water use at a key soil water content.

5 Advanced techniques in abiotic stress research

- Shen et al. discovered that precisely introducing a regulatory element into a target gene's 5'UTR might effectively boost the protein abundance of that gene in rice. The research offered a fresh method to control protein translation for crop breeding by demonstrating the viability of such in-locus editing to improve protein expression.

- Si et al. found that virus-induced gene silencing (VIGS) is continuously tracked by a visible gland in cotton. The enhanced VIGS technology will provide another tool for the quick functional identification of many genomes' undiscovered genes.

6 Prospect

It is crucial to comprehend how general and stress-specific response pathways interact since plants must deal with numerous abiotic stresses at once in their natural habitat. Similar to this, stomatal closure and ROS generation are examples of regulatory nodes at which plant responses to abiotic stimuli may also converge. These numerous reactions, as well as the crosstalk between them, maybe simultaneously triggered and result in additive, synergistic, or antagonistic effects, which could improve or impair stress resistance. In order to discover essential molecular targets for breeding stress-resistant crops in the field, it will be necessary to untangle plant responses to various stresses at the molecular level by using multiomics analysis and advanced techniques.

Author contributions

TZ: Formal Analysis, Software, Supervision, Writing – original draft. XW: Data curation, Funding acquisition, Investigation, Project administration, Writing – original draft. MJ: Conceptualization, Funding acquisition, Methodology, Validation, Writing – review & editing.

Funding

This Research Topic was supported by the Research Startup Funding from the Hainan Institute of Zhejiang University (0201-6602-A12203) received by MJ and Zhejiang Science and Technology Major Program on Agricultural New Variety (2021C02067-7) received by XW.

Acknowledgments

We extend our heartfelt thanks to all authors and reviewers for their invaluable input and contributions. Additionally, we are grateful to the Journal Committee for providing us the opportunity to develop this Research Topic.

Conflict of interest

The authors declare that the research was conducted in the absence of any commercial or financial relationships that could be construed as a potential conflict of interest.

Publisher's note

All claims expressed in this article are solely those of the authors and do not necessarily represent those of their affiliated organizations, or those of the publisher, the editors and the reviewers. Any product that may be evaluated in this article, or claim that may be made by its manufacturer, is not guaranteed or endorsed by the publisher.

References

Chang, Y. N., Zhu, C., Jiang, J., Zhang, H., Zhu, J. K., and Duan, C. G. (2020). Epigenetic regulation in plant abiotic stress responses. *J. Integr. Plant Biol.* 62 (5), 563–580. doi: 10.1111/jipb.12901

Gong, Z., Xiong, L., Shi, H., Yang, S., Herrera-Estrella, L. R., Xu, G., et al. (2020). Plant abiotic stress response and nutrient use efficiency. *Sci. China Life Sci.* 63 (5), 635–674. doi: 10.1007/s11427-020-1683-x

Mittler, R., Zandalinas, S. I., Fichman, Y., and Van Breusegem, F. (2022). Reactive oxygen species signalling in plant stress responses. *Nat. Rev. Mol. Cell Biol.* 23 (10), 663–679. doi: 10.1038/s41580-022-00499-2

Waadt, R., Seller, C. A., Hsu, P. K., Takahashi, Y., Munemasa, S., and Schroeder, J. I. (2022). Plant hormone regulation of abiotic stress responses. *Nat. Rev. Mol. Cell Biol.* 23 (10), 680–694. doi: 10.1038/s41580-022-00479-6

Zhang, H., Zhu, J., Gong, Z., and Zhu, J. K. (2022). Abiotic stress responses in plants. *Nat. Rev. Genet.* 23 (2), 104–119. doi: 10.1038/s41576-021-00413-0

frontiers | Frontiers in Plant Science

TYPE Original Research
PUBLISHED 16 September 2022
DOI 10.3389/fpls.2022.1020841

Check for updates

OPEN ACCESS

EDITED BY
Xinyang Wu,
China Jiliang University, China

REVIEWED BY
Jun Zhao,
Zhenjiang Institute of Agricultural Sciences, China
Lianguang Shang,
Agricultural Genomics Institute at Shenzhen (CAAS), China

*CORRESPONDENCE
Tianzhen Zhang
cotton@zju.edu.cn
Yan Hu
0016211@zju.edu.cn

†These authors have contributed equally to this work

SPECIALTY SECTION
This article was submitted to Plant Abiotic Stress, a section of the journal Frontiers in Plant Science

RECEIVED 16 August 2022
ACCEPTED 29 August 2022
PUBLISHED 16 September 2022

CITATION
Si Z, Wu H, Tian Y, Zhang Z, Zhang T and Hu Y (2022) Visible gland constantly traces virus-induced gene silencing in cotton.
Front. Plant Sci. 13:1020841.
doi: 10.3389/fpls.2022.1020841

COPYRIGHT
© 2022 Si, Wu, Tian, Zhang, Zhang and Hu. This is an open-access article distributed under the terms of the Creative Commons Attribution License (CC BY). The use, distribution or reproduction in other forums is permitted, provided the original author(s) and the copyright owner(s) are credited and that the original publication in this journal is cited, in accordance with accepted academic practice. No use, distribution or reproduction is permitted which does not comply with these terms.

Visible gland constantly traces virus-induced gene silencing in cotton

Zhanfeng Si[1†], Huaitong Wu[1,2†], Yue Tian[3†], Zhiyuan Zhang[4], Tianzhen Zhang[1,4*] and Yan Hu[1,4*]

[1]Department of Agronomy, College of Agriculture and Biotechnology, Zhejiang University, Hangzhou, China, [2]Key Laboratory for Tree Breeding and Germplasm Improvement, Southern Modern Forestry Collaborative Innovation Center, College of Forestry, Nanjing Forestry University, Nanjing, China, [3]College of Biotechnology, Jiangsu University of Science and Technology, Zhenjiang, China, [4]Hainan Institute of Zhejiang University, Sanya, China

A virus-induced gene silencing (VIGS) system was established to induce endogenous target gene silencing by post-transcriptional gene silencing (PTGS), which is a powerful tool for gene function analysis in plants. Compared with stable transgenic plant *via Agrobacterium-mediated* gene transformation, phenotypes after gene knockdown can be obtained rapidly, effectively, and high-throughput through VIGS system. This approach has been successfully applied to explore unknown gene functions involved in plant growth and development, physiological metabolism, and biotic and abiotic stresses in various plants. In this system, *GhCLA1* was used as a general control, however, silencing of this gene leads to leaf albino, wilting, and plant death ultimately. As such, it cannot indicate the efficiency of target gene silencing throughout the whole plant growth period. To address this question, in this study, we developed a novel marker gene, *Gossypium PIGMENT GLAND FORMATION GENE* (*GoPGF*), as the control to trace the efficiency of gene silencing in the infected tissues. *GoPGF* has been proved a key gene in gland forming. Suppression of *GoPGF* does not affect the normal growth and development of cotton. The number of gland altered related to the expression level of *GoPGF* gene. So it is a good marker that be used to trace the whole growth stages of plant. Moreover, we further developed a method of friction inoculation to enhance and extend the efficiency of VIGS, which facilitates the analysis of gene function in both the vegetative stage and reproductive stage. This improved VIGS technology will be a powerful tool for the rapid functional identification of unknown genes in genomes.

KEYWORDS

cotton, gene function analyses, VIGS (virus-induced gene silencing), marker gene, gland trait

Introduction

As a kind of hereditary immune mechanism prevalent in plants, virus-induced gene silencing (VIGS) belongs to post-transcriptional gene silencing (PTGS) (Lu et al., 2003). When carrying a vector with endogenous gene fragments of the host plant infection, VIGS can activate the plant's own immune system. Plants recognize and degrade viral RNA, and also produce microRNAs that contain endogenous genes of interest. Through binding to the mRNAs of the target genes, these microRNAs can form a hairpin structure which is then degraded by the Dicer enzyme, leading to a decrease in the expression level of the gene of interest or loss of function (Senthil-Kumar and Mysore, 2011).

As one of the most widely used gene silencing systems, the tobacco rattle virus-induced gene silencing system (TRV-VIGS) has the advantages of high silencing efficiency, long duration, light symptoms of the host plant viruses, and no cover of the phenotype in various organizations that produce gene silencing. Above all, as it does not require the development of stable transformants, it is very suitable for characterizing gene function in plants with low transformation efficiency. Therefore, due to its validity and rapidity, TRV-VIGS has been successfully used in various plants, such as *Nicotiana tabacum*, *Solanum lycopersicum*, *Gossypium hirsutum*, *Arabidopsis*, *Capsicum annuum,* etc. (Tian et al., 2014).

The VIGS method utilizes the *Cloroplastos alterados 1* gene (*CLA1*) as a common positive control, which results in photobleaching of the silenced regions (Gao et al., 2011a). Recently, VIGS technology has been used extensively to study the gene function of cotton, due to its discrete characters verification, such as Red plant (R_1) (Cai et al., 2014), Okra leaf ($L_2{}^0$) (Chang et al., 2016; Andres et al., 2017), Glandless ($Gl_2{}^e$) (Ma et al., 2016), Ligon-lintless (Li_1) (Thyssen et al., 2017), Naked seed (N_1) (Wan et al., 2016), Lint fiber development (Li_3) (Wu et al., 2018), Axillary flowering (*GbAF*) (Si et al., 2018), Coiled-coil nucleotide-binding site leucine-rich repeat (*CC-NBS-LRR*) (Deng et al., 2019), APETALA 2/ethylene-responsive factor (*AP2/ERF*) (Pei et al., 2021), UBX-Domain Containing10 (Zang et al., 2021a) and novel stem pigment gland-forming gene (*GoSPGF*) (Zang et al., 2021b). There are many studies on the analysis of gene function in biotic and abiotic resistances including disease (Gao et al., 2011b), drought (Chen et al., 2015) and low temperature (Liu et al., 2015). However, after the whitening of the individual plants, the treated plants grow slowly and weakly compared to normal plants, due to their inability to complete the photosynthesis process. Finally, after the albino plant grows for about 2 months, it gradually withers (**Figure 1**). Therefore, this positive control is suitable only for identifying the phenotype at the seedling stage, and is not conducive to the study of the phenotype at the middle or late growth stage. Here, we report on a novel positive control gene *GoPGF* (Ma et al., 2016), which could constantly trace virus-induced gene silencing visually throughout the entire range of plant growth stages. Thus, it is suitable for studying traits such as buds, flowering, and fiber.

Materials and methods

Plant materials

The materials used in the experiments were TM-1 with glands. TM-1 is a standard genetic line of Upland cotton and has broad leaves. The seeds were germinated and grown in a greenhouse. The seedlings from the cotyledon expansion to 4th true leaf emergence were used for the VIGS assays. Infiltrated plants were grown in a growth chamber at 23°C with a 16/8 h light/dark photoperiod. *N. benthamiana* was grown at 25°C in a semi-controlled walk-in chamber with a 16/8 h light to dark photoperiod for the generation of transgenic plants or agroinfiltration.

Recombinant virus-induced gene silencing vectors

The pTRV1, pTRV-*CLA1*, and pTRV-*GoPGF* vectors were stored in our laboratory. The three vectors were transformed into *Agrobacterium tumefaciens* strains GV3101.

Agrobacterium infiltration

pTRV1, pTRV-*CLA1,* and pTRV-*GoPGF* were grown overnight at 28°C in an antibiotic selection medium containing rifampicin and kanamycin at a concentration of 50 mg l^{-1}. *Agrobacterium* cells were collected and resuspended in an infiltration medium (10 mM $MgCl_2$, 10 mM MES and 200 μM acetosyringone), and adjusted OD_{600} to OD_{600} 1.5. When silencing *GoPGF* gene separately *Agrobacterium* strains to contain the TRV1 and TRV-*GoPGF* vectors were mixed at a ratio of 1:1. While silencing the *CLA1* and *GoPGF* genes at the same time, in the case of the *Agrobacterium* strains carrying pTRV-*CLA1*, pTRV- *GoPGF*, and pTRV1 vectors were mixed at a ratio of 1: 1: 2 and then injected into the cotton cotyledons. The treated cotton seedlings were grown in a growth chamber at 23°C with a 16/8 h light/dark photoperiod.

Friction inoculation in the virus-induced gene silencing system

The tobacco (*N. benthamiana*) grows to 6 leaves in a greenhouse at 25°C in a semi-controlled walk-in chamber with a 16/8 h light to dark photoperiod. TRV1 and TRV-*CLA1*

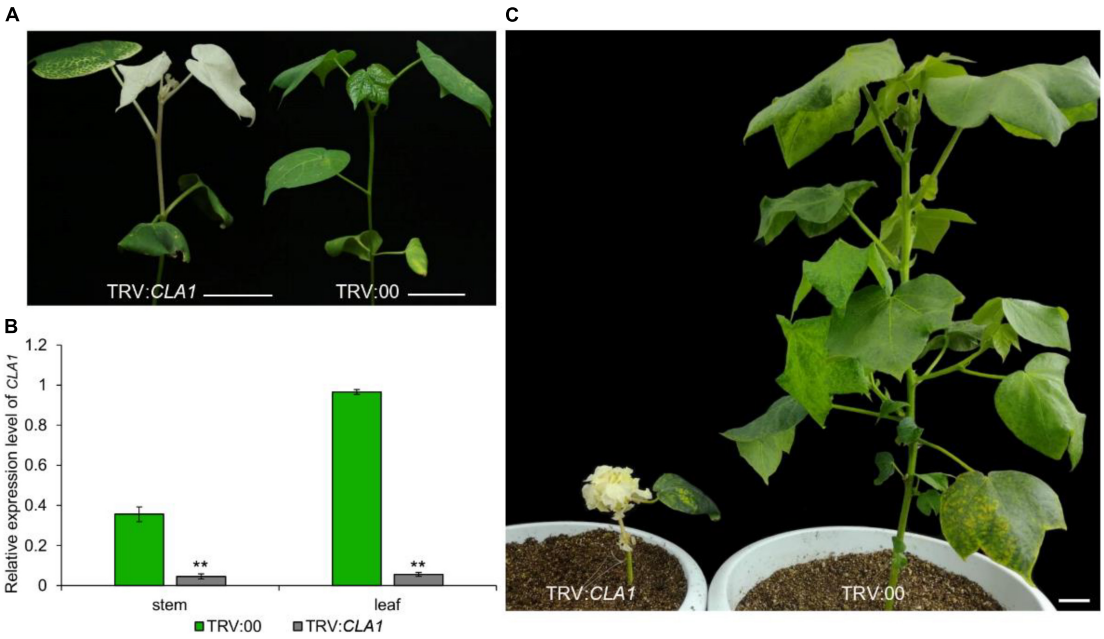


FIGURE 1
The gene expression and phenotype of the *CLA1*- silenced plants. **(A)** After 2 weeks of silencing the *CLA1* gene, the leaves showed an albino phenotype. **(B)** After 2 weeks of silencing the *CLA1* gene, the expression of genes in young leaves and young stems of albino and empty control plants were analyzed. **(C)** The phenotype of the plant was observed after silencing the *CLA1* gene for 2 months. Error bars are s.d. of three biological repeats. $^{**}P < 0.01$; Student's *t*-test, $n = 3$. Bars = 5 cm.

were grown overnight at 28°C in a LB medium containing antibiotics (50 μg/ml kanamycin, 25 μg/ml gentamicin), 10 mM MES and 20 μM acetosyringone. The cells were pelleted by centrifugation at 1,200 × *g* at room temperature for 8 min, and resuspended in an MMA (10 mM MES, 10 mM MgCl2, 200 μM acetosyringone) solution to the final OD_{600} of 1.5. Cell suspensions were incubated at room temperature for at least 3 h without shaking. The *Agrobacterium* strains containing the TRV1 and pTRV-*CLA1* vectors were mixed at a ratio of 1:1 and infiltrated into tobacco leaves using a needleless syringe. The treated tobacco was grown in a greenhouse at 23°C with a 16/8 h light/dark photoperiod.

Tobacco was placed in the greenhouse after 2 weeks of growth, with the new leaves showing white spots. In the mortar, white-spotted tobacco leaves were added, along with a little 400 mesh quartz sand and 10 ml 0.01M phosphate buffer solution (PBS). These were then ground into a homogenate.

In the cotton plant, only the completely unfolded leaves were chosen, and a small quantity of 400 mesh quartz sand was sprinkled over the above mixture. A pestle was used to divert the prepared homogenate to gently rub over the selected cotton leaves. Friction control was implemented in order to penetrate the leaves, so that the leaves would be damaged to the epidermis. The purpose was intended to invade cotton leaves with the tobacco containing virus. The treated cotton was placed in a greenhouse at 23°C with a 16/8 h light/dark photoperiod. After 2–3 weeks, the new growing cotton leaves displayed whitening phenotypes.

RNA extraction and quantitative real-time PCR analysis

RNA was extracted from the stem, leaf, bract, and calyculus of TM-1 using the Biospin Plant Total RNA Extraction Kit (Hangzhou Bori Technology Co. Ltd, Hangzhou, China, cat: BSC65S1). First-strand cDNA was generated using a TransScript® One-Step gDNA Removal Kit and a cDNA Synthesis SuperMix (TransGen Biotech Co. Ltd, Beijing China, cat: AT311) according to the manufacturer's instructions. The cotton *Histone 3* gene (AF024716) was used as the housekeeping gene. The primers' sequences were listed in **Supplementary Table 1**.

Results

The number of glands on the plants reflects the silencing efficiency of virus-induced gene silencing

The *Gossypium* species are characterized by the presence of small and darkly pigmented lysigenous glands on the surface of

almost all the organs (**Figure 2A** and **Supplementary Figure 1**). Using a dominant glandless mutant Hai-1, we cloned the pigment gland formation regulator *GoPGF* which encodes a *basic helix-loop-helix* (*bHLH*) transcription factor (Ma et al., 2016). It is expressed in a constitutive manner in most organs and tissues including the stem, leaf, bract, etc. (**Figure 2B**), consistent with the presence of glands (Ma et al., 2016). *GoPGF* was proven to be specific to gland development and had no noticeable effect on plant growth and development (Gao et al., 2022). The silencing of *GoPGF* can lead to a complete glandless phenotype. However, we observed that there was a noticeable difference in the silencing efficiency in different VIGS-treated plants even though this applied to the same receptor material and was implemented with the same silencing vector injection. For example, a VIGS-silenced *GoPGF* plant displayed different gland phenotypes using the cotton genetic standard line TM-1 as the receptor. Some *GoPGF*-silenced plants did not develop glands at all, suggesting that *GoPGF* is completely silenced, while some plants showed reduced glands (**Figure 2C**). The relative expression of *GoPGF* gene is also down-regulated with a decrease in the number of glands (**Figure 2D**). Thus, the *GoPGF* gene can be utilized as a positive control and internal indicator to trace the silencing efficiency of the target gene through phenotype observation of the absence or presence of the gland and variation of gland numbers throughout the entire VIGS stage.

Assessment of degree and specificity of virus-induced endogenous *GoPGF* gene silencing in cotton

The pTRV-*GoPGF* silencing vector was constructed and injected into TM-1 to observe the glandular phenotype during the completed sequence of developmental stages. Silencing of the *GoPGF* gene resulted in the glandless phenotype in the new leaves and stems after 2–3 weeks of inoculation, while plants inoculated with empty vectors and the control plants displayed a glanded phenotype (**Supplementary Figures 2A,B**). qPCR analysis revealed that the transcripts of the *GoPGF* gene were significantly decreased in the glandless plants (**Supplementary Figure 2**). At the flowering stage, some *GoPGF*-silenced plants began to develop a few glands only in the 5-day-old young boll, but no glands were found in the top, middle and lower parts of the stems, the penultimate leaves and the sepals (**Figure 3**). The expression of the *GoPGF* gene in the six examined tissues was significantly lower than that of the empty vector control (**Supplementary Figure 3**). Therefore, the silencing efficiency of the endogenous gene can be maintained till the flowering stage. Moreover, when the *GoPGF* gene served as the internal control, the silencing efficiency of the target gene in the plant was directly reflected by the existence and the number variation of glands.

GoPGF can be considered as an internal reference gene in a cotton virus-induced gene silencing system

According to previous reports, two target gene fragments can be constructed on one TRV vector to achieve the purpose of simultaneously silencing two genes (Pang et al., 2013). In this study, a mixed VIGS system was designed by equally mixing *Agrobacterium* containing TRV vectors of different target genes. We utilized the silencing of the *CLA1* gene in order to produce leaf albino and silenced the *GoPGF* gene in order to create glandless traits to validate the above ideas. *Agrobacterium* strains carrying pTRV-*CLA1*, pTRV-*GoPGF* and pTRV1 vectors were mixed at the ratio of 1: 1: 2 and then injected into cotton cotyledons. At the same time, the *Agrobacterium* carrying pTRV-*CLA1* and pTRV-*GoPGF* vectors were, respectively injected into the cotton cotyledons, and the TRV2 empty vector was adopted as the negative control. Two weeks later, the phenotype of the treated plants was observed. The RNA was extracted from the penultimate leaves of cotton plants, and the expression patterns of the *CLA1* and *GoPGF* genes were analyzed. The plants injected with pTRV-*CLA1* had an albino phenotype, while those plants injected with pTRV-*GoPGF* exhibited a glandless phenotype (**Figure 4A**). Meanwhile, the plants injected with pTRV-*CLA1* mixed with pTRV-*GoPGF* exhibited the white and glandless phenotype simultaneously (**Figure 4A**). The phenotype of negative control did not change at all (**Figure 4A**). Expression pattern analysis confirmed that the expression of *CLA1* and *GoPGF* was strongly inhibited when silencing these two genes independently (**Figures 4B,C**). By silencing pTRV-*CLA1* and pTRV-*GoPGF* at the same time, the expression of both genes was also completely inhibited (**Figures 4B,C**). Moreover, it is completely feasible to determine the efficiency of the target gene silencing method using the *GoPGF* gene as an internal reference gene by alteration of the gland number.

Friction inoculation can extend the duration of silencing of target genes

Though the VIGS method has a high silencing efficiency in cotton seedlings, the silencing efficiency after flowering is significantly reduced. Therefore, in order to render this method applicable to the study of gene function in flowering or the fiber elongation stage, we applied a friction inoculation method to extend the duration of silencing of target genes. In addition, the modified method can extend the duration of the VIGS in other plants (Becker and Lange, 2010; Senthil-Kumar and Mysore, 2011). With TM-1 as the receptor material, the *CLA1* gene was used for validating the effectiveness of this approach (Gao et al., 2011a). First, the *Agrobacterium strains* carrying the *CLA1*

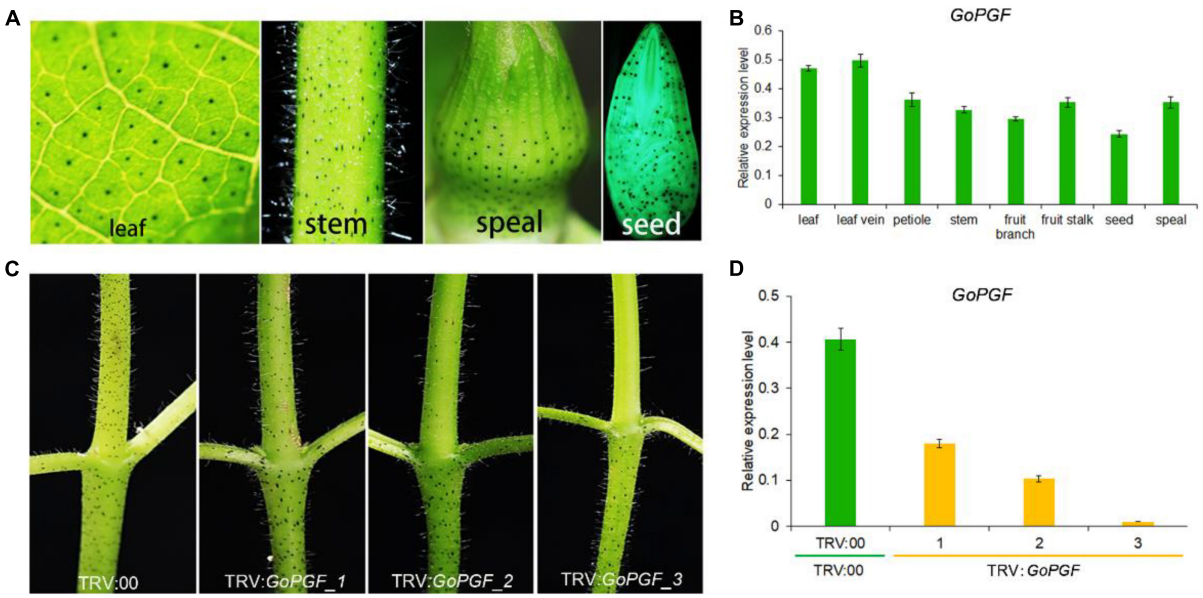


FIGURE 2
Gland phenotypes and gene expression level in different tissues of *GoPGF*-silenced plants. **(A)** Distribution of glandular phenotype in different tissues of cotton including leaf, stem, bud and seed. **(B)** Relative expression of the *GoPGF* gene in different tissues of cotton. Error bars are s.d. of three biological repeats. **(C)** Comparison of silencing efficiency in different VIGS plants. **(D)** The relative expression of the *GoPGF* gene was analyzed in the stems of different VIGS plants in panel **(C)**. Error bars are s.d. of three biological repeats.

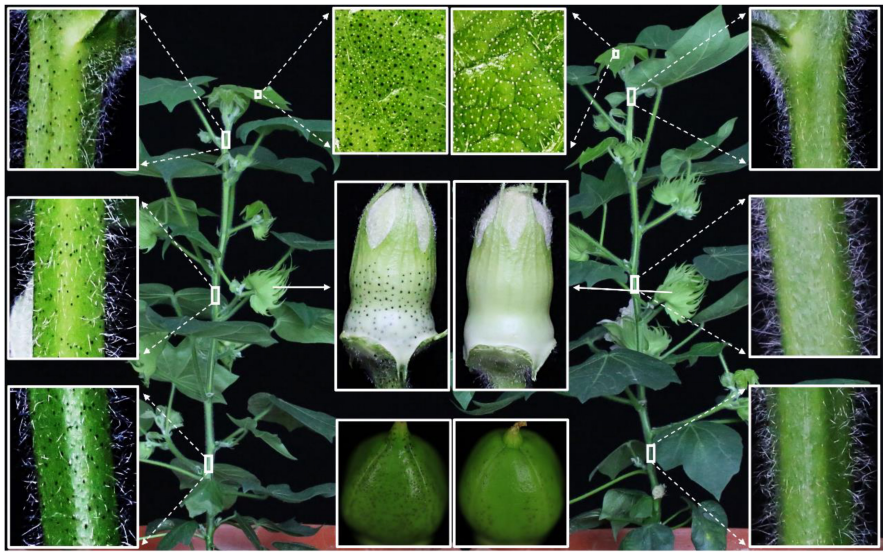


FIGURE 3
Comparison of the glandular phenotype of different tissues from *GoPGF*-VIGS plants and control at flowering stage. The tissues marked in the white box showed an enlargement of corresponding tissues including leaf, stem, bud and boll from the TRV:00 and TRV:*PGF* whole plants, respectively. The boll was collected 5 days after flowering.

gene vector were injected into the *Nicotiana tabacum*, and then after 2 weeks, the newly grown tobacco leaf displayed a macular phenotype (**Supplementary Figure 4A**). Next, 1–3 g of tobacco leaves with the macular phenotype were collected and placed in a mortar. A small amount of PBS (0.01 M, pH = 7.2) was added and ground into juice. The cotton leaves were vaccinated and sprinkled with a trace of 500 mesh diamond. Upon dipping into the juice with a pestle and gently rubbing on the leaves, the leaves exhibited micro-wounds, but epidermal cells were not destroyed.

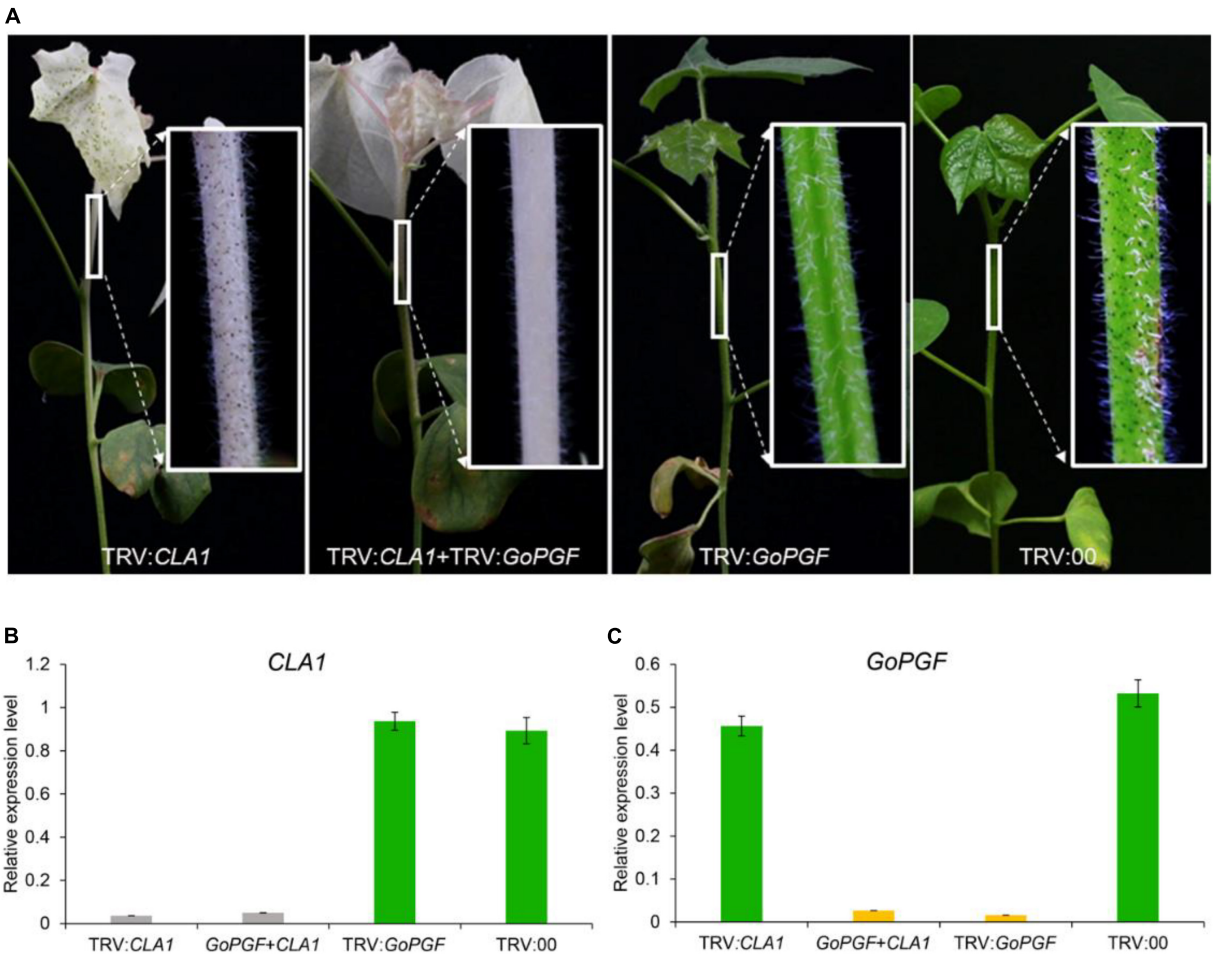


FIGURE 4
Phenotype and gene expression level of VIGS plants silenced by various combinations of the *CLA1* and *GoPGF* gene. **(A)** Phenotype of VIGS plants silenced by *CLA1* or *GoPGF* gene and both *CLA1*–silenced plants display a typical albino phenotype; the *GoPGF*-silenced plants show a glandless phenotype; VIGS plants showed albino and glandless phenotype when both were silenced simultaneously. **(B)** *CLA1* gene relative expression in the stem marked white box in panel **(A)**. Error bars are s.d. of three biological repeats. **(C)** *GoPGF* gene relative expression in the stem marked white box in panel **(A)**. Error bars are s.d. of three biological repeats.

Finally, the treated cotton plants were further grown in a greenhouse. After 2 weeks, the new cotton leaves grew albino (**Supplementary Figure 4B**). The relative expression of the *CLA1* gene was analyzed by the whitening and normal leaves in the same position of the cotton plants. The expression of the *CLA1* gene in the white leaves was significantly decreased (**Supplementary Figure 4C**). This result revealed that the friction inoculation method could prolong the silence duration of the target gene in the cotton plants.

Discussion and conclusions

The earliest application of VIGS in cotton was to construct a *CLA1* gene fragment into a TRV vector and then transform it into *Agrobacterium* to inject cotton cotyledons. After 2–3 weeks, the whitening phenotype of the new leaves was observed, and the target gene was highly efficient (Gao et al., 2011a). Since then, many researchers have used this method for functional gene research and used the *CLA1* gene as a positive control. For example, *GhMLP28* is involved in resistance to *Verticillium wilt* (Yang et al., 2015), *LMI1* regulates the development of the okra leaf (Chang et al., 2016; Andres et al., 2017) and *GhSnRK2* participates in the regulation of drought resistance (Bello et al., 2014), etc. In *Gossypium barbadense*, VIGS systems were established using multiple marker genes, including *GaPDS*, *GaCLA1*, *GaANS*, and *GaANR* (Pang et al., 2013). In the above method, although the high silencing efficiency of the target gene in cotton VIGS system was established, the selection of the marker gene is not perfect. These marker genes

have certain defects: *CLA1* and *PDS* gene silencing plants have a whitening phenotype, but do not maintain long-term growth; in *GaANS* gene silencing plants, the leaves need to be treated before the phenotype can be observed. Compared with them, as a marker gene, *GoPGF* can well solve the above-mentioned limitations. When the expression of the *GoPGF* gene is silenced, it does not affect the normal growth of the cotton plant, and gene silencing efficiency can be visually observed through the number variation of glands.

In our study, after inoculation of two *Agrobacterium strains* (containing pTRV-*CLA1* and pTRV-*GoPGF* plasmids, respectively) into the same plant, both whitening and glandless phenotypes appeared at the same time. It was demonstrated that mixing two gene-silencing vectors in VIGS can also silence two target genes simultaneously. This result was consistent with previous reports (Gao et al., 2011a). During the VIGS process, the growth environment of the plant determines the silencing efficiency of the target gene. Even though treated with the same material as inoculation receptor, silencing efficiency of target genes still exists individual difference. Therefore, *GoPGF* as an internal reference gene can reflect the silencing efficiency of the target gene in real time according to the number variation of glands in the newly grown tissue of the plant. Although the VIGS system can be applied to the study of the cotton growth period after flowering, the silencing efficiency of its target gene is much lower than that at the seedling stage (Wan et al., 2016). Thus, we developed an improved method of friction inoculation based on the principle that plant viruses can be transmitted between plants. We successfully verified the feasibility of cotton (Wu et al., 2018; Zang et al., 2021a). The method is to inoculate a TRV virus in the bud stage of cotton and to increase the silencing efficiency of the target gene in the newly grown fruit branch by spreading the virus in the cotton plant. Up to now, many genomes of many cotton species have been released and tens of thousands predicated coding genes have been annotated. However, the function of most genes is unknown, and it needs to be proved by experiments. As we all know, gain of function through transgenic expression of the candidate gene in the mutant varieties is the most direct and effective method for functional validation. But it is time consuming and laborious work and sometime difficult to implement because of genotype dependence of genetic transformation in cotton. Obviously, VIGS is a practicable method for quick gene function verification. Here, this improved VIGS method will facilitates the rapid validation of gene function especially during the development of cotton fiber initiation, elongation, lipid metabolism or under biotic and abiotic stresses.

In summary, we employed the *GoPGF* gene as a positive control and an internal reference gene during the VIGS process, so as to reflect the silencing efficiency of the target gene through existence and number variations of glands. The friction inoculation method is a necessary supplement and helps to investigate phenotype at later stages of development in cotton.

Data availability statement

The original contributions presented in this study are included in the article/**Supplementary material**, further inquiries can be directed to the corresponding authors.

Author contributions

ZS, HW, and YT conceived and designed the experiments. YH, ZS, and HW performed the experiments and wrote the manuscript. YT and ZZ participated in the experiments. ZS, HW, YT, TZ, and YH edited the manuscript. All authors read and approved the last version.

Funding

This work was financially supported in part by grants National Natural Science Foundation of China (31970320), the Fundamental Research Funds for the Central Universities (2021QN81011), the Xinjiang Production and Construction Corps (project of 2021AB008), the Hainan Yazhou Bay Seed Lab (project of B21HJ0223), and the Leading Innovative and Entrepreneur Team Introduction Program of Zhejiang (2019R01002).

Conflict of interest

The authors declare that the research was conducted in the absence of any commercial or financial relationships that could be construed as a potential conflict of interest.

Publisher's note

All claims expressed in this article are solely those of the authors and do not necessarily represent those of their affiliated organizations, or those of the publisher, the editors and the reviewers. Any product that may be evaluated in this article, or claim that may be made by its manufacturer, is not guaranteed or endorsed by the publisher.

Supplementary material

The Supplementary Material for this article can be found online at: https://www.frontiersin.org/articles/10.3389/fpls.2022.1020841/full#supplementary-material

References

Andres, R. J., Coneva, V., Frank, M. H., Tuttle, J. R., Samayoa, L. F., Han, S.-W., et al. (2017). Modifications to a Late Meristem Identity1 gene are responsible for the major leaf shapes of Upland cotton (*Gossypium hirsutum* L.). *Proc. Natl. Acad. Sci. U S A.* 114, E57–E66. doi: 10.1073/pnas.1613593114

Becker, A., and Lange, M. (2010). Vigs–genomics goes functional. *Trends Plant Sci.* 15, 1–4. doi: 10.1016/j.tplants.2009.09.002

Bello, B., Zhang, X., Liu, C., Yang, Z., Yang, Z., Wang, Q., et al. (2014). Cloning of *Gossypium hirsutum* sucrose non-fermenting 1-related protein kinase 2 gene (GhSnrk2) and its overexpression in transgenic *Arabidopsis* escalates drought and low temperature tolerance. *PLoS One* 9:e112269. doi: 10.1371/journal.pone.0112269

Cai, C., Zhang, X., Niu, E., Zhao, L., Li, N., Wang, L., et al. (2014). Ghpsy, a phytoene synthase gene, is related to the red plant phenotype in upland cotton (*Gossypium hirsutum* L.). *Mol. Biol. Rep.* 41, 4941–4952. doi: 10.1007/s11033-014-3360-x

Chang, L., Fang, L., Zhu, Y., Wu, H., Zhang, Z., Liu, C., et al. (2016). Insights into interspecific hybridization events in allotetraploid cotton formation from characterization of a gene-regulating leaf shape. *Genetics* 204, 799–806. doi: 10.1534/genetics.116.193086

Chen, T., Li, W., Hu, X., Guo, J., Liu, A., and Zhang, B. (2015). A cotton Myb transcription factor, Gbmyb5, is positively involved in plant adaptive response to drought stress. *Plant Cell Physiol.* 56, 917–929. doi: 10.1093/pcp/pcv019

Deng, J., Fang, L., Zhu, X., Zhou, B., and Zhang, T. (2019). A Cc-Nbs-Lrr gene induces hybrid lethality in cotton. *J. Exp. Bot.* 70, 5145–5156. doi: 10.1093/jxb/erz312

Gao, W., Zhu, X., Ding, L., Xu, B., Gao, Y., Cheng, Y., et al. (2022). Development of the engineered "glanded plant and glandless seed" cotton. *Food Chem. Mol. Sci.* 5:100130. doi: 10.1016/j.fochms.2022.100130

Gao, X., Britt, R. C. Jr., Shan, L., and He, P. (2011a). Agrobacterium-mediated virus-induced gene silencing assay in cotton. *J. Vis. Exp.* 54:e2938. doi: 10.3791/2938

Gao, X., Wheeler, T., Li, Z., Kenerley, C. M., He, P., and Shan, L. (2011b). Silencing Ghndr1 and Ghmkk2 compromises cotton resistance to *Verticillium* wilt. *Plant J.* 66, 293–305. doi: 10.1111/j.1365-313X.2011.04491.x

Liu, T., Guo, S., Lian, Z., Chen, F., Yang, Y., Chen, T., et al. (2015). A P4-Atpase gene Gbpatp of cotton confers chilling tolerance in plants. *Plant Cell Physiol.* 56, 549–557. doi: 10.1093/pcp/pcu200

Lu, R., Martin-Hernandez, A. M., Peart, J. R., Malcuit, I., and Baulcombe, D. C. (2003). Virus-induced gene silencing in plants. *Methods* 30, 296–303.

Ma, D., Hu, Y., Yang, C., Liu, B., Fang, L., Wan, Q., et al. (2016). Genetic basis for glandular trichome formation in cotton. *Nat. Commun.* 7:10456. doi: 10.1038/ncomms10456

Pang, J., Zhu, Y., Li, Q., Liu, J., Tian, Y., Liu, Y., et al. (2013). Development of Agrobacterium-mediated virus-induced gene silencing and performance evaluation of four marker genes in Gossypium barbadense. *PLoS One* 8:e73211. doi: 10.1371/journal.pone.0073211

Pei, Y., Zhang, J., Wu, P., Ye, L., Yang, D., Chen, J., et al. (2021). GoNe encoding a class Viiib Ap2/Erf is required for both extrafloral and floral nectary development in *Gossypium*. *Plant J.* 106, 1116–1127. doi: 10.1111/tpj.15223

Senthil-Kumar, M., and Mysore, K. S. (2011). New dimensions for Vigs in plant functional genomics. *Trends Plant Sci.* 16, 656–665.

Si, Z., Liu, H., Zhu, J., Chen, J., Wang, Q., Fang, L., et al. (2018). Mutation of Self-Pruning homologs in cotton promotes short-branching plant architecture. *J. Exp. Bot.* 69, 2543–2553. doi: 10.1093/jxb/ery093

Thyssen, G. N., Fang, D. D., Turley, R. B., Florane, C. B., Li, P., Mattison, C. P., et al. (2017). A Gly65Val substitution in an actin, Ghact_Li1, disrupts cell polarity and F−actin organization resulting in dwarf, lintless cotton plants. *Plant J.* 90, 111–121. doi: 10.1111/tpj.13477

Tian, J., Pei, H., Zhang, S., Chen, J., Chen, W., Yang, R., et al. (2014). Trv–Gfp: a modified Tobacco rattle virus vector for efficient and visualizable analysis of gene function. *J. Exp. Bot.* 65, 311–322. doi: 10.1093/jxb/ert381

Wan, Q., Guan, X., Yang, N., Wu, H., Pan, M., Liu, B., et al. (2016). Small interfering Rna s from bidirectional transcripts of Gh Mml 3_A12 regulate cotton fiber development. *New Phytol.* 210, 1298–1310. doi: 10.1111/nph.13860

Wu, H., Tian, Y., Wan, Q., Fang, L., Guan, X., Chen, J., et al. (2018). Genetics and evolution of Mixta genes regulating cotton lint fiber development. *New Phytol.* 217, 883–895.

Yang, C.-L., Liang, S., Wang, H.-Y., Han, L.-B., Wang, F.-X., Cheng, H.-Q., et al. (2015). Cotton major latex protein 28 functions as a positive regulator of the ethylene responsive factor 6 in defense against *Verticillium dahliae*. *Mol. Plant* 8, 399–411. doi: 10.1016/j.molp.2014.11.023

Zang, Y., Hu, Y., Xu, C., Wu, S., Wang, Y., Ning, Z., et al. (2021a). Ghubx controlling helical growth results in production of stronger cotton fiber. *iscience* 24:102930. doi: 10.1016/j.isci.2021.102930

Zang, Y., Xu, C., Xuan, L., Ding, L., Zhu, J., Si, Z., et al. (2021b). Identification and characteristics of a novel gland-forming gene in cotton. *Plant J.* 108, 781–792. doi: 10.1111/tpj.15477

frontiers | Frontiers in Plant Science

TYPE Review
PUBLISHED 07 October 2022
DOI 10.3389/fpls.2022.1019414

Check for updates

OPEN ACCESS

EDITED BY
Meng Jiang,
Zhejiang University, China

REVIEWED BY
Adrian A. Moreno,
Universidad Andres Bello, Chile
Baris Uzilday,
Ege University, Turkey
Renu Srivastava,
Iowa State University, United States

*CORRESPONDENCE
Yan Bao
yanbao@sjtu.edu.cn

†These authors have contributed equally to this work

SPECIALTY SECTION
This article was submitted to Plant Abiotic Stress, a section of the journal Frontiers in Plant Science

RECEIVED 15 August 2022
ACCEPTED 05 September 2022
PUBLISHED 07 October 2022

CITATION
Liu Y, Lv Y, Wei A, Guo M, Li Y, Wang J, Wang X and Bao Y (2022) Unfolded protein response in balancing plant growth and stress tolerance.
Front. Plant Sci. 13:1019414.
doi: 10.3389/fpls.2022.1019414

COPYRIGHT
© 2022 Liu, Lv, Wei, Guo, Li, Wang, Wang and Bao. This is an open-access article distributed under the terms of the Creative Commons Attribution License (CC BY). The use, distribution or reproduction in other forums is permitted, provided the original author(s) and the copyright owner(s) are credited and that the original publication in this journal is cited, in accordance with accepted academic practice. No use, distribution or reproduction is permitted which does not comply with these terms.

Unfolded protein response in balancing plant growth and stress tolerance

Yao Liu[1†], Yonglun Lv[1†], An Wei[1], Mujin Guo[1], Yanjie Li[1], Jiaojiao Wang[1], Xinhua Wang[1] and Yan Bao[1,2*]

[1]School of Agriculture and Biology, Shanghai Jiao Tong University, Shanghai, China, [2]Shanghai Collaborative Innovation Center of Agri-Seeds, Joint Center for Single Cell Biology, Shanghai Jiao Tong University, Shanghai, China

The ER (endoplasmic reticulum) is the largest membrane-bound multifunctional organelle in eukaryotic cells, serving particularly important in protein synthesis, modification, folding and transport. UPR (unfolded protein response) is one of the systematized strategies that eukaryotic cells employ for responding to ER stress, a condition represents the processing capability of ER is overwhelmed and stressed. UPR is usually triggered when the protein folding capacity of ER is overloaded, and indeed, mounting studies were focused on the stress responding side of UPR. In plants, beyond stress response, accumulating evidence suggests that UPR is essential for growth and development, and more importantly, the necessity of UPR in this regard requires its endogenous basal activation even without stress. Then plants must have to fine tune the activation level of UPR pathway for balancing growth and stress response. In this review, we summarized the recent progresses in plant UPR, centering on its role in controlling plant reproduction and root growth, and lay out some outstanding questions to be addressed in the future.

KEYWORDS

UPR – unfolded protein response, ER stress, IRE1, bZIP, pollen, root

What is UPR?

ER stress response refers to an action of protective mechanism, which can be triggered by various environmental stresses or protein folding problems in the ER. In order to cope with ER stress and maintain ER homeostasis, an efficient mechanism termed ERQC (ER quality control) is configured for ER stress response (Chen et al., 2020; Sun et al., 2021). Eukaryotic cells repair or clear damaged proteins through a series of ERQC systems to maintain homeostasis in the ER. UPR (unfolded protein response) is one of the key ERQC strategies that can effectively respond to ER stress. UPR is highly conserved among eukaryotes, and during ER stress, UPR modulates downstream targets

to increase the folding capacity of ER and protect the organism from stress. In metazoans, the three canonical UPR sensors IRE1 (Inositol-requiring enzyme 1), ATF6 (Activating transcription factor 6) and PERK (Protein kinase R (PKR)-like ER kinase) are ER membrane localized, and have the ability to sense unfolded or misfolded proteins in ER and transduce downstream UPR signals (Doultsinos et al., 2017). Type I membrane proteins include IRE1 and PERK, which contain an N-terminal ER lumenal sensing domain, a transmembrane domain, and a C-terminal cytosolic domain for signal output. While ATF6 belongs to a type II membrane protein, which is structurally similar to type I membrane protein except that its N-terminus is in the cytosol and the C-terminus in the ER lumen. Alternatively, in other events, ER stress signals can also be transduced *via* noncanonical UPR pathways, independent of the three classic UPR sensors (Yu et al., 2022).

Two branches of canonical UPR in plants

No clear PERK homologs were found in plants and, to date, only two branches of plant UPR pathway have been discovered. In Arabidopsis, the first branch of UPR is mediated by AtIRE1a and AtIRE1b (Figure 1A), two homologues of metazoan IRE1, which are close in protein structure and function (Koizumi et al., 2001; Noh, 2002). During ER stress, AtIRE1a and AtIRE1b work redundantly to cleave the mRNA of basic leucine zipper family member *bZIP60* (*bZIP60u*) with unconventional splicing. Post to the cleavage of 23 bp (base pair) nucleotides from *bZIP60u*, a t-RNA ligase called RLG1 will re-join the two segments and produce *bZIP60s* (spliced form of *bZIP60* mRNA) (Nagashima et al., 2016). Spliced *bZIP60s* encodes the active form of bZIP60 transcription factor, which

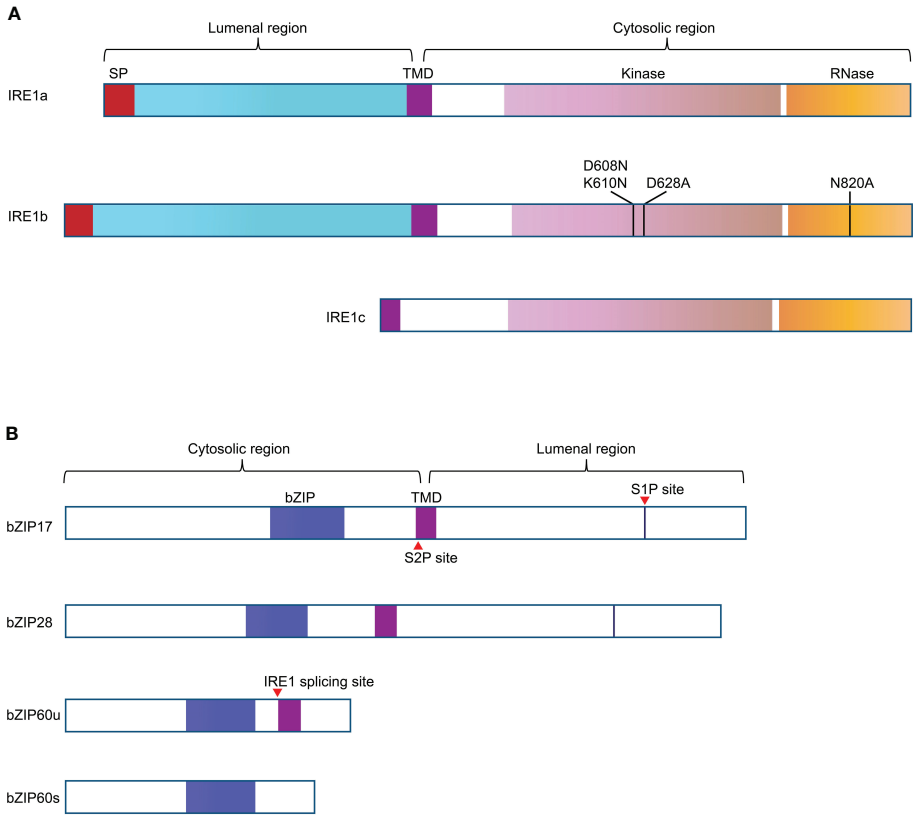


FIGURE 1
Schematic representation of the structural features of the UPR signal transducers in Arabidopsis. **(A)** A transmembrane domain (TMD) divides IRE1a and IRE1b into two segments. The N-terminal region of IRE1 has a signal peptide (SP, in red) and a sensing domain, facing the ER lumen. The C-terminal region of IRE1 contains the protein kinase domain (in light purple) and RNase domain (in orange), facing the cytosol. The mutation D608N K610N in IRE1b was supposed to be able to block its nucleotide binding activity, D628A mutation in IRE1b can interfere with the protein kinase activity of IRE1b, and N820A mutation knocks out the RNase activity of IRE1b. IRE1c is plant unique as it only has the corresponding TMD and cytosolic region. **(B)** bZIP transcriptional factors of UPR pathway have N-term cytosolic bZIP domain and C-term luminal region. The blue boxes represent bZIP domains, the purple boxes indicate the TMD, the red triangle arrows represent the corresponding cleavage or splicing site. bZIP60s (active form) and bZIP60u are spliced and unspliced forms of bZIP60.

can move into the nucleus to induce the expression of target genes (Iwata et al., 2008; Deng et al., 2011; Nagashima et al., 2011). In addition, under ER stress, the activated IRE1 also targets other mRNAs and degrades them, ultimately inhibiting the synthesis of new proteins, a process termed RIDD (regulated IRE1-dependent RNA decay) (Figure 2) (Mishiba et al., 2013).

The second branch of Arabidopsis UPR is carried out by membrane-associated transcription factors AtbZIP17 and AtbZIP28 (Figure 1B), which are functional homologs of metazoan ATF6 (Liu et al., 2007a; Liu et al., 2007b). ATF6 confers ER localization through its transmembrane domain (Haze et al., 1999). In plants, Arabidopsis AtbZIP17 and AtbZIP28 are activated in similar ways to that of ATF6. Under ER stress conditions, ER-localized AtbZIP17 and AtbZIP28 were induced to transport to the Golgi, where they are sequentially hydrolyzed by S1P (site 1 protease) and S2P (site 2 protease) (Kinch et al., 2006), freeing the AtbZIP17p and/or AtbZIP28p to function as transcription factors in the nucleus (Figure 2). However, it has been demonstrated that activation of Arabidopsis bZIP28 is mediated by S2P rather than S1P (Iwata et al., 2017), thus, the underlying basis for this sequential activation needs further investigation.

The function of canonical UPR under ER stress has been extensively studied. However, in recent years, the research of non-canonical UPR pathways in plant growth and stress responding has also been intensified. In addition to bZIP family transcriptional factors, plant unique NAC (No apical meristem (NAM), Arabidopsis transcription activation factor (ATAF), and Cup-shaped cotyledon (CUC)) family transcriptional factors are also involved in UPR response. To

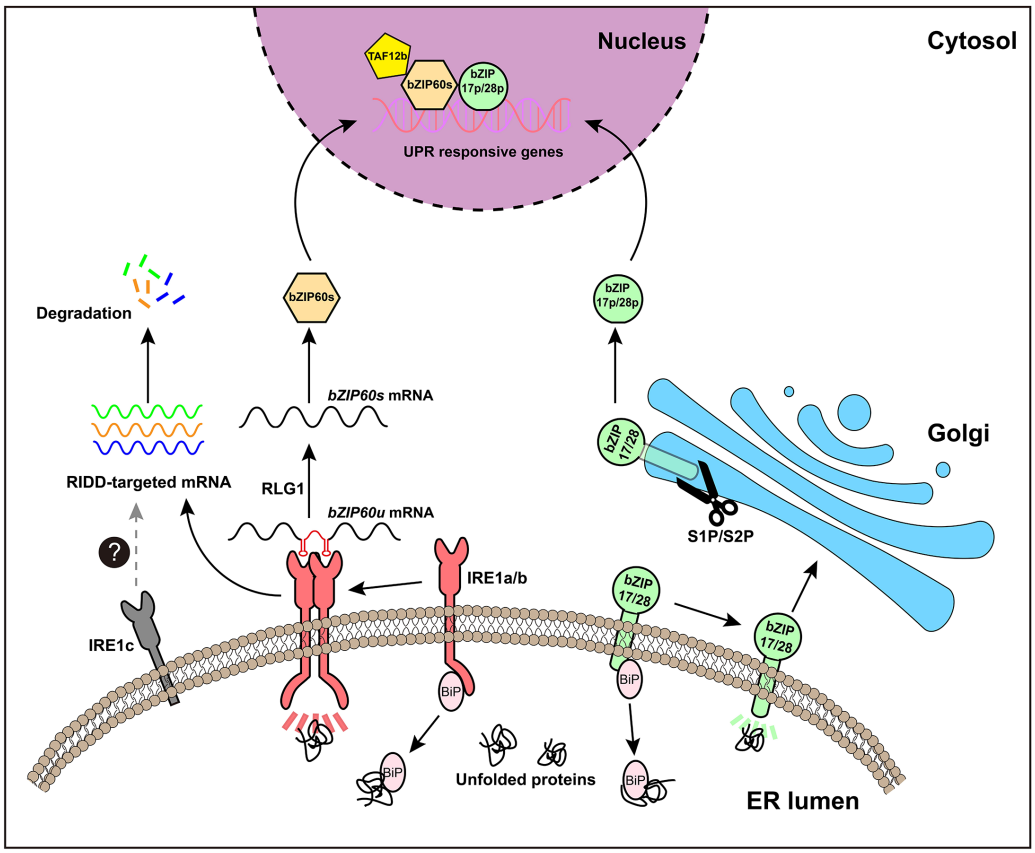


FIGURE 2
An overview of UPR signaling pathway in Arabidopsis. The plant UPR signaling pathway has two branches. The first branch is mediated by IRE1a and IRE1b. Under ER stress, the chaperone protein BiP, binds to unfolded proteins, thereby releasing IRE1 to form an active dimeric or polymeric form. Activated IRE1 splices the mRNA of *bZIP60u* to produce *bZIP60s*, releasing a hairpin RNA (in red). The spliced fragments of bZIP60 mRNA will be reunited by t-RNA ligase RLG1. *bZIP60s* mRNA encodes the active transcription factor bZIP60s, which can enter the nucleus to induce the expression of related UPR target genes. In addition, activated IRE1 is involved in another process, known as RIDD (regulated IRE1-dependent decay), which degrades other mRNAs and ultimately reduces the synthesis of new proteins. The second branch is mediated by bZIP17 and bZIP28, two ER membrane-localized transcription factors. Under ER stress conditions, bZIP17 and/or bZIP28 are relocated from the ER to the Golgi, where they are hydrolyzed by S1P and S2P protease, and subsequently their hydrolyzed TF domains (bZIP17p and/or bZIP28p) are released for further importing to the nucleus to regulate the expression of ER stress responsive genes. IRE1c is a recently discovered plant-specific IRE1 subtype, but the exact function of IRE1c and its role in plant UPR pathway need to be further examined.

date, three NAC transcription factors AtNAC062 (plasma membrane tethered), AtNAC089 (ER-localized) and AtNAC103 (cytosolic) were reported to be implicated in ER stress response via the regulation of UPR responsive genes in Arabidopsis (Sun et al., 2013; Yang et al., 2014a; Yang et al., 2014b).

Beyond transcriptional level of regulation, a variety of strategies were employed for noncanonical UPR responding. For instance, study of plant-specific, PIP binding SVB (Small Trichomes with Variable Branches) family proteins suggests a connection between PIP signaling and UPR response (Marks et al., 2009; Oxley et al., 2013; Yu and Kanehara, 2020; Yu et al., 2021). In addition, plant G protein signaling participates in ER stress response via collaboration with IRE1 (Wang et al., 2007; Chen and Brandizzi, 2012; Afrin et al., 2022). Arabidopsis BLISTER (BLI) protein affects plant growth via negative regulation of IRE1 (Hong et al., 2019), while IRE1-mediated ER stress signal output in rice is negatively regulated by SQUAMOSA PROMOTER-BINDING PROTEIN-LIKE 6 (SPL6) (Wang et al., 2018). Recently, UPR-related BiP2 and ERDJ3a were detected in SGs (Stress Granules), suggesting the potential of SG formation in UPR regulation (Advani and Ivanov, 2020; Maruri-Lopez et al., 2021).

UPR in plant stress response

As stated above, accumulation of misfolded proteins in the ER can activate UPR pathway, which in turn regulates the expression of UPR responsive genes and helps to maintain ER homeostasis. Both environmental stresses and genetic disorders can cause misfolded proteins to trigger UPR. Protein folding is a delicate and complex process that is influenced by a variety of environmental factors. For example, salt, heat, drought and some biotic stresses all provoke UPR in plants. The studies regarding UPR in plant stress response have been extensively discussed (Howell, 2017; Manghwar and Li, 2022), which will not be the focus of this review.

UPR in regulating plant root growth

Accumulating evidence suggests that plant UPR pathway components are closely involved in regulating plant root growth. Single Arabidopsis UPR mutants (*ire1a, ire1b, bzip17, bzip28, bzip60*) do not affect primary root growth under normal condition, but high order UPR mutants have additive effect on limiting primary root elongation (Figure 3). Compared with wild-type, the *ire1a ire1b* double mutant shows shorter primary root, and this effect is exemplified after DTT (Dithiothreitol, a redox reagent) or Tm (Tunicamycin, an inhibitor of N-linked glycosylation) treatment (Deng et al., 2013; Chen et al., 2014). IRE1-regulated root growth seems independent of its classic

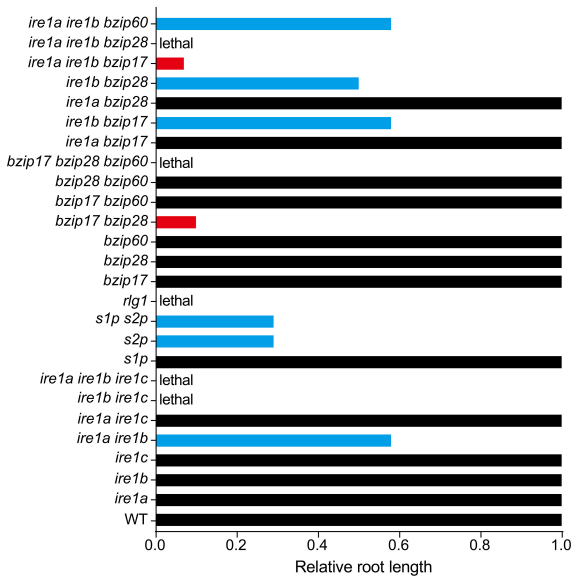


FIGURE 3
Relative root length of Arabidopsis canonical UPR pathway mutants. Root length of WT is set as 1.0, and the black columns indicate the root growth of relevant UPR mutants are not significantly affected. The blue columns represent about 50% reduction of root length in the relevant mutants. The red columns show stunted root length in two triple knock-out mutants *17ab* (*ire1a ire1b bzip17*, ~5% of WT) and *bzip17 bzip28* (*bz1728*, ~10% of WT). Data shown in this figure are based on published results regarding the root length of relevant UPR mutants compared with their corresponding WT.

target *bZIP60*, as *bzip60* mutants act the same as wild-type in controlling primary root growth with or without ER stress. Moreover, introducing *bzip60* into *ire1a ire1b* background does not further reduce the root length of *ire1a ire1b*, again suggesting a limited role of bZIP60 in this process.

The other arm of UPR is the S1P/S2P-mediated proteolytic cleavage of bZIP17 and bZIP28. Single mutants of *s1p* have little effect on primary root elongation under non-stress condition, just like the single mutant *bzip17* or *bzip28*. However, *s1p* shows shorter root under salt stress when compared with that of the corresponding wild-type (Liu et al., 2007b). The single mutants of *s2p* have a profound effect on limiting primary root elongation under normal conditions, retaining its root length 30% of the wild-type, while the shoot of *s2p* is not significantly affected (Che et al., 2010). In addition, *s1p s2p* double mutant behaves a similar root growth rate to that of the *s2p* under normal condition (Kim et al., 2018), suggesting a major role of S2P in controlling root growth. The *bzip17 bzip28* double mutant exhibits stunted short root phenotype, even shorter than that of *s2p* or *s1p s2p*, along with dwarfed plant and delayed germination, indicating there is an unknown S1P/S2P-independent path for controlling bZIP17/28-mediated root growth. In the recent study, Kim et al. (2022)

further found that NOBIRO6/TAF12b (TBP-ASSOCIATED FACTOR 12b (TAF12b)), a general transcription factor component, may function as a cofactor of bZIP60 for maintaining favorable level of UPR signal output. Regarding the rate of root recovery in *nobiro6 bzip17 bzip28*, bZIP60-independent pathway for controlling root growth is still yet to be identified.

Although each arm of plant UPR plays specific functions in certain pathways or conditions, both arms also have overlapping functions. For instance, bZIP28 works cooperatively with IRE1 and bZIP60 in ER stress responses (Liu and Howell, 2010; Howell, 2013). The *ire1b bzip28* double mutant exhibits a phenotype similar to that of the *ire1a ire1b* double mutant (Figure 3), inhibiting primary root elongation under both stress and non-stress conditions. Interestingly, the *bzip28 bzip60* double mutant does not affect root elongation under normal conditions. However, under ER stress, the *bzip28 bzip60* double mutant inhibits primary root elongation profoundly. As bZIP60 is a direct and classic target of IRE1, therefore, the author believes that the promoting effect of IRE1b on roots is unrelated to bZIP60 under non-stress conditions (Deng et al., 2013). bZIP17 was shown to function redundantly with bZIP28 in controlling plant root growth (Kim et al., 2018), but when combined with b*zip60*, the relevant *bzip17 bzip60* double mutant does not interfere with the elongation of primary root under non-stress condition. However, during ER stress, the primary root of *bzip17 bzip60* is significantly reduced, but not as profound as that of *bzip28 bzip60* (Deng et al., 2013; Kim et al., 2018; Bao et al., 2019). The primary root of *ire1b bzip17* is also significantly shorter than that of the wild-type, but this difference was neither observed in *ire1a bzip17* nor in *ire1a bzip28* (Bao et al., 2019). *ire1a ire1b bzip17* (*17ab*) triple mutant is viable and has very stunted primary root (5% of that in the wild-type, shorter than that of *bzip17 bzip28*), while *ire1a ire1b bzip28* is lethal. All above discoveries suggest a major role of IRE1b and bZIP28 in UPR-regulated root growth. Of note, *bzip17 bzip28 bzip60* triple mutant is not obtainable (Kim et al., 2018), implying the high redundance and essential role of those three transcriptional factors in regulating plant growth.

As mentioned above, elongation of primary roots under non-stress conditions depends on IRE1. IRE1 is a dual protein kinase and RNase, therefore, it is necessary to explore the influence of its different specific functions on root growth. Using site-directed mutagenesis, Deng et al. (2013) showed that disrupting the nucleotide binding activity (D608N K610N) or RNase activity (N820A) of IRE1b cannot restore the stress sensitive phenotype of *ire1a ire1b*, while the IRE1b kinase-dead variant (D628A) and nonmutated form can. However, none of the three mutated forms of IRE1b can restore the *17ab* dwarf phenotype or its root growth defects, suggesting the impacts of corresponding domains in IRE1 may vary depends on different genetic backgrounds applied. More importantly, the active nucleus-targeted forms of bZIP17, bZIP28 and bZIP60 can all restore growth defects of *17ab*, but the Golgi-detained bZIP17G372A cannot, suggesting UPR-associated bZIP transcriptional factors have shared functions and need to be activated for sustaining root growth, even without stress (Bao et al., 2019). Interestingly, in the previous research, Liu et al. (2007b) reported that constitutive over expression of the active form of bZIP17 can inhibit plant growth in the wild-type. Opposite function of bZIP17 in different genetic backgrounds looks intriguing but may somehow reflect the dual role of UPR in balancing plant growth and stress response.

IRE1c is a recently discovered plant-specific isoform of IRE1 family. The root length of *ire1c* single mutant is similar to that of the wild-type under ER stress or normal conditions. *ire1a ire1c* behaves the same as *ire1c*, however, *ire1b ire1c* and *ire1a ire1b ire1c* are lethal (Pu et al., 2019). The underlying mechanism of IRE1c in controlling plant root growth and UPR signaling is puzzling and yet to be verified.

UPR in controlling plant reproduction

Pollen abortion is one of the most influential factors that can cause crop yield reduction. A variety of genetic and environmental factors can affect the normal development of pollen in flowering plants, including high temperature, drought, high light and beyond. Studies have shown that the temperature requirements during plant development are very strict, and pollen development is very sensitive to high temperature. Some transcription factors and RNA splicing factors are closely involved in the UPR and play a vital role in pollen resistance to heat stress (Table 1). IRE1, a major component of the UPR pathway, relies on its ribonuclease activity for splicing mRNA to protect male fertility from heat stress (Deng et al., 2016). Arabidopsis *ire1a ire1b* double mutant has normal and vigorous pollen development under normal growth conditions, while during heat stress, the double mutant has defective growth and exhibits temperature-sensitive male sterility traits. Intriguingly, overexpression of *SEC31A*, a COPII membrane vesicle trafficking protein and potential target of UPR pathway, rescued male sterility in the *ire1a ire1b* double mutant (Deng et al., 2016). Not coincidentally and pollen development under high temperature stress is also closely linked to bZIP28 on the other arm of plant UPR. Arabidopsis *bzip28 bzip60* double mutant plants exhibit a hypersensitive phenotype to high temperature stress, such as shorter cuticles and reduced fertility (Zhang et al., 2017). In the *ire1b bzip28* double mutant, pollen development is also slightly affected. Homozygous *ire1a ire1b bzip28* triple mutant is not viable, but pollens from the *ire1a ire1b bzip28*+/- mutant plant showed approximately 50% pollen abortion. Thus, it is concluded that IRE1b protein kinase and RNase activity are essential for male

TABLE 1 Reproduction property of Arabidopsis canonical UPR pathway mutants.

Genotype (Gene ID)	Normal condition	Heat stress	Reference
ire1a (AT2G17520)	normal	\	Mishiba et al., 2019
ire1b (AT5G24360)	normal	\	Mishiba et al., 2019
ire1c (AT3G11870)	normal	\	Mishiba et al., 2019
ire1a ire1b	normal	defective pollen, low fertility	Deng et al., 2016; Mishiba et al., 2019
ire1a ire1c	normal	\	Mishiba et al., 2019
ire1b ire1c+/-	aborted pollen; homozygous lethal	\	Pu et al., 2019
ire1a ire1b ire1c+/-	aborted pollen; short stamens; homozygous lethal	\	Mishiba et al., 2019; Pu et al., 2019
s1p (AT5G19660)	\	\	Liu et al., 2007b
s2p (AT4G20310)	\	\	Kinch et al., 2006
s1p s2p	\	\	Che et al., 2010; Kim et al., 2018
rlg1+/- (AT1G07910)	homozygous lethal	homozygous lethal	Nagashima et al., 2016
bzip17 (AT2G40950)	normal	low fertility	Gao et al., 2022
bzip28 (AT3G10800)	normal	\	Liu et al., 2007a; Gao et al., 2008
bzip60 (AT1G42990)	normal	\	Iwata et al., 2008; Deng et al., 2011
bzip17 bzip28	\	\	Kim et al., 2018
bzip17 bzip60	normal	\	Deng et al., 2013; Bao et al., 2019
bzip28 bzip60	normal	low fertility	Deng et al., 2013; Zhang et al., 2017
bzip60 bzip17 bzip28+/-	heteromorphic flower; short stamens; homozygous lethal	\	Kim et al., 2018
ire1a bzip17	normal	\	Bao et al., 2019
ire1b bzip17	normal	\	Bao et al., 2019
ire1a bzip28	normal	\	Bao et al., 2019
ire1b bzip28	normal	\	Deng et al., 2013; Bao et al., 2019
ire1a ire1b bzip17	\	\	Bao et al., 2019
ire1a ire1b bzip28+/-	reduced pollen viability; homozygous lethal	\	Deng et al., 2013
ire1a ire1b bzip60	normal	\	Deng et al., 2013

+/-, heterozygote; /, not investigated.

gametophyte establishment (Deng et al., 2013). Compared with the wild-type, Arabidopsis *bzip17* mutant is found to be sensitive to heat stress in affecting silique length and fertility. ChIP-Seq (chromatin immuno-precipitation coupled with high-throughput sequencing) found that 1645 genes are direct target genes of bZIP17 under heat stress. Among them, 113 genes are up-regulated by bZIP17 in flowers under heat stress. These results demonstrate that bZIP17 also plays an important role in maintaining plant fertility under heat stress (Gao et al., 2021).

Previous studies have shown that BiP (Binding Protein) proteins function coordinately in well-developed pollen and pollen tubes. Pollens from *bip1 bip2* double mutant plants are normal, but pollens from *bip1 bip2 bip3* triple mutant are lethal (Maruyama et al., 2014). Arabidopsis HOP3 (HSP70/HSP90 organizing protein 3) is a BiP interacting cytosolic cochaperone protein, whose expression is both transcriptional and translationally regulated by IRE1 during ER stress. When knocked out, *hop3* shows defects in pollen development and inability to resist ER stress (Fernandez-Bautista et al., 2017). In line with the above findings, TMS1 (Thermosensitive Male Sterile 1), another heat shock protein, acts downstream of *bZIP28* and *bZIP60* during heat stress and function as physical partners of BiP proteins in sustaining protein folding capacity for plant thermotolerance (Ma et al., 2015).

As mentioned above, the pollen development process is closely linked to the fertilization process, and the normal development of the endosperm in flowering plants cannot be achieved without the UPR, and key regulatory genes from both arms of UPR pathways are also involved in the regulation of rice grain chalkiness (Vitale and Boston, 2008; Zhang et al., 2017; Sandhu et al., 2021). *OsbZIP60* (a homolog of *AtbZIP28*), an important regulator of heat stress and drought stress response in rice, also regulates rice grain chalking. Loss of *OsbZIP60* gene results in hyper ER stress sensitivity during endosperm development. In the *osbzip60* mutant, UPR-associated genes *OsbZIP50* (a homolog of *AtbZIP60*) and *OsBiP2/3/4/5* are overactivated in endosperm cells and lead to a severe grain chalkiness phenotype. In addition, OsbZIP50 also amplifies ER stress signal by promoting its own transcription. And overexpression of *OsBiP2/3/4/5* leads to different degrees of chalkiness in grains, respectively. This further suggests that UPR activation in *osbzip60* mutant is inseparable from OsbZIP50, and that OsbZIP60 balances endosperm

development and grain chalkiness by suppressing the overexpression of OsbZIP50 (Hayashi et al., 2012; Wakasa et al., 2012; Yang et al., 2022). Moreover, OsbZIP60 activates the expression of *Chalk5*, a master effector gene that regulates chalkiness traits in rice. Chalk5 disrupts protein biosynthesis in the rice endosomal system by acting as a vacuolar H^+ transport pyrophosphatase (V-PPase), and overexpression of *Chalk5* enhances the endosperm and grain chalkiness phenotypes (Li et al., 2014).

Recent studies revealed a unique plant IRE1 subtype, AtIRE1c, which is only found in *Brassica* species. IRE1c and IRE1b have unexpected functional coordination in controlling gametogenesis in Arabidopsis (Table 1), however, there is no clear evidence of IRE1c in modulating canonical UPR (Mishiba et al., 2019; Pu et al., 2019). Functional diversification of IRE1c and its exact role in UPR pathway thus warrants further explorations.

Discussions and future perspectives

After decades of efforts committed in studying Arabidopsis and some other plant species, great progresses were achieved in our understanding of plant UPR pathway. Attributing to the sessile feature of plants, UPR pathway components and the relevant mechanism of activation have been extensively investigated in environment-derived ER stress responding. In recent years, more and more evidence suggests that UPR is strongly involved in plant growth and development. Studies from (Bao et al., 2019) clearly suggested that, even without stress, endogenous basal activation of UPR pathway is required for maintaining normal plant growth, functional UPR thus plays dual roles in controlling growth and stress responding. How plants manipulate the same set of UPR components and fine-tune the level of UPR activation for balancing growth and stress response is ambiguous, but the underlying mechanism will be exciting to explore. Like UPR, autophagy also plays dual roles in regulating plant growth and stress response. ER stress-mediated autophagy activation seems IRE1 dependent and bZIP60 independent (Bao et al., 2018), reinforcing the critical role of IRE1-associated RIDD pathway in this process. Decoding the exact function of relevant RIDD targets is challenging but will be helpful in dissecting the principles of RIDD-mediated UPR regulation. In addition to UPR and autophagy, other ERQC system like ERAD (ER-associated degradation) was also showed to be involved in plant growth and stress responding (Chen et al., 2020). How plants leverage and coordinate each pathway for maintaining ER homeostasis is a long outstanding but critical question to be addressed. IRE1c family proteins were found to be unique for *Brassicaceae* species, which lack an ER lumenal sensing domain (Mishiba et al., 2019). Essential role of IRE1c will appear when acting in combination with IRE1b (Pu et al., 2019), but how does IRE1c exert its function with IRE1b is quite interesting and definitely justified for further investigations. Persistent ER stress and ER stress recovery are recent new trends in studying plant UPR pathway (Ruberti and Brandizzi, 2018; Srivastava et al., 2018; Ko and Brandizzi, 2022a; Ko and Brandizzi, 2022b), interpreting the relevant working language in UPR pathway will advance our understanding of plant environment adaptions and accelerate the breeding of stress-resistant crops.

Author contributions

YB concepted the topic of this manuscript with YLiu. YL and YLL drafted the manuscript with YB. YB revised the manuscript. All authors contributed to the article and approved the submitted version.

Funding

This research is supported by China Agriculture Research System of MOF and MARA.

Conflict of interest

The authors declare that the research was conducted in the absence of any commercial or financial relationships that could be construed as a potential conflict of interest.

Publisher's note

All claims expressed in this article are solely those of the authors and do not necessarily represent those of their affiliated organizations, or those of the publisher, the editors and the reviewers. Any product that may be evaluated in this article, or claim that may be made by its manufacturer, is not guaranteed or endorsed by the publisher.

References

Advani, V. M., and Ivanov, P. (2020). Stress granule subtypes: An emerging link to neurodegeneration. *Cell Mol. Life Sci.* 77 (23), 4827–4845. doi: 10.1007/s00018-020-03565-0

Afrin, T., Costello, C. N., Monella, A. N., Korner, C. J., and Pajerowska-Mukhtar, K. M. (2022). The interplay of GTP-binding protein AGB1 with ER stress sensors IRE1a and IRE1b modulates *arabidopsis* unfolded protein response and bacterial

immunity. *Plant Signal Behav.* 17 (1), 2018857. doi: 10.1080/15592324.2021.2018857

Bao, Y., Bassham, D. C., and Howell, S. H. (2019). A functional unfolded protein response is required for normal vegetative development. *Plant Physiol.* 179 (4), 1834–1843. doi: 10.1104/pp.18.01261

Bao, Y., Pu, Y., Yu, X., Gregory, B. D., Srivastava, R., Howell, S. H., et al. (2018). IRE1B degrades RNAs encoding proteins that interfere with the induction of autophagy by ER stress in *arabidopsis thaliana*. *Autophagy* 14 (9), 1562–1573. doi: 10.1080/15548627.2018.1462426

Che, P., Bussell, J. D., Zhou, W., Estavillo, G. M., Pogson, B. J., and Smith, S. M. (2010). Signaling from the endoplasmic reticulum activates brassinosteroid signaling and promotes acclimation to stress in *arabidopsis*. *Sci. Signal* 3 (141), ra69. doi: 10.1126/scisignal.2001140

Chen, Y., Aung, K., Rolcik, J., Walicki, K., Friml, J., and Brandizzi, F. (2014). Inter-regulation of the unfolded protein response and auxin signaling. *Plant J.* 77 (1), 97–107. doi: 10.1111/tpj.12373

Chen, Y., and Brandizzi, F. (2012). AtIRE1A/AtIRE1B and AGB1 independently control two essential unfolded protein response pathways in *arabidopsis*. *Plant J.* 69 (2), 266–277. doi: 10.1111/j.1365-313X.2011.04788.x

Chen, Q., Yu, F., and Xie, Q. (2020). Insights into endoplasmic reticulum-associated degradation in plants. *New Phytol.* 226 (2), 345–350. doi: 10.1111/nph.16369

Deng, Y., Humbert, S., Liu, J. X., Srivastava, R., Rothstein, S. J., and Howell, S. H. (2011). Heat induces the splicing by IRE1 of a mRNA encoding a transcription factor involved in the unfolded protein response in *arabidopsis*. *Proc. Natl. Acad. Sci. U.S.A.* 108 (17), 7247–7252. doi: 10.1073/pnas.1102117108

Deng, Y., Srivastava, R., and Howell, S. H. (2013). Protein kinase and ribonuclease domains of IRE1 confer stress tolerance, vegetative growth, and reproductive development in *arabidopsis*. *Proc. Natl. Acad. Sci. U.S.A.* 110 (48), 19633–19638. doi: 10.1073/pnas.1314749110

Deng, Y., Srivastava, R., Quilichini, T. D., Dong, H., Bao, Y., Horner, H. T., et al. (2016). IRE1, a component of the unfolded protein response signaling pathway, protects pollen development in *arabidopsis* from heat stress. *Plant J.* 88 (2), 193–204. doi: 10.1111/tpj.13239

Doultsinos, D., Avril, T., Lhomond, S., Dejeans, N., Guedat, P., and Chevet, E. (2017). Control of the unfolded protein response in health and disease. *SLAS. Discov* 22 (7), 787–800. doi: 10.1177/2472555217701685

Fernandez-Bautista, N., Fernandez-Calvino, L., Munoz, A., and Castellano, M. M. (2017). HOP3, a member of the HOP family in *arabidopsis*, interacts with BiP and plays a major role in the ER stress response. *Plant Cell Environ.* 40 (8), 1341–1355. doi: 10.1111/pce.12927

Gao, H., Brandizzi, F., Benning, C., Larkin, R.M., and Liu, J.-X. (2008). A membrane-tethered transcription factor defines a branch of the heat stress response in *Arabidopsis thaliana*. *Proc. Natl. Acad. Sci. USA* 105 (42), 16398–403. doi: 10.1073/pnas.0808463105

Gao, J., Wang, M.-J., Wang, J.-J., Lu, H.-P., and Liu, J.-X. (2022). bZIP17 regulates heat stress tolerance at reproductive stage in *arabidopsis*. *aBIOTECH* 3 (1), 1–11. doi: 10.1007/s42994-021-00062-1

Hayashi, S., Wakasa, Y., Takahashi, H., Kawakatsu, T., and Takaiwa, F. (2012). Signal transduction by IRE1-mediated splicing of bZIP50 and other stress sensors in the endoplasmic reticulum stress response of rice. *Plant J.* 69 (6), 946–956. doi: 10.1111/j.1365-313X.2011.04844.x

Haze, K., Yoshida, H., Yanagi, H., Yura, T., Mori, K., and Silver, P. (1999). Mammalian transcription factor ATF6 is synthesized as a transmembrane protein and activated by proteolysis in response to endoplasmic reticulum stress. *Mol. Biol. Cell* 10 (11), 3787–3799. doi: 10.1091/mbc.10.11.3787

Hong, Z. H., Qing, T., Schubert, D., Kleinmanns, J. A., and Liu, J. X. (2019). BLISTER-regulated vegetative growth is dependent on the protein kinase domain of ER stress modulator IRE1A in *arabidopsis thaliana*. *PloS Genet.* 15 (12), e1008563. doi: 10.1371/journal.pgen.1008563

Howell, S. H. (2013). Endoplasmic reticulum stress responses in plants. *Annu. Rev. Plant Biol.* 64, 477–499. doi: 10.1146/annurev-arplant-050312-120053

Howell, S. H. (2017). When is the unfolded protein response not the unfolded protein response? *Plant Sci.* 260, 139–143. doi: 10.1016/j.plantsci.2017.03.014

Iwata, Y., Ashida, M., Hasegawa, C., Tabara, K., Mishiba, K. I., and Koizumi, N. (2017). Activation of the *arabidopsis* membrane-bound transcription factor bZIP28 is mediated by site-2 protease, but not site-1 protease. *Plant J.* 91 (3), 408–415. doi: 10.1111/tpj.13572

Iwata, Y., Fedoroff, N. V., and Koizumi, N. (2008). *Arabidopsis* bZIP60 is a proteolysis-activated transcription factor involved in the endoplasmic reticulum stress response. *Plant Cell* 20 (11), 3107–3121. doi: 10.1105/tpc.108.061002

Kim, J. S., Sakamoto, Y., Takahashi, F., Shibata, M., Urano, K., Matsunaga, S., et al. (2022). *Arabidopsis* TBP-ASSOCIATED FACTOR 12 ortholog NOBIRO6 controls root elongation with unfolded protein response cofactor activity. *Proc. Natl. Acad. Sci. U.S.A.* 119 (6), e2120219119. doi: 10.1073/pnas.2120219119

Kim, J. S., Yamaguchi-Shinozaki, K., and Shinozaki, K. (2018). ER-anchored transcription factors bZIP17 and bZIP28 regulate root elongation. *Plant Physiol.* 176 (3), 2221–2230. doi: 10.1104/pp.17.01414

Kinch, L. N., Ginalski, K., and Grishin, N. V. (2006). Site-2 protease regulated intramembrane proteolysis: Sequence homologs suggest an ancient signaling cascade. *Protein Sci.* 15 (1), 84–93. doi: 10.1110/ps.051766506

Ko, D. K., and Brandizzi, F. (2022a). Advanced genomics identifies growth effectors for proteotoxic ER stress recovery in *arabidopsis thaliana*. *Commun. Biol.* 5 (1), 16. doi: 10.1038/s42003-021-02964-8

Ko, D. K., and Brandizzi, F. (2022b). Transcriptional competition shapes proteotoxic ER stress resolution. *Nat. Plants* 8 (5), 481–490. doi: 10.1038/s41477-022-01150-w

Koizumi, N., Martinez, I. M., Kimata, Y., Kohno, K., Sano, H., and Chrispeels, M. J. (2001). Molecular characterization of two *arabidopsis* Ire1 homologs, endoplasmic reticulum-located transmembrane protein kinases. *Plant Physiol.* 127 (3), 949–962. doi: 10.1104/pp.010636

Li, Y., Fan, C., Xing, Y., Yun, P., Luo, L., Yan, B., et al. (2014). Chalk5 encodes a vacuolar H^+-translocating pyrophosphatase influencing grain chalkiness in rice. *Nat. Genet.* 46 (4), 398–404. doi: 10.1038/ng.2923

Liu, J. X., and Howell, S. H. (2010). bZIP28 and NF-y transcription factors are activated by ER stress and assemble into a transcriptional complex to regulate stress response genes in *arabidopsis*. *Plant Cell* 22 (3), 782–796. doi: 10.1105/tpc.109.072173

Liu, J. X., Srivastava, R., Che, P., and Howell, S. H. (2007a). An endoplasmic reticulum stress response in *arabidopsis* is mediated by proteolytic processing and nuclear relocation of a membrane-associated transcription factor, bZIP28. *Plant Cell* 19 (12), 4111–4119. doi: 10.1105/tpc.106.050021

Liu, J. X., Srivastava, R., Che, P., and Howell, S. H. (2007b). Salt stress responses in *arabidopsis* utilize a signal transduction pathway related to endoplasmic reticulum stress signaling. *Plant J.* 51 (5), 897–909. doi: 10.1111/j.1365-313X.2007.03195.x

Ma, Z. X., Leng, Y. J., Chen, G. X., Zhou, P. M., Ye, D., and Chen, L. Q. (2015). The THERMOSENSITIVE MALE STERILE 1 interacts with the BiPs *via* DnaJ domain and stimulates their ATPase enzyme activities in *arabidopsis*. *PloS One* 10 (7), e0132500. doi: 10.1371/journal.pone.0132500

Manghwar, H., and Li, J. (2022). Endoplasmic reticulum stress and unfolded protein response signaling in plants. *Int. J. Mol. Sci.* 23 (2), 828. doi: 10.3390/ijms23020828

Marks, M. D., Wenger, J. P., Gilding, E., Jilk, R., and Dixon, R. A. (2009). Transcriptome analysis of *arabidopsis* wild-type and gl3-sst sim trichomes identifies four additional genes required for trichome development. *Mol. Plant* 2 (4), 803–822. doi: 10.1093/mp/ssp037

Maruri-Lopez, I., Figueroa, N. E., Hernandez-Sanchez, I. E., and Chodasiewicz, M. (2021). Plant stress granules: Trends and beyond. *Front. Plant Sci.* 12. doi: 10.3389/fpls.2021.722643

Maruyama, D., Sugiyama, T., Endo, T., and Nishikawa, S. (2014). Multiple BiP genes of *arabidopsis thaliana* are required for male gametogenesis and pollen competitiveness. *Plant Cell Physiol.* 55 (4), 801–810. doi: 10.1093/pcp/pcu018

Mishiba, K. I., Iwata, Y., Mochizuki, T., Matsumura, A., Nishioka, N., Hirata, R., et al. (2019). Unfolded protein-independent IRE1 activation contributes to multifaceted developmental processes in *arabidopsis*. *Life Sci. Alliance.* 2 (5), e201900459. doi: 10.26508/lsa.201900459

Mishiba, K. I., Nagashima, Y., Suzuki, E., Hayashi, N., Ogata, Y., Shimada, Y., et al. (2013). Defects in IRE1 enhance cell death and fail to degrade mRNAs encoding secretory pathway proteins in the *arabidopsis* unfolded protein response. *Proc. Natl. Acad. Sci. U.S.A.* 110 (14), 5713–5718. doi: 10.1073/pnas.1219047110

Nagashima, Y., Iwata, Y., Mishiba, K., and Koizumi, N. (2016). *Arabidopsis* tRNA ligase completes the cytoplasmic splicing of bZIP60 mRNA in the unfolded protein response. *Biochem. Biophys. Res. Commun.* 470 (4), 941–946. doi: 10.1016/j.bbrc.2016.01.145

Nagashima, Y., Mishiba, K., Suzuki, E., Shimada, Y., Iwata, Y., and Koizumi, N. (2011). *Arabidopsis* IRE1 catalyses unconventional splicing of bZIP60 mRNA to produce the active transcription factor. *Sci. Rep.* 1, 29. doi: 10.1038/srep00029

Noh, S. (2002). Characterization of two homologs of Ire1p, a kinase/endoribonuclease in yeast, in *arabidopsis thaliana*. *Biochim. Biophys. Acta (BBA). - Gene Structure Expression* 1575 (1-3), 130–134. doi: 10.1016/s0167-4781(02)00237-3

Oxley, D., Ktistakis, N., and Farmaki, T. (2013). Differential isolation and identification of PI(3)P and PI(3,5)P2 binding proteins from *arabidopsis thaliana* using an agarose-phosphatidylinositol-phosphate affinity chromatography. *J. Proteomics* 91, 580–594. doi: 10.1016/j.jprot.2013.08.020

Pu, Y., Ruberti, C., Angelos, E. R., and Brandizzi, F. (2019). AtIRE1C, an unconventional isoform of the UPR master regulator AtIRE1, is functionally

associated with AtIRE1B in *arabidopsis* gametogenesis. *Plant Direct.* 3 (11), e00187. doi: 10.1002/pld3.187

Ruberti, C., and Brandizzi, F. (2018). Unfolded protein response in *arabidopsis*. *Methods Mol. Biol.* 1691, 231–238. doi: 10.1007/978-1-4939-7389-7_18

Sandhu, J., Irvin, L., Liu, K., Staswick, P., Zhang, C., and Walia, H. (2021). Endoplasmic reticulum stress pathway mediates the early heat stress response of developing rice seeds. *Plant Cell Environ.* 44 (8), 2604–2624. doi: 10.1111/pce.14103

Srivastava, R., Li, Z., Russo, G., Tang, J., Bi, R., Muppirala, U., et al. (2018). Response to persistent ER stress in plants: A multiphasic process that transitions cells from prosurvival activities to cell death. *Plant Cell* 30 (6), 1220–1242. doi: 10.1105/tpc.18.00153

Sun, J. L., Li, J. Y., Wang, M. J., Song, Z. T., and Liu, J. X. (2021). Protein quality control in plant organelles: Current progress and future perspectives. *Mol. Plant* 14 (1), 95–114. doi: 10.1016/j.molp.2020.10.011

Sun, L., Yang, Z. T., Song, Z. T., Wang, M. J., Sun, L., Lu, S. J., et al. (2013). The plant-specific transcription factor gene NAC103 is induced by bZIP60 through a new cis-regulatory element to modulate the unfolded protein response in *arabidopsis*. *Plant J.* 76 (2), 274–286. doi: 10.1111/tpj.12287

Vitale, A., and Boston, R. S. (2008). Endoplasmic reticulum quality control and the unfolded protein response: Insights from plants. *Traffic* 9 (10), 1581–1588. doi: 10.1111/j.1600-0854.2008.00780.x

Wakasa, Y., Hayashi, S., and Takaiwa, F. (2012). Expression of OsBiP4 and OsBiP5 is highly correlated with the endoplasmic reticulum stress response in rice. *Planta* 236 (5), 1519–1527. doi: 10.1007/s00425-012-1714-y

Wang, S., Narendra, S., and Fedoroff, N. (2007). Heterotrimeric G protein signaling in the *arabidopsis* unfolded protein response. *Proc. Natl. Acad. Sci. U.S.A.* 104 (10), 3817–3822. doi: 10.1073/pnas.0611735104

Wang, Q. L., Sun, A. Z., Chen, S. T., Chen, L. S., and Guo, F. Q. (2018). SPL6 represses signalling outputs of ER stress in control of panicle cell death in rice. *Nat. Plants* 4 (5), 280–288. doi: 10.1038/s41477-018-0131-z

Yang, Z. T., Lu, S. J., Wang, M. J., Bi, D. L., Sun, L., Zhou, S. F., et al. (2014a). A plasma membrane-tethered transcription factor, NAC062/ANAC062/NTL6, mediates the unfolded protein response in *arabidopsis*. *Plant J.* 79 (6), 1033–1043. doi: 10.1111/tpj.12604

Yang, Z. T., Wang, M. J., Sun, L., Lu, S. J., Bi, D. L., Sun, L., et al. (2014b). The membrane-associated transcription factor NAC089 controls ER-stress-induced programmed cell death in plants. *PloS Genet.* 10 (3), e1004243. doi: 10.1371/journal.pgen.1004243

Yang, W., Xu, P., Zhang, J., Zhang, S., Li, Z., Yang, K., et al. (2022). OsbZIP60-mediated unfolded protein response regulates grain chalkiness in rice. *J. Genet. Genomics* 49 (5), 414–426. doi: 10.1016/j.jgg.2022.02.002

Yu, C. Y., Cho, Y., Sharma, O., and Kanehara, K. (2022). What's unique? The unfolded protein response in plants. *J. Exp. Bot.* 73 (5), 1268–1276. doi: 10.1093/jxb/erab513

Yu, C. Y., and Kanehara, K. (2020). The unfolded protein response modulates a phosphoinositide-binding protein through the IRE1-bZIP60 pathway. *Plant Physiol.* 183 (1), 221–235. doi: 10.1104/pp.19.01488

Yu, C. Y., Sharma, O., Nguyen, P. H. T., Hartono, C. D., and Kanehara, K. (2021). A pair of DUF538 domain-containing proteins modulates plant growth and trichome development through the transcriptional regulation of GLABRA1 in *arabidopsis thaliana*. *Plant J.* 108 (4), 992–1004. doi: 10.1111/tpj.15487

Zhang, S. S., Yang, H., Ding, L., Song, Z. T., Ma, H., Chang, F., et al. (2017). Tissue-specific transcriptomics reveals an important role of the unfolded protein response in maintaining fertility upon heat stress in *arabidopsis*. *Plant Cell* 29 (5), 1007–1023. doi: 10.1105/tpc.16.00916

frontiers | Frontiers in Plant Science

TYPE Original Research
PUBLISHED 18 November 2022
DOI 10.3389/fpls.2022.1059749

Check for updates

OPEN ACCESS

EDITED BY
Xinyang Wu,
China Jiliang University, China

REVIEWED BY
Changquan Zhang,
Yangzhou University, China
Yihua Wang,
Nanjing Agricultural University, China
Xiangjin Wei,
State Key Laboratory of Rice Biology and Chinese National Center for Rice Improvement (CAAS), China

*CORRESPONDENCE
Xiaoli Shu
shuxl@zju.edu.cn

†These authors have contributed equally to this work

SPECIALTY SECTION
This article was submitted to Plant Abiotic Stress, a section of the journal Frontiers in Plant Science

RECEIVED 02 October 2022
ACCEPTED 21 October 2022
PUBLISHED 18 November 2022

CITATION
Zhou Y, Cheng Z, Jiang S, Cen J, Wu D and Shu X (2022) High temperature boosts resistant starch content by altering starch structure and lipid content in rice *ssIIIa* mutants. *Front. Plant Sci.* 13:1059749. doi: 10.3389/fpls.2022.1059749

COPYRIGHT
© 2022 Zhou, Cheng, Jiang, Cen, Wu and Shu. This is an open-access article distributed under the terms of the Creative Commons Attribution License (CC BY). The use, distribution or reproduction in other forums is permitted, provided the original author(s) and the copyright owner(s) are credited and that the original publication in this journal is cited, in accordance with accepted academic practice. No use, distribution or reproduction is permitted which does not comply with these terms.

High temperature boosts resistant starch content by altering starch structure and lipid content in rice *ssIIIa* mutants

Yufeng Zhou[1†], Zhenfeng Cheng[1,2†], Shuo Jiang[1], Jinxi Cen[1,2], Dianxing Wu[1,2] and Xiaoli Shu[1,2*]

[1]State Key Laboratory of Rice Biology and Key Lab of the Ministry of Agriculture for Nuclear Agricultural Sciences, Institute of Nuclear Agricultural Sciences, Zhejiang University, Hangzhou, China, [2]Hainan Institute, Zhejiang University, Yazhou Bay Science and Technology City, Sanya, China

High temperature (HT) during grain filling had adverse influences on starch synthesis. In this study, the influences of HT on resistant starch (RS) formation in rice were investigated. Most genes in *ssIIIa* mutants especially in RS4 were upregulated under Normal Temperature (NT) while downregulated under HT when compared with those of wild parent R7954. *ssIIIa* mutants had higher RS content, more lipid accumulation, higher proportion of short chains of DP 9–15, and less long chains of DP ≥37. *ssIIIa* mutation exacerbated the influences of HT on starch metabolite and caused larger declines in the expression of *BEI*, *BEIIa*, *BEIIb*, and *SSIVb* when exposed to HT. HT reduced the contents of total starch and apparent amylose significantly in wild type but not in mutants. Meanwhile, lipids were enriched in all varieties, but the amounts of starch–lipid complexes and the RS content were only heightened in mutants under HT. HT led to greatest declines in the amount of DP 9–15 and increases in the proportion of fb3 (DP ≥37); the declines and increases were all larger in mutants, which resulted in varied starch crystallinity. The increased long-chain amylopectin and lipids may be the major contributor for the elevated RS content in mutants under HT through forming more starch–lipid complexes (RSV).

KEYWORDS

resistant starch, high temperature, amylopectin, chain length distribution, rice

Introduction

Rice (*Oryza sativa*) is an extremely important cereal and is the main food for more than 50% of the population worldwide. As the major components in rice grains, starch mainly comprises amylose and amylopectin molecules. The ratio of amylose to amylopectin and the structure of starch granules are key factors influencing rice quality. Meanwhile, amylose content and the distributions of branch lengths in both amylose and amylopectin influence starch digestibility (Syahariza et al., 2014; Raigond et al., 2015). The rate and extent of digestibility of starch in the small intestine determine the eventual glucose level in blood, which is of great interest in the context of worldwide health concerns.

Although starch is a homopolysaccharide of glucose, a proportion of starch, namely, resistant starch (RS), is not digested in the small intestine and passed into the large intestine to produce short-chain fatty acids (Englyst and Hudson, 1996; Hu et al., 2016). Due to its digestion resistance, RS is beneficial for inflammatory bowel disease, glycemic index, cholesterol levels, coronary heart disease, and other conditions (Shen et al., 2022). Based on different origins and characteristics, RS can be classified into RSI, RSII, RSIII, RSIV, and RSV five types. RSII consists of native starch granules with a compact structure, majorly exists in raw potatoes, peas, and green bananas (Sajilata et al., 2006), and can become digestible after traditional cooking. RSIII consists of retrograded starches that are principally recrystallized amylose produced after heating starchy food, such as in rice. RSV is a complex of amylose and lipids that improve antidigestion capabilities through forming double helical structures (Hasjim et al., 2010).

Food high in RS is associated with improved cardiovascular health, gut health, and glycemic response, while RS contents in rice and other cereal crops are generally below 3% (Xia et al., 2018; Kumar et al., 2018) and affected by amylose content, starch granule structure, fine structure of amylopectin, and other metabolites such as lipids and sugars (Shen et al., 2022). Apparent amylose content (AAC) and amylopectin with degree of polymerization (DP) 8–12 have been found to be positively related to RS content (Shu et al., 2006; Shu et al., 2007; Shen et al., 2022). RS is decisive in determining the glycemic index of rice (Kumar et al., 2018). Nowadays, several genes involved in starch biosynthesis have been found to be responsible for RS formation in rice grains. The *Wx* gene may regulate RS formation by tuning the amylose content (Itoh et al., 2003; You et al., 2022). *BEIIb* may play an important role in RS formation through modulating the distribution of long and intermediate debranched amylopectin chains (Butardo et al., 2011; Guo et al., 2020; Miura et al., 2021) and tuning other metabolites such as sugar, lipid, and protein contents (Baysal et al., 2020). *be1be2b* double mutant shows higher RS content than the *be2b* mutant (Miura et al., 2021). *SSIIIa* has been verified to be a key gene responsible for the RS content; the loss-of-function of SSIIIa gives rise to a high RS content in rice grain, but the effect of *SSIIIa* on RS content depends partly on the functional *Wx* gene (Wx^a) (Zhou et al., 2016). Double repression of *SSIIa* and *SSIIIa* resulted in higher AAC and RS content (Zhang et al., 2011).

In a preliminary study, we developed a series of rice mutants high in RS (Shu et al., 2007; Shu et al., 2009; Ding et al., 2019). These mutants have significantly lower digestibility (Shu et al., 2009; Zhou et al., 2016) and show great potentialities in lowering the serum glucose level of Type II diabetes patients. However, the absolute content of RS in these mutants showed fluctuations among different growing years or locations (data not published). Bao et al. (2020) also found that the RS content of three chalky mutants derived from R9311 differed significantly between two environments (Hangzhou and Hainan). Among environmental factors, temperature is the most important for rice kernel development. It is proposed that temperature may influence the RS formation and the functional properties of high-RS rice.

With global warming, high temperature (HT) during grain filling has become a great threat for rice production. HT during grain filling can lead to reduced yield, increased chalkiness, and varied amylose content (AC) and starch structure (Zhang et al., 2016). AC has been found either increased or decreased when exposed to HT depending on rice variety (Cheng et al., 2005; Lin et al., 2010; Liu et al., 2021). Zhao et al. (2020) found that *ssIIIa*-RNAi affected the susceptibility of grain chalky occurrence to HT exposure due to the relatively sensitive response of ADP-glucose pyrophosphorylase (AGPase) and SSI to HT exposure and induced significant decreases in AAC and a larger decline in the proportion of DP <12 under HT relative to wild type (WT). Although the formation of RS in rice grain has been investigated in detail from the intrinsic properties of starch, storage and processing conditions, and external factors such as non-starch components (Shen et al., 2022), few concerns have been paid on the growth environment such as temperature. In view of extreme climate change, understanding the influences of temperature on RS formation will provide valuable clues for breeding high-RS rice with improved quality. In the present study, genetic *SSIIIa* mutations in high-RS rice mutants RS111 and RS4 were detected. The main reserve substances in rice under two growth conditions with different day/night temperatures are measured. Furthermore, the expression levels of genes involved in starch synthesis, amylopectin chain length (CL) distribution, X-ray diffraction (XRD) analysis and Fourier transform infrared (FTIR) spectroscopy, and thermal and pasting properties of starch were investigated. In addition, a possible mechanism of temperature affecting RS formation was proposed. The results in this study give some evidence for the impacts of temperature on RS formation in rice grain and provide alternative thoughts on improving the quality of rice high in RS under global climate warming.

Materials and methods

Plant materials and growth conditions

Three indica rice varieties with different RS contents were used in this study, including R7954 (WT) and RS111 and RS4 (mutants). RS111 was derived from R7954 through 300 Gy 60-Cobalt γ-ray mutagenesis, and RS4 was obtained from RS111 by irradiation (Shu et al., 2006; Shu et al., 2009); the two mutants have been planted for more than 15 generations. All varieties were grown in artificial climatic chambers with a relative humidity of 80% under a photon flux density of 630–720 $\mu mol \cdot m^{-1} \cdot s^{-1}$. The growth cabinets were maintained at an average air temperature of 25°C (NT, ranging from 20°C to 30°C, 12-h day/12-h night cycles) until flowering. Then, half of the plants were transferred to another growth cabinet with an average air temperature of 30°C (HT, ranging from 25°C to 35°C, 12-h day/12-h night cycles). Individual panicles were labeled on the day of flowering. Grains at 8 days after flowering (DAF) were collected and immediately frozen in liquid nitrogen and stored at -80°C until use. Mature grains were harvested and dried under 37°C, then the glume and aleurone were detached using Satake rice machine (Satake Corp., Japan). After polishing, the white rice was ground into flour, passed through a 150-μm sieve and stored in a drier until use.

DNA extraction and sequencing

The total genomic DNA of rice leaf was extracted using Tris physiological saline (TPS) (1 M Tris-HCl pH 8, 0.5 M EDTA pH 8, 5 M KCl) according to the procedure modified by Xin et al. (2003). The PCR products amplified with SSIIIa CAPS primer were digested using restriction enzyme TSP509i as previously reported (Zhou et al., 2016) and separated using 2% agarose gel. Genomic *SSIIIa* was amplified using gSSIIIa primer, and the PCR products were sequenced using Genetic Analyzer (3730XL-96, ABI, USA). All primers used are listed in Table S1.

RNA extraction and quantitative real-time PCR

The total RNA from dehulled seeds at 8 DAF was extracted using Plant RNA Extraction Kit (9769, Takara, Japan), and cDNA was synthesized using FastKing RT Kit (KR116, TIANGEN Biotech, China) following the manufacturer's protocol. Quantitative real-time PCR (qRT-PCR) was performed with SYBR Green Premix Pro Taq HS qPCR Kit (AG11701, Accurate Biotech, China) on the CFX96 Real-time system (Bio-Rad, USA). The rice *Actin* gene (LOC_Os0350885) was used as internal reference. qPCR primers of 27 starch-related genes were referred to Ohdan et al. (2005) and listed in Table S1.

Sample preparation and starch extraction

Starch was isolated using NaOH as follows. The flour and NaOH solution (0.3%, w/v) were mixed (1:20, w/v) thoroughly, shaking at 180 rpm and 4°C for 16 h. Then, the mixture was filtered with a 150-μm sieve, and the filtered solution was centrifuged at 5,000 g for 10 min. The yellow layer in the precipitation was scraped carefully, then the precipitation was suspended with ddH_2O, and the pH of the slurry was adjusted to neutral. Repeated centrifugation and rinsing with ddH_2O were done several times until the precipitation was clearly white. Then, the obtained starch was dried at 37°C, ground, and filtered with a 150-μm sieve. The isolated starch was used for XRD, FTIR, differential scanning calorimetry (DSC), and amylopectin chain length (CL) profile analyses.

Major reserves and RS measurement

AAC and total starch content were measured according to the methods described by Shu et al. (2014). The total protein was measured using Digestor (DT208, FOSS, Denmark) and automatic Kjeldahl nitrogen analyzer (Foss8400, FOSS, Denmark) based on the principle of Kjeldahl method. Lipid content was measured using a fat analyzer (SOX406, Hanon Group, China) based on Soxhlet extraction method.

RS content was measured according to Shu et al. (2014), but the released glucose content was measured using Glucose Assay Kit (Ningbo Saike Biological Technology, China). The glucose content was converted to starch content by a factor of 0.9.

Amylopectin chain length distribution

Amylopectin was extracted from starch using a fractionation method according to the procedure described by Kong et al. (2008). Purified amylopectin was debranched with pullulanase (E-PULKP, Megazyme, USA) and isoamylase (E-ISAMYHP, Megazyme, USA) using the method described by Kong et al. (2016). The CL distributions of debranched amylopectin were determined using high-performance anion-exchange chromatography (HPAEC) (DionexICS-5000+, Sunnyvale, CA, USA) with BioLC gradient pump and a pulsed amperometric detector (PAD) (Kong et al., 2016).

X-ray diffraction

The X-ray powder diffractometer (Bruker D8 Advance, Brucker, Germany) was used for XRD analysis. Starch samples were packed into a round glass sample holder and scanned from 4° to 70° 2θ with a step of 0.02°/2 s. The relative crystallinity (RC; %) was calculated using MDI Jade 6.5.

Fourier transform infrared spectroscopy

Starch granule short-range ordered structure was detected with the FTIR spectrometer (NICOLET iS50FT-IR, Thermo Scientific, USA). The resolution of the instrument is 4 cm^{-1}, and the scanning range is from 4,000 cm^{-1} to 400 cm^{-1}. The relative absorbances at 1,045, 1,022 and 995 cm^{-1} were extracted from the deconvoluted spectra and were measured from the baseline to the peak height.

Differential scanning calorimetry

The thermal properties of starch were determined using DSC (Q20, TA Instruments, Newcastle, DE, USA) according to the method described by Shu et al. (2009). The enthalpy change (ΔH), onset temperature (To), peak temperature (Tp), and conclusion temperature (Tc) were calculated using Universal Analysis 2000 program (Version 4.4A).

Rapid viscosity analysis

The pasting properties of rice flours were measured using a rapid visco analyzer (Model 4500, Perten Instruments, Sweden) according to the procedure described by Bao et al. (2004). Peak viscosity (PV), hot paste viscosity (HPV), cold paste viscosity (CPV), breakdown value (BD = PV-HPV), and setback value (SB = CPV-PV) were recorded.

Statistical analysis

All experiments have biological triplicates. One-way analysis of variance followed by the least significant difference (LSD) test ($P < 0.05$ or $P < 0.01$) was performed using SPSS 22 (IBM, USA).

Results

Genotypes of RS111 and RS4

SSIIIa has been confirmed to be a key gene for RS formation in rice, as RS111 and RS4 are both derived from R7954 as *b10*, whether they are allelic *ssIIIa* mutations was detected first. Compared with R7954, RS4 and RS111 carried a G/A mutation in the fifth intron of *SSIIIa*, which caused varied splicing and led to a 4-bp deletion in the coding sequence (Figures 1A, B). With the SSIIIa CAPS marker developed based on this Single

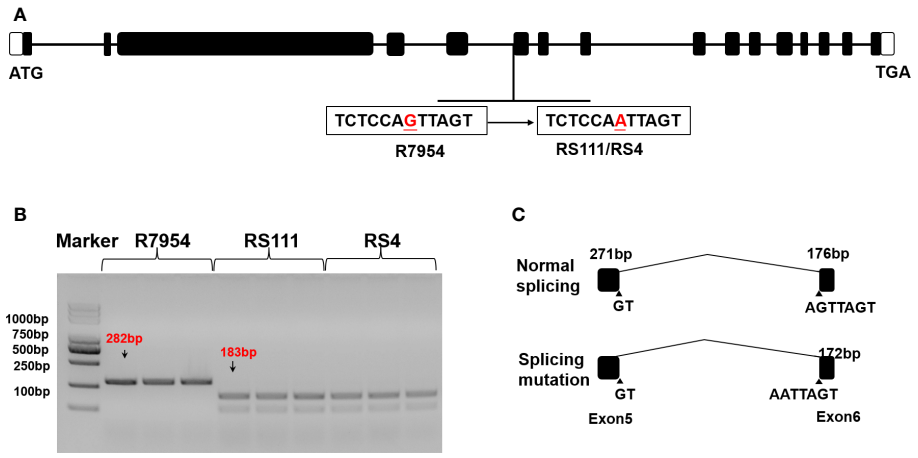


FIGURE 1
SSIIIa sequence variations in wild type (WT) (R7954) and mutants (RS111 and RS4). **(A)** Genomic sequencing of WT and mutants. **(B)** Genotyping of *SSIIIa* alleles using the *SSIIIa* CAPS marker. **(C)** Varied splicing of transcripts in WT and mutants.

Nucleotide Polymorphism (SNP), the PCR products were digested into two shorter products by TSP509i (Figure 1C). This proved that RS4 and RS111 carried the same mutation in *SSIIIa* gene as *b10* (Zhou et al., 2016) and are two allelic *ssIIIa* mutants.

Main reserve substances in the grains under different temperatures

The main reserves in grains of mutants RS111 and RS4 differed significantly from those in R7954, such as decreased starch content, elevated AAC, RS and lipid contents (Table 1). While RS4 and RS111 also showed differences in the contents of the main components, except total starch (Table 1). The RS content in RS4 under NT reached up to 7.76% and the lipid content was high up to 2.19%, which was almost two times and three times as high as those in RS111, respectively. In addition, the protein in RS4 was the least but that in RS111 was the highest. Meanwhile, RS4 showed almost transparent grain under NT, although both mutants showed serious chalk under HT (Figure S1). It is noteworthy that although both RS4 and RS111 had the same *ssIIIa* mutations, other genes related to starch or lipid metabolites might be mutated in RS4.

Under HT, the protein content was decreased in all three varieties and the lipid contents were all increased. The lipid content in R7954 increased up to 0.91%, close to that in RS111, and the lipid content in RS4 reached up to 3.0%. However, the total starch content and AAC in R7954 were reduced by 3.92% and 2.17%, respectively, while those in RS111 and RS4 are similar as those at NT. HT elevated the RS content only in RS111 and RS4 but not in R7954; the RS content increased from 3.97% to 4.83% and from 7.76% to 8.42% in RS111 and RS4, respectively (Table 1). This indicated that HT played different influences on the storage accumulations among R7954, RS111, and RS4, although they have the same genetic background.

Expression pattern of genes involved in starch synthesis

Among the detected 27 starch synthesis-related genes, the expression of *SSIIIa* was significantly downregulated in both RS111 and RS4, indicating that the mutation of *SSIIIa* diminished its transcript. Compared with R7954, most genes in mutants especially in RS4 were upregulated under NT, while these were downregulated under HT (Figure 2). However, the expressions of *SSIIIb*, *AGPL4*, and *SSIIa* were lower in RS4 than those in RS111 and R7954; the expression level of *SSIIa* in RS111 was the highest under both NT and HT (Figure 2A).

Upon HT, the expressions of starch-related genes showed different responses among R7954, RS111, and RS4. According to their expressions under NT and HT, all genes tested could be categorized into five groups (Figure 2B). *SSIIIa* and *SSIIIb* exhibited higher expressions in R7954 at HT than those at NT but showed similar or even lower expressions in RS111 and RS4 at HT. *AGPL4* and *SSIVa* were upregulated under HT in all three varieties. Group III contains most of the genes, including *SSIIa*, *BEI*, and *SBEIIb*; the expressions of these genes in the three varieties all declined to a certain extent under HT, although the attenuated expression of some genes in R7954 was slight. *ssIIIa* mutation increased the susceptibility of genes, such as *GBSSI*, *SSIVb*, *ISA1*, *BEIIb*, and *BEIIa*, to HT exposure, bringing up larger declines in the expression of most genes detected.

Amylopectin chain length distributions

Based on the DP, the side chains of amylopectin can be classified into four fractions, namely, fa with DP 6–12, fb1 with DP 13–24, fb2 with DP 25–36, and fb3 with DP ≥37, which correspond to A, B1, B2, and B3 together with longer chains, respectively (Nakamura et al., 1997). The proportions of fa, fb1, fb2, and fb3 from the three varieties under NT and HT were presented in Table 2. Among the three varieties, RS4 had the highest proportion of fa and the lowest amount of fb3, followed by RS111 and R7954. High-RS mutants RS111 and RS4 had reduced average chain length of amylopectin (Table 2). The varietal differences in amylopectin CL among R7954, RS111, and RS4 were consistent at either NT or HT; mutants had more chains of DP 9–15 and DP 20–30, with the greatest increases in DP 9–12 and less chains of DP ≥37 (Figures 3A, B). These results were basically similar to previous results (Fujita et al., 2007; Shu et al., 2007; Zhao et al., 2020). Under HT, the amounts of fa and fb1

TABLE 1 Main components of the three varieties under NT and HT*.

Varieties	Total starch (%)	AAC (%)	RS (%)	Protein (%)	Free lipids (%)
R7954-NT	77.27 ± 1.45a	24.91 ± 0.55c	0.75 ± 0.02e	5.44 ± 0.012c	0.30 ± 0.01e
R7954-HT	73.35 ± 0.66ab	22.74 ± 0.39d	0.79 ± 0.03e	5.31 ± 0.009d	0.91 ± 0.04cd
RS111-NT	67.06 ± 1.07c	27.03 ± 0.14b	3.97 ± 0.04d	5.80 ± 0.01a	0.69 ± 0.04d
RS111-HT	68.82 ± 1.29bc	27.69 ± 0.28b	4.83 ± 0.16c	5.59 ± 0.012b	1.08 ± 0.09c
RS4-NT	67.72 ± 1.26c	32.42 ± 0.10a	7.76 ± 0.2b	4.88 ± 0.005e	2.19 ± 0.07b
RS4-HT	68.81 ± 1.38bc	31.65 ± 0.44a	8.42 ± 0.28a	4.79 ± 0.009f	3.00 ± 0.05a

*The same small letter in the same column indicated that there were no significant differences among different samples at the $P < 0.05$ level. AAC, apparent amylose content; RS, resistant starch; NT, normal temperature; HT, high temperature.

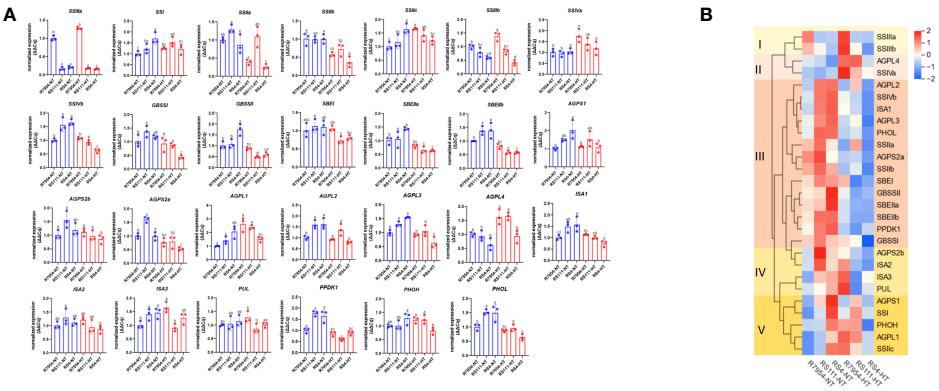


FIGURE 2
Expression levels of different genes in the three varieties under normal temperature (NT) and high temperature (HT) **(A)** and the clustering according to their expression levels **(B)**. The same small letter indicated that there were no significant differences among different samples at the $P < 0.05$ level.

were decreased and fb2 and fb3 were increased for all three varieties (Table 2), with the greatest decreases in DP 9–19 and increases in DP ≥37 (Figure 3C). Obvious decreases in fa under HT were also found in *ssIIIa*-RNAi rice (Zhao et al., 2020). It is noteworthy that the increase or decrease of the proportion of each chain at HT did not correspond to the borders of the fractions. HT resulted in an increase in the proportion of DP 20–30 in R7954 but not in RS111 and RS4 (Figure 3C). Several studies also found that HT decreased the proportion of fa and increased the proportions of fb2 and fb3 (Umemoto et al., 1999; Jiang et al., 2003; Zhang et al., 2016). The similar trends of decline in the proportion of chains with DP 9–19 in all three varieties indicated that the mechanism causing the temperature-dependent variation of CL is different from the one specifically regulating the proportions of fa and fb1 caused by the mutation of *ssIIIa*.

Long-range and short-range ordered structure

XRD can be used to measure the helices that are packed in regular arrays (in the long-range distance) forming crystallinity (Man et al., 2012). The XRD pattern of all starches showed diffraction peaks at ca. 15°, 23° and an unresolved doublet at ca. 17° and 18° (Figure 4A), which are the typical A-type crystalline pattern (Pérez and Bertoft, 2010). In addition, all XRD patterns showed a diffraction peak around 2θ 20°, which indicated the existence of the amylose–lipid complex (Putseys et al., 2010). RS4 had the lowest RC, but the most starch–lipid complexes, especially under HT (Table 3). This might be due to the higher lipid content and AAC in RS4 and RS111 (Table 1). Under HT, RC and the starch–lipid complexes of RS111 and RS4 were elevated but not for R7954 (Table 3).

With FTIR, short-range ordered structure of starch granule can be observed, the ratio of absorption at 1,045/1,022 cm^{-1} and 1,022/995 cm^{-1} can reflect the degree of order structure and the proportion of amorphous to ordered carbohydrate structure in starch granule external region, respectively (Sevenou et al., 2002). All three varieties showed similar FTIR profiles under both NT and HT; no new peaks appeared (Figure 4B). RS111 and RS4 showed higher 1,045/1,022 cm^{-1} ratio but lower 1,022/995 cm^{-1} ratio under NT (Table 3), indicating that there were more short-range order helical structure in the external region

TABLE 2 Chain length distribution of amylopectin in all rice materials, as determined by HPAEC-PAD analysis*.

Varieties	fa (6≤DP≤12) (%)	fb1 (13≤DP≤24) (%)	ffb2 (25≤DP≤36) (%)	fb3 (37≤DP) (%)	Peak DP	Average CL	fa/fb1	fa/fb1-2	fa/fb1-3
R7954-NT	24.76 ± 0.17c	48.01 ± 0.33ab	12.53 ± 0.25b	14.7 ± 0.52ab	12	20.77 ± 0.35	0.52	0.41	0.33
R7954-HT	23.4 ± 0.53d	47.22 ± 0.84b	13.28 ± 0.15a	16.1 ± 1.44a	12	22.12 ± 0.21	0.5	0.39	0.31
RS111-NT	26.59 ± 0.17b	48.79 ± 0.16ab	12.79 ± 0.15ab	11.83 ± 0.36cd	12	18.17 ± 0.13	0.54	0.43	0.36
RS111-HT	25.95 ± 0.12b	47.48 ± 0.16ab	13.16 ± 0.14ab	13.41 ± 0.18abc	12	20.73 ± 0.11	0.55	0.43	0.35
RS4-NT	28.25 ± 0.2a	49.14 ± 0.16a	12.76 ± 0.11ab	9.84 ± 0.31d	12	18.26 ± 0.29	0.57	0.46	0.39
RS4-HT	26.66 ± 0.07b	47.19 ± 0.03b	12.91 ± 0.04ab	13.24 ± 0.07bc	12	20.18 ± 0.21	0.56	0.44	0.36

*The same small letter in the same column indicated that there were no significant differences among different samples at the P < 0.05 level. CL, chain length.

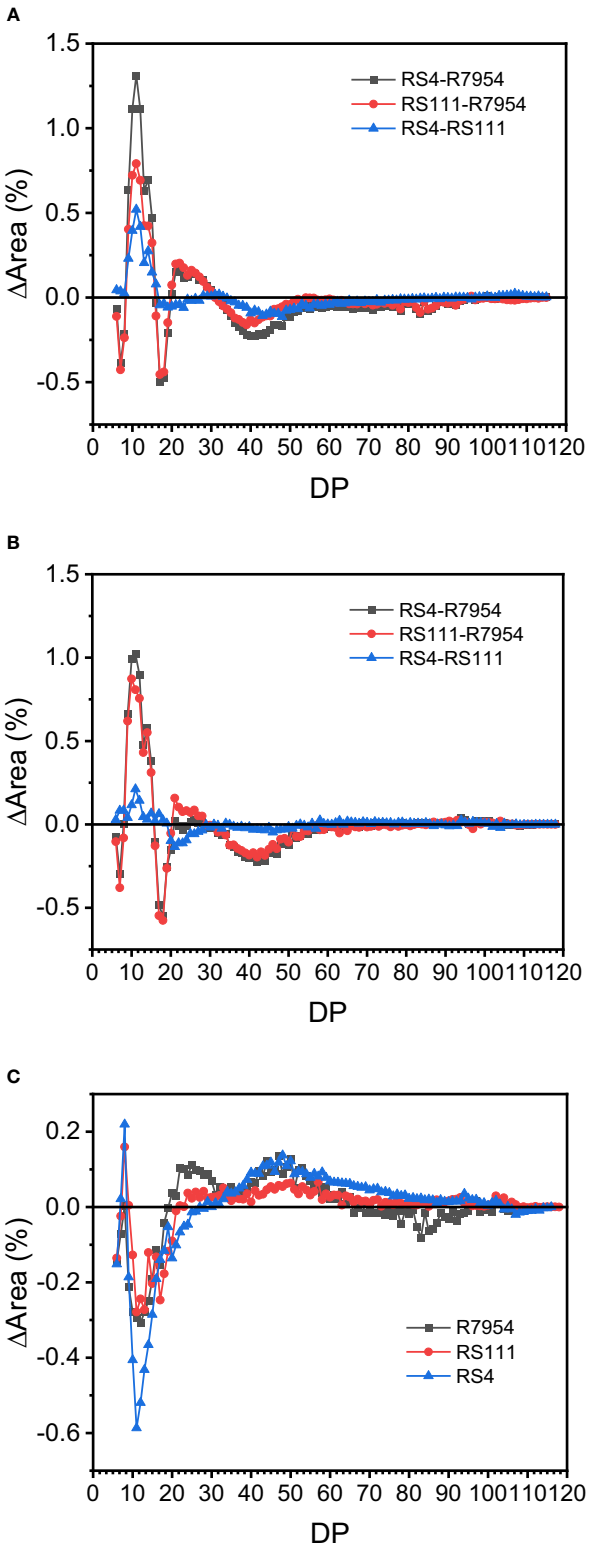


FIGURE 3
Comparison of the chain length distribution patterns of amylopectin among rice at normal temperature (NT) **(A)**, high temperature (HT) **(B)**, and between HT and NT **(C)**.

10.3389/fpls.2022.1059749

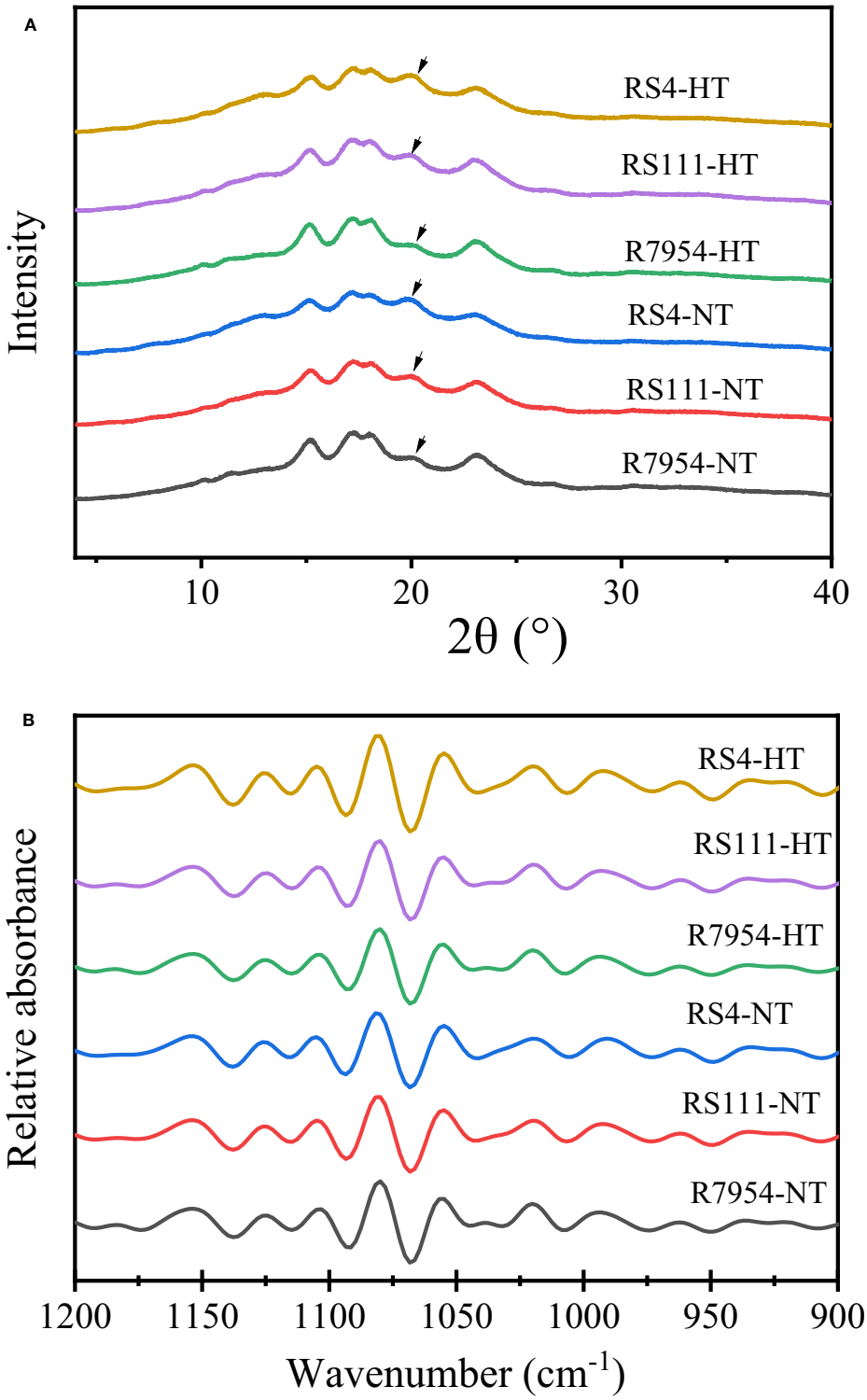


FIGURE 4
X-ray diffraction (XRD) spectra **(A)** and deconvoluted Fourier transform infrared (FTIR) spectroscopy spectra **(B)** of starches from wild type (WT) and mutants at normal temperature (NT) and high temperature (HT). The arrow in panel **(A)** indicated the peaks of starch–lipid complexes.

10.3389/fpls.2022.1059749

TABLE 3 RC and IR ratios of starches from R7954, RS111 and RS4 at NT and HT*.

Sample	RC (%)	Starch–lipid complexes (%)	IR ratio 1,045/1,022 (cm^{-1})	IR ratio 1,022/995 (cm^{-1})
R7954-NT	30.62 ± 0.15a	1.05 ± 0.01a	0.648 ± 0.0004e	1.137 ± 0.0021a
R7954-HT	30.13 ± 0.31a	1.10 ± 0.01a	0.664 ± 0.0004d	1.106 ± 0.0016b
RS111-NT	27.82 ± 0.26b	1.66 ± 001b	0.668 ± 0.0007c	1.058 ± 0.001e
RS111-HT	30.34 ± 0.11a	1.94 ± 0.03c	0.663 ± 0.0003d	1.099 ± 0.0006c
RS4-NT	25.42 ± 0.11c	2.46 ± 0.05d	0.68 ± 0.0005a	1.04 ± 0.0008f
RS4-HT	27.11 ± 0.09b	2.76 ± 0.04e	0.674 ± 0.0009b	1.078 ± 0.0014d

*The same small letter in the same column indicated that there were no significant differences among different samples at the $P < 0.05$ level.
RC, relative crystallinity; NT, normal temperature; HT, high temperature.

and less proportion of amorphous to ordered structure in the mutants. Under HT, the 1,045/1,022 cm^{-1} ratio of R7954 was elevated but that of RS111 and RS4 lessened (Table 3), indicating that the short-range ordered structure especially in the external region of the starch granule in RS111 and RS4 was slightly attenuated. HT played more apparent influences on starch ordered structure in mutants than in R7954, especially on long-range ordered structure.

Thermal properties and pasting properties

At NT, RS111 and RS4 had lower To, Tp, and ΔH than R7954. Compared with the values of To (58.91°C–61.02°C), Tp (63.33°C–65.52°C), Tc (69.55°C–74.29°C), and ΔH (5.68–8.65 J/g) at NT, it is obvious that HT significantly elevated the gelatinization temperature (GT) and ΔH (Table 4).

As for the paste viscosity, RS111 and RS4 showed significantly lower paste viscosity than R7954 regardless of whether at NT or HT (Table 5). The PV of R7954, RS111, and RS4 at NT was 1,787 cP, 277 cP, and 200.5 cP, respectively. BD and SB of RS111 and RS4 were also lower than those of R7954. Other *ssIIIa* mutants also showed very low viscosity (Fujita et al., 2007; Zhang et al., 2011). Under HT, the PV, HPV, CPV, and SB values were decreased in all three varieties, indicating that HT contributed greatly to pasting properties of rice starches, and the cooking quality of rice grain decreased under HT. Decreased paste viscosity of rice under HT had also been observed by Zhang et al. (2020).

Discussion

The influences of ssIIIa mutation and high temperature on RS and other accumulations in rice grains

The *SSIIIa* gene has been identified as the key gene for RS formation in rice grains (Zhou et al., 2016). RS111 and RS4 are two *ssIIIa* allelic mutants, and the increased AAC and RS content in RS111 and RS4 (Table 1) might be majorly due to the mutation of *SSIIIa* (Figure 1). However, RS4 had higher RS and lipid contents (Table 1) that contribute to its greatest starch–lipid complexes (Table 3), as AAC can complex with lipids to form RSV (Hasjim et al., 2010; Zhou et al., 2016). This indicated that, besides *SSIIIa*, other genes involved in starch synthesis or lipid metabolites might also contribute to RS formation in rice grains.

During grain development, an increment in temperature of 1.6°C–3.1°C can disturb the accumulation of storage materials (Liu et al., 2021). Previous studies showed that HT can increase protein content (Lin et al., 2010) and was unfavorable for lipid accumulation during rice grain ripening. However, HT showed negative influences on protein content and stimulated lipid accumulation in this study (Table 1),

TABLE 4 Thermal properties of R7954, RS111, and RS4 at NT and HT*.

Varieties	T_o (°C)	T_p (°C)	T_c (°C)	ΔH (J/g)
R7954-NT	61.02 ± 0.08c	65.52 ± 0.03c	71.13 ± 0.11d	8.65 ± 0.07b
R7954-HT	63.25 ± 0.13a	69.06 ± 0.05b	75.72 ± 0.14b	10.46 ± 0.04a
RS111-NT	58.89 ± 0.04e	63.33 ± 0.05e	69.55 ± 0.22e	7.07 ± 0.01d
RS111-HT	60.16 ± 0.04d	65.12 ± 0.04d	71.9 ± 0.39d	8.46 ± 0.03c
RS4-NT	58.91 ± 0.1e	65.09 ± 0.55d	74.29 ± 1.25c	5.68 ± 0.4e
RS4-HT	61.68 ± 0.01b	69.89 ± 0.21a	79.53 ± 0.36a	7.2 ± 0.05d

*The same small letter in the same column indicated that there were no significant differences among different samples at the $P < 0.05$ level.

10.3389/fpls.2022.1059749

TABLE 5 Viscosity parameters of R7954, RS111, and RS4 under NT and HT*.

Varieties	PV (cP)	HPV (cP)	CPV (cP)	BD (cP)	SB (cP)
R7954-NT	1787 ± 12.26a	1658 ± 20.27a	2680 ± 39.13a	129 ± 8.01b	893 ± 26.87a
R7954-HT	1701 ± 26.4b	1496 ± 16.5b	2213 ± 0.94b	205 ± 9.9a	512 ± 27.34b
RS111-NT	277 ± 7.54c	269 ± 5.66c	413.5 ± 14.85c	8 ± 1.89c	136.5 ± 7.31c
RS111-HT	241 ± 1.41dcd	239 ± 1.89cd	314.5 ± 0.24d	2 ± 0.47c	73.5 ± 1.65cd
RS4-NT	220.5 ± 2.12d	217.5 ± 2.12d	255.5 ± 2.59de	3.33 ± 0.27c	35 ± 0.47de
RS4-HT	204.5 ± 2.59d	200.5 ± 2.59d	209 ± 2.36e	4.33 ± 0.27c	4.5 ± 0.24e

*The same small letter in the same column indicated that there were no significant differences among different samples at the $P < 0.05$ level. PV, peak viscosity; HPV, hot paste viscosity; CPV, cold paste viscosity; BD, breakdown value; SB, setback value.

although the decreased protein content is small in absolute values. This might be due to different varieties studied. Variations in AAC under HT may also be dependent on rice varieties. Cheng et al. (2005) found that HT increased the AC in high-AC varieties, while Liu et al. (2021) found that AC decreased under elevated temperatures. The different responses of AAC in R7954 and mutants RS111 and RS4 to HT (Table 1) might be because of the increased sensitivity of amyloplast enzymes in RS111 and RS4 exposed to HT. AAC has been thought to be a key determinant for RS formation; higher AAC always related to higher RS content (Raigond et al., 2015). The inconsistent decreases or increases in AAC and RS in the three varieties under HT indicated that, besides amylose, other factors such as lipids also play important roles in RS formation under HT.

Impacts of *ssIIIa* mutation and high temperature on the expressions of genes involved in starch synthesis and amylopectin fine structure

SSIIIa is a key enzyme responsible for the elongation of long branched amylopectin; it might regulate the whole cascade of starch biosynthesis through the formation of large enzyme complexes with other enzymes (Crofts et al., 2012; Crofts et al., 2015). Loss-of-function mutation of *SSIIIa* results in abnormal starch metabolites in RS111 and RS4, resulting in a lower total starch content, higher AAC and lipid content, and more proportion of DP 9–15 and DP 20–30 when compared with those of R7954 (Figure 3). The enhanced expression of *SSIIa* in RS111 might partly compensate for the loss-of-function of *SSIIIa*, as they play partially overlapping roles during starch synthesis (Zhang et al., 2011), which might partially explain the differences in CL distribution of amylopectin between RS111 and RS4 (Figure 2).

Generally, HT leads to a declined expression of many starch biosynthesis genes such as *GBSSI*, *BEs*, *cyPPDK* (Jiang et al., 2003; Yamakawa et al., 2007; Zhang et al., 2021) and *SSs* like *SSIIIa*, *SSII*, and *SSIV* (Liu et al., 2021). SSI, SSIIa, SSIIIa, BEI, and BEIIb function specifically in elongating or synthesizing A chains, B1 chains, B2 chains, or longer chains (Nakamura et al., 2005; Fujita et al., 2006; Fujita et al., 2007; Jeon et al., 2010). The decreased transcripts of starch synthase and branching enzyme genes (Figure 2) in all varieties resulted in decreases in the amount of fa and fb1 under HT (Table 2, Figure 3) (Jiang et al., 2003). Meanwhile, lower expression levels of *SSI*, *SSIIc*, and some other genes in RS4 under HT (Figure 2) might be responsible for its noticeable decreases in amylopectin short chains. The more pronounced decreases in the expression of several genes such as *BEIIb*, *BEI* and *BEIIa* in RS111 and RS4 indicated that *ssIIIa* mutation exacerbated the influences of HT on starch metabolites.

Influences of high temperature on starch crystalline

Crystallinity was influenced majorly by fine amylopectin structure and AC (Man et al., 2014; Bertoft, 2017). More AAC and shorter amylopectin usually lead to a defective crystallite (Luo et al., 2021). The lower RC in RS111 and RS4 might be due to their higher AAC (Table 1) and more short chains of amylopectin (Table 2). The increased RC in RS4 and RS111 at HT was consistent with the pronouncedly decreased amount of fa and fb1 and increased proportion of fb2 and fb3 at HT (Table 2). Although amylopectin long chains are of benefit for the formation of double helices, complexing with non-starchy compounds increased short-range ordered structure (Chi et al., 2021). The increased starch–lipid complexes in RS111 and RS4 might contribute to the increased 1,045/1,022 cm^{-1} ratio (Table 3).

Previous studies indicated that slower digestibility of processed starch is usually related to the short-range ordered structures; however, the reassembled ordered molecular aggregation architecture showed more pronounced starch digestibility. Compared with long-range ordered structures, short-range ordered structures exhibited a weaker effect on starch digestibility (Chi et al., 2021). The increased RC in RS4 and RS111 under HT might partly contribute to their enhanced

RS content, as an increase in the degree of crystallinity can result in a reduction in starch digestibility *in vitro* and *in vivo* (Rombo et al., 2001; García-Rosas et al., 2009), and the amorphous matrix might be more susceptible to enzyme attack (Chung et al., 2006).

Influences of high temperature on starch thermal and paste viscosity

GT has been found to be related to crystallinity associated with molecular order (Table 3). The amount of short-chain amylopectin (DP ≤12) was negatively correlated with GT; starch with relatively high levels of long branch chains (13 ≤ DP ≤ 24) requires higher temperatures for complete dissociation (Zhang et al., 2020). The higher AAC (Table 1) and the more proportion of fa in mutants (Table 2, Figure 3) indicated that they have shorter double helices formed between adjacent chains in the crystalline lamellae (Jeon et al., 2010), leading to a lower starch GT and ΔH (Table 4). The enhanced GT under HT may be due to the increased crystallites and double helices (Table 3). Under HT, the increased proportion of amylopectin long chains that span at least two crystalline lamellae and more ordered structures can form more stable double helices; hence, a higher GT would be required to disorder the ordered structure (Witt et al., 2012). A previous study also found that HT exposure led to a significantly higher GT (Pang et al., 2021). Furthermore, the variations of GT between NT and HT were larger than those among varieties (Table 4), indicating that the influences of temperature on GT were more obvious than that of *ssIIIa* mutation.

The very low viscosity of RS111 and RS4 might be due to their high AAC and lipids (Table 1), as lipids and amylose complexes formed during cooking can render entanglements with amylopectin molecules and restrict the swelling of granules, causing incomplete gelatinization during cooking (Sun et al., 2018), which results in a higher pasting temperature and a lower PV (Ai and Jane, 2015). Increased lipids under HT (Table 1) might be responsible partially for the decreased viscosity. Previous studies have found that *Wx* and *SSIIa* were the main genes involved in many grain quality properties such as gelatinization and paste viscosity (Kharabian-Masouleh et al., 2012); significantly different expressions of *GBSSI* and *SSIIa* among R7954, RS4, and RS111 at both NT and HT might explain the different viscosity among them.

Proposed regulations of high temperature on RS formation in rice

Rice high in RS had a relatively higher proportion of DP 8–12 and less DP ≥37 (Shu et al., 2007). Among the three varieties, the higher the RS content, the most the proportion of DP 9–15 and the least the proportion of DP ≥37. While under HT, the amylopectin chains with DP 9–15 in RS4 and RS111 were greatly decreased and chains with DP ≥37 were increased, but the RS contents in RS111 and RS4 under HT were significantly increased (Table 1). The incongruent correlation between RS and DP 9–15 and DP ≥37 under HT indicated that the mechanism causing enhanced RS under HT should be different from that caused by loss of function of *SSIIIa*, which might be due to the differences in stability or temperature preference of starch synthase and starch branching enzyme (Umemoto et al., 1999).

The synthesis of amylose and amylopectin might compete for substrates and enzymes (Han et al., 2019) and maintain equilibrium under normal conditions. While inactivation of *SSIIIa* results in varied transcripts of genes related to starch synthesis (Figure 2), leading to more substrates synthetized by GBSSI into amylose (Figure 5). Furthermore, inactive SSIIIa facilitated the synthesis of DP 10–15 chains from short DP 6–9 chains of A chains and DP 20–30 chains from DP 16–19 chains of B1 chains of amylopectin by enhancing the endogenous SSI

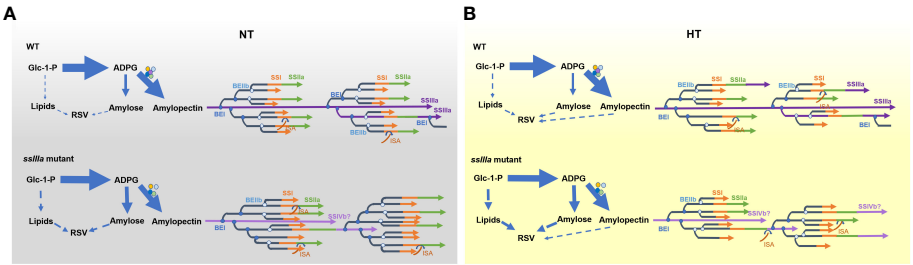


FIGURE 5
Proposed processes of RS formation in rice. **(A)** The loss-of-function mutation of SSIIIa causes repartition of carbohydrate, breaks the equibrium synthesis of amylose and amylopectin, and leads to higher AAC and lipid content that promote the formation of starch–lipid complexes. **(B)** Loss-of-function mutation of SSIIIa leads to more short chains of DP 9–15 both under NT and high temperature (HT). HT decreases the branching, resulting in less proportion of short chains and more long chains. The increased long chains and enhanced lipid content under HT stimulate more RS accumulation.

activity and reduced the formation of DP >35 chains (Fujita et al., 2007) (Table 2, Figure 5B). Enhanced transcripts of SSIVb or other enzymes might partially compensate for the elongation of B2-B4 in the *ssIIIa* mutant (Figure 5). Concurrently, the increased expression levels of *BEs* such as *BEI* and *BEIIb* (Figure 2) might increase the branching frequency and enhance the proportion of short chains further (Table 2, Figure 5). Less proportion of short-chain DP 10–15 is an important determinant for high RS (Table 1) (Shu et al., 2007; Shu et al., 2009). Additionally, pyruvate phosphate dikinase (PPDK) presented in the complex with AGPase may enable G-1-P channel to lipid, while the starch biosynthetic complexes are proposed to inhibit the activity of PPDK and AGPase, the absence of SSIIIa enhanced the expression of *PPDK* (Figure 2) and promoted lipid accumulation (Figure 5). The high levels of amylose and lipids in mutants especially in RS4 can form more amylose–lipid complexes (RSV) (Table 3).

Under HT, the altered transcripts of several genes in R7954 led to aberrant starch synthesis (Table 1). Fan et al. (2019) found that the ratio of SBE activity to that of GBSS was increased under HT. Downregulation of the *Wx* gene due to transcript inhibition or posttranscriptional regulation (Zhang et al., 2021) caused less synthesis of amylose, while for *ssIIIa* mutants, although the expression levels of most genes were also reduced, amylopectin and amylose biosynthesis maintained a relative balance, but the starch enzyme complexes might be disrupted further due to the lower activity of most amyloplast enzymes and more carbon were partitioned into lipid metabolites, leading to the synthesis of more lipids (Table 1, Figure 5). Furthermore, decreases in the transcripts of *BEI* and *BEIIb* (Figure 2) resulted in lower branching frequency (Figure 5) and produced fewer short chains of DP ≤19, with the greatest decreases in chains of DP 9–19 (Figure 3). The increased transcripts of *SSIIIa* in R7954 and *SSIVb* in mutants under HT (Figure 2) might also partially contribute to the increased proportion of long chains (DP >37) (Figure 3, Table 2), reflected as intensified crystallinity in mutants (Table 3). Longer amylopectin side chains might also be involved in RS formation, although the short chains of DP 9–15 are the major determinants for RS properties, as retrograded amylopectin may also reduce enzyme susceptibility (Eerlingen and Delcour, 1995). Moreover, aside from amylose, long chains of amylopectin may also complex with the increased free lipids and lead to increases in the contents of RSV at HT (Table 3). The molecular mechanisms of RS produced in high-RS rice mutants under HT might not be uniform with that under NT. Trimming the fine structure of amylopectin and regulating lipid metabolites through biological means might be alternative ways to obtain rice rich in RS with acceptable palatability under global climate change.

In conclusion, RS4 and RS111 are two *ssIIIa* allelic mutants as *b10* (Zhou et al., 2016). Meanwhile, other mutations responsible for RS formation might exist in RS4, as the RS in RS4 was significantly higher than that in RS111. Loss-of-function mutation of *SSIIIa* boosted the expressions of most genes involved in starch biosynthesis under NT, such as *PhoI*, *SSI*, *BEIIb*, and *SSIVb*. The varied expressions of genes involved in starch biosynthesis in *ssIIIa* mutants caused the increases in AAC and lipid content, more proportion of DP 9–15, and less proportion of DP >37, which finally led to enhanced RS. However, most of the genes upregulated under NT in *ssIIIa* mutants especially in RS4 were downregulated under HT, such as *GBSSI*, *SSI*, *BEI*, *BEIIb*, and *ISA*. The decreased activities of SSs and BEs under HT caused greatest decreases in chains of DP 9–19 and produced more proportion of long chains (DP >37) in all materials, but only reduced AAC and total starch content in R7954. Moreover, the varied transcripts of genes involved in starch biosynthesis under HT channeled more carbon flux to lipid synthesis, promoting lipid accumulation. The varied starch structure and lipid content under HT resulted in increased crystallinity, GT, ΔH and reduced viscosity. The high AAC and enhanced long amylopectin chains and lipid content in RS111 and RS4 under HT might boost the starch–lipid complexes further and contribute to the elevated RS.

Data availability statement

The original contributions presented in the study are included in the article/Supplementary Material. Further inquiries can be directed to the corresponding author.

Author contributions

YZ: Investigation, Data curation, Formal analysis, Writing-original draft. ZC: Investigation, Data curation, Formal analysis, Writing-original draft. SJ: Investigation. JC: Investigation. DW: Funding acquisition, material bred. XS: Conceptualization, Formal analysis, Writing-review and editing, Supervision and Funding acquisition. All authors contributed to the article and approved the submitted version.

Funding

This project was financially supported by grants from the National Key Research and Development Program of China (2021YFF100020), Functional Rice Breeding and germplasm enhancement (2022C02011, 2021C02063), National Natural Science Foundation of China (32072038) and Administration Bureau of Yazhou Bay Science Technology City (SKJC-2020-02-010).

Conflict of interest

The authors declare that the research was conducted in the absence of any commercial or financial relationships that could be construed as a potential conflict of interest.

Publisher's note

All claims expressed in this article are solely those of the authors and do not necessarily represent those of their affiliated organizations, or those of the publisher, the editors and the reviewers. Any product that may be evaluated in this article, or claim that may be made by its manufacturer, is not guaranteed or endorsed by the publisher.

Supplementary material

The Supplementary Material for this article can be found online at: https://www.frontiersin.org/articles/10.3389/fpls.2022.1059749/full#supplementary-material

References

Ai, Y., and Jane, J. L. (2015). Gelatinization and rheological properties of starch. *Starch/Staerke* 67, 213–224. doi: 10.1002/star.201400201

Bao, J., Kong, X., Xie, J., and Xu, L. (2004). Analysis of genotypic and environmental on rice starch. 1. apparent amylose content, pasting viscosity, and gel texture. *J. Agric. Food Chem.* 52, 6010–6016. doi: 10.1021/jf049234i

Bao, J., Ying, Y., Zhou, X., Xu, Y., Wu, P., Xu, F., et al. (2020). Relationships among starch biosynthesizing protein content, fine structure and functionality in rice. *Carbohydr. Polym.* 237, 116118. doi: 10.1016/j.carbpol.2020.116118

Baysal, C., He, W., Drapal, M., Villorbina, G., Medina, V., Capell, T., et al. (2020). Inactivation of rice starch branching enzyme IIb triggers broad and unexpected changes in metabolism by transcriptional reprogramming. *Proc. Natl. Acad. Sci. U. S. A.* 117, 26503–26512. doi: 10.1073/pnas.2014860117

Bertoft, E. (2017). Understanding starch structure: Recent progress. *Agronomy* 7, 56. doi: 10.3390/agronomy7030056

Butardo, V. M., Fitzgerald, M. A., Bird, A. R., Gidley, M. J., Flanagan, B. M., Larroque, O., et al. (2011). Impact of down-regulation of starch branching enzyme IIb in rice by artificial microRNA-and hairpin RNA-mediated RNA silencing. *J. Exp. Bot.* 62, 4927–4941. doi: 10.1093/jxb/err188

Cheng, F., Zhong, L., Zhao, N., Liu, Y., and Zhang, G. (2005). Temperature induced changes in the starch components and biosynthetic enzymes of two rice varieties. *Plant Growth Regul.* 46, 87–95. doi: 10.1007/s10725-005-7361-6

Chi, C., Li, X., Huang, S., Chen, L., Zhang, Y., Li, L., et al. (2021). Basic principles in starch multi-scale structuration to mitigate digestiblity: A review. *Trends Food Sci. Technol.* 109, 154–168. doi: 10.1016/j.tifs.2021.01.024

Chung, H. J., Lim, H. S., and Lim, S. T. (2006). Effect of partial gelatinization and retrogradation on the enzymatic digestion of waxy rice starch. *J. Cereal Sci.* 43, 353–359. doi: 10.1016/j.jcs.2005.12.001

Crofts, N., Abe, K., Aihara, S., Itoh, R., Nakamura, Y., Itoh, K., et al. (2012). Lack of starch synthase IIIa and high expression of granule-bound starch synthase I synergistically increase the apparent amylose content in rice endosperm. *Plant Sci.*, 193–194, 62–69. doi: 10.1016/j.plantsci.2012.05.006

Crofts, N., Abe, N., Oitome, N. F., Matsushima, R., Hayashi, M., Tetlow, I. J., et al. (2015). Amylopectin biosynthetic enzymes from developing rice seed form enzymatically active protein complexes. *J. Exp. Bot.* 66, 4469–4482. doi: 10.1093/jxb/erv212

Ding, Y., Huang, J., Zhang, N., Rasmussen, S. K., Wu, D., and Shu, X. (2019). Physiochemical properties of rice with contrasting resistant starch content. *J. Cereal Sci.* 89, 102815. doi: 10.1016/j.jcs.2019.102815

Eerlingen, R., and Delcour, J. (1995). Formation, analysis, structure and properties of type III enzyme resistant starch. *J. Cereal Sci.* 22, 129–138. doi: 10.1016/0733-5210(95)90042-X

Englyst, H. N., and Hudson, G. J. (1996). The classification and measurement of dietary carbohydrates. *Food Chem.* 57, 15–21. doi: 10.1016/0308-8146(96)00056-8

Fan, X., Li, Y., Lu, Y., Zhang, C., Li, E., Li, Q., et al. (2019). The interaction between amylose and amylopectin synthesis in rice endosperm grown at high temperature. *Food Chem.* 301, 125258. doi: 10.1016/j.foodchem.2019.125258

Fujita, N., Yoshida, M., Asakura, N., Ohdan, T., Miyao, A., Hirochika, H., et al. (2006). Function and characterization of starch synthase I using mutants in rice. *Plant Physiol.* 140, 1070–1084. doi: 10.1104/pp.105.071845

Fujita, N., Yoshida, M., Kondo, T., Saito, K., Utsumi, Y., Tokunaga, T., et al. (2007). Characterization of SSIIIa-deficient mutants of rice: the function of SSIIIa and pleiotropic effects by SSIIIa deficiency in the rice endosperm. 144, 2009–2023.doi: 10.1104/pp.107.102533

García-Rosas, M., Bello-Pérez, A., Yee-Madeira, H., Ramos, G., Flores-Morales, A., and Mora-Escobedo, R. (2009). Resistant starch content and structural changes in maize (Zea mays) tortillas during storage. *Starch/Staerke* 61, 414–421. doi: 10.1002/star.200800147

Guo, D., Ling, X., Zhou, X., Li, X., Wang, J., Qiu, S., et al. (2020). Evaluation of the quality of a high-resistant starch and low-glutelin rice (Oryza sativa l.) generated through CRISPR/Cas9-mediated targeted mutagenesis. *J. Agric. Food Chem.* 68, 9733–9742. doi: 10.1021/acs.jafc.0c02995

Han, H., Yang, C., Zhu, J., Zhang, L., Bai, Y., Li, E., et al. (2019). Competition between granule bound starch synthase and starch branching enzyme in starch biosynthesis. *Rice* 12, 96–105. doi: 10.1186/s12284-019-0353-3

Hasjim, J., Lee, S. O., Hendrich, S., Setiawan, S., Ai, Y., and Jane, J. L. (2010). Characterization of a novel resistant-starch and its effects on postprandial plasma-glucose and insulin responses. *Cereal Chem.* 87, 257–262. doi: 10.1094/CCHEM-87-4-0257

Hu, Y., Leu, R. K. L., Christophersen, C. T., Somashekar, R., Conlon, M. A., Meng, X. Q., et al. (2016). Manipulation of the gut microbiota using resistant starch is associated with protection against colitis-associated colorectal cancer in rats. *Carcinogenesis* 37, 366–375. doi: 10.1093/carcin/bgw019

Itoh, K., Ozaki, H., Okada, K., Hori, H., Takeda, Y., and Mitsui, T. (2003). Introduction of wx transgene into rice wx mutants leads to both high- and low-amylose rice. *Plant Cell Physiol.* 44, 473–480. doi: 10.1093/pcp/pcg068

Jeon, J. S., Ryoo, N., Hahn, T. R., Walia, H., and Nakamura, Y. (2010). Starch biosynthesis in cereal endosperm. *Plant Physiol. Biochem.* 48, 383–392. doi: 10.1016/j.plaphy.2010.03.006

Jiang, H., Dian, W., and Wu, P. (2003). Effect of high temperature on fine structure of amylopectin in rice endosperm by reducing the activity of the starch branching enzyme. *Phytochemistry* 63, 53–59. doi: 10.1016/S0031-9422(03)00005-0

Kharabian-Masouleh, A., Waters, D. L. E., Reinke, R. F., Ward, R., and Henry, R. J. (2012). SNP in starch biosynthesis genes associated with nutritional and functional properties of rice. *Sci. Rep.* 2, 1–9. doi: 10.1038/srep00557

Kong, X., Bertoft, E., Bao, J., and Corke, H. (2008). Molecular structure of amylopectin from amaranth starch and its effect on physicochemical properties. *Int. J. Biol. Macromol.* 43, 377–382. doi: 10.1016/j.ijbiomac.2008.07.018

Kong, X., Kasapis, S., Zhu, P., Sui, Z., Bao, J., and Corke, H. (2016). Physicochemical and structural characteristics of starches from Chinese hull-less barley cultivars. *Int. J. Food Sci. Technol.* 51, 509–518. doi: 10.1111/ijfs.12984

Kumar, A., Sahoo, U., Baisakha, B., Okpani, O. A., Ngangkham, U., Parameswaran, C., et al. (2018). Resistant starch could be decisive in determining the glycemic index of rice cultivars. *J. Cereal Sci.* 79, 348–353. doi: 10.1016/j.jcs.2017.11.013

Lin, C. J., Li, C. Y., Lin, S. K., Yang, F. H., Huang, J. J., Liu, Y. H., et al. (2010). Influence of high temperature during grain filling on the accumulation of storage proteins and grain quality in rice (Oryza sativa l.). *J. Agric. Food Chem.* 58, 10545–10552. doi: 10.1021/jf101575j

Liu, W., Yin, T., Zhao, Y., Wang, X., Wang, K., Shen, Y., et al. (2021). Effects of high temperature on rice grain development and quality formation based on proteomics comparative analysis under field warming. *Front. Plant Sci.* 12. doi: 10.3389/fpls.2021.746180

Luo, X., Cheng, B., Zhang, W., Shu, Z., Wang, P., and Zeng, X. (2021). Structural and functional characteristics of japonica rice starches with different amylose contents. *CYTA - J. Food* 19, 532–540. doi: 10.1080/19476337.2021.1927194

Man, J., Lin, G., Wang, Z., Wang, Y., Liu, Q., and Wei, C. (2014). Different structures of heterogeneous starch granules from high-amylose rice. *J. Agric. Food Chem.* 62, 11254–11263. doi: 10.1021/jf503999r

Man, J., Yang, Y., Zhang, C., Zhou, X., Dong, Y., Zhang, F., et al. (2012). Structural changes of high-amylose rice starch residues following *in vitro* and *in vivo* digestion. *J. Agric. Food Chem.* 60, 9332–9341. doi: 10.1021/jf302966f

Miura, S., Koyama, N., Crofts, N., Hosaka, Y., Abe, M., and Fujita, N. (2021). Generation and starch characterization of non-transgenic BEI and BEIIb double mutant rice (Oryza sativa) with ultra-high level of resistant starch. *Rice* 14, 3. doi: 10.1186/s12284-020-00441-0

Nakamura, Y., Francisco, P. B.Jr., Hosaka, Y., Sato, A., Sawada, T., Kubo, A., et al. (2005). Essential amino acids of starch synthase IIa differentiate amylopectin structure and starch quality between japonica and indica rice varieties. *Plant Mol. Biol.* 58, 213–227. doi: 10.1007/sl

Nakamura, Y., Kubo, A., Shimamune, T., Matsuda, T., Harada, K., and Satoh, H. (1997). Correlation between activities of starch debranching enzyme and α-polyglucan structure in endosperms of sugary-1 mutants of rice. *Plant J.* 12, 143–153. doi: 10.1046/j.1365-313X.1997.12010143.x

Ohdan, T., Francisco, P. B., Sawada, T., Hirose, T., Terao, T., Satoh, H., et al. (2005). Expression profiling of genes involved in starch synthesis in sink and source organs of rice. *J. Exp. Bot.* 56, 3229–3244. doi: 10.1093/jxb/eri292

Pang, Y., Hu, Y., and Bao, J. (2021). Comparative phosphoproteomic analysis reveals the response of starch metabolism to high-temperature stress in rice endosperm. *Int. J. Mol. Sci.* 22. doi: 10.3390/ijms221910546

Pérez, S., and Bertoft, E. (2010). The molecular structures of starch components and their contribution to the architecture of starch granules: A comprehensive review. *Starch/Staerke* 62, 389–420. doi: 10.1002/star.201000013

Putseys, J. A., Lamberts, L., and Delcour, J. A. (2010). Amylose-inclusion complexes: Formation, identity and physico-chemical properties. *J. Cereal Sci.* 51, 238–247. doi: 10.1016/j.jcs.2010.01.011

Raigond, P., Ezekiel, R., and Raigond, B. (2015). Resistant starch in food: A review. *J. Sci. Food Agric.* 95, 1968–1978. doi: 10.1002/jsfa.6966

Rombo, G. O., Taylor, J. R. N., and Minnaar, A. (2001). Effect of irradiation, with and without cooking of maize and kidney bean flours, on porridge viscosity and *in vitro* starch digestibility. *J. Sci. Food Agric.* 81, 497–502. doi: 10.1002/jsfa.838

Sajilata, M. G., Singhal, R. S., and Pushpa, R. K. (2006). Resistant starch — a review. *Compr. Rev. Food Sci. Food Saf.* 5, 1–17. doi: 10.1111/j.1541-4337.2006.tb00076.x

Sevenou, O., Hill, S. E., Farhat, I. A., and Mitchell, J. R. (2002). Organisation of the external region of the starch granule as determined by infrared spectroscopy. *Int. J. Biol. Macromol.* 31, 79–85. doi: 10.1016/S0141-8130(02)00067-3

Shen, L., Li, J., and Li, Y. (2022). Resistant starch formation in rice: Genetic regulation and beyond. *Plant Commun.* 3, 100329. doi: 10.1016/j.xplc.2022.100329

Shu, X., Jia, L., Gao, J., Song, Y., Zhao, H., Nakamura, Y., et al. (2007). The influences of chain length of amylopectin on resistant starch in rice (Oryza sativa l.). *Starch - Stärke* 59, 504–509. doi: 10.1002/star.200700640

Shu, X., Jiao, G., Fitzgerald, M. A., Yang, C., Shu, Q., and Wu, D. (2006). Starch structure and digestibility of rice high in resistant starch. *Starch/Staerke* 58, 411–417. doi: 10.1002/star.200600501

Shu, X., Jia, L., Ye, H., Li, C., and Wu, D. (2009). Slow digestion properties of rice different in resistant starch. *J. Agric. Food Chem.* 57, 7552–7559. doi: 10.1021/jf900988h

Shu, X., Sun, J., and Wu, D. (2014). Effects of grain development on formation of resistant starch in rice. *Food Chem.* 164, 89–97. doi: 10.1016/j.foodchem.2014.05.014

Sun, J., Wang, Y., Zhang, X., Rasmussen, S. K., Jiang, X., Song, W., et al. (2018). Dependence of physiochemical, functional and textural properties of high-resistant starch rice on endogenous nonstarch polysaccharides. *Int. J. Food Sci. Technol.* 53, 1079–1086. doi: 10.1111/ijfs.13686

Syahariza, Z. A., Sar, S., Warren, F. J., Zou, W., Hasjim, J., Tizzotti, M. J., et al. (2014). Erratum: The importance of amylose and amylopectin fine structures for starch digestibility in cooked rice grains. *Food Chem.* 136, 617–618. doi: 10.1016/j.foodchem.2012.08.053

Umemoto, T., Nakamura, Y., Satoh, H., and Terashima, K. (1999). Differences in amylopectin structure between two rice varieties in relation to the effects of temperature during grain-filling. *Starch/Staerke* 51, 58–62. doi: 10.1002/(SICI)1521-379X(199903)51:2<58::AID-STAR58>3.0.CO;2-J

Witt, T., Doutch, J., Gilbert, E. P., and Gilbert, R. G. (2012). Relations between molecular, crystalline, and lamellar structures of amylopectin. *Biomacromolecules* 13, 4273–4282. doi: 10.1021/bm301586x

Xia, J., Zhu, D., Wang, R., Cui, Y., and Yan, Y. (2018). Crop resistant starch and genetic improvement : a review of recent advances. *Theor. Appl. Genet.* 131, 2495–2511. doi: 10.1007/s00122-018-3221-4

Xin, Z., Velten, J. P., Oliver, M. J., and Burke, J. J. (2003). High-throughput DNA extraction method suitable for PCR. *Biotechniques* 34, 820–826. doi: 10.2144/03344rr04

Yamakawa, H., Hirose, T., Kuroda, M., and Yamaguchi, T. (2007). Comprehensive expression profiling of rice grain filling-related genes under high temperature using DNA microarray. *Plant Physiol.* 144, 258–277. doi: 10.1104/pp.107.098665

You, H., Liang, C., Zhang, O., Xu, H., Xu, L., Chen, Y., et al. (2022). Variation of resistant starch content in different processing types and their starch granules properties in rice. *Carbohydr. Polym.* 276, 118742. doi: 10.1016/j.carbpol.2021.118742

Zhang, G., Cheng, Z., Zhang, X., Guo, X., Su, N., Jiang, L., et al. (2011). Double repression of soluble starch synthase genes *SSIIa* and *SSIIIa* in rice (*Oryza sativa* l.) uncovers interactive effects on the physicochemical properties of starch. *Genome* 54, 448–459. doi: 10.1139/g11-010

Zhang, H., Xu, H., Jiang, Y., Zhang, H., Wang, S., Wang, F., et al. (2021). Genetic control and high temperature effects on starch biosynthesis and grain quality in rice. *Front. Plant Sci.* 12. doi: 10.3389/fpls.2021.757997

Zhang, C., Yang, Y., Chen, Z., Chen, F., Pan, L., Lu, Y., et al. (2020). Characteristics of grain physicochemical properties and the starch structure in rice carrying a mutated ALK/SSIIa gene. *J. Agric. Food Chem.* 68, 13950–13959. doi: 10.1021/acs.jafc.0c01471

Zhang, C., Zhou, L., Zhu, Z., Lu, H., Zhou, X., Qian, Y., et al. (2016). Characterization of grain quality and starch fine structure of two japonica rice (Oryza sativa) cultivars with good sensory properties at different temperatures during the filling stage. *J. Agric. Food Chem.* 64, 4048–4057. doi: 10.1021/acs.jafc.6b00083

Zhao, Q., Ye, Y., Han, Z., Zhou, L., Guan, X., Pan, G., et al. (2020). SSIIIa-RNAi suppression associated changes in rice grain quality and starch biosynthesis metabolism in response to high temperature. *Plant Sci.* 294. doi: 10.1016/j.plantsci.2020.110443

Zhou, H., Wang, L., Liu, G., Meng, X., Jing, Y., Shu, X., et al. (2016). Critical roles of soluble starch synthase SSIIIa and granule-bound starch synthase waxy in synthesizing resistant starch in rice. *Proc. Natl. Acad. Sci.* 113, 12844–12849. doi: 10.1073/pnas.1615104113

frontiers | Frontiers in Plant Science

TYPE Original Research
PUBLISHED 23 November 2022
DOI 10.3389/fpls.2022.1066752

Check for updates

OPEN ACCESS

EDITED BY
Tianlun Zhao,
Zhejiang University, China

REVIEWED BY
Xuechen Zhang,
The State of Queensland, Australia
Yao Fangjie,
Sichuan Agricultural University, China
Jindong Liu,
Institute of Crop Sciences, Chinese Academy of Agricultural Sciences, China

*CORRESPONDENCE
Meixue Zhou
meixue.zhou@utas.edu.au
Wenying Zhang
wyzhang@yangtzeu.edu.cn

†These authors have contributed equally to this work

SPECIALTY SECTION
This article was submitted to Plant Abiotic Stress, a section of the journal Frontiers in Plant Science

RECEIVED 11 October 2022
ACCEPTED 08 November 2022
PUBLISHED 23 November 2022

CITATION
Xu L, Zhao C, Pang J, Niu Y, Liu H, Zhang W and Zhou M (2022) Genome-wide association study reveals quantitative trait loci for waterlogging-triggered adventitious roots and aerenchyma formation in common wheat.
Front. Plant Sci. 13:1066752.
doi: 10.3389/fpls.2022.1066752

COPYRIGHT
© 2022 Xu, Zhao, Pang, Niu, Liu, Zhang and Zhou. This is an open-access article distributed under the terms of the Creative Commons Attribution License (CC BY). The use, distribution or reproduction in other forums is permitted, provided the original author(s) and the copyright owner(s) are credited and that the original publication in this journal is cited, in accordance with accepted academic practice. No use, distribution or reproduction is permitted which does not comply with these terms.

Genome-wide association study reveals quantitative trait loci for waterlogging-triggered adventitious roots and aerenchyma formation in common wheat

Le Xu[1,2†], Chenchen Zhao[2†], Jiayin Pang[3], Yanan Niu[2], Huaqiong Liu[1], Wenying Zhang[1*] and Meixue Zhou[2*]

[1]MARA Key Laboratory of Sustainable Crop Production in the Middle Reaches of the Yangtze River (Co-construction by Ministry and Province), College of Agriculture, Engineering Research Centre of Ecology and Agricultural Use of Wetland, Ministry of Education, Yangtze University, Jingzhou, China, [2]Tasmanian Institute of Agriculture, University of Tasmania, Launceston, TAS, Australia, [3]The UWA Institute of Agriculture and School of Agriculture and Environment, The University of Western Australia, Perth, WA, Australia

Waterlogging severely affects wheat growth and development. Limited availability of oxygen in the root zone negatively affects the metabolism of plants. The formation of adventitious roots (ARs) and root cortical aerenchyma (RCA) are the most important adaptive trait contributing to plants' ability to survive in waterlogged soil conditions. This study used a genome-wide association study (GWAS) approach with 90K single nucleotide polymorphisms (SNPs) in a panel of 329 wheat genotypes, to reveal quantitative trait loci (QTL) conferring ARs and RCA. The wheat genotypes exposed to waterlogging were evaluated for ARs and RCA in both field and glasshouse over two consecutive years. Six and five significant marker-trait associations (MTAs) were identified for ARs and RCA formation under waterlogging, respectively. The most significant MTA for AR and RCA was found on chromosome 4B. Two wheat cultivars with contrasting waterlogging tolerance (tolerant: H-242, sensitive: H-195) were chosen to compare the development and regulation of aerenchyma in waterlogged conditions using staining methods. Results showed that under waterlogging conditions, H_2O_2 signal generated before aerenchyma formation in both sensitive and tolerant varieties with the tolerant variety accumulating more H_2O_2 and in a quicker manner compared to the sensitive one. Several genotypes which performed consistently well under different conditions can be used in breeding programs to develop waterlogging-tolerant wheat varieties.

KEYWORDS

waterlogging, wheat, aerenchyma, ethylene, adventitious roots

Introduction

Waterlogging is a major constraint to the production of winter wheat (*Triticum aestivum* L.) worldwide such as in the Yangtze River valley of China, the USA, Australia, Europe and Japan. Waterlogging occurs due to intermittent rainfall, irrigation practices, and/or poor soil drainage (Liu and Bassham, 2012; Manik et al., 2019). Waterlogging is deleterious to the growth and yield of wheat crops (Li et al., 2001; Setter and Waters, 2003). In Australia, about one million ha of wheat cropping area is affected by waterlogging, which causes 20%-50% of yield losses (Manik et al., 2019). The principal cause of damage to plants under waterlogging/saturated soil is due to inadequate oxygen supply since gas diffusion in water is tremendously slower than that in the air (Loreti et al., 2016).

Plants have developed several adaptive metabolic strategies to cope with oxygen deprivation under hypoxia/anoxic (Bailey-Serres et al., 2012; Voesenek and Bailey-Serres, 2013; Abbas et al., 2015). These include anatomical changes such as the formation of a barrier against radial oxygen loss, the development of adventitious roots (ARs) and root cortical aerenchyma (RCA) (Armstrong, 1971; Malik et al., 2003; Vidoz et al., 2010; Nelson et al, 2018; Zhang et al., 2015; Kim et al., 2015; Pan et al., 2019). The importance of AR in alleviating waterlogging stress has been observed in rice (*Oryza Sativa*; Lorbiecke and Sauter, 1999), *Rumex* spp. (Visser et al., 1996), tamarack (*Larix laricina*; Calvo-Polanco et al., 2012), *Eucalyptus* spp. (Argus et al., 2015), and tomato (*Solanum lycopersicum*). Adventitious roots enhance gas exchange, and water/nutrient uptake, thus contributing to plants' survival under waterlogging (Steffens and Rasmussen, 2016). Root cortical aerenchyma, a special plant tissue containing enlarged gas space, facilitates oxygen delivery from above ground to root zones thus maintaining a sustainable root growth rate under hypoxia (Armstrong, 1979; Evans, 2003). Positive correlations between the proportion/area of aerenchyma and waterlogging tolerance have been witnessed in multiple crops, such as oats (*Avena sativa* L), triticale, wheat, cotton (*Anemone vitifolia Buch*), and barley (Pan et al., 2019; Thomson et al., 1992; Huang et al., 1994; Setter and Waters, 2003; Zhang et al., 2015). There are two types of aerenchyma according to the developmental process: lysigeny and schizogeny (Evans, 2003; Haque et al., 2010). Lysigenous aerenchyma is generally referred to as the aerenchyma developed in non-wetland species, such as wheat (Trought and Drew, 1980), barley (Benjamin and Greenway, 1979), and maize (Drew et al., 1979), when exposed to low oxygen environments. Schizogenous aerenchyma is generally the constitutive aerenchyma, formed by the separation of cells and growth patterns without cell death taking place. Schizogenous aerenchyma occurs in many species under non-waterlogged conditions, though in some species it can be increased in extent in waterlogged conditions (Evans, 2003).

Many other different agronomic and physiological traits have been used as indicators for plant waterlogging tolerance. These include leaf chlorosis (Li et al., 2008), ion toxicity (Pang et al., 2007; Huang et al., 2018), survival rate, germination rate index, leaf chlorophyll content, plant height index, dry matter weight (Yu and Chen, 2013), ROS formation (Gill et al., 2019), membrane potential maintenance (Gill et al., 2017), K^+ retention in barley roots (Zeng et al., 2014). Using these traits, many QTL for waterlogging tolerance have been reported in barley (Li et al., 2008; Zhou, 2011; Broughton et al., 2015; Manik et al., 2022b), wheat (Yu et al., 2014; Ballesteros et al., 2015), maize (Qiu et al., 2007; Campbell et al., 2015) and other crops. Among the major QTL for wheat waterlogging tolerance, the one on chromosome 7A explained 23.92% of the phenotypic variance of germination rate index (Yu et al., 2014), and another QTL on chromosome 1BL explained 14 - 32% of phenotypic variation in chlorophyll and root/shoot dry matter under waterlogged conditions (Ballesteros et al., 2015). From a cross between a winter spelta (*T. spelta* L) and a winter wheat, more than 10 QTL associated with seedling survival and seedling growth index under waterlogging have been identified on different chromosomes with spelta providing most QTL for waterlogging tolerance (Burgos et al., 2001).

Fast formation of aerenchyma in adventitious roots is critical for root survival and waterlogging tolerance in cereal crops under waterlogged conditions (Zhang et al., 2016). However, there are limited reports on QTL for RCA and ARs, or the genetic control of waterlogging tolerance in wheat when compared to the significant amount of literature on other crops, such as rice (Toojinda et al., 2003), barley (Zhu et al, 2008; Manik et al., 2022b), soybean (Cornelious et al., 2005) and maize (Qiu et al., 2007). GWAS could be conducted using a diverse range of varieties without the development of a population (Buckler and Thornsberry, 2002). By using a large number of varieties, it facilitates the exploration of more genetic variations, including those with small effects and allelic diversity (Zhu et al., 2008; Juliana et al., 2018). Moreover, GWAS provides higher resolution mapping for identifying candidate genes (Nelson et al., 2018). The aim of this study was to link two-year phenotyping data from both the field and glasshouse with genotyping data using GWAS, therefore identifying potential QTL and searching for candidate genes associated with adventitious roots, cortical aerenchyma and root survival in wheat under waterlogging conditions.

Materials and methods

Plant materials and genotyping

A set of 335 wheat genotypes collected worldwide were used to evaluate their waterlogging tolerance. All these genotypes were obtained from China and Australian Grains GenBank.

Genotyping of these accessions has been described in Kang et al. (2020) and Choudhury et al. (2019). Briefly, all accessions were genotyped using the Illumina iSelect 90,000 SNP bead chip assay described in Wei et al, 2019. A total of 38,379 SNPs were identified to be polymorphic in the population. For quality control, markers with a less than 90% call rate across samples, a minor allele frequency less than 0.05, or that were redundant were removed. Finally, 4,560 markers were selected for marker trait association analysis.

Growth conditions, waterlogging treatment and assessment for aerenchyma formation and root survival

Two glasshouse tank trials and one outdoor tank trial were undertaken at the University of Tasmania, Australia in 2021. For the experiment in the glasshouse, plants were grown in 60 cm × 120 cm × 60 cm bins, filled with soil from the field site prone to waterlogging. The outside tank experiment was performed in big cement tanks (120 cm x 240 cm x 70 cm), also filled with soil from the site prone to waterlogging. For all the glasshouse and tank experiments, waterlogging treatment was imposed at the 2-3 leaf stage. For the waterlogging treatment, the water was maintained at the soil surface level. The experiment was repeated three times in all the trials. Root samples were harvested when the roots of the most sensitive genotypes died (two weeks after waterlogging in glasshouse tank experiments and eight weeks after waterlogging in the outdoor tank experiment). Root survival was scored from 1 to 10 after terminating waterlogging treatment (Figure 1) with the most tolerant varieties being scored 1 (well-developed ARs and no dead roots) and the most sensitive/intolerant plants being scored 10 (all roots died) based on the methods by (Manik et al., 2022b). Aerenchyma formation was detected based on the method by Zhang et al. (2016). Root cortical aerenchyma formation in adventitious roots was checked 10 days after waterlogging. Approximately 2 cm long root segments were taken from the mature zone which was about 6 cm from the root apex. Cross sections were cut manually using razor blades and photographed under a bright field light microscope (Olympus BXBX53, Japan). The proportion of aerenchyma was visually scored based on digital images and the criteria are as followed: 0 = no aerenchyma, 4 = well-formed aerenchyma (Zhang et al., 2016).

Genome-wide association analysis

For population correction, PCA (principal component analysis) was calculated using SNPRelate package as described in the previous publication (Kang et al., 2020), the optimum number of PCs (Principal components) was fixed in association models. GWAS was conducted using the rMVP package of R as described earlier (Yin et al., 2021; Manik et al., 2022b). In the association study, the notional p-value threshold to indicate a significant MTA was set to -Log10(p) ≥ 3.5.

In our study, GLM, MLM, and FarmCPU models were used for analysing the data on adventitious root development and root cortical aerenchyma formation scored from the 329 accessions and 18,132 SNPs. The best model was selected



FIGURE 1
Root damage scores under waterlogging conditions. Damage score of 1: highly tolerant; damage score of 10: severely damaged with no survived roots.

based on quantile-quantile (Q-Q) plots (Figure S2). The outcome variable in each model was the average of AR or RCA values from different trials.

The FarmCPU model was found to be the most suitable one which had a small number of extreme p-values. The FarmCPU method iteratively performs marker tests with pseudo-quantitative trait nucleotides (QTNs) as covariates in a fixed-effect model and keeps optimizing pseudo-QTNs in a random-effect model, and this process continues until no new pseudo QTNs are added (Liu et al., 2016). The joint capabilities of removing confounding effects between testing markers and kinship, preventing model overfitting, and controlling false positives have made the FarmCPU method one of the most efficient methods in modern GWAS (Knoch et al., 2020). Within our implementation of the rMVP model we used the following settings: default imputation, no principal components were adduced, "max Loop" was set to 10 (this exceeded what was required for our data), and the internal "FaST-LMM" method was used. Significant markers were visualized with a Manhattan plot and important p-value distributions from all the GLM, MLM and FarmCPU results (expected vs. observed p-values on a -log10 scale) were shown with Q-Q plots.

Estimation of allelic effects on waterlogging tolerance

The allele at the locus of the detected SNPs responsible for increasing waterlogging tolerant (lower visual scoring (healthier roots or greater proportion of RCA)) is referred to as a "positive allele (T or TT)" while the allele associated with increasing waterlogging sensitivity was classified as a "negative allele (S or SS)". The effects of SNPs were determined based on average matching scores of positive alleles and those of negative alleles.

Candidate gene associated with waterlogging tolerance

SNPs at a level of -Log10(p) ≥ 5.5 were considered highly significant and were used to identify candidate genes. We used the physical chromosome positions and sequence of significant SNPs within the LD interval to identify the annotation of the high-confidence (HC) candidate genes. Based on the physical position of these SNPs (through blasting wheat genome on gramene.org), wheat gene IDs located either up or down 1 Mb of the physical position were searched for functional annotation. Gene functional annotation was obtained from the public database of wheat genome from 1 Kb (https://db.cngb.org/onekp/). Candidate genes with a possible connection to waterlogging tolerance were taken into consideration with high confidence.

Statistical analysis and heritability

Phenotypic traits were summarised with descriptive statistics (mean and standard deviation).

Histological staining

Aerenchyma formation follows programmed cell death (PCD) induced by histological metabolic changes, typically, the production of H_2O_2 under waterlogging (Cheng et al., 2016). To confirm this, the adventitious roots of wheat seedlings were sampled 1, 3, 5, and 7 d after waterlogging to examine aerenchyma development. Aerenchyma formation of wheat roots after 1 d, 3 d, 5 d, and 7 d waterlogging treatment was scored according to Zhang et al. (2016). Root cross sections at 40 mm above the root tip were sampled to study the characteristics of cells that develop aerenchyma using light micrographs. We used three pairs of wheat varieties showing different waterlogging tolerance (tolerant, AUS19402, H-242, KZYL-SARK, and sensitive, H-195, YU-1, H-197) for cell acidification staining and diaminobenzidine (DAB) staining. Among these pairs, H-242 and H-195 showed the greatest differences thus being selected for further studies.

DAB staining was performed as described previously (Xu et al., 2019). Briefly, cross sections of wheat roots sampled after 1 d, 2 d, 3 d and 7 d waterlogging treatment were incubated in 1 mg/ml DAB solution (pH = 5.5) for 1 h and then immersed in 75% ethanol. The localization of H_2O_2 signal (indicated by the pink or brown color) was monitored under a light microscope (Leica M205C, Germany).

To study cell acidification, the root cross sections sampled after 1, 2, 3 and 7 d waterlogging treatment were stained with 1% neutral red in 10 mM Tris-HCl (pH 7.0) for 5 s. Then the sections were placed in the petri dish with clean water and washed for 3 times. Excess water was removed and photos were taken under a light microscope (Xu et al., 2013).

Results

Waterlogging tolerance of wheat accessions

The frequency distributions of root survival scores and aerenchyma formation of the 329 accessions are presented in Figure 2. Most of the genotypes formed aerenchyma with only 25 having the aerenchyma score of < 1 (Figure 2A). For root survival, most of the germplasm showed medium tolerance to waterlogging with less than 10% showing damage scores of < 3 and > 8, respectively (Figure 2B). The broad-sense heritability (h_B^2) for root survival was 0.37. Among those tolerant lines,

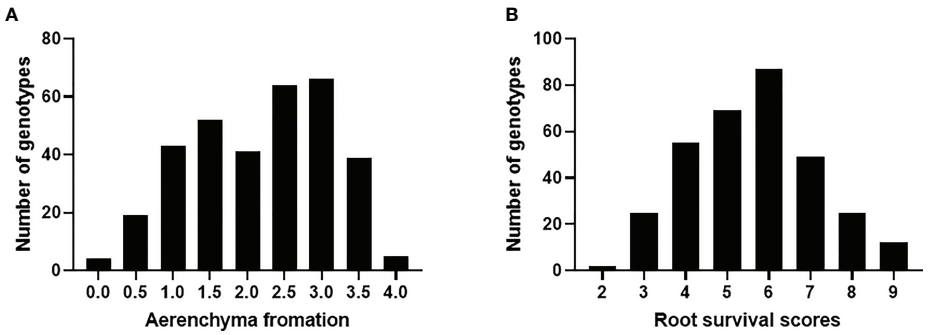


FIGURE 2
Distribution of aerenchyma formation **(A)** and root survival under waterlogging condition **(B)**.

Afghanistan 7, H-023, H-054, H-056, H-074, H-114, H-115, H-119, H-197, and Yu-03 showed consistently better root survival in both glasshouse trials and the tank trial while the roots of B-T-35, B-T-38, Bukovinka, CAZ53, H-083, H-249, H-251, H-252, IG43428, and Surhak 5688 died in all trials. Surprisingly, aerenchyma formation under waterlogging stress showed no significant correlation with root survival (R^2 = 0.008, Figure S1). Some genotypes such as H-074 had no aerenchyma (aerenchyma score = 0.67) but showed good root survival, while some genotypes such as IG43428 and Surhak 5688 had aerenchyma scores of >3 but no roots survived. Detailed genotypic, phenotypic data and genetic map for the 329 common wheats are provided in Supplementary Tables S1–S3.

Genome wide association study in wheat under waterlogging conditions

We use the same population as Kang et al. (2020), and the effect of population structure in our study was not significant. Three different GWAS models including generalised linear models (GLM), mixed linear models with random effects (MLM) and FarmCPU models were initially used and compared. The Q-Q plots from the three models were shown in Figure S2. FarmCPU was shown to be the best fitted model and thus we focused on the SNPs identified from the Farm CPU modelling.

Using the Farm CPU model, five significant MTAs were identified based on average scores of roots cortical aerenchyma (Figure 3A). The threshold for selecting the significant QTL is -log10(p) is equal or larger than 3.8. These MTAs were located on chromosomes 2D, 4A, 4B, 7A, and 7D (Table 1; Figures 3A, Figure 4). SNPIWB11078, SNPIWA8342 and SNPIWB7934 were the most significant MTAs. Overall, genotypes with the tolerance alleles (marked with T) showed a significantly higher proportion of aerenchyma than those with sensitive alleles (marked with S). These alleles had additive effects and all genotypes with three tolerant alleles had a greatest proportion of RCA (Figure 3B).

Six significant MTAs were identified based on mean root survival scores, and these MTAs were located on chromosomes 2A (two), 2B, 4B, 5A and 5B (Figures 4, 5A). The genotypes with tolerance alleles (marked with T) showed significantly better root survival than those with sensitive alleles (marked with S) and the combination of all three different tolerance alleles also improved root survival (Figure 5B). Among all the MTAs, only one MTA for root survival on 4B was located very close to one MTA for aerenchyma formation, confirming the non-significant correlation between aerenchyma formation and root survival.

Histological staining during aerenchyma formation

The root cross-section taken at 4 cm from the root tips showed that the root cells remained intact thus no aerenchyma was formed even after five days of waterlogging treatment in sensitive variety H-195 (Figure 6). In tolerant variety H-242, aerenchyma formation started on the third day after waterlogging (Figure 6), and ~70% and >80% of the root cross-section area consisted of aerenchyma on the fifth and seventh day after waterlogging, respectively. This indicated an earlier formation of aerenchyma and larger proportion of aerenchyma in root cross-section of H-242 relative to H-195 (Figure 6). Evidence regarding the programmed root cell death was witnessed from the neutral red staining which similarly reflects the cell death scenario (Figure 7). Root cross-section of H-242 showed a higher accumulation of neutral staining, suggesting that a higher proportion of root cells were dying during waterlogging, consistent with the mechanism of

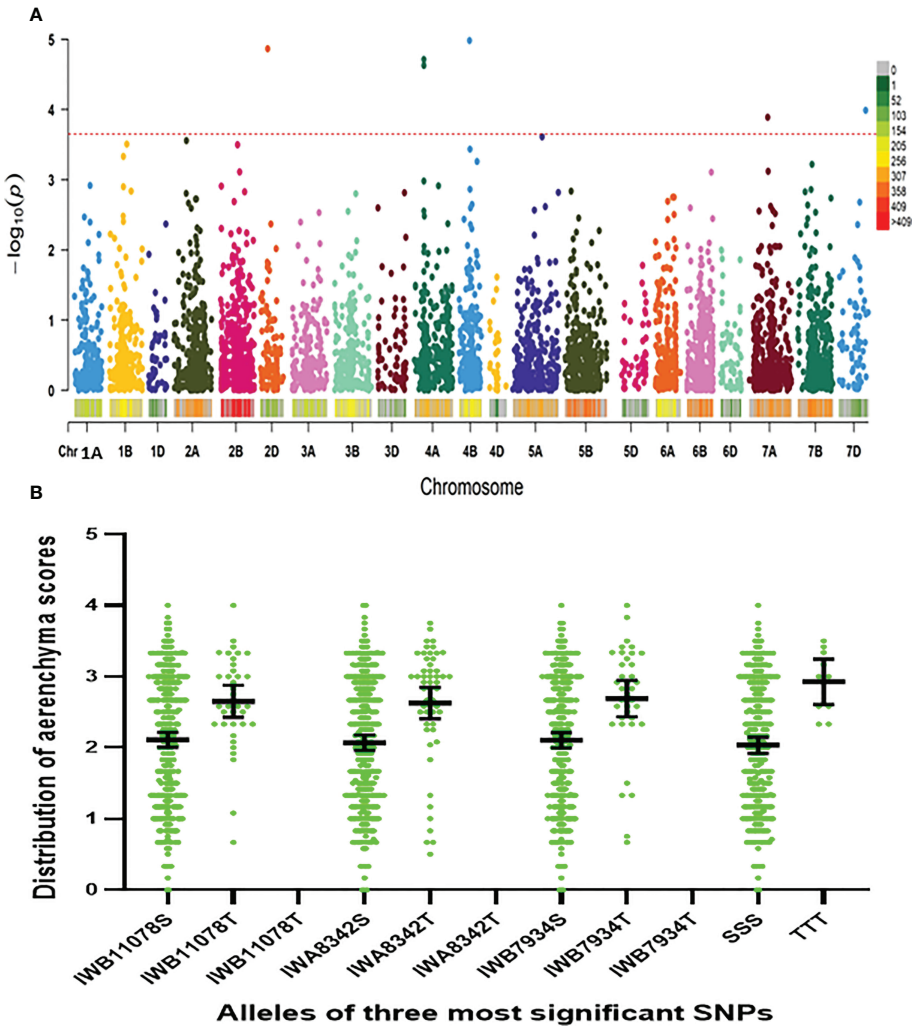


FIGURE 3
Marker-trait (aerenchyma formation) associations. **(A)**: GWAS aerenchyma formation using FarmCPU: Lod values of all the markers; **(B)**: distribution of aerenchyma formation of genotypes with three markers significantly correlated with aerenchyma formation and the combination of all three markers. T, tolerance allele; S, sensitive allele; TTT, tolerance alleles of all three markers; SSS, sensitive alleles of all three markers.

aerenchyma formation against waterlogging in wheat (Figure 7). To further confirm whether reactive oxygen species (ROS) was involved in aerenchyma formation (PCD induced), histological staining was applied to monitor H_2O_2 production in the root cross-sections on selected representative waterlogging days. H_2O_2 was abundantly detected in the central cortical cells (the pre-aerenchyma cells) and was also seen in the vasculature with tolerant variety H-242 showing quicker response and accumulating more H_2O_2 than sensitive variety H-195 (Figure 8). All these observations indicated that under waterlogging, the waterlogging tolerant variety employs the PCD process to produce aerenchyma induced by H_2O_2.

Discussion

QTL for root traits associated with wheat waterlogging tolerance

Very few studies have investigated root physiological or morphological traits to identify QTL associated with waterlogging tolerance in wheat due to the difficulty of phenotyping. Instead, leaf physiological traits have been more often used for assessing wheat waterlogging tolerance. For example, by assessing leaf chlorosis at the maturity stage of wheat crops utilizing the SC (SHWL1 × Chuanmai 32) wheat

10.3389/fpls.2022.1066752

TABLE 1 QTL and associated markers for different traits.

Associated markers	Chromosome	Physical position (Mb)	Additive effect	Marker significance level	R^2	minor allele frequency (MAF)
		Root survival under waterlogging stress				
IWA2092	2A	388.71	0.69	1.0E-04	0.011	0.25
IWB11193	2A	413.64	0.55	8.9E-05	0.026	0.16
IWA3325	4B	193.52	0.73	4.1E-05	0.036	0.29
IWB22137	5A	374.32	-0.64	1.0E-04	0.013	0.22
IWB10994	5B	54.30	-0.61	7.2E-05	0.098	0.40
		Aerenchyma formation under waterlogging stress				
IWB11078	2D	117.32	-0.59	1.4E-05	0.035	0.11
IWA8342	4A	185.89	0.50	2.4E-05	0.052	0.16
IWB41008	4A	185.89	-0.45	1.9E-05	0.043	0.17
IWB7934	4B	168.86	-0.53	1.0E-05	0.042	0.11
IWB33938	7A	325.39	-0.29	1.3E-04	0.029	0.50
IWB16121	7D	427.90	-0.43	1.0E-04	0.014	0.18

population, 10 QTL were identified responsible for waterlogging tolerance (Yu and Chen, 2013). Furthermore, Yu and Chen (2013) assessed waterlogging tolerance using the wheat ITMI population W7984/Opata85 at the early growth stage, and found 36 QTL associated with aboveground traits (including survival rate, germination rate index, leaf chlorophyll content, plant height index, dry matter weight) on 18 chromosomes. Burgos et al. (2001) found that QTL associated with seedling survival/seedling growth index under waterlogging are on chromosomes 2A, 2B, 3A, 3B, 4B, 5A, 6A and 7S which explained 35.5% of the phenotypic variance (Burgos et al., 2001). Using recombinant inbred lines (RILs) derived from USG3209 × Jaypee, 48 QTL clustering into 10 genomic regions were consistently detected both in greenhouse and field trials, among which three QTL were identified on chromosome 1BL, explaining 22-32% phenotypic variance, and a major QTL (*QSpad3.ua-1D.5*) for chlorophyll content on chromosome 1D explained 24% phenotypic variance under environment-controlled greenhouse conditions (Ballesteros et al., 2015). However, none of those authors have investigated root aerenchyma formation in response to waterlogging.

Our findings offer a strong explanation that the variations in leaf survival performance is highly due to the difference in root aerenchyma development under waterlogging. MTAs for root survival performance were identified on chromosomes 2B and 5A in our study, which were consistent with results of Burgos et al. (2001). This highlights the possible linkage between root aerenchyma development and leaf growth under waterlogging. Besides, a major QTL on chromosome 7A associated with germination rate index was found under waterlogging conditions, explaining 23.92% of phenotypic variance in wheat (Yu et al., 2014). This QTL is located at a close position to the

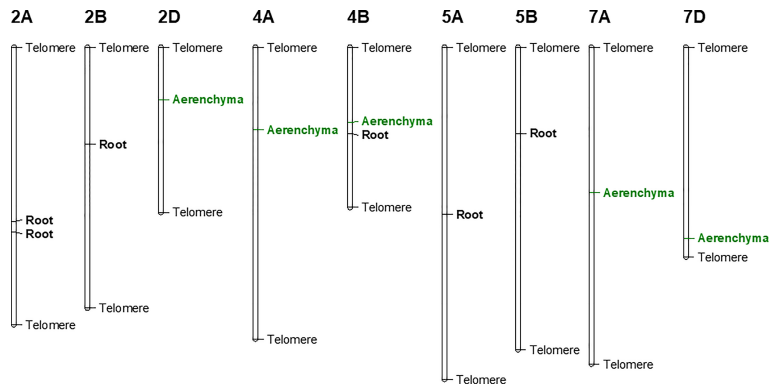


FIGURE 4
Genetic linkage map of identified MTAs. Root: markers associated with root survival under waterlogging condition; Aerenchyma: markers associated with aerenchyma formation under waterlogging condition.

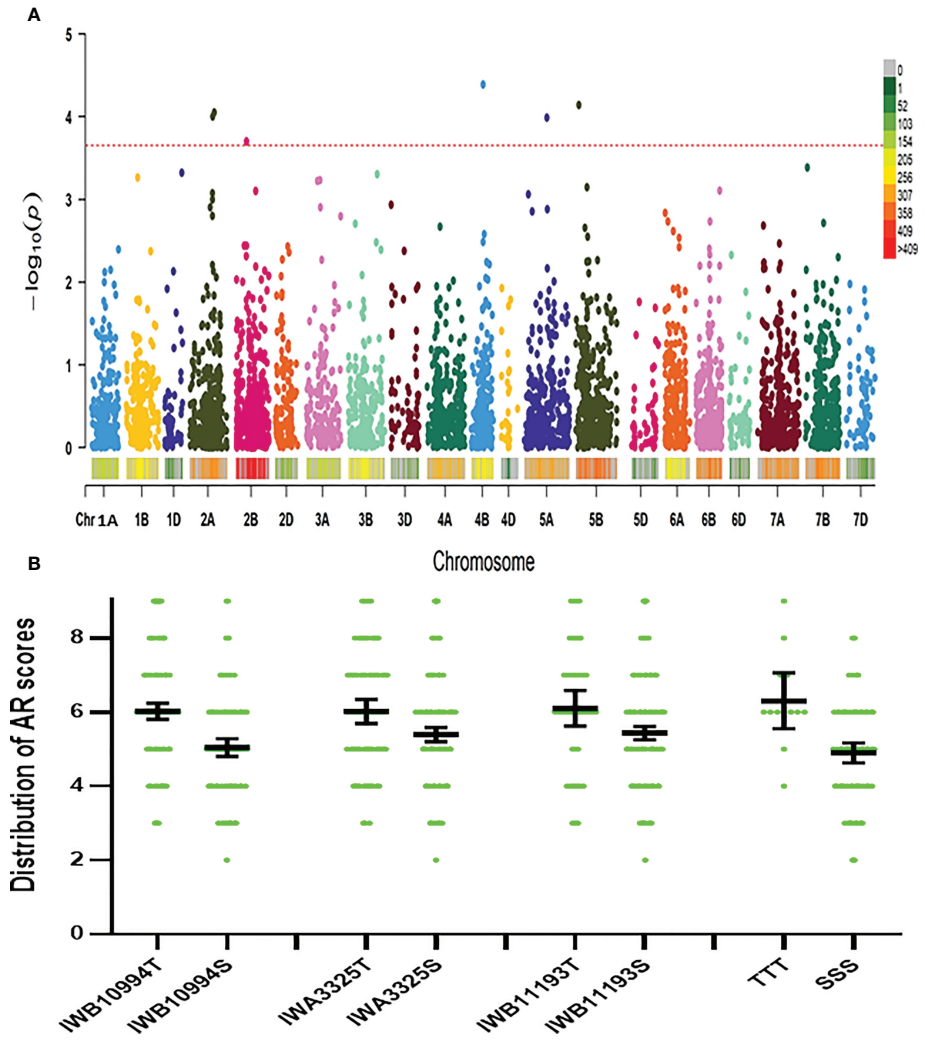


FIGURE 5
Marker-trait (root survival) associations. **(A)**: GWAS for root survival using FarmCPU: Lod values of all the markers; **(B)**: distribution of root survival scores of genotypes with three markers significantly correlated with root survival and the combination of all three markers. T, tolerance allele; S, sensitive allele; TTT, tolerance alleles of all three markers; SSS, sensitive alleles of all three markers.

MTA for aerenchyma formation on 7A from our study (Figure 4). However, most of the QTL for root traits identified in our study were different from the previously reported QTL in wheat waterlogging utilizing leaf physiological traits (Tong et al., 2021). Therefore, our study case offers novelty in finding specific root survival related QTL in wheat responsible for waterlogging tolerance.

Candidate genes

Based on the physical positions of markers that were significantly linked with those identified QTL, we further investigated candidate genes by investigating the annotated genes within these zones (± 1 cM from the maker position). Annotated genes functioning in ROS production, Ca^{2+} binding, and ethylene metabolism were highly regarded as potential candidate genes. Therefore, a total of 38 annotated wheat genes were identified from the proposed QTL in this study (Table S1). Of which, eight genes were highlighted as the potential candidate genes associated with ROS production according to annotated gene functions. ROS plays an important role in inducing PCD for aerenchyma development (Cheng et al., 2016). Within the QTL on chromosome 4B, gene *TraesCS4B02G176900* (encodes peroxidase) was co-located in the same zone, indicating that ROS metabolism is potentially involved in wheat waterlogging tolerance. *TraesCS2B02G229100* (encodes detoxification protein) correlates with the QTL on

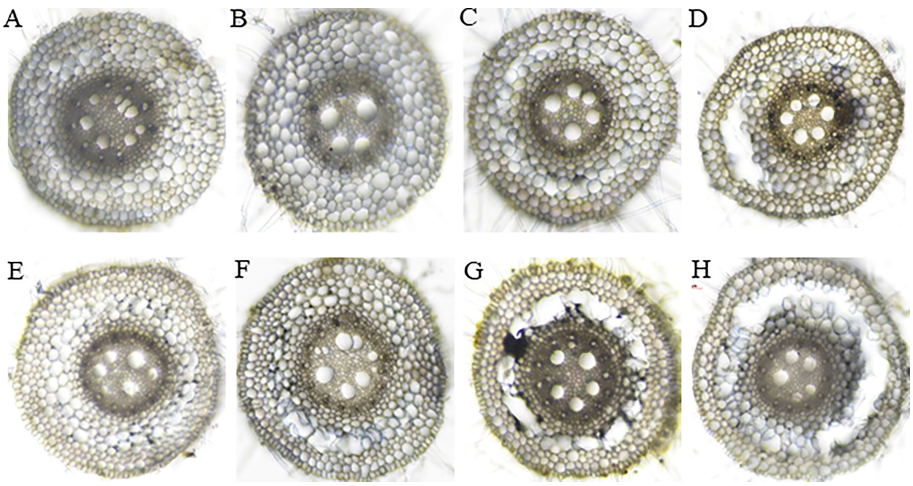


FIGURE 6
Aerenchyma formation in the root cross-section sampled at 4 cm from the root tips in wheat genotypes with different degrees of aerenchyma formation after waterlogging treatment. Upper panel: H-195; Bottom panel: H-242. **(A, E)**, **(B, F)**, **(C, G)**, and **(D, H)**: waterlogging for 1, 3, 5 and 7 days, respectively.

chromosome 2B and is potentially involved in the degradation of ROS under waterlogging (Li et al., 2018). Another gene *TraesCS2B02G230100* (encodes Histone H4) within the same QTL could also be a potential candidate gene. Direct evidence has been supplied that histone maintains a role in deciding cell wall degradation and thus participating in aerenchyma formation in wheat seminal roots (Li et al., 2019) under waterlogging. *TraesCS4A02G067800* encoding histone located on 4A is also a candidate gene (Table S1).

Ethylene response factor (ethylene related signaling components) is a representative regulator for crop waterlogging tolerance. Through maintaining the constitutive expression of ERFVII (group VII ethylene response factor) in transgenic wheat plants, waterlogging tolerance is significantly enhanced without grain yield penalty (Wei et al., 2019). In the present study, *TraesCS5B02G214400* (directly encoding ethylene responsive factor 5a) linked with the QTL on 5B was a most likely candidate gene. Besides, hormonal regulation under waterlogging is one of the

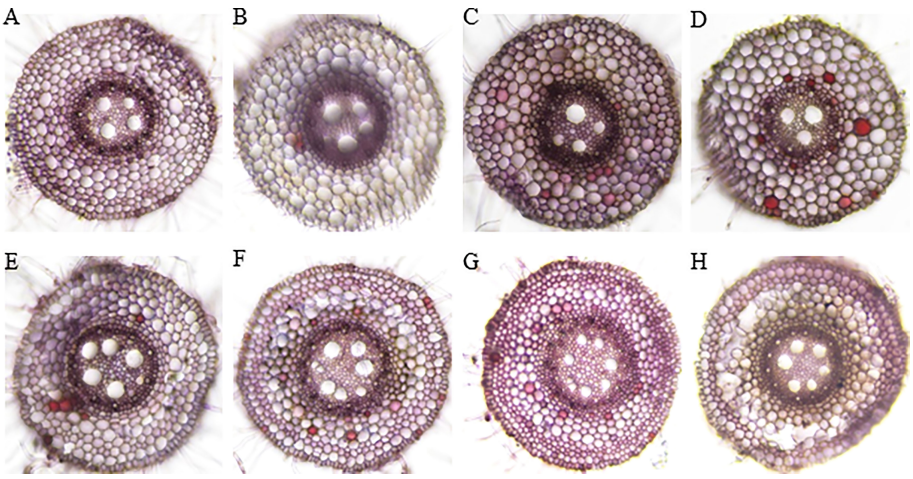


FIGURE 7
Neutral red staining for cell acidification. Upper panel: H-195; Bottom panel: H-242. **(A, E)**, **(B, F)**, **(C, G)**, and **(D, H)**: waterlogging for 1 to 4 d, respectively.

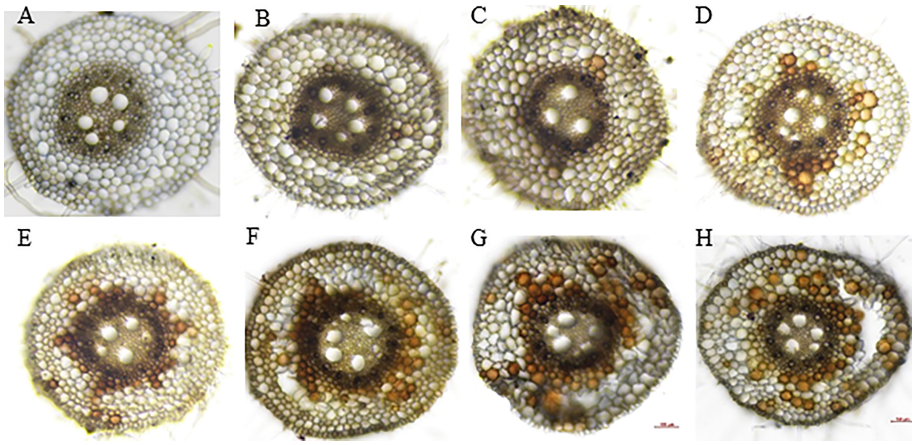


FIGURE 8
DAB staining for H_2O_2 signal. Upper panel: H-195; Bottom panel: H-242. **(A, E)**, **(B, F)**, **(C, G)** and **(D, H)**: waterlogging for 1 to 4 days, respectively.

mechanisms that plants utilize to fight against waterlogging (Nguyen et al., 2018). ABA biosynthesis genes, such as NCED1 and NCED2, are important in wheat waterlogging tolerance (Nguyen et al., 2018). Thus ABI3 (ABA insensitive 3, ABI interacting protein) encoded by *TraesCS5B02G214500* (within the QTL on 5B) was a potential candidate gene. Alanine aminotransferase links glycolysis and TCA cycle (tricarboxylic acid cycle) under hypoxia induced by waterlogging (Rocha et al., 2010), thus, *TraesCS5B02G214700* on 2D (encodes alanine aminotransferase) could contribute to RCA QTL on 2D (Table S1).

Mechanisms for aerenchyma formation

Histochemical staining results in our study aligned with the mechanism of ROS-induced PCD for aerenchyma formation. Consistent with their findings of Xu et al. (2013) showing that ROS accumulation starts in the mid-cortex cells along with the development of aerenchyma in wheat, our results indicated that early cortical cell death started from the mid-cortex (Figures 6, 7) along with the development of aerenchyma (Figure 6). The neutral red staining under waterlogging conditions further illustrated the dying cell (Figure 7). Furthermore, lysigenous aerenchyma formation in wheat was reported to be regulated through ROS signaling (Yamauchi et al., 2014), further indicating the strong links between ROS production and aerenchyma formation. In our study, ROS accumulation under waterlogging was evidenced by DAB staining (for H_2O_2 detection) (Figure 8). H_2O_2 was abundantly detected (reflected by the brown precipitate) in the central cortical cells (pre-aerenchymal cells) (Figure 8). Our results suggested that aerenchyma development in wheat roots began in the central cortical cells (pre-aerenchymal cells) with further expansion to its surrounding cells, consistent with the previous report (Xu et al., 2013). Moreover, DAB staining also indicated the strong involvement of H_2O_2 induced PCD during aerenchyma formation (Xu et al., 2013). A similar mechanism has been confirmed by Steffens and Sauter (2005) and Steffens et al. (2011), showing that H_2O_2 is required for ethylene-induced epidermal death which is responsible for aerenchyma development in rice stems.

The relationship between aerenchyma formation and root survival

Our results showed significant variation in root survival in response to waterlogging among 329 wheat genotypes with diverse genetic background, however, there was lack of correlation between root survival and aerenchyma formation in the present study, indicating that multiple mechanisms underlying root survival are involved.

Many studies show that aerenchyma formation and root survival are highly related (Thomson et al., 1990; Haque et al., 2012), and the aerenchyma formation greatly contributes to the survival of root system (Thomson et al., 1990; Haque et al., 2012). For example, newly produced adventitious roots are adapted with more aerenchyma than seminal roots in waterlogged soil or O_2-deficient solutions, along with consecutive root elongation under saturated conditions (Thomson et al., 1992; Malik et al., 2002). In our study, fast aerenchyma development was observed in tolerant variety H-242 under waterlogging, along with the highly induced H_2O_2 accumulation (Figure 6) and greater root cell death (Figure 7), suggesting that root aerenchyma formation is involved in wheat waterlogging tolerance. These observations

highly aligned with the classic defense mechanism that waterlogging triggers reactive oxygen species production which led to PCD for root aerenchyma formation under waterlogging (Cheng et al., 2016). Other than aerenchyma formation, other alternative waterlogging tolerance mechanisms were also reported. For example, root architecture was found to contribute to waterlogging tolerance (Haque et al., 2012). Root architecture involves axile and surface adventitious roots development induced by salicylic acid (SA). The reduction in redox potential due to waterlogging caused accumulation of toxin ions and secondary metabolites, which inhibit plant growth under waterlogging, skeletons as another defense mechanism. It was found that barley genotypes with better tolerance to Mn^{2+} or Fe^{2+} toxicity perform better in waterlogging soil (Pang et al., 2007; Hossein and Rengel, 2010; Hossein et al., 2012). Similarly, some barley genotypes with no RCA also show a degree of waterlogging tolerance (Manik et al., 2022a), suggesting that the tolerance to toxicity contributes to waterlogging resistance. In wheat, varieties tolerant to ion toxicities usually grow better under waterlogging-affected acid soil, disclosing the contribution of resistance to toxic compounds under waterlogging (Hossein and Rengel, 2010; Hossein et al., 2012). However, root aerenchyma development under waterlogging still serves as the primary mechanism for defending which involves ethylene biosynthesis (Koramutla et al., 2022). Barley varieties having QTL associated with root cortical aerenchyma showed better waterlogging tolerance, reflected by the higher aerenchyma area, more white (healthy and functional) adventitious roots, higher shoot biomass (Manik et al., 2022a). QTL responsible for root survival and root aerenchyma development identified in our study (Figure 4) provide multiple mechanisms that can be were utilized by crops while under waterlogging.

Factors influence the assessment of waterlogging tolerance and the development of aerenchyma

Factors affecting the assessment of waterlogging can be simply categorized into underground and aboveground. Leaf traits aboveground for assessing waterlogging damage are mainly utilized for QTL detection in wheat (Burgos et al., 2001; Yu and Chen, 2013). However, given the hypoxia environment (induced by waterlogging) in soil that initially limited/affected root growth due to oxygen deficiency (or soil toxicity), root damage may have occurred at early waterlogging stress stage before leaf related traits become affected. Therefore, only focusing on leaf related traits for waterlogging QTL detections has limitations. In our research, we primarily investigated root survival and root aerenchyma development under wheat waterlogging stress, which identified the QTL for root development under waterlogging (Figure 4).

Aerenchyma formation is determined by a combination of variable aspects. The porosity of adventitious root increases due to the formation of aerenchyma, which depends on genotype, plant developmental stage, duration of O_2 deficiency, and treatment method (Thomson et al., 1990; Huang et al., 1997; Wiengweera et al., 1997; Malik et al., 2001; Malik et al., 2002; Manik et al., 2019; Tong et al, 2021). Genetic variation is the dominant factor that determines aerenchyma development under waterlogging, which is also the key basis for GWAS/QTL analysis. Previous research has illustrated the importance of root aerenchyma for waterlogging tolerance. For instance, waterlogging-tolerant genotypes always had higher root porosities than sensitive genotypes if growing in an N_2-flushed nutrient solution for 20 days, demonstrating the importance of genotypic variation under waterlogging (Boru et al., 2003). Besides, plant growth stages differ in aerenchyma development. Seminal roots of young seedlings form aerenchyma whereas older seminal roots lose this capacity (Thomson et al., 1990; Xu et al., 2013; Tong et al., 2021). Our research not only confirmed the importance of aerenchyma formation in wheat waterlogging tolerance, but also agrees with previous research cases that the involvement of H_2O_2 induced PCD is critical for aerenchyma development (Xu et al., 2013; Cheng et al., 2016).

Conclusions

Waterlogging seriously affected wheat root growth. GWAS analysis identified six and five MTAs/QTL in wheat associated with the formation of adventitious roots and aerenchyma formation, respectively, under waterlogging stress. Several genotypes consistently produced a large number of adventitious roots and formed a large proportion of aerenchyma in root cortical cells could be used in breeding programs to develop waterlogging tolerant wheat varieties. Through histochemical staining, our study confirmed that H_2O_2 induced PCD led to aerenchyma formation in wheat adventitious roots. Candidate genes for these QTL are most likely ROS, ethylene or ABA related regulatory elements. Our research also illustrated an alternative tolerance mechanism that may involve soil toxicity tolerance under waterlogged soil. Similarly, wheat lines which don't have aerenchyma but indicated stable tolerance to waterlogging can be used to pyramid different waterlogging tolerance mechanisms. As healthy root development under waterlogging conditions is the ultimate waterlogging tolerance indicator, future research should concentrate more on roots and mechanisms for root survival and development under the hypoxia environment. The combination of QTL for aerenchyma formation and soil toxicity tolerance can be more effectively used to improve wheat waterlogging tolerance.

Data availability statement

The data presented in the study are deposited in the Dryad repository, accession number doi:10.5061/dryad.wh70rxwrk.

Author contributions

MZ acquired the funding, and participated in supervision; WZ participated in supervision, LX, YN, and CZ conducted the field trials and data collection and data analysis; LX, YN, and CZ carried out data visualization; HL collected the data; LX, MZ, and JP wrote, reviewed and edited the draft. All authors contributed to the article and approved the submitted version.

Funding

This project is funded by the Grains Research and Development Corporation (GRDC) of Australia and Hubei Key Research and Development Program (2021BBA225).

Conflict of interest

The authors declare that the research was conducted in the absence of any commercial or financial relationships that could be construed as a potential conflict of interest.

Publisher's note

All claims expressed in this article are solely those of the authors and do not necessarily represent those of their affiliated organizations, or those of the publisher, the editors and the reviewers. Any product that may be evaluated in this article, or claim that may be made by its manufacturer, is not guaranteed or endorsed by the publisher.

Supplementary material

The Supplementary Material for this article can be found online at: https://www.frontiersin.org/articles/10.3389/fpls.2022.1066752/full#supplementary-material

References

Abbas, M., Berckhan, S., Rooney, D. J., Gibbs, D. J., Vicente, C. J., Sousa, C. C., et al. (2015). Oxygen sensing coordinates photomorphogenesis to facilitate seedling survival. *Curr. Biol.* 25, 1483–1488. doi: 10.1093/jxb/eraa442

Argus, R. E., Colmer, T. D., and Grierson, P. F. (2015). Early physiological flood tolerance is followed by slow post-flooding root recovery in the dryland riparian tree *Eucalyptus camaldulensis subsp refulgens*. *Plant Cell Environ.* 36, 1189–1199. doi: 10.1111/pce.12473

Armstrong, W. (1971). Radial oxygen losses from intact rice roots as affected by distance from the apex, respiration and water logging. *Physiol. Plant* 25, 192–197. doi: 10.1111/j.1399-3054.1971.tb01427.x

Armstrong, W. D. (1979). Aeration in higher plants. *Adv. Bot. Res.* 7, 225–332. doi: 10.1016/S0065-2296(08)60089-0

Bailey-Serres, J., Lee, S. C., and Brinton, E. (2012). Waterproofing crops: Effective flooding survival strategies. *Plant Physiol.* 160, 1698–1709. doi: 10.2307/41812018

Ballesteros, D. C., Mason, R. E., Addison, C. K., Andrea Acuña, M., Nelly Arguello, M., Subramanian, N., et al. (2015). Tolerance of wheat to vegetative stage soil waterlogging is conditioned by both constitutive and adaptive QTL. *Euphytica.* 201, 329–343. doi: 10.1007/s10681-014-1184-3

Benjamin, L. R., and Greenway, H. (1979). Effects of a range of O_2 concentrations on porosity of barley roots and on their sugar and protein concentrations. *Ann. Bot.* 43, 383–391. doi: 10.1093/oxfordjournals.aob.a085646

Boru, G., van Ginkel, M., Trethowan, R. M., Boersma, L., and Kronstad, W. E. (2003). Oxygen use from solution by wheat genotypes differing in tolerance to waterlogging. *Euphytica.* 132, 151–158. doi: 10.1023/A:1024622405505

Broughton, S., Zhou, G. F., Teakle, L. N., Matsuda, R., Zhou, M. X., O'Leary, A. R., et al. (2015). Waterlogging tolerance is associated with root porosity in barley (*Hordeum vulgare* l.). *Mol. Breed.* 35, 27.doi: 10.1007/s11032-015-0243-3

Buckler, E. S., and Thornsberry, J. M. (2002). Plant molecular diversity and applications to genomics. *Curt Opin. Plant Biol.* 5, 107–111. doi: 10.1016/S1369-5266(02)00238-8

Burgos, M. S., Messmer, M. M., Stamp, P., and Schmid, J. E. (2001). Flooding tolerance of spelt (*Triticum spelta* l.) compared to wheat (*Triticum aestivum* l.)- a physiological and genetic approach. *Euphytica.* 122, 287–295. doi: 10.1023/a:1012945902299

Calvo-Polanco, M., Señorans, J., and Zwiazek, J. J. (2012). Role of adventitious roots in water relations of tamarack (*Larix laricina*) seedlings exposed to flooding. *BMC Plant Biol.* 12, 99. doi: 10.1186/1471-2229-12-99

Campbell, M. T., Proctor, C. A., Dou, Y., Schmitz, A. J., Phansak, P., Kruger, G. R., et al. (2015). Genetic and molecular characterization of submergence response identifies Subtol6 as a major submergence tolerance locus in maize. *PloS One* 10, e120385. doi: 10.1371/journal.pone.0120385

Cheng, X. X., Yu, M., Zhang, N., Zhou, Z. Q., Xu, Q. T., Mei, Z. F., et al. (2016). Reactive oxygen species regulate programmed cell death progress of endosperm in winter wheat (*Triticum aestivum* l.) under waterlogging. *Protoplasma.* 253, 311–327. doi: 10.1007/s00709-015-0811-8

Choudhury, S., Hu, H., Fan, Y., Larkin, P., Hayden, M., Forrest, K., et al. (2019). Identification of new QTL contributing to barley yellow dwarf virus-PAV (BYDV-PAV) resistance in wheat. *Plant Dis.* 103 (11), 2798–2803. doi: 10.1094/PDIS-02-19-0271-RE

Cornelious, B., Chen, P., Chen, Y., Leon, N., Shannon, J. G., and Wang, D. (2005). Identification of QTLs underlying water-logging tolerance in soybean. *Mol. Breed.* 16, 103–112. doi: 10.1007/s11032-005-5911-2

Drew, M. C., Jackson, M. B., and Giffard, S. (1979). Ethylene-promoted adventitious rooting and development of cortical air spaces (aerenchyma) in roots may be adaptive responses to flooding in *Zea mays* l. *Planta.* 147, 83–88. doi: 10.1007/BF00384595

Evans, D. E. (2003). Aerenchyma formation. *New Phytol.* 161, 35–49. doi: 10.1046/j.1469-8137.2003.00907.x

Gill, M. B., Zeng, F., Shabala, L., Zhang, G., Fan, Y., Shabala, S., et al. (2017). Cell-based phenotyping reveals QTL for membrane potential maintenance associated with hypoxia and salinity stress tolerance in barley. *Front. Plant Sci.* 8. doi: 10.3389/fpls.2017.01941

Gill, M. B., Zeng, F., Shabala, L., Zhang, G., Yu, M., Demidchik, V., et al. (2019). Identification of QTL related to ROS formation under hypoxia and their association with waterlogging and salt tolerance in barley. *Int. J. Mol. Sci.* 20, 699. doi: 10.3390/ijms20030699

Haque, M. E., Abe, F., and Kawaguchi, K. (2010). Formation and extension of lysigenous aerenchyma in seminal root cortex of spring wheat (*Triticum aestivum* cv. bobwhite line SH 98 26) seedlings under different strengths of waterlogging. *Plant Root.* 4, 31–39. doi: 10.3117/plantroot.4.31

Haque, M. E., Oyanagi, A., and Kawaguchi, K. (2012). Aerenchyma formation in the seminal roots of Japanese wheat cultivars in relation to growth under waterlogged conditions. *Plant Prod Sci.* 15, 164–173. doi: 10.1626/pps.15.164

Hossein, K. S., Barker, S. J., and Rengel, Z. (2012). Tolerance to ion toxicities enhances wheat (*Triticum aestivum* l.) grain yield in waterlogged acidic soils. *Plant Soil.* 354, 371–381. doi: 10.1007/s11104-011-1073-7

Hossein, K. S., and Rengel, Z. (2010). Aluminum, manganese, and iron tolerance improves performance of wheat genotypes in waterlogged acidic soils. *J. Plant Nutr. Soil Sci.* 173, 461–468. doi: 10.1002/jpln.200900316

Huang, X., Fan, Y., Shabala, L., Rengel, Z., Shabala, S., and Zhou, M. X. (2018). A major QTL controlling the tolerance to manganese toxicity in barley (*Hordeum vulgare* l.). *Mol. Breed* 38, 16. doi: 10.1007/s11032-017-0767-9

Huang, B. R., Johnson, J. W., Box, J. E., and NeSmith, D. S. (1997). Root characteristics and hormone activity of wheat in response to hypoxia and ethylene. *Crop Sci.* 37, 812–818. doi: 10.2135/cropsci1997.0011183X003700030020x

Huang, B. R., Johnson, J. W., Nesmith, D. S., and Bridges, D. C. (1994). Root and shoot growth of wheat genotypes in response to hypoxia and subsequent resumption of aeration. *Crop Sci.* 34, 1538–1544. doi: 10.2135/cropsci1994.0011183X003400060023x

Juliana, P., Singh, R. P., Singh, P. K., Poland, J. A., Bergstrom, G. C., Huerta-Espino, J., et al. (2018). Genome-wide association mapping for resistance to leaf rust, stripe rust and tan spot in wheat reveals potential candidate genes. *Theor. Appl. Genet.* 131, 1405–1422. doi: 10.1007/s00122-018-3086-6

Kang, Y., Barry, K., Cao, F., and Zhou, M. (2020). Genome-wide association mapping for adult resistance to powdery mildew in common wheat. *Mol. Biol. Rep.* 47, 1241–1256. doi: 10.1007/s11033-019-05225-4

Kim, Y. H., Hwang, S. J., Waqas, M., Khan, A. L., Lee, J. H., Lee, J. D., et al. (2015). Comparative analysis of endogenous hormones level in two soybean (*Glycine max* l.) lines differing in waterlogging tolerance. *Front. Plant Sci.* 6. doi: 10.3389/fpls.2015.00714

Knoch, D., Abbadi, A., Grandke, F., Meyer, R. C., Samans, B., Werner, C. R., et al. (2020). Strong temporal dynamics of QTL action on plant growth progression revealed through high-throughput phenotyping in canola. *Plant Biotechnol. J.* 18, 68–82. doi: 10.1111/pbi.13171

Koramutla, M. K., Tuan, P. A., and Ayele, B. T. (2022). Salicylic acid enhances adventitious root and aerenchyma formation in wheat under waterlogged conditions. *Int. J. Mol. Sci.* 23, 1243. doi: 10.3390/ijms23031243

Li, J. C., Dong, Q., and Yu, S. L. (2001). Effects of waterlogging at different growth stages on photosynthesis and yield of different wheat cultivars. *Acta Agronomica Sinica.* 27, 434–441. doi: 10.1136/bmj.2.6096.1220

Li, C., Liu, D., Lin, Z., Guan, B., Liu, D., Yang, L., et al. (2019). Histone acetylation modification affects cell wall degradation and aerenchyma formation in wheat seminal roots under waterlogging. *Plant Growth Regul.* 87, 149–163. doi: 10.1007/s10725-018-0460-y

Liu, Y., and Bassham, D. C. (2012). Autophagy: pathways for self-eating in plant cells. *Ann. Rev. Plant Biol.* 63, 215–237. doi: 10.1146/annurev-arplant-042811-105441

Liu, X., Huang, M., Fan, B., Buckler, E. S., and Zhang, Z. (2016). Iterative usage of fixed and random effect models for powerful and efficient genome-wide association studies. *PloS Genet.* 12, e1005767. doi: 10.1371/journal.pgen.1005767

Li, H., Vaillancourt, R., Mendham, N., and Zhou, M. (2008). Comparative mapping of quantitative trait loci associated with waterlogging tolerance in barley (*Hordeum vulgare* l.). *BMC Genom.* 9, 401. doi: 10.1186/1471-2164-9-401

Lorbiecke, R., and Sauter, M. (1999). Adventitious root growth and cell cycle induction in deepwater rice. *Plant Physiol.* 119, 21–29. doi: 10.1104/pp.119.1.21

Loreti, E., van Veen, H., and Perata, P. (2016). Plant responses to flooding stress. *Curr. Opin. Plant Biol.* 33, 64–71. doi: 10.1016/j.pbi.2016.06.005

Malik, A. I., Colmer, T. D., Lambers, H., and Schortemeyer, M. (2001). Changes in physiological and morphological traits of roots and shoots of wheat in response to different depths of waterlogging. *Aus J. Plant Physiol.* 28, 1121–1131. doi: 10.1016/S0014-5793(97)00086-0

Malik, A. I., Colmer, T. D., Lambers, H., and Schortemeyer, M. (2003). Aerenchyma formation and radial O_2 loss along adventitious roots of wheat with only the apical root portion exposed to O_2 deficiency. *Plant Cell Environ.* 26, 1713–1722. doi: 10.1046/j.1365-3040.2003.01089.x

Malik, A. I., Setter, T. L., Colmer, T. D., Lambers, H., and Schortemeyer, M. (2002). Short-term waterlogging has long-term effects on the growth and physiology of wheat. *New Phytol.* 153, 225–236. doi: 10.2307/1513791

Manik, S. M. N., Pengilley, G., Dean, G., Field, B., Shabala, S., and Zhou, M. (2019). Soil and crop management practices to minimize the impact of waterlogging on crop productivity. *Front. Plant Sci.* 10. doi: 10.3389/fpls.2019.00140

Manik, S. M. N., Quamruzzaman, M., Livermore, M., Zhao, C., Johnson, P., Hunt, I., et al. (2022a). Impacts of barley root cortical aerenchyma on growth, physiology, yield components, and grain quality under field waterlogging conditions. *Field Crops Res.* 279, 108461. doi: 10.1016/j.fcr.2022.108461

Manik, S. M. N., Quamruzzaman, M., Zhao, C. C., Johnson, P., Hunt, I., Shabala, S., et al. (2022b). Genome-wide association study reveals marker trait associations (MTA) for waterlogging-triggered adventitious roots and aerenchyma formation in barley. *Int. J. Mol. Sci.* 23, 3341. doi: 10.3390/ijms23063341

Nelson, R., Wiesner-Hanks, T., Wisser, R., and Balint-Kurti, P. (2018). Navigating complexity to breed disease-resistant crops. *Nat. Rev. Genet.* 19, 21–33. doi: 10.1038/nrg.2017.82

Nguyen, T., Tuan, P., Mukherjee, S., Son, S., and Ayele, B. (2018). Hormonal regulation in adventitious roots and during their emergence under waterlogged conditions in wheat. *J. Exp. Bot.* 69 (16), 4065–4082. doi: 10.1093/jxb/ery190

Pang, J., Cuin, T. A., Shabala, L., Zhou, M., Mendham, N., and Shabala, S. (2007). Effect of secondary metabolites associated with anaerobic soil conditions on ion fluxes and electrophysiology in barley roots. *Plant Physiol.* 145, 266–276. doi: 10.1104/pp.107.102624

Pan, R., He, D., Xu, L., Zhou, M., Li, C., Wu, C., et al. (2019). Proteomic analysis reveals response of differential wheat (*Triticum aestivum* l.) genotypes to oxygen deficiency stress. *BMC Genomics* 20, 60. doi: 10.1186/s12864-018-5405-3

Qiu, F., Zheng, Y., Zhang, Z., and Xu, S. (2007). Mapping of QTL associated with waterlogging tolerance during the seedling stage in maize. *Ann. Bot.* 99, 1067–1081. doi: 10.1093/aob/mcm055

Rocha, M., Licausi, F., Araújo, W. L., Nunes-Nesi, A., Sodek, L., Fernie, A. R., et al. (2010). Glycolysis and the tricarboxylic acid cycle are linked by alanine aminotransferase during hypoxia induced by waterlogging of lotus japonicus. *Plant Physiol.* 152, 1501–1513. doi: 10.1104/pp.109.150045

Setter, T. L., and Waters, I. (2003). Review of prospects for germplasm improvement for waterlogging tolerance in wheat, barley and oats. *Plant Soil.* 253, 1–34. doi: 10.1023/A:1024573305997

Steffens, B., Geske, T., and Sauter, M. (2011). Aerenchyma formation in the rice stem and its promotion by H_2O_2. *New Phytol.* 190, 369–378. doi: 10.1111/j.1469-8137.2010.03496.x

Steffens, B., and Rasmussen, A. (2016). The physiology of adventitious roots. *Plant Physiol.* 170, 603–617. doi: 10.1104/pp.15.01360

Steffens, B., and Sauter, M. (2005). Epidermal cell death in rice (*Oryza sativa* l.) is regulated by ethylene, gibberellin and abscisic acid. *Plant Physiol.* 139, 713–721. doi: 10.1104/pp.105.064469

Thomson, C. J., Armstrong, W., Waters, I., and Greenway, H. (1990). Aerenchyma formation and associated oxygen movement in seminal and nodal roots of wheat. *Plant Cell Environ.* 13, 395–403. doi: 10.1111/j.1365-3040.1990.tb02144.x

Thomson, C. J., Colmer, T. D., Watkins, E. L. J., and Greenway, H. (1992). Tolerance of wheat (*Triticum aestivum* cvs. gamenya and kite) and triticale (*Triticosecale* cv. Muir) to waterlogging. *New Phytol.* 120, 335–344. doi: 10.1111/j.1469-8137.1992.tb01073.x

Tong, C., Hill, C. B., Zhou, G., Zhang, X. Q., and Li, C. (2021). Opportunities for improving waterlogging tolerance in cereal crops-physiological traits and genetic mechanisms. *Plants.* 10, 1560. doi: 10.3390/plants10081560

Toojinda, T., Siangliw, M., Tragoonrung, S., and Vanavichit, A. (2003). Molecular genetics of submergence tolerance in rice: QTL analysis of key traits. *Ann. Bot.* 91, 243–253. doi: 10.1093/aob/mcf072

Trought, M. C. T., and Drew, M. (1980). The development of waterlogging damage in wheat seedlings (*Triticum aestivum* l.). *Plant Soil.* 56, 187–199. doi: 10.0032-079X/80/0563-0187S01.95

Vidoz, M. L., Loreti, E., Mensuali, A., Alpi, A., and Perata, P. (2010). Hormonal interplay during adventitious root formation in flooded tomato plants. *Plant J.* 63, 551–562. doi: 10.1111/j.1365-313x.2010.04262.x

Visser, E. J. W., Cohen, J. D., Barendse, G. W. M., Blom, C. W. P. M., and Voesenek, L. A. C. J. (1996). An ethylene-mediated increase in sensitivity to auxin induces adventitious root formation in flooded rumex palustris Sm. *Plant Physiol.* 112, 1687–1692. doi: 10.1104/pp.112.4.1687

Voesenek, L., and Bailey-Serres, J. (2013). Flooding tolerance: O_2 sensing and survival strategies. *Curr. Opin. Plant Biol.* 16, 647–653. doi: 10.1016/j.pbi.2013.06.008

Wei, X., Xu, H., Rong, W., Ye, X., and Zhang, Z. (2019). Constitutive expression of a stabilized transcription factor group VII ethylene response factor enhances waterlogging tolerance in wheat without penalizing grain yield. *Plant Cell Environ.* 42, 1471–1485. doi: 10.1111/pce.13505

Wiengweera, A., Greenway, H., and Thomson, C. J. (1997). The use of agar nutrient solution to simulate lack of convection in waterlogged soils. *Ann. Bot.* 80, 115–123. doi: 10.1006/anbo.1996.0405

Xu, L., Pan, R., Shabala, L., Shabala, S., and Zhang, W. Y. (2019). Temperature influences waterlogging stress-induced damage in arabidopsis through the

regulation of photosynthesis and hypoxia-related genes. *Plant Growth Regul.* 89, 143–152. doi: 10.1007/s10725-019-00518-x

Xu, Q. T., Yang, L., Zhou, Z. Q., Mei, F. Z., Qu, L. H., and Zhou, G. S. (2013). Process of aerenchyma formation and reactive oxygen species induced by waterlogging in wheat seminal roots. *Planta.* 238, 969–982. doi: 10.1007/s00425-013-1947-4

Yamauchi, T., Watanabe, K., Fukazawa, A., Mori, H., Abe, F., Kawaguchi, K., et al. (2014). Ethylene and reactive oxygen species are involved in root aerenchyma formation and adaptation of wheat seedlings to oxygen-deficient conditions. *J. Exp. Bot.* 65, 261–273. doi: 10.1093/jxb/ert371

Yin, L. L., Zhang, H., Tang, Z. S., Xu, J. Y., Yin, D., Zhang, Z. W., et al. (2021). rMVP: a memory-efficient, visualization-enhanced, and parallel-accelerated tool for genome-wide association study. *Genom proteom bioinf.* 19, 619–628. doi: 10.1016/j.gpb.2020.10.007

Yu, M., and Chen, G. Y. (2013). Conditional QTL mapping for waterlogging tolerance in two RILs populations of wheat. *SpringerPlus.* 2, 1–7. doi: 10.1186/2193-1801-2-245

Yu, M., Mao, S. L., Chen, G. Y., Liu, Y. X., Li, W., Wei, Y. M., et al. (2014). QTLs for waterlogging tolerance at germination and seedling stages in population of recombinant inbred lines derived from a cross between synthetic and cultivated wheat genotypes. *J. Integr. Agric.* 13, 31–39. doi: 10.1016/S2095-3119(13)60354-8

Zeng, F., Konnerup, D., Shabala, L., Zhou, M., Colmer, T.D., Zhang, G., et al. (2014). Linking oxygen availability with membrane potential maintenance and K+ retention of barley roots: implications for waterlogging stress tolerance. *Plant Cell Environ.* 37, 2325–2338. doi: 10.1111/pce.12422

Zhang, X., Shabala, S., Koutoulis, A., Shabala, L., Johnson, P., Hayes, D., et al. (2015). Waterlogging tolerance in barley is associated with faster aerenchyma formation in adventitious roots. *Plant Soil.* 394, 355–372. doi: 10.1007/s11104-015-2536-z

Zhang, X., Zhou, G., Shabala, S., Koutoulis, A., Shabala, L., Johnson, P., et al. (2016). Identification of aerenchyma formation-related QTL in barley that can be effective in breeding for waterlogging tolerance. *Theor. Appl. Genet.* 129, 1167–1177. doi: 10.1007/s00122-016-2693-3

Zhou, M. (2011). Accurate phenotyping reveals better QTL for waterlogging tolerance in barley. *Plant Breed.* 130, 203–208. doi: 10.1111/j.1439-0523.2010.01792.x

Zhu, C. S., Gore, M., Buckler, E. S., and Yu, J. M. (2008). Status and prospects of association mapping in plants. *Plant Genome.* 1, 5–20. doi: 10.3835/plantgenome2008.02.0089

frontiers | Frontiers in Plant Science

TYPE Original Research
PUBLISHED 24 November 2022
DOI 10.3389/fpls.2022.1074132

Check for updates

OPEN ACCESS

EDITED BY
Tianlun Zhao,
Zhejiang University, China

REVIEWED BY
Syed Tahir Ata-Ul-Karim,
The University of Tokyo, Japan
Wenguang Wu,
China Academy of Chinese Medical Sciences, China
Da Li,
Zhejiang Academy of Agricultural Sciences, China

*CORRESPONDENCE
Chong Wu
WuchongSDIP@outlook.com

†These authors have contributed equally to this work

SPECIALTY SECTION
This article was submitted to Plant Abiotic Stress, a section of the journal Frontiers in Plant Science

RECEIVED 19 October 2022
ACCEPTED 09 November 2022
PUBLISHED 24 November 2022

CITATION
Jiang L, Sun T, Wang X, Zong X and Wu C (2022) Functional physiological phenotyping and transcriptome analysis provide new insight into strawberry growth and water consumption.
Front. Plant Sci. 13:1074132.
doi: 10.3389/fpls.2022.1074132

COPYRIGHT
© 2022 Jiang, Sun, Wang, Zong and Wu. This is an open-access article distributed under the terms of the Creative Commons Attribution License (CC BY). The use, distribution or reproduction in other forums is permitted, provided the original author(s) and the copyright owner(s) are credited and that the original publication in this journal is cited, in accordance with accepted academic practice. No use, distribution or reproduction is permitted which does not comply with these terms.

Functional physiological phenotyping and transcriptome analysis provide new insight into strawberry growth and water consumption

Lili Jiang[1†], Ting Sun[2†], Xiaofang Wang[1], Xiaojuan Zong[1] and Chong Wu[1*]

[1]Shandong Institute of Pomology, Taian, Shandong, China, [2]Key Laboratory of Specialty Agri-product Quality and Hazard Controlling Technology of Zhejiang Province, College of Life Sciences, China Jiliang University, Hangzhou, China

Global warming is expected to increase agricultural water scarcity; thus, optimized irrigation schedules are important and timely for sustainable crop production. Deficit irrigation, which balances crop growth and water consumption, has been proposed, but the critical threshold is not easily quantified. Here, we conducted experiments on strawberry plants subjecting progressive drought following various water recovery treatments on the high-throughput physiological phenotyping system "Plantarray". The critical soil water contents (θ_{cri}), below which the plant transpiration significantly decreased, were calculated from the inflection point of the transpiration rate (Tr) - volumetric soil water content (VWC) curve fitted by a piecewise function. The physiological traits of water relations were compared between the well-watered plants (CK), plants subjecting the treatment of rewatering at the point of θ_{cri} following progressive drought (WR_θ_{cri}), and the plants subjecting the treatment of rewatering at severe drought following progressive drought (WR_SD). The results showed that midday Tr, daily transpiration (E), and biomass gain of the plants under WR_θ_{cri} treatment were equivalent to CK during the whole course of the experiment, but those under WR_SD treatment were significantly lower than CK during the water stress phase that could not recover even after rehydration. To explore the gene regulatory mechanisms, transcriptome analysis of the samples collected 12 h before, 12 h post and 36 h post water recovery in the three treatments was conducted. GO and KEGG enrichment analyses for the differentially expressed genes indicated that genes involved in mineral absorption and flavonoid biosynthesis were among the most striking transcriptionally reversible genes under the WR_θ_{cri} treatment. Functional physiological phenotyping and transcriptome data provide new insight into a potential, quantitative, and balanceable water-saving strategy for strawberry irrigation and other agricultural crops.

KEYWORDS

strawberry, irrigation, critical soil water content, balance, growth, phenotyping

1 Introduction

Human-induced global warming is presently increasing, which increases the odds of worsening drought (Falkland and White, 2020). The total land area subject to drought will increase, and agricultural droughts will become more frequent and severe due to the increasing evapotranspiration associated with enhanced temperature, decreased relative humidity and increasing net radiation under global warming (IPCC, 2021). In the summer of recent years, La Niña typically leads to warm temperatures and accompanying drought across the Northern Hemisphere, which increases the likelihood of severe impacts on agriculture and ecosystems (Cates et al., 2022). Agricultural water use for irrigation accounts for 70% of the total water consumption worldwide, followed by industrial and municipal use (Chen et al., 2018); therefore, optimizing agricultural water use is of great significance for alleviating water scarcity.

Strawberry (*Fragaria* × *annanasa* Duch.) is one of the most economically important horticultural crops in the world. Shallow rooting systems, high leaf area and large fruit result in strawberry being a water-intensive crop (Ali Sarıdaş et al., 2021). Consumptive water use of strawberry has been reported to be between ~300 and ~800 mm (Lozano et al., 2016). As a protected cultivation fruit, strawberry is generally grown under plastic tunnels during the entire season (Galati et al., 2020); thus, intensive use of water will significantly reduce planting costs and save water resources. To date, most irrigation scheduling is intuitive or qualitative, which generally leads to overirrigation (Kapur et al., 2018). The irrigation scheduling recommended by the FAO depends on the soil water balance with crop water demand, i.e., reference crop evapotranspiration (ET_c) calculated by the Penman–Monteith equation (Steduto et al., 2012). This approach was recently applied to strawberry in southern Spain, which saved water by ~40% (Gavilán et al., 2021). Nevertheless, prolonged soil saturation under water balance is not entirely satisfactory because of various root diseases and nutrient leaching (Villa et al., 2022). Deficit irrigation, an irrigation practice in which a crop is watered below full crop water demand, is reported to significantly increase fruit quality, such as sugars (Zarrouk et al., 2015), without compromising production (Mirás-Avalos et al., 2016; Permanhani et al., 2016). Rodríguez Pleguezuelo et al. (2018) set the deficit irrigation condition to 33%, 50%, and 75% of the ET_c and found that 50% deficit irrigation obtained the highest mango yield. Williams et al. (2009) studied the response of vines to different irrigation inputs between 20 and 140% of the ET_c in a California environment and found that maximum yields were achieved at 60–80% of the ET_c. In a case study of strawberry irrigation regimes in a Mediterranean environment, the maximum total berry yield was attained at 75% of the ET_c, while there was a significant decrease at 50% and no benefit at 100% and 125% of the ET_c (Kapur et al., 2018). Deficit irrigation is reported as an effective technology to improve water use efficiency and reduce water waste on the premise of maintaining the quality of agricultural products, especially in the horticultural crops represented by fruits and vegetables (Yang et al., 2022); however, by far, the threshold of water deficit balancing plant growth and water saving is still expertise-based when scheduling water application.

With the rapid development of phenomics in recent years, functional physiological traits, such as diurnal transpiration (Tr), could be nondestructively monitored with a high-throughput method (Halperin et al., 2017; Li et al., 2020; Gosa et al., 2022). Plant water use behavior is then detected *via* the dynamic response of transpiration to a progressively decreasing soil water content (SWC) (Vadez et al., 2014; Halperin et al., 2017). It has widely been observed that there was no significant difference in whole-plant transpiration rates during the initial days of irrigation reduction, and stomatal conductance (g_s) is limited and transpiration significantly decreased only under lower SWCs (Halperin et al., 2017; Luo et al., 2022). The response curves of transpiration against water stress are generally described as a piecewise function in crop models (e.g., AquaCrop) or physiological studies of water response (Steduto et al., 2012; Vadez et al., 2014), where Tr decreased linearly after SWC exceeded a critical threshold (θ_{cri}). θ_{cri} is a genotype-dependent parameter that indicates conservative and profligate water use strategies for drought tolerance (Casadebaig et al., 2008; Luo et al., 2022). Based on high-throughput lysimeter systems, genotypic differences in θ_{cri} in different populations have been detected and used for genome-wide association studies (GWAS) (Xu et al., 2015; Wu et al., 2021). Water deficit reaches a tipping point, below which crop growth will be significantly influenced by stomatal closure; hence, genotype-dependent θ_{cri} could be a quantifiable threshold for deficit irrigation. Nevertheless, to date, θ_{cri} has rarely been applied to irrigation practices as a threshold. To test this hypothesis, we conducted progressive drought experiments with three genotypes of strawberry, which has different drought tolerances. The physiological parameters obtained by the high-throughput physiological phenotypic platform were compared for two sets of progressive drought experiments where water recovery was conducted at θ_{cri} and severe water deficit. RNA-seq experiments were also conducted before and after water recovery to gain insights into the gene regulatory profiles under the respective conditions, and thus underlying mechanism governing the association between soil water content on growth and water consumption of strawberry will be revealed. Our study provided a potential, quantitative, and balanceable water-saving strategy for strawberry irrigation and other agricultural crops.

2 Materials and methods

2.1 Plant materials, cultivation and management

Three varieties of strawberry, i.e., Xiangye, Hongyan, and ZhangJi, introduced from Japan and widely cultivated in China were used in this study, which differ in drought-tolerance according to the preliminary screening by field survey. The experiments were carried out in a semi-controlled greenhouse (L×W×H: 10 m×5 m×4 m) in January and April of 2022 in Huai'an (119°01′E, 33°35′N), Jiangsu Province, China. One seedling at the four-leaf stage was transplanted per pot (upper diameter 16 cm, lower diameter 13 cm, height 18 cm, 1.5 L in total) with profile porous ceramic substrate (PPC, diameter: 0.2 mm, pH: 5.5 ± 1, porosity: 74, and CEC: 33.6 mEq/100 g). Seven replicates (three for destructive sampling) for each genotype were set in a completely randomized design on the high-throughput physiological phenotyping platform, also known as 'Plantarray' (Figure 1A, Plant-Ditech, Israel, Halperin et al., 2017). Water and nutrient supplements (Yamazaki nutrient solution) were controlled by the automatic irrigation system of "Plantarray" (Xu et al., 2015).

2.2 Experimental design

As shown in Figure 1B, the irrigation regimes were scheduled as sufficient irrigation across the whole period (CK), water recovery following progressive drought at the critical threshold (θ_{cri}) when Tr starts to reduce significantly (WR_θ_{cri}), and water recovery following progressive drought at severe drought (WR_SD), where the wilting leaves were observed. Experiments of WR_θ_{cri} and WR_SD included three phases, i.e., sufficient irrigation, progressive drought and water recovery. The water supply of the WR_SD treatment was stopped 5 days earlier than WR_θ_{cri} (according to the preliminary experiment) to guarantee the same day of water recovery; thus, the functional physiological traits of different treatments could be compared under the same environmental conditions. At the sufficient irrigation and water recovery phases, nutrient solution was provided by irrigation for 240 seconds (oversaturated) at 0:00, 1:00, 2:00, and 3:00 hours, and no nutrient solution was supplied during the progressive drought phase.

2.3 Meteorological and functional physiological parameter acquisition

Air temperature (T_{air}, °C) and relative humidity (RH, %), photosynthetically active radiation (PAR, $\mu molm^{-2}\ s^{-1}$) above the canopy, and soil volumetric water content (VWC, $m^3\ m^{-3}$) in each pot were measured by the VP-4 sensor (Decagon Devices, Pullman, Wash, USA), 5TM sensor (Decagon Devices, Pullman, Wash, USA) and PYR solar radiation sensor (Decagon Devices, Pullman, Wash, USA), respectively. Diurnal

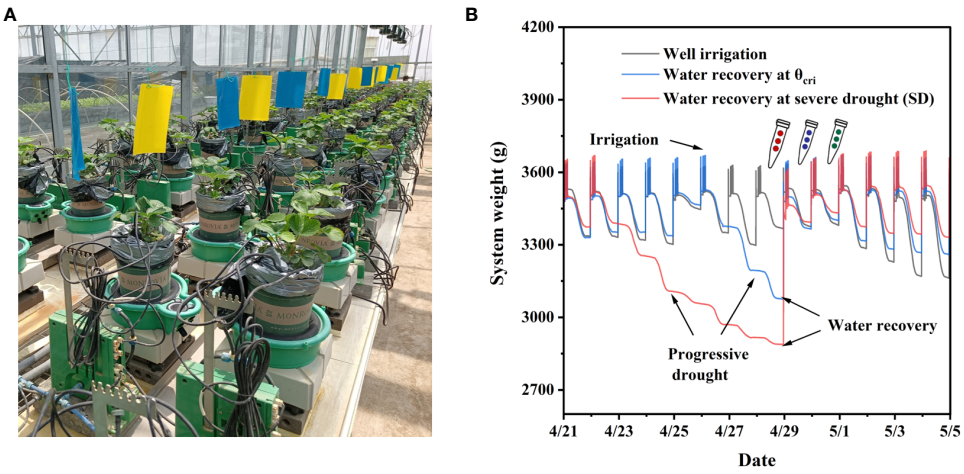


FIGURE 1
Strawberry experiments conducted with the high-throughput phenotyping platform "Plantarray". **(A)**, Overview of the automated physiological phenotyping array loaded with strawberry seedlings. **(B)**, System weights that were recorded every 3 minutes during the experimental course. Three irrigation regimes are scheduling as well irrigation across the whole period (CK), water recovery at the critical threshold (θ_{cri}) when Tr starts to reduce significantly (WR_θ_{cri}), and water recovery at severe drought (WR_SD). The WR_θ_{cri} and WR_SD experiments were divided into the well-irrigated, progressive drought, and water recovery phases.

variations in T_{air}, RH and PAR during the spring growth season are exhibited in Figure 2. The vapor pressure deficit (VPD, kPa) was calculated according to Halperin et al. (2017).

The physiological parameters for plant water relations were obtained from the "Plantarray" system. This system provides a simultaneous measurement and detailed physiological response profile for plants in each pot in the array over time periods ranging from a few minutes to the entire growing season under normal, stress and recovery conditions and at any phenological stage (Li et al., 2020). The whole-plant transpiration rates (Tr, g min^{-1}), daily whole-plant transpiration (E, g d^{-1}), and daily fresh plant growth (PG, g d^{-1}, only under overirrigated conditions) were calculated using the SPAC software implemented in the "Plantarray" system according to the continuously monitored system weight. Briefly, Tr was computed by multiplying the first derivative of the measured system weight by -1. E was calculated by the difference in the measured system weight at predawn (averaged between 4:00 and 4:30) and that at evening (averaged between 19:00 and 19:30). During the well irrigation phase, the PG was calculated as the difference in the predawn system weights on two adjacent days. Difference between measurement data were compared through analysis of variance and that between groups with Q test.

2.4 Critical soil water content (θ_{cri}) determined by the dynamic water response curve

Daily whole-plant midday transpiration (Tr_m, averaged over the period between 12:00 and 14:00) was fitted to a two-piecewise linear function of the corresponding soil volumetric water content (VWC) during the dynamic period of water deficit, which was described in our previous study (Wu et al., 2021). To offset the influence of daily environmental variation, Tr_m is normalized to VPD ($Tr_{m,VPD}$). The dynamic water response function is then determined using the following equation:

$$Tr_{m,VPD} = \begin{cases} a, & VWC \geq \theta_{cri} \\ a + k \times (VWC - \theta_{cri}), & VWC < \theta_{cri} \end{cases} \quad (1)$$

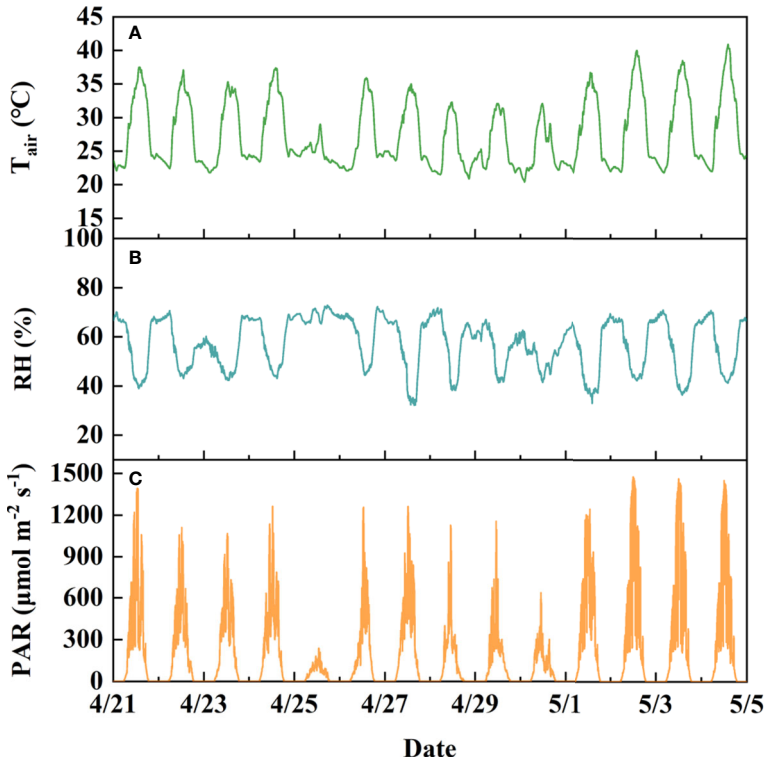


FIGURE 2
Parameters of the soil–plant–atmosphere continuum monitored by "Plantarray". **(A)**, air temperature (T_{air}, °C). **(B)**, Relative humidity (RH, %). **(C)**, Photosynthetic active radiation (PAR, μmol m^{-2} s^{-1}). The data shown in the graph were obtained from the spring-season experiment in 2022.

where θ_{cri} is the critical soil water content quantified by the VWC in this study, a is the maximum $Tr_{m,VPD}$, *k* is the decreasing slope of $Tr_{m,VPD}$ when VWC is below θ_{cri}.

2.5 Sampling and RNA isolation and RNA-seq

New fully expanded leaves of strawberry variety Xiangye of CK, WR_θ_{cri} and WR_SD treatments were sampled at approximately 12:00 am the day before water recovery around the end of progressive drought (12 h before water recovery, i.e., CK 12 h-, WR_θ_{cri} 12 h-, WR_SD 12 h-), the day of water recovery (12 h after water recovery, i.e., CK 12 h+, WR_θ_{cri} 12 h+, WR_SD 12 h+), and the day after water recovery (36 h after water recovery, i.e., CK 36 h+, WR_θ_{cri} 36 h+, WR_SD 36 h+), respectively. Three biological replicates (pots) were set for each treatment. Total RNA was extracted using TRIzol reagent (Invitrogen, Carlsbad, CA). Five micrograms of total RNA from each sample was used to construct an RNA-Seq library by using the TruSeq RNA Sample Preparation Kit according to the manufacturer's instructions (Illumina, San Diego, CA). A total of 27 libraries were constructed and then sequenced on the Novaseq 6000 platform. The accession number for the sequence data is PRJNA891140 (https://www.ncbi.nlm.nih.gov/search/all/?term=PRJNA891140).

2.6 Raw data processing, pairwise differential expression analysis and functional analysis

The raw reads were filtered and trimmed using SeqPrep (https://github.com/jstjohn/SeqPrep) and Sickle (https://github.com/najoshi/sickle) with default parameters. The clean reads were combined and aligned to the strawberry reference genomes (https://www.rosaceae.org/Analysis/9642085). The count of the mapped reads from each sample was derived and normalized to fragments per kilobase of transcript length per million mapped reads (FPKM) for each predicted transcript using Cufflinks (v2.2.1).

Pairwise comparisons were made between samples collected at the same timepoint and different phases. To reduce noise and false results, only genes having an FPKM ≥ 1 in at least 3 of the 6 samples of a comparison (3 replicates each sample) and a coefficient of variation (CV)< 0.2 in the 3 replicates were considered. The genes exhibiting a difference of at least twofold change with the corrected *P* value after adjusting with false discovery rate (FDR) ≤ 0.05 were considered significantly differentially expressed.

Gene functional categories (GO enrichments) were analyzed using AgriGO V2.0 (Tian et al., 2017) under a *q*-value threshold of 0.01 for statistical significance. Unigenes were annotated to corresponding KEGG gene/KEGG ortholog descriptions and their associated pathways using the KEGG Automatic Annotation Server (KAAS, http://www.genome.jp/tools/kaas/) (Moriya et al., 2007). The list of gene identifiers and log2FC values from each treatment were imported into MapMan software version 3.5.1R2 and assigned to functional categories using the strawberry mapping file obtained by Mercator 4.

3 Results

3.1 Dynamic patterns of Tr in response to soil water contents decline

The midday Tr normalized to VPD ($Tr_{m,VPD}$) and soil VWC averaged between 12:00 and 14:00 were well fitted with a

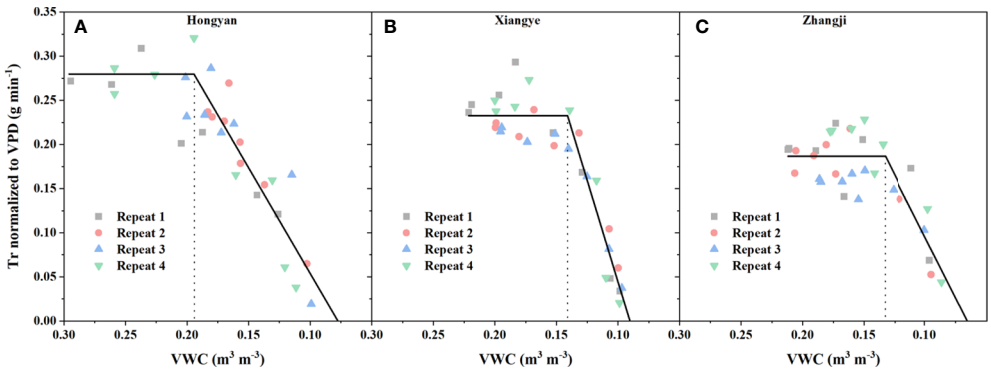


FIGURE 3
Midday Tr normalized to VPD ($Tr_{m,VPD}$) against soil water content (VWC) for different strawberry varieties. The $Tr_{m,VPD}$ and VWC data were both averaged between 12:00 and 14:00 and then fitted with a piecewise function (Eq. 1). The inflection point of the fitting curve was determined as the critical soil water content, i.e., θ_{cri}, below which $Tr_{m,VPD}$ decreased linearly. Three strawberry varieties, i.e., Hongyan **(A)**, Xiangye **(B)** and Zhangji **(C)**, were used in the experiment.

piecewise function (Figure 3, R^2 ranged from 0.82 to 0.91 for the dataset obtained from spring season). The transpiration variation caused by environmental fluctuations, as shown in Figure 2, was largely smoothed by dividing by VPD, where $Tr_{m,VPD}$ remained relatively stable when there was no severe water deficit (Figure 3). The inflection point of the fitting curve was determined as the critical soil water content, i.e., θ_{cri} in Eq. 1, below which $Tr_{m,VPD}$ decreased linearly. θ_{cri}, which represents the sensitivity of stomatal closure (Halperin et al., 2017), varied within different varieties of strawberry. The θ_{cri} of Hongyan was highest (0.1944 ± 0.0087, Figure 3A), followed by Xiangye (0.1410 ± 0.0031, Figure 3B), and Zhangji (0.1327 ± 0.0087, Figure 3C), indicating that within the three strawberry varieties, Hongyan was most sensitive to water deficit and reduced Tr the earliest to survive under drought. In addition, the descending slope, i.e., k in Eq. 1 also differed within varieties, where Xiangye (4.6011 ± 0.4396, Figure 3B) was significantly different from the other two (Hongyan: 2.3915 ± 0.3178, Figure 3C; Zhangji: 2.7851 ± 0.7534, Figure 3A), suggesting a faster process of stomatal closure. There was no significant difference between θ_{cri} of a particular variety obtained from the winter season and spring season, but there was little difference for k. That is, $\theta_{cri}$is a relatively conservative, genotype-independent parameter that characterizes the dynamic pattern of Tr in response to the soil water content.

3.2 Physiological traits before and after water recovery

The midday Tr (Tr_m) and daily transpiration (E) of treatments with three irrigation schedules, i.e., well irrigation (CK), water recovery at θ_{cri} (WR_θ_{cri}), and water recovery under severe drought (WR_SD), were compared, as shown in Figure 4 for Hongyan, Xiangye, and Zhangji. There was no significant difference in Tr_m or E during the period before progressive drought treatment within all three varieties (Figure 4). With the experiment, WR_θ_{cri} was close to or slightly slower than CK (no significant difference in two-way ANOVA), where Tr_m and E were both reduced by ~6% averaged for three varieties across the progressive drought phase (blue line in shaded area of Figure 4). However, the Tr_m and E of WR_SD both decreased significantly compared to CK ($P<0.01$), by ~37% and ~35%, respectively (red line in shaded area of Figure 4). Within the three varieties, the Tr_m of Hongyan, which is highly sensitive to water deficit according to θ_{cri}, decreased the most during the progressive

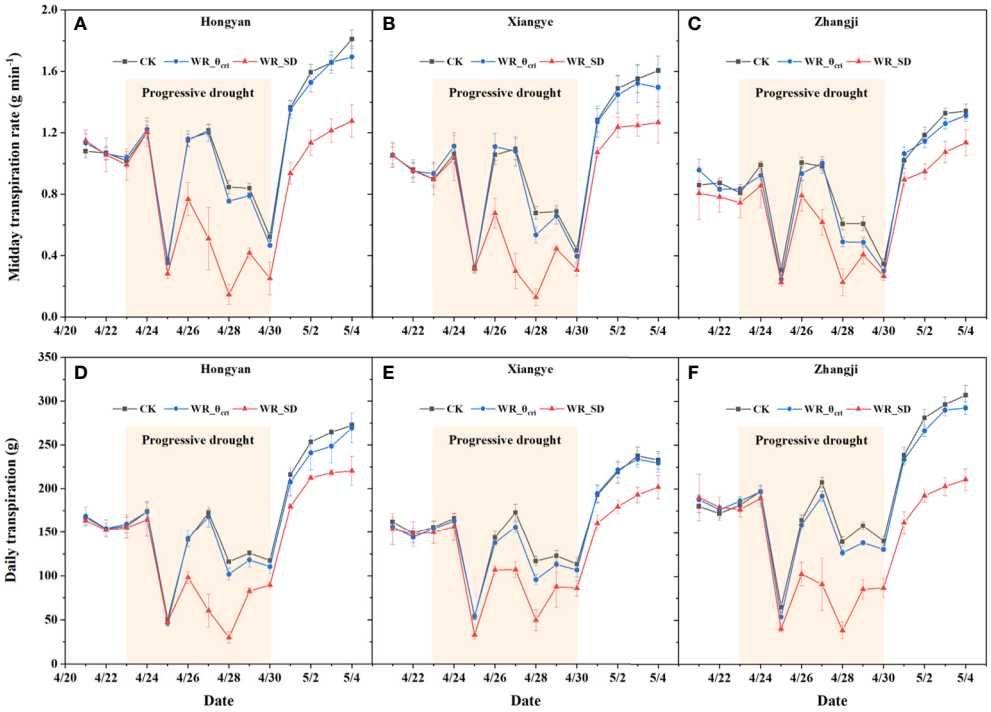


FIGURE 4
Midday transpiration rate (Tr_m) and daily transpiration (E) of different treatments during the spring season for strawberry varieties. Three treatments, i.e., well irrigation across the whole period (CK), water recovery at the critical threshold (θ_{cri}) when Tr started to reduce significantly (WR_θ_{cri}), and water recovery under severe drought (WR_SD), are shown in the graph. Three strawberry varieties, i.e., Hongyan **(A, D)**, Xiangye **(B, E)** and Zhangji **(C, F)**, were used in the experiment.

10.3389/fpls.2022.1074132

TABLE 1 Daily Plant growth and WUE during the period after water recovery.

Variety		Xiangye			Hongyan			Zhangji		
Treatment		CK	WR_θ_{cri}	WR_SD	CK	WR_θ_{cri}	WR_SD	CK	WR_θ_{cri}	WR_SD
Plant growth (g)	4/30	5.47 ± 0.58	5.22 ± 0.35	4.16 ± 0.39	5.91 ± 0.35	5.68 ± 0.17	3.99 ± 0.81	5.6 ± 0.38	4.51 ± 0.34	4.15 ± 0.74
	5/1	9.36 ± 0.97	9.56 ± 1.08	7.94 ± 0.89	10.99 ± 0.68	10.13 ± 0.81	7.14 ± 0.85	8.24 ± 0.58	9.16 ± 0.44	7.04 ± 0.97
	5/2	11.33 ± 1.14	11.1 ± 1.22	9.61 ± 0.29	13.2 ± 0.92	12.95 ± 0.91	7.88 ± 0.6	9.95 ± 0.88	10.6 ± 0.5	8.36 ± 1.87
	5/3	11.89 ± 1.04	10.9 ± 1.13	9.88 ± 1.02	13.02 ± 0.84	13.35 ± 0.13	9.18 ± 1.13	11.21 ± 0.65	11.5 ± 0.27	8.18 ± 0.79
	5/4	11.89 ± 1.08	12.05 ± 0.83	9.39 ± 0.83	13.3 ± 0.41	13.07 ± 0.64	9.81 ± 1.35	10.53 ± 0.74	10.98 ± 0.43	8.41 ± 1.55
WUE (g g-1)	5 day	0.044 ± 0.003	0.045 ± 0.003	0.044 ± 0.001	0.045 ± 0.004	0.044 ± 0.001	0.044 ± 0.002	0.045 ± 0.002	0.048 ± 0.003	0.043 ± 0.001

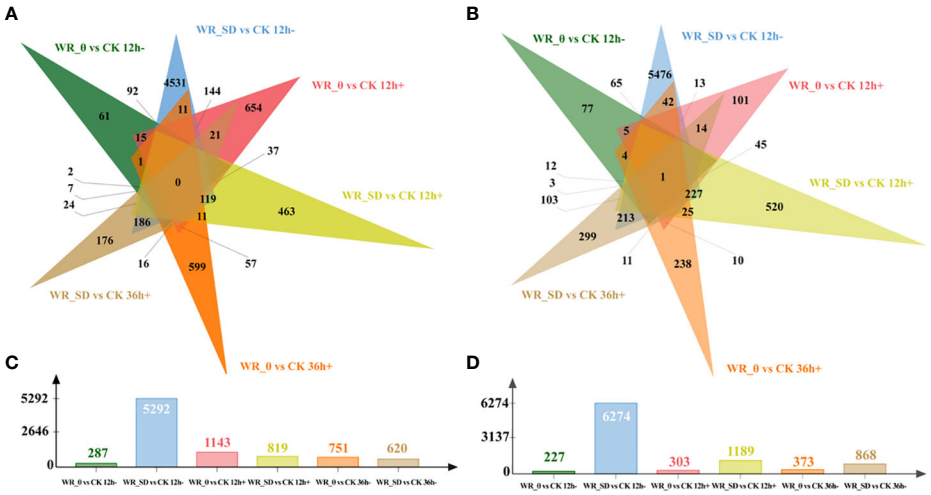


FIGURE 5
Overview of DEGs before and after water recovery. a-b, Venn diagrams for upregulated **(A)** and downregulated **(B)** DEGs of pairwise comparisons within the entire WR_θ_{cri} vs. CK set and WR_SD vs. CK. c-d, Number of upregulated **(C)** and downregulated **(D)** DEGs of pairwise comparisons within the entire WR_θ_{cri} vs. CK set and WR_SD vs. CK. "CK 12 h-, WR_θ_{cri} 12 h-, WR_SD 12 h-", "CK 12 h+, WR_θ_{cri} 12 h+, WR_SD 12 h+", and "CK 36 h+, WR_θ_{cri} 36 h+, WR_SD 36 h+" indicate samples obtained at 12 h before, 12 h after and 36 h after water recovery in the CK, WR_θ_{cri}, and WR_SD treatments, respectively.

drought period in the WR_SD treatment (~42%, Figure 4A), followed by Xiangye (~37%, Figure 4B) and Zhangji (~31%, Figure 4C), but was different for E (Zhangji: reduced by ~41%, Figure 4D; Hongyan: reduced by ~34%, Figure 4E; Xiangye: reduced by ~31%, Figure 4F). After water recovery, the Tr_m and E of WR_θ_{cri} recovered rapidly to levels similar to those of CK, where Tr_m and E only decreased by ~2% averaged for the three varieties across the water recovery phase (Figure 4). In accordance with Tr_m and E during the progressive drought phase, the recovery of Tr_m was poorest for Hongyan (reduced by ~29%, Figure 4A), followed by Xiangye (~18%, Figure 4B) and Zhangji (~16%, Figure 4C), while there was the largest gap between the E values of WR_SD and CK for Zhangji (reduced by ~32%, Figure 4F), followed by Hongyan (~17%, Figure 4D) and Xiangye (~16%, Figure 4E).

Daily plant growth (fresh weight, g) was also detected nondestructively by the "Plantarray" system during the water recovery phase, and water use efficiency (WUE) during the 5-day window after water recovery was also calculated by accumulated plant growth and E. The daily plant growth of WR_SD during the water recovery phase was significantly lower than WR_θ_{cri} and CK in all three varieties, mainly due to the daily

transpiration, as there was no significant difference in WUE either between varieties or treatment (Table 1).

3.3 Overview of differentially expressed genes before and after water recovery

Physiological traits before and after water recovery indicated that there is an essential difference for strawberry growth between WR_θ_{cri} and WR_SD. To gain insights into the gene regulatory profiles under the respective conditions, gene expressions 12 h before (end of progressive drought, 12 h-), 12 h after (12 h+), and 36 h after (36 h+) water recovery in the WR_θ_{cri} and WR_SD treatments were compared with CK based on RNA-Seq data. An overview of pairwise comparisons is shown in Figure 5. The number of both upregulated and downregulated DEGs of WR_SD at 12 h before water recovery compared to CK (WR_SD vs. CK 12 h-) were greatest, while the opposite was true for WR_θ vs. CK 12 h-.

3.4 Functional analysis of DEGs identified from different comparisons

3.4.1 Gene ontology enrichment analysis

We performed GO enrichment analysis on the entire set of DEGs upregulated and downregulated by WR_θ and WR_SD compared to CK at different time points (12 h-, 12 h+ and 36 h +). The top 30 enriched GO terms were selected from each set (FDR<0.05, Figure 6). Interestingly, over two-thirds of the top 30 GO terms related to iron homeostasis and transport were enriched in upregulated DEGs of WR_θ vs. CK 12 h- (Figure 6A). After water recovery, the abovementioned GO terms were enriched in the upregulated DEGs of WR_θ vs. CK 12 h+ but not significantly enriched in WR_θ vs. CK 36 h+, except for the molecular functions 'heme binding', 'iron ion binding', 'metal ion binding', 'cation binding', and 'transition metal ion binding' (Figure 6A). In addition, GO enrichment analysis of upregulated DEGs of WR_θ vs. CK 12 h- showed enrichment for the biological processes 'phloem development', 'phloem or xylem histogenesis', and 'tissue development' but could not be retrieved for that of WR_θ vs. CK 12 h+ or WR_θ vs. CK 36 h+ (Figure 6A).

Stimulus response-related GO terms (e.g., biological processes 'response to auxin', 'response to hormone', 'response to endogenous stimulus', 'response to organic substance', 'response to chemical', and 'response to stimulus'; molecular functions 'receptor regulator activity', 'receptor ligand activity', 'signaling receptor activator activity', and 'signaling receptor binding') and cell growth-related GO terms (e.g., biological processes 'cell wall organization or biogenesis'; molecular functions 'growth factor activity'; and cellular component 'intracellular membrane-bounded organelle' and 'nucleus') were enriched in downregulated DEGs of WR_θ vs. CK 12 h- but not significantly in WR_θ vs. CK 12 h+ and WR_θ vs. CK 36 h+ (Figure 6B). In contrast, cell wall-related GO terms (e.g., biological processes 'xyloglucan metabolic process', 'cell wall biogenesis', 'cell wall polysaccharide metabolic process', 'cellular component biogenesis; molecular functions 'xyloglucan: xyloglucosyl transferase activity'; and cellular component 'external encapsulating structure', and 'cell wall') were specific for downregulated DEGs of WR_θ vs. CK 36 h+ (Figure 6B).

The top 30 GO terms enriched in upregulated DEGs of WR_SD vs. CK 12 h- and WR_SD vs. CK 12 h+ were relevant to reactive oxygen species, e.g., biological processes 'regulation of removal of superoxide radicals', 'positive regulation of response to oxidative stress', 'regulation of reactive oxygen species metabolic process', 'positive regulation of cellular response to oxidative stress', 'positive regulation of oxidoreductase activity', 'regulation of superoxide metabolic process', 'positive regulation

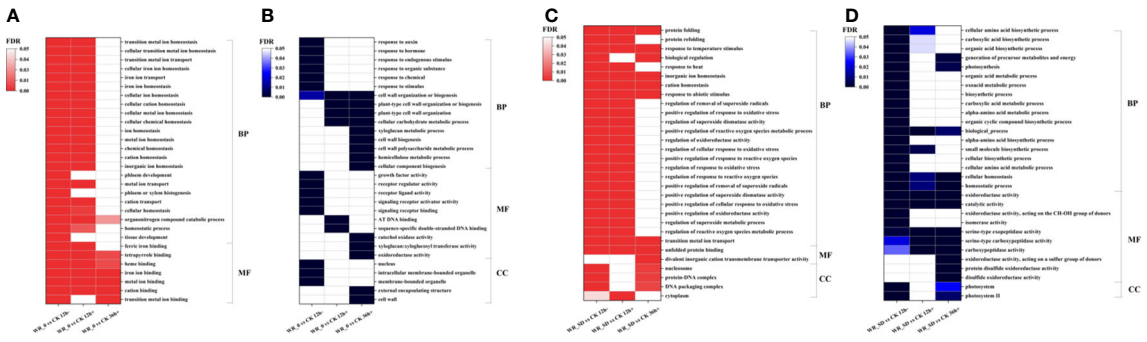


FIGURE 6
GO terms enriched in DEGs of pairwise comparisons within the entire WR_θ_{cri} vs. CK set and WR_SD vs. CK set. **(A)**, GO terms enriched in upregulated DEGs within the WR_θ_{cri} vs. CK set. **(B)**, GO terms enriched in downregulated DEGs within the WR_θ_{cri} vs. CK set. **(C)**, GO terms enriched in upregulated DEGs within the WR_SD vs. CK set. **(D)**, GO terms enriched in downregulated DEGs within the WR_SD vs. CK set. The top 30 significant (P<0.01) GO terms are shown in the graph, and the FDR value of each item was used to draw a heatmap.

of response to reactive oxygen species', 'regulation of cellular response to oxidative stress', 'positive regulation of reactive oxygen species metabolic process', 'regulation of response to oxidative stress', 'regulation of response to reactive oxygen species', 'positive regulation of superoxide dismutase activity', 'regulation of oxidoreductase activity', and 'positive regulation of removal of superoxide radicals' (Figure 6C). These GO terms could not be retrieved for the upregulated DEGs of WR_SD vs. CK 36 h+ (Figure 6C). Furthermore, the iron transport-related biological processes 'inorganic ion homeostasis', 'cation homeostasis', and 'transition metal ion transport' were always enriched in upregulated DEGs of samples of all time points within the WR_SD vs. CK set (Figure 6C).

Many biological processes related to carbohydrate and amino acid metabolism, such as 'organic acid metabolic process', 'oxoacid metabolic process', 'biosynthetic process', 'carboxylic acid metabolic process', 'alpha-amino acid metabolic process', 'organic cyclic compound biosynthetic process', 'alpha-amino acid biosynthetic process', 'cellular biosynthetic process', and 'cellular amino acid metabolic process', were enriched in downregulated DEGs of WR_SD vs. CK 12 h- and recovered in WR_SD vs. CK 12 h+ and WR_SD vs. CK 36 h+ (Figure 6D). However, biological progress 'cellular homeostasis', 'homeostatic process', and molecular functions 'oxidoreductase activity', 'catalytic activity', 'serine-type exopeptidase activity', 'serine-type carboxypeptidase activity', 'carboxypeptidase activity' were always enriched in downregulated DEGs of samples of all time points within the WR_SD vs. CK set (Figure 6D). Some photosynthesis-related GO terms were enriched in the downregulated DEGs of WR_SD vs. CK 12 h- and recovered in WR_SD vs. CK 12 h+; however, they still exhibited enrichment in WR_SD vs. CK 36 h + (Figure 6D).

3.4.2 KEGG pathway enrichment analysis

To understand the metabolic or signaling pathways involved in the response to drought and water recovery, we mapped upregulated and downregulated DEGs to the Kyoto Encyclopedia of Genes and Genomes (KEGG) database to retrieve the pathways involved in each comparison. In total, 21 and 1 significantly (FDR<0.05) enriched pathways were identified for all upregulated and downregulated DEGs in the WR_θ vs. CK set, respectively (Figure 7). Upregulated DEGs of WR_θ vs. CK 12 h- were involved in mineral absorption, flavonoid biosynthesis, ferroptosis, necroptosis, ubiquinone and other terpenoid-quinone biosynthesis, and linoleic acid metabolism. After water recovery, necroptosis, ubiquinone and other terpenoid-quinone biosynthesis were no longer significantly enriched in WR_θ vs. CK 12 h+, while in WR_θ vs. CK 36 h+, mineral absorption, ferroptosis, and linoleic acid metabolism were no longer enriched (Figure 7A). Cutin, suberine and wax biosynthesis; flavone and flavonol biosynthesis; fatty acid biosynthesis; and peroxisome biosynthesis were only enriched in WR_θ vs. CK 36 h+. Downregulated DEGs were enriched only in the KEGG pathway of isoquinoline alkaloid biosynthesis in WR_θ vs. CK 36 h+ (Figure 7B).

Most upregulated DEGs were significantly enriched in WR_SD vs. CK 12 h- but no longer significant in WR_SD vs. CK 12 h+ and WR_SD vs. CK 36 h+, e.g., spliceosome, protein processing in endoplasmic reticulum, plant hormone signal transduction, ubiquitin-mediated proteolysis, mTOR signaling pathway, and terpenoid backbone biosynthesis (Figure 7C). Notably, mineral absorption, necroptosis, and ferroptosis were all enriched in the WR_SD vs. CK set. Moreover, chlorocyclohexane and chlorobenzene degradation, fluorobenzoate degradation, toluene degradation, and

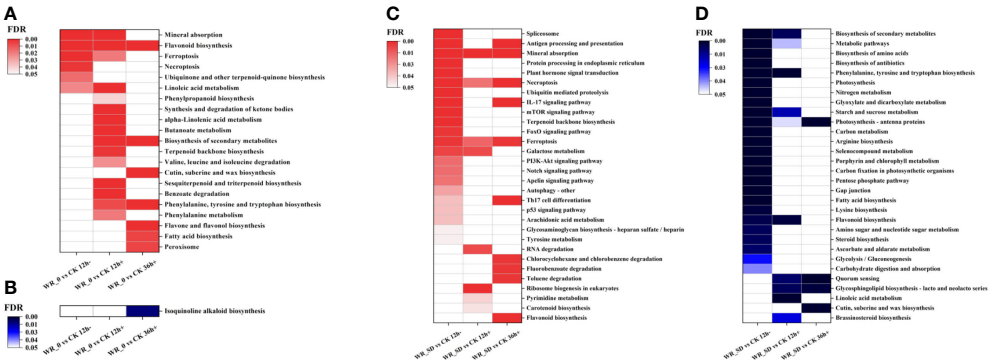


FIGURE 7
KEGG pathways enriched in DEGs of pairwise comparisons within the entire WR_θ_{cri} vs. CK set and WR_SD vs. CK set. **(A)**, KEGG pathways enriched in upregulated DEGs within the WR_θ_{cri} vs. CK set. **(B)**, KEGG pathways enriched in downregulated DEGs within the WR_θ_{cri} vs. CK set. **(C)**, KEGG pathways enriched in upregulated DEGs within the WR_SD vs. CK set. **(D)**, KEGG pathways enriched in downregulated DEGs within the WR_SD vs. CK set. The top 30 significant (P<0.01) KEGG pathways are shown in the graph, and the FDR value of each item was used to draw a heatmap.

flavonoid biosynthesis were enriched only in WR_SD vs. CK36 h + (Figure 7C).

Similarly, most downregulated DEGs were enriched only in WR_SD vs. CK 12 h-, which are nitrogen- or carbon-related pathways, e.g., 'biosynthesis of amino acids', 'photosynthesis', 'nitrogen metabolism', 'carbon metabolism', 'arginine biosynthesis', 'carbon fixation in photosynthetic organisms', 'pentose phosphate pathway', 'lysine biosynthesis', 'amino sugar and nucleotide sugar metabolism', 'glycolysis/gluconeogenesis', and 'carbohydrate digestion and absorption' (Figure 7D). Some secondary metabolism pathways were significant in WR_SD vs. CK 12 h- and WR_SD vs. CK 12 h+, such as 'flavonoid biosynthesis'. Moreover, 'cutin, suberine and wax biosynthesis' was only enriched in WR_SD vs. CK 36 h + (Figure 7D).

3.4.3 DEG visualization for metabolism pathway

We then visualized DEGs enriched in metabolic pathways using MapMan, and the metabolism overview of different comparisons is shown in Figure 8. For DEGs of the WR_θ vs. CK set, we focused on the transition metal homeostasis and terpenoids category, where large numbers of DEGs were significantly enriched. DEGs related to negative regulators of iron deficiency responses 'HRZs/BTS', bHLH-Ib-class transcriptional regulator, and metal cation transporter 'NRAMP' were downregulated, while metallothionein 'MT', iron storage protein 'ferritin', ferric cation-chelator transporter 'YSL', and iron transporters 'VIT' were upregulated. In contrast, in WR_θ vs. CK 36 h+, DEGs related to metallothionein 'MT' were all significantly downregulated, and those of bHLH-Ib-class transcriptional regulators were upregulated. In the tetrapyrrole category, DEGs related to flavonoid biosynthesis, e.g., chalcone synthase (CHS), flavanone 3-hydroxylase (F3H), dihydroflavonol-4-reductase (DFR), anthocyanidin synthase (ANS), leucoanthocyanidin reductase (LAR), and CoA biosynthesis, e.g., cinnamate 4-hydroxylase (C4H), and 4-coumarate-CoA ligase (4CL), were upregulated in WR_θ vs. CK 12 h-. In WR_θ vs. CK 12 h+ and WR_θ vs. CK 36 h+, in addition to the above flavonoid biosynthesis- and CoA biosynthesis-related genes, upregulated DEGs related to the mevalonate pathway, terpene biosynthesis, and cycloartenol biosynthesis were observed.

For DEGs of the WR_θ vs. CK set, DEGs in the protein homeostasis, nitrogen assimilation, transition metal homeostasis, and terpenoid categories were considered. In WR_SD vs. CK 12 h-, genes in the protein homeostasis category were significantly regulated, as a large number of upregulated DEGs were enriched in ER quality control (ERQC) machinery (e.g., membrane-anchored lectin chaperone 'CNX', ER luminal lectin chaperone 'CRT'), mitochondrial Hsp70 chaperone system, Hsp90 chaperone system, Hsp60 chaperone system, N-degron pathways (e.g., GID ubiquitination complex), ubiquitin-fold protein conjugation (e.g., ubiquitin-conjugating enzyme), ATG8-phosphatidylethanolamine conjugation system, cysteine-type peptidase activities (e.g., subclass CTB cysteine protease, subclass SAG12 cysteine protease, subclass RD19 cysteine protease). However, in WR_SD vs. CK 12 h+ and WR_SD vs. CK 36 h+, DEGs enriched in the above pathway were significantly reduced. In the entire WR_SD vs. CK set, in addition to the aforementioned genes enriched in the transition metal homeostasis category of the WR_θ vs. CK set, genes related to the nitrate uptake system (e.g., nitrate transporter 'NRT1.1', 'NRT2', and 'NRT3', signaling factor 'NRG2', transcriptional repressor 'NIGT', signaling factor 'NRG2'), ammonium assimilation (e.g., cytosolic glutamine synthetase 'GLN1', glutamate dehydrogenase), sulfate uptake system (sulfate transporter 'SULTR1', sulfite oxidase, regulatory protein 'SDI'), and phosphate signaling

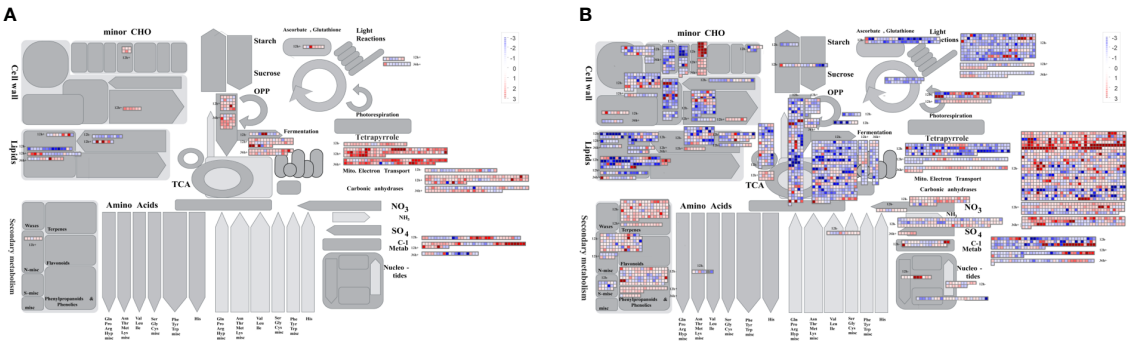


FIGURE 8
Visualization of DEGs of pairwise comparisons within the entire WR_θ_{cri} vs. CK set **(A)** and WR_SD vs. CK **(B)** set enriched in metabolism pathways. The list of gene identifiers and log2FC values from each treatment were imported into MapMan software version 3.5.1R2 and assigned to functional categories using the strawberry mapping file obtained by Mercator 4.

(transcription factor 'PHR1', regulatory protein 'SPX', phosphate transporter 'PHT1', 'PHO1') were enriched. In the terpenoid classification, DEGs of WR_SD vs. CK 12 h- and WR_SD vs. CK 12 h+ were enriched in the mevalonate pathway, methylerythritol phosphate (MEP) pathway, isoprenyl diphosphate biosynthesis, terpene biosynthesis, CoA biosynthesis, and flavonoid biosynthesis, which were mostly downregulated. Similar to WR_SD vs. CK 12 h-, in WR_SD vs. CK 36 h-, DEGs were enriched in the flavonoid biosynthesis pathway, and most of them were upregulated.

4 Discussion

4.1 The potential of θ_{cri} as the threshold for deficit irrigation

Previous studies have reported that water recovery under moderate drought will not reduce and even increase crop growth and yield, but the threshold of deficit irrigation is unclear or determined empirically according to different ratios of ETc (Williams et al., 2009; Kapur et al., 2018). Our study determined the inflection point (θ_{cri}) of the $Tr_{m,VPD}$-VWC curve fitted by a piecewise function as the critical soil water content under drought (Figure 3) and explored the potential of θ_{cri} as the threshold of deficit irrigation. Midday Tr, daily E before and after water recovery, and daily plant growth and WUE after water recovery obtained from the "Plantarray" phenotyping system indicated that there was no significant difference in physiological traits between water recovery at θ_{cri} (WR_θ_{cri}) and CK, but they were significantly reduced when water recovery occurred under severe drought except WUE (Figure 4, Table 1). In modeling studies, Tr/VPD is scaled to biomass accumulation (Steduto et al., 2012; Vadez et al., 2014); therefore, θ_{cri} also represents the threshold when water stress significantly affects biomass assimilation. GO and KEGG analyses also supported that photosynthesis-related processes and carbohydrate pathways were downregulated in the WR_SD vs. CK set but not significant in the WR_θ_{cri} vs. CK set (Figures 6, 7). Our study indicated that θ_{cri} was a genotype-independent parameter characterizing dynamic plant water use behavior. With the rapid development of phenomics, high-throughput screening of θ_{cri} has been realized with low cost, thus making it possible to make irrigation schedules individually according to the θ_{cri} of various varieties (Li et al., 2020). As no irrigation was applied during the progressive drought phase of WR_θ_{cri}, this method was obviously more water-saving than the ET_c methods depending on daily reference evapotranspiration.

4.2 Molecular mechanism underlying WR_θ_{cri} distinguished from WR_SD

GO terms and KEGG pathways both indicated that mineral absorption is a vital physiological process influenced by drought, not only in the WR_θ_{cri} vs. CK set but also in WR_SD vs. CK (Figures 6, 7). A series of DEGs visualized in the metabolism overview also included YSL, NRAMP and VIT, which are widely known as Fe transporters. Iron plays an irreplaceable role in alleviating the stress imposed by drought (Tripathi et al., 2018; Rai et al., 2021). Many studies have demonstrated that the application of Fe nutrition to plants under drought conditions enhances tolerance, yield and yield components (Di Caterina et al., 2007; Pourgholam et al., 2013; Mirjahanmardi and Ehsanzadeh, 2016). Recently, Xu et al. (2021) found that iron homeostasis is disrupted by drought stress in sorghum roots using time-series root RNA-Seq data and that loss of a plant phytosiderophore iron transporter impacts microbial community composition, leading to significant increases in the drought-enriched lineage Actinobacteria. Mineral absorption-related genes were upregulated in WR_θ_{cri} vs. CK 12 h- and WR_θ_{cri} vs. CK 12 h+, but entire WR_SD vs. CK set, suggesting that iron homeostasis was repaired in WR_θ_{cri} treatment 36 h after, while not recovered at severe drought treatment even 36 h after water recovery (Figure 7A, C). Moreover, necroptosis and ferroptosis, which are related to programmed cell death, were significantly enriched in upregulated DEGs of the entire WR_SD vs. CK set but were not retrieved after water recovery in WR_θ_{cri} treatment, indicating the reversible injury of WR_θ_{cri} treatment (Figure 7A, C). This is also why Tr and plant growth were not recovered in the WR_SD treatment (Figure 4, Table 1).

Drought stress triggering the biosynthesis of secondary metabolites has been widely reported (Yadava et al., 2019). Flavonoids are low-molecular-weight polyphenolic secondary metabolic compounds and play important roles in drought tolerance (Yadava et al., 2019). Ma et al. (2014) found that flavonoid pathway gene expression and the accumulation of flavonoid compounds were closely related to drought tolerance in wheat. Yang et al. (2020) found that *B. chinense* adapts to drought stress through physiological changes and the regulation of flavonoids in different plant tissues. Meng et al. (2021) demonstrated a role for the CcCIPK14-CcCBL1 complex in drought stress tolerance through the regulation of flavonoid biosynthesis in pigeon pea. Li et al. (2021) researched an overly insensitive drought mutant and indicated that flavonoids improve the drought tolerance of maize seedlings by regulating the homeostasis of reactive oxygen species. Flavonoids prevent stomatal closure by reducing the H_2O_2

level in guard cells and alleviate drought-induced ROS damage. Interestingly, our results indicated that DEGs related to flavonoid biosynthesis were upregulated in the entire WR_θ vs. CK set and WR_SD vs. CK 36 h+ but downregulated in WR_SD vs. CK 12 h- and WR_SD vs. CK 12 h+. Although it is more common for genes enriched in flavonoid biosynthesis to be upregulated under drought, key enzyme genes in flavonoid biosynthesis, e.g., F3H, 4CL, IFS, and DFR, have also been observed to be downregulated under severe drought (Gu et al., 2020; Yang et al., 2020). We hypothesize that moderate drought triggers flavonoid biosynthesis to defend against the negative effects of water stress but is inhibited under severe drought until 36 h after water recovery. Shojaie et al. (2016) observed that the total flavonoid concentrations in roots and shoots both reached their highest levels under mild drought stress (Ψw = −0.5 MPa) at the end of the drought experiment, while that of severe drought (Ψw = −0.9 MPa) significantly dropped after it peaked in the early stage, which is in accordance with our results.

5 Conclusion

The critical soil water content (θ_{cri}) was obtained as the inflection point of the $Tr_{m,VPD}$-VWC curve fitted by a piecewise function, depending on the high-throughput physiological phenotyping system. θ_{cri}, below which Tr significantly decreased, highly dependent on the varieties of strawberry. The physiological traits of water relations were compared between the well-watered plants (CK), plants subjecting the treatment of rewatering at the point of θ_{cri} following progressive drought (WR_θ_{cri}), and the plants subjecting the treatment of rewatering at severe drought following progressive drought (WR_SD). The results showed that the midday Tr and daily E and plant growth of WR_θ_{cri} were slightly lower or close to those of CK (not significant in two-way ANOVA) during the progressive drought and water recovery phases, but those of WR_SD were significantly lower than those of CK during water stress and did not recover after rehydration. Obviously, WR_θ_{cri} is a potential choice for irrigation schedules, which balances crop growth and water consumption. To detect the molecular mechanism underlying progressive drought and water recovery, transcriptome analysis of samples obtained 12 h before, 12 h after and 36 h after water recovery in the WR_θ_{cri}, WR_SD, and CK treatments was conducted. GO terms and KEGG pathways indicated that mineral absorption and flavonoid biosynthesis were significantly regulated under drought. Mineral absorption-related genes were upregulated in WR_θ_{cri} vs. CK 12 h- and WR_θ_{cri} vs. CK 12 h+, but entire WR_SD vs. CK set, suggesting that iron homeostasis process was repaired in WR_θ_{cri} treatment 36 h after, while not recovered at severe drought treatment even 36 h after water recovery. Flavonoid biosynthesis was triggered by moderate drought to defend against the negative effects of water stress and remained after water recovery but was inhibited under severe drought until 36 h after water recovery. In summary, genes involved in mineral absorption and flavonoid biosynthesis were among the most striking transcriptionally reversible genes under the WR_θ_{cri} treatment. Therefore, functional physiological phenotyping and transcriptome data indicated that irrigation at the critical soil water content will reduce water consumption without sacrificing plant growth, which provides a potential, quantitative, and balanceable water-saving strategy for strawberry irrigation and other agricultural crops.

Data availability statement

The original contributions presented in the study are included in the article/supplementary material. Further inquiries can be directed to the corresponding author.

Author contributions

LJ, TS, and CW contributed to conception and design of the study. XW organized the database. XZ performed the statistical analysis. TS and CW wrote the draft of the manuscript. All authors contributed to manuscript revision, read, and approved the submitted version.

Funding

This work was supported by Agricultural Science and Technology Innovation Project of Shandong Academy of Agricultural Sciences (CXGC2022F05), the central government guides local special projects for science and technology development (YDZX2021101), National Key Research & Development Program of China (China-Israel 2021YFE19800 and 3013005724), Zhejiang Science and Technology Major Program on Agricultural New Variety (2021C02067-7, 2021C02066-5).

Conflict of interest

The authors declare that the research was conducted in the absence of any commercial or financial relationships that could be construed as a potential conflict of interest.

Publisher's note

All claims expressed in this article are solely those of the authors and do not necessarily represent those of their affiliated organizations, or those of the publisher, the editors and the reviewers. Any product that may be evaluated in this article, or claim that may be made by its manufacturer, is not guaranteed or endorsed by the publisher.

References

Ali Sarıdaş, M., Kapur, B., Çeliktopuz, E., Şahiner, Y., and Kargı, S. P. (2021). Land productivity, irrigation water use efficiency and fruit quality under various plastic mulch colors and irrigation regimes of strawberry in the eastern Mediterranean region of Turkey. *Agric. Water Manage.* 245, 106568. doi: 10.1016/j.agwat.2020.106568

Casadebaig, P., Debaeke, P., and Lecoeur, J. (2008). Thresholds for leaf expansion and transpiration response to soil water deficit in a range of sunflower genotypes. *Eur. J. Agron.* 28, 646–654. doi: 10.1016/j.eja.2008.02.001

Cates, J., Baker, J. M., Almendares, O., Kambhampati, A. K., Burke, R. M., Balachandran, N., et al. (2022). Rare 'triple' la niña climate event looks likely — what does the future hold? *Nature* 607, 852–858. doi: 10.1038/d41586-022-01668-1

Chen, B., Han, M., Peng, K., Zhou, S., Shao, L., Wu, X., et al. (2018). Global land-water nexus: Agricultural land and freshwater use embodied in worldwide supply chains. *Sci. Total Environ.* 613, 931–943. doi: 10.1016/j.scitotenv.2017.09.138

Di Caterina, R., Giuliani, M. M., Rotunno, T., De Caro, A., and Flagella, Z. (2007). Influence of salt stress on seed yield and oil quality of two sunflower hybrids. *Ann. Appl. Biol.* 151, 145–154. doi: 10.1111/j.1744-7348.2007.00165.x

Falkland, T., and White, I. (2020). "Freshwater availability under climate change," in *Climate change and impacts in the pacific*. Ed. L. Kumar (Cham: Springer International Publishing), 403–448.

Galati, A., Sabatino, L., Prinzivalli, C. S., D'Anna, F., and Scalenghe, R. (2020). Strawberry fields forever: That is, how many grams of plastics are used to grow a strawberry? *J. Environ. Manage.* 276, 111313. doi: 10.1016/j.jenvman.2020.111313

Gavilán, P., Ruiz, N., Miranda, L., Martínez-Ferri, E., Contreras, J., Baeza, R., et al. (2021). Improvement of strawberry irrigation sustainability in southern Spain using FAO methodology. *Water* 13, 833. doi: 10.3390/w13060833

Gosa, S. C., Koch, A., Shenhar, I., Hirschberg, J., Zamir, D., and Moshelion, M. (2022). The potential of dynamic physiological traits in young tomato plants to predict field yield performance. *Plant Sci.* 315, 111122. doi: 10.1016/j.plantsci.2021.111122

Gu, H., Wang, Y., Xie, H., Qiu, C., Zhang, S., Xiao, J., et al. (2020). Drought stress triggers proteomic changes involving lignin, flavonoids and fatty acids in tea plants. *Sci. Rep.* 10, 15504. doi: 10.1038/s41598-020-72596-1

Halperin, O., Gebremedhin, A., Wallach, R., and Moshelion, M. (2017). High-throughput physiological phenotyping and screening system for the characterization of plant-environment interactions. *Plant J.* 89, 839–850. doi: 10.1111/tpj.13425

IPCC (2021). *Climate change 2021: the physical science basis. contribution of working group I to the sixth assessment report of the intergovernmental panel on climate change* (Cambridge, United Kingdom and New York, NY, USA: Cambridge University Press).

Kapur, B., Celiktopuz, E., Sandas, M. A., and Kargi, S. P. (2018). Irrigation regimes and bio-stimulant application effects on yield and morpho-physiological responses of strawberry. *Hortic. Sci. Technol.* 36, 313–325.

Li, B., Fan, R., Sun, G., Sun, T., Fan, Y., Bai, S., et al. (2021). Flavonoids improve drought tolerance of maize seedlings by regulating the homeostasis of reactive oxygen species. *Plant Soil* 461, 389–405. doi: 10.1007/s11104-020-04814-8

Li, Y., Wu, X., Xu, W., Sun, Y., Wang, Y., Li, G., et al. (2020). High-throughput physiology-based stress response phenotyping: Advantages, applications and prospective in horticultural plants. *Hortic. Plant J.* 7, 181–187. doi: 10.1016/j.hpj.2020.09.004

Lozano, D., Ruiz, N., and Gavilán, P. (2016). Consumptive water use and irrigation performance of strawberries. *Agric. Water Manage.* 169, 44–51. doi: 10.1016/j.agwat.2016.02.011

Luo, T., Hu, L., and Zhang, H. (2022). Genotypic variation of conservative and profligate water use in the vegetative and reproductive stages of canola (Brassica napus l.). *Funct. Plant Biol.* 49, 231–244. doi: 10.1071/FP21239

Ma, D., Sun, D., Wang, C., Li, Y., and Guo, T. (2014). Expression of flavonoid biosynthesis genes and accumulation of flavonoid in wheat leaves in response to drought stress. *Plant Physiol. Biochem.* 80, 60–66. doi: 10.1016/j.plaphy.2014.03.024

Meng, D., Dong, B., Niu, L., Song, Z., Wang, L., Amin, R., et al. (2021). The pigeon pea CcCIPK14-CcCBL1 pair positively modulates drought tolerance by enhancing flavonoid biosynthesis. *Plant J.* 106, 1278–1297. doi: 10.1111/tpj.15234

Mirás-Avalos, J. M., Trigo-Córdoba, E., da Silva-Dias, R., Varela-Vila, I., and García-Tomillo, A. (2016). Multifractal behaviour of the soil water content of a vineyard in northwest Spain during two growing seasons. *Nonlinear Process. Geophys.* 23, 205–213. doi: 10.5194/npg-23-205-2016

Mirjahanmardi, H., and Ehsanzadeh, P. (2016). Iron supplement ameliorates drought-induced alterations in physiological attributes of fennel (*Foeniculum vulgare*). *Nutr. Cycl. Agroecosys.* 106, 61–76. doi: 10.1007/s10705-016-9789-7

Moriya, Y., Itoh, M., Okuda, S., Yoshizawa, A. C., and Kanehisa, M. KAAS: an automatic genome annotation and pathway reconstruction server. *Nucleic Acids Res.* (2007) 35 (Web Server issue), W182–W185. doi: 10.1093/nar/gkm321

Permanhani, M., Costa, J. M., Conceição, M. A. F., de Souza, R. T., Vasconcellos, M. A. S., and Chaves, M. M. (2016). Deficit irrigation in table grape: eco-physiological basis and potential use to save water and improve quality. *Theor. Exp. Plant Physiol.* 28, 85–108. doi: 10.1007/s40626-016-0063-9

Pourgholam, M., Nemati, N., and Oveysi, M. (2013). Effect of zinc and iron under the influence of drought on prolin, protein and nitrogen leaf of rapeseed (*Brassica napus*). *Ann. Biol. Res.* 4, 200–203.

Rai, S., Singh, P. K., Mankotia, S., Swain, J., and Satbhai, S. B. (2021). Iron homeostasis in plants and its crosstalk with copper, zinc, and manganese. *Plant Stress* 1, 100008. doi: 10.1016/j.stress.2021.100008

Rodríguez Pleguezuelo, C. R., Cárceles Rodríguez, B., García Tejero, I. F., Gálvez Ruíz, B., Franco Tarifa, D., Francia Martínez, J. R., et al. (2018). "Irrigation strategies for mango (mangifera indica l.) under water-scarcity scenario in the mediterranean subtropical environment," in *Water scarcity and sustainable agriculture in semiarid environment*, 299–316. doi: 10.1016/B978-0-12-813164-0.00013-2

Shojaie, B., Mostajeran, A., and Ghanadian, M. (2016). Flavonoid dynamic responses to different drought conditions: amount, type, and localization of flavonols in roots and shoots of arabidopsis thaliana l. *Turkish J. Biol.* 40, 612–622. doi: 10.3906/biy-1505-2

Steduto, P., Hsiao, T. C., Fereres, E., and Raes, D. (2012). *Crop yield response to water* (Rome: FAO).

Tian, T., Liu, Y., Yan, H., You, Q., Yi, X., Du, Z., et al. AgriGO v2.0: a GO analysis toolkit for the agricultural community, 2017 update. *Nucleic Acids Res.* (2017) 45 (W1), W122–W129. doi: 10.1093/nar/gkx382

Tripathi, D. K., Singh, S., Gaur, S., Singh, S., Yadav, V., Liu, S., et al. (2018). Acquisition and homeostasis of iron in higher plants and their probable role in abiotic stress tolerance. *Front. Environ. Sci.* 5, 86. doi: 10.3389/fenvs.2017.00086

Vadez, V., Kholova, J., Medina, S., Kakkera, A., and Anderberg, H. (2014). Transpiration efficiency: new insights into an old story. *J. Exp. Bot.* 65, 6141–6153. doi: 10.1093/jxb/eru040

Villa, B. d., Petry, M. T., Santos, M., Martins, J. D., Lago, I., Moura, M., et al. (2022). Water deficit and excess and the main physiological disorders in agricultural crops. *J. Agric. Sci.* 14, 166. doi: 10.5539/jas.v14n8p166

Williams, L. E., Grimes, D. W., and Phene, C. J. (2009). The effects of applied water at various fractions of measured evapotranspiration on reproductive growth and water productivity of Thompson seedless grapevines. *Irrig. Sci.* 28, 233–243. doi: 10.1007/s00271-009-0173-0

Wu, X., Sun, T., Xu, W., Sun, Y., Wang, B., Wang, Y., et al. (2021). Unraveling the genetic architecture of two complex, stomata-related drought-responsive traits by high-throughput physiological phenotyping and GWAS in cowpea (Vigna. unguiculata l. walp). *Front. Genet.* 12. doi: 10.3389/fgene.2021.743758

Xu, L., Dong, Z., Chiniquy, D., Pierroz, G., Deng, S., Gao, C., et al. (2021). Genome-resolved metagenomics reveals role of iron metabolism in drought-induced rhizosphere microbiome dynamics. *Nat. Commun.* 12, 3209. doi: 10.1038/s41467-021-23553-7

Xu, P., Moshelion, M., Wu, X., Halperin, O., Wang, B., Luo, J., et al. (2015). Natural variation and gene regulatory basis for the responses of asparagus beans to soil drought. *Front. Plant Sci.* 6, 891. doi: 10.3389/fpls.2015.00891

Yadava, P., Singh, A., Kumar, K., Sapna,, and Singh, I. (2019). "Plant senescence and agriculture," in *Senescence signalling and control in plants*. (Academic Press), 283–302. doi: 10.1016/B978-0-12-813187-9.00018-4

Yang, B., Fu, P., Lu, J., Ma, F., Sun, X., and Fang, Y. (2022). Regulated deficit irrigation: An effective way to solve the shortage of agricultural water for horticulture. *Stress Biol.* 2, 28. doi: 10.1007/s44154-022-00050-5

Yang, L. L., Yang, L., Yang, X., Zhang, T., Lan, Y. M., Zhao, Y., et al. (2020). Drought stress induces biosynthesis of flavonoids in leaves and saikosaponins in roots of *Bupleurum chinense* DC. *Phytochemistry* 177, 112434. doi: 10.1016/j.phytochem.2020.112434

Zarrouk, O., Costa, J. M., Francisco, R., Lopes, C., and Chaves, M. M. (2015). "Drought and water management in Mediterranean vineyards," in *Grapevine in a changing environment*, 38–67. doi: 10.1002/9781118735985.ch3

frontiers | Frontiers in Plant Science

TYPE Original Research
PUBLISHED 24 November 2022
DOI 10.3389/fpls.2022.1065261

Check for updates

OPEN ACCESS

EDITED BY
Meng Jiang,
Zhejiang University, China

REVIEWED BY
Yuchun Wang,
Tea Research Institute (CAAS), China
Ying Gao,
Beijing Forestry University, China
Wenjun Qian,
Qingdao Agricultural University, China

*CORRESPONDENCE
Gaojie Hong
gjhong@126.com

SPECIALTY SECTION
This article was submitted to Plant Abiotic Stress, a section of the journal Frontiers in Plant Science

RECEIVED 09 October 2022
ACCEPTED 07 November 2022
PUBLISHED 24 November 2022

CITATION
Zhang X, Li L, Lang Z, Li D, He Y, Zhao Y, Tao H, Wei J, Li Q and Hong G (2022) Genome-wide characterization of NAC transcription factors in *Camellia sinensis* and the involvement of CsNAC28 in drought tolerance. *Front. Plant Sci.* 13:1065261. doi: 10.3389/fpls.2022.1065261

COPYRIGHT
© 2022 Zhang, Li, Lang, Li, He, Zhao, Tao, Wei, Li and Hong. This is an open-access article distributed under the terms of the Creative Commons Attribution License (CC BY). The use, distribution or reproduction in other forums is permitted, provided the original author(s) and the copyright owner(s) are credited and that the original publication in this journal is cited, in accordance with accepted academic practice. No use, distribution or reproduction is permitted which does not comply with these terms.

Genome-wide characterization of NAC transcription factors in *Camellia sinensis* and the involvement of CsNAC28 in drought tolerance

Xueying Zhang[1], Linying Li[1], Zhuoliang Lang[1,2], Da Li[3], Yuqing He[1], Yao Zhao[1], Han Tao[1], Jiqian Wei[4], Qingsheng Li[2] and Gaojie Hong[1*]

[1]Key Laboratory for Managing Biotic and Chemical Threats to the Quality and Safety of Agro-products, Key Laboratory of Biotechnology in Plant Protection of Ministry of Agriculture and Rural Affairs, Key Laboratory of Biotechnology in Plant Protection of Zhejiang Province, Institute of Virology and Biotechnology, Zhejiang Academy of Agricultural Sciences, Hangzhou, China, [2]College of Advanced Agricultural Sciences, Zhejiang A&F University, Hangzhou, China, [3]Institute of Sericulture and Tea, Zhejiang Academy of Agricultural Sciences, Hangzhou, China, [4]Ecology and Energy Section, Hangzhou Agricultural Technology Extension Center, Hangzhou, China

The NAM, ATAF1/2, and CUC2 (NAC) transcription factors, which are members of a plant-specific gene family, play critical roles during the growth and development of plants and in their adaption to environmental stress. Few NAC transcription factors have been functionally characterized in tea plants (*Camellia sinensis*). Based on the analysis of the gene structure, motif pattern, and evolutionary relationship, we identified 104 NAC genes in *C. sinensis*. Among them, *CsNAC28* is constitutively expressed in all organs, and most significantly, exhibiting remarkable responsiveness to abscisic acid (ABA) treatment and drought stress. ABA is a primary stress-related hormone. Recently, ABA-responsive element binding factor 2 (*CsABF2*) was identified in the ABA pathway of *C. sinensis*. However, the involvement of the *CsABF2*-mediated ABA pathway in regulating CsNACs was not known. Herein, a series of biochemical and genetic approaches supported the fact that *CsNAC28* could potentially act as a transcription factor in the downstream of *CsABF2*. Furthermore, we investigated the function of *CsNAC28* in the adapting of a plant to drought stress. The results showed that overexpression of *CsNAC28* in Arabidopsis conferred hypersensitivity to ABA treatment and decreased the accumulation of reactive oxygen species (ROS), resulting in improved dehydration tolerance. Under conditions of drought, the expression levels of ABA pathway-related genes and drought stress–inducible genes were greater in *CsNAC28* overexpression lines than in the wild type. Our study's

comprehensive characterization of NAC genes in *C. sinensis* could serve as a foundation for exploring the molecular mechanism of CsNAC-mediated drought responsiveness.

KEYWORDS

***Camellia sinensis*, expression pattern, NAC transcription factor, drought stress, abscisic acid**

Introduction

The tea plant *C. sinensis* is a major crop harvested for tea that is consumed worldwide, and it has been widely cultivated in tropical and subtropical areas (Liu et al., 2015). Its abundance of secondary metabolites contribute to the nutrients, a clean taste, and rich flavors beneficial to human health (Yang and Hong, 2013; Zhao et al., 2020). In recent years, the increasing frequency of extreme temperatures and drought stress affected the yield and quality of tea leaves (Wang et al., 2016a). Transcription factors play critical roles in activating gene transcripts through binding to the target gene promoter regions and regulating the plant growth, development, and biotic and abiotic stress processes (Pandey and Shukla, 2015).

NAC (NAM-ATAF1/2-CUC) transcription factors constitute one of the most diverse transcription factor families in plants; they contain highly conserved N-terminal DNA binding domains (150 amino acids) but relatively variable C-terminal regions (Souer et al., 1996; Ooka et al., 2003; Ernst et al., 2004). The N-terminal areas contain five subdomains (A, B, C, D and E), such as NAM (no apical meristem) in a petunia mutant and ATAF1/2 and CUC2 (cup-shaped cotyledon) in Arabidopsis. Subdomains B and E are divergent and may be associated with the NAC gene's functional diversity, whereas subdomains A, C, and D are generally conserved (Olsen et al., 2005). The C-terminal regions are responsible for activating or repressing the expression of downstream genes (Kjaersgaard et al., 2011; Lindemose et al., 2014). Additionally, some NAC transcription factors have transmembrane motifs, which function as endoplasmic or plasma membrane anchors at the C-terminal (Seo et al., 2008; Li et al., 2016).

The NAC transcription factors regulate many critical biological processes that are commonly associated with stress resistance, and they have been extensively identified in Arabidopsis (105), rice (138), maize (147), sunflowers (151), tomatoes (93), bananas (167), peppers (104), *Populus trichocarpa* (163), and apples (180) because of the availability of their whole-genome sequences (Ooka et al., 2003; Hu et al., 2010; Nuruzzaman et al., 2010; Su et al., 2013; Cenci et al., 2014; Diao et al., 2018; Jin et al., 2020; Wang et al., 2020; Bengoa Luoni et al., 2021). Many studies have demonstrated that NAC transcription factors increase resistance to drought by activating downstream genes involved in the ABA pathway. In Arabidopsis, ATAF1, ATAF2, ANAC019, ANAC055, RD26/ANAC072, and ANAC096 contribute to drought tolerance through an ABA-mediated pathway (Fujita et al., 2004; Tran et al., 2004; Jiang et al., 2009; Jensen et al., 2010; Xu et al., 2013; Liu et al., 2016; Jiang et al., 2019). Overexpression of OsNAC5, OsNAC6, and OsNAC9 increases the sensitivity to ABA and results in enhanced tolerance to drought in rice (Redillas et al., 2012; Lee et al., 2017; Bang et al., 2022). In wheat, TaSNAC8-6A, TaASNAC4-3A, and TaNAC069 could activate the expression of drought-related genes (Xue et al., 2011; Mao et al., 2020; Mei et al., 2021). In maize, ZmSNAC1, ZmNAC33, ZmNAC49, ZmNAC55, ZmNAC84, and ZmNAC111 drive drought responses through the ABA pathway (Lu et al., 2012; Mao et al., 2015; Mao et al., 2016; Liu et al., 2019; Han et al., 2021; Xiang et al., 2021). In the tea plant, the involvement of CsNAC in responding to drought stress has not been determined.

The high-quality genome sequences of tea plants have been published, and, therefore, it was possible to identify 104 CsNACs by scanning the genome at the chromosome level (Wei et al., 2018). We analyzed the gene structure, motif pattern, chromosome distribution, synteny, and evolutionary relationship among Arabidopsis, *P. trichocarpa*, and *C. sinensis*. To investigate the involvement of CsNACs in the adaption to drought stress, we chose *CsNAC28* as a candidate. The results showed that *CsNAC28* localized in the nucleus and possessed transactivation activity. Furthermore, the overexpression of *CsNAC28* in Arabidopsis enhanced ABA sensitivity and upregulated the expression of drought-tolerance-related genes, thus improving the dehydration tolerance. This work improved our understanding of CsNAC transcription factors and the function of NACs in the adaption to drought stress, thereby contributing to tea plant breeding programs.

Materials and methods

Identification and structure analysis of NAC genes in *C. sinensis*

To identify the tea plant (*C. sinensis* cv. ShuChaZao) NAC genes, the hidden Markov model (HMM) profile of the NAC

domain (PF00170) was downloaded from Pfam (http://pfam.xfam.org/) and the NAC protein sequences were searched with an e-value cutoff of $1e^{-5}$. Then, to determine their presence and completeness of the NAC domain, all of the putative NAC genes were identified manually one by one (E value<1.0) in INTERPORSCAN and SMART (http://smart.embl-heidelberg.de/). Molecular weight, isoelectric points, subcellular localization, and transmembrane helices of candidate NAC proteins were detected in ExPASy (http://expasy.org/tools/), WoLF PSORT (http://wolfpsort.org/) and TMHMM (http://www.cbs.dtu.dk/services/TMHMM/) server v2.0.

Phylogenetic, gene structure and motifs composition of CsNACs

The NAC sequences of coding proteins from Arabidopsis, *Oryza sativa* and *C. sinensis* were aligned using ClustalX 2.0. A phylogenetic tree consisting of 345 NACs was constructed by MEGA7.0 using the neighbor-joining (NJ) tree with default parameters. 1000 replicates were used to produce bootstrap values. The exon/intron structure of NAC genes was displayed by the Gene Structure Display Server program (GSDS http://gsds.cbi.pku.edu.cn/) platform, and the NAC conserved motif was characterized by MEME, with a cap of motifs set to 10.

Chromosomal mapping and gene duplication analysis

The NAC genes were mapped by MapInspect (http://www.plantbreeding.wur.nl/UK/software_mapinspect.html) with the *C. sinensis* genome database. The gene duplication events of NAC genes were examined by MCScanX software with default parameters. To visualize the duplicated regions in the *C. sinensis* genome, the Circos-0.67 program (http://circos.ca/) was used to draw between matching genes. The homology of the NAC genes between *C. sinensis* and the other species (*Arabidopsis thaliana*, *Oryza sativa and Populus trichocarpa*) was analyzed by Dual Synteny Plotter of TBtools (Chen et al., 2020).

NAC transcription factors expression pattern in *C. sinensis*

The expression pattern data from distinct tissues (Root, Stem, Old leaf, Mature leaf, Young leaf, Apical bud, Folwer and Fruit) have been previously reported in the genome sequencing research of 'ShuChaZao', which was downloaded from http://tpia.teaplant.org/index.html (Wei et al., 2018). The NAC genes expression level were evaluated using fragments per kilobase per million reads mapped (FPKM) and the data were displayed as Log_{10} $^{(FPKM\ value)}$ in a heat map using the Mev4.9.0 software. The leaves of tea plant (*C. sinensis* vs LongJing43) were sprayed with 100 μM ABA for ABA treatments (ddH_2O as control). The roots of tea plant seedlings were irrigated with 20% PEG for drought treatments (ddH_2O as a mock control). The real-time PCR primers for the CsNACs of interest were designed by Beacon Designer 7.0 software (Supplementary Table S1). Glyceraldehyde-3-phosphate dehydrogenase (GAPDH, accession number: KA295375.1) was employed as an internal reference. SYBR Green (Roche, Basel, Switzerland) was used in real-time PCR on an ABI7900HT Sequence Detection System (Applied Biosystems, Waltham, MA, USA).

Transcriptional self-activating of NACs proteins and subcellular localization

The cDNA of CsNAC28 were inserted into the pGBK vector digested with BamH I and Nde I. pGBK-CsNAC28 and pGBK-Lam were transformed into the yeast strain Y_2H and plated on the SD/-Trp plates individually. Colonies were further transferred to SD/-Trp/ABA (250ng) medium for 3-5 days at 30°C.

The binary vector PCV-eGFP -N1 was digested with Apa I enzyme before the cDNA of CsNAC28 was inserted. PCV-CsNAC28-eGFP-N1 and PCV-eGFP-N1 vectors were introduced into *Agrobacterium tumefaciens* strain GV3101, then transiently transformed into tobacco. The GFP fluorescence was imaged at 495-545 nm using a Leica TCS SP5 (Leica Microsystems, Bannockburn, IL, USA) confocal laser-scanning microscope after infiltrating 44-48h.

Yeast one-hybrid assay

The cDNA of CsABF2 was inserted into a pGAD vector digested with BamH I and Nde I. The *CsNAC28* promoter was inserted into the pABAi vector digested with Hind III and Sal I. CsNAC28p-pABAi were linearized with Bstb I, then transformed into Y1H strain and plated on SD/-Ura medium. Colonies containing the CsNAC28 promoter were used to generate receptor states, which were then transformed with the CsABF2- pGAD (pGAD plasmid as a control) and plated into SD/-Leu medium. Colonies were further transferred to SD/-Leu medium with 300ng/ml ABA for three days.

Dual-luciferase assay for CsNAC28

Dual-luciferase assays were conducted in accordance with He et al. (2021). The pGreenII0800- LUC vector was digested with Pst I and Nco I and used to insert the 1388 bp promoter region of CsNAC28. The pCambia2300 vector was digested with Kpn I and Bam HI and used to insert the cDNA of CsABF2. Dual-Luciferase Reporter Assay kit (Promega, Madison, WI,

USA) was used to measure the ratio of firefly luciferase to renilla luciferase of the CsNAC28 promoters with and without the effect of CsABF2.

Transient gene suppression in tea plants

Gene suppression assays were carried out as described by Hu et al. (2022). *CsABF2* was used as input sequences to design candidate antisense oligonucleotides (AsODNs) with the Soligo software (Ding and Lawrence, 2003) (Supplementary Table S1). Both sense oligonucleotides (sODNs) and gene-specific AsODNs were infiltrated with at least ten individual tea plants. The leaves were harvested after 24 h treatment, quick-frozen in liquid nitrogen, and stored at -80°C.

Plant phenotype under ABA and drought treatments

The cDNA of CsNAC28 was cloned into the pCambia1300 vector under the control of the 35s promoter, Transgenic plants of CsNAC28-Flag (three copies of the flag in tandem) overexpressing in Col-0 were generated. The *Agrobacterium* strains GV3101 containing CsNAC28-pCambia1300 were introduced into Arabidopsis plants by the *Agrobacterium tumefaciens*-mediated floral dip method (Clough and Bent, 1998). Hygromycin resistance was used to screen out of ten independent transgenic lines. T3 homozygous progenies of transgenic lines (OE1, OE2 and OE3) were chosen to be studied further. The sequence of primers used in this investigation is listed in Supplementary Table S1.

To conduct the germination experiment, the cleaned seeds were sown on 1/2MS solid medium (90 seeds were sown for each line), which contained ABA (0 and 5μM) and mannitol (0, 100 and 200 mM) in varying concentrations, respectively. Then the mediums were placed in a refrigerator at 4°C for three days to break seed dormancy and transferred into a greenhouse 22°C under long-day ling conditions (16h light/8h dark). The germination number and root length were recorded once daily. The 4-week-old seedlings were dehydrated for 14 days for drought stress treatment, and re-water. Each experiment was repeated three times (Chen et al., 2017).

Measurement of reactive oxygen species

WT and transgenic plants were subjected to drought stress and three individual plant leaves were sampled. To determine the hydrogen peroxide (H_2O_2) and superoxide (O^{2-}) content, the leaves were stained by 3,3'-diaminobenzidine (DAB) and nitroblue tetrazolium (NBT) according to previously described methods (Yang et al., 2018).

Statistical analysis

All experiments were carried out with at least three independent biological replicates. Each measurement was carried out in triplicate. Data represent the mean ± sd of three biological replicates. Data were statistically analyzed by one-way analysis of variance (ANOVA) performed using SPSS.

Results

Identification of NACs in *C. sinensis*

The genome database of "*C. sinensis*" allows for the identification of NAC gene members in the tea plant (Wei et al., 2018). A total of 104 NACs was characterized with a conserved NAC domain (PF01849) or NAM domain (PF02365). The NACs' amino acid residue counts ranged from 134 to 679, their putative molecular weights ranged from 15.37 to 77.14 KDa, and their isoelectric points (pIs) were 4.6 to 9.91. An examination of their chromosomal locations showed that 104 NACs were matched to the 15 chromosomes of the *C. sinensis* genome and that the number of NACs in each chromosome differed, ranging from 3 (chr15) to 15 (chr09) (Supplementary Figure S1). According to the chromosomal position, which was named CsNAC1 to CsNAC104 (Supplementary Table S2), the 104 NAC proteins were predicted to be located in the nucleus or cytoplasm. Additionally, eight NACs contained a transmembrane domain. *CsNAC20, CsNAC64, CsNAC74*, and *CsNAC99* had transmembrane domains at the C-terminal, *CsNAC55* had two transmembrane domains, and *CsNAC2, CsNAC68*, and *CsNAC100* had transmembrane domains at the N-terminal.

Phylogenetic and gene structure analysis of CsNAC genes

To evaluate the phylogenetic relationship of the NAC proteins in *C. sinensis* and other species, an unrooted neighbor-joining tree was created with 345 NAC proteins from three plant species (i.e., 78 from Arabidopsis, 163 from *P. trichocarpa*, and 104 from *C. sinensis*). The results showed that 345 NAC proteins were grouped into 13 subfamilies, named subfamilies A to M. All of them were unevenly distributed in 11 subfamilies; subfamily L contained 17 PNACs and 7 CsNACs, whereas subfamily K contained only 4 PNACs but no AtNACs

or CsNACs. Generally, the CsNAC proteins had closer relationships with the NACs from *P. trichocarpa* than those from Arabidopsis, and this was confirmed by the current plant evolutionary history and provided more useful references for functional identification in tea plants (Figure 1).

To further explore the evolution of the NAC gene family, we analyzed the structural features of the NAC genes in *C. sinensis*. *CsNAC41* has a gene structure that is longer than 20 kb, whereas *CsNAC66* has the shortest structure, at 405 bp. Of all the NAC genes, *CsNAC59* contained the most (10) exons. No introns were found in *CsNAC66;* over half (54, or approximately 51.9%) of the NAC genes had three exons; and most of the NAC genes shared a common exon/intron structure and had intron phases that were clustered in the same subgroup (Figure 2). In addition, 10 conserved motifs of the 104 NAC genes were investigated by the MEME program to explore genetic diversification in *C. sinensis*. The lengths of these conserved motifs ranged from 11 to 50 amino acids, with a highly diverse distribution. *CsNAC33* only contained one motif, whereas eight similarly ordered motifs (motifs 3, 8, 4, 1, 6, 5, 2, 7) were present in most NACs. Except for the fourth subgroup, the compositions of the conserved motifs and orders of the NAC protein sequences in the same group were similar. Motifs 9 and 10 were unique to subgroup four, suggesting that they had specific functions that benefited this group (Figure 2). An analysis of the exon/intron and motif compositions further showed that the genes that have developed in offspring may have functional redundancy.

Syntenic analysis of NAC genes in *C. sinensis* and other species

Intrachromosomal and interchromosomal evolutionary research showed that 9 pairs of tandem duplicate events occurred in the same chromosome (tandem duplications were defined as genes on the same chromosome that were mapped at a distance ≤ 100 kb) and that 49 segmental duplication events occurred on all chromosomes, which suggested that the expansion of the CsNAC family was mainly the result of interchromosomal duplication events (Supplementary Figure S2).

A collinearity assay of the NAC gene family in *C. sinensis*, Arabidopsis, *Oryza sativa*, and *P. trichocarpa* was carried out to explore the species' evolutionary relationships, and it found 101, 45, and 165 homologous pairs between *C. sinensis* and the other three species, respectively. The results

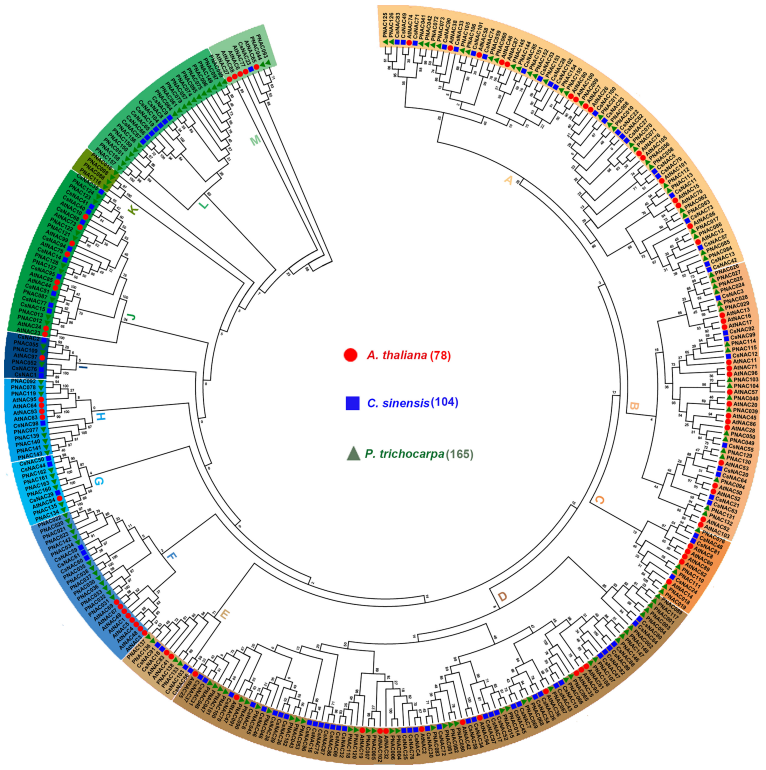


FIGURE 1
Phylogenetic tree of NACs from *Arabidopsis thaliana*, *Populus trichocarpa* and *C. sinensis*. Amino acid sequences were aligned using Clustal X software and subjected to phylogenetic analysis using MEGA X software by the NJ method with 1,000 bootstrap replicates.

10.3389/fpls.2022.1065261

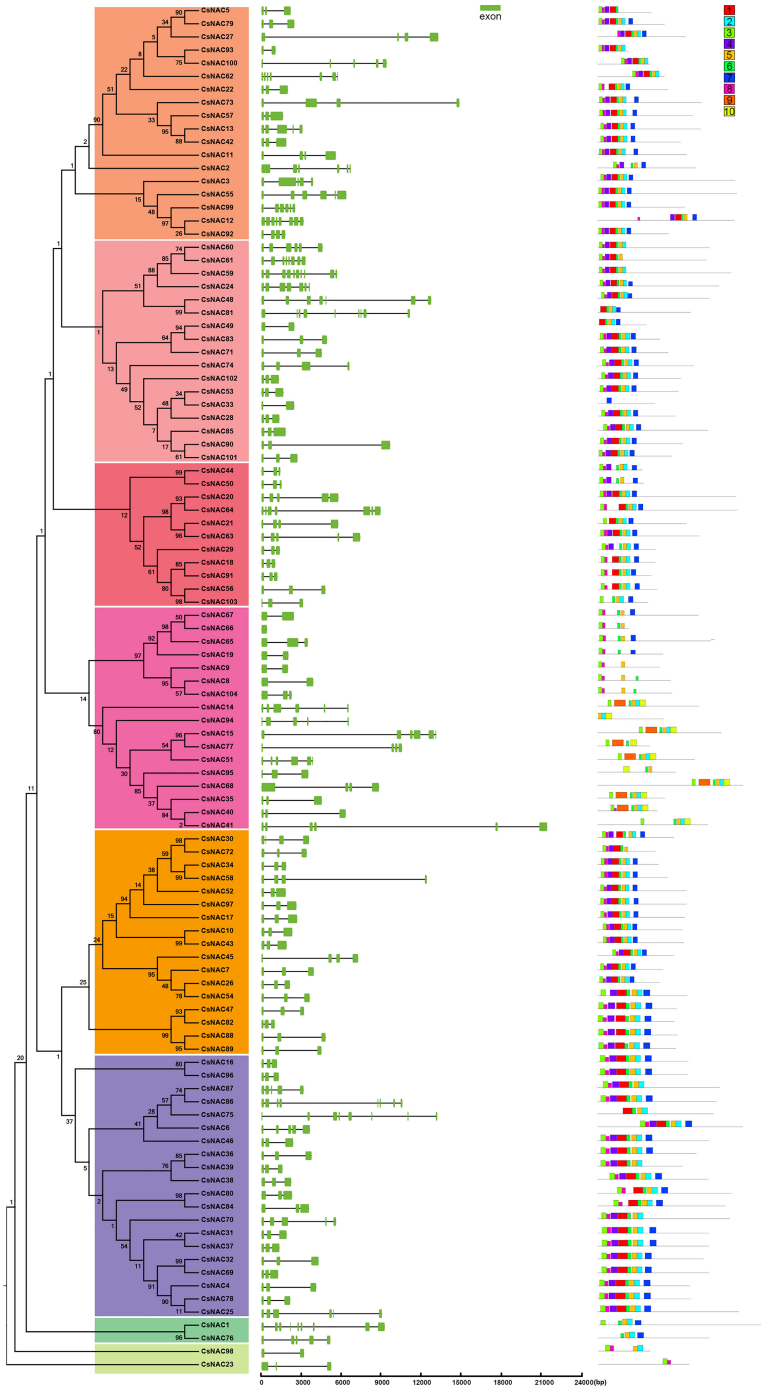


FIGURE 2
Gene structure and motif organization of *NAC* genes in *C. sinensis*. Intron and exon structures of NACs are graphically represented by black lines and orange boxes, respectively. The protein sequences of NACs was used to predict the conserved regions and motifs. Conserved motifs are indicated by a colored box numbered 1 to 10.

showed that *C. sinensis* and *P. trichocarpa* had more homologous genes, which was consistent with their phylogenetic relationship (Figure 3).

Tissue-specific expression profiles of NACs in *C. sinensis*

Cultivated tea tree species differ greatly in terms of plant morphology and economic characteristics. We determined the abundance of NAC transcripts in various tissues, including the apical bud, young leaf, mature leaf, flower, fruit, old leaf, stem, and root tissue of *C. sinensis* cv. ShuChaZao, to explore the tissue specificity. As shown in Figure 4, the expression levels of 16 *CsNACs* (*CsNAC8/9/23/34/38/39/46/58/65/66/67/80/86/87/84/98*) were very low or undetectable in all tested tissues, possibly due to the fact that they were pseudogenes; 88 CsNAC members were expressed in at least one of the organs of *C. sinensis*; and 14 *CsNACs* (*CsNAC1/3/4/15/18/20/21/24/28/63/64/69/78/91*) were predominantly expressed in all tissues with a Log_{10} (FPKM value) of greater than 1. Ten *CsNACs* (*CsNAC7/10/25/29/35/36/43/45/48/59*) were highly expressed in buds and leaves. The transcripts of 18 CsNACs were found in the roots, and the transcripts of 20 CsNACs were found in the flowers or fruits (Figure 4).

AREB *cis*-acting elements of CsNAC gene promoter regions

ABA-responsive element-binding factors (AREB/ABFs) are master regulators of the transcriptional response to ABA. Most of them activate the expression of drought-responsive genes *via* the direct binding of the ABA-responsive element (ABRE: PyACGTGG/TC) to improving drought tolerance (Fujita et al., 2011). Thus, we analyzed a sequence 2 kb upstream from the translation initiation site of the CsNACs. The results showed that 78 of the CsNAC promoters contained at least one ABRE element. The number of ABRE elements ranged from one to eight. Specifically, 27 of the CsNAC promoters had one ABRE element, 17 contained two ABRE elements, and 11 contained three or five ABRE elements. The other CsNAC promoters contained four, six, or seven ABRE elements, and only *CsNAC78* contained eight ABRE elements (Supplementary Figure S3A). To further examine the potential role of CsNACs

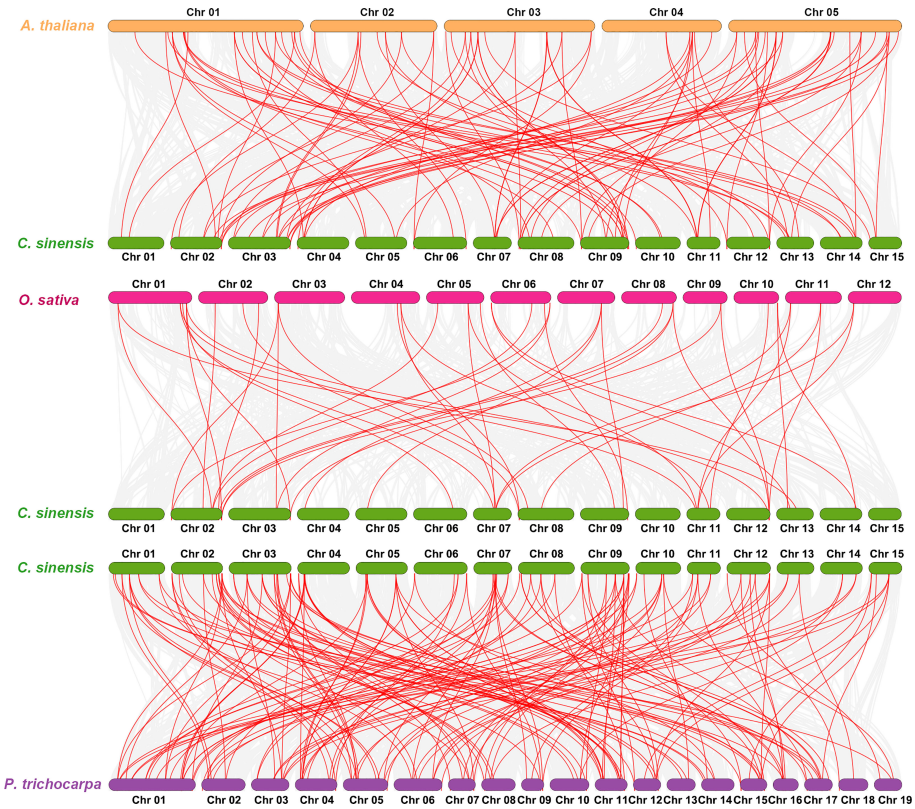


FIGURE 3
Synteny analysis of NAC genes between *C. sinensis* and three representative species. Red lines highlight the syntenic NAC gene pairs with the *Camellia sinensis* and other plant genomes, whereas gray lines in the background indicate the collinear blocks.

10.3389/fpls.2022.1065261

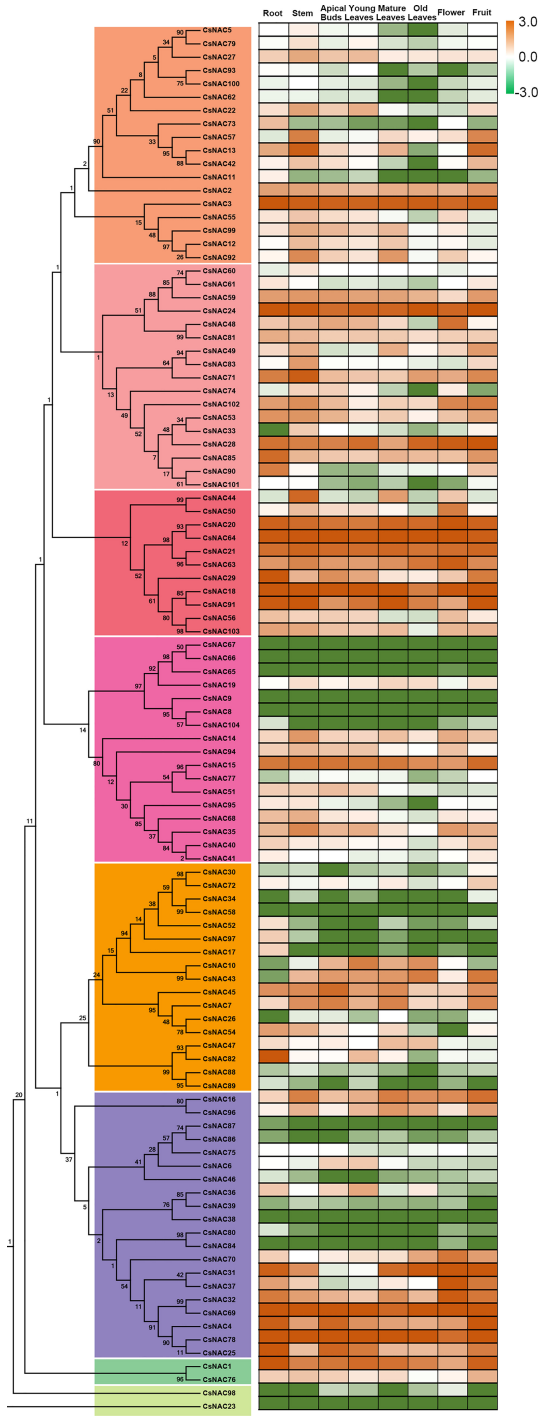


FIGURE 4
Expression patterns of CsNACs in different tissues of *C. sinensis*. The expression patterns of CsNACs genes in eight tissues (Root, Stem, Old leaf: germinated in previous years; Mature leaf: geminated in the spring and harvested in the autumn; Young leaf: the first and second leaves follow the apical bud; Apical bud: unopened leaves on the top of activity growing shoots, Flower and Fruit) of tea plant were calculated using $Log_{10}^{(FPKM)}$. The most of the data were distributed between -3 and +3, which indicated high and low expression levels.

in the response to drought stress, transcriptome data for tea plants under drought stress treatment were acquired from the Tea Plant Information Archive (http://tpdb.shengxin.ren/index.html). The expression patterns of 50 CsNAC genes in response to drought stress are shown in Supplementary Figure S3B. The expression of 20 of these CsNACs was induced significantly, and the expression of 15 of these was high after 24 hours of drought treatment.

Considering the expression pattern of the CsNACs and the existence of ABRE elements in their promoters, seven CsNACs were selected for attempts to detect their responsiveness to ABA treatment and drought stress through the quantitative real-time polymerase chain reaction (qRT-PCR). In most of the selected candidate genes, expression was significantly induced after exposure to ABA treatment and drought stress. The expression levels of *CsNAC20*, *CsNAC25*, *CsNAC28*, *CsNAC32*, and *CsNAC69* were upregulated two-fold to four-fold at 1 hour (H), *CsNAC25* were induced after 3 H of ABA treatment. The gene expression of most CsNACs had similar profiles for ABA treatment and drought stress, although drought stress exhibited a certain lag effect on the induction of expression of CsNACs. To be specific, the expression of *CsNAC20* and *CsNAC25* was upregulated three-fold and nine-fold at 24 H, respectively; that of *CsNAC28*, *CsNAC32*, and *CsNAC69* was significantly increased at 3 H; and that of *CsNAC29* was upregulated at 12 H. The expression of *CsNAC3* was repressed by ABA and drought stress, and the peak values of relative expression appeared at 1 H and 3 H, respectively (Figure 5). The results showed that the expression of most NACs was induced by ABA treatment and drought stress.

Subcellular localization and transcriptional activation ability of CsNAC proteins

Both *CsNAC28* and *CsNAC69* were constitutively expressed in all organs, and their expression was further induced by ABA treatment and drought stress. Because *CsNAC69* is the homologue of *ANAC019*, which confers drought tolerance in Arabidopsis (Jensen et al., 2010), we investigated whether *CsNAC28* participated in the drought stress response in tea. The full-length *CsNAC28* was fused into the DNA binding domain to investigate the transcriptional activation of *CsNAC28*. Each CsNAC-pGBK-pGAD pair was individually co-transformed into the yeast cells Y_2H and further selected on a quadruple dropout medium. As shown in Figure 6A, the negative control did not grow but the *CsNAC28* transformant grew well, indicating that *CsNAC28* acts as a transcription factor with transcriptional activity in yeast strains.

To explore the sub-localization of *CsNAC28*, *Agrobacterium tumefacient* strains GV3101 containing either a GFP empty vector or a *CsNAC28*-GFP vector were introduced into

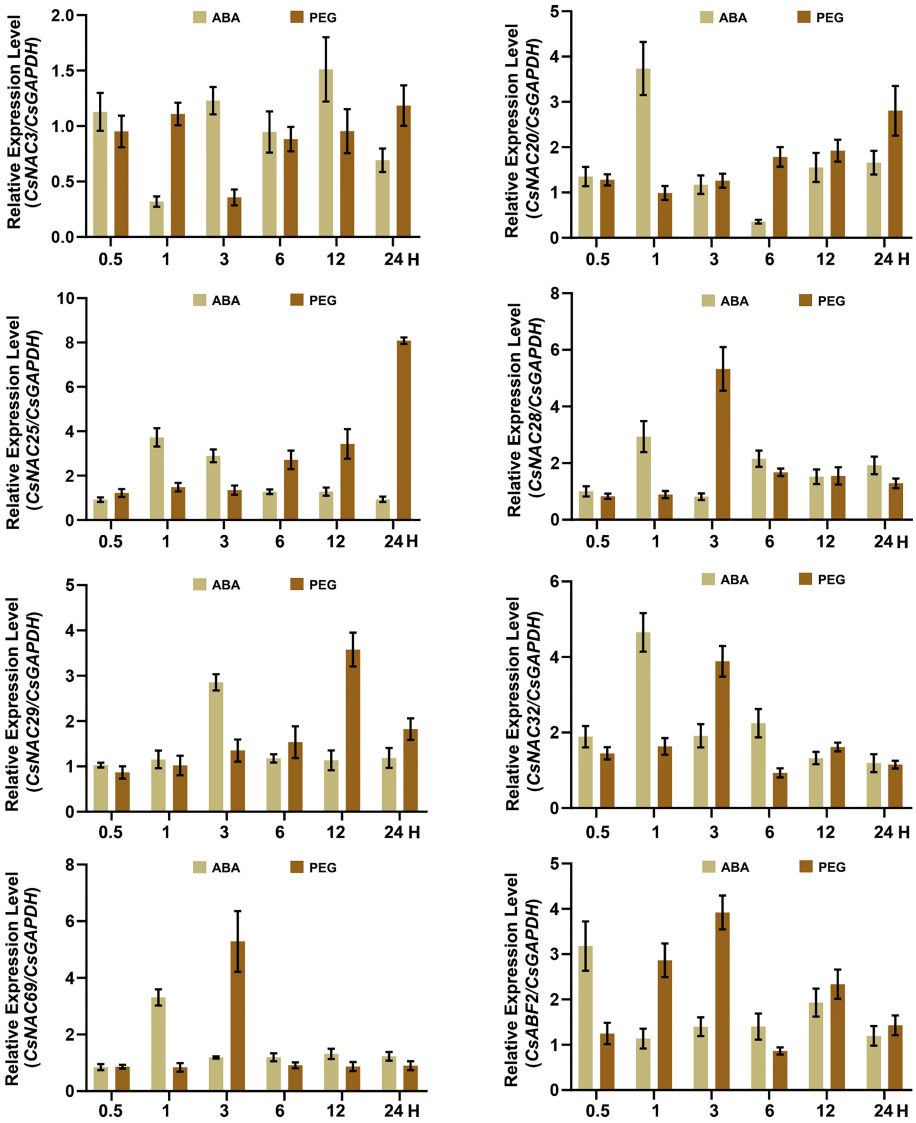


FIGURE 5
Expression patterns of CsNACs in *C. sinensis* under ABA and PEG. Error bars indicate SD of three biological replicates.

tobacco leaves. The GFP fluorescence of the *CsNAC28*-GFP vector was detected in the nucleus, while the GFP signals of the empty vector were detected in the nucleus and cytoplasm (Figure 6B). The results are consistent with the predicted role of CsNAC28 as a transcription activator.

CsABF2 binds and activates *CsNAC28* expression

CsABF2 was examined as a key transcription factor in regulating the tea cultivar's drought tolerance (Lu et al., 2021). To verify whether the ABRE element on CsNAC promoters could be recognized and bonded by *CsABF2*, the 1388-bp length of the *CsNAC28* promoter was fused to the *Aureobasidin A* (AbA) gene to generate the *CsNAC28Pro-pABAi* vectors that confer resistance to AbA. Then, the linearized *CsNAC28Pro-pABAi* vector (digested by BstB I) was co-transformed with the *CsABF2*-pGAD vector and tested on SD/-Trp/150mM AbA media (Figure 6C). The result showed that CsABF2 could recognize and bind the *cis*-element in the promoter of *CsNAC28 in vitro*. Then, to explore the effect of *CsABF2* on *CsNAC28* transcription *in vivo*, we cloned the promoter regions of *CsNAC28* to fuse them into the LUC reporter vector. Compared with the control, the co-expression of *CsABF2* dramatically increased the promoter activity of *CsNAC28* by

3.6-fold (Figure 6D). Furthermore, we transiently silenced *CsABF2* in tea plants to investigate the relationship between *CsABF2* and *CsNAC28*. Compared with *CsABF2/sODN* tea plants, *CsABF2* and *CsNAC28* were decreased by 60% and 41%, respectively, in *CsABF2/AsODN* tea plants (Figure 6E). Altogether, the results suggested that *CsABF2* could recognize the ABRE element on the promoter of *CsNAC28* and activate the expression of *CsNAC28*.

Overexpression of *CsNAC28* enhances drought tolerance in transgenic Arabidopsis

The ABA signaling pathway is critical for plant adaptation to drought stress. When a plant is subjected to drought stress, ABA rapidly accumulates in the roots and leaves (Finkelstein et al., 2002; Kuromori et al., 2018). To explore the role of *CsNAC28* in the adaption to drought stress in plants, we heterogeneously expressed *CsNAC28* in Arabidopsis. Three overexpression lines with relatively higher expression levels were selected for further analysis (Supplementary Figure S4). Since the expression of *CsNAC28* was upregulated by ABA treatment, we spotted the seeds of the wild type (WT) and three *CsNAC28/OE* lines on 1/2MS medium with or without the addition of 5 μM ABA. As the results showed, no significant difference in growth phenotype and germination rate was observed in the WT and *CsNAC28/OE* transgenic lines on the 1/2MS medium. However, when grown on 1/2MS medium with 5 μM ABA added, three *CsNAC28/OE* lines had lower germination rates than the WT (Figures 7A, B) to different degrees. Moreover, the roots of the WT were longer than the roots of the three *CsNAC28/OE* lines (Figures 7C, D). Our data indicated that *CsNAC28* overexpression in Arabidopsis increased the sensitivity to ABA.

To further examine the drought tolerance of the *CsNAC28/OE* lines, mannitol treatment was used to simulate drought stress. Three *CsNAC28/OE* lines and the WT were sown on 1/2MS medium containing 0 mM, 100 mM, or 200 mM mannitol. Under normal growth conditions, there was no obvious difference in the germination rate (Figures 8A, B) or root length (Figures 8C, D) between the transgenic Arabidopsis and the WT. When grown on the 1/2MS medium plus 100 mM mannitol, the germination rate of the WT was 80% and the root growth was slightly impaired. Compared with the influence on the WT, the germination percentages of the three *CsNAC28/OE* lines were higher (84%, 92%, and 96%), and consistently, the

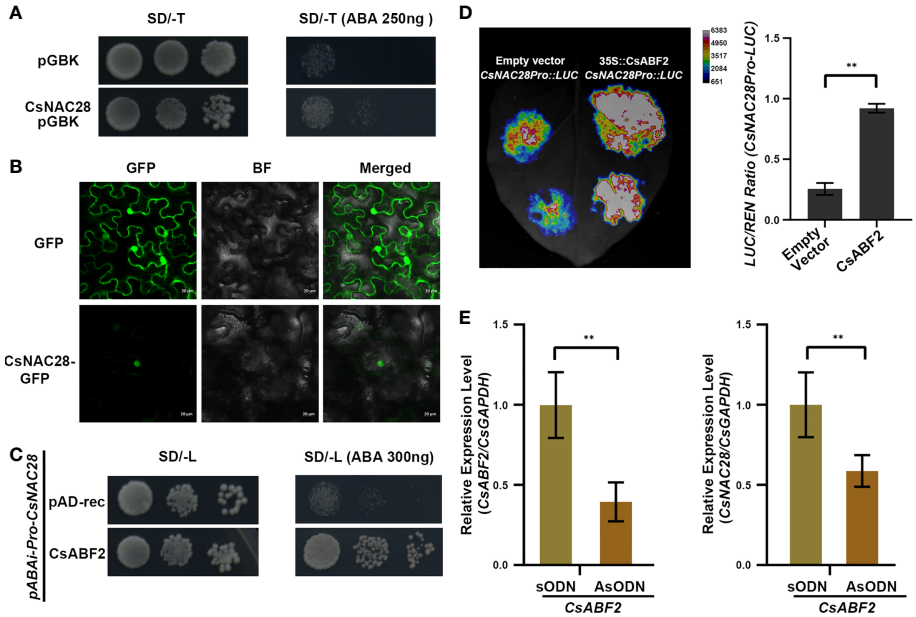


FIGURE 6
The potential function of CsNAC28 in tea plant. **(A)** Transactivation analyses of CsNAC28 in yeast. Negative control, and the fusion constructs were transformed into the Y_2H strain and successively incubated in SD/-Trp media and SD-Trp/ABA (250ng) plate. **(B)** Subcellular localization of CsNAC28. GFP and CsNAC28-GFP were transiently expressed in tobacco leaves. GFP, Green fluorescence image; BF, Bright-field microscopy image; Merge, Merged bright-field and green fluorescence images. **(C)** Yeast one-hybrid assay to confirm binding of CsABF2 to the *CsNAC28* promoter. **(D)** Relative LUC/REN ratio from transient expression assays of the *CsNAC28* promoter in the present of CsABF2. Error bars indicate the SD of three biological replicates. **(E)** *CsABF2* and *CsNAC28* expression in control (*CsABF2*/sODN) and *CsABF2/AsODN* tea leaves. Error bars indicate the SD of three biological replicates. **Student's test, $P < 0.01$.

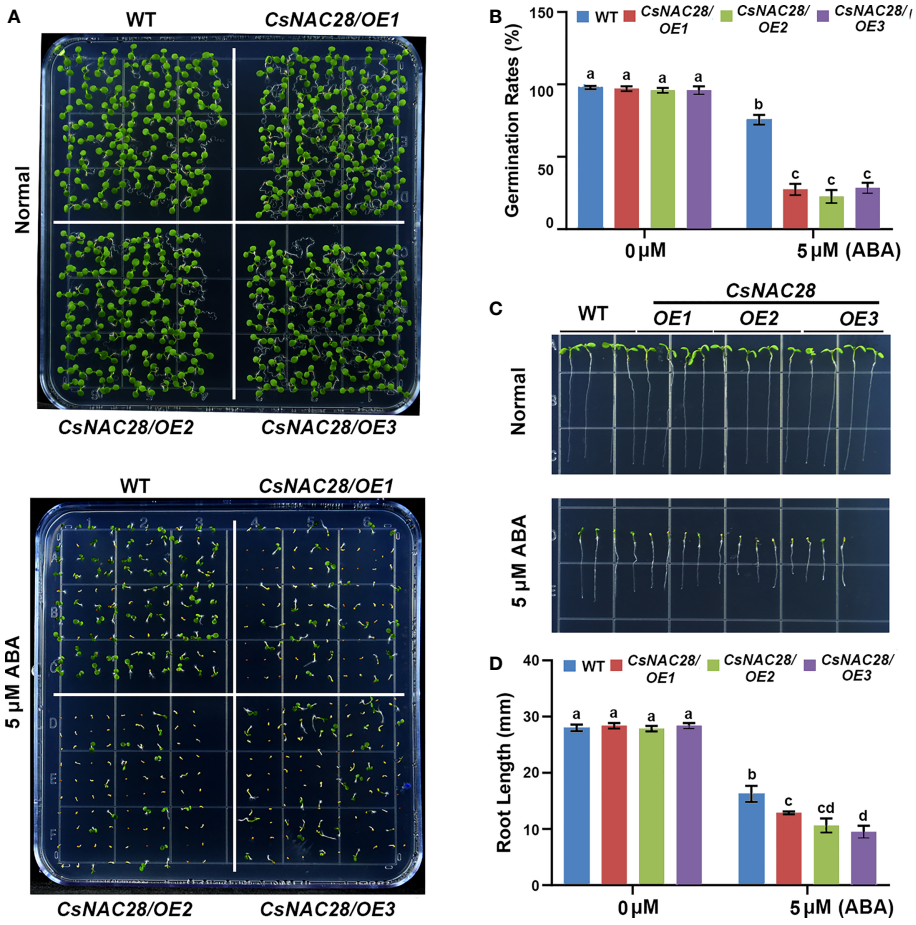


FIGURE 7
Overexpression of CsNAC28 increases ABA sensitivity in transgenic Arabidopsis. **(A)** Germination assays for each lines under different concentrations of ABA treatments. **(B)** Germination percentage of each line under different concentrations of ABA treatments. **(C)** Root length assays for different lines under different concentrations of ABA treatments. **(D)** Quantification of root length under different concentrations of ABA treatments.

root lengths were longer (Figure 8). When the concentration of mannitol increased to 200 mM, the germination rate of the WT fell to 65% and the root growth was severely retarded. In this condition, the *CsNAC28/OE* lines with higher germination rates (Figures 8A, B) and longer root lengths exhibited resistance to mannitol treatment (Figures 8C, D).

Four-week-old seedlings were subjected to drought stress to further identify the function of *CsNAC28* in drought stress during the adult stage. The majority of the WT leaves were seriously wilted and unable to recover after re-watering or were dead. Only 53% of the WTs subjected to drought treatment survived. However, the transgenic lines (*CsNAC28/OE1, CsNAC28/OE2*, and *CsNAC28/OE3*) wilted only slightly after drought treatment and grew normally after re-watering; For them the final average survival percentages were 80%, 86%, and 91%, respectively (Figure 9A). In addition, we measured the hydrogen peroxide (H_2O_2) and O^{2-} content in leaves under normal and drought conditions using DAB and NBT staining to see whether those levels were associated with improved drought tolerance. Under normal conditions, the WT and three *CsNAC28/OE* lines had little staining. When exposed to drought stress, the staining of the WT leaves was substantially greater than of the leaves of the *CsNAC28/OE* lines (Figure 9B).

It is well known that *ABI1* and *DREB2A* are involved in ABA signaling transduction and that *RD22* (responsive to dehydration 22) and *RD29B* are marker genes in the ABA pathway (Yamaguchi and Shinozaki, 1993; Liu et al., 2020; Yu et al., 2021; Sun et al., 2022). To further explore the role of *CsNAC28* overexpression in drought response pathways, the expression of these genes was analyzed. Under normal conditions, there was no obvious difference in expression pattern between the *CsNAC28/OE* and the WT plants. Under drought conditions, however, the expression of all these genes was significantly induced. Furthermore, the expression levels

10.3389/fpls.2022.1065261

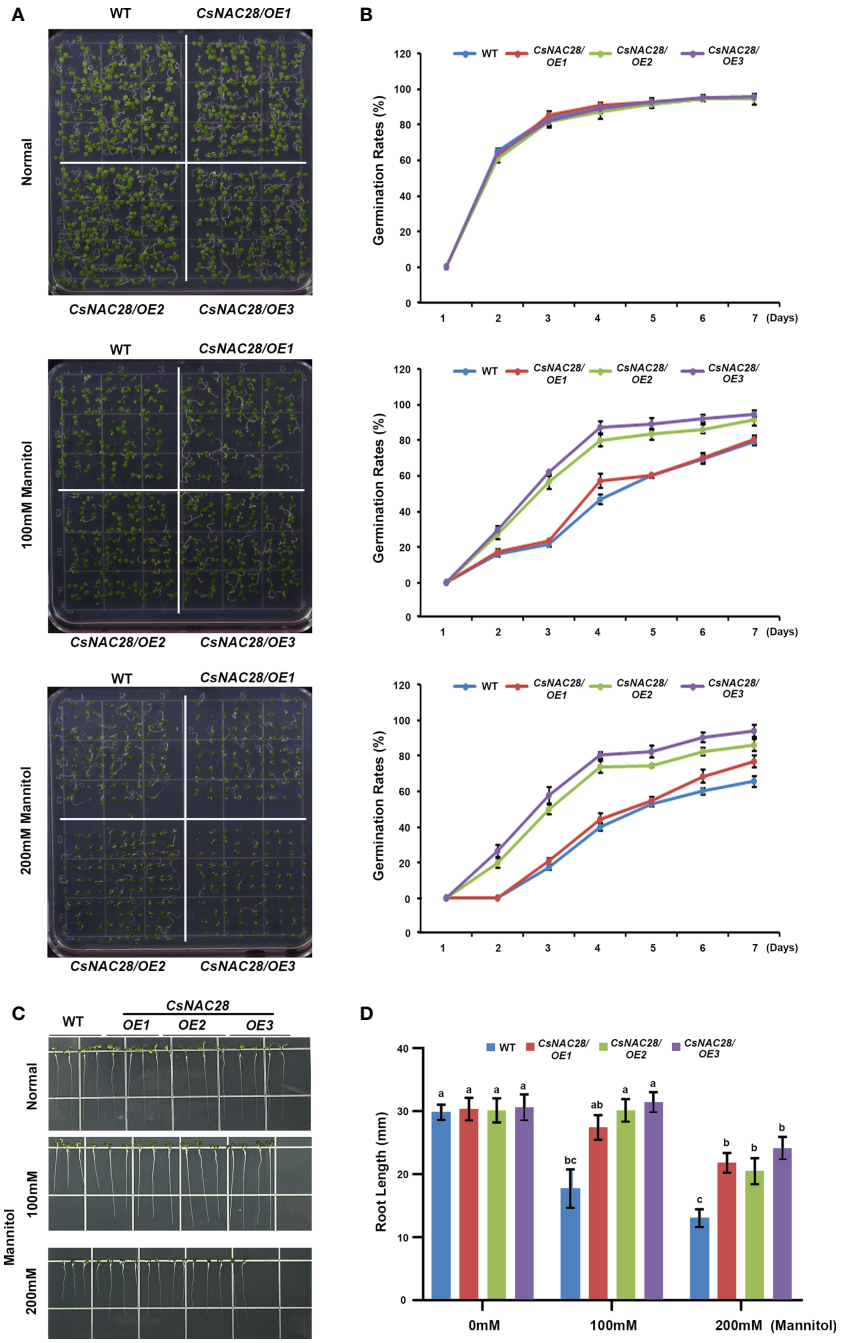


FIGURE 8
CsNAC28 overexpression promotes seed germination under simulated drought conditions. **(A)** Germination assay under different concentrations of mannitol treatments. **(B)** Germination percentage of each line after 7-day simulated drought treatment. **(C)** Root elongation assays under different concentrations of mannitol treatments. **(D)** Quantification of root length under different concentrations of mannitol treatments. Different letters indicate significant differences at P-value<0.05.

were higher in the *CsNAC28/OE* plants than in the WT plants. These results demonstrated that *CsNAC28* overexpression resulted in the additional upregulation of drought-responsive genes during drought treatment (Figure 9C).

Discussion

NAC transcription factors make up the most abundant plant-specific transcription family that plays a central role in

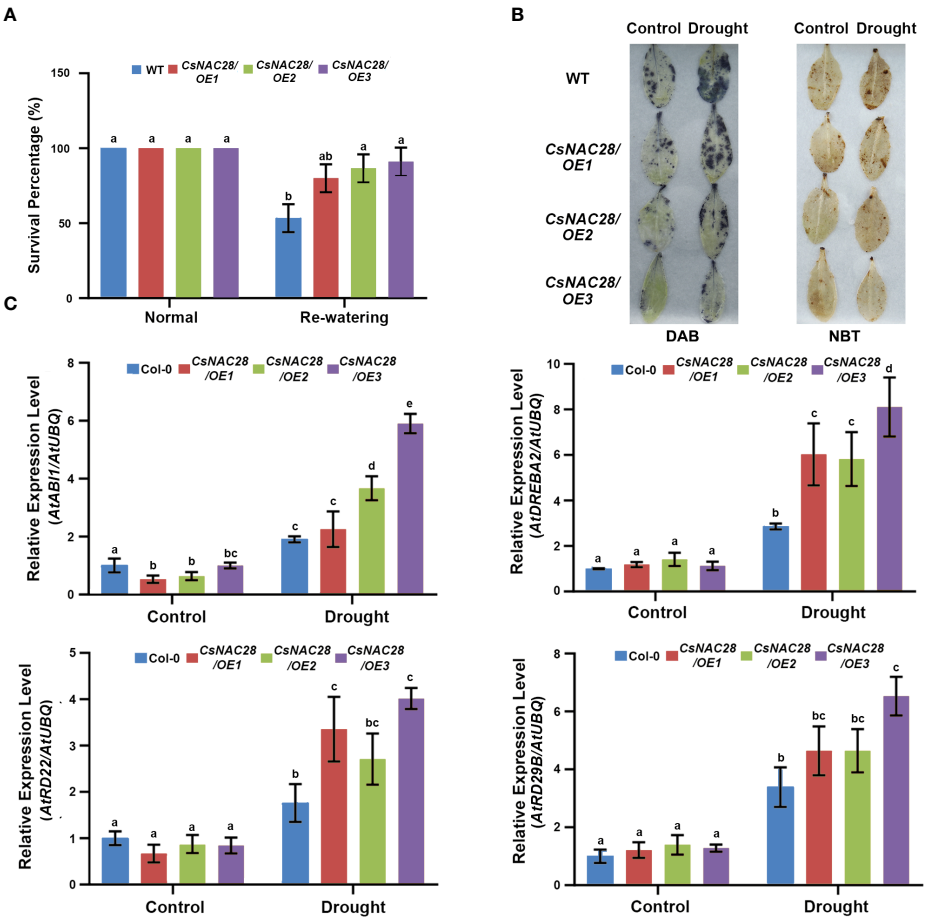


FIGURE 9
Overexpression of CsNAC28 improves drought stress tolerance in transgenic Arabidopsis. **(A)** Survival rates of the WT and transgenic lines at 7d of re-water. **(B)** Histochemical detection of hydrogen peroxide (H_2O_2) and superoxide (O^{2-}) using DAB staining and NBT staining. **(C)** The relative expression of four abiotic stress-responsive genes in transgenic lines and the WT under normal and drought stress conditions. Error bars indicate the SD of three biological replicates.

plants' growth, development, and response to environmental stimuli. Previous reports showed that 45 putative NAC sequences were identified in the tea plant (Wang et al., 2016b). In the current study, a total of 104 members of the enlarged NAC gene family were identified in *C. sinensis*. The genome sizes of Arabidopsis (125 Mb), *O. sativa* (480 Mb), and *P. trichocarpa* (1.07 Gb) are smaller than the genome size of *C. sinensis*, whereas the members of the NAC gene family of Arabidopsis (105), rice (151), and *P. trichocarpa* (167) are more numerous than in the tea plant (104) (Guillaume et al., 2003; Ooka et al., 2003; Tuskan et al., 2006; Hu et al., 2010; Korbinian et al., 2011; Nuruzzaman et al., 2010; Schneeberger et al., 2011). In particular, the CsNAC genes in subgroups B, F, and H are far fewer than in Arabidopsis and *P. trichocarpa*. The exon/intron location patterns of CsNACs were unified in all the phylogenetic subfamilies studied. Similar exon/intron structures were observed in the same subgroups as in Arabidopsis, *O. sativa*, and *P. trichocarpa* (Ooka et al., 2003; Hu et al., 2010; Nuruzzaman et al., 2010).

Genome duplication events have increased the evolution and expansion speed of these essential genes, which might provide genetic diversity and a greater ability for plants to survive under a variety of environmental pressures (Blanc et al., 2003; Crow et al., 2006). There are 49 segmental duplications found in the tea plants, and many species such as Arabidopsis, *O. sativa*, *P. trichocarpa*, and potatoes experienced an abundance of segmental duplication events (Olsen et al., 2005; Hu et al., 2006; Hu et al., 2010; Yan et al., 2021). Therefore, segment gene duplication plays a vital role in NAC gene family expansion. However, in comparing the size of the genome with NAC genes in different species, the low number of NAC genes in *C. sinensis* might be due to the whole-genome duplication events.

Drought stress is one of the most severe difficulties encountered by land plants; it disrupts plants' metabolism,

photosynthesis, and cell structure, thereby impairing plants' productivity (Pandey and Shukla, 2015; Chen et al., 2017; Qing et al., 2022). Recently, many studies have shown that NACs can upgrade the drought resistance of Arabidopsis, rice, wheat, and maize (Tran et al., 2004; Hu et al., 2006; Huang et al., 2015; Zhu et al., 2016). However, the research on stress-related NAC genes in tea plants was limited. NAC genes operate at multiple levels in ABA signaling networks (Fujita et al., 2011; Kuromori et al., 2018). Many NAC transcription factors have been reported to be upregulated by exogenous ABA and involved in an ABA-dependent signaling pathway in response to drought stress (Fujita et al., 2004; Ding et al., 2019; Chen et al., 2021). Herein, we showed that the expression of *CsNAC28* was strongly induced by treatment with ABA and PEG. The fact that the peak values of relative expression were different between them may be due to the fact that exogenous ABA induces conduction faster than drought stress induces endogenous signaling. Previous works indicated that ABF could bind to the ABRE *cis*-acting element in the promoter of NAC and thereby became involved in a drought stress response (Jia et al., 2022). Our study found that *CsABF2* could bind to the ABRE *cis*-acting element in the promoter of *CsNAC28* and activate *CsNAC28* expression.

ABA is the phytohormone most closely related to drought stress responses in plants. It causes stomatal closure, which decreases water loss, and is thus critical for drought resistance (Wu et al., 2019). Overexpression of *CsNAC28* in Arabidopsis reduced germination rates and shortened root lengths when ABA medium was added. Our study supported the finding that *CsNAC28* overexpression in Arabidopsis resulted in increased sensitivity to ABA and promoted ABA-mediated stomatal closure, which helped plants conserve water and have improved survival rates. Overexpression of *CsNAC28* in Arabidopsis upregulated the expression of drought-responsive genes (*ABI1*, *DREB2A*, *RD22*, and *RD29B*) and enhanced plants' survival rates under drought stress conditions. Our study found that *CsNAC28* was involved in the response to drought stress dependent on the ABA signal transduction pathway.

In contrast to the highly conserved NAC-binding domain at the N-terminal of NAC family proteins, the C-terminal transcription regulatory region is highly variable and usually functions as a transcriptional repressor or activator (Puranik et al., 2012). In this study, we demonstrated that *CsNAC28* was located in the nucleus and functioned as a transcriptional activator to modulate abiotic stress tolerance positively. Drought stress causes the excessive accumulation of ROS, which destroys plant performance and thus reduces crop yields. Hence, having an ROS scavenging system is crucial for plants to cope with drought stress (Verslues et al., 2006; Guo et al., 2022). The role of NAC transcription factors in regulating ROS scavenging systems under drought stress has been explored in other species. The Arabidopsis NAC transcription Jungbrunnen1 is induced by H_2O_2 and reduces the level of H_2O_2 in cells and improves various degrees of abiotic stress tolerance (Wu et al., 2012). In rice, *SNAC3* confers drought tolerance through the modulation of ROS (Fang et al., 2015). We found that compared with WT plants, *CsNAC28/OE* plants had a significantly reduced ROS content under drought stress. These findings indicated that WT plants suffered more serious oxidative damage than *CsNAC28* transgenic plants during the drought stress response. The improved antioxidant capability of *CsNAC28/OE* plants enhanced the drought resistance of transgenic Arabidopsis at the cellular level, laying the foundation for its drought-tolerant phenotype.

Conclusion

NAC plays an essential role in responses to abiotic stresses. Herein, we have identified 104 NAC transcription factors in *C. sinensis* and presented a comprehensive analysis of them. Importantly, our findings suggested that *CsNAC28* contributes to drought tolerance by regulating the expression of ABA-related genes and the antioxidant system. These results provide physiological and molecular evidence for the participation of *CsNAC28* in plants' drought tolerance.

Data availability statement

The original contributions presented in the study are included in the article/Supplementary Material. Further inquiries can be directed to the corresponding author.

Author contributions

XZ and GH designed the research and performed most of the experiments. LL, ZL, DL, YH, YZ, HT, JW and QL performed some of the experiments. XZ and GH were responsible for data analysis and wrote the manuscript. The authors agree with the content of the manuscript. All authors contributed to the article and approved the submitted version.

Funding

This work was funded by the National Natural Science Foundation of China under Grant No. 32000234, and the Zhejiang Provincial Natural Science Foundation of China under Grant No. LR22C02003, the Major Science and Technology Special Project of Variety Breeding of Zhejiang Province (2021C02067-7), and the State Key Laboratory for Managing Biotic and Chemical Threats to the Quality and Safety of Agro-products under Grant No. 2021DG700024-KF202102.

Conflict of interest

The authors declare that the research was conducted in the absence of any commercial or financial relationships that could be construed as a potential conflict of interest.

Publisher's note

All claims expressed in this article are solely those of the authors and do not necessarily represent those of their affiliated organizations, or those of the publisher, the editors and the reviewers. Any product that may be evaluated in this article, or claim that may be made by its manufacturer, is not guaranteed or endorsed by the publisher.

Supplementary material

The Supplementary Material for this article can be found online at: https://www.frontiersin.org/articles/10.3389/fpls.2022.1065261/full#supplementary-material

References

Bang, S. W., Choi, S., Jin, X., Jung, S. E., Choi, J. W., Seo, J. S., et al. (2022). Transcriptional activation of rice CINNAMOYL-CoA REDUCTASE 10 by OsNAC5, contributes to drought tolerance by modulating lignin accumulation in roots. *Plant Biotechnol. J.* 20, 736–747. doi: 10.1111/pbi.13752

Bengoa Luoni, S. A., Cenci, A., Moschen, S., Nicosia, S., Radonic, L. M., Sabio, Y., et al. (2021). Genome-wide and comparative phylogenetic analysis of senescence-associated NAC transcription factors in sunflower (*Helianthus annuus*). *BMC Genomics* 22, 893. doi: 10.1186/s12864-021-08199-5

Blanc, G., Hokamp, K., and Wolfe, K. H. (2003). A recent polyploidy superimposed on older large-scale duplications in the arabidopsis genome. *Genome Res.* 13, 137–144. doi: 10.1101/gr.751803

Cenci, A., Guignon, V., Roux, N., and Rouard, M. (2014). Genomic analysis of NAC transcription factors in banana (*Musa acuminata*) and definition of NAC orthologous groups for monocots and dicots. *Plant Mol. Biol.* 85, 63–80. doi: 10.1007/s11103-013-0169-2

Chen, C., Chen, H., Zhang, Y., Thomas, H. R., Frank, M. H., He, Y., et al. (2020). TBtools: An integrative toolkit developed for interactive analyses of big biological data. *Mol. Plant* 13, 1194–1202. doi: 10.1016/j.molp.2020.06.009

Chen, J., Gong, Y., Gao, Y., Zhou, Y. B., Chen, M., Xu, Z. S., et al. (2021). TaNAC48 positively regulates drought tolerance and ABA responses in wheat (L.). *Crop J.* 9, 785–793. doi: 10.1016/j.cj.2020.09.010

Chen, J., Nolan, T. M., Ye, H., Zhang, M., Tong, H., Xin, P., et al. (2017). Arabidopsis WRKY46, WRKY54, and WRKY70 transcription factors are involved in brassinosteroid-regulated plant growth and drought responses. *Plant Cell* 29, 1425–1439. doi: 10.1105/tpc.17.00364

Clough, S. J., and Bent, A. F. (1998). Floral dip: a simplified method for agrobacterium-mediated transformation of *Arabidopsis thaliana*. *Plant J.* 16, 735–743. doi: 10.1046/j.1365-313x.1998.00343.x

Crow, K. D., Wagner, G. P.Investigators, S. T.-N. Y. (2006). What is the role of genome duplication in the evolution of complexity and diversity? *Mol. Biol. Evol.* 23, 887–892. doi: 10.1093/molbev/msj083

Diao, W., Snyder, J. C., Wang, S., Liu, J., Pan, B., Guo, G., et al. (2018). Genome-wide analyses of the NAC transcription factor gene family in pepper (*Capsicum annuum* l.): Chromosome location, phylogeny, structure, expression patterns, cis-elements in the promoter, and interaction network. *Int. J. Mol. Sci.* 19, 1028. doi: 10.3390/ijms19041028

Ding, Y., and Lawrence, C. E. (2003). A statistical sampling algorithm for RNA secondary structure prediction. *Nucleic Acids Res.* 31, 7280–7301. doi: 10.1093/nar/gkg938

Ding, A., Li, S., Li, W., Hao, Q., Wan, X., Wang, K., et al. (2019). RhNAC31, a novel rose NAC transcription factor, enhances tolerance to multiple abiotic stresses in arabidopsis. *Acta Physiol. Plant* 41, 1–16. doi: 10.1007/s11738-019-2866-1

Ernst, H. A., Olsen, A. N., Larsen, S., and Lo Leggio, L. (2004). Structure of the conserved domain of ANAC, a member of the NAC family of transcription factors. *EMBO Rep.* 5, 297–303. doi: 10.1038/sj.embor.7400093

Fang, Y., Liao, K., Du, H., Xu, Y., Song, H., Li, X., et al. (2015). A stress-responsive NAC transcription factor SNAC3 confers heat and drought tolerance through modulation of reactive oxygen species in rice. *J. Exp. Bot.* 66, 6803–6817. doi: 10.1093/jxb/erv386

Finkelstein, R. R., Gampala, S. S., and Rock, C. D. (2002). Abscisic acid signaling in seeds and seedlings. *Plant Cell* 14, S15–S45. doi: 10.1105/tpc.010441

Fujita, M., Fujita, Y., Maruyama, K., Seki, M., Hiratsu, K., Ohme-Takagi, M., et al. (2004). A dehydration-induced NAC protein, RD26, is involved in a novel ABA-dependent stress-signaling pathway. *Plant J.* 39, 863–876. doi: 10.1111/j.1365-313X.2004.02171.x

Fujita, Y., Fujita, M., Shinozaki, K., and Yamaguchi-Shinozaki, K. (2011). ABA-mediated transcriptional regulation in response to osmotic stress in plants. *J. Plant Res.* 124, 509–525. doi: 10.1007/s10265-011-0412-3

Guillaume, B., Karsten, H., and Kenneth, H. W. (2003). A recent polyploidy superimposed on older large-scale duplications in the Arabidopsis genome. *Genome Res.* 13, 137–144.

Guo, X., Yu, X., Xu, Z., Zhao, P., Zou, L., Li, W., et al. (2022). CC-type glutaredoxin, MeGRXC3, associates with catalases and negatively regulates drought tolerance in cassava (*Manihot esculenta crantz*). *Plant Biotechnol. J.* 1–17. doi: 10.1111/pbi.13920

Han, T., Yan, J., Xiang, Y., and Zhang, A. (2021). Phosphorylation of ZmNAC84 at ser-113 enhances the drought tolerance by directly modulating ZmSOD2 expression in maize. *Biochem. Biophys. Res. Commun.* 567, 86–91. doi: 10.1016/j.bbrc.2021.06.026

He, Y., Zhang, X., Li, L., Sun, Z., Li, J., Chen, X., et al. (2021). SPX4 interacts with both PHR1 and PAP1 to regulate critical steps in phosphorus-status-dependent anthocyanin biosynthesis. *New Phytol.* 230, 205–217. doi: 10.1111/nph.17139

Huang, Q., Wang, Y., Li, B., Chang, J., Chen, M., Li, K., et al. (2015). TaNAC29, a NAC transcription factor from wheat, enhances salt and drought tolerance in transgenic arabidopsis. *BMC Plant Biol.* 15, 268. doi: 10.1186/s12870-015-0644-9

Hu, H., Dai, M., Yao, J., Xiao, B., Li, X., Zhang, Q., et al. (2006). Overexpressing a NAM, ATAF, and CUC (NAC) transcription factor enhances drought resistance and salt tolerance in rice. *Proc. Natl. Acad. Sci. U. S. A.* 103, 12987–12992. doi: 10.1073/pnas.0604882103

Hu, R., Qi, G., Kong, Y., Kong, D., Gao, Q., Zhou, G., et al. (2010). Comprehensive analysis of NAC domain transcription factor gene family in *Populus trichocarpa*. *BMC Plant Biol.* 10, 145. doi: 10.1186/1471-2229-10-145

Hu, Y., Zhang, M., Lu, M., Wu, Y., Jing, T., Zhao, M., et al. (2022). Salicylic acid carboxyl glucosyltransferase UGT87E7 regulates disease resistance in *Camellia sinensis*. *Plant Physiol.* 188, 1507–1520. doi: 10.1093/plphys/kiab569

Jensen, M. K., Kjaersgaard, T., Nielsen, M. M., Galberg, P., Petersen, K., O'Shea, C., et al. (2010). The *Arabidopsis thaliana* NAC transcription factor family: structure-function relationships and determinants of ANAC019 stress signalling. *Biochem. J.* 426, 183–196. doi: 10.1042/BJ20091234

Jiang, H., Li, H., Bu, Q., and Li, C. (2009). The RHA2a-interacting proteins ANAC019 and ANAC055 may play a dual role in regulating ABA response and jasmonate response. *Plant Signal Behav.* 4, 464–466. doi: 10.4161/psb.4.5.8543

Jiang, H., Tang, B., Xie, Z., Nolan, T., Ye, H., Song, G. Y., et al. (2019). GSK3-like kinase BIN2 phosphorylates RD26 to potentiate drought signaling in arabidopsis. *Plant J.* 100, 923–937. doi: 10.1111/tpj.14484

Jia, X., Zeng, Z., Lyu, Y., and Zhao, S. (2022). Drought-responsive NAC transcription factor RcNAC72 is recognized by RcABF4, interacts with RcDREB2A to enhance drought tolerance in arabidopsis. *Int. J. Mol. Sci.* 23, 1755. doi: 10.3390/ijms23031755

Jin, J. F., Wang, Z. Q., He, Q. Y., Wang, J. Y., Li, P. F., Xu, J. M., et al. (2020). Genome-wide identification and expression analysis of the NAC transcription

factor family in tomato (*Solanum lycopersicum*) during aluminum stress. *BMC Genomics* 21, 288. doi: 10.1186/s12864-020-6689-7

Kjaersgaard, T., Jensen, M. K., Christiansen, M. W., Gregersen, P., Kragelund, B. B., and Skriver, K. (2011). Senescence-associated barley NAC (NAM, ATAF1, 2, CUC) transcription factor interacts with radical-induced cell death 1 through a disordered regulatory domain. *J. Biol. Chem.* 286, 35418–35429. doi: 10.1074/jbc.M111.247221

Korbinian, S., Stephan, O., Felix, O., Klein, J. D., Xi, W., Christa, L., et al. (2011). Reference-guided assembly of four diverse Arabidopsis thaliana genomes. *Proc. Natl. Acad. Sci. U.S.A.* 108, 10249–10254.

Kuromori, T., Seo, M., and Shinozaki, K. (2018). ABA transport and plant water stress responses. *Trends Plant Sci.* 23, 513–522. doi: 10.1016/j.tplants.2018.04.001

Lee, D. K., Chung, P. J., Jeong, J. S., Jang, G., Bang, S. W., Jung, H., et al. (2017). The rice OsNAC6 transcription factor orchestrates multiple molecular mechanisms involving root structural adaptions and nicotianamine biosynthesis for drought tolerance. *Plant Biotechnol. J.* 15, 754–764. doi: 10.1111/pbi.12673

Li, X., Li, X., Li, M., Yan, Y., Liu, X., Li, L., et al. (2016). Dual function of NAC072 in ABF3-mediated ABA-responsive gene regulation in arabidopsis. *Front. Plant Sci.* 7, 1075. doi: 10.3389/fpls.2016.01075

Lindemose, S., Jensen, M. K., Van de Velde, J., O'Shea, C., Heyndrickx, K. S., Workman, C. T., et al. (2014). A DNA-binding-site landscape and regulatory network analysis for NAC transcription factors in *Arabidopsis thaliana*. *Nucleic Acids Res.* 42, 7681–7693. doi: 10.1093/nar/gku502

Liu, W., Sikora, E., and Park, S. W. (2020). Plant growth-promoting rhizobacterium, paenibacillus polymyxa CR1, upregulates dehydration-responsive genes, RD29A and RD29B, during priming drought tolerance in arabidopsis. *Plant Physiol. Biochem.* 156, 146–154. doi: 10.1016/j.plaphy.2020.08.049

Liu, Y., Sun, J., and Wu, Y. (2016). Arabidopsis ATAF1 enhances the tolerance to salt stress and ABA in transgenic rice. *J. Plant Res.* 129, 955–962. doi: 10.1007/s10265-016-0833-0

Liu, S. C., Yao, M. Z., Ma, C. L., Jin, J. Q., Ma, J. Q., Li, C. F., et al. (2015). Physiological changes and differential gene expression of tea plant under dehydration and rehydration conditions. *Sci. Hortic.* 184, 129–141. doi: 10.1016/j.scienta.2014.12.036

Liu, W., Zhao, B. G., Chao, Q., Wang, B., Zhang, Q., Zhang, C., et al. (2019). Function analysis of ZmNAC33, a positive regulator in drought stress response in arabidopsis. *Plant Physiol. Biochem.* 145, 174–183. doi: 10.1016/j.plaphy.2019.10.038

Lu, J., Du, J., Tian, L., Li, M., Zhang, X., Zhang, S., et al. (2021). Divergent response strategies of CsABF facing abiotic stress in tea plant: Perspectives from drought-tolerance studies. *Front. Plant Sci.* 12, 763843. doi: 10.3389/fpls.2021.763843

Lu, M., Ying, S., Zhang, D. F., Shi, Y. S., Song, Y. C., Wang, T. Y., et al. (2012). A maize stress-responsive NAC transcription factor, ZmSNAC1, confers enhanced tolerance to dehydration in transgenic arabidopsis. *Plant Cell Rep.* 31, 1701–1711. doi: 10.1007/s00299-012-1284-2

Mao, H., Li, S., Wang, Z., Cheng, X., Li, F., Mei, F., et al. (2020). Regulatory changes in TaSNAC8-6A are associated with drought tolerance in wheat seedlings. *Plant Biotechnol. J.* 18, 1078–1092. doi: 10.1111/pbi.13277

Mao, H., Wang, H., Liu, S., Li, Z., Yang, X., Yan, J., et al. (2015). A transposable element in a NAC gene is associated with drought tolerance in maize seedlings. *Nat. Commun.* 6, 8326. doi: 10.1038/ncomms9326

Mao, H., Yu, L., Han, R., Li, Z., and Liu, H. (2016). ZmNAC55, a maize stress-responsive NAC transcription factor, confers drought resistance in transgenic arabidopsis. *Plant Physiol. Biochem.* 105, 55–66. doi: 10.1016/j.plaphy.2016.04.018

Mei, F., Chen, B., Li, F., Zhang, Y., Kang, Z., Wang, X., et al. (2021). Overexpression of the wheat NAC transcription factor TaSNAC4-3A gene confers drought tolerance in transgenic arabidopsis. *Plant Physiol. Biochem.* 160, 37–50. doi: 10.1016/j.plaphy.2021.01.004

Nuruzzaman, M., Manimekalai, R., Sharoni, A. M., Satoh, K., Kondoh, H., Ooka, H., et al. (2010). Genome-wide analysis of NAC transcription factor family in rice. *Gene.* 465, 30–44. doi: 10.1016/j.gene.2010.06.008

Olsen, A. N., Ernst, H. A., Leggio, L. L., and Skriver, K. (2005). NAC transcription factors: structurally distinct, functionally diverse. *Trends Plant Sci.* 10, 79–87. doi: 10.1016/j.tplants.2004.12.010

Ooka, H., Satoh, K., Doi, K., Nagata, T., Otomo, Y., Murakami, K., et al. (2003). Comprehensive analysis of NAC family genes in *Oryza sativa* and *Arabidopsis thaliana*. *DNA Res.* 10, 239–247. doi: 10.1093/dnares/10.6.239

Pandey, V., and Shukla, A. (2015). Acclimation and tolerance strategies of rice under drought stress. *Rice Sci.* 22, 147–161. doi: 10.1016/j.rsci.2015.04.001

Puranik, S., Sahu, P. P., Srivastava, P. S., and Prasad, M. (2012). NAC proteins: regulation and role in stress tolerance. *Trends Plant Sci.* 17, 369–381. doi: 10.1016/j.tplants.2012.02.004

Qing, Y., Wang, S., Ancell, B. C., and Yang, Z. L. (2022). Accelerating flash droughts induced by the joint influence of soil moisture depletion and atmospheric aridity. *Nat. Commun.* 13, 1139. doi: 10.1038/s41467-022-28752-4

Redillas, M. C., Jeong, J. S., Kim, Y. S., Jung, H., Bang, S. W., Choi, Y. D., et al. (2012). The overexpression of OsNAC9 alters the root architecture of rice plants enhancing drought resistance and grain yield under field conditions. *Plant Biotechnol. J.* 10, 792–805. doi: 10.1111/j.1467-7652.2012.00697.x

Schneeberger, K., Ossowski, S., Ott, F., Klein, J. D., Wang, X., Lanz, C., et al. (2011). Reference-guided assembly of four diverse *Arabidopsis thaliana* genomes. *Proc. Natl. Acad. Sci. U. S. A.* 108, 10249–10254. doi: 10.1073/pnas.1107739108

Seo, P. J., Kim, S. G., and Park, C. M. (2008). Membrane-bound transcription factors in plants. *Trends Plant Sci.* 13, 550–556. doi: 10.1016/j.tplants.2008.06.008

Souer, E., van, H. A., Kloos, D., Mol, J., and Koes, R. (1996). The no apical meristem gene of petunia is required for pattern formation in embryos and flowers and is expressed at meristem and primordia boundaries. *Cell* 85, 159–170. doi: 10.1016/S0092-8674(00)81093-4

Sun, Z., Feng, Z., Ding, Y., Qi, Y., Jiang, S., Li, Z., et al. (2022). RAF22, ABI1 and OST1 form a dynamic interactive network that optimizes plant growth and responses to drought stress in arabidopsis. *Mol. Plant* 15, 1192–1210. doi: 10.1016/j.molp.2022.06.001

Su, H., Zhang, S., Yuan, X., Chen, C., Wang, X. F., and Hao, Y. J. (2013). Genome-wide analysis and identification of stress-responsive genes of the NAM-ATAF1, 2-CUC2 transcription factor family in apple. *Plant Physiol. Biochem.* 71, 11–21. doi: 10.1016/j.plaphy.2013.06.022

Tran, L. S., Nakashima, K., Sakuma, Y., Simpson, S. D., Fujita, Y., Maruyama, K., et al. (2004). Isolation and functional analysis of arabidopsis stress-inducible NAC transcription factors that bind to a drought-responsive cis-element in the early responsive to dehydration stress 1 promoter. *Plant Cell* 16, 2481–2498. doi: 10.1105/tpc.104.022699

Tuskan, G. A., Difazio, S., Jansson, S., Bohlmann, J., Grigoriev, I., Hellsten, U., et al. (2006). The genome of black cottonwood, *Populus trichocarpa*. *Science* 313, 1596–1604. doi: 10.1126/science.1128691

Verslues, P. E., Agarwal, M., Katiyar-Agarwal, S., Zhu, J., and Zhu, J. K. (2006). Methods and concepts in quantifying resistance to drought, salt and freezing, abiotic stresses that affect plant water status. *Plant J.* 45, 523–539. doi: 10.1111/j.1365-313X.2005.02593.x

Wang, Y. X., Liu, Z. W., Wu, Z. J., Li, H., and Zhuang, J. (2016b). Transcriptome-wide identification and expression analysis of the NAC gene family in tea plant [*Camellia sinensis* (L.) o. kuntze]. *PloS One* 11, e0166727. doi: 10.1371/journal.pone.0166727

Wang, W., Xin, H., Wang, M., Ma, Q., Wang, L., Kaleri, N. A., et al. (2016a). Transcriptomic analysis reveals the molecular mechanisms of drought-Stress-Induced decreases in *Camellia sinensis* leaf quality. *Front. Plant Sci.* 7, 385. doi: 10.3389/fpls.2016.00385

Wang, G., Yuan, Z., Zhang, P., Liu, Z., Wang, T., and Wei, L. (2020). Genome-wide analysis of NAC transcription factor family in maize under drought stress and rewatering. *Physiol. Mol. Biol. Plants* 26, 705–717. doi: 10.1007/s12298-020-00770-w

Wei, C., Yang, H., Wang, S., Zhao, J., Liu, C., Gao, L., et al. (2018). Draft genome sequence of *Camellia sinensis* var. *sinensis* provides insights into the evolution of the tea genome and tea quality. *Proc. Natl. Acad. Sci. U. S. A.* 115, E4151–E4158. doi: 10.1073/pnas.1719622115

Wu, A., Allu, A. D., Garapati, P., Siddiqui, H., Dortay, H., Zanor, M. I., et al. (2012). JUNGBRUNNEN1, a reactive oxygen species-responsive NAC transcription factor, regulates longevity in arabidopsis. *Plant Cell* 24, 482–506. doi: 10.1105/tpc.111.090894

Wu, Q., Wang, M., Shen, J., Chen, D., Zheng, Y., Zhang, W., et al. (2019). ZmOST1 mediates abscisic acid regulation of guard cell ion channels and drought stress responses. *J. Integr. Plant Biol.* 61, 478–491.

Xiang, Y., Sun, X., Bian, X., Wei, T., Han, T., Yan, J., et al. (2021). The transcription factor ZmNAC49 reduces stomatal density and improves drought tolerance in maize. *J. Exp. Bot.* 72, 1399–1410. doi: 10.1093/jxb/eraa507

Xue, G. P., Way, H. M., Richardson, T., Drenth, J., Joyce, P. A., and McIntyre, C. L. (2011). Overexpression of TaNAC69 leads to enhanced transcript levels of stress up-regulated genes and dehydration tolerance in bread wheat. *Mol. Plant* 4, 697–712. doi: 10.1093/mp/ssr013

Xu, Z. Y., Kim, S. Y., Hyeon, D. Y., Ki, D. H., Dong, T., Park, Y., et al. (2013). The arabidopsis NAC transcription factor ANAC096 cooperates with bZIP-type transcription factors in dehydration and osmotic stress responses. *Plant Cell* 25, 4708–4724. doi: 10.1105/tpc.113.119099

Yamaguchi, S. K., and Shinozaki, K. (1993). The plant hormone abscisic acid mediates the drought-induced expression but not the seed-specific expression of rd22, a gene responsive to dehydration stress in *Arabidopsis thaliana*. *Mol. Gen. Genet.* 238, 17–25. doi: 10.1007/BF00279525

Yang, X. W., He, K., Chi, X. Y., Chai, G. H., Wang, Y. P., Jia, C. L., et al. (2018). Miscanthus NAC transcription factor MlNAC12 positively mediates abiotic stress tolerance in transgenic arabidopsis. *Plant Sci.* 277, 229–241. doi: 10.1016/j.plantsci.2018.09.013

Yang, C. S., and Hong, J. (2013). Prevention of chronic diseases by tea: possible mechanisms and human relevance. *Annu. Rev. Nutr.* 33, 161–181. doi: 10.1146/annurev-nutr-071811-150717

Yan, H., Ma, G., Silva, J. A. T. D., Qiu, L., Xu, J., Zhou, H., et al. (2021). Genome-wide identification and analysis of NAC transcription factor family in two diploid wild relatives of cultivated sweet potato uncovers potential NAC genes related to drought tolerance. *Front. Genet.* 12, 744220. doi: 10.3389/fgene.2021.744220

Yu, M., Liu, J., Du, B., Zhang, M., Wang, A., and Zhang, L. (2021). NAC transcription factor PwNAC11 activates ERD1 by interaction with ABF3 and DREB2A to enhance drought tolerance in transgenic arabidopsis. *Int. J. Mol. Sci.* 22, 6952. doi: 10.3390/ijms22136952

Zhao, J., Li, P., Xia, T., and Wan, X. (2020). Exploring plant metabolic genomics: chemical diversity, metabolic complexity in the biosynthesis and transport of specialized metabolites with the tea plant as a model. *Crit. Rev. Biotechnol.* 40, 667–688. doi: 10.1080/07388551.2020.1752617

Zhu, Y., Yan, J., Liu, W., Liu, L., Sheng, Y., Sun, Y., et al. (2016). Phosphorylation of a NAC transcription factor by a Calcium/Calmodulin-dependent protein kinase regulates abscisic acid-induced antioxidant defense in maize. *Plant Physiol.* 171, 1651–1664. doi: 10.1104/pp.16.00168

frontiers | Frontiers in Plant Science

TYPE Original Research
PUBLISHED 12 December 2022
DOI 10.3389/fpls.2022.1078330

Check for updates

OPEN ACCESS

EDITED BY
Meng Jiang,
Zhejiang University, China

REVIEWED BY
Feng Xue,
Qingdao Agricultural University, China
Faisal Islam,
Zhejiang University, China
Erli Niu,
Zhejiang Academy of Agricultural Sciences, China

*CORRESPONDENCE
Jun Huang
huangjun@zust.edu.cn
hjunlzr@163.com

SPECIALTY SECTION
This article was submitted to Plant Abiotic Stress, a section of the journal Frontiers in Plant Science

RECEIVED 24 October 2022
ACCEPTED 28 November 2022
PUBLISHED 12 December 2022

CITATION
Zhao Q, Li Q, Lin S, Hou R, Liu J, Tao Y, Li Y, Zhou Y, Ye Z, Yu X and Huang J (2022) *De Novo* transcriptome combined with physiological analyses revealed key genes for cadmium accumulation in Zhe-Maidong (*Ophiopogon japonicus*). *Front. Plant Sci.* 13:1078330. doi: 10.3389/fpls.2022.1078330

COPYRIGHT
© 2022 Zhao, Li, Lin, Hou, Liu, Tao, Li, Zhou, Ye, Yu and Huang. This is an open-access article distributed under the terms of the Creative Commons Attribution License (CC BY). The use, distribution or reproduction in other forums is permitted, provided the original author(s) and the copyright owner(s) are credited and that the original publication in this journal is cited, in accordance with accepted academic practice. No use, distribution or reproduction is permitted which does not comply with these terms.

De Novo transcriptome combined with physiological analyses revealed key genes for cadmium accumulation in Zhe-Maidong (*Ophiopogon japonicus*)

Qian Zhao[1], Qing Li[1], Shuting Lin[1], Ruijun Hou[1], Jianying Liu[1], Yachen Tao[1], Ye Li[1], Yifeng Zhou[1], Zihong Ye[2], Xiaoping Yu[2] and Jun Huang[1]*

[1]School of Biological and Chemical Engineering, Zhejiang University of Science and Technology, Hangzhou, China, [2]College of Life Science, China Jiliang University, Hangzhou, China

Introduction: Cadmium (Cd) is a toxic heavy metal that severely threatens safe food production. Zhe-Maidong, a well-known Chinese traditional herbal medicine, is susceptible to Cd stress. However, the characteristics of Cd transformation and migration, as well as the regulatory system for genes conferring Cd accumulation of Zhe-Maidong, remains an essential issue to be addressed.

Methods: Zhe-Maidong seedling growth in Cd-contaminated and uncontaminated soil was conducted for 90 days. The Cd concentration was determined by inductively coupled plasma-mass spectrometry, and the Cd^{2+} fluorescence probe detected Cd distributions. The root transcriptome of Zhe-Maidong was then evaluated using various Cd stress hydroponic treatments designated Cd-0, Cd-M, and Cd-H.

Results and discussion: The enrichment factor (EF) value in the root was four times that of the leaves, indicating that the root has a high ability to absorb and accumulate Cd. The Cd^{2+} were mainly distributed in the root hair and the epidermis in both roots and leaves, revealing that the epidermal cells of roots may collect Cd^{2+} and also have an outstanding role in Cd^{2+} uptake. A total of 50 DEGs involved in Cd translocation and accumulation were identified. Among these DEGs, ANN, ABCC2/4, HMA1- 5, and CCX gene expression were positively correlated with EF-root, EF-leaf, EF-total, Cd-leaf, Cd-root, and Cd-plant, indicating their role in Cd transport and accumulation under Cd-stress. These data could be helpful in uncovering the Cd accumulation characteristics in Zhe-Maidong, as well as provide a bioinformatic foundation for investigations on finding gene functions and the screening of candidate genes related to Cd accumulation.

KEYWORDS

Zhe-Maidong (Ophiopogon japonicus), cadmium stress, cadmium accumulation and distribution, transcriptome, transporters

1 Introduction

Zhe-Maidong (*Ophiopogon japonicus* (L.f.) Ker-Gawl) is a prominent Chinese traditional herbal medicine that has been widely used in China for more than 2000 years (Liu et al., 2017). According to traditional Chinese medical theory, it replenishes the *yin*, enhances body fluid production, moistens the lung, and relieves heartburn (Yu et al., 2021). Zhe-Maidong contains a range of phytochemicals like as flavonoids, saponin, and polysaccharides, and it has antioxidation, anti-inflammation, immunomodulation, cardiovascular protection, and anticancer properties (Liu et al., 2017). In recent years, with the growth of the traditional Chinese medicine industry and the expansion of global commerce (Fu et al., 2021), the planting area of Zhe-Maidong has extended steadily. However, most farmers cultivate Zhe-Maidong in a dispersed manner, and soil and climate conditions were not considered before planting, resulting in poor quality and heavy metal residues in Zhe-Maidong (Jiang et al., 2018).

Rapid industrialization in China during the last three decades has resulted in widespread contamination of Cadmium (Cd) in agricultural soils (Wang et al., 2019a; Fu et al., 2021). Due to the high mobility, Cd is easily absorbed by plants, posing a severe threat to safe food production (Chihmin et al., 2021). Zhe-Maidong is primarily and widely planted in Zhejiang Province, and its grade quality is superior to all other *O. japonicus* produced in China. However, previous research has found that the rate of Cd concentrations exceeding the Chinese herbal medical limit is around 16.67% during 2003–2020 in Zhejiang province (Wang et al., 2019b; Chao et al., 2021). Moreover, Cd content detection on several batches of *O. japonicus* revealed that a portion of the product exceeded the threshold for the Cd limit (Wang et al., 2021). In light of the nutritional significance of Zhe-Maidong, it is urgent to comprehend the mechanism of cadmium absorption and transport to provide a crucial foundation for alleviating cadmium accumulation.

To date, numerous studies have been undertaken to investigate relationships between plant and soil Cd levels on the factors of the metal availability in soil, the root uptake processes, Cd distribution in plant organs, as well as mechanisms of Cd adsorption and essential genes for Cd transport in various plant species. Multiple pieces of research have demonstrated that Cd distribution in plants varies significantly between species and within a species, depending on the population or cultivar. (Florijn and Van Beusichem, 1993; Greger and Löfstedt, 2004; Laporte et al., 2015; Lewis et al., 2018; Huang et al., 2020; Zhang et al., 2022; Chi et al., 2022). In addition, several studies have explored the biological mechanisms of Cd accumulation in plants, emphasizing identifying the genes and proteins involved in Cd absorption, transport, storage, and detoxification in plant tissues. A number of genes were responsible for Cd uptake, transportation, and phloem loadings, such as IRT1 (iron-regulated transporter-ZIP family), natural resistance-associated macrophage protein (NRAMP), the heavy metal ATPase (HMA) transporters, and ABC transporters in rice, barley, *Arabidopsis thaliana*, and *Sedum plumbizincicola* (Sterckeman and Thomine, 2020). However, the characteristics of Cd transformation and migration, as well as the regulatory system for genes conferring Cd accumulation of Zhe-Maidong, remains an essential issue to be addressed.

We conducted different Cd treatments in the present study using two culture systems (soil cultivation and hydroponics). Initially, Zhe-Maidong growth in Cd-contaminated soil was employed to evaluate the regularities of transformation and migration, as well as the distribution of Cd in Zhe-Maidong tissues. Following that, RNA sequencing (RNA-Seq) techniques were used to identify candidate genes related to Cd accumulation in the root of Zhe-Maidong treated by hydroponic. And the expression of critical genes associated with Cd accumulation was further validated by quantitative real-time PCR (qRT-PCR). Finally, to screen the core genes closely related to Cd accumulation, we performed a correlation coefficient analysis on the relative expression of several essential genes and the Cd accumulation main feature of Zhe-Maidong under Cd-contaminated soil. These data could be helpful in uncovering the Cd accumulation characteristics in Zhe-Maidong, as well as provide a bioinformatic foundation for investigations on the finding of gene functions and the screening of candidate genes connected to Cd absorption and translocation.

2 Materials and methods

2.1 Plant materials and treatments

Zhe-Maidong was collected from Cixi, Zhejiang Province, PR China. All the samples were authenticated by Prof. Fangmin Cheng (Zhejiang University, Zhejiang, PR China). 1-year-old seedlings with uniformity development were selected. We only preserved 5-6 inner leaves, cut off the underground part at the stem's base, and kept 10-12 cm of the leaves. Then the plants were conducted with different Cd^{2+} treatments.

Experiment I:

The contaminated soil (CS) and uncontaminated soil (UCS) were collected from Fuyang, Zhejiang province. As shown in Table 1, the Cd content of CS exceeds the national Grade II value for soil Cd levels in China (0.3 mg/kg). One hundred seedlings were randomly separated into two groups (CS treatment or UCS treatment) and then transplanted into 10 L plastic pots (two plants per pot) filled with the corresponding soil (CS or UCS). The pots were placed in a greenhouse with natural light conditions and an average daily temperature of 25°C to 28°C. And the plants were uniformly managed and usually irrigated every 2-3 days, depending on requirements. Plants were grown for 90 days before harvesting.

TABLE 1 Cd concentrations and physicochemical properties of tested soils.

Soil	Cd concentration (mg/kg)	Available Cd concentration (mg/kg)	Moisture content (%)	pH	Total nitrogen (g/kg)	Available phosphorus (mg/kg)	Available potassium (mg/kg)
CS	0.38 ± 0.03*	0.21 ± 0.01*	44.60 ± 0.05	5.65 ± 0.06	1.98 ± 0.19	26.75 ± 2.5	134.00 ± 10.83
USC	0.11 ± 0.01	0.11 ± 0.00	46.72 ± 0.1	5.88 ± 0.24	1.98 ± 0.29	25.50 ± 2.89	125.25 ± 5.50

CS and UCS indicated contaminated soil and uncontaminated soil, respectively. * Indicate significant differences at $p< 0.05$ level among different treatments.

Experiment II:

The obtained seedlings were initially pre-cultured on the artificial substrate for 15 days. For hydroponic experiments, seedlings with uniform morphology were selected. The seedlings were transplanted to 15 L plastic pots (12 plants per pot) containing 10L 1/2-strength Hoagland's nutrient solution under daily conditions of 25°C to 28°C. Then the plants grown in different pots were randomly classified into three groups. The treatments were the control (Cd-0), 1 mg/L Cd (Cd-M) (the maximum permitted Cd content in soil for agriculture), and 10 mg/L Cd (Cd-H), with three replicate pots for each treatment. The pH of the nutrient solution was adjusted to pH 6.0 ± 0.1. Plants were cultured in a greenhouse under natural light conditions and with an average diurnal temperature of 25°C to 28°C. The nutrient solution was renewed every three days. After 30 days of treatments, the roots were sampled and immediately frozen in liquid nitrogen and then stored at −80°C for RNA extraction.

2.2 Cd concentration detection and calculation of enrichment factor and transfer factor

Dried samples were digested in concentrated nitric acid (HNO_3) and hydrogen peroxide (H_2O_2) at 120°C by Digi-Block ED54 digestion system (LabTech, Wilmington, MA, USA). According to (Pan et al., 2021), the Cd concentration was determined by inductively coupled plasma-mass spectrometry (ICP-MS; XSeries 2, Thermo, Waltham, MA, USA). Three biological replicates were used in each experiment.

The enrichment factor (EF) indices were calculated as follows:

$$EF_{root} = C_{root}/C_{soil}$$

$$EF_{leaf} = C_{leaf}/C_{soil}$$

$$EF_{plant} = (C_{root} + C_{leaf})/C_{soil}$$

The transfer factor (TF) indices were calculated as follows:

$$TF = C_{leaf}/C_{root}$$

Where C_{root}, C_{leaf}, and C_{soil} (mg/kg) represent the metal concentration in the dried samples of root, leaf, and soil, respectively.

2.3 Intracellular Cd localization

Fresh samples were placed in a small box filled with an optimal cutting temperature compound (OCT), which was then frozen with liquid nitrogen. The tissue blocks were sliced by a frozen section machine (CM1950, Leica, USA) at 10 μm and placed on slides. Detection of Cd^{2+} distribution and its fluorescence intensity in developing anthers was performed according to previous studies (Xue et al., 2020). Frozen sections were rinsed with PBS three times before incubating in a Cd^{2+} probe (Life Leadmium™ Green AM dye) at 28°C in the dark for 10 min. The fluorescence signals were observed by using confocal microscopy (Eclipse NI, Nikon, Japan).

2.4 RNA extraction, library preparation, and sequencing

The total RNA was isolated from the roots of Zhe-Maidong using a Trizol Plant RNA Extraction Kit (Takara Bio, Japan). Utilizing the RNA Nano 6000 Assay Kit of the Bioanalyzer 2100, the total quantities and integrity of RNA were determined (Agilent Technologies, CA, USA). According to the manufacturer's instructions, mRNA was enhanced with oligo (dT) beads and fragmented into small fragments. mRNA was reverse transcribed into cDNA using random primers (Illumina, Inc., San Diego, United States). Illumina NovaSeq 6000 equipment was used to sequence the cDNA library products in paired-end sequencing technology with read lengths of 150 bp by Novogene Co. (Guangzhou, China). Each experiment included three biological replicates.

2.5 Filtering of sequencing data and *de novo* assembly

Low-quality reads (Q-value ≤ 20) and reads containing more than 10% ambiguous 'N' bases were declared poor-quality reads

and deleted, leaving the remaining clean reads. The clean reads were used for *de novo* assembly using Trinity software (v2.6.6). Contigs were clustered and constructed based on paired-end information. Trinity found extended non-terminal sequences of contigs, and the resulting sequences were designated as unigenes. All assembled unigenes were searched using BLASTX against public protein databases with an E-value of less than 1.0×10^{-5}; the databases included the Nr (NCBI non-redundant protein database), Nt String (NCBI non-redundant nucleotide sequences), Pfam (Protein family), KOG/COG (Clusters of Orthologous Groups of proteins), Swiss-Prot (A manually annotated and reviewed protein sequence database), KO (KEGG Ortholog database), and GO (Gene Ontology).

2.6 Differential expression analysis

Differential expression analysis of two treatments (three biological replicates per condition) was performed using the DESeq2 R package (1.20.0). DESeq2 provides statistical routines for determining differential expression in digital gene expression data using a model based on the negative binomial distribution. The resulting P-values were adjusted using Benjamini and Hochberg's approach for controlling the false discovery rate. The threshold for significantly different expressions was set as padj0.05 and $|\ Log_2\ (foldchange)| > 1$.

2.7 qRT-PCR analysis

The cDNA preparation was carried out as described by the instructions (TaKaRa, Japan). SYBR Green real-time PCR Master Mix reagent Kit was used for qRT-PCR (Toyobo, Osaka, Japan). Reactions were performed using the Bio-Rad CFX96 real-time system (Bio-Rad, USA) according to the manufacturer's protocol. Supplemental Table S1 lists the gene-specific primer pairs utilized in this study. Tublin (Cluster-21637.82800) expression was used to normalize the amplification of genes, and their relative expression levels were calculated using the 2 (-CT) method. The mean values and standard errors were calculated using three separate biological replicates in triplicate.

2.8 Statistical analysis

Data were presented as the means of three biological repetitions ± standard deviation. Data were analyzed by one-way analysis of variance (ANOVA) using SPSS 19.0 (IBM, Portsmouth, UK). Correlation effects were calculated by Origin software. Different letters and * indicate significant differences at $p< 0.05$ level among different treatments.

3 Results

3.1 Cd accumulation and distribution in Zhe-Maidong leaves and roots

According to the results presented in Figure 1 and Table 2, the Cd content in the root and leaf tissues of Zhe-Maidong was significantly increased after being treated with cadmium-contaminated soil (CS). And the rise in Cd content was markedly more significant in the root than in the leaf. The Cd content of Zhe-Maidong roots and leaves was 1.14 mg/kg and 0.16 mg/kg, respectively, when the soil Cd concentration was 0.375 mg/kg and the available Cd concentration was 0.207 mg/kg after 90 days of CS treatment. The enrichment factor (EF) was increased significantly with the CS treatment, especially in the root. The total EF of Zhe-Maidong under CS treatment was 2.34, of which the EF of roots was as high as 1.88, while the EF of leaves was 0.46 (Table 2). The EF value of the roots was almost four times higher than that of the leaves. It was noteworthy that the transfer factor (TF) was significantly lower in the CS treatment than in the UCS, which was mainly attributed to the extremely low and similar Cd content deposited in the roots and leaves of Zhe-Maidong in the UCS.

Cd distributions in the leaf and root tissues were detected by the Cd^{2+} fluorescence probe, as shown in Figure 1. The result showed that the preferential Cd^{2+} fluorescence in the leaves was distributed to the upper epidermis, xylem, phloem, and lower epidermis, while the Cd^{2+} in the roots were mainly distributed in root hair, epiblema, and metaxylem. In addition, we found that the intensity of Cd^{2+} fluorescence was most noticeable in the hair and epidermis of the root, followed by the epidermis, xylem, and phloem in the leaf. It was suggested that these tissues/cells were significant sites for the Cd^{2+} uptake and accumulation in Zhe-Maidong.

3.2 Sequencing and *de novo* transcriptome assembly

Various Cd stress hydroponic treatments, designated Cd-0, Cd-M, and Cd-H, were performed to evaluate the root transcriptome of Zhe-Maidong under Cd stress (Figure 2A). There were no discernible differences in the biomass, morphology, plant length, and so on among Cd-0, Cd-M, and Cd-H (data not shown). However, under Cd stress (Cd-M and Cd-H), the root tips of Zhe-Maidong turned somewhat yellow, indicating an unhealthy situation. The Cd^{2+} fluorescence was detectable in the Zhe-Maidong roots subjected to various Cd stress hydroponic treatments with the intensity order Cd-H > Cd-M (Figure 2B).

Total RNA was isolated from the roots and subjected to various Cd stress hydroponic treatments to determine RNA

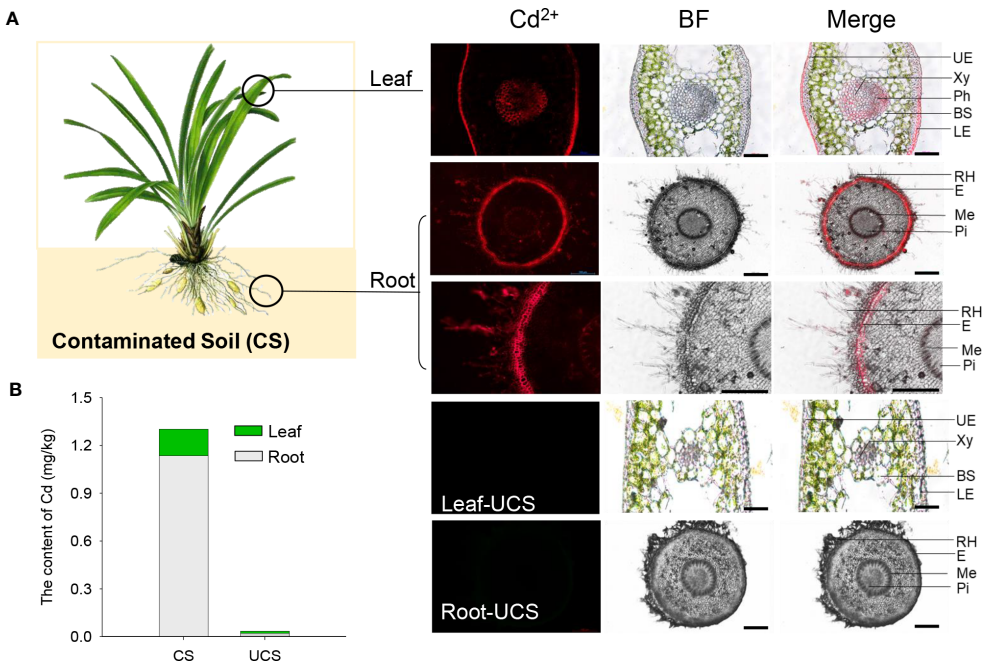


FIGURE 1
Analyses of Cd accumulation and distribution in Zhe-Maidong. **(A)** The distribution of Cd^{2+} in Zhe-Maidong leaves and roots using Leadmium Green AM dye. BF, bright field; Merge, the overlap of Cd^{2+} fluorescence and bright field. For each treatment, images from three technical replicates for three biological repeats were collected. UE, upper epidermis; Xy, xylem; Ph, phloem; BS, bundle sheath; LE, lower epidermis; RH, root hair; E, epiblema; Me, metaxylem; Pi, pith. Bars = 100 μm. **(B)** The Cd content in different tissues of Zhe-Maidong. CS, contaminated soil; UCS, uncontaminated soil.

sequencing and then performed on the Illumina NovaSeq 6000 equipment. After filtering sequencing data, a total of 212,557,374 clean reads of 9 samples were retained, with more than 92% Q30 bases acquired (Supplemental Table S2). The assembled unigenes were searched against several databases, including NR, NT, KOG, Pfam, and Go by BLAST. There were 68,148 (40.43%), 38,358 (22.76%), 47,628 (28.25%), 15,310 (9.08%), and 47,625 (28.25%) unigenes annotated by the NR, NT, Pfam, KOG, and Go databases, respectively (Figure 2C). Compared with the other databases, the NR database presented the highest proportion of annotations. Overall, the unigene sequences exhibited the most similar BLASTx matches to gene sequences from *Asparagus officinalis* (34,542), followed by *Elaeis guineensis* (3,206), *Phoenix dactylifera* (3,177), *Ananas comosus* (1,419), *Vitis vinifera* (1,155), *Musa acuminata* (1,134), and so on (Figure 2D).

3.3 Annotation and classification of Zhe-Maidong unigenes

GO analysis was used to classify the functions of the Zhe-Maidong unigenes. There were 183,939 unigenes successfully classified into 42 functional groups, which were further subdivided into three core GO categories: biological processes, cell components, and molecular function (Figure 2E). The dominant subcategories of the classified genes included 'cellular process' (26,640) and 'metabolic process' (23,932) in

TABLE 2 Cd contents in Zhe-Maidong with different soil.

Soil	Cd content (mg/kg)			EF			TF
	Root	Leaf	Plant	Root	Leaf	Total	
CS	0.68 ± 0.01*	0.17 ± 0.01*	0.85 ± 0.02*	1.88 ± 0.05*	0.46 ± 0.04*	2.34 ± 0.09*	0.24 ± 0.02
UCS	0.03 ± 0.00	0.02 ± 0.00	0.04 ± 0.00	0.25 ± 0.03	0.15 ± 0.01	0.40 ± 0.04	0.62 ± 0.07*

CS and UCS indicated contaminated soil and uncontaminated soil, respectively. * Indicate significant differences at $p < 0.05$ level among different treatments.

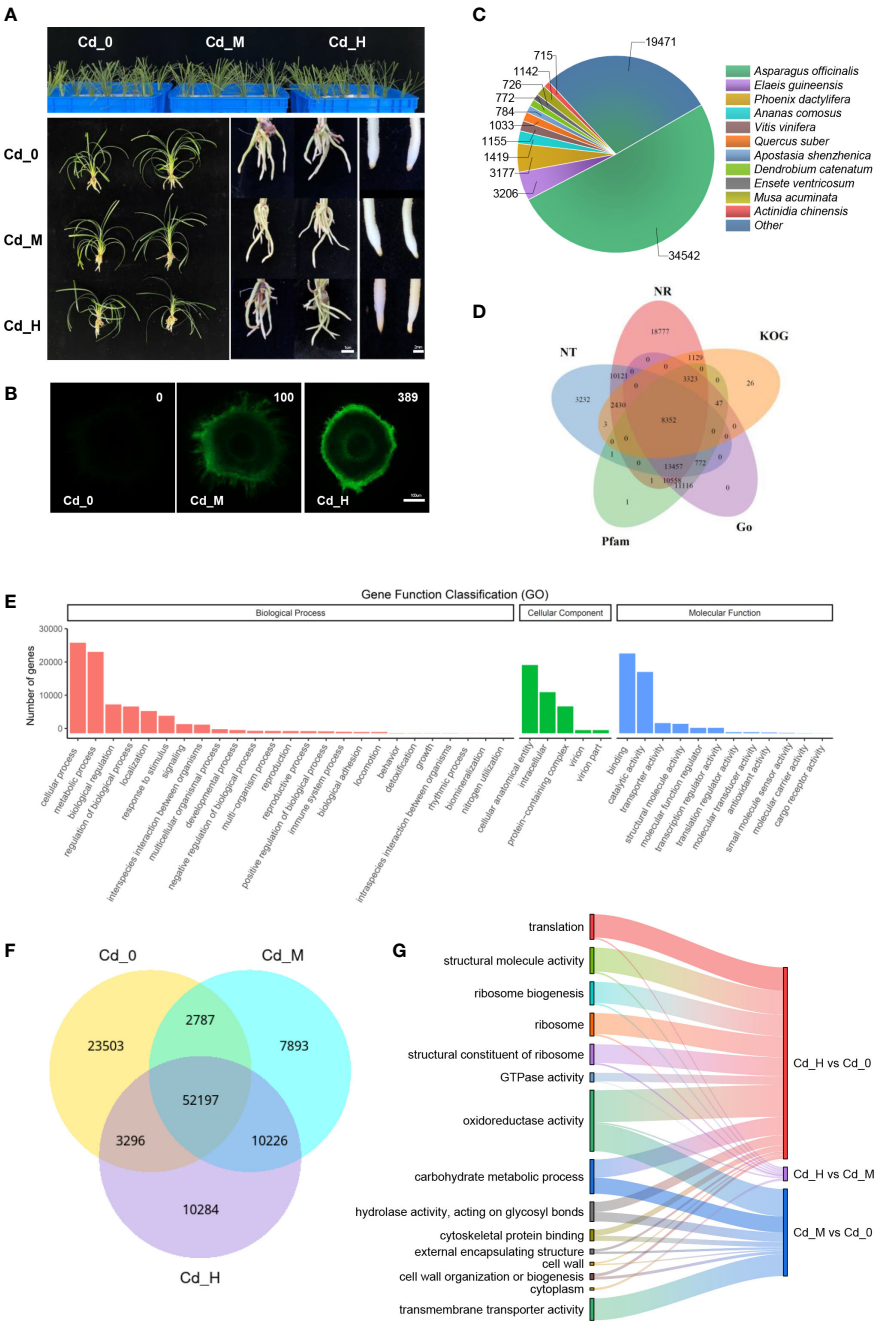


FIGURE 2
The phenotype and DEGs analysis of Zhe-Maidong exposed to three different Cd concertation. **(A)** The phenotype of Zhe-Maidong exposed to three different Cd concertation by hydroponics. The treatments were control (Cd-0), 1 mg/L Cd (Cd-M), and 10 mg/L Cd (Cd-H). **(B)** The distribution of Cd^{2+} in Zhe-Maidong leaves and roots using Leadmium Green AM dye. For each treatment, images from three technical replicates for three biological repeats were collected. The relative fluorescence intensities of Cd-0, Cd-M, and Cd-H were 0, 100, and 389, respectively. Bars = 100 μm. **(C)** Species distribution of homologous proteins of unigenes. The different color blocks represent different species. **(D)** Distribution of functionally annotated unigenes in the Go, KOG, NR, NT, and Pfam databases. **(E)** Functional annotation of unigenes based on Gene Ontology (GO) categorization. **(F)** DEGs under different Cd stress in Zhe-Maidong. **(G)** Go enrichment analysis of DEGs following the Cd stress treatment. The most significant 15 terms were chosen to be displayed.

the 'Biological processes' category; 'cellular anatomical entity' (20,070), 'intracellular' (8,171) and 'protein-containing complex' (7,901) in the 'Cellular Component category; 'binding' (23,483) and 'catalytic activity' (18,043) in the 'Molecular Function' category. A detailed Venn diagram depicts the number of transcripts shared by different Cd treatments (Cd-0, Cd-M, and Cd-H) of Zhe-Maidong (Figure 2F). The Venn diagram illustrates the effect of Cd stress on Zhe-Maidong is very complex, with 52,197 transcripts commonly expressed among different Cd treatments. There were also numerous specific transcripts expressed at Cd-0, Cd-M, or Cd-H.

All test samples were divided into three comparisons (Cd-H vs. Cd-0, Cd-H vs. Cd-M, and Cd-M vs. Cd-0), and each with upregulated and downregulated genes. In total, 24,222 differentially expressed genes (DEGs) (12,146 upregulated and 12,076 downregulated), 21,987 DEGs (10,679 upregulated and 11,308 downregulated), and 481 DEGs (319 upregulated and 162 downregulated) were found between Cd-H vs. Cd-0, Cd-H vs. Cd-M, and Cd-M vs. Cd-0, respectively (Table 3). Then, all differentially expressed genes (DEGs) following the Cd stress treatment were annotated by Go enrichment analysis. The most significant 15 terms were chosen to be displayed (Figure 2G). Among all DEGs from Cd-H vs. Cd-0, Cd-H vs. Cd-M, and Cd-M vs. Cd-0 were substantially enriched in oxidoreductase activity, carbohydrate metabolic process, structural molecule activity, and transmembrane transporter activity.

3.4 DEGs involved in Cd translocation and accumulation

To better understand the DEGs related to Cd accumulation of Zhe-Maidong and their corresponding functions, we illustrated a brief diagram of the transporters/proteins involved in Cd accumulation according to previous studies (Takahashi et al., 2012; Song et al., 2017; Sterckeman and Thomine, 2020) (Figure 3A), including root uptake and sequestration, xylem loading, shoot sequestration, and phloem loading. These processes are mediated by several proteins/transporters, such as natural resistance-associated macrophage protein (NRAMP), glutamate receptors (GLR), annexin (ANN), ATP binding cassettes (PDR/ABC), Cys-rich peptide (CDT), defensin-like protein (CAL), multidrug resistance-associated protein (MRP/ABCC), P18-type metal transporter ATPase (HMAs), and cation/calcium (Ca) exchanger (CCX).

Based on the Cd accumulation pathway in higher plants (Figure 3A), 50 DEGs involved in Cd uptake, transport, and accumulation were identified at a threshold of $|\mathrm{Log_2}$ (foldchange)| > 2 with padj<0.05 in the comparisons of Cd-H vs. Cd-0 and Cd-M vs. Cd-0 (Figure 3B). These DEGs were found to be sequence similarity to the 9 family genes associated with Cd accumulation: *NRAMP, GLR, ANN, PDR, CDT, CAL, MRP, HMA*, and *CCX*, which can be divided into 5 groups based on their expression patterns. Four genes from the first group (excluding MRP), all 19 genes in the second group, and five genes in the third group were considerably upregulated by Cd stress treatments (Cd-M and Cd-H). Among all the upregulated genes, there were eleven *HMA* genes, five *MRP* genes, three *PDR* genes, two *CAL* genes, two *CDT* genes, two *ANN* genes, one *GLR* gene, and one *CCX* gene. In contrast, 20 DEGs were significantly downregulated in the fourth and fifth groups after Cd exposure. Furthermore, we found that DEGs expression patterns under moderate Cd exposure (Cd-M) were highly comparable to those under high Cd stress (Cd-H) (Figure 3B).

To validate the RNA-seq results, qRT-PCR was utilized to quantify the expression of 7 DEGs associated with Cd accumulation. The qRT-PCR results of these DEGs were mostly compatible with the RNA-seq data, as shown in Supplemental Figure S1. The correlation coefficient (R^2 = 0.8628) indicated that the DEGs expression pattern obtained by RNA-seq and qRT-qPCR results were in good concordance, which supports the reliability of the RNA-seq data.

3.5 Correlation coefficient analysis between Cd accumulation and the expression of Cd accumulation-related genes

We measured the relative expression levels of the obtained 21 genes that have the prediction cDNA sequence by RNA-seq in CS and UCS to determine their roles in Cd accumulation (Supplemental Table S1). As shown in Figure 4, all 21 genes were significantly upregulated when CS was compared to UCS. Under CS treatment, the relative gene expression levels of *ANN*, *PDR3*, *CDT1*, *ABCC1*, and *HMA1/2/4/5* increased the most. Then, we performed a correlation coefficient analysis between Cd accumulation (EF-root, EF-leaf, EF-total, TF, Cd-leaf, Cd-root, and Cd-plant) and the related gene expression (Figure 5). The results showed that the gene expressions of *ANN, PDR3, CDT1,*

TABLE 3 Total number of differentially expressed genes (DEGs).

Compare	All	Up	Down	Threshold
Cd-H vs. Cd-0	24,222	12,146	12,076	DESeq2 padj<0.05 $\lvert\mathrm{Log_2FoldChange}\rvert$>1
Cd-M vs. Cd-0	21,987	10,679	11,308	DESeq2 padj<0.05 $\lvert\mathrm{Log_2FoldChange}\rvert$>1
Cd-H vs. Cd-M	481	319	162	DESeq2 padj<0.05 $\lvert\mathrm{Log_2FoldChange}\rvert$>1

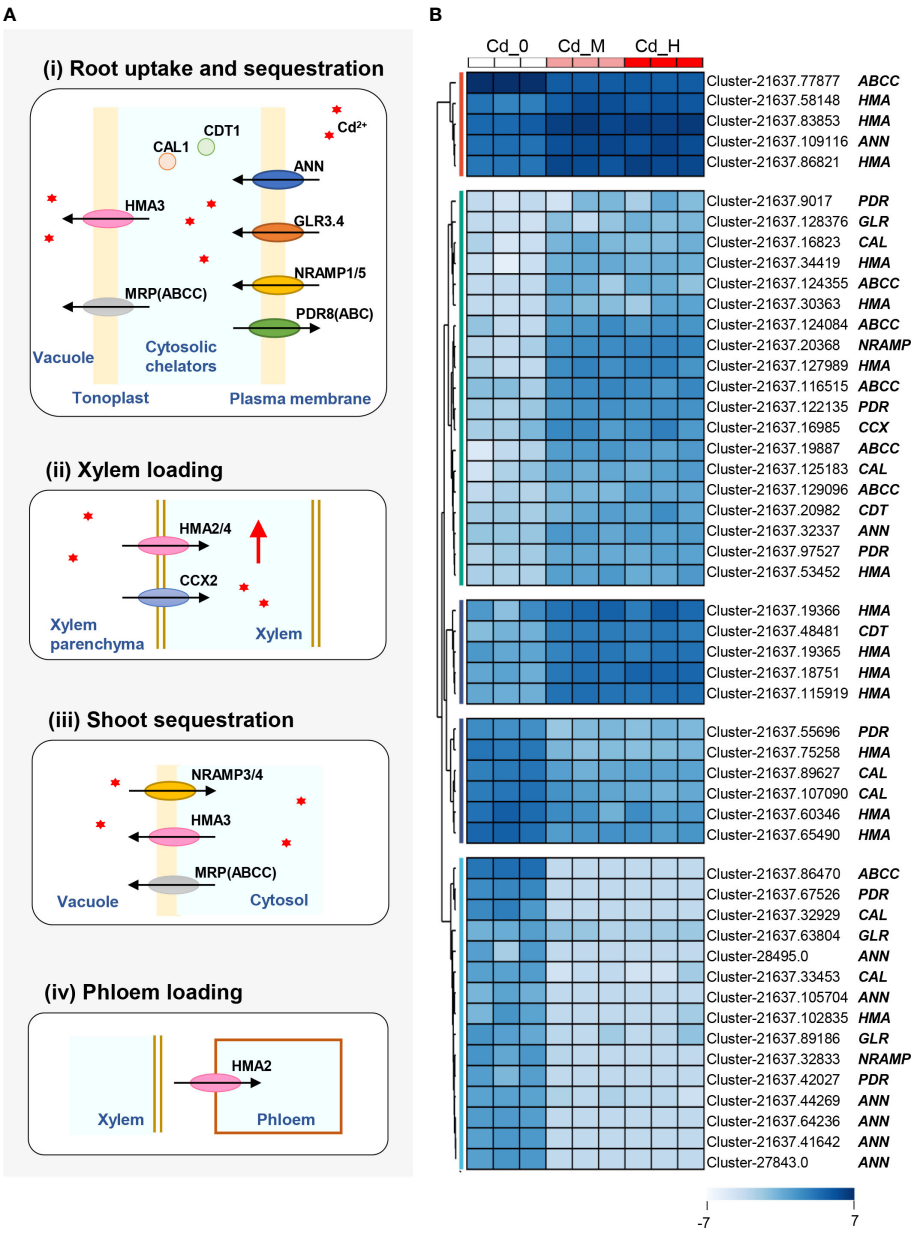


FIGURE 3
The DEGs of transporters/proteins involved in Cd accumulation. **(A)** The brief diagram of the transporters/proteins involved in Cd accumulation. **(B)** DEGs of transporters/proteins involved in Cd accumulation. The expression levels of DEGs were recorded as Log_2 (FPKM). $Cd^{2+}$was symbolized by red *.

ABCC2/4, HMA1-5, and *CCX* were statistically and positively correlated with EF-root, EF-leaf, EF-total, Cd-leaf, Cd-root, and Cd-plant in the root of Zhe-Maidong under Cd-stress. Therefore, we inferred that higher gene expressions of *ANN, ABCC2/4, HMA1-5*, and *CCX* in the root of Zhe-Maidong under the Cd-stress were strongly responsible for Cd transport and accumulation. Interestingly, most gene expression levels were negatively correlated with TF coefficients, which we hypothesize is due to the fact that Cd accumulation in *Ophiopogon japonicus* roots was significantly higher than in leaves, causing TF values in plants with high Cd accumulation to be reversed.

4 Discussion

Previous studies reported that heavy metal contents in herbs whose roots are used as medicinal parts are higher than those in whole-grass herbs (Wang et al., 2019b). The root is the main

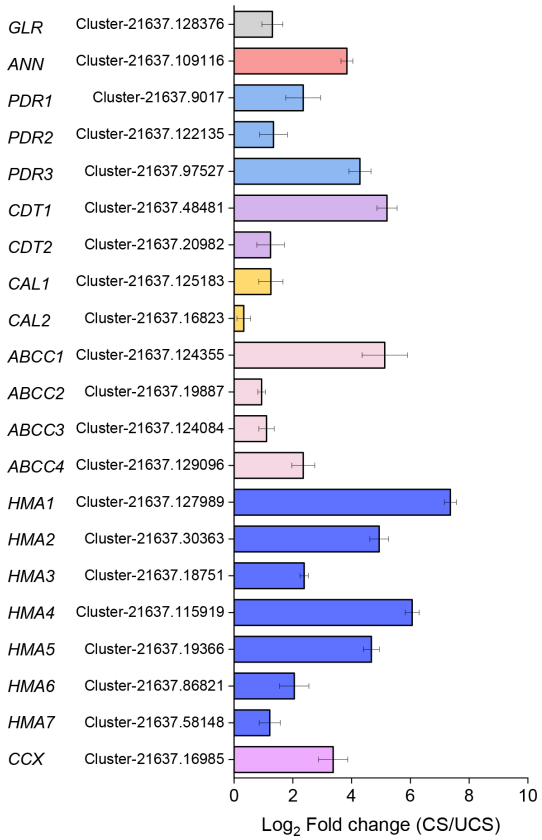


FIGURE 4
The relative gene expression levels of transporters/proteins involved in Cd accumulation under CS treatment as determined by qRT-PCR.

organ for heavy metal uptake (Pál et al., 2006). In our present study, the Cd content of Zhe-Maidong roots was much more than that in leaves after exposure to CS for 90 days (Figure 1, Table 2). When exposed to CS, the EF value in the root was four times that of the leaves, whereas the TF value was only approximately 0.24. As a result, we suggested that the root can absorb and accumulate Cd while possessing a poor capacity for Cd transport from roots to leaves (Table 2). This finding was similar to recent studies on rice and 60 kinds of Chinese herbal medicines (Wang et al., 2019b; Li et al., 2022), which found that Cd is rarely translocated to aerial tissues and primarily accumulates in the roots. It could be attributable to Cd retention during long-distance transport from roots to leaves of Zhe-Maidong. Previous studies suggested that Cd is accumulated in the roots among most plants, which serves as a protective mechanism against Cd toxicity in whole plants (Zhou et al., 2017). However, for Zhe-Maidong, whose main edible parts are root organs, the massive accumulation of cadmium in the roots poses a threat to human health.

Cd subcellular distribution has been shown to be intimately related to tolerance mechanisms (Lu et al., 2017). Our result showed that the intensity of Cd^{2+} fluorescence was most noticeable in the root hair, as well as the epidermis in both roots and leaves (Figure 1). The root hairs are the most active regions for absorbing ions from the soil. These structures may facilitate the absorption of the majority of Cd from the soil (Sterckeman and Thomine, 2020). Similar characteristics have been detected in the root of various plants, such as rice (Chen et al., 2018) and sunflowers (Laporte et al., 2013). These findings can be related to the increased activity of transport systems near the root hair, where they may be expressed at higher levels and/or benefit from additional energy (Chen et al., 2018). Subsequently, Cd^{2+} entry into the root epidermis layer through the apoplast pathway (adsorption process) or the symplast pathway (through the appropriate ion channels) (Song et al., 2017; Sterckeman and Thomine, 2020). Cd accumulation in the epidermal cell layer was also identified in *Zea mays* seedlings grown in heavy metal-polluted soils, which is consistent with our test results (Seregin and Kozhevnikova, 2004). Previous studies revealed that the epidermal cell layer in plants is thought to be an absorbing tissue because it contains a more active system of membrane transporters (Sridhar et al., 2005). Thus, we proposed that the epidermal cells of roots in Zhe-Maidong not only have the potential to accumulate Cd^{2+},

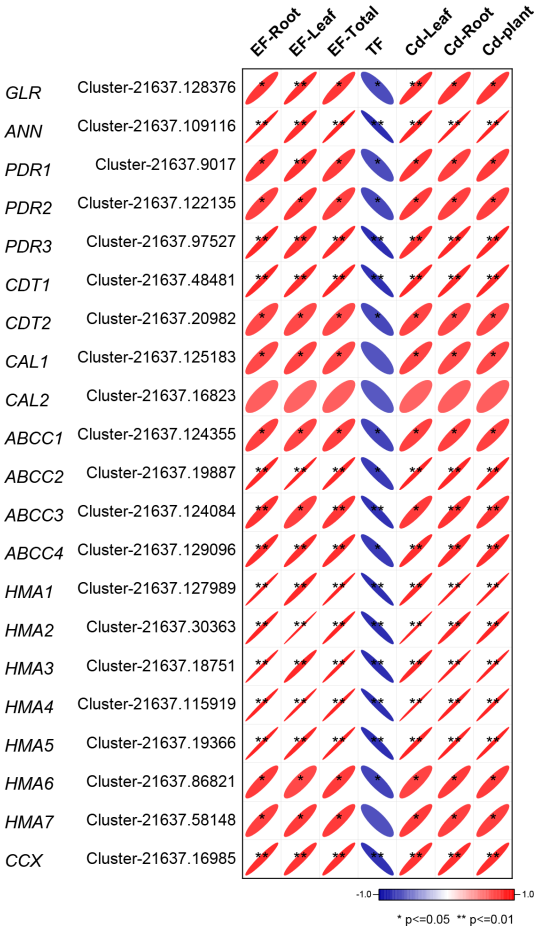


FIGURE 5
The correlation coefficient between Cd accumulation and the relative gene expression. * and ** denote statistically significant differences at the p<0.05 and p<0.01 levels, respectively.

but also have an excellent feature for ion uptake. This also explains why the intensity of cadmium fluorescence in root epidermal cells is considerably higher than in leaf epidermal cells.

Transporters are necessary for the Cd translocation and accumulation processes (Sterckeman and Thomine, 2020) (Figure 3). In this study, RNA-Seq techniques were used to identify candidate genes related to Cd translocation and accumulation in the root of Zhe-Maidong treated by hydroponic. In the comparisons of Cd-H vs. Cd-0 and Cd-M vs. Cd-0, a total of 50 DEGs involved in Cd translocation and accumulation were identified at a threshold of $|Log_2$ (foldchange)| > 2 with padj<0.05 (Figure 3B). Among all the DEGs, upregulated genes included eleven *HMA* genes, five *MRP* genes, three *PDR* genes, two *CAL* genes, two *CDT* genes, two *ANN* genes, one *GLR* gene, and one *CCX* gene. There were 20 DEGs significantly downregulated in the fourth and fifth groups after Cd exposure (Figure 3B). Additionally, a total of 21 predicted cDNA sequences by RNA-seq were used to determine their roles in Cd accumulation in the root of Zhe-Maiddong under CS for 90 days. According to Figure 4, the gene expressions of *ANN, ABCC2/4, HMA1-5*, and *CCX* were statistically and positively correlated with EF-root, EF-leaf, EF-total, Cd-leaf, Cd-root, and Cd-plant in Zhe-Maidong under Cd stress. These findings suggest that *ANN, ABCC2/4, HMA1-5*, and *CCX* genes were strongly responsible for Cd transport and accumulation in the root of Zhe-Maidong under Cd stress. In contrast to CAX, HMA, and ABCCs, the PDR8 protein (pleiotropic drug resistance) belongs to a wide family of ATP-binding cassette (ABC) transporters that are prominent in the root hairs and epidermis and have been linked to Cd efflux (Kim et al., 2007). Furthermore, *OsCDT1* may restrict cellular Cd accumulation by limiting Cd uptake by chelating the metal at the cellular surface, therefore improving Cd tolerance (Kuramata et al., 2009). In this paper, PDR3 (Cluster-21637.97527) and CDT1 (Cluster-21637.48481) gene expression levels were

drastically upregulated in response to Cd stress, showing that they play an essential role in avoiding Cd stress and promoting Cd tolerance.

Based on our findings, we developed a schematic model of Cd accumulation in Zhe-Maidong (Figure 6). Cd^{2+} from the soil can diffuse or be carried passively by water flow in the apoplast of the root cortex (apoplastic pathway). Furthermore, Cd^{2+} entrance might occur through Ca^{2+} channels in root cell plasma membranes, which are permeable to a broad range of monovalent and divalent cations (Chen et al., 2018). Here, we supposed that ANN (Cluster-21637.109116) plays a vital role in Cd uptake in Zhe-Maidong. The study on rice indicates that the Ca^{2+} channels *OsANN4* can mediate Cd uptake in rice roots after exposure to 20 μM Cd (Chen et al., 2018). In plants, the vacuole is the primary organelle for Cd storage. HMA1-5 (Cluster-21637.127989, Cluster-21637.30363, Cluster-21637.18751, Cluster-21637.115919, Cluster-21637.19366) and ABCC2/4 (Cluster-21637.19887, Cluster-21637.129096) were considered to bind Cd and induce its influx from the cytoplasm to the vacuole in roots. HMA transporters also play an essential role in the loading of Cd in xylem vessels and phloem loading. Members of the HMA family have been identified in a variety of plant species, including *A. thaliana* (Wong and Cobbett, 2009), rice (Treesubsuntorn and Thiravetyan, 2019), barley (Zhang et al., 2021), and wheat (Kintlová et al., 2021). As ATPases, they can transport the cation from the cytosol into the xylem sap against its electrochemical gradient. MRP transporters (ABCC) were responsible for the influx of PC-Cd complexes into the vacuole (Brunetti et al., 2015). Overall, we identified the major transporters related to Cd uptake and accumulation in the root of Zhe-Maidong, providing the putative genes for genetic improvement under Cd stress.

5 Conclusions

In this study, we evaluated the regularities of Cd transformation and distribution and developed a schematic model of Cd accumulation in Zhe-Maidong. The EF value in the root was four times that of the leaves, which shows that the root has a high ability to absorb and accumulate Cd. The Cd^{2+} distribution revealed that the epidermal cells of roots not only have the potential to accumulate Cd^{2+} but also have an excellent feature for Cd^{2+} uptake. *ANN, ABCC2/4, HMA1-5*, and *CCX* gene expression were positively correlated with EF-root, EF-leaf, EF-total, Cd-leaf, Cd-root, and Cd-plant, indicating their role in

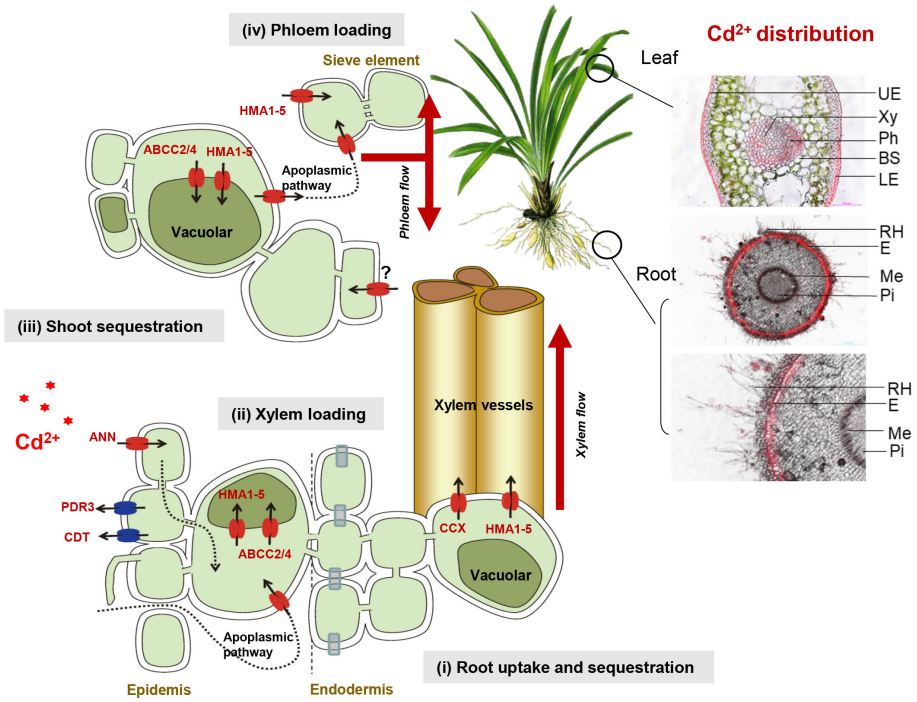


FIGURE 6
A schematic model of Cd uptake and accumulation in Zhe-Maidong. Cd^{2+} from the soil can diffuse or be carried passively by water flow in the apoplast of the root cortex (apoplastic pathway). ANN plays a vital role in Cd uptake in Zhe-Maidong. HMA1-5 could bind Cd and induce Cd^{2+} influx from the cytoplasm to the vacuole. In addition, HMA transporters also play an essential role in loading Cd in xylem vessels and phloem loading. MRP transporters (ABCC) were responsible for the influx of PC-Cd complexes into the vacuole. The PDR8 and CDT1 may be crucial in Cd efflux, in contrast to CAX, HMA, and ABCCs.

Cd transport and accumulation under Cd-stress. However, PDR3 and CDT gene expression were drastically upregulated in response to Cd stress, showing that they play a crucial role in avoiding Cd stress and promoting Cd tolerance. Our study lays the groundwork for future research into discovering novel genes and improving plant tolerance to Cd stress through selective breeding.

Data availability statement

The original contributions presented in the study are publicly available. The raw sequence data reported in this paper have been deposited in the Genome Sequence Archive in National Genomics Data Center (Nucleic Acids Res 2022), China National Center for Bioinformation / Beijing Institute of Genomics, Chinese Academy of Sciences (GSA: CRA008254) that are publicly accessible at https://ngdc.cncb.ac.cn/gsa.

Author contributions

Conceived and designed the experiments: QZ. Performed the experiments: QZ, QL, and SL. Analyzed the data: QZ, RH, JL, YT, YL, ZY, and XY. Wrote the paper: QZ, YZ, and JH. All authors contributed to the article and approved the submitted version.

Funding

This work was supported by the Key Research and Development Program of Zhejiang Province (2020C02024).

Conflict of interest

The authors declare that the research was conducted in the absence of any commercial or financial relationships that could be construed as a potential conflict of interest.

Publisher's note

All claims expressed in this article are solely those of the authors and do not necessarily represent those of their affiliated organizations, or those of the publisher, the editors and the reviewers. Any product that may be evaluated in this article, or claim that may be made by its manufacturer, is not guaranteed or endorsed by the publisher.

Supplementary material

The Supplementary Material for this article can be found online at: https://www.frontiersin.org/articles/10.3389/fpls.2022.1078330/full#supplementary-material

References

Brunetti, P., Zanella, L., De Paolis, A., Di Litta, D., Cecchetti, V., Falasca, G., et al. (2015). Cadmium-inducible expression of the ABC-type transporter AtABCC3 increases phytochelatin-mediated cadmium tolerance in arabidopsis. *J. Exp. Bot.* 66, 3815–3829. doi: 10.1093/jxb/erv185

Chen, X., Ouyang, Y., Fan, Y., Qiu, B., Zhang, G., and Zeng, F. (2018). The pathway of transmembrane cadmium influx *via* calcium-permeable channels and its spatial characteristics along rice root. *J. Exp. Bot.* 69, 5279–5291. doi: 10.1093/jxb/ery293

Chihmin, Y., Chien, M., Chao, P., Huang, C., and Chen, C. (2021). Investigation of toxic heavy metals content and estimation of potential health risks in Chinese herbal medicine. *J. Hazard. Mater.* 412, 125142. doi: 10.1016/j.jhazmat.2021.125142

Chi, Y., You, Y., Wang, J., Chen, X., Chu, S., Wang, R., et al. (2022). Two plant growth-promoting bacterial bacillus strains possess different mechanisms in affecting cadmium uptake and detoxification of *Solanum nigrum* l. *Chemosphere* 305, 135488. doi: 10.1016/j.chemosphere.2022.135488

Florijn, P., and Van Beusichem, M. (1993). Uptake and distribution of cadmium in maize inbred lines. *Plant Soil* 150, 25–32. doi: 10.1007/BF00779172

Fu, T., Zhao, R., Hu, B., Jia, X., Wang, Z., Zhou, L., et al. (2021). Novel framework for modelling the cadmium balance and accumulation in farmland soil in zhejiang province, East China: Sensitivity analysis, parameter optimisation, and forecast for 2050. *J. Cleaner Product.* 279, 123674. doi: 10.1016/j.jclepro.2020.123674

Greger, M., and Löfstedt, M. (2004). Comparison of uptake and distribution of cadmium in different cultivars of bread and durum wheat. *Crop Sci.* 44, 501–507. doi: 10.2135/cropsci2004.5010

Huang, F., Zhou, H., Gu, J., Liu, C., Yang, W., Liao, B., et al. (2020). Differences in absorption of cadmium and lead among fourteen sweet potato cultivars and health risk assessment. *Ecotoxicol. Environ. Saf.* 203, 111012. doi: 10.1016/j.ecoenv.2020.111012

Jiang, C. (2008). Study on the accumulation and distribution of cadmium in the effect of Ophiopogon Japonicus, Houttuynia Cordata, and Duchesnea Indica Focke (dissertation/ master's thesis). Guangxi Province, China: University of Guangxi. doi: 10.7666/d.Y2887866

Kim, D. Y., Bovet, L., Maeshima, M., Martinoia, E., and Lee, Y. (2007). The ABC transporter AtPDR8 is a cadmium extrusion pump conferring heavy metal resistance. *Plant J.* 50, 207–218. doi: 10.1111/j.1365-313X.2007.03044.x

Kintlová, M., Vrána, J., HOBZA, R., BLAVET, N., and HUDZIECZEK, V. (2021). Transcriptome response to cadmium exposure in barley (*Hordeum vulgare* l.). *Front. Plant Sci.* 12. doi: 10.3389/fpls.2021.629089

Kuramata, M., Masuya, S., Takahashi, Y., Kitagawa, E., Inoue, C., Ishikawa, S., et al. (2009). Novel cysteine-rich peptides from digitaria ciliaris and oryza sativa enhance tolerance to cadmium by limiting its cellular accumulation. *Plant Cell Physiol.* 50, 106–117. doi: 10.1093/pcp/pcn175

Laporte, M. A., Denaix, L., Sterckeman, T., Flénet, F., Dauguet, S., and Nguyen, C. (2013). Longitudinal variation in cadmium influx in intact first order lateral roots of sunflower (Helianthus annuus. l). *Plant Soil* 372, 581–595. doi: 10.1007/s11104-013-1756-3

Laporte, M. A., Sterckeman, T., Dauguet, S., Denaix, L., and Nguyen, C. (2015). Variability in cadmium and zinc shoot concentration in 14 cultivars of sunflower (*Helianthus annuus* l.) as related to metal uptake and partitioning. *Environ. Exp. Bot.* 109, 45–53. doi: 10.1016/j.envexpbot.2014.07.020

Lewis, C., Lennon, A. M., Eudoxie, G., and Umaharan, P. (2018). Genetic variation in bioaccumulation and partitioning of cadmium in *Theobroma cacao* l. *Sci. Total Environ.* 640, 696–703. doi: 10.1016/j.scitotenv.2018.05.365

Li, X., Teng, L., Fu, T., He, T., and Wu, P. (2022). Comparing the effects of calcium and magnesium ions on accumulation and translocation of cadmium in rice. *Environ. Sci. Pollut. Res.* 29, 41628–41639. doi: 10.1007/s11356-021-17923-3

Liu, H., Wang, Y., Wang, T., Ying, X., Wu, R., and Chen, H. (2017). *De novo* assembly and annotation of the zhe-maidong (*Ophiopogon japonicus* (Lf) ker-gawl) transcriptome in different growth stages. *Sci. Rep.* 7, 1–15. doi: 10.1038/s41598-017-03937-w

Lu, H., Li, Z., Wu, J., Shen, Y., Li, Y., Zou, B., et al. (2017). Influences of calcium silicate on chemical forms and subcellular distribution of cadmium in amaranthus hypochondriacus l. *Sci. Rep.* 7, 1–9. doi: 10.1038/srep40583

Pál, M., Horváth, E., JANDA, T., Páldi, E., and SZALAI, G. (2006). Physiological changes and defense mechanisms induced by cadmium stress in maize. *J. Plant Nutr. Soil Sci.* 169, 239–246. doi: 10.1002/jpln.200520573

Pan, J., Guan, M., Xu, P., Chen, M., and Cao, Z. (2021). Salicylic acid reduces cadmium (Cd) accumulation in rice (*Oryza sativa* l.) by regulating root cell wall composition *via* nitric oxide signaling. *Sci. Total Environ.* 797, 149202. doi: 10.1016/j.scitotenv.2021.149202

Seregin, I., and Kozhevnikova, A. (2004). Strontium transport, distribution, and toxic effects on maize seedling growth. *Russian J. Plant Physiol.* 51, 215–221. doi: 10.1023/B:RUPP.0000019217.89936.e7

Song, Y., Jin, L., and Wang, X. (2017). Cadmium absorption and transportation pathways in plants. *Int. J. Phytoremediation* 19, 133–141. doi: 10.1080/15226514.2016.1207598

Sridhar, B. M., Diehl, S., Han, F., Monts, D., and Su, Y. (2005). Anatomical changes due to uptake and accumulation of zn and cd in Indian mustard (*Brassica juncea*). *Environ. Exp. Bot.* 54, 131–141. doi: 10.1016/j.envexpbot.2004.06.011

Sterckeman, T., and Thomine, S. (2020). Mechanisms of cadmium accumulation in plants. *Crit. Rev. Plant Sci.* 39, 322–359. doi: 10.1080/07352689.2020.1792179

Takahashi, R., Bashir, K., Ishimaru, Y., Nishizawa, N. K., and Nakanishi, H. (2012). The role of heavy-metal ATPases, HMAs, in zinc and cadmium transport in rice. *Plant Signaling Behav.* 7, 1605–1607. doi: 10.4161/psb.22454

Treesubsuntorn, C., and Thiravetyan, P. (2019). Calcium acetate-induced reduction of cadmium accumulation in oryza sativa: Expression of auto-inhibited calcium-ATP ase and cadmium transporters. *Plant Biol.* 21, 862–872. doi: 10.1111/plb.12990

Wang, C., Chang, L., Qing, H., Hong, W., and Jingyang, G. (2021). Pollution status of heavy metals in herbal medicine and their traceability & control in the whole chain production process. *Chin. J. Environ. Eng.* doi: 10.12030/j.cjee.202012116

Wang, P., Chen, H., Kopittke, P. M., and Zhao, F.-J. (2019a). Cadmium contamination in agricultural soils of China and the impact on food safety. *Environ. Pollut.* 249, 1038–1048. doi: 10.1016/j.envpol.2019.03.063

Wang, Z., Wang, H., Wang, H., Li, Q., and Li, Y. (2019b). Heavy metal pollution and potential health risks of commercially available Chinese herbal medicines. *Sci. Total Environ.* 653, 748–757. doi: 10.1016/j.scitotenv.2018.10.388

Wong, C. K. E., and Cobbett, C. S. (2009). HMA p-type ATPases are the major mechanism for root-to-shoot cd translocation in *Arabidopsis thaliana*. *N. Phytol.* 181, 71–78. doi: 10.1111/j.1469-8137.2008.02638.x

Xue, W., Jiang, Y., Shang, X., and Zou, J. (2020). Characterisation of early responses in lead accumulation and localization of *Salix babylonica* l. roots. *BMC Plant Biol.* 20, 1–15. doi: 10.1186/s12870-020-02500-6

Yu, K., Liu, W., Zhang, N., Cheng, X., Zhou, S., Zuo, T., et al. (2021). A novel method to identify three quality grades of herbal medicine ophiopogonis radix by microscopic quantification. *Front. Pharmacol.* 11, 591310. doi: 10.3389/fphar.2020.591310

Zhang, C., Yang, Q., Zhang, X., Zhang, X., Yu, T., Wu, Y., et al. (2021). Genome-wide identification of the HMA gene family and expression analysis under cd stress in barley. *Plants* 10, 1849. doi: 10.3390/plants10091849

Zhang, J., Zhu, Y., Yu, L., Yang, M., Zou, X., Yin, C., et al. (2022). Research advances in cadmium uptake, transport and resistance in rice (*Oryza sativa* l.). *Cells* 11, 569. doi: 10.3390/cells11030569

Zhou, J., Wan, H., He, J., Lyu, D., and Li, H. (2017). Integration of cadmium accumulation, subcellular distribution, and physiological responses to understand cadmium tolerance in apple rootstocks. *Front. Plant Sci.* 8, 966. doi: 10.3389/fpls.2017.00966

frontiers | Frontiers in Plant Science

TYPE Original Research
PUBLISHED 13 December 2022
DOI 10.3389/fpls.2022.1088281

Check for updates

OPEN ACCESS

EDITED BY
Xinyang Wu,
China Jiliang University, China

REVIEWED BY
Chenchen Zhao,
University of Tasmania, Australia
Shengchun Xu,
Zhejiang Academy of Agricultural Sciences, China

*CORRESPONDENCE
Quanxiang Tian
quanxiang@hznu.edu.cn
Dawei Xue
dwxue@hznu.edu.cn

†These authors have contributed equally to this work and share first authorship

SPECIALTY SECTION
This article was submitted to Plant Abiotic Stress, a section of the journal Frontiers in Plant Science

RECEIVED 03 November 2022
ACCEPTED 23 November 2022
PUBLISHED 13 December 2022

CITATION
Yu T, Cen Q, Kang L, Mou W, Zhang X, Fang Y, Zhang X, Tian Q and Xue D (2022) Identification and expression pattern analysis of the *OsSnRK2* gene family in rice.
Front. Plant Sci. 13:1088281.
doi: 10.3389/fpls.2022.1088281

COPYRIGHT
© 2022 Yu, Cen, Kang, Mou, Zhang, Fang, Zhang, Tian and Xue. This is an open-access article distributed under the terms of the Creative Commons Attribution License (CC BY). The use, distribution or reproduction in other forums is permitted, provided the original author(s) and the copyright owner(s) are credited and that the original publication in this journal is cited, in accordance with accepted academic practice. No use, distribution or reproduction is permitted which does not comply with these terms.

Identification and expression pattern analysis of the *OsSnRK2* gene family in rice

Tongyuan Yu†, Qiwen Cen†, Lihua Kang, Wangshu Mou, Xiaoqin Zhang, Yunxia Fang, Xian Zhang, Quanxiang Tian* and Dawei Xue*

College of Life and Environmental Sciences, Hangzhou Normal University, Hangzhou, China

Sucrose non-fermenting-1-related protein kinase 2 (SnRK2) is a class of plant-specific serine/threonine (Ser/Thr) protein kinase that plays an important role in rice stress tolerance, growth and development. However, systematic bioinformatics and expression pattern analysis have not been reported. In the current study, ten *OsSnRK2* genes were identified in the rice genome and located on 7 chromosomes, which can be classified into three subfamilies (I, II, and III). Many *cis*-regulatory elements were identified in the promoter region of *OsSnRK2* genes, including hormone response elements, defense and stress responsive elements, indicating that the *OsSnRK2* family may play a crucial role in response to hormonal and abiotic stress. Quantitative tissue analysis showed that *OsSnRK2* genes expressed in all tissues of rice, but the expression abundance varied from different tissues and showed varietal variability. In addition, expression pattern of *OsSnRK2* were analyzed under abiotic stress (salt, drought, salt and drought) and showed obvious difference in diverse abiotic stress. In general, these results provide useful information for understanding the *OsSnRK2* gene family and analyzing its functions in rice in response to ABA, salt and drought stress, especially salt-drought combined stress.

KEYWORDS

rice, *OsSnRK2*, genome–wide, abiotic stress, expression patterns

Introduction

Plants are exposed to various biotic and abiotic stresses in the natural environment that inhibit normal growth and development. During the evolution, plants have developed complicated and sophisticated mechanisms to cope with various adversity stresses. Protein kinase phosphorylation plays an important role in the signaling pathway, plant growth and development, hormone response and anti-stress by modifying the activity of translated proteins, regulatory enzymes, and various

functional proteins (Umezawa et al., 2013; Mao et al., 2020; Sharif et al., 2020; Maszkowska et al., 2021).

Sucrose non-fermenting-1-related protein kinase (SnRK) is a class of serine/threonine (Ser/Thr) protein kinases and widely observed in plants. According to the conservation of the active domain of the kinase, it can be classified into three subfamilies: SnRK1, SnRK2, and SnRK3 (Hrabak et al., 2003). The SnRK2 gene family is a family of plant-specific protein kinases and involved in stress responsive processes. Recent studies have shown that members of the SnRK2 gene family play an important role in stress response by phosphorylation modifications and regulating protein activity and gene expression, thereby participating in the regulation of osmotic stress, stomatal movement through signal transduction (Riichiro et al., 2002; Taishi et al., 2004; Cheng et al., 2017; Fatima et al., 2020; Xu et al., 2020).

As one of important phytohormones, abscisic acid (ABA) is not only involved in plant growth and development but also plays an essential role in plant response to biotic and abiotic stresses (Mahadi et al., 2022). ABA signaling pathway is consisted of ABA receptor, protein phosphatase type 2C and SNF1-related protein kinase (SnRK2) (Li et al., 2000; Taishi et al., 2004; Zhang et al., 2020). In the absence of ABA, PP2C interacts with OsSnRK2 and inhibits its kinase activity, which shuts down the ABA signaling pathway; in the presence of ABA, the PYR/PYL/RCAR receptor protein binds to the hormone to form a complex, which in turn binds to PP2C, relieving its inhibition on SnRK2 and activating the ABA signaling pathway. Therefore, SnRK2 is a key factor with positive regulation of ABA signaling, and the activity of SnRK2 kinase is critical for ABA signaling on/off and abiotic stress response in plants (Fujii et al., 2007; Cheng et al., 2017).

Salt stress and drought stress have become major factors in inhibiting plant growth, development and crop yield. The main risks that the plants suffered from high concentrations of salt in the soil include osmotic stress, ion poisoning, water losing, wilting and metabolic disruption (Kawa et al., 2020; Zelm et al., 2020). In addition, salt stress causes oxidative stress, which destabilizes cell membranes (Munns and Tester, 2008). Drought stress also causes osmotic stress, which leads to the reduction of plant height, leaf area and stomatal conductance, as well as affecting plant root development (Khatun et al., 2021). Numerous studies have reported that SnRK2 is involved in plant responses to salt stress and drought stress. Under salt stress, overexpressing *OsSAPK4* reduces the accumulation of Na^+ and Cl^- in rice leaves than the wild type and promote germination, growth and development (Diedhiou et al., 2008). Among the 11 SnRK2 members in maize, the expression of *ZmSnRK2.3* and *ZmSnRK2.6* were activated and significantly up-regulated by salt stress (Huai et al., 2008). In recent years, it was found that expression of most *VrSnRK2* genes was induced by drought stress, suggesting their potential function in drought stress response; with *VrSnRK2.6c* being most significantly (12-fold) induced by drought stress (Fatima et al., 2020). Overexpression of *TaSnRK2.9* in tobacco enhanced the tolerance of tobacco seedlings and mature plants to drought and salt stress, and increased tobacco survival, seed germination, and root length (Feng et al., 2019). Then, it has been shown that overexpressing *MpSnRK2.10* in *Malus prunifolia* exhibit enhanced drought tolerance in phenotypic appearance associated with drought stress damage, i.e. most of the leaves of transgenic plants appear healthy upon rehydration after drought, while the leaves of wild-type plants show extensive necrosis. Moreover, transgenic plants were observed with less accumulation of ROS and MDA than WT under drought stress (Shao et al., 2018). It has also been confirmed that transgenic plants overexpressing *OsSGT1* showed less tolerant to salt stress and that *OsSAPK9* can act as a positive regulator for salt stress response and disease resistance by interacting with *OsSGT1* (Zhang et al., 2019). All the above results implied that OsSnRK2 family may plays a crucial role in regulating plant response to salt stress and drought stress.

To better understand the OsSnRK2 family members and their responses to abiotic stress, bioinformatics analysis was performed in this study including the physicochemical properties, conserved sequences, gene structures, *cis*-acting elements, expression profiles, and phylogeny of *OsSnRK2*. In addition, the expression pattern of *OsSnRK2* in different tissues and under different stresses (ABA, salt, drought and salt-drought double) were investigated by qRT-PCR. The results will help to enrich the understanding of the *OsSnRK2* gene family and provide a theoretical basis for further studying the function of OsSnRK2 in abiotic stress response of rice.

Materials and methods

Gene identification and chromosome localization

The candidate OsSnRK2 protein sequences were searched for structural domains using the online website SMART: Main page (http://smart.embl-heidelberg.de/) to confirm the presence of the conserved SnRK family domain S_TKc. Based on the OsSnRK2 protein sequences reported in the literature (Yuhko et al., 2004), after collecting the gene information through the online website RiceDate (https://www.ricedata.cn/gene/), TBtools (Chen et al., 2020) was used to chromosome localization maps.

Gene structure and conserved motifs analysis

The protein-coding regions (CDS) and DNA sequences of *OsSnRK2* were downloaded in FASTA format from the Whole Genome Data Ensembl website (http://plants.ensembl.org/index.html). The distribution of introns and exons and non-

coding regions of the genes were mapped using TBtools. Conserved motifs of the proteins were analyzed online *via* the MEME website (http://meme-suite.org/) with Motif set to 12 and parameters set to default values, and conserved motifs were mapped using TBtools.

Protein sequence alignment, phylogenetic tree, gene duplication and synteny analysis

Sequence alignment and output of the conserved structural domain of OsSnRK2 proteins were completed by MEGA7 software and geneDoc software and construction of phylogenetic relationships of the OsSnRK2 family, *Arabidopsis thaliana* and *Hordeum vulgare* was completed using MEGA7 software. The segmental repeat events of the *OsSnRK2* genes were analyzed using TBtools and presented in the form of Circos plots. Also, TBtools was used to do synteny analysis of *SnRK2* genes in genomes.

Protein physicochemical properties, subcellular localization, secondary and 3D structure prediction

Protein physicochemical property analysis *via* ExPASy (https://web.expasy.org/protparam/) online, subcellular localization and nuclear localization were analysis by WoLF (https://wolfpsort.hgc.jp/) and NucPred (https://nucpred.bioinfo.se/uncared/) online respectively. Secondary structure predictive of protein was performed by the SOPMA website (https://npsa-prabi.ibcp.fr/cgi-bin/npsa_automat.pl?page=npsa_sopma.html). Protein 3D structure prediction for OsSnRK2 gene families using the UniProt website (https://www.uniprot.org/).

Protein interaction and *cis*-acting elements in the promoter region of the *OsSnRK2* gene analysis

The STRING (https://cn.string-db.org/) website was used to predict the putative protein-protein interaction networks with *Oryza sativa* SnRK2 proteins using default settings. Optimising protein-protein interaction networks with Cytoscape (Doncheva et al., 2019).

The sequence of the 2000 bp region upstream of the start codon of the rice OsSnRK2 family gene was downloaded from the whole genome data Ensembl website (http://plants.ensembl.org/index.html) as the promoter sequence. Prediction analysis of *cis*-acting elements in the promoter region of the gene was performed through the PlantCare website (http://bioinformatics.psb.ugent.be/webtools/plantcare/html/) and promoter *cis*-acting elements were mapped by TBtools.

Plant growth and stress treatments

The rice material used in this study was japonica rice Nipponbare. The International Rice Research Institute (IRRI) nutrient solution (the pH adjusted to 5.0-5.5 with KOH) was used as the hydroponic medium and changed every 3 days. The seedlings were grown in an artificial climate chamber under light conditions of 14 h at 28°C and 10 h in darkness at 24°C and 70% humidity.

ABA treatment: Rice seedlings of two leaves stage were transferred to a hydroponic medium containing 0 μM, 50 μM and 100 μM ABA respectively and the shoots were taken after 24 h for gene expression analysis.

Salt, drought, and salt-drought combined stress treatments: Rice seedlings grown hydroponically to the two leaves stage were transferred to rice nutrient solutions containing 200 mM NaCl (salt treatment), 13% PEG 6000 (drought treatment) and 200 mM NaCl and 13% PEG 6000 (salt-drought double treatment) for treatment, and shoots were collected 48 h later for gene expression analysis.

Tissue expression and expression profiling of the *OsSnRK2* gene

RNA was extracted from roots, stems, leaves, leaf sheath and panicles at the tassel stage, and then analyzed for the expression of *OsSnRK2* genes in different tissue using qRT-PCR. The primers used in this assay were listed in Supplementary Table 1.

The CREP database (http://crep.ncpgr.cn/crep-cgi/home.pl) was searched for full fertility expression profile data of the indica rice variety *MingChuan63* to obtain the expression of *OsSnRK2* genes in five mature organs and 24 different developmental periods, which were clustered hierarchically using TBtools.

RNA extraction and qRT-PCR analysis

Fluorescent quantitative PCR primers were designed by Primer Premier 5 and *OsUBQ5* was selected as the internal reference gene. Total RNA was extracted from rice samples using the Total Plant RNA Kit (Tiangen Biochemical Technology Co., Ltd.) and reverse transcribed into cDNA using the AMV First Strand cDNA Synthesis Kit. PCR amplification was performed using the CFX96 Real-Time PCR Detection System (Bio-Rad, USA). The reaction conditions were pre-denaturation at 95 °C for 5 min, denaturation at 94 °C for 35 s, annealing at 63 °C for 40 s, and extension at 72 °C for 20 s. 38 amplification cycles were performed with 4 replicates for each sample and $2^{-\Delta\Delta Ct}$ was used for data processing.

Results

Gene identification and chromosome localization analysis of *OsSnRK2*

Referring to the *OsSAPK1-10* names reported in the published literature (Huai et al., 2008), bioinformatics analysis was performed after collecting gene information *via* the online website RiceData (https://www.ricedata.cn/gene/). The detailed information of genes was listed in Tables 1, 2. Fox example, the amino acid lengths of the OsSnRK2 family proteins ranged from 334 to 371 aa. Meanwhile, the molecular weight is ranged from 36.99 to 41.18 kDa. The isoelectric points and the hydrophobicity values of OsSnRK2 were ranged from 4.80 to 6.06 and -0.621 to -0.208, respectively. The negative hydrophobicity values means that the OsSnRK2 proteins are all hydrophilic.

Chromosome localization analysis revealed that the 10 genes of *OsSnRK2* were distributed on seven chromosomes (Figure 1 and Supplementary Table 2), with *OsSAPK1*, *OsSAPK8*, and *OsSAPK10* on chromosome 3, *OsSAPK5* and *OsSAPK7* on chromosome 4, *OsSAPK4*, *OsSAPK6*, *OsSAPK2*, *OsSAPK3* and *OsSAPK9* are located on chromosomes 1, 2, 7, 10 and 12 respectively.

TABLE 1 *OsSnRK2* family gene information.

Gene Name	Gene ID	Accession number
OsSAPK1	Os03g0390200	LOC_Os03g27280
OsSAPK2	Os07g0622000	LOC_Os07g42940
OsSAPK3	Os10g0564500	LOC_Os10g41490
OsSAPK4	Os01g0869900	LOC_Os01g64970
OsSAPK5	Os04g0691100	LOC_Os04g59450
OsSAPK6	Os02g0551100	LOC_Os02g34600
OsSAPK7	Os04g0432000	LOC_Os04g35240
OsSAPK8	Os03g0764800	LOC_Os03g55600
OsSAPK9	Os12g0586100	LOC_Os12g39630
OsSAPK10	Os03g0610900	LOC_Os03g41460

Gene structure and protein motif analysis of OsSnRK2

The gene structure analysis of the *OsSnRK2* family members showed that the length of the family genes ranged from 1875 (*OsSAPK5*) to 5459 bp (*OsSAPK7*). *OsSAPK5* and *OsSAPK10* had four and seven exons respectively, and the rest of the *OsSnRK2* genes all contained nine exons. In addition, the last exon of most *OsSnRK2* genes was longer (Figure 2A).

Analysis of gene conserved motifs is useful for exploring the structural composition of proteins. We used MEME online software to analyze the number and distribution of motifs of the *OsSnRK2* gene family members, and identified a total of nine motifs, named Motif 1~Motif 9. The results showed that Motif 3 is the most conserved, and the Motif 6 ranked as the second; except for *OsSAPK3* which missing the Motif 9 conserved motif, all the other *OsSnRK2* genes contain the same number of motifs with the same order arrangement of gene structure (Figure 2B and Supplementary Table 3). The similarities and diversity of these conserved motifs may result from the evolutionary adaptation of the gene functions in *OsSnRK2* family.

Protein sequence alignment, phylogenetic relationships, gene duplication and synteny analysis of OsSnRK2

The alignment of amino acid composition of the OsSnRK2 protein sequences showed the presence of a highly conserved S_TKc structural domain in the OsSnRK2 proteins (Figure 3A),

TABLE 2 Sequence characteristics, predicted subcellular and nuclear localization of OsSnRK2.

Gene Name	Protein Number	Length(aa)	MW(kDa)	PI	GRAVY	Subcelluar Location	NLS predicts
OsSAPK1	Q75LR7	342	37.79	5.43	-0.208	cytoplasm	NA
OsSAPK2	Q0D4J7	339	37.63	5.31	-0.248	cytoskeleton	NA
OsSAPK3	P0C5D6	334	36.99	5.67	-0.424	cytoplasm	NA
OsSAPK4	Q5N942	360	40.99	6.06	-0.616	cytoskeleton	NA
OsSAPK5	Q7XKA8	370	41.18	5.99	-0.501	cytoskeleton	NA
OsSAPK6	Q6ZI44	365	40.82	5.72	-0.621	cytoskeleton	NA
OsSAPK7	Q7XQP4	359	40.36	5.83	-0.567	cytoskeleton	NA
OsSAPK8	Q7Y0B9	371	40.75	4.85	-0.303	cytoskeleton	NA
OsSAPK9	Q75V57	361	39.68	4.81	-0.272	cytoskeleton	NA
OsSAPK10	Q75H77	362	39.75	4.80	-0.281	cytoskeleton	NA

"NA" is an abbreviation for "Not Available" and indicating no predicted nuclear localization sequences.

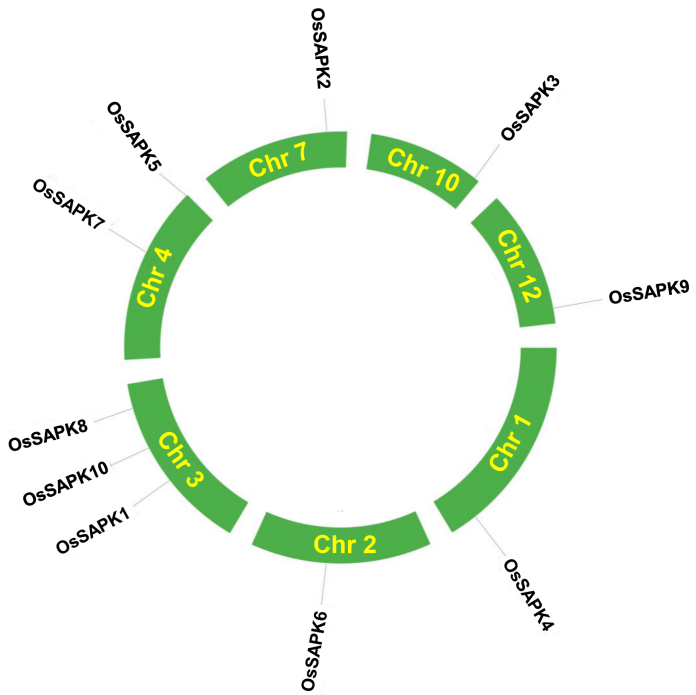


FIGURE 1
Distribution of *OsSnRK2* genes in rice chromosomes. Only show the chromosomes where located the *OsSnRK2* gene. The yellow font represents chromosome numbers and Green arc length indicate chromosome size.

which is closely related to their highly conserved function during evolution.

To further investigate the evolutionary relationships of the OsSnRK2, phylogenetic analysis was performed with amino acid sequences of 10 OsSnRK2 and several important SnRK2 proteins from *Arabidopsis thaliana* and *Hordeum vulgare* (Figure 3B). The results showed that the OsSnRK2 proteins could be classified into three subfamilies according to their affinities, with *OsSAPK1*, *OsSAPK2* and *OsSAPK3* belonged to subfamily I, *OsSAPK4*, *OsSAPK5*, *OsSAPK6*, *OsSAPK7* belonged to subfamily II, and *OsSAPK8*, *OsSAPK9* and *OsSAPK10* belonged to subfamily III. The OsSnRK2 family members are closely related to the *Arabidopsis thaliana* and *Hordeum vulgare* SnRK2 family members, suggesting that they might have conserved physiological and biochemical functions.

Three segmental duplication events were identified in *OsSnRK2* family by the MCScanX function of the software TBtools (Figure 3C) and involving six genes of ten *OsSnRK2*. All segmental duplication events happened between different chromosomes, but all occur within the same subfamily.

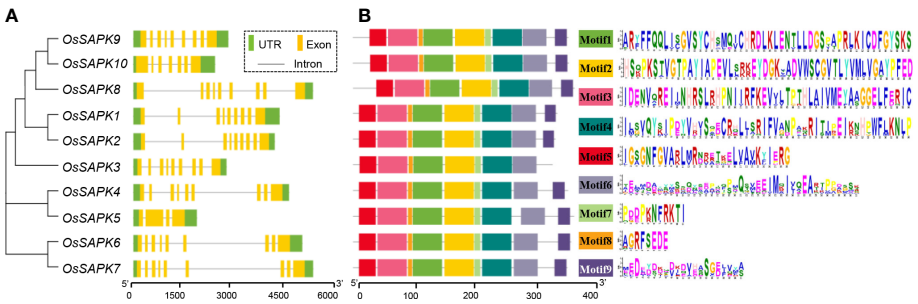


FIGURE 2
Gene structure and conserved motif analysis of the *OsSnRK2* gene. **(A)** Gene structure analysis of the *OsSnRK2*. Green boxes, yellow boxes and black lines represent UTR, Exon and Introns respectively. **(B)** Conserved motif analysis of the *OsSnRK2* gene.

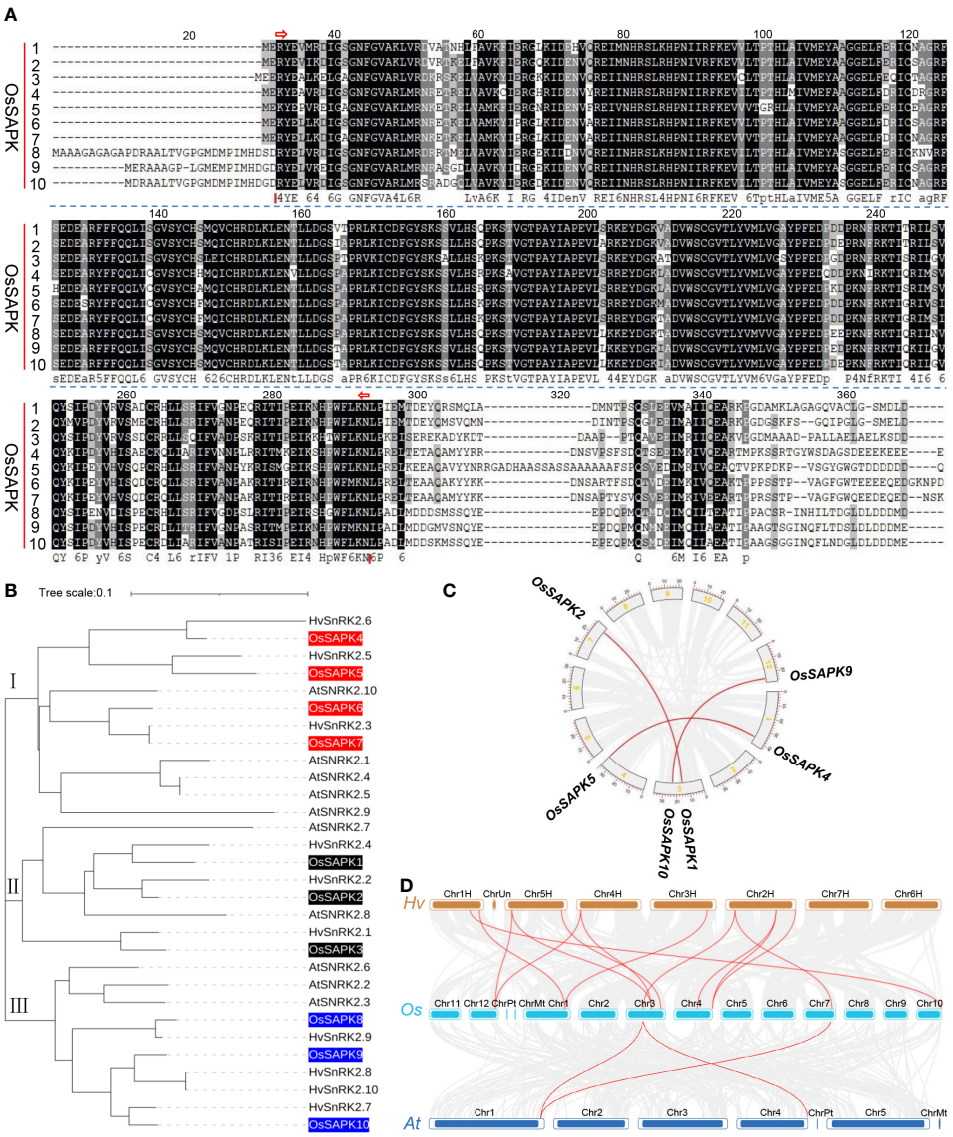


FIGURE 3
protein sequence alignment, phylogenetic relationships and gene duplication analysis of OsSnRK2. **(A)** Sequence alignment of the conserved structural domains of the *OsSnRK2* gene family, S_TKc structural domain, position 33-292, interval shown by red arrows. **(B)** Phylogenetic relationships analysis of SnRK2 in *Oryza sativa*, *Arabidopsis thaliana* and *Hordeum vulgare*. **(C)** Gene segmental duplication analysis of *OsSnRK2* in rice. Gray lines indicate all synteny blocks in the rice genome, and the red lines indicate duplicated *OsSnRK2* gene pairs. The chromosome number is indicated at the gray arc. The scale at the periphery of the chromosome represents the physical location (Kb). **(D)** Synteny analysis of *SnRK2* genes in the genomes between *Hordeum vulgare* and *Oryza sativa* or *Arabidopsis thaliana*. The gray lines show collinear blocks. The red lines indicate the syntenic gene pairs between *Hordeum vulgare* and *Oryza sativa* or *Arabidopsis thaliana*, respectively.

The above results demonstrate that a number of *OsSnRK2* genes maybe appear in the course of gene duplication, and the segmental duplication events may be responsible for the expansion of *SnRK2* genes in rice.

The colinearity of *OsSnRK2* gene pairs between *Oryza sativa*, *Hordeum vulgare* and *Arabidopsis thaliana* was compared. The result showed that 2 *OsSnRK2* genes exhibited syntenic relationship with *AtSnRK2*. However, 9 *OsSnRK2* genes showed syntenic relationship with *HvSnRK2* (Figure 3D and Supplementary Table 4), implying that these genes may play a critical role in evolution of *OsSnRK2* family.

Subcellular localization, secondary and 3D structure prediction of OsSnRK2

The predicted subcellular localization results showed that *OsSAPK1* and *OsSAPK3* proteins were localized in the

cytoplasm, the remaining OsSnRK2 proteins were localized in the cytoskeleton. The NucPred scores of the OsSnRK2 family proteins were all below 0.6, indicating no predicted nuclear localization sequences (marked with "NA" in Table 2).

Secondary structures of OsSnRK2 proteins were analyzed by the SOPMA online website (https://npsa-prabi.ibcp.fr/cgi-bin/npsa_automat.pl?page=npsa_sopma.html). All OsSnRK2 proteins were consisted of four secondary structures: alpha helix, extended helix, random coil, and extended strand (Figure 4), and the proportions of alpha helix > random coil > extended strand > extended helix. It is assumed that the alpha helix and random coil are the main conformations of the OsSnRK2 protein. The results of protein 3D structure prediction shows that all OsSnRK2 proteins have similar 3D structure (Figure 5).

Protein-protein interaction analysis of OsSnRK2 proteins

To identify potential interacting proteins with the OsSnRK2 proteins, a protein - protein interaction (PPI) network was generated with the STRING database (Figure 6). Notably, several proteins belonging to OsBZIP and OsPP2C proteins interacted with OsSAPK1, OsSAPK2, OsSAPK3, OsSAPK5, OsSAPK6, OsSAPK7, OsSAPK9, OsSAPK10, suggested their regulatory role in ABA signaling. Furthermore, there are other potential interacting proteins for OsSnRK2 proteins. Among them, OsDOS (a CCCH-Type Zinc Finger Protein) and OsDjC28 (belongs to heat shock protein DnaJ), are both showing tight relationships with different OsSnRK2 proteins, respectively.

Cis-elements analysis in *OsSnRK2* promoters

To explore the underlying function of the *OsSnRK2* genes, Plant-CARE was adopted for the analysis of *cis*-elements in their promoter region. The sequence of 2000 bp upstream of the *OsSnRK2* gene start codon was downloaded from the whole genome data Ensembl website and submitted for the *cis*-elements assay. The promoter sequences of the *OsSnRK2* gene contained a number of light-responsive *cis*-acting elements (e.g. AE-box, Box4, G-Box, GT1-motif, sp1), ABA-responsive *cis*-acting elements (ABRE), stress-responsive *cis*-acting elements (DRE, LTR, MYB, MYC, TC-rich repeats), salicylic acid response-related elements (TCA-element), MeJA-related elements (CGTCA-motif, TGACG-motif) and meristematic tissue expression elements (CAT-box) (Figure 7 and Supplementary Table 5). This indicates that *OsSnRK2* genes may be by exogenous factors such as light, hormones, stress and involved in the stress response.

Tissue expression and expression profile analysis of *OsSnRK2*

The expression patterns of the *OsSnRK2* gene were investigated in different tissues (root, stem, leaf, sheath and

Gene Name	Percentage (%)				Distribution of Secondary Structure Elements
	Hh	Tt	Cc	Ee	
OsSAPK1	36.84	5.56	40.35	17.25	
OsSAPK2	35.99	6.49	39.23	18.29	
OsSAPK3	45.81	5.99	33.83	14.37	
OsSAPK4	40.56	5.56	39.44	14.44	
OsSAPK5	41.08	4.59	39.19	15.14	
OsSAPK6	39.18	6.58	39.45	14.79	
OsSAPK7	39.00	5.57	40.11	5.32	
OsSAPK8	35.85	8.89	38.81	6.44	
OsSAPK9	37.95	6.93	39.34	5.79	
OsSAPK10	35.91	7.46	40.61	6.02	

FIGURE 4
Secondary structure analysis of OsSnRK2 proteins. The blue color represents alpha helix (Hh), the green color represents extended helix (Tt), the yellow color represents random coil (Cc) and the red color represents extended strand (Ee).

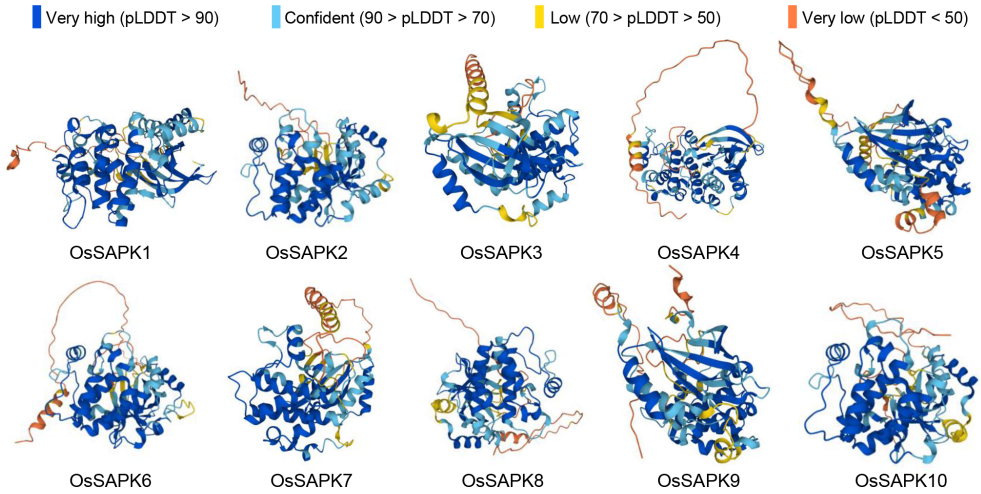


FIGURE 5
Protein 3D structure prediction model of *OsSnRK2* gene families. AlphaFold produces a per-residue confidence score (pLDDT) between 0 and 100.

panicle) of rice (Nipponbare) (Figure 8A). It was found that *OsSAPK2* and *OsSAPK7* were most abundantly expressed in the root and expressed at the lowest level in the panicle; *OsSPK3*, *OsSAPKA4*, and *OsSAPK9* were the most highly expressed in the stem, *OsSAPK3*, *OsSAPK4* were the least expressed in panicle and *OsSAPK9* was the least expressed in leaf sheath; *OsSAPK1*, *OsSAPK5*, *OsSAPK8*, and *OsSAPK10* were the most highly expressed in leaves, *OsSAPK1*, *OsSAPK5* and *OsSAPK8* were the least expressed in panicle and *OsSAPK10* was the least expressed in stems. These results indicated that the expression

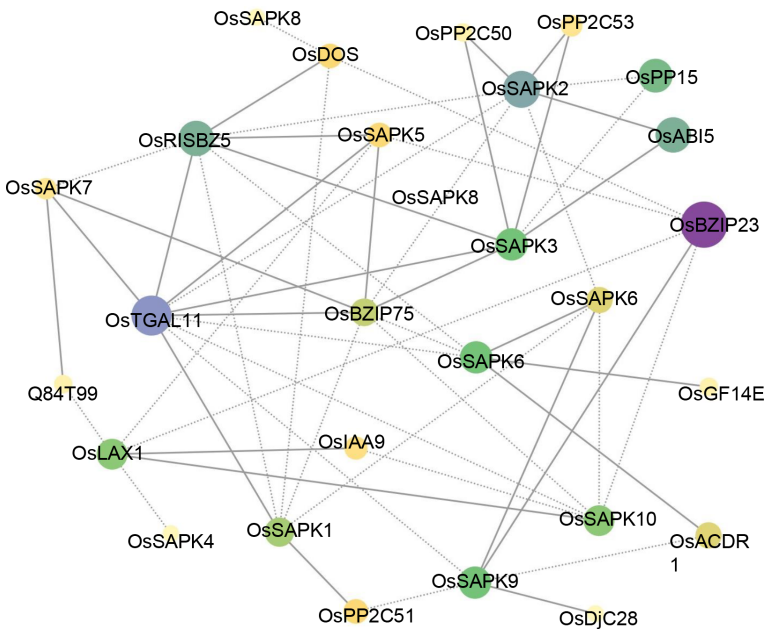


FIGURE 6
Protein-protein interaction network assembly of OsSnRK2 proteins. The area and color of the circles represent the number of interacting proteins, the larger area and darker color of the circles indicate more interacting proteins. The dashed lines represent protein interaction score ≤ 0.5, and solid lines means protein interaction score > 0.5.

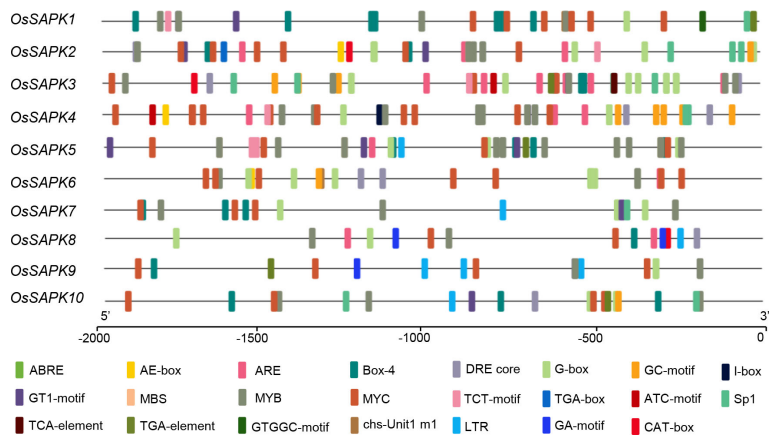


FIGURE 7
Predicted *cis*-acting elements in *OsSnRK2* promoter. Promoter sequences (–2 Kb) of 10 *OsSnRK2* were analyzed by PlantCARE. Different *cis*-elements are represented by different colors.

pattern of the ten *OsSnRK2* genes were tissue-specific, suggesting that *OsSnRK2* might play distinct roles in different tissue in growth and stress response of rice.

The expression file of the *OsSnRK2* genes of Indica rice *Mingchu 63* obtained from the CREP database (https://ricexpro.dna.affrc.go.jp/data-set.html) was hierarchically clustered in root, stem, leaf blade, leaf sheath, and panicle (Figure 8B and Supplementary Table 6), and the results showed that the expression level of *OsSAPK1* and *OsSAPK10* were highest in leaves, *OsSAPK2* was highest in stems and *OsSAPK8* was lowest in panicles, and these were consistent with the expression pattern of the *OsSnRK2* genes that we showed in the japonica rice variety Nipponbare. However, the expression pattern of *OsSAPK7* and *OsSAPK9* obtained from the CREP database in *Mingchu* 63 differed dramatically from that in Nipponbare, with *OsSAPK7* and *OsSAPK9* in *Mingchu* 63 having the highest expression in the panicle. Taken together, the results indicate that there is some variability in the tissue expression of *OsSnRK2* among different rice varieties.

Meanwhile, the expression of the *OsSnRK2* family genes of Indica rice *Mingchu 63* obtained from the CREP database was hierarchically clustered at 24 different developmental stages (Figure 8B and Supplementary Table 6). On the basis of the expression patterns of the *OsSnRK2* genes in the reproductive period, they could be classified into three groups. Group 1 had low expression in all periods and contained *OsSAPK1*. Group 2 include *OsSAPK2*, *OsSAPK5*, *OsSAPK7*, and *OsSAPK8*, and they were expressed at relatively high level in most periods. The rest of *OsSnRK2* genes were belong to the Group 3 and had moderate expression during all the periods. These results implied that *OsSnRK2* showed different expression level in different developmental periods.

Expression patterns of *OsSnRK2* under ABA and abiotic stress

To investigate the response of the *OsSnRK2* genes to ABA, the expression level of *OsSnRK2* genes in rice seedlings after 24 h treatment with different concentrations of ABA (0 μM, 50 μM, 100 μM) was analyzed (Figure 9). The results showed that the expression of *OsSAPK3* and *OsSAPK8* remained unchanged under different concentrations of ABA applications; the expression trends of *OsSAPK2*, *OsSAPK4*, *OsSAPK7*, and *OsSAPK9* were significantly lower than that of the control with 50 μM ABA treatment. The expression of *OsSAPK2*, *OsSAPK4*, *OsSAPK7*, and *OsSAPK9* was 0.002-fold, 0.31-fold, 0.37-fold, and 0.51-fold lower than the control with 50 μM ABA treatment, respectively; the expression of *OsSAPK1* and *OsSAPK6* tended to increase and then decrease with increasing concentration of ABA treatment. The expression levels of *OsSAPK1* and *OsSAPK6* in 50 μM ABA treatment were 1.66 and 4.32 times higher than the control group, respectively. The expression levels of *OsSAPK5* and *OsSAPK10* were enhanced as the ABA concentration increased, and the levels of *OsSAPK5* and *OsSAPK10* in 100 μM ABA treatment were 1.85 and 1.77 times higher than the control group, respectively.

To investigate the gene expression of *OsSnRK2* gene under salt and drought stress, the transcription level of the *OsSnRK2* gene in rice seedlings under three different treatments of 200 mM NaCl (salt treatment), 13% PEG 6000 (drought treatment) and 200 mM NaCl combined with 13% PEG 6000 (salt-drought double treatment) was compared using qRT-PCR (Figure 10). Under salt stress, the expression level of *OsSAPK1*, *OsSAPK2*, *OsSAPK4*, *OsSAPK6*, *OsSAPK7* and *OsSAPK8* were dramatically increased. In contrast, *OsSAPK3* and *OsSAPK5* were significantly decreased. However, the expression of other *OsSnRK2*s were not

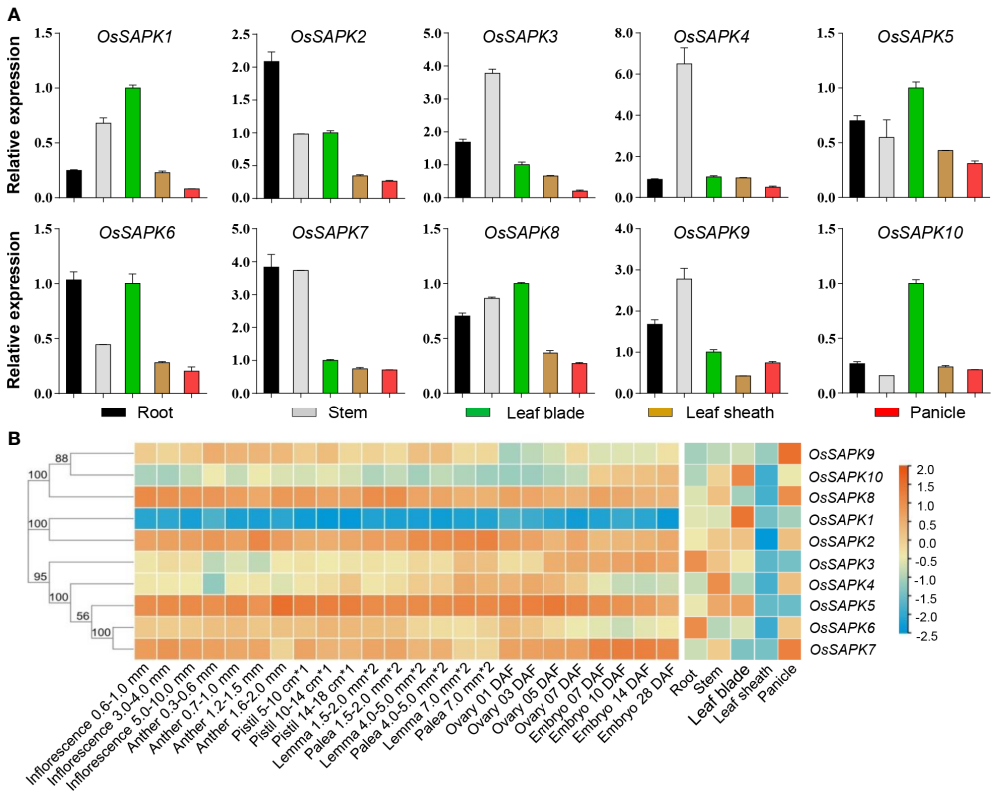


FIGURE 8
Expression analysis of the *OsSnRK2* in different tissues. **(A)** Expression analysis of *OsSnRK2* in root, stem, leaf blade, leaf sheath and panicle by qRT-PCR. *OsUBQ5* was used for normalization. The data represent means ± standard deviation (n = 3). **(B)** Expression profiles of *OsSnRK2* in an indica rice variety Minghui 63 obtained from CREP database. The color scale represents relative expression levels from low (blue) to high (red).

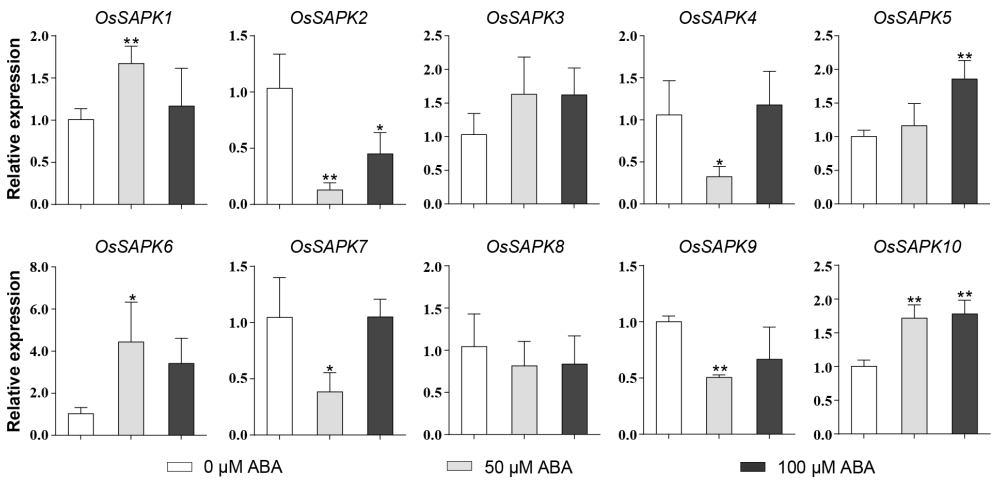


FIGURE 9
Expression analysis of *OsSnRK2* under different ABA concentration treatments. *OsUBQ5* was used for normalization. Total RNA was extracted from shoots of 14-day-old rice seedlings that were treatment or not. The data bars indicated Mean ± SD of three replicates. Asterisks represents significant differences from 0 μM ABA treatment (*p < 0.05; **p < 0.01) by Student's *t* test.

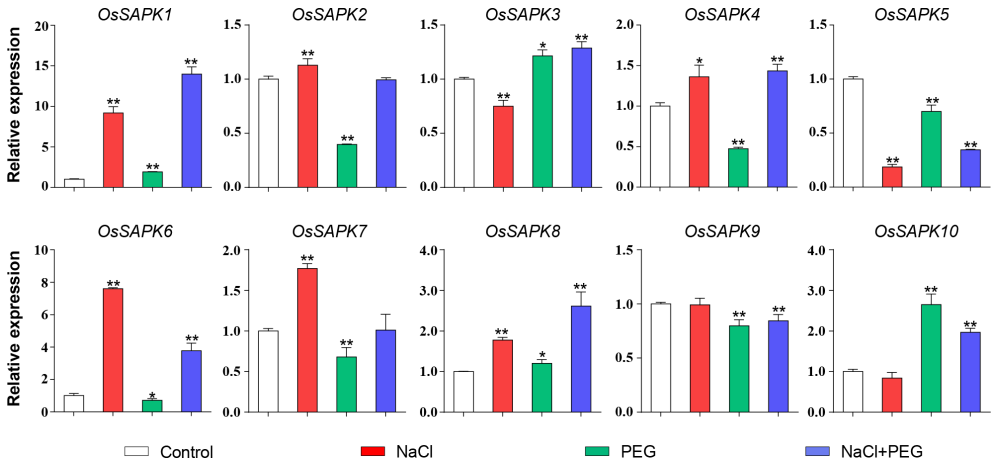


FIGURE 10
Expression analysis of *OsSnRK2* under salt, drought and salt-drought double stress. *OsUBQ5* was used for normalization. Total RNA was extracted from shoots of 14-day-old rice seedlings that were treatment or not. The data bars indicated Mean ± SD of three replicates. Asterisks represents significant differences from Control (*p < 0.05; **p < 0.01) by Student's t test.

altered by salt stress. Under drought stress, *OsSAPK10* was observed significantly up-regulated, which was 2.65-fold higher than the control. Some of the *OsSnRK2* genes were inhibited by drought stress, with *OsSAPK2* and *OsSAPK4* being 0.40 and 0.48 times than the control, respectively. The expression of *OsSAPK1* and *OsSAPK6* was significantly up-regulated than the other genes under the salt-drought double stress, with 13.96 and 3.75 times higher than the control, respectively. The above results demonstrate the potential important role of the *OsSnRK2* family in response to abiotic stress.

Discussion

Detailed characterization and evolution of *SnRK2* in rice

SnRK2 genes were found only in the plant kingdom and play a crucial role in plant growth, stress response, and have been identified in a variety of plants, such as *Arabidopsis thaliana*, *oat*, *Hevea brasiliensis* (Cheng et al., 2017; Shao et al., 2018; Wang et al., 2019), etc. Researchers has also identified *OsSnRK2* in rice, but not systematically. In the current study, ten *OsSnRK2* gene (named *OsSAPK1-OsSAPK9*) sequences were obtained from website RiceDate for detailed bioinformatics analysis. Ten *OsSnRK2* genes were unevenly distributed on seven chromosomes (Figure 1). The same subfamily genes often share similar intron-exon organization and motif (Zhang et al., 2022), For example, most *SnRK2* genes have 9 exons in *Nicotiana tabacum* (Li et al., 2022). In this study, we found that majority of *OsSnRK2* genes have 9 exons and the same motif arranged in the same order (Figure 2). The similarity shown above implied the functional redundancy among the members of *OsSnRK2* gene family. However, there were differences in the structure of individual *OsSnRK2* compared with genes of the same subclade. For example, the number of exons of *OsSAPK5* is significantly less than other members in the same subfamily, which only has 5 exons, and *OsSAPK3* has 8 motif, but others member have 9 motif. It is speculated that *OsSnRK2* members may have new functions by increased or decreased introns in the process of evolution to adapt to environmental changes.

Multiple sequence alignment of OsSnRK2 proteins showed that the N-terminus of this family was highly conserved protein kinase catalytic domain (S_TKc structural) and contained similar motif composition, which has also been reported in pepper (*Capsicum annuum* L.) (Wu et al., 2020; Figure 3). In the analysis of gene duplication and collinearity of *OsSnRK2*, we identified three pairs of segmental duplication events in ten genes, which speculated that segmental duplication may be the main way of *SnRK2* gene expansion in rice. A pair of duplication events, *OsSAPK1* and *OsSAPK2*, have been confirmed to act synergistically and become positive regulators of salt tolerance in rice (Lou et al., 2018). Moreover, the more syntenic gene pairs between *Hordeum vulgare* and *Oryza sativa* than between *Oryza sativa* and *Arabidopsis thaliana*, illustrating the greater affinity between *Hordeum vulgare* and *Oryza sativa*, which was further demonstrated by the results of phylogenetic relationships analysis (Figure 3).

OsSnRK2 genes play important roles in ABA pathway

The results of protein-protein interaction analysis show that the OsSnRK2 proteins are closely related to the OsBZIP and

OsPP2C proteins (Figure 6). Among the OsBZIP proteins, OsBZIP23 and OsBZIP46 are positive regulators in ABA-mediated drought resistance and are involved in ABA signaling (Yoshida et al., 2010; Guo et al., 2013; Vanitha et al., 2022). In addition, among the OsPP2C protein family, there are key players in ABA signal transduction, including OsPP2C50 and OsPP2C53, which act by negatively regulating ABA responses (Rodriguez et al., 1998; Merlot et al., 2001; Ma et al., 2009; Li et al., 2015; Zhao et al., 2021). These proteins have been shown to interact with some of the OsSnRK2 family proteins, suggesting that the OsSnRK2 family proteins are widely involved in the ABA signaling pathway.

Cis-acting elements are important switches in the regulation of gene transcription. Analysis of *cis*-acting elements of *OsSnRK2* promoter showed that there were enriched in *cis*-elements for the responses to ABA, such as ABRE, AER, etc. (Figure 7). This results are similar to those in pepper (Wu et al., 2020), Brassica napus (Yoo et al., 2016), *Ammopiptanthus nanus* (Tang et al., 2021). Further analysis revealed that 90% of *OsSnRK2* genes had ABRE, an ABA-related regulatory element (Kazuo and Kazuko, 2013), suggesting that the potential involvement of *OsSnRK2* family genes in ABA response. For example, mutations in ABA-activated SNF1-associated protein kinase 2 (SnRK2s) – SRK2D/SnRK2.2, SRK2E/SnRK2.6/OST1 and SRK2I/SnRK2.3 in *Arabidopsis thaliana* cause up-regulation of ABA repressor gene expression and down-regulation of ABA activator gene expression, resulting in severe growth defects during seed development, such as loss of dormancy function (Kazuo et al., 2009).

Protein interaction and *cis*-acting elements analysis of OsSnRK2 indicate that this family likely involved in ABA signaling transduction pathway, which was further confirmed by the expression analysis of *OsSnRK2* gene under ABA treatment. Most *OsSnRK2* genes expression were significantly altered by exogenous ABA, some were up-regulated (*OsSAPK1*, *6*, *5*, *10*) and some were down-regulated (OsSAPK*2*, *4*, *7*, *9*), indicating that *OsSnRK2* genes play a dual role in ABA response and plant growth (Figure 9). Mahadi et al. demonstrate this point and proposed that *OsSnRK2* can promote plant growth under normal conditions and while inhibiting plant growth in the absence of ABA (Mahadi et al., 2022).

OsSnRK2 genes play important roles in salt and drought stress responses

In the natural environment, plants are subjected to various abiotic stresses, such as drought, salinity low temperature, etc. As protein kinases, OsSnRK2 can phosphorylate or dephosphorylate the interacting proteins and involved in signal transduction, which is essential for plants to sense and adapt to various stress (Lou et al., 2017; Wang J et al., 2020; Wang Y et al., 2020; Li et al., 2021; Jia et al., 2022). In current study, we identified kinds of potential interacting factor for OsSnRK2 proteins including heat shock protein DnaJ and bZIP transcription factors that play a crucial role in salt and drought stress, and indicating OsSnRK2 involved in stress response (Figure 6). In addition, a large number of *cis*-acting elements were found in the *SnRK2* genes promoters, which is important in response to different hormones and abiotic stresses in wheat, potato, cotton (Zhang et al., 2016; Bai et al., 2017; Liu et al., 2017). Similar results were also verified in rice. The promoters of almost all *OsSnRK2* contain drought and salt stress response *cis*-acting elements, such as ABRE, G-box, and DRE, indicated that *OsSnRK2* family play a crucial role in the process of rice adaptive stress.

Previous studies have demonstrated that *SnRK2* genes are involved in a various of abiotic stresses responses (Ding et al., 2015; Soma et al., 2017; Tan et al., 2018). AtSnRK2.4 and AtSnRK2.10 are rapidly and transiently activated and regulate ROS homeostasis involved salt stress in *Arabidopsis* (Szymańska et al., 2019). The expression of *TaSnRK2* genes was induced by drought and salt, and overexpression of *TaSnRK2.4* in *Arabidopsis* significantly increased salt tolerance (Zhang et al., 2016). Under salt and PEG treatment, five *GhSnRK2* genes expression were found notably upregulated in cotton (*Gossypium hirsutum*) (Liu et al., 2017). In *Populus trichocarpa*, heterologously overexpression of *PtSnRK2.5* and *PtSnRK2.7* genes could enhance *Arabidopsis* salt stress tolerance (Song et al., 2016). In rice, several *SnRK2* genes have also been identified to be involved in stress responses. For example, overexpression of *OsSAPK4*, *OsSAPK6* or *OsSAPK7* in rice could increase salt tolerance (Diedhiou et al., 2008; Nam et al., 2012; Zeng et al., 2021), and overexpression *OsSAPK2* could improve grain yield by regulating nitrogen utilization under reproductive drought stress (RDS) (Lou et al., 2020). However, there is no systematic gene expression analysis under abiotic stress, especially under salt-drought combined stress, though they can coexist in the agroecosystem. In our results, almost all *OsSnRK2* members responded to salt and drought treatment simultaneously, except *OsSAPK9* and *OsSAPK10* which only responded to drought stress. Some *OsSnRK2*s showed opposite responses to salt and drought, but some are the same. For example, *OsSAPK1* and *OsSAPK8* expression were up-regulated by salt and drought simultaneously, and *OsSAPK2*, *OsSAPK4*, *OsSAPK6* and *OsSAPK7* were up-regulated by salt and down-regulated by drought stress (Figure 10). Under salt and drought stress, most *OsSnRK2* genes, including *OsSAPK1*, *OsSAPK3*, *OsSAPK4*, *OsSAPK6*, *OsSAPK8* and *OsSAPK10*, were up-regulated and two genes (*OsSAPK5*/*9*) were significantly down-regulate than control(Figure 10). The gene expressions of *OsSAPK1* and *OsSAPK8* under salt-drought combined stress were significantly higher than those under single stress (salt or drought). In addition, *OsSAPK1* and *OsSAPK8* were highly induced by salt and drought simultaneously, which suggested that *OsSAPK1* and *OsSAPK8* may play an important positive

regulatory role in response to salt-drought combined stress, and overexpression of *OsSAPK1* or *OsSAPK8* in rice may significantly improve the salt and drought tolerance and increase rice yield. The above results showed that *OsSnRK2* genes exhibit different expression profiles in response to salt and drought, which indicated that *OsSnRK2* genes play different role, and may be have different mechanisms in response to salt and drought stress.

Conclusion

Here, we studied the *SnRK2* gene family in rice by bioinformatics method. The results revealed the characteristics of the *OsSnRK2* gene in terms of physicochemical properties, phylogenetic relationships, structural domain distribution, chromosomal localization, motif composition, intron-exon structure, tissue expression, etc. In addition, the tissue-specific expression and response of the *OsSnRK2* gene to ABA, salt, drought, and salt-drought double stress were analyzed using qRT-PCR. The results showed that *OsSnRK2* genes were expressed in rice roots, stems, leaves, leaf sheaths and panicles, but the expression levels varied from different tissues and varieties. The expression level of most *OsSnRK2* genes were induced by ABA, salt, drought, and salt-drought double stress, indicating that *OsSnRK2* genes may be extensively involved in stress response. In summary, this study adopted bioinformatics way and qRT-PCR to unveil the physicochemical properties, tissue expression patterns, and responses of the *OsSnRK2* gene to different stresses, expanding the understanding of *SnRK2* gene family in rice and providing a reference for further investigation of their functions in response to ABA treatment and different abiotic stress.

Data availability statement

The datasets presented in this study can be found in online repositories. The names of the repository/repositories and accession number(s) can be found in the article/Supplementary Material.

Author contributions

DX, QT, and TY conceived and designed the research; TY, QC, LK, WM, XQZ, YF, XZ, and QT performed the experiments and data analyses. DX supervised the experiments and gave advice on laboratory work. TY and QT wrote the manuscript. DX, QT, and WM revised the manuscript. All authors read and approved the final article.

Funding

This work is supported by the Natural Science Foundation of Zhejiang province in China (LY21C130007; LY20C140003; LY19C130001), Hangzhou Scientific and Technological Major Project (202203A01) and Hangzhou Scientific and Technological Project (20201203B107).

Conflict of interest

The authors declare that the research was conducted in the absence of any commercial or financial relationships that could be construed as a potential conflict of interest.

Publisher's note

All claims expressed in this article are solely those of the authors and do not necessarily represent those of their affiliated organizations, or those of the publisher, the editors and the reviewers. Any product that may be evaluated in this article, or claim that may be made by its manufacturer, is not guaranteed or endorsed by the publisher.

Supplementary material

The Supplementary Material for this article can be found online at: https://www.frontiersin.org/articles/10.3389/fpls.2022.1088281/full#supplementary-material

References

Bai, J., Mao, J., Yang, H., Khan, A., Fan, A., Liu, S., et al. (2017). Sucrose non-ferment 1 related protein kinase 2 (SnRK2) genes could mediate the stress responses in potato (*Solanum tuberosum l.*). *BMC Genet.* 18, 41. doi: 10.1186/s12863-017-0506-6

Chen, C., Chen, H., Zhang, Y., Thomas, H. R., Frank, M. H., He, Y., et al. (2020). TBtools: An integrative toolkit developed for interactive analyses of big biological data. *Mol. Plant* 13, 1194–1202. doi: 10.1016/j.molp.2020.06.009

Cheng, C., Wang, Z., Ren, Z., Zhi, L., Yao, B., Su, C., et al. (2017). SCFAtPP2-B11 modulates ABA signaling by facilitating *SnRK2.3* degradation in *Arabidopsis thaliana*. *PloS Genet.* 13, e1006947. doi: 10.1371/journal.pgen.1006947

Diedhiou, C. J., Popova, O. V., Dietz, K. J., and Golldack, D. (2008). The SNF1-type serine-threonine protein kinase SAPK4 regulates stressresponsive gene expression in rice. *BMC Plant Bio.* 8, 49. doi: 10.1186/1471-2229-8-49

Ding, S., Zhang, B., and Qin, F. (2015). *Arabidopsis* RZFP34/CHYR1, a ubiquitin E3 ligase, regulates stomatal movement and drought tolerance *via* SnRK2.6-mediated phosphorylation. *Plant Cell.* 27, 3228–3244. doi: 10.1105/tpc.15.00321

Doncheva, N. T., Morris, J. H., Gorodkin, J., and Jensen, L. J. (2019). Cytoscape StringApp: Network analysis and visualization of proteomics data. *J. Proteome Res.* 18, 623–632. doi: 10.1021/acs.jproteome.8b00702

Fatima, A., Khan, M. J., Awan, H. M., Akhtar, M. N., Bibi, N., Sughra, K., et al. (2020). Genome-wide identification and expression analysis of *SnRK2* gene family in mungbean (*Vigna radiata)* in response to drought stress. *Crop Pasture Sci.* 71, 469–476. doi: 10.1071/CP19392

Feng, J., Wang, L., Wang, L., Wu, Y., Luo, Q., Zhang, Y., et al. (2019). *TaSnRK2.9*, a sucrose non-fermenting 1-related protein kinase gene, positively regulates plant response to drought and salt stress in *Transgenic tobacco*. *Front. Plant Sci.* 9. doi: 10.3389/fpls.2018.02003

Fujii, H., Verslues, P., and Zhu, J.-K. (2007). Identification of two protein kinases required for abscisic acid regulation of seed germination, root growth, and gene expression in *Arabidopsis*. *Plant Cell* 19, 485–494. doi: 10.1105/tpc.106.048538

Guo, C., Ge, X., and Ma, H. (2013). The rice *OsDIL* gene plays a role in drought tolerance at vegetative and reproductive stages. *Plant Mol. Biol.* 82, 239–253. doi: 10.1007/s11103-013-0057-9

Hrabak, E. M., Chan, C. W., Gribskov, M., Harper, J. F., Choi, J. H., Halford, N., et al. (2003). The Arabidopsis CDPK-SnRK superfamily of protein kinases. *Plant Physiol* 132 (2), 666–80. doi: 10.1104/pp.102.011999

Huai, J., Wang, M., He, J., Zheng, J., Dong, Z., Lv, H., et al. (2008). Cloning and characterization of the *SnRK2* gene family from *Zea mays*. *Plant Cell Rep.* 27, 1861–1868. doi: 10.1007/s00299-008-0608-8

Jia, M., Meng, X., Song, X., Zhang, D., Kou, L., Zhang, J., et al. (2022). Chilling-induced phosphorylation of IPA1 by *OsSAPK6* activates chilling tolerance responses in rice. *Cell Discovery* 8, 71. doi: 10.1038/s41421-022-00413-2

Kawa, D., Meyer, A. J., Dekker, H. L., Abd-El-Haliem, A. M., Gevaert, K., Slijke, E. V. D., et al. (2020). SnRK2 protein kinases and mRNA decapping machinery control root development and response to salt. *Plant Physiol.* 182, 361–377. doi: 10.1104/pp.19.00818

Kazuo, N., and Kazuko, Y.-S. (2013). ABA signaling in stress-response and seed development. *Plant Cell Rep.* 32, 959–970. doi: 10.1007/s00299-013-1418-1

Kazuo, N., Yasunari, F., Norihito, K., Takeshi, K., Taishi, U., Satoshi, K., et al. (2009). Three *Arabidopsis* SnRK2 protein kinases, SRK2D/SnRK2.2, SRK2E/SnRK2.6/OST1 and SRK2I/SnRK2.3, involved in ABA signaling are essential for the control of seed development and dormancy. *Plant Cell Physiol.* 50, 1345–1363. doi: 10.1093/pcp/pcp083

Khatun, M., Sarkar, S., Era, F. M., Mominul Islam, A. K. M., Anwar, P., Fahad, H., et al. (2021). Drought stress in *Grain legumes*: Effects, tolerance mechanisms and management. *Agronomy.* 11, 2374. doi: 10.3390/AGRONOMY11122374

Li, C., Shen, H., Wang, T., and Wang, X. (2015). ABA regulates subcellular redistribution of OsABI-LIKE2, a negative regulator in ABA signaling, to control root architecture and drought resistance in *Oryza sativa*. *Plant Cell Physiol.* 56, 2396–2408. doi: 10.1093/pcp/pcv154

Li, J., Song, J., Li, C., Ma, J., Liu, J., Zhu, X., et al. (2022). Genome-wide identification and expression profile analysis of the *SnRK2* gene family in *Nicotiana tabacum*. *Biochem. Genet.* 60, 1511–1526. doi: 10.1007/s10528-021-10170-8

Liu, Z., Ge, X., Yang, Z., Zhang, C., Zhao, G., Chen, E., et al. (2017). Genome-wide identification and characterization of *SnRK2* gene family in cotton (*Gossypium hirsutum l.*). *BMC Genet.* 18 (1), 54. doi: 10.1186/s12863-017-0517-3

Li, J., Wang, X., Watson, M. B., and Assmann, S. M. (2000). Regulation of abscisic acid-induced stomatal closure and anion channels by guard cell AAPK kinase. *Science.* 287, 300–303. doi: 10.1126/science.287.5451.300

Li, X., Yu, B., Wu, Q., Min, Q., Zeng, R., Xie, Z., et al. (2021). *OsMADS23* phosphorylated by SAPK9 confers drought and salt tolerance by regulating ABA biosynthesis in rice. *PloS Genet.* 17, e1009699. doi: 10.1371/journal.pgen.1009699

Lou, D., Chen, Z., Yu, D., and Yang, X. (2020). SAPK2 contributes to rice yield by modulating nitrogen metabolic processes under reproductive stage drought stress. *Rice.* 13, 35. doi: 10.1186/s12284-020-00395-3

Lou, D., Wang, H., Liang, G., and Yu, D. (2017). *OsSAPK2* confers abscisic acid sensitivity and tolerance to drought stress in rice. *Front. Plant Sci.* 8. doi: 10.3389/fpls.2017.00993

Lou, D., Wang, H., and Yu, D. (2018). The sucrose non-fermenting-1-related protein kinases SAPK1 and SAPK2 function collaboratively as positive regulators of salt stress tolerance in rice. *BMC Plant Biol.* 18, 203. doi: 10.1186/s12870-018-1408-0

Mahadi, H. M., Xudong, L., Muhammed, W., Yao, G., Alabdallah, N. M., Shah, J. M., et al. (2022). ABA activated SnRK2 kinases: An emerging role in plant growth and physiology. *Plant Signal. Behav.* 17, 2071024. doi: 10.1080/15592324.2022.2071024.

Mao, X., Li, Y., Rehman, S. U., Miao, L., Zhang, Y., Chen, X., et al. (2020). The sucrose non-fermenting 1-related protein kinase 2 (*SnRK2*) genes are multifaceted players in plant growth, development and response to environmental stimuli. *Plant Cell Physiol.* 61, 225–242. doi: 10.1093/pcp/pcz230

Maszkowska, J., Szymańska, K. P., Kasztelan, A., Krzywińska, E., Sztatelman, O., and Dobrowolska, G. (2021). The multifaceted regulation of SnRK2 kinases. *Cells.* 10, 2180. doi: 10.3390/cells10092180

Ma, Y., Szostkiewicz, I., Korte, A., Moes, D. L., Yang, Y., Christmann, A., et al. (2009). Regulators of PP2C phosphatase activity function as abscisic acid sensors. *Science.* 324, 1064–1068. doi: 10.1126/science.1172408

Merlot, S., Gosti, F., Guerrier, D., Vavasseur, A., and Giraudat, J. (2001). The ABI1 and ABI2 protein phosphatases 2C act in a negative feedback regulatory loop of the abscisic acid signalling pathway. *Plant J.* 25, 295–303. doi: 10.1046/j.1365-313x.2001.00965.x

Munns, R., and Tester, M. (2008). Mechanisms of salinity tolerance. *Annu. Rev. Plant Biol.* 59, 651–681. doi: 10.1146/annurev.arplant.59.032607.092911

Nam, M. H., Huh, S. M., Kim, K. M., Park, W. J., Seo, J. B., Cho, K., et al. (2012). Comparative proteomic analysis of early salt stress-responsive proteins in roots of SnRK2 transgenic rice. *Proteome Sci.* 10, 25. doi: 10.1186/1477-5956-10-25

Riichiro, Y., Tokunori, H., Kazuya, I., Tsuyoshi, M., Fuminori, T., Jose, A., et al. (2002). ABA-activated SnRK2 protein kinase is required for dehydration stress signaling in *Arabidopsis*. *Plant Cell Physiol.* 43, 1473–1483. doi: 10.1093/pcp/pcf188

Rodriguez, P. L., Benning, G., and Grill, E. (1998). ABI2, a second protein phosphatase 2C involved in abscisic acid signal transduction in *Arabidopsis*. *FEBS Lett.* 421, 185–190. doi: 10.1016/s0014-5793(97)01558-5

Shao, Y., Zhang, X., Nocker, S. V., Gong, X., and Ma, F. (2018). Overexpression of a protein kinase gene *MpSnRK2.10* from *Malus prunifolia* confers tolerance to drought stress in transgenic *Arabidopsis thaliana* and apple. *Gene.* 692, 26–34. doi: 10.1016/j.gene.2018.12.070

Sharif, R., Xie, C., Wang, J., Cao, Z., Zhang, H., Chen, P., et al. (2020). Genome wide identification, characterization and expression analysis of HD-ZIP gene family in *Cucumis sativus l.* under biotic and various abiotic stresses. *Int. J. Biol. Macromol.* 158, 502–520. doi: 10.1016/j.ijbiomac.2020.04.124

Soma, F., Mogami, J., Yoshida, T., Abekura, M., Takahashi, F., Kidokoro, S., et al. (2017). ABA unresponsive SnRK2 protein kinases regulate mRNA decay under osmotic stress in plants. *Nat. Plants.* 3, 16204. doi: 10.1038/nplants.2016.204

Song, X., Yu, X., Hori, C., Demura, T., Ohtani, M., and Zhuge, Q. (2016). Heterologous overexpression of poplar SnRK2 genes enhanced salt stress tolerance in *Arabidopsis thaliana*. *Front. Plant Sci.* 7. doi: 10.3389/fpls.2016.00612

Szymańska, K. P., Polkowska-Kowalczyk, L., Lichocka, M., Maszkowska, J., and Dobrowolska, G. (2019). SNF1-related protein kinases SnRK2.4 and SnRK2.10 modulate ROS homeostasis in plant response to salt stress. *Int. J. Mol. Sci.* 20, 143. doi: 10.3390/ijms20010143

Taishi, U., Riichiro, Y., Kyonoshin, M., Kazuko, Y.-S., and Kazuo, S. (2004). SRK2C, a SNF1-related protein kinase 2, improves drought tolerance by controlling stress-responsive gene expression in *Arabidopsis thaliana*. *P Natl. Acad. Sci. U.S.A.* 101, 17306–17311. doi: 10.1073/pnas.0407758101

Tang, Y., Lu, F., Feng, W., Liu, Y., Cao, Y., Li, W., et al. (2021). Genome-wide identification and expression analyses of *AnSnRK2* gene family under osmotic stress in *Ammopiptanthus nanus*. *Plants.* 10, 882. doi: 10.3390/PLANTS10050882

Tan, W., Zhang, D., Zhou, H., Zheng, T., Yin, Y., and Lin, H. (2018). Transcription factor *HAT1* is a substrate of SnRK2.3 kinase and negatively regulates ABA synthesis and signaling in *Arabidopsis* responding to drought. *PloS Genet.* 14, e1007336. doi: 10.1371/journal.pgen.1007336

Umezawa, T., Sugiyama, N., Takahashi, F., Anderson, J. C., Ishihama, Y., Peck, S. C., et al. (2013). Genetics and phosphoproteomics reveal a protein phosphorylation network in the abscisic acid signaling pathway in *Arabidopsis thaliana*. *Sci. Signal.* 6, rs8. doi: 10.1126/scisignal.2003509

Vanitha, P., Preethi, V., Akshay, U., Akashata, D., Sujitha, D., Ashwin, V., et al. (2022). Novel small molecules targeting *bZIP23* TF improve stomatal conductance and photosynthesis under mild drought stress by regulating ABA. *FEBS J.* 289, 6058–6077. doi: 10.1111/febs.16461

Wang, Y., Hou, Y., Qiu, J., Wang, H., Wang, S., Tang, L., et al. (2020). Abscisic acid promotes jasmonic acid biosynthesis *via* a 'SAPK10-bZIP72-*AOC*' pathway to synergistically inhibit seed germination in rice (*Oryza sativa*). *New Phytol.* 228, 1336–1353. doi: 10.1111/nph.16774

Wang, J., Ren, Y., Liu, X., Luo, S., Zhang, X., Liu, X., et al. (2020). Transcriptional activation and phosphorylation of *OsCNGC9* confer enhanced chilling tolerance in rice. *Mol. Plant* 14, 315–329. doi: 10.1016/j.molp.2020.11.022

Wang, X., Wu, Q., and Yuan, H. (2019). Cloning, prokaryotic expression and purification of *SnRK2.6* in *Hevea brasiliensis*. *MPB.* 17, 2828–2834. doi: 10.13271/j.mpb.017.002828

Wu, Z., Cheng, J., Hu, F., Qin, C., Xu, X., and Hu, K. (2020). The SnRK2 family in pepper (*Capsicum annuum* l.): genome-wide identification and expression analyses during fruit development and under abiotic stress. *Genes Genom.* 42, 1117–1130. doi: 10.1007/s13258-020-00968-y

Xu, P., Zhang, X., Su, H., Liu, X., Wang, Y., and Hong, G. (2020). Genome-wide analysis of *PYL-PP2C-SnRK2s* family in *Camellia sinensis*. *Bioengineered.* 11, 103–115. doi: 10.1080/21655979.2019.1710932

Yoo, M.-J., Ma, T., Zhu, N., Liu, L., Harmon, A. C., Wang, Q., et al. (2016). Genome-wide identification and homeolog-specific expression analysis of the

SnRK2 genes in *Brassica napus* guard cells. *Plant Mol. Biol.* 91, 211–227. doi: 10.1007/s11103-016-0456-9

Yoshida, T., Fujita, Y., Sayama, H., Kidokoro, S., Maruyama, K., Mizoi, J., et al. (2010). AREB1, AREB2, and ABF3 are master transcription factors that cooperatively regulate ABRE-dependent ABA signaling involved in drought stress tolerance and require ABA for full activation. *Plant J.* 61, 672–685. doi: 10.1111/j.1365-313X.2009.04092.x

Yuhko, K., Shuhei, Y., Hideyuki, M., Yasuaki, K., and Tsukaho, H. (2004). Differential activation of the rice sucrose nonfermenting1-related protein kinase2 family by hyperosmotic stress and abscisic acid. *Plant Cell.* 16, 1163–1177. doi: 10.1105/tpc.019943

Zelm, E. V., Zhang, Y., and Testerink, C. (2020). Salt tolerance mechanisms of plants. *Annu. Rev. Plant Biol.* 71, 403–433. doi: 10.1146/annurev-arplant-050718-100005

Zeng, D., Wang, C., Xie, J., Zhang, F., Lu, J., and Shi, X. (2021). Stress-activated protein kinase OsSAPK7 regulates salt-stress tolerance by modulating diverse stress-defensive responses in rice. *Rice Sci.* 28, 547–594. doi: 10.1016/j.rsci.2021.09.003

Zhang, Z., Ali, S., Zhang, T., Wang, W., and Xie, L. (2020). Identification, evolutionary and expression analysis of *PYL-PP2C-SnRK2s* gene families in soybean. *Plants.* 9, 1356. doi: 10.3390/plants9101356

Zhang, J., Liao, J., Ling, Q., Xi, Y., and Qian, Y. (2022). Genome-wide identification and expression profiling analysis of maize AP2/ERF superfamily genes reveal essential roles in abiotic stress tolerance. *BMC Genom.* 23, 125–125. doi: 10.1186/s12864-022-08345-7

Zhang, H., Li, W., Mao, X., Jing, R., and Jia, H. (2016). Differential activation of the wheat SnRK2 family by abiotic stresses. *Front. Plant Sci.* 7. doi: 10.3389/fpls.2016.00420

Zhang, F., Zeng, D., Huang, L., Shi, Y., Chen, T., Zhang, F., et al. (2019). Stress-activated protein kinase *OsSAPK9* regulates tolerance to salt stress and resistance to bacterial blight in rice. *Rice.* 12, 80. doi: 10.1186/s12284-019-0338-2

Zhao, J., Zhang, W., da Silva, J. A. T., Liu, X., and Duan, J. (2021). Rice histone deacetylase HDA704 positively regulates drought and salt tolerance by controlling stomatal aperture and density. *Planta.* 254, 79. doi: 10.1007/s00425-021-03729-7

frontiers | Frontiers in Plant Science

TYPE Review
PUBLISHED 04 January 2023
DOI 10.3389/fpls.2022.1052569

Check for updates

OPEN ACCESS

EDITED BY
Tianlun Zhao,
Zhejiang University, China

REVIEWED BY
Hao Chen,
Guangdong Academy of Agricultural Sciences (GDAAS), China
Dexin Liu,
Southwest University, China
Rasim Unan,
University of California, Davis

*CORRESPONDENCE
Hong Yang
yang@hubu.edu.cn
Li Liu
liuli2020@hubu.edu.cn

SPECIALTY SECTION
This article was submitted to Plant Abiotic Stress, a section of the journal Frontiers in Plant Science

RECEIVED 24 September 2022
ACCEPTED 01 December 2022
PUBLISHED 04 January 2023

CITATION
Chen L, Duan L, Sun M, Yang Z, Li H, Hu K, Yang H and Liu L (2023) Current trends and insights on EMS mutagenesis application to studies on plant abiotic stress tolerance and development.
Front. Plant Sci. 13:1052569.
doi: 10.3389/fpls.2022.1052569

COPYRIGHT
© 2023 Chen, Duan, Sun, Yang, Li, Hu, Yang and Liu. This is an open-access article distributed under the terms of the Creative Commons Attribution License (CC BY). The use, distribution or reproduction in other forums is permitted, provided the original author(s) and the copyright owner(s) are credited and that the original publication in this journal is cited, in accordance with accepted academic practice. No use, distribution or reproduction is permitted which does not comply with these terms.

Current trends and insights on EMS mutagenesis application to studies on plant abiotic stress tolerance and development

Liuzhu Chen[1], Liu Duan[1], Minghui Sun[1], Zhuo Yang[1], Hongyu Li[1], Keming Hu[2,3], Hong Yang[1]* and Li Liu[1]*

[1]State Key Laboratory of Biocatalysis and Enzyme Engineering, Hubei Collaborative Innovation Center for Green Transformation of Bio-Resources, Hubei Key Laboratory of Industrial Biotechnology, School of Life Sciences, Hubei University, Wuhan, China, [2]Jiangsu Key Laboratory of Crop Genomics and Molecular Breeding/Key Laboratory of Plant Functional Genomics of the Ministry of Education, College of Agriculture, Yangzhou University, Yangzhou, China, [3]Co-Innovation Center for Modern Production Technology of Grain Crops of Jiangsu Province/Key Laboratory of Crop Genetics and Physiology of Jiangsu Province, Yangzhou University, Yangzhou, China

Ethyl methanesulfonate (EMS)-induced mutagenesis is a powerful tool to generate genetic resource for identifying untapped genes and characterizing the function of genes to understand the molecular basis of important agronomic traits. This review focuses on application of contemporary EMS mutagenesis in the field of plant development and abiotic stress tolerance research, with particular focuses on reviewing the mutation types, mutagenesis site, mutagen concentration, mutagenesis duration, the identification and characterization of mutations responsible for altered stress tolerance responses. The application of EMS mutation breeding combined with genetic engineering in the future plant breeding and fundamental research was also discussed. The collective information in this review will provide good insight on how EMS mutagenesis is efficiently applied to improve abiotic stress tolerance of crops with the utilization of Next-generation sequencing (NGS) for mutation identification.

KEYWORDS

ethyl methane sulfonate, molecular breeding, abiotic stress tolerance, plant development, mutation breeding

1 Overview of EMS mutagenesis

Ethyl methanesulfonate (EMS) is one of the most common used alkylating agents that can induce chemical modification of nucleotides through the introducing active alkyl group, which creates base changes and nucleotide mutations (Sabetta et al., 2011; Arisha et al., 2014; Gillmor and Lukowitz, 2020). Modifications caused by alkylating agents

include the N^7 and O^6 of guanine (G), N^3 and N^7 of adenine (A), N^3, O^2, and O^4 of thymine (T), N^3, O^2, and N^4 of cytosine (C), and the phosphonate backbone (Murray, 1987; Fu et al., 2012). The EMS primarily induces the changes in guanine (Boysen et al., 2009). Compared to cytosine, the O^6-exhalation pair is more stable than the thymine pair, so during replication the O^6-GC pair is regularly converted into an AT pair. A lot of studies for EMS in the genotoxic activity *in vivo* and *in vitro* provide clear evidence, that EMS is a carcinogenic chemical and it is necessary to be very careful when using it (Gocke et al., 2009).

In the vast majority of cases, the mutant phenotype is due to premature stop codons, splice site disruption, deleterious amino acid substitutions, and loss of gene function (Sabetta et al., 2011). Therefore, it is critical to ensure that a large quantity of mutant alleles are present in a small mutant population and that the requirements for efficient homogenization are adequately met.

EMS is a type of non-transgenic chemical mutagen, and EMS mutagenesis is an important way to obtain mutations and the discovery of new genes for plants. Special protocols have been established for many plant species (Unan et al., 2021). The first commercial rice varieties CL112 and CL141, which were M_2 from Clearfield rice varieties AS350, promoted the imidazolinone (IMI) resistant commercial progress and has important significance for rice research (Sudianto et al., 2013). Treatment with EMS is inexpensive, easy to implement, and induces point mutations at high rates and with good agreement in most species with different genetic backgrounds (Gillmor and Lukowitz, 2020). Currently, EMS mutagenesis can achieve a large number of mutants in a short period of time, which can facilitate the study of stress tolerance in plants. Moreover, it is necessary to strengthen research of phenomics, transcriptomics, proteomics, metabolomics, and other methods in EMS mutant screening and gene function analysis. It is significant carrying out research on stress tolerance breeding from different directions, and tap the potential of EMS mutagenesis in abiotic stress tolerance research.

2 The application of EMS mutagenesis

When EMS mutates seeds or tissues, several key parameters need to be considered, such as the uniformity of the material to be mutated and the optimization of EMS dose. In a perfect world, mutagenic material should be homologous and isogenic would facilitate evaluation using molecular markers (Sabetta et al., 2011). The use of homogeneous materials reduces the ambiguity between phenotype and genotype. After mutagenizing a plant, the first generation of seeds can be selected and selfed in successive rounds to create a large near-isogenic homozygous seed bank (Till et al., 2003). Homozygote is difficult to achieve in obligate vegetative breeding species, such as bananas (Wang X et al., 2021). However, homogeneous populations with fixed heterozygote and common features in all plants can be produced by clonal reproduction.

The second key parameter and main troubleshooting area in mutagenesis experimentation is optimization of EMS dose. The accumulation of induced mutation densities must be balanced against the viability or fecundity of the material so as to be feasible under existing resource conditions. Unan et al. (2021) believe that rice seed pre-soaking for 12 hours, can effectively promote the mutagenic effect of EMS, and establish the standard of rice EMS mutagenesis. Additionally, the shelf life of EMS is critical. Once the mutagen is turned on, EMS can interact with the outside air, which may reduce its activity.

2.1 EMS is applied to plant research

EMS mutagenesis is suitable for most plants (Kim et al., 2006). For crops, vegetables, and fruits, the purpose of mutagenesis is to obtain varieties with excellent traits. By identifying the agronomic and quality traits of progeny, a population of progeny with the visible mutation type is obtained, followed by further gene function research. As another example, improving ornamental plant ornamental value and stress resistance is a primary purpose of mutagenesis research. For example, common ornamental plants such as *Chrysanthemum*, moss, and jasmine were applied mutagenesis to obtain new landscape plant varieties (Hossain et al., 2006).

EMS mutagenesis has been used for multi-omits combined analysis, and related genes are obtained by reverse genetics. Subsequently, gene-editing technology is used for research. Editing and recombining genes are the basis for an ideal breeding method, which will bring infinite possibilities and breakthrough developments for human beings in plant genetics. In recent years, these are the primary methods of forwarding genetics among model plants.

2.2 Various plant tissues could be used for mutagenesis

Mutagens can make abundant mutations in different organs of plants, such as seeds, bulbs, callus, pollen, etc. (Mba et al., 2010). Plants make different mutagenesis sites, which can be selected according to the needs of the experiment, and EMS can be used for mutagenesis.

Jankowicz-Cieslak et al. (2012) considered that seeds are the most common mutagenic plant materials, and there is also a wealth of data in other plant species on doses used to achieve high densities of induced mutations. In general, for plants propagated by seeds, their seeds are usually preferentially selected mutagenic material (Gottwald et al., 2009). At present, reports on seed mutations are multifarious, and the materials

cover a wide range, including food crops, cash crops, vegetables, fruits, and flowers (Chen et al., 2021). During mutagenesis, seeds are soaked in the mutagenesis solution, and the mutagenesis of plants can be achieved by changing the concentration of EMS and the mutagenesis duration. Mutagenesis of plant seeds is relatively convenient and quick, and not only are the steps simple, the workload is small, and it is suitable for the experimental research that requires the mutagenesis of most plants. Of course, we prefer the method of seed mutagenesis, but some plants may not be able to use the traditional method of seed mutagenesis due to different experimental purposes. It is not easy to obtain homozygous offspring from seeds, and it needs to be screened by techniques such as hybridization. At this time, pollen, callus, spores, plant fragments, etc. can also be selected for mutagenesis, and the mutagenesis method is relatively complicated. Compared with EMS mutagenesis of seeds, EMS mutagenesis of plant pollen has a large workload and complex operation in the process of mutagenesis. A common method is *in vivo* mutagenesis, that is, mutagenesis is carried out in a pollen tube. Meanwhile, other mutagenesis sites are usually selected for *ex vivo* mutagenesis methods.

3 The principles, methods and process of EMS mutagenesis

3.1 The concentration of the chemical and the duration of mutation

There is a strict correlation between EMS concentration, mutagenesis duration and lethality. Singh and Sadhukhan (2019) used EMS to mutate three diverged genotypes of grasspea, viz *Nirmal*, *Biol-212* and *Berhampur local*. The results showed that when the EMS concentration of *Nirmal* and *Biol-212* was higher than 0.5% and that of *Berhampur local* was higher than 1%, it was found to be fatal (Singh and Sadhukhan, 2019). The most effective concentration of EMS was 0.5%. In addition, with the increase in EMS concentration, the mutagenic efficiency increased and the effectiveness decreased (Singh and Sadhukhan, 2019). Ghosh et al. (2020) treated terminal cuttings with 0.25%, 0.30%, 0.35% and 0.40% of EMS, respectively. They concluded that morphological as well as flowering parameters, namely flower bud length, plant height, leaf area, flower yield and number of primary branches, decreased with increasing mutagenic dose. The study by Roychowdhury and Tah (2011) showed that germination and survival rates were significantly reduced with increasing EMS levels. The tolerance of plants to EMS varies widely, for example, in *Arabidopsis*, a 0.25-0.5% EMS mutation rate is high, tomato farming populations are constructed by 0.7% and 1% EMS, while in cucumber, 1.5-2% EMS (Greene et al., 2003; Minoia et al., 2010). In common plants, the larger the seed, the higher the EMS concentration required, and the longer the mutagenesis duration necessary, in order to achieve a certain mutation effect.

Mutagenesis duration is also different for different plants. In general, the higher the mutagenesis concentration selected, the shorter the mutagenesis duration. Conversely, the longer the mutagenesis duration, the lower the mutagenesis concentration used. The mutagenesis concentration required for different mutagenesis positions is also different. The mutagenesis concentration of seed mutagenesis and stem node mutagenesis is relatively high, while that of pollen mutagenesis is relatively low. When using plant seeds for mutagenesis, rice was mutagenized with 0.7% EMS, while pepper was mutagenized with 0.02% EMS concentration (Dwinianti et al., 2019; Yan W et al., 2021). The choice of concentration may also be related to the size of the seeds. Mutagenesis may also be affected by the mutagenic environment, which has not been proven due to the uncertain outcome of mutagenesis. When experimenters conduct EMS mutagenesis, they generally refer to published data and make appropriate choices based on the actual situation, instead of blindly conducting experiments according to the published data. In general, 50% of the lethality can be a good mutagenesis effect (Ke et al., 2019). In fact, in order to pursue higher mutation efficiency, the lethality rate we choose generally reaches 80%. Although the specific operation process is different, the basic steps are almost the same, as shown in Figure 1. The EMS mutagenesis concentrations of common plants are shown in Table 1.

3.2 Screening and analysis of the mutation lines

Chemical mutagenesis of seeds results in a long period of duration before full display. In experiments, identification of a population of plant mutants suitable for genotypic or phenotypic screening requires at least the production of M_2 or later progeny. The duration required to generate a suitable mutagenize population depends on the choice of mutagenic material, and addressing the issue of heterozygote and homozygote is critical.

Plant materials must be non-chimeric before phenotypic or genotype screening, and the duration required varies depending on the species and tissue culture method used. While chimeras may disintegrate in meristem cells within a month of treatment, one or more rounds of post-EMS meristem dissociation and cutting may be required to ensure that all tissues in the resulting plant are genetically homogeneous (Jankowicz-Cieslak et al., 2012). In recent years, the EMS mutagenesis of some plants is shown in Table 1.

Mutagenesis using physical mutagens has been used to generate mutant populations in various plants (Stadler, 1929; Chawade et al., 2010). However, gamma irradiation and high-speed neutrons can lead to greater DNA inversion and deletion, which hinders the recognition of genes under the mutant phenotype (Espina et al., 2018). As an alternative, EMS is a chemical reagent commonly used to induce seed mutations. EMS induces high-frequency random point mutations, some of

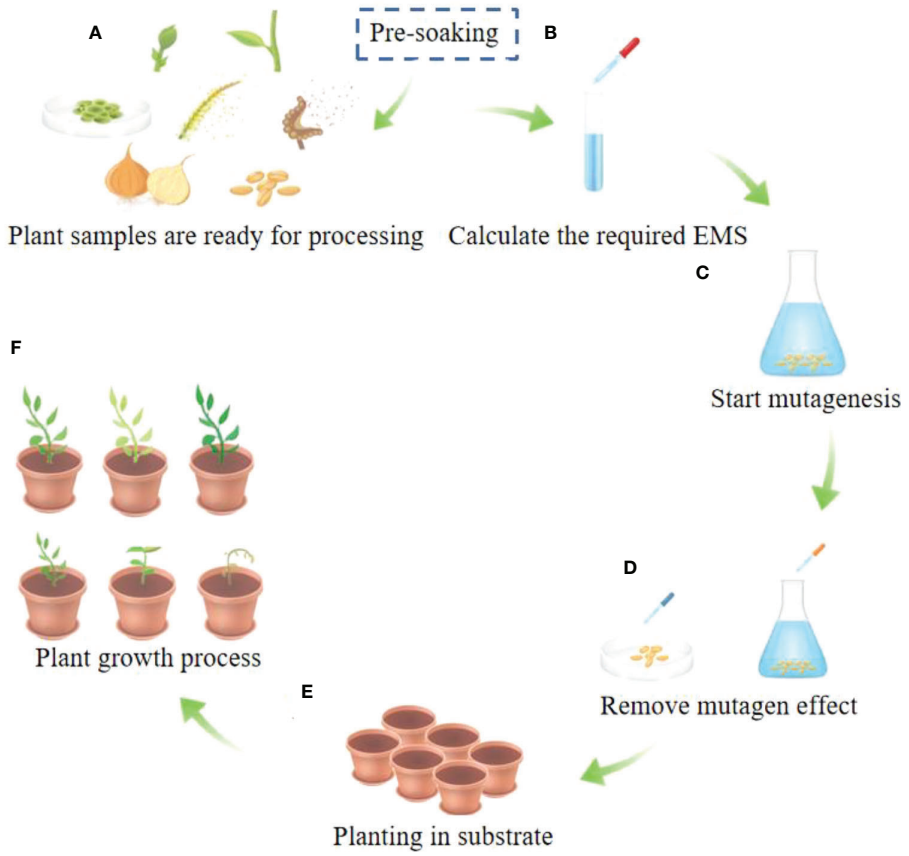


FIGURE 1
General steps of EMS mutagenesis. **(A)** Different prats of plants can be used for mutagenesis. The parts of the plant shown in A are buds, branches, callus, pollen, spores, bulbs, seeds and other parts of the plant tissue. **(B)** Determine the required EMS mutagenesis concentration and mutagenesis duration to profrom mutagenesis, and perform the mutagenesis. The preferred mutagenesis concentration range is 0.01%-4% and the duration range is 0.5h-12h. **(C)** Start mutagenesis with plant seeds as an example. **(D)** Rinse after mutagenesis or add mutagenesis terminator. **(E)** Planting in culture substrate. **(F)** After the seedlings grow, various phenotype can appear and carry out identification and further experiments.

which can produce new termination codons in genes of interest (Jankowicz-Cieslak and Till, 2015).

EMS has been successfully applied to *Solanaceae*, resulting in morphological diversity that promotes improvements in fruit quality, yield, and desirable traits such as male sterility and disease resistance. The expected result of EMS treatment of seeds or vegetative tissues is that plant populations contain high-density induced point mutations. Due to the existence of homologous sequences, the density of polyploid plants is higher. As toddlers first observe phenotype, increased ploidy confers greater tolerance to mutations (Stadler, 1929). The mutation density of triploid banana is 1/57 KB, that of tetraploid wheat is 1/40 KB, and that of hexaploid wheat and oats is 1/24 KB (Slade et al., 2005; Chawade et al., 2010; Jankowicz-Cieslak et al., 2012). The evaluation of tillering mutants density usually involves screening a small number of target gene mutations in hundreds of plants. Alternatively, less representative genome sequencing of the full genome or fewer plants can be used to estimate mutation density (Henry et al., 2014). Stable phenotypic variation should be observed in the first non-chimeric generation (M_2 for seed mutation) and can be used to determine whether the population is sufficiently mutated (Haughn and Somerville, 1987; Caldwell et al., 2004; Sabetta et al., 2011). The fertility of mutant populations should be reduced in early generations (Gottwald et al., 2009).

The traits mutated by EMS mainly include yield, quality, and resistance (Wang H et al., 2016). EMS has been successfully applied to a large number of plants to produce morphological diversity and promote the improvement of ideal traits (Lethin et al., 2020). Based on the mutation of agronomic and yield traits, new materials with excellent quality can be screened from the mutated offspring after multiple generations of screening and identification.

When a laboratory technician treated saffron with colchicine and EMS together, *ALDH*, *BGL*, and *CCD2* gene expression

TABLE 1 EMS mutagenesis study in different plants.

Plant species	Mutagenic concentration and duration	Combined with other technologies	Mutagenic significance	Reference
Four *Chrysanthemum* cultivars (‘*Homa*’, *‘Fariba2’*, *‘Arina’*, and *‘Delkash’*)	0%, 0.125%, 0.25%, and 0.5%	Genetic polymorphism among mutants and their parents was detected using inter simple sequence repeat (ISSR) and inter-retrotransposon amplified polymorphism (IRAP) molecular markers.	A wide range of phenotypic leaf and inflorescence variability was obtained.	Nasri et al., 2022
Marigold (*Tagetes* sp.)	0%, 0.2%, 0.4%, 0.6%, 0.8%, 1.0%, 1.5%, 2.0%, and 3.0%; 4 hours (The acute mutation technique), 6 hours, 24 hours and 48 hours (The chronic mutation technique)	Observations were made on the percentage of surviving plants, quantitative and qualitative characters.	Increasing the diversity of marigold (*Tagetes* sp.).	Lenawaty et al., 2022
Sweet wormwood (*Artemisia annua* L.)	100 Gy, 200 Gy, 300 Gy and combination treatments with 100 Gy + 0.1%EMS, 200 Gy + 0.1% EMS, 300 Gy + 0.1%EMS	Meiotic study was done and various cytological aberrations were observed. In addition, quantitative analysis of chl pigments was also done.	Increasing the genetic variability and induces new trait.	Singh and Kumar, 2022
Four watermelon accessions named *G42*, *97103*, *PI 595203* and *PI 296341-FR*	0%, 0.1%, 0.15% and 0.2%; 0, 40, 60 and 80 min	Incorporating the high-coverage and accurate long-read sequence data.	Elongated fruit shape and male sterility (*ClMS1*).	Deng et al., 2022
Cotton (*Gossypium hirsutum* L.)	–	Correlation coefficients were used to study the association between fiber traits.	One (Population R) focused on improving four fiber attributes (micronaire, length, strength and elongation) and the other (population S) to pyramid superior alleles for fiber length.	Patel et al., 2022
Chinese cabbage (*Brassica rapa ssp. Pekinensis*)	0.4% EMS at room temperature in the dark for 16 h	A total of 300 M_2 to M_5 EMS mutants were phenotypically screened and then sequenced. A forward-genetics approach and reverse-genetics approach were used.	Facilitating gene mining of Chinese cabbage and might also be useful for the study of other *Brassica crops*.	Sun et al., 2022
Aerobic rice cultivar *Nagina 22*	–	Molecular genetics approaches	Salinity tolerance	Shankar et al., 2021
Oilseed rape (*Brassica napus*)	–	Genomic background selection combined with marker-assisted selection	Inducing random mutations throughout the genome with high mutation density	Karunarathna et al., 2021
Maize inbred line *Jing 724*	–	Bulk-segregant RNA sequencing and Kompetitive Allele-Specific PCR assays	Identifying genomic loci regulating Genic male sterility (GMS)	Shi et al., 2021
Sunflower variety *BARI Surjamukhi-2*	0.2%, 0.4%, 0.5%, 0.6% EMS	Quadratic regression analysis	Qermination rate, survival rate and early seedling growth rate	Habib et al., 2021
Indica variety *HHZ*	0.7% EMS solution for 12 h	The whole genome resequencing and single nucleotide polymorphic sites (SNPs).	DNA repair	Yan W et al., 2021
Common wheat (*T. aestivum* L.)	0.5% EMS for 12 h	Genomic DNA extraction, PCR amplification, and sequence analyses	Herbicide-resistant	Chen et al., 2021
Groundnut	1.2% and 0.4% EMS	Targeting Induced Local Lesions in Genomes (TILLING) approach	Reducing allergenicity and increasing oleic content	Karaman et al., 2021
Short day Indian onion cultivar *Bhima dark red*	0%, 0.2%, 0.4%, 0.6%, 0.8%, 1.0%, 1.2% EMS	Probit Analysis based on germination percentage	Mutagenic agent significantly reduced seed germination and seedling growth parameters in terms of shoot and root length	Singh et al., 2021
Chickpea (*Cicer arietinum* L.)	4% EMS for 10 h	Genetic transformation of tobacco plants	Providing resistance to IMI herbicides	Galili et al., 2021

(Continued)

TABLE 1 Continued

Plant species	Mutagenic concentration and duration	Combined with other technologies	Mutagenic significance	Reference
Cucumber (*Cucumis sativus* L.)	–	Genetic analysis, MutMap+ and Kompetitive Allele Specific PCR (KASP) genotyping	Reducing lethality during seed germination in cucumber.	Wang C et al., 2021
Chinese cabbage (*Brassica campestris* L. *ssp. Pekinensis*)	–	Genetic analysis	Breeding new varieties exhibiting a wax deficient phenotype	Liu et al., 2021
Barley (‘*Hordeum vulgare*’ L.)	Five EMS dosages (0.1%, 0.3%, 0.5%, 0.7% and 0.9%) and five exposure times (0.5 hr, 1 hr, 1.5 hr, 2 hrs and 2.5 hrs)	Data was recorded for percent germination, seedling survival, shoot height, root height, shoot and root biomass.	Selecting fodder barley mutants with high biomass yield	Sharamo et al., 2021
Rice (*Oryza sativa L.*)	3% EMS	Being characterized for phenotypic, biochemical and grain qualities	Inducing early flowering mutants in popular rice variety *Bapatla 2231* (*BPT 2231*)	Gautam et al., 2021
Wheat (*Triticum aestivum* L.)	0.5% EMS	Measuring their impact on coleoptile length, gibberellic acid (GA) sensitivity, and DELLA/GID1 interaction	Increasing wheat yields	Jobson et al., 2021
Kharif sorghum (*Sorghum bicolor* L.)	0.1%, 0.2%, 0.3% EMS	Chlorophyll mutation frequency and spectrum	Chlorophyll mutants	Thange et al., 2021
Fenugreek (*Trigonella foenum-graecum* L.)	0.1%, 0.2%, 0.3%, and 0.4% EMS	LSD test	Increaseing grain yield and secondary metabolites	Parchin et al., 2021
Two *Chrysanthemum* cultivars, ‘*Jaguar Pink*’ and ‘*Reagent Pink*’	0.1%, 0.2%, 0.3% 0.4%, 0.5% and 0.6% EMS	Data on the number of survival callus, number of germinating callus, and number of callus with shoots after exposure to different concentrations of EMS were noted.	Obtaining genetic diversity in chrysanthemums	Aisyah et al., 2021
Maize	1% for 2 h	Transcriptomic and metabolic changes	The characterization of flavonoid biosynthesis	Dong et al., 2021
Ajara ghansal	EMS 0.8%, SA 0.006%, and gamma rays 200 Gy	Seed germination (%), lethality (%), chromosomal abnormality (%), chlorophyll deficient sector (%), pollen sterility (%), and plant survival were determined	The improvement of non-basmati aromatic landrace *Ajara ghansal*	Desai et al., 2021
The four dwarf wheat mutants, *dm1*, *dm2*, *dm3* and *dm4*	1–1.5% EMS for the duration of 4–8 h	Kyoto Encyclopedia of Genes and Genomes (KEGG) analyses	Great advancements in yield improvement	Xiong et al., 2020
Jasminum grandiflorum cv.	0.25%, 0.3%, 0.35% and 0.4% of EMS	Molecular analysis based on ISSR data	Developing new cultivars especially in ornamental crops	Ghosh et al., 2020
Triticum aestivum (wheat)	1% EMS	Field trials and principal component analysis, DNA sequencing, Alignment of reads to reference genome, SNP calling	Further increasing salt tolerance	Lethin et al., 2020
Capsicum annuum pepper “*Micro-Pep*”	0.3% EMS	Targeting Induced Local Lesions IN Genomes (TILLING)	Genetic diversity in useful traits	Siddiqe MI et al., 2020
The bred new wheat line *KD527*	0.3% EMS for 4 ~ 6 h	Chromosomal location analysis	Lesion-mimic and premature aging	Kong et al., 2020
Seeds of carrot inbred line “*17005*”	0.5% EMS for 6 h	Genetic analysis	Enriching the carrot germplasm	Wu et al., 2020
Brassica napus	0.4%, 0.8%, 1.2% and 1.6% EMS	Whole-genome sequencing and GC-FID analysis	Genetic improvement of seed oil content and fatty acid composition of *B. Napus*	Van Zelm et al., 2020

(Continued)

TABLE 1 Continued

Plant species	Mutagenic concentration and duration	Combined with other technologies	Mutagenic significance	Reference
Hyoscyamus niger	0.00% 0.01%, 0.02%, 0.03%, 0.04%, 0.05%, 0.06%, 0.70%, 0.08%, 0.09% and 0.1% EMS for 1 hr	PCR analysis, DNase treatment and cDNA synthesis and Quantitative real–time PCR	Increased accumulation of scopolamine and hyoscyamine	He et al., 2018
Sorghum	0.00%, 0.5% and 1.0% EMS	Germination percentage and Emergence percentage	Induce genetic variation in the tested sorghum genotypes	Wanga et al., 2020
Cotton (*G. hirsutum* L.)	0.5%, 1.5%, 2.5% and 3.5% EMS for 3 and 6 h	HRM analysis on DNA base level variation, Genome sequencing and SNP identification	Abundant EMS mutant libraries (approximately 12 000) in allotetraploid cotton were successfully obtained.	Lian et al., 2020
Chili Pepper (*Capsicum frutescens* L.)	0%, 0.01%, 0.02%, 0.04% EMS	SSR molecular marker analysis	Increasing genetic variation in chili pepper plants	Dwinianti et al., 2019
Sesame (*Sesamum indicum* L. *Vartilottama; family: Pedaliaceae*)	0.25%, 0.50% and 1.00% EMS for 2, 4 and 6h durations	Phenotypic variables on which observations were performed included plant height (cm), number of primary and total branches per plant, number of capsules per plant, number of seeds per capsule and per plant and total seed yield per plant (g)	Yield and six yield contributing traits	Saha, 2019
The two upland rice genotypes *Dawk pa-yawm* (white rice) and *Dawk kha 50* (red rice)	EMS at the concentration of 0.5%, 0.75%, 1% and 1.25%	Phenotypic variability among mutants	To create new and diverse characters to a natural population	Awais et al., 2019
Vernonia (*Centrapalus pauciflorus (Willd.) H.Rob.*)	0.372% EMS for 1 h and 2 h	Determination of seed oil content and fatty acids	Altering seed oil content and fatty acid compositions in selected *Vernonia* accessions	Hadebe et al., 2019

increased by 2-fold (Samadi et al., 2022). Mutations of beneficial characteristics for wheat include dwarfing, early maturity, large grain, and more tillers (Ferrie et al., 2020). In the report of Kuraparthy et al. (2007) single tillering mutants were screened from the diploid wheat EMS mutant library by molecular technology, and the exact location of tiller-related genes on the chromosome was determined. Related experimenters identified a new type of rice precocious leaf 85 (*psl85*) mutant in the rice mutant population, showing an obvious premature senescence leaf phenotype and dwarfism, and the expression of senescence-related genes was up-regulated. Furthermore, genetic analysis showed that the senescent leaf phenotype is controlled by a single recessive nuclear gene, and further studies on senescence genes in rice were conducted (He et al., 2018). Yan W et al. (2021) randomly induced G/C to A/T conversion in rice genome by EMS. Whole-genome resequencing of 52 rice EMS mutants to investigate potential EMS mutational bias and its possible correlation with sequence background and chromatin structure.

After EMS mutagenesis treatment, experimenters observed a significant increase in the average number of shoots and roots of Hyoscyamus, and the EMS treatment also increased the accumulation of scopolamine and scopolamine in the explants compared to control (Shah et al., 2020).

After EMS, sodium azide (NaN_3) or gamma-rays mutagenesis, chlorophyll-deficient mutants were most efficiently generated in EMS mutagenesis, three mutants were obtained from soybean seeds, and the progeny isolation of non-nodule mutant plants was completed (Carroll et al., 1986). The experimenter used EMS to mutagenize wheat cv. *Gao 8901*, and isolated the waxy mutant (*Wx-null*) by screening the progeny seeds with KI-I, and there was no significant difference in seed morphology and size compared with the wild type, but the mutants contained more B-type starch granules, while the amylose content was reduced (Pang et al., 2010). In the rape study, the Korean rape variety *Tamla* was used for EMS mutagenesis. The screened mutants were slightly smaller

than the control in the early vegetative growth stage, but the oleic acid content in the mutants increased by about 7%. The mutants will be used for developed high oleic rapeseed varieties and conduct related research (Lee et al., 2018). Experimenters performed EMS mutagenesis on 5500 *Gossypium herbaceum* seeds, and about 5% of the progeny showed visible phenotype, such as leaf shape changes and sterility. The morphological and phenotypic evaluation of more than 4,000 plant materials of progeny was carried out, and the results showed significant differences (Kumar et al., 2022). Munda et al. (2022) treated seeds with different doses of EMS, induced morphological mutants of citronella, analyzed the morphological and physiological characteristics of the obtained mutants, increased herbage yield and citronellal content, and increased economic value. In the EMS mutagenesis of *Brassica napus* plants, a dwarf mutant *bnd2* was successfully isolated. Compared with the wild type, the mutant has a shorter hypocotyl and a reduced plant height, and verified that *bnd2* is a single-site recessive mutation that can be used research on the genetic mechanism of Brassica napus (Li et al., 2021). According to official data released by the FAO/IAEA project, 16 pepper varieties have been bred so far through mutation techniques (http://mvd.iaea.org). In pepper mutagenesis, several studies have used high-quality mutant populations obtained from EMS mutagenesis (Arisha et al., 2014). In particular, the EMS mutant population of sweet pepper variety *'Maoer'* was established to study the genes regulating flower and plant structure (Siddiqe MI et al., 2020).

Nasri et al. (2022) mutated four *Chrysanthemum* varieties ("*Homa*", "*Fariba2*", "*Arina*", and "*Delkash*") with EMS (0-0.5%) as mutagens and leaf discs as explants to obtain new varieties. In addition, ISSR and IRAP molecular markers were used to detect the genetic polymorphism between the mutant and its parents. The ISSR and IRAP primers used can classify *Chrysanthemum* mutants according to varieties and some extent according to the EMS concentration used, to confirm their effectiveness in distinguishing real mutants, and to allow them to select in advance and reduce the size of the mutant population. In *in vitro* mutagenesis, EMS-induced mutations may be a useful tool to aid in breeding programs for new generation *Chrysanthemum* varieties.

4 Recent studies in plants using EMS mutagenesis

Plants are sessile, and they have to withstand various stress tolerance, which largely limit the way plants can survive, so it is crucial to improve their tolerance to stress tolerance. At present, research to screen resistant mutants by mutagenesis has attracted much attention, and stress-tolerant mutants have been successfully screened in many plants (Ge et al., 2018). Improving plant stress tolerance is a powerful measure to improve plant yield. Moreover, there are many studies on improving resistance through EMS mutagenesis (Thangwana et al., 2021; Li et al., 2022).

Salt tolerance has a great impact on plant yield traits, especially the genetic basis of salt tolerance (Costa and Farrant, 2019). However, in *Arabidopsis*, salt tolerant mutants caused by monocyte mutation have been previously reported, revealing the complexity of the genetic basis of plant salt tolerance. The results show that osmotic pressure, osmotic protectant, free radical detoxification, ion transport system, hormone level changes, and hormone-guided communication are all related to salt stress, which further affects plant yield traits (Quesada et al., 2000; Zhao et al., 2021). EMS induction of 275 mutants has been used in different levels of salinity response study, and research shows *N22-L-1013*, *N22-L-806*, and *N22-L-1010* were identified as typical Na excluders (Shankar et al., 2021). After four generations of choice, and in the field experiment carried out, the EMS wheat mutants, showed good salt-tolerant phenotypes (Lethin et al., 2020). *Hitomebore Salt Tolerant 1* (*hst1*) of rice mutants from the 6000 EMS by Takagi et al. (2015) in the mutant screening, and researchers verified the *OsRR22* role in the process response to salt stress. Due to the complexity of plant salt-tolerant and limited experimental data from previous studies, the NaCl tolerance mechanism of the mutants needs to be further investigated. Salt-tolerant crops play an important role in the use of saline-alkali land for agricultural production (Van Zelm et al., 2020).

EMS-induced yellow seeded *Brassica napus* was used to analyze the drought tolerance of mutants at the bud stage and seedling stage, and successfully screened for mutants with strong drought resistance (Tang et al., 2020). Screening in mutant nightshade populations restored alleles with improved content comprised of phenolic compounds, namely anthocyanin and chlorogenic acid (CGA) (Xi-Ou et al., 2017). In this study, the author performed High Performance Liquid Chromatography (HPLC) to determine the concentration of the anthocyanin, and the results showed that the CGA content of mutant was significantly higher than that of WT. RT-PCR anlysis showed that levels of expression of anthocyanin biosynthetic genes were increased in *S9-1*, with the exception of *SmPAL* (Xi-Ou et al., 2017). After EMS mutagenesis, glyphosate-resistant mutant lines were selected from the M_4 generation of soybean seeds with excellent agronomic characteristics. Wheat and *Chickpea cicer arietinum* L. Plants. beans also won the IMI mutants in this way (Chen et al., 2021; Galili et al., 2021).

In the process of mutant screening, some physiological indexes can be used as stress resistance indexes for resistance screening under different stress conditions (Friesen and Wall, 1986; Sebastian and Chaleff, 1987). Li et al. (2019) induced radish mutation with EMS, which is suitable for obtaining the target characteristics of new radish materials. *DY13* radish seeds were treated with 0.5% EMS to produce sterile mutants.

Morphological observation showed that the anthers of these male sterile lines were curled, browned and wrinkled, and their disease resistance and drought tolerance were enhanced. The male sterile line was successfully selected from *DY13* radish, which provides a new and effective method for the selection of the radish male sterile line.

Munda et al. (2022) used an EMS chemical mutagen to induce the morphological mutant of citronella Indus. The mutant has high puncture strength and an enhanced anti-penetration ability due to a curved stem, which further proves the reliability of practical physiological index analysis of stress-resistant mutants. A large number of studies have shown that it is very reliable to screen the resistance of mutated plants according to physiological indexes, and this will speed up the process of plant stress resistance breeding.

In recent years, various attempts have been made to cultivate crops that are tolerant to herbicide doses, which are usually fatal to weeds (Prakash et al., 2020). Different scientific methods have been used to genetically modify crops to cultivate herbicide-tolerant/herbicide-resistant crops (Halford and Shewry, 2000). Herbicide-resistant mutant plants have been found in many crops, such as corn, wheat, cotton, sorghum, sunflower, lentil, and soybean (Anderson and Georgeson, 1989; Newhouse et al., 1991; Rajasekaran et al., 1996). Rizwan et al. (2017) developed an imidazolinone-resistant lentil mutant (*RH44*) through EMS mutation. In general, it is not easy to develop crops with high-dose herbicide resistance. Such herbicides can kill all types of weeds at one duration. However, to improve the resistance of crops to higher herbicide doses, new strategies are being adopted, such as large-scale screening of mutagenic populations, re-mutation of independently isolated mutations, screening, and gene polymerization, and selecting hypothetical herbicide-resistant mutants in different crops (Piquerez et al., 2014).

Among various mutagenic methods, chemical reagents that can produce genetic variation in crops have been widely popular for many years. A mutation strategy is considered to be an important step for producing new and valuable genetic variations (Wei et al., 2022. Many important crops, such as wheat, sesame, rice, grapefruit, cotton, and bananas, have produced mutant-derived varieties. In tomato, EMS-based mutations have been used to generate specific alleles such as a purple leaf color, smaller leaves, and early fruit (Silué et al., 2013). Through EMS mutagenesis, researchers have cultivated Targeting Induced Local Lesions IN Genomes (TILLING) populations containing a mutant phenotype of various quality traits in cucumber and pumpkin (Kami et al., 2000; Prakash et al., 2020). Some M_1 plants showed chimerism caused by a recessive gene mutation. Some M_1 plants showed variation in flower organs, delayed flowering and a pale leaf color at maturity. Fruit color and shape also changed in M_1 plants, consistent with EMS-induced changes in tomato fruit (Gauffier et al., 2016). Because EMS can cause morphological variation in fruit, we believe that EMS mutation may have potential value in fruit quality (Bhat et al., 2017).

5 Molecular technology promotes application of EMS mutagenesis technology

In recent years, research on EMS mutagenesis has continued to develop, and the mutagenesis of some plants is shown in Table 1. EMS mutagenesis has been widely studied in mutant screening and mutant library construction. At present, some research progress has been made in *Arabidopsis*, rice, soybean, and other plants (DeMarini, 2020). Identifying mutants by plant phenotype is the most direct method, but this has significant limitations, and it is easy to miss important mutations. In addition, some researchers have used molecular markers to analyze the EMS mutants of wheat, and to screen mutants with different glutenin subunit deletions from a wheat EMS mutant library (Grover and Sharma, 2016). With the rapid development of molecular sequencing technology, research is also intensifying to identify mutants with TILLING technology (Manzanares et al., 2016; Taheri et al., 2017). Reverse genetics is a potentially important approach to identify new mutations in genes of interest. Reverse genetics can be applied to plant tillering, regardless of the level of plant genome structure (Kurowska et al., 2011). In contrast to other reverse genetics methods (such as RNAi technology) and T-DNA insertional mutagens, this non-transgenic method does not require transformation (Krysan et al., 1999; Travella et al., 2006). TILLING aims to find nucleotide changes caused by chemical mutagenesis in target genes, to enable changes in protein function (Till et al., 2004). The development of molecular technology will be beneficial to the identification of EMS mutagenesis mutants and promote the application of EMS mutagenesis technology.

EMS is the mutagen of choice, which induces single-nucleotide variation through the titillation of a specific nucleoside, resulting in a broad spectrum of mutations (Henikoff et al., 2004). This may be silencing, nonsense, missed, and splicing mutations in the gene coding region (Boualem et al., 2014). TILLING has been applied to different plants, such as Archbishops thali, rapeseed, soybean, rice, wheat, tomato, sunflower, and tobacco, indicating that this method is an important alternative method for plant species function analysis (Till et al., 2007; Reddy et al., 2012; Bovina et al., 2014; Yan Z et al., 2021). The mutant population induced by EMS was used to target induced local damage (TILLING) in the genome. Further screening and identification of EMS mutants were identified by the combination of morphological analysis and biotechnology,

which will facilitate the screening of abiotic stress tolerance mutants, and the preliminary screening of mutants in a more efficient and targeted manner.

6 Conclusion

The development of EMS mutagenesis promoted the rapid development of plant functional genomics, resulting in the birth of map-based cloning technology and directed induced local mutation technology (Kim et al., 2006). The latter one effectively combines traditional chemical mutagenesis with mutant screening skills. EMS mutagenesis cause high throughput mutation with low cost, which tremendously speeds up the research for plant genomics and promotes the development of molecular breeding for abiotic stress tolerance plants.

Similar to other breeding methods, EMS mutation also has limitations, including a high level of randomness, low mutation efficiency, and few beneficial mutations. Additionally, it is still difficult to identity, clone and characterize mutations, resulting in limited application of this method in plant species with complicated or polyploid genomes. Although the latest gene editing technology, such as the CRISPR/Cas9 system, which is faster, more accurate, and is widely used in plant abiotic stress tolerance research by altering individual gene loci, it is difficult for genetic improvement of traits controlled by multiple sites. Moreover, the CRISPR/Cas9 system is difficult to apply to the species with little genomic information. On the contrary, EMS mutagenesis results mutation at multi-sites and can obtain abundant traits, which is difficult to be replaced by other mutagenesis breeding. It is also noteworthy that although the CRISPR/Cas9 technology has been widely used in gene editing, EMS mutagenesis is a non-GMO application, which could meet the strict laws for genetic modification of genes.

Author contributions

LC prepared an outline, first draft. LD, MS, ZY, KH, HL, HY, and LL provided literature support, and prepared the figure and table. HY and LL are corresponding to overall editing and finalization of paper drafts. All authors read and approved the published version of the manuscript.

Funding

This work was supported by the National Natural Science Foundation of China (31971410).

Acknowledgments

We would like to express our sincere thanks to everyone who assisted us with this paper.

Conflict of interest

The authors declare that the research was conducted in the absence of any commercial or financial relationships that could be construed as a potential conflict of interest.

Publisher's note

All claims expressed in this article are solely those of the authors and do not necessarily represent those of their affiliated organizations, or those of the publisher, the editors and the reviewers. Any product that may be evaluated in this article, or claim that may be made by its manufacturer, is not guaranteed or endorsed by the publisher.

References

Anderson, P., and Georgeson, M. (2011). Herbicide-tolerant mutants of corn. *Genome* 31 (2), 994–999. doi: 10.1139/g89-173

Arisha, M. H., Liang, B. K., Muhammad Shah, S. N., Gong, Z. H., and Li, D. W. (2014). Kill curve analysis and response of first generation *Capsicum annuum* l. B12 cultivar to ethyl methane sulfonate. *Genet. Mol. Res.* 13 (4), 10049–10061. doi: 10.4238/2014.November.28.9

Ashrafi Parchin, R., Nasrollahnezhad Ghomi, A. A., Naghdi Badi, H., Navabpour, S., Mehrafarin, A., and Eskandari, A. (2021). Investigation effect of ethyl methane sulfonate (EMS) on some of morphophysiological and phytochemical traits of fenugreek (*Trigonella foenum-graecum* l.). *Ind. Crops* 162, 113239. doi: 10.1016/j.indcrop.2021.113239

Awais, A., Nualsri, C., and Soonsuwon, W. (2019). Induced mutagenesis for creating variability in thailand's upland rice (cv. *Dawk pa-yawm* and *Dawk kha 50*) using ethyl methane sulphonate (EMS). *Sarhad J. Agric.* 35 (1), 293–301. doi: 10.17582/journal.sja/2019/35.1.293.301

Bhat, S., Sharma, S., and Sharma, V. K. (2017). Effect of EMS induced morphological mutation in strawberry. *J. Hill Agric.* 8 (1), 50–55. doi: 10.5958/2230-7338.2017.00020.9

Boualem, A., Fleurier, S., Troadec, C., Audigier, P., Kumar, A. P., Chatterjee, M., et al. (2014). Development of a *Cucumis sativus* TILLING platform for forward and reverse genetics. *PloS One* 9 (5), e97963. doi: 10.1371/journal.pone.0097963

Boysen, G., Pachkowski, B., Nakamura, J., and Swenberg, J. (2009). The formation and biological significance of N^7-guanine adducts. *Mutat. Res.* 678, 76–94. doi: 10.1016/j.mrgentox.2009.05.006

Caldwell, D. G., McCallum, N., Shaw, P., Muehlbauer, G. J., Marshall, D. F., Waugh, R., et al. (2004). A structured mutant population for forward and reverse genetics in barley (*Hordeum vulgare* L.). *Plant J.* 40 (1), 143–150. doi: 10.1111/j.1365-313X.2004.02190.x

Carroll, B. J., McNeil, D. L., and Gresshoff, P. M. (1986). Mutagenesis of soybean (*Glycine max (L.) merr.*) and the isolation of non-nodulating mutants. *Plant Sci.* 47, 109–114. doi: 10.1016/0168-9452(86)90057-9

Chawade, A., Sikora, P., Bräutigam, M., Larsson, M., Vivekanand, V., Nakash, M. A, et al. (2010). Development and characterization of an oat TILLING-population and identification of mutations in lignin and β-glucan biosynthesis genes. *BMC Plant Biol.* 10, 86. doi: 10.1186/1471-2229-10-86

Chen, Z., Wang, Z., Heng, Y., Li, J., Pei, J., Cao, Y., et al. (2021). Generation of a series of mutant lines resistant to imidazolinone by screening an EMS-based mutant library in common wheat. *Crop J.* 9 (5), 1030–1038. doi: 10.1016/j.cj.2020.11.001

Costa, M.-C. D., and Farrant, J. M. (2019). Plant resistance to abiotic stresses. *Plants* 8, 553. doi: 10.3390/plants8120553

DeMarini, D. M. (2020). The mutagenesis moonshot: The propitious beginnings of the environmental mutagenesis and genomics society. *Environ. Mol. Mutag.* 61 (1), 8–24. doi: 10.1002/em.22313

Deng, Y., Liu, S., Zhang, Y., Tan, J., Li, X., Chu, X., et al. (2022). A telomere-to-telomere gap-free reference genome of watermelon and its mutation library provide important resources for gene discovery and breeding. *Mol. Plant* 15 (8), 1268–1284. doi: 10.1016/j.molp.2022.06.010

Desai, S. P., Jadhav, A. G., Ramteke, A. R., Dhole, V. J., Bapat, V. A., and Gaikwad, N. J. A. R. J., et al. (2021). Differential effects of gamma rays, EMS, and SA on biological parameters of ajara ghansal a non-*Basmati* aromatic rice landrace from kolhapur, maharashtra.

Dong, H., Li, H., Xue, Y., Su, S., Li, S., Shan, X., et al. (2021). *E183K* mutation in chalcone synthase C2 causes protein aggregation and maize colorless. *Front. Plant Sci.* 12, 679654. doi: 10.3389/fpls.2021.679654

Dwinianti, E. F., Mastuti, R., and Arumingtyas, E. L. J. J. o. T. L. S. (2019). Genetic variation analysis of ems-induced chili pepper (*Capsicum frutescens l.*) mutants using SSR markers. *J. Trop. Life Sci.* 9 (3), 223–228.

Espina, M. J., Ahmed, C. M.S., Bernardini, A., Adeleke, E., Yadegari, Z., Arelli, P., et al. (2018). Development and phenotypic screening of an ethyl methane sulfonate mutant population in soybean. *Front. Plant Sci.* 9, 394. doi: 10.3389/fpls.2018.00394

Ferrie, A. M. R., Bhowmik, P., Rajagopalan, N., Kagale, S., et al. (2020). "CRISPR/Cas9-mediated targeted mutagenesis in wheat doubled haploids," in *Cereal genomics* (Springer), 183–198. doi: 10.1007/978-1-4939-9865-4_15

Fora, F., Shimelis, H., Olaolorun, B., Korir, H., Indetie, A., Mashilo, J., et al. (2021). Determining ethyl methane sulfonate-mediated (EMS) mutagenesis protocol for inducing high biomass yield in fodder barley (*'Hordeum vulgare'* l.). *Aust. J. Crop Sci.* 15 (7), 983–989. doi: 10.21475/ajcs.21.15.07.p2877

Friesen, G., and Wall, D. A. (1986). Tolerance of lentil (*Lens culinaris medik.*) to herbicides. *Can. J. Plant Sci.* 66 (1), 131–139. doi: 10.4141/cjps86-017

Fu, D., Calvo, J. A., and Samson, L. D. (2012). Balancing repair and tolerance of DNA damage caused by alkylating agents. *Nat. Rev. Cancer.* 12 (2), 104–120. doi: 10.1038/nrc3185

Galili, S., Hershenhorn, J., Edelman, M., Sobolev, V., Smirnov, E., Amir-Segev, O., et al. (2021). Novel mutation in the acetohydroxyacid synthase (AHAS), gene confers imidazolinone resistance in *Chickpea cicer arietinum* l. *Plants. Plants* 10 (12), 2791. doi: 10.3390/plants10122791

Gauffier, C., Lebaron, C., Moretti, A., Constant, C., Moquet, F., Bonnet, G., et al. (2016). A TILLING approach to generate broad-spectrum resistance to potyviruses in tomato is hampered by *eIF4E* gene redundancy. *Plant J.* 85 (6), 717–729. doi: 10.1111/tpj.13136

Gautam, V., Swaminathan, M., Akilan, M., Gurusamy, A., Suresh, M., Kaithamalai, B., et al. (2021). Early flowering, good grain quality mutants through gamma rays and EMS for enhancing per day productivity in rice (*Oryza sativa* L.). *Int. J. Radiat. Biol.* 97 (12), 1716–1730. doi: 10.1080/09553002.2021.1987563

Ge, F.-y., Zheng, N., Zhang, L.-p., Huang, W.-k., Peng, D.-l., Liu, S.-m, et al. (2018). Chemical mutagenesis and soybean mutants potential for identification of novel genes conferring resistance to soybean cyst nematode. *J. Integr. Agric.* 17 (12), 2734–2744. doi: 10.1016/S2095-3119(18)62105-7

Ghosh, S., Ganga, M., S K, S., Kumar, A., Kapoor, M., et al. (2020). Induction of mutation in *Jasminum grandiflorum* with gamma rays and EMS and identification of novel mutants using molecular markers and SEM imaging. *Indian J. Hortic.* 77 (4), 695–703. doi: 10.5958/0974-0112.2020.00101.2

Gillmor, C. S., and Lukowitz, W. (2020). "EMS mutagenesis of arabidopsis seeds," in *Plant embryogenesis* (Springer), 15–23. doi: 10.1007/978-1-0716-0342-0_2

Gocke, E., Bürgin, H., Müller, L., and Pfister, T. (2009). Literature review on the genotoxicity, reproductive toxicity, and carcinogenicity of ethyl methanesulfonate. *Toxicol. Lett.* 190 (3), 254–265. doi: 10.1016/j.toxlet.2009.03.016

Gottwald, S., Bauer, P., Komatsuda, T., Lundqvist, U., Stein, N., et al. (2009). TILLING in the two-rowed barley cultivar '*Barke*' reveals preferred sites of functional diversity in the gene *HvHox1*. *BMC Res. Notes* 2 (1), 1–14. doi: 10.1186/1756-0500-2-258

Greene, E. A., Codomo, C. A., Taylor, N. E., Henikoff, J. G., Till, B. J., Reynolds, S. H., et al. (2003). Spectrum of chemically induced mutations from a large-scale reverse-genetic screen in *Arabidopsis*. *BMC Plant Biol.* 164 (2), 731–740. doi: 10.1093/genetics/164.2.731

Grover, A., and Sharma, P. c (2016). Development and use of molecular markers: past and present. *Crit. Rev. Biotechnol.* 36 (2), 290–302. doi: 10.3109/07388551.2014.959891

Habib, S. H., Akanda, M. A.L., Roy, P., Kausar, H., et al. (2021). Effect of different dosage of EMS on germination, survivability and morpho-physiological characteristics of sunflower seedling. *Helia* 44 (75), 167–180. doi: 10.1515/helia-2021-0008

Hadebe, S., Hadebe, S., Modi, A. T., Hugo, A., Shimelis, H. A, et al. (2019). Seed oil content and fatty acid composition response to ethyl methanesulphonate mutagenesis in vernonia. *South Afr. J. Plant Soil* 36 (5), 375–380. doi: 10.1080/02571862.2019.1631399

Halford, N. G., and Shewry, P. R. (2000). Genetically modified crops: methodology, benefits, regulation and public concerns. *Br. Med. Bull.* 56 (1), 62–73. doi: 10.1258/0007142001902978

Haughn, G., and Somerville, C. R. (1987). *Selection for herbicide resistance at the whole-plant level* (ACS Publications) American Chemical Society. 334 98–107.

He, Y., Zhang, Z., Li, L., Tang, S., Wu, J. L, et al. (2018). Genetic and physio-biochemical characterization of a novel premature senescence leaf mutant in rice (*Oryza sativa* l.). *Int. J. Mol. Sci.* 19 (8), 2339. doi: 10.3390/ijms19082339

Henikoff, S., Till, B. J., and Comai, L. (2004). TILLING. traditional mutagenesis meets functional genomics. *Plant Physiol.* 135 (2), 630–636. doi: 10.1104/pp.104.041061

Henry, I. M., Nagalakshmi, U., Lieberman, M. C., Ngo, K. J., Krasileva, K. V., Vasquez-Gross, H., et al. (2014). Efficient genome-wide detection and cataloging of EMS-induced mutations using exome capture and next-generation sequencing. *Plant Cell* 26 (4), 1382–1397. doi: 10.1105/tpc.113.121590

Hossain, Z., Mandal, A. K., Datta, S. K., Biswas, A. K., et al. (2006). Development of NaCl-tolerant strain in *Chrysanthemum* morifolium ramat. through *in vitro* mutagenesis. *Plant Biol.* 8 (04), 450–461.

Jankowicz-Cieslak, J., Huynh, O. A., Brozynska, M., Nakitandwe, J., Till, B. J., et al. (2012). "Induction, rapid fixation and retention of mutations in vegetatively propagated banana," in *Advances in plant breeding strategies: breeding, biotechnology*, vol. 10. , 1056–1066. doi: 10.1111/j.1467-7652.2012.00733.x

Jankowicz-Cieslak, J., and Till, B. J. (2015). "Forward and reverse genetics in crop breeding," in J. M. Al-Khayri, S. M. Jain, D. V. Johnson , et al (Eds.), *Advances in plant breeding strategies: breeding, biotechnology molecular tools*, 215–240. Cham: Springer International Publishing.

Jobson, E. M., Martin, J. M., Sharrock, R., Hogg, A. C., Giroux, M. J., et al. (2021). Identification and molecular characterization of novel *Rht-1* alleles in hard red spring wheat. *Crop Sci.* 61 (2), 1030–1037. doi: 10.1002/csc2.20375

Kami, J., and Gepts, P. (2000). Development of a BAC library in common bean genotype BAT93. *Annu. Rep. Bean Improv. Coop.* 43 (2), 208–209. doi: 10.1002/csc2.20375

Karaman, K., Kizil, S., Başak, M., Uzun, B., and Yol, E., et al. (2021). Development of EMS-induced mutagenized groundnut population and discovery of point mutations in the *ahFAD2* and *Ara h 1* genes by TILLING. *J. Oleo Sci.* 70 (11), 1631–1640. doi: 10.5650/jos.ess21075

Karunarathna, N. L., Patiranage, D. S.R., Harloff, H. J., Sashidhar, N., Jung, C., et al. (2021). Genomic background selection to reduce the mutation load after random mutagenesis. *Sci. Rep.* 11 (1), 1–8. doi: 10.1038/s41598-021-98934-5

Ke, C., Guan, W., Bu, S., Li, X., Deng, Y., Wei, Z., et al. (2019). Determination of absorption dose in chemical mutagenesis in plants. *PloS One* 14, e0210596. doi: 10.1371/journal.pone.0210596

Kim, Y., Schumaker, K. S., and Zhu, J.-K. (2006). EMS mutagenesis of arabidopsis. *Methods Mol. Biol.* 323, 101–103. doi: 10.1385/1-59745-003-0:101

Kong, W., Wang, L., Cao, P., Li, X., Ji, J., Dong, P, et al. (2020). Identification and genetic analysis of EMS-mutagenized wheat mutants conferring lesion-mimic premature aging. *BMC Genet.* 21 (1), 1–11. doi: 10.1186/s12863-020-00891-x

Krysan, P. J., Young, J. C., and Sussman, M. R. (1999). T-DNA As an insertional mutagen in *Arabidopsis*. *The plant cell* 11, 12, 2283–2290. doi: 10.1105/tpc.11.12.2283

Kumar, U., Padhan, B., Tripathi, A., Choudhary, J., Kumar, D., Prakash, N., et al. (2022). Breeding for herbicide tolerance in crops: a review. *Res. J. Biotech.* 15, 154–162.

Kumar, U., Chavan, N. S., Sawant, S. V., Kumar Yadav, H., et al. (2022). Evaluation and characterization of EMS induced mutant population of gossypium herbaceum. *Vegetos* 35 (4), 1036–1046. doi: 10.1007/s42535-022-00385-4

Kuraparthy, V., Sood, S., Dhaliwal, H. S., Chhuneja, P., Gill, B. S., et al. (2007). Identification and mapping of a tiller inhibition gene (*tin3*) in wheat. *Theor. Appl. Genet.* 114 (2), 285–294. doi: 10.1007/s00122-006-0431-y

Kurowska, M., Daszkowska-Golec, A., Gruszka, D., Marzec, M., Szurman, M., Szarejko, I., et al. (2011). TILLING-a shortcut in functional genomics. *J. Appl. Genet.* 52 (4), 371–390. doi: 10.1007/s13353-011-0061-1

Lee, Y.-H., Park, W., Kim, K.-S., Jang, Y.-S., Lee, J.-E., Cha, Y.-L., et al. (2018). EMS-induced mutation of an endoplasmic reticulum oleate desaturase gene (*FAD2-2)* results in elevated oleic acid content in rapeseed (*Brassica napus* L.). *Euphytica* 214 (2), 1–12. doi: 10.1007/s10681-017-2106-y

Lenawaty, D. Y., Sukma, D., Syukur, M., Suprapta, D., Nurcholis, W., Aisyah, S, et al. (2022). Increasing the diversity of marigold (*Tagetes* sp.*)* by acute and chronic chemical induced mutation of EMS (Ethyl methane sulfonate). *Biodiversitas J. Biol. Diversity* 23 (3). doi: 10.13057/biodiv/d230326

Lethin, J., Shakil, S. S.M., Hassan, S., Sirijovski, N., Töpel, M., Olsson, O., et al. (2020). Development and characterization of an EMS-mutagenized wheat population and identification of salt-tolerant wheat lines. *BMC Plant Biol.* 20 (1), 1–15. doi: 10.1186/s12870-019-2137-8

Li, S., Zhang, N., Li, J., Xiang, J., et al. (2019). A new male sterile line of "*Duanye-13*" radish (*Raphanus sativus* l.) produced by ethyl methanesulfonate mutagenesis. *Genet. Resour. Crop Evol.* 66 (5), 981–987. doi: 10.1007/s10722-019-00772-y

Li, X., Xiang, F., Zhang, W., Yan, J., Li, X., Zhong, M., et al. (2021). Characterization and fine mapping of a new dwarf mutant in *Brassica napus*. *BMC Plant Biol.* 21 (1), 1–12. doi: 10.1186/s12870-021-02885-y

Li, Z., Zhu, L., Zhao, F., Li, J., Zhang, X., Kong, X, et al. (2022). Plant salinity stress response and nano-enabled plant salt tolerance. *Front. Plant Sci.* 13, 843994. doi: 10.3389/fpls.2022.843994

Lian, X., Liu, Y., Guo, H., Fan, Y., Wu, J., Guo, H., et al. (2020). Ethyl methanesulfonate mutant library construction in *Gossypium hirsutum* l. for allotetraploid functional genomics and germplasm innovation. *Plant J.* 103 (2), 858–868. doi: 10.1111/tpj.14755

Liu, C., Song, G., Wang, N., Huang, S., Gao, Y., Fu, W., et al. (2021). A single SNP in *Brcer1* results in wax deficiency in Chinese cabbage (*Brassica campestris* l. *ssp. pekinensis*). *Sci Hortic.* 282, 110019. doi: 10.1016/j.scienta.2021.110019

Manzanares, C., Yates, S., Ruckle, M., Nay, M., and Studer, B. (2016). TILLING in forage grasses for gene discovery and breeding improvement. *New Biotechnol.* 33 (5), 594–603. doi: 10.1016/j.nbt.2016.02.009

Mba, C., Afza, R., Bado, S., and Mohan Jain, S. (2010). Induced mutagenesis in plants using physical and chemical agents. *Plant Cell culture: Essential Methods* 20, 111–130. doi: 10.1002/9780470686522.ch7

Minoia, S., Petrozza, A., D'Onofrio, O., Piron, F., Mosca, G., Sozio, G., et al. (2010). A new mutant genetic resource for tomato crop improvement by TILLING technology. *BMC Res. Notes* 3 (1), 1–8. doi: 10.1186/1756-0500-3-69

Munda, S., Begum, T., Gogoi, A., Pandey, S. K., Sarma, N., Lal, M., et al. (2022). Induced variations by gamma radiation and EMS on the agronomic traits, essential oil yield with its quality and their exploitation in Java citronella (*Cymbopogon winterianus jowitt*). *Int. J. Radiat. Biol.* 98 (8), 1376–1387. doi: 10.1080/09553002.2022.2038805

Murray, V. (1987). O6-methylguanine specifically induces AT-GC transition mutations. *Mutat. Res.* 190 (4), 267–270. doi: 10.1016/0165-7992(87)90007-8

Nasri, F., Zakizadeh, H., Vafaee, Y., Mozafari, A. A., et al. (2022). In vitro mutagenesis of *Chrysanthemum* morifolium cultivars using ethyl methane sulphonate (EMS) and mutation assessment by ISSR and IRAP markers. *Plant Cell Tissue Organ Culture* 149 (3), 657–673. doi: 10.1007/s11240-021-02163-7

Newhouse, K., Singh, B., Shaner, D., and Stidham, M. (1991). Mutations in corn (*Zea mays* l.) conferring resistance to imidazolinone herbicides. *Theor. Appl. Genet.* 83 (1), 65–70.

Pang, H., Li, W. H., Zhang, H. B., Wang, L., Yin, Y. A., Yuan, H. G., et al. (2010). Inheritance analysis of resistant starch content in kernels of wheat. *Yi Chuan= Hereditas* 32 (2), 170–176. doi: 10.3724/SP.J.1005.2010.00170

Patel, J., Chandnani, R., Khanal, S., Adhikari, J., Brown, N., Chee, P. W., et al. (2022). Pyramiding novel EMS-generated mutant alleles to improve fiber quality components of elite upland cotton germplasm. *Ind. Crops Products* 178, 114594. doi: 10.1016/j.indcrop.2022.114594

Piquerez, S. J., Harvey, S. E., Beynon, J. L., and Ntoukakis, V. (2014). Improving crop disease resistance: lessons from research on *Arabidopsis* and tomato. *Front. Plant Sci.* 5, 671. doi: 10.3389/fpls.2014.00671

Prakash, N. R., et al. (2020). Breeding for herbicide tolerance in crops: A review. *Res. J. Biotechnol.* 15 (4).

Quesada, V., Ponce, M. R., and Micol, J. L. (2000). Genetic analysis of salt-tolerant mutants in *Arabidopsis thaliana*. *Genetics* 154 (1), 421–436. doi: 10.1093/genetics/154.1.421

Rajasekaran, K., Grula, J. W., and Anderson, D. M. (1996). Selection and characterization of mutant cotton (*Gossypium hirsutum* l.) cell lines resistant to sulfonylurea and imidazolinone herbicides. *Plant Science* 119 (1), 115–124. doi: 10.1016/0168-9452(96)04444-5

Reddy, T. V., Dwivedi, S., and Sharma, N. K. (2012). Development of TILLING by sequencing platform towards enhanced leaf yield in tobacco. *Ind. Crops Products* 40, 324–335. doi: 10.1016/j.indcrop.2012.03.031

Rizwan, M., Aslam, M., Asghar, M. J., Abbas, G., Shah, T. M., and Shimelis, H. (2017). Pre-breeding of lentil (*Lens culinaris medik.*) for herbicide resistance through seed mutagenesis. *PloS One* 12 (2), e0171846. doi: 10.1371/journal.pone.0171846

Roychowdhury, R., and Tah, J. (2011). Germination behaviors in M_2 generation of *Dianthus* after chemical mutagenesis. *Intern. J. Adv. Sci. Tech. Res.* 2 (1), 448–454.

Sabetta, W., Alba, V., Blanco, A., and Montemurro, C. J. P. M. (2011). sunTILL: a TILLING resource for gene function analysis in sunflower. *Plant Methods* 7 (1), 1–13. doi: 10.1186/1746-4811-7-20

Saha, A. (2019). EMS induced polygenic mutation in tilottama cultivar of *Sesamum indicum*. *Plant Arch.* 19 (1), 630–632.

Samadi, N., Naghavi, M. R., Moratalla-López, N., Alonso, G. L., and Shokrpour, M. (2022). Morphological, molecular and phytochemical variations induced by colchicine and EMS chemical mutagens in *Crocus sativus* l. *Food Chem.: Mol. Sci.* 4, 100086. doi: 10.1016/j.fochms.2022.100086

Sebastian, S. A., and Chaleff, R. S. (1987). Soybean mutants with increased tolerance for sulfonylurea herbicides 1. *Crop Sci.* 27 (5), 948–952. doi: 10.2135/cropsci1987.0011183X002700050025x

Shah, D., Kamili, A. N., Wani, A. A., Majeed, U., Wani, Z. A., Sajjad, N., et al. (2020). Promoting the accumulation of scopolamine and hyoscyamine in *Hyoscyamus niger* l. through EMS based mutagenesis. *Mutat. Research/Reviews Genet. Toxicol.* 15 (5), e0231355.

Shankar, A., Choudhary, O., and Singh, K. (2021). Effect of EMS induced mutation in rice cultivar nagina 22 on salinity tolerance. *bioRxiv*. doi: 10.1101/2021.08.03.455004

Shi, Z., Ren, W., Zhao, Y., Wang, X., Zhang, R., Su, A., et al. (2021). Identification of a locus associated with genic male sterility in maize *via* EMS mutagenesis and bulked-segregant RNA-seq. *Crop J.* 9 (6), 1263–1269. doi: 10.1016/j.cj.2020.09.007

Siddique, M. I., Back, S., Lee, J. H., Jo, J., Jang, S., Han, K., et al. (2020). Development and characterization of an ethyl methane sulfonate (EMS) induced mutant population in *Capsicum annuum* l. *Plants* 9 (3), 396. doi: 10.3390/plants9030396

Silué, S., Nafan, D., Fofana, I., Muhovski, Y., Toussaint, A., Guy, M., et al. (2013). Description of *Phaseolus vulgaris* l. aborting embryos from ethyl methanesulfonate (EMS) mutagenized plants. *Biotechnol agronomie société environnement*, 17(4).

Singh, H., Verma, P., Lal, S., and Khar, A. (2021). Optimization of EMS mutagen dose for short day onion. *Indian J. Hortic.* 78 (1), 35–40. doi: 10.5958/0974-0112.2021.00005.0

Singh, R., and Kumar, G. (2022). Analyzing frequency and spectrum of chlorophyll mutation induced through gamma ray and combination treatment (Gamma + EMS) on genetic paradigm of *Artemisia annua* l.: Effect of gamma and gamma + EMS on the frequency and spectrum of chlorophyll mutation in *Artemisia annua* l. *Caryologia*.

Singh, P. K., and Sadhukhan, R. (2019). Ems and gamma radiation induced mutation in grasspea (*Lathyrus sativus* l.). *Legume Res.* 42, 300–307.

Slade, A. J., Fuerstenberg, S. I., Loeffler, D., Steine, M. N., and Facciotti, D. (2005). A reverse genetic, nontransgenic approach to wheat crop improvement by TILLING. *Nat. Biotechnol.* 23 (1), 75–81. doi: 10.1038/nbt1043

Stadler, L. J. (1929). Chromosome number and the mutation rate in avena and *Triticum*. *Proc. Natl. Acad. Sci.* 15 (12), 876–881. doi: 10.1073/pnas.15.12.876

Sudianto, E., Song, B.-K., Neik, T.-X., Saldain, N. E., Scott, R. C., and Burgos, N. R. (2013). Clearfield® rice: Its development, success, and key challenges on a global perspective. *Crop Protection* 49, 40–51. doi: 10.1016/j.cropro.2013.02.013

Sun, X., Li, X., Lu, Y., Wang, S., Zhang, X., Zhang, K., et al. (2022). Construction of a high-density mutant population of Chinese cabbage facilitates the genetic dissection of agronomic traits. *Mol. Plant* 15 (5), 913–924. doi: 10.1016/j.molp.2022.02.006

Taheri, S., Abdullah, T. L., Jain, S. M., Sahebi, M., and Azizi, P. (2017). TILLING, high-resolution melting (HRM), and next-generation sequencing (NGS) techniques in plant mutation breeding. *Mol. Breed.* 37 (3), 1–23. doi: 10.1007/s11032-017-0643-7

Takagi, H., Tamiru, M., Abe, A., Yoshida, K., Uemura, A., Yaegashi, H., et al. (2015). MutMap accelerates breeding of a salt-tolerant rice cultivar. *Nat. Biotechnol.* 33 (5), 445–449. doi: 10.1038/nbt.3188

Tang, S., Liu, D. X., Lu, S., Yu, L., Li, Y., Lin, S., et al. (2020). Development and screening of EMS mutants with altered seed oil content or fatty acid composition in *Brassica napus*. *Plant J.* 104 (5), 1410–1422. doi: 10.1111/tpj.15003

Thange, V., Bagade, A., and Wankhade, M. (2021). Evaluation of mutagenic effects on frequency and spectrum of chlorophyll mutation in sorghum (*Sorghum bicolor (L.)* Moench).

Thangwana, A., Gwata, E. T., and Zhou, M. M. (2021). Impact of chemical mutagenesis using ethyl methane sulphonate on tepary bean seedling vigour and adult plant performance. *Heliyon* 7 (1), e06103. doi: 10.1016/j.heliyon.2021.e06103

Till, B. J., Reynolds, S. H., Greene, E. A., Codomo, C. A., Enns, L. C., Johnson, J. E., et al. (2003). Large-Scale discovery of induced point mutations with high-throughput TILLING. *J. Genome Res.* 13 (3), 524–530. doi: 10.1101/gr.977903

Till, B. J., Reynolds, S. H., Weil, C., Springer, N., Burtner, C., Young, K., et al. (2004). Discovery of induced point mutations in maize genes by TILLING. *BMC Plant Biol.* 4 (1), 12. doi: 10.1186/1471-2229-4-12

Till, B. J., Cooper, J., Tai, T. H., Colowit, P., Greene, E. A., Henikoff, S., et al. (2007). Discovery of chemically induced mutations in rice by TILLING. *BMC Plant Biol.* 7 (1), 19. doi: 10.1186/1471-2229-7-19

Travella, S., Klimm, T. E., and Keller, B. (2006). RNA Interference-based gene silencing as an efficient tool for functional genomics in hexaploid bread wheat. *Plant Physiol.* 142 (1), 6–20. doi: 10.1104/pp.106.084517

Unan, R., Deligoz, I., Al-Khatib, K., and Mennan, H. (2021). Protocol for ethyl methanesulphonate (EMS) mutagenesis application in rice. *Open Res. Europe* 1, 19. doi: 10.12688/openreseurope.13317.1

Van Zelm, E., Zhang, Y., and Testerink, C. (2020). Salt tolerance mechanisms of plants. *Annu. Rev. Plant Biol.* 71, 403–433. doi: 10.1146/annurev-arplant-050718-100005

Wanga, M. A., Shimelis, H., Horn, L. N., and Sarsu, F. (2020). The effect of single and combined use of gamma radiation and ethylmethane sulfonate on early growth parameters in sorghum. *Plants* 9 (7), 827. doi: 10.3390/plants9070827

Wang, H., Huang, C., Zhao, W., Dai, B., Shen, C., Zhang, B., et al. (2016). Identification of QTL for fiber quality and yield traits using two immortalized backcross populations in upland cotton. *PloS One* 11 (12), e0166970. doi: 10.1371/journal.pone.0166970

Wang, C., Hao, N., Xia, Y., Du, Y., Huang, K., Wu, T., et al. (2021). CsKDO is a candidate gene regulating seed germination lethality in cucumber. *Breed. Sci.* 71 (4), 417–425. doi: 10.1270/jsbbs.20149

Wang, X., Wang, A., Li, Y., Xu, Y., Wei, Q., Wang, J., et al. (2021). A novel banana mutant "*RF 1*"(*Musa* spp. *ABB, pisang awak subgroup*) for improved agronomic traits and enhanced cold tolerance and disease resistance. *Front. Plant Sci.* 12, 730718. doi: 10.3389/fpls.2021.730718

Wei, Y., Liu, Y., Ali, A. M., Xiao, R., Liang, C., Meng, Z., et al. (2022). Rich variant phenotype of *Gossypium hirsutum* l. saturated mutant library provides resources for cotton functional genomics and breeding. *Ind. Crops Products* 186, 115232. doi: 10.1016/j.indcrop.2022.115232

Wu, Z., Liu, Z., Chang, S., and Zhao, Y. (2020). An EMS mutant library for carrot and genetic analysis of some mutants. *Breed. Sci* 70 (5), 540–546. doi: 10.1270/jsbbs.20020

Xiong, H., Zhou, C., Guo, H., Xie, Y., Zhao, L., Gu, J., et al. (2020). Transcriptome sequencing reveals hotspot mutation regions and dwarfing mechanisms in wheat mutants induced by γ-ray irradiation and EMS. *J. Radiat. Res.* 61 (1), 44–57. doi: 10.1093/jrr/rrz075

Xi-Ou, X., Wenqiu, L., Wei, L., Xiaoming, G., Lingling, L., Feiyue, M., et al. (2017). The analysis of physiological variations in M_2 generation of *Solanum melongena* l. mutagenized by ethyl methane sulfonate. *Front. Plant Sci.* 8, 17. doi: 10.3389/fpls.2017.00017

Yan, W., Deng, X. W., Yang, C., and Tang, X. (2021). The genome-wide EMS mutagenesis bias correlates with sequence context and chromatin structure in rice. *Front. Plant Sci.* 12, 579675. doi: 10.3389/fpls.2021.579675

Yan, Z., Appiano, M., van Tuinen, A., Meijer-Dekens, F., Schipper, D., Gao, D., et al. (2021). Discovery and characterization of a novel tomato mlo mutant from an ems mutagenized micro-tom population. *Genes* 12 (5), 719. doi: 10.3390/genes12050719

Zhao, S., Zhang, Q., Liu, M., Zhou, H., Ma, C., and Wang, P. (2021). Regulation of plant responses to salt stress. *Int. J. Mol. Sci.* 22 (9), 4609. doi: 10.3390/ijms22094609

frontiers | Frontiers in Plant Science

TYPE Original Research
PUBLISHED 13 January 2023
DOI 10.3389/fpls.2022.1110724

Check for updates

OPEN ACCESS

EDITED BY
Xinyang Wu,
China Jiliang University, China

REVIEWED BY
Tao Wu,
Jilin University, China
Han Jiang,
Shandong Agricultural University, China

*CORRESPONDENCE
Minghui Zhao
mhzhao@syau.edu.cn
Dianrong Ma
madianrong@syau.edu.cn

SPECIALTY SECTION
This article was submitted to Plant Abiotic Stress, a section of the journal Frontiers in Plant Science

RECEIVED 29 November 2022
ACCEPTED 21 December 2022
PUBLISHED 13 January 2023

CITATION
Gu S, Zhuang J, Zhang Z, Chen W, Xu H, Zhao M and Ma D (2023) Multi-omics approach reveals the contribution of *OsSEH1* to rice cold tolerance.
Front. Plant Sci. 13:1110724.
doi: 10.3389/fpls.2022.1110724

COPYRIGHT
© 2023 Gu, Zhuang, Zhang, Chen, Xu, Zhao and Ma. This is an open-access article distributed under the terms of the Creative Commons Attribution License (CC BY). The use, distribution or reproduction in other forums is permitted, provided the original author(s) and the copyright owner(s) are credited and that the original publication in this journal is cited, in accordance with accepted academic practice. No use, distribution or reproduction is permitted which does not comply with these terms.

Multi-omics approach reveals the contribution of *OsSEH1* to rice cold tolerance

Shuang Gu, Jia Zhuang, Zhe Zhang, Wanchun Chen, Hai Xu, Minghui Zhao* and Dianrong Ma*

Rice Research Institute/Collaborative Innovation Center for Genetic Improvement and High Quality and Efficiency Production of Northeast Japonica Rice in China, Shenyang Agricultural University, Shenyang, China

As low environmental temperature adversely affects the growth, development and geographical distribution, plants have evolved multiple mechanisms involving changing physiological and metabolic processes to adapt to cold stress. In this study, we revealed that nucleoporin-coding gene *OsSEH1* was a positive regulator of cold stress in rice. Physiological assays showed that the activity of antioxidant enzymes showed a significant difference between *osseh1* knock-out lines and wild type under cold stress. Metabolome analysis revealed that the contents of large-scale flavonoids serving as ROS scavengers were lower in *osseh1* mutants compared with wild type under cold stress. Transcriptome analysis indicated that the DEGs between *osseh1* knock-out lines and wild type plants were enriched in defense response, regulation of hormone levels and oxidation-reduction process. Integration of transcriptomic and metabolic profiling revealed that *OsSEH1* plays a role in the oxidation-reduction process by coordinately regulating genes expression and metabolite accumulation involved in phenylpropanoid and flavonoid biosynthetic pathway. In addition, Exogenous ABA application assays indicated that *osseh1* lines had hypersensitive phenotypes compared with wild type plants, suggesting that *OsSEH1* may mediate cold tolerance by regulating ABA levels.

KEYWORDS

***OsSEH1*, cold tolerance, metabolome, transcriptome, ROS, phenylpropanoid**

Introduction

Rice (*Oryza sativa* L.), a staple food crop that feeds over half of the world's population, originates from tropical and subtropical regions and is sensitive to cold stress (Sasaki and Burr, 2000). Cold stress has been identified as one of the main factors restricting the growth, development, production, and geographical distribution of rice

(Sperotto et al., 2018). In Northeast China, the growth and development of rice are seriously affected by cold stress at the seedling and booting stages (Sun et al., 2022). As a result of severe cold disasters, rice production in Northeast China was drastically reduced by 42% in 1972 and 37% in 1976 (Yang et al., 2017a). Therefore, it is important to mine cold-tolerant genes and elucidate their regulatory mechanisms for national food security and sustainable agricultural development.

Plants exposed to cold stress suffer from wilting, discoloration, leaf margin drying, accelerated aging, incomplete ripening, and even death (Zhang et al., 2016). Various evaluation indices were used to reflect cold tolerance at the seedling stage, including survival rate, leaf withering degree, proline content, soluble sugar content, and the activity of antioxidant enzymes (Han et al., 2020). The survival rate and degree of leaf withering reflect the external phenotype of seedlings under cold stress. As cytoplasmic osmotic pressure regulators, proline and soluble sugars can enhance cold tolerance (Ma et al., 2009; Gaveliene et al., 2014). Under normal conditions, reactive oxygen species (ROS) are well known to act as molecular signals or secondary messengers that regulate plant growth at lower concentrations (Mittler, 2017). However, under cold conditions, overaccumulation of ROS degrades polyunsaturated lipids, oxidizes proteins, and damages cells (Han et al., 2017). Antioxidant enzymes play an important role in maintaining cellular redox homeostasis. The activity of antioxidant enzymes, such as superoxide dismutase (SOD), peroxidase (POD), ascorbate peroxidase (APX), and catalase (CAT), reflects the ability of plants to mitigate ROS under cold stress (Noctor and Foyer, 1998).

Plants synthesize a variety of secondary metabolites from the amino acid phenylalanine, including benzenoids, coumarins, flavonoids, hydroxycinnamates, and lignin (Vogt, 2010). These compounds are collectively referred to as phenylpropanoids and play an essential role in plant development and plant–environment interactions (Dong and Lin, 2021). For example, lignins are a large group of aromatic polymers that are deposited in the plant cell wall, serving as both structural support and a plant defense mechanism (Boerjan et al., 2003; Vanholme et al., 2019). The synthesis of lignin can be induced by many types of abiotic stressors, such as drought, cold stress, and mineral deficiency, as well as biotic stresses, including infection by fungi, bacteria, or viruses (Moura et al., 2010). Flavonoids, another important class of soluble phenylpropanoids, have long been suggested to have multiple functions in plant development and adaptation to environmental stress (Agati et al., 2012; Agati et al., 2013; Nakabayashi et al., 2014). Under unfavorable conditions, such as UV light, drought, and biotic stress, flavonoids accumulate in plants to protect cells from oxidative damage (Treutter, 2005; Hassan and Mathesius, 2012; Agati et al., 2013; Nakabayashi et al., 2014). Recently, phenylpropanoid responses to environmental temperature in plants, which are considered to play a vital role in cold stress, have gathered more attention (Sudheeran et al., 2018; Zhang et al., 2022).

Cold tolerance is a complex agronomic trait controlled by multiple genes (Guo et al., 2018; Shi et al., 2018). Traditional genetic and molecular analysis has been used to identify major QTLs/genes controlling cold tolerance in rice, including *low-temperature germinability on chromasome 3* (*qLTG3*), *low temperature growth 1* (*LTG1*), *chilling tolerance divergence 1* (*COLD1*), *cold tolerance at booting stage 4a* (*CTB4a*), *basic leucine zipper 73* (*bZIP73*), and *HAN1* ("han" is termed "chilling" in Chinese) (Fujino et al., 2008; Lu et al., 2014; Ma et al., 2015; Zhang et al., 2017; Liu et al., 2018; Liu et al., 2019; Mao et al., 2019). Nuclear pore complexes (NPCs), consisting of multiple nucleoporins (Nups), play vital roles in the exchange of macromolecules, such as RNAs and proteins (Parry, 2015; Yang et al., 2017b). Some studies have suggested that Nups also play an important role in regulating cold tolerance. For instance, *NUP160* was shown to be involved in cold stress responses, since the *nup160* lines impaired the expression of the *CBF3-LUC* reporter gene and cold response (*COR*) genes, resulting in hypersensitivity to cold stress (Dong et al., 2006b). In addition, *high expression of osmotically responsive genes 1* (*HOS1*) is considered a negative regulator of cold signaling (Ishitani et al., 1998). The expression of *COR* genes in *hos1* mutants was higher than that in wild-type (WT) plants (Lee et al., 2001). HOS1 was further shown to modulate the protein levels of ICE1 (inducer of CBF expression 1) by ubiquitination to attenuate cold signaling (Lee et al., 2001; Dong et al., 2006a). However, the functions of other nucleoporins in cold signaling remain poorly understood, especially in rice.

Our previous study detected QTLs for cold tolerance at the seedling stage through genome-wide association studies using Ting's rice core collection (Song et al., 2018). At all these QTLs, a major locus on chromosome 1 explained 27% of phenotypic variance. We subsequently analyzed candidate genes within this locus and noticed that the expression of the nucleoporin-coding gene *OsSEH1* was dramatically induced by cold stress. Hence, our previous results indicate that *OsSEH1* is a potential candidate gene for cold tolerance in rice. However, further characterization of gene function and its regulatory mechanism in response to cold stress in rice requires further investigation. In the current study, we revealed by combining transcriptomic and metabolomic methods that *OsSEH1* regulates many genes and metabolites involved in the phenylpropanoid pathway in response to cold stress. Moreover, we showed that exogenous abscisic acid (ABA) increased the cold tolerance of *osseh1* knockout lines, but had little effect on WT plants. This study advances our understanding of the function of plant nucleoporins in cold stress and provides a potential genetic resource for generating cold-tolerant rice varieties.

Materials and methods

Plant materials and growth conditions

Two rice genotypes, wild type MangShuiDao (MSD) and its mutant *osseh1*, were selected for use in this study. MSD is a cold tolerant temperate *Japonica* landrace from Yangtze River region, China. The mutant *osseh1* lines were generated by CRISPR/Cas9 previously. The mutation sites in the *osseh1* knock-out lines were showed in Supplementary Figure 1.

Seeds were surface sterilized with 5% (w/v) sodium hypochlorite for 3 min and then soaked in the water at 28°C for 5 days in the dark. The germinated seeds were transferred to 96-well plates and then grown hydroponically in the solution of International Rice Research Institute (IRRI). The 96-well plates were placed in a plant growth chamber (14h-light/10h-dark conditions) with temperatures of 28°C and 25°C for the light and dark conditions, respectively.

For cold stress at the seedling stage, the seedlings of wild type and *osseh1* mutants were used to test the cold tolerance. The seedlings were transferred to a growth chamber at 4°C for 7 days after knowing which plants were able to recover at 28°C for 7 days, and the survival rates were calculated. Cold treatment was treated at the 16^{th} days of rice seedling growth. The sampling time of physiological indicators was 0 h and 48 h after cold stress.

For the germination assay, sterilized seeds were put in the 0 μM, 1 μM, 10 μM, 100 μM or 150 μM ABA. The germination rates were assessed at 0, 36, 48, 60, 72, 84, 96 h. Three replicate assays were conducted with at least 200 seeds each time.

Measurement of soluble sugar content

The soluble sugar content was measurement was performed according to the previous study (Yoshida et al., 1971) with some modification. Briefly, leaf sample (0.2 g fresh weight) was fixed in 4 ml 80% ethanol. After centrifugation at 5000 × g for 10 min, added 2.5 ml of anthrone to the supernatant (0.5 ml) and kept in a water bath at 40°C for 30 min. After cooling, measure the optical density of the mixture at 625 nm.

Measurement of proline content

The proline content was determined according to the previous study (Bates et al., 1973) with some modification. Leaf samples (0.5 g) were boiled in 10ml 3% sulfosalicylic acid and then the cooling homogenate was centrifuged at 3000×g for 10 min. The supernatant (1 ml) was treated with 1 ml acetic acid and 2 ml 2.5% ninhydrin, boiled for 1 h, and absorbance was determined at 520 nm.

Measurement of ROS content

The ROS content was determined by plant ROS enzyme-linked immunity kit (Jiangsu Meimian Industrial Co., Ltd., Yancheng, China) according to the manufacturer's protocol. Double antibody sandwich method was used in the kit to determine the content of plant ROS in the leaves sample. Purified plant ROS antibodies were placed in the microporous plate to form solid-phase antibodies. Use purified ROS antibody to coat the microplate to prepare solid phase antibody. Add ROS to the microplate coated with monoclonal antibody in turn, and then combine with HRP (horse radish peroxidase) labeled ROS antibody to form antibody antigen enzyme labeled antibody complex. After thorough washing, add substrate TMB (3, 3′,5,5′-Tetramethylbenzidine) for color development. TMB is catalyzed by HRP enzymes to turn blue and converted to the final yellow color by acid. The shade of color was positively correlated with ROS in the sample. The absorbance (OD) was measured at 450nm and the concentration of ROS was calculated by standard curve.

Measurements for antioxidative enzyme activity

Fresh leaves (about 0.2 g) were ground in cold 2 mL 50 mM PBS solution. Centrifuged homogenate at 8000 r/min for 20 min at 4°C. The supernatant was kept measure the antioxidant enzyme activity. For SOD activity measurement, 50 μL supernatant was added to 5 mL nitroblue tetrazolium (NBT) reaction buffer and then the reaction mixture was kept under 4000 lux lights for 20 min and analyzed at 560 nm using a spectrophotometer (Polle et al., 1989). For POD activity measurement, 50 μL supernatant was added to 5 mL guaiacol reaction buffer and analyzed at 470 nm using a spectrophotometer (Fecht-Christoffers et al., 2006). For CAT activity measurement, 50 μL supernatant was added to 5 mL reaction buffer in the presence of H_2O_2 and analyzed at 240 nm using a spectrophotometer (Verma and Dubey, 2003). For APX activity measurement, 50 μL supernatant was added to 5 mL ascorbate reaction buffer and analyzed at 290 nm using a spectrophotometer (Vanacker et al., 1998). All treatments had three biological and three technical replicates.

Metabolite profiling analysis

Metabolomic profiling was performed using a widely targeted metabolome technology with three independent biological replicates at MetWare Biotechnology Co., Ltd. (Wuhan, China) (Li et al., 2022a). Briefly, the leaves samples were ground using the MM 400 Mixer Mill (Retsch Technology,

Haan, Germany) with a zirconia bead for 1.5 min. Then, 100 mg freeze-dried powder was weighted for metabolites extraction with 500 µL of 80% aqueous methanol containing 0.1 mg/L lidocaine at 4°C for 8h. Following centrifugation at 10000g for 15 min, the supernatant was filtered *via* a syringe filter (SCAA-104, 0.22-µm pore size; ANPEL, Shanghai, China) before LC-MS/MS analysis. Quality Control (QC) samples were mixed with all samples to test the reproducibility of the entire experiment. Differentially accumulated metabolites (DAMs) were identified using the t-test < 0.05 and variable importance in projection (VIP) ≥ 1.

Transcriptome and bioinformatics analysis

RNA-Seq sequencing and analyses were performed by Gene Denovo Biotechnology Co., (Guangzhou, China) as described previously (Li et al., 2022b; Yan et al., 2022). Briefly, total RNA was extracted from the four-leaf stage seedlings using the Trizol Reagent Kit (Invitrogen, Carlsbad, CA, USA) according to the manufacturer's protocol, with three biological replicates each containing 50 plants. RNA quality and integrity were assessed on the Agilent 2100 Bioanalyzer (Agilent Technologies, Palo Alto, CA, USA). Gene Denovo Biotechnology Co. (Guangzhou, China) performed RNA-Seq sequencing and analyses using the Illumina HiSeq2500 platform. Differentially expressed genes (DEGs) between the *osseh1* mutants and the wild type were identified with false discovery rate (FDR) < 0.05 and absolute fold change ≥ 2. DEGs were then analyzed by Gene Ontology (GO) functions and Kyoto Encyclopedia of Genes and Genomes (KEGG) pathway.

RNA extraction and RT-qPCR

Total RNA was extracted from the rice seedling leaves using the TransZol Up Plus RNA kit (TransGen Biotech, China) according to the manufacturer's protocol. RNA quality and concentration were quantified using a NanoDrop 8000 spectrophotometer (Thermo Fisher Scientific). Total RNA was reverse-transcribed to cDNA using One-Step gDNA Removal and cDNA Synthesis SuperMix (TransGen Biotech, China). RT-qPCR was carried out using the PerfectStart Green qPCR SuperMix (TransGen Biotech, China) protocol and the QuantStudio 3 System (Applied Biosystems, USA). Rice *ACTIN1* gene was used as the internal control. Data were analyzed following the relative quantification method (Livak and Schmittgen, 2001). Primer used for RT-qPCR are listed in Supplementary Table 9. The experiments were repeated at least three times.

Exogenous ABA treatment

Hormone treatments were conducted by spraying the leaves of 12-day old seedlings with 1 µM, 10 µM, 100 µM and 150 µM ABA containing 0.1% (v/v) Tween 20 as the surfactant. The seedlings were sprayed with the mixture of different concentration of ABA at 9 a.m. for 3 days and then transferred to a growth chamber at 4°C for 2 days. ABA (Sigma) was dissolved in methanol. The identical volume of the blank methanol containing 0.1% (v/v) Tween20 was used as a mock treatment.

Endogenous ABA measurement

The ABA content was determined by plant ABA enzyme-linked immunity kit (Jiangsu Meimian Industrial Co., Ltd., Yancheng, China) according to the manufacturer's protocol. Double antibody sandwich method was used in the kit to determine the content of plant ABA in the leaves sample.

Statistical analysis

A two-tailed Student's *t*-test was used to compare the difference of data from two groups, and analysis of variance (ANOVA) one-way comparison followed by Duncan's tests ($p<0.05$) was used to compare the difference of data from multiple groups, using SPSS version 26 ((IBM Corp., Armonk, NY, USA).

Results

Morphological and physiological characteristics are altered in *osseh1* knock-out lines under cold stress

In order to dissect the function of *OsSEH1* in rice, we examined the cold tolerance of wild type (WT) and *osseh1*lines. After 7-day cold treatment and a 7-day recovery, only 41.67% of the *osseh1* seedlings survived, in contrast to 87.5% of the WT plants (Figures 1A, B). Further, we measured the physiological parameters of WT plants and *osseh1* knock-out lines before and after cold treatment. The growth performance was assessed by evaluating plant height, root length, shoot fresh and dry weight, root fresh and dry weight. We sampled and measured the parameters at three time points and the first sampling point is the 14^{th} day of the rice seedling (Supplementary Figure 2A). For both WT and *osseh1* lines, shoot fresh weight, root fresh weight, shoot dry weight and

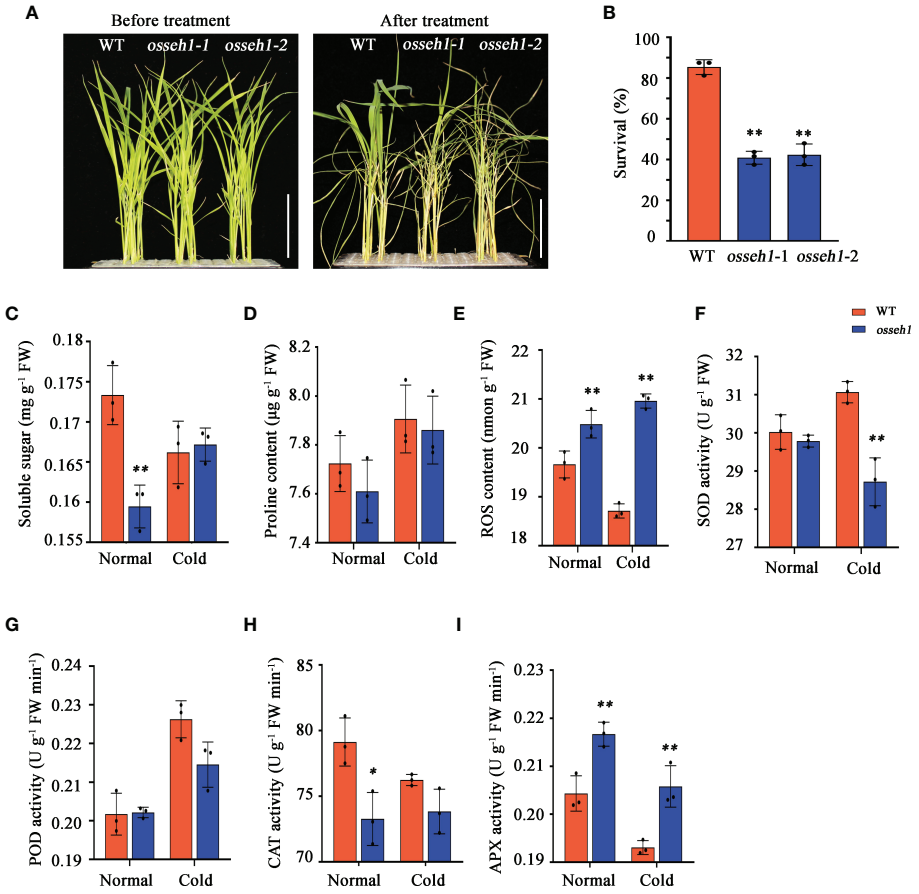


FIGURE 1
Comparison of morphological and physiological indexes between *osseh1* knock-out lines and WT plants under cold stress. **(A)** Phenotypes of *osseh1* knock-out lines and WT plants under cold tolerance. **(B)** Survival rates of *osseh1* knock-out lines and WT plants recovered for 7 days after cold treatment. Statistical analysis of **(C)** soluble sugar, **(D)** proline content, **(E)** ROS content, **(F)** SOD activity, **(G)** POD activity, **(H)** CAT activity and **(I)** APX activity. Data represents means ± SEM (n = 3). *P < 0.05, **P < 0.01. Scale bars, 5cm. WT, wild type; *osseh1*, knockout lines; ROS, reactive oxygen species. SOD, superoxide dismutase; POD, peroxidase; CAT, catalase; APX, ascorbate peroxidase.

root dry weight showed similar rising tendency during cold treatment compared with that during normal condition (Supplementary Figures 2B–E). However, the plant height and root length of *osseh1* lines was significantly inhibited under cold stress compared with that of WT (Supplementary Figure 2F, G).

In addition, we measured soluble sugar content, proline content, ROS content, superoxide dismutase (SOD) activity, peroxidase (POD) activity, ascorbate peroxidase (APX) activity and catalase (CAT) activity in the leaves of WT and *osseh1* lines under normal and cold condition. Compared with the WT lines, the soluble sugar content of *osseh1* lines decreased significantly under normal condition, while there was no significant difference between them under cold stress (Figure 1C). The proline content of both WT and *osseh1* lines were increased after cold stress, while there was no significant difference between them under normal and cold condition (Figure 1D). Our results also revealed that the ROS content in *osseh1* knock-out lines was significantly higher than that in WT plants, suggesting that *osseh1* lines were subjected to more severe oxidative stress under cold stress (Figure 1E). After 2-day 4°C cold stress, the SOD activity in the leaves of *osseh1* is significantly lower than that of WT (Figure 1F). The POD activity was no difference between WT and *osseh1* lines under normal and cold condition (Figure 1G). The CAT activity of *osseh1* was lower compared to that of WT under normal condition, while there was no significant difference between them under cold condition (Figure 1H). The APX activity of *osseh1* lines was significantly higher than that of WT under both normal and cold condition (Figure 1I). These results indicated that *OsSEH1* play a role in regulating rice development and physiological characteristics.

10.3389/fpls.2022.1110724

OsSEH1 regulates a broad range of the metabolite accumulation

To reveal the role of *OsSEH1* underlying cold treatment at the metabolic profile, we performed widely targeted metabolomics assay for wild type plants and *osseh1* knock-out mutants. We used an ultra-performance liquid chromatography-tandem mass spectrometry (UPLC-MS) method to identify changes in metabolite levels. Principal component analysis (PCA) indicated that the metabolites of different genotypes and treatments were significantly different (Figure 2A). Cluster analysis was also performed, and 12 samples were clearly divided into four groups, indicating significant differences in metabolites among four experiment groups (Figure 2B). A total of 806 metabolites were detected with this approach, including 31 different types of substances, among these metabolites, 110 were phenolic acids, 108 were flavonoid metabolites, 75 were organic acids, 73 were amino acids and derivatives, and 54 were free fatty acids (Supplementary Table 1; Supplementary Figure 3). In positive ion mode, the metabolites were

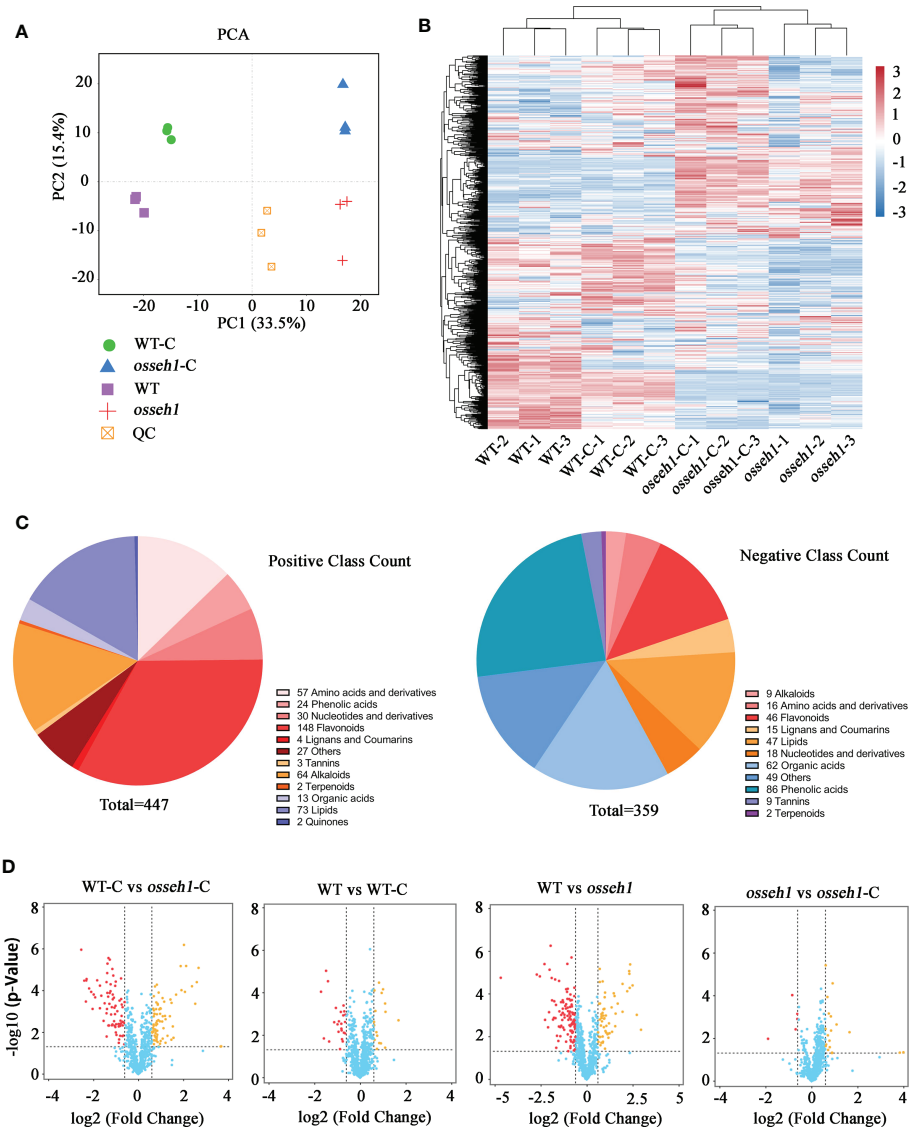


FIGURE 2
Overview of the metabolite accumulation under normal and cold condition. **(A)** Principal component analysis (PCA) of the metabolic profiles. PC1 and PC2 indicate principal component 1 and principal component 2, respectively. The quality control sample (QC) was prepared by mixing aliquots of all of the samples. **(B)** Heat map visualization of metabolites. The content of each metabolite was normalized to complete linkage hierarchical clustering. **(C)** Classification map of metabolites under positive and negative iron mode. **(D)** Volcano plots of the metabolites from the comparison of WT-C vs. *osseh1*-C, WT vs. WT-C, WT vs. *osseh1* and *osseh1* vs. *osseh1*-C, respectively. WT, WT under normal condition. WT-C, WT under cold treatment. *osseh1*, *osseh1* lines under normal condition. *osseh1*-C, *osseh1* lines under cold treatment.

categorized into 12 classes, while in negative ion mode, the metabolites were categorized into 11 classes (Figure 2C).

A total of 102 differently accumulated metabolites (DAMs) (32 upregulated and 70 downregulated metabolites) were identified between WT under normal condition and *osseh1* under normal condition (WT vs *osseh1*; variable importance (VIP) scores ≥1 and T-test P<0.05; Figure 2D; Supplementary Table 2). 81 DAMs (53 upregulated and 28 downregulated metabolites) were identified between the WT under normal condition and WT under cold stress (WT vs WT-C; variable importance (VIP) scores ≥1 and T-test P<0.05; Figure 2D; Supplementary Table 3). 59 DAMs (54 upregulated and 5 downregulated metabolites) were identified between the *osseh1* under normal condition and *osseh1* under cold stress (*osseh1* vs *osseh1*-C; variable importance (VIP) scores ≥1 and T-test P<0.05; Figure 2D; Supplementary Table 4). 100 DAMs (47 upregulated and 53 downregulated metabolites) were identified between WT and *osseh1*under cold stress (WT-C vs *osseh1*-C; variable importance (VIP) scores ≥1 and T-test P<0.05; Figure 2D; Supplementary Table 5). These results suggested that *OsSEH1* regulate a broad range of the metabolite accumulation.

Differentially regulated metabolites by *OsSEH1* under cold stress

The DAMs between WT and *osseh1* lines under normal and cold condition were analyzed further. As expected, the metabolites expression patterns were similar between the biological replicates but differed significantly between the WT and *osseh1* mutant lines (Figures 3A, C). We detected the different accumulation pattern of a wide range of the amino acids, flavonoids, organic acids, alkaloids, phenolic acids and lipids between WT and *osseh1* mutants (Figures 3A, C). Kyoto

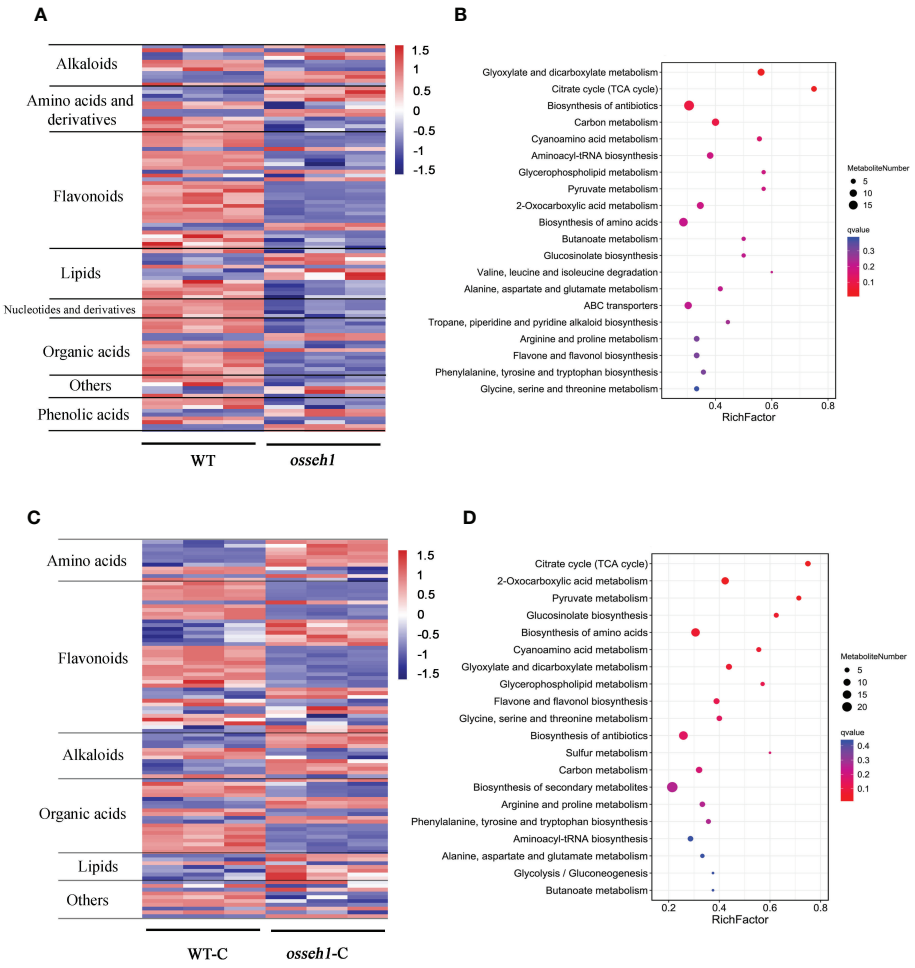


FIGURE 3
Differentially accumulated metabolites (DAMs) between *osseh1* lines and WT plants under normal condition and cold stress. **(A)** Heatmap of DAMs between *osseh1* lines and WT plants under normal condition. **(B)** The top 20 KEGG pathways of DAMs under normal condition. **(C)** Heatmap of DAMs between *osseh1* lines and WT plants under cold stress. **(D)** The top 20 KEGG pathways of DAMs under cold stress. WT, WT under normal condition. WT-C, WT under cold treatment. *osseh1*, *osseh1* lines under normal condition. *osseh1*-C, *osseh1* lines under cold treatment.

Encyclopedia of Genes and Genomes (KEGG) pathway analysis demonstrated that glyoxylate and dicarboxylate metabolism, citrate cycle (TCA cycle) and biosynthesis of antibiotics were the most significantly changed pathways in the noncold treatment WT vs *osseh1* comparison (Figure 3B). However, the DAMs participating in citrate cycle (TCA cycle), 2-Oxocarboxylic acid metabolism, Pyruvate metabolism were mainly enriched under cold stress (Figure 3D). Further, some primary metabolic pathway that are essential for plant growth and development were also significantly enriched under cold stress, including biosynthesis of amino acids, flavone and flavonol biosynthesis and carbon metabolism. Flavonoids serve as ROS scavengers by locating and neutralizing radicals before they damage the cell thus important for plants (Agati et al., 2012). The contents of large-scale flavonoids were lower in *osseh1* mutants compared to WT plants under cold treatment (Figure 3C), suggesting that the *OsSEH1* may be involved in the regulation of flavone and flavonol biosynthesis.

Overview of RNA-seq data analysis

We also performed a transcriptome assay using WT plants and *osseh1* mutants, in parallel with metabolomics. Under normal condition, we depicted 683 differently expressed genes (DEGs) that were up-regulated and 496 down-regulated (fold change > 2 or < 0.5, FDR<0.05; Supplementary Figure 4A; Supplementary Table 6) in the WT vs. *osseh1* comparison. Gene ontology (GO) analyses revealed that these DEGs were enriched in defense response, regulation of hormone levels, benzene-containing compound metabolic process, response to stimulus and oxidation-reduction process biological processes (Figure 4A). KEGG pathway analysis showed that photosynthesis (ko00195), flavonoid biosynthesis (ko00941) and stilbenoid, diarylheptanoid and gingerol biosynthesis (ko00945) were the most significantly changed pathways (Figure 4B).

Under cold condition, we depicted 514 differently expressed genes (DEGs) that were up-regulated and 429 down-regulated (fold change>2 or < 0.5, FDR<0.05; Supplementary Figure 4B; Supplementary Table 7) in the WT-C vs *osseh1*-C comparison. GO analyses revealed that these DEGs were enriched in multiple biological process, including defense response, photosynthetic electron transport chain, toxin metabolic process, zinc ion transmembrane transport and oxidation-reduction process (Figure 4C). KEGG pathway analysis demonstrated that photosynthesis (ko00195), metabolic pathways (ko01100) and flavonoid biosynthesis (ko00941) were the most significantly changed pathways in the WT-C vs *osseh1*-C comparison (Figure 4D). These results are consistent with our proposed role for *OsSEH1* in the regulation of cold stress tolerance.

To further understand the regulatory network of *OsSEH1* in the cold stress, we conducted transcription factor analysis on the differently expression genes between WT and *osseh1* lines. The results showed that significant changes in the expression level of many different types of transcription factors, including *bHLH* family, *ERF* family, *NAC* family, C2H2 family and MYB family (Figure 4E). The results indicated that OsSEH1 may regulate the expression of a large number transcription factors.

In view of the differences in physiological characteristics between WT and *osseh1* lines, we also focused on the term of oxidation-reduction process. We found that a total of 59 DEGs involved in oxidation-reduction process, including multiple genes encoding oxidoreductase (Figure 5A; Supplementary Table 8). The result indicated a role of *OsSEH1* in the control of redox homeostasis. To confirm this possibility, we analyzed the expression levels of 14 genes by RT-qPCR (six genes in the DEGs analysis and eight other ROS-related genes) in WT and *osseh1* lines under normal condition and cold stress (Figure 5B). Of the 14 tested genes, *FeSOD*, *SODcc1*, *POD1*, *POX22.3, LOX10, ANS, Prx30, OPR1 and GRL8* were significantly lower in *osseh1* lines than in WT plants under cold stress, while the expression of *APx1*, *APx8*, *CATB* and *OPR8* were significantly higher in the *osseh1* lines than WT plants and the expression of *Perox4* was not significantly different between the *osseh1* lines and WT plants.

Transcriptomic and metabolic profile of phenylpropanoid biosynthesis modulated by *OsSEH1*

To better characterize the role of *OsSEH1* in regulating genes and metabolites under cold stress, we conducted Pearson's correlation analysis based on the transcriptomic and metabolomic data. The KEGG analysis of the correlated DEGs and DAMs showed that phenylpropanoid biosynthesis, metabolic pathways and flavonoid biosynthesis were the most enriched pathway under cold treatment (Figure 6A). Further, we performed an integrated Two-way Orthogonal Partial Least Squares (O2PLS) analysis of the transcriptome and metabolome Tables (Figure 6B). Consistent with the result of KEGG analysis, 11 of the top 25 metabolites were highly correlated with phenylpropanoid biosynthesis and flavonoid biosynthesis, including Isovitexin-2''-O-(6'''-p-coumaroyl) glucoside (Zmhp003322), Isovitexin-2''-O-(6'''-feruloyl) glucoside (Zmhp003186), Swertiajaponin (pmp000233), 4'-Hydroxy-5,7-dimethoxyflavanone (pmc1990), Tricin-4'-O-(guaiacylglycerol) ether-7-O-glucoside (pmb1312), Tricin-7-O-Glucoside (pmb0736), Tricin-4'-O-(syringyl alcohol) ether-5-O-glucoside (pmb0719), Isoorientin-7-O-(6''-p-coumaroyl) glucoside (pmb0660), Tricin-4'-O-glucoside (Lmhp206353), L-Phenylalanine (pme0021) (Figure 6B).

Moreover, we screened DEGs and DAMs in relation to their corresponding positions in the phenylpropanoid biosynthesis pathway. Metabolite analysis showed that (S)-alpha-Amino-beta-phenylpropionic acid (pme0021), Tyrosine (mws0250), 5-O-Caffeoylshikimic acid (Hmln002806), Apigenin 8-C-glucoside

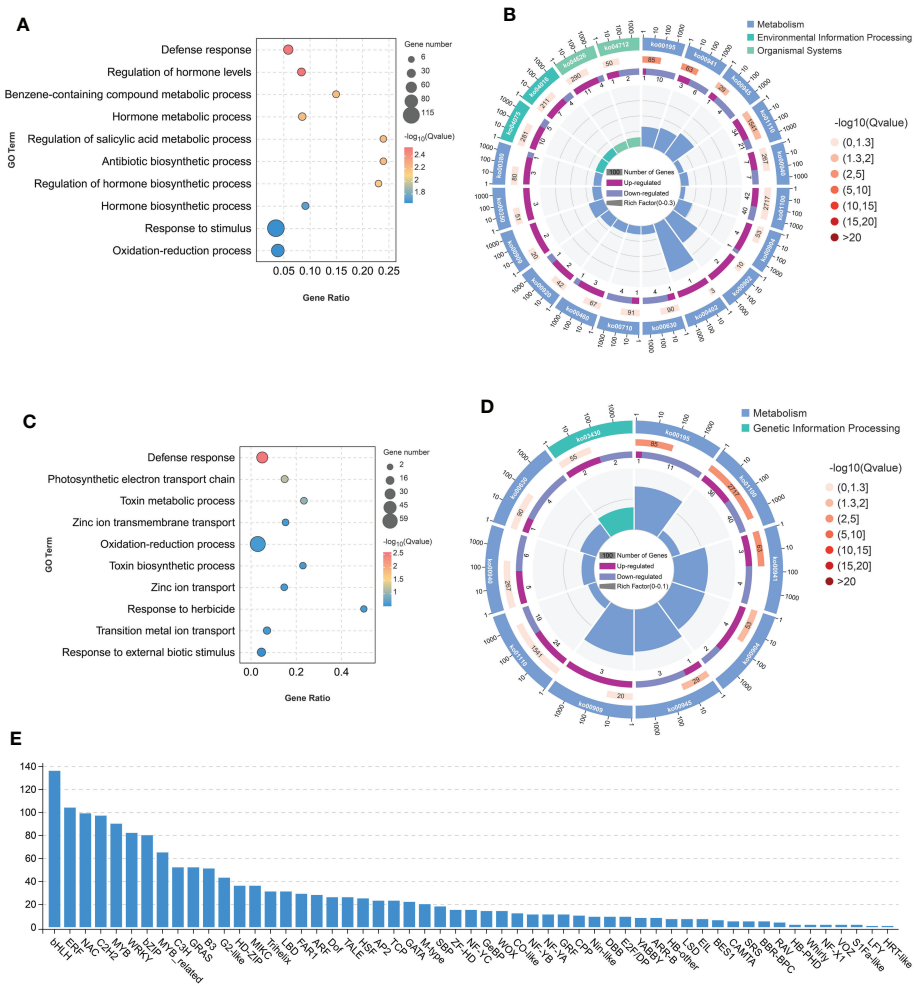


FIGURE 4
Differentially expressed genes (DEGs) between *osseh1* lines and WT plants under normal condition and cold stress. **(A)** The Gene Ontology (GO) enrichment of DEGs between *osseh1* lines and WT plants under normal condition. **(B)** The KEGG enrichment of the DEGs between *osseh1* lines and WT plants under normal condition. **(C)** The Gene Ontology (GO) enrichment of DEGs between *osseh1* lines and WT plants under cold stress. **(D)** The KEGG enrichment of the DEGs between *osseh1* lines and WT plants under cold stress. **(E)** Transcription factor analysis on the DEGs between *osseh1* lines and WT plants under cold stress.

(mws0048) and 5,7,3',4'-Tetrahydroxyflavone (pme0088) were all down-regulated in the *osseh1* lines compared with that of WT plants under cold treatment (Figure 7). Then, a total of 31 DEGs were identified in the phenylpropanoid biosynthesis pathway between the WT and *osseh1* lines under cold treatment. 16 genes encoding core players in the phenylpropanoid biosynthesis pathway, such as *PAL* (Os04g0518400), *ANS* (Os01g0372500), *4CL* (Os01g0901600), *prx30* (Os02g0240100), *prx38* (Os03g0235000), *prx45* (Os03g0368900), *prx58* (Os04g0656800), *prx72* (Os05g0162000), *prx115* (Os07g0677600) and *prx117* (Os08g0113000) were significantly down-regulated in *osseh1* lines compared with that in WT plants under cold stress (Figure 7). These evidences supported the conclusion that *OsSEH1* may play an essential role in the phenylpropanoid biosynthesis pathway in response to cold stress.

Exogenous ABA increased the cold tolerance of *osseh1* knock-out lines

The growth and adaptation to stress of plants are commonly regulated by multiple phytohormones. Meanwhile, we noticed that the DEGs between WT and *osseh1* knock-out lines were significantly enriched in regulation of hormone levels and hormone metabolic process (Figure 4A) and we thus speculated that *OsSEH1* may play a role in regulation of phytohormones. To verify our speculation, we separately sprayed exogenous indole-3-acetic acid (IAA), 2, 4-Epibrassinolide and abscisic acid (ABA) onto the leaves of WT and *osseh1* knock-out lines under cold stress. The cold tolerance of WT plants and *osseh1* knock-out lines sprayed with ABA was significantly improved compared with that without exogenous

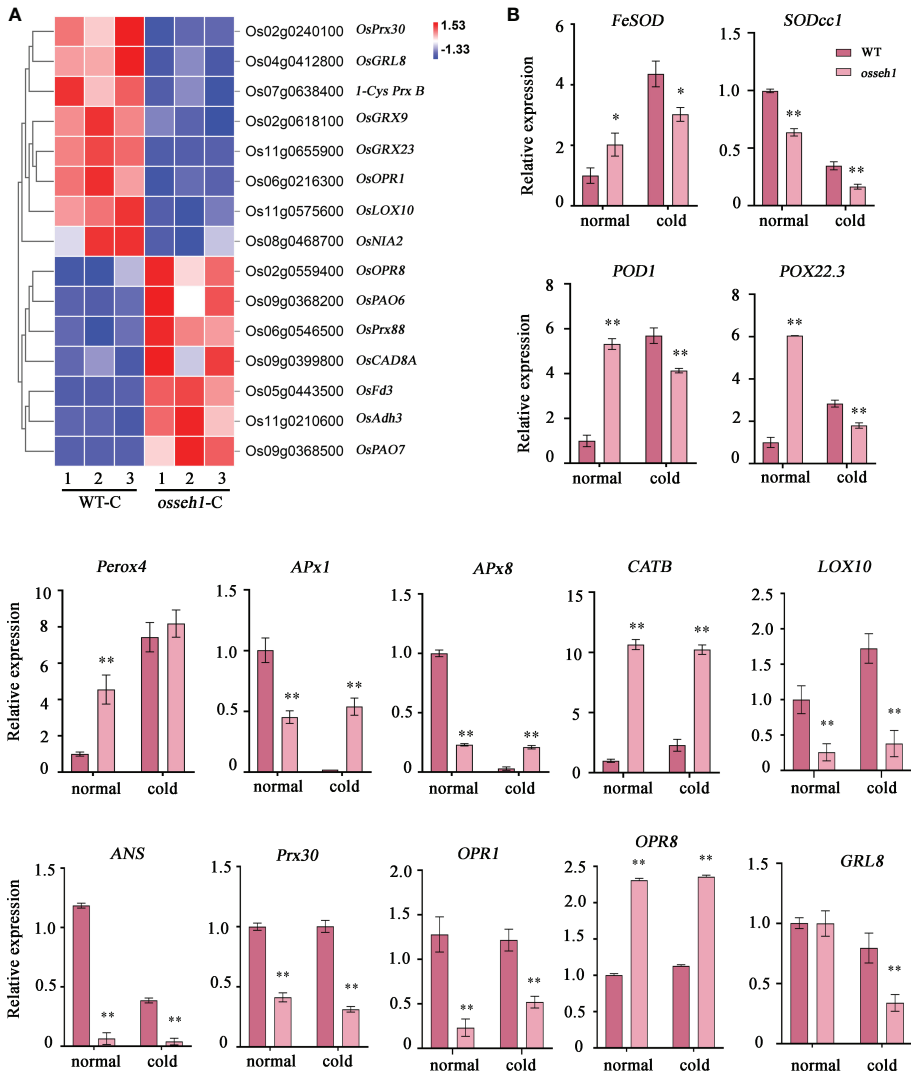


FIGURE 5
DEGs between *osseh1* knock-out lines and WT plants were involved in oxidation-reduction process. **(A)** Heatmap showing the enriched genes in the term of oxidation-reduction process. **(B)** Transcript levels of genes related to ROS scavenging in *osseh1* knock-out lines and WT plants under normal condition and cold stress. Data represents means ± SEM (n = 3). *P < 0.05, **P < 0.01. WT-C, WT under cold treatment. *osseh1*-C, *osseh1* lines under cold treatment.

hormone, but not with IAA or 2, 4-Epibrassinolide. To test a potential connection between *OsSEH1* and ABA, we further determined that the survival of WT plants increased by 0.70%, 5.56%, 11.11%, -1.39% in the 1 μM, 10 μM, 100 μM and 150 μM ABA treatments, respectively, compared with that of the 0 μM ABA treatment, while those of *osseh1* lines were 12.5%, 18.06%, 21.54%, 11.81% respectively (Figures 8A, B). To further verify the sensitivity of WT and *osseh1* lines to exogenous ABA, we calculated the germination rates of seeds grown on 0 μM, 1 μM or 10 μM ABA. In the absence of ABA, there was no significant difference between *osseh1* mutants and WT plants (Figures 8C, D). However, the germination rates of *osseh1* seeds treated with 1 μM and 10 μM ABA were significantly inhibited compared with that of WT plants (Figures 8C, D). These results indicated that *osseh1* knock-out lines had ABA hypersensitive phenotypes compared with that WT lines.

Further, we measured soluble sugar content, proline content, ROS content, SOD activity, POD activity, APX activity and CAT activity in the leaves treated with different ABA concentrations of WT and *osseh1* lines. We measured the endogenous ABA content in the *osseh1* knock-out lines and WT plants to verify the effectiveness of exogenous ABA application. The endogenous ABA content of *osseh1* knock-out lines was significantly higher than that of WT plants before and after treatment (Supplementary Figure 5A). The content of soluble sugar in WT plants was increased as the ABA concentrations was increased, while it was

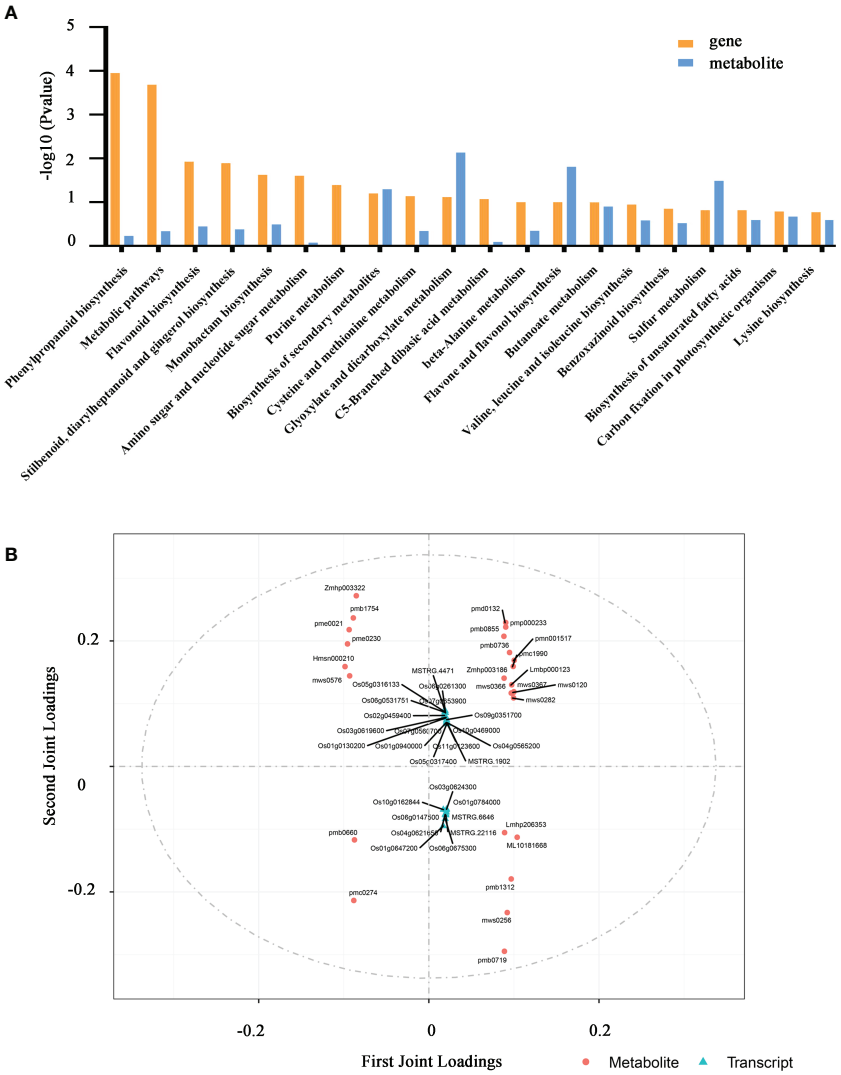


FIGURE 6
Combined analysis of the transcriptome and metabolome. **(A)** KEGG enrichment analysis of DAMs and DEGs between *osseh1* lines and WT plants under cold stress. **(B)** Loading values representation of genes and metabolites from transcriptome and metabolome Tables based on two-way orthogonal partial least squares (O2PLS) analysis.

almost no difference in *osseh1* lines under cold stress (Figure 8E). The trends of the proline content in both WT and *osseh1* lines showed no difference with the increase in ABA concentration (Figure 8F). The content of ROS in WT plants was increased as the ABA concentrations was increased, while it decreased significantly at the concentration of 1 μM and 10 μM in *osseh1* lines (Figure 8G). The activity of SOD in WT increased slowly as the ABA concentrations was increased, reaching a maximum with the spraying of 150 μM^*L^{-1} ABA. In contrast, the activity of SOD in *osseh1* lines increase to a maximum with the spraying of 10 μM^*L^{-1} ABA (Supplementary Figure 5B). Interestingly, in WT plants, the activity of POD was decreased as the ABA concentration was increased under cold stress, while it increased in *osseh1* plants (Supplementary Figure 5C). The activity of CAT and APX in both WT and *osseh1* plants increased with the increase in ABA concentration under cold stress (Supplementary Figures 5D, E). These results suggested that WT and *osseh1* knock-out plants differ in the sensitivity to exogenous ABA.

Discussion

Low environmental temperature limits plant growth and development, so plants have evolved multiple response mechanism to adapt to cold stress. However, the mechanisms of perception and response to cold stress in rice remain largely

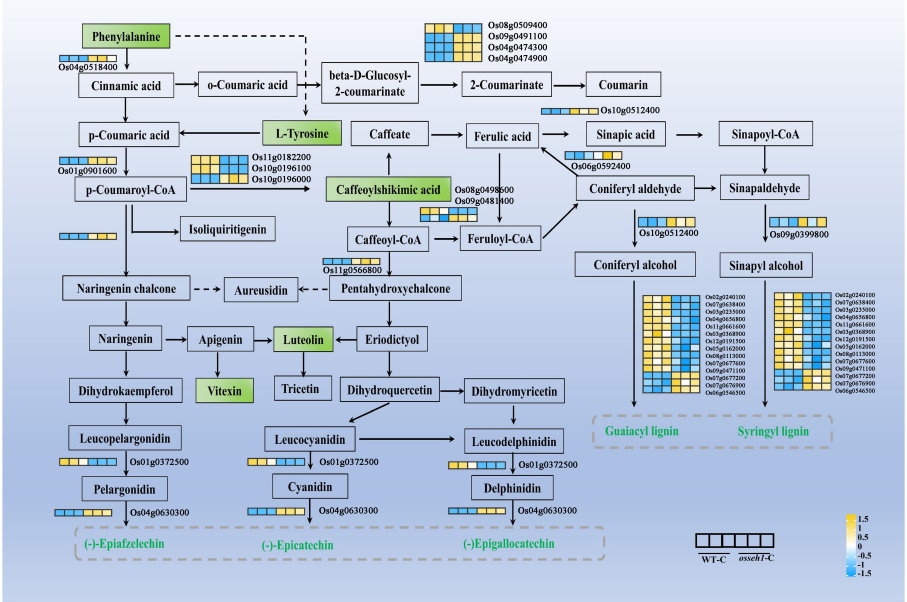


FIGURE 7
Different accumulation and expression patterns of metabolites and genes related to the phenylpropanoid biosynthesis pathway. Rectangle in the pathway indicates metabolite. The differentially accumulated metabolites are shown in green. The expression levels of genes are shown from yellow to blue (high to low) in the comparison of WT-C vs. *osseh1*-C. Gene heatmap shows the value of Log 2 (FPKM) in WT (left panel) and *osseh1* knock-out lines (right panel). WT-C, WT under cold treatment. *osseh1*-C, *osseh1* lines under cold treatment.

unknown. Therefore, it is of interest to identify the cold-tolerant genes and their regulatory network in cold stress. In previous studies, we presented evidence that *OsSEH1* was a potential gene involved in the regulation of cold stress at the seedling stage (Song et al., 2018). In this study, we performed physiological, metabolomic and transcriptomic analyses of the leaves from *osseh1* knock-out lines and WT plants under normal and cold condition to understand the regulatory role in the cold stress of rice. Moreover, we provide several lines of evidence that *OsSEH1* functions in the oxidation-reduction process to regulate cold tolerance in rice. First, the content of ROS and the activity of antioxidant enzymes showed significant differences between *osseh1* knock-out lines and WT plants under cold stress (Figures 1E–I). Second, metabolomics analysis revealed that the contents of large-scale flavonoids serving as ROS scavengers were lower in *osseh1* mutants compared to wild type under cold treatment (Figure 3C). Finally, Transcriptome analysis revealed that the DEGs between *osseh1* knock-out lines and WT plants were enriched in oxidation-reduction process (Figure 4C).

Nuclear pore complex (NPC), located within invaginations of the nuclear envelope, is the key subcellular structure to ensure the normal working of nuclear function and cell activities. NPC connects cytoplasm and nucleoplasm serving as the only channel for the exchange of macromolecules (Meier and Brkljacic, 2009). NPC is composed of multiple copies of approximately 30 diverse proteins termed nucleoporins (Nups) (Rout et al., 2000; Zimmerli et al., 2021). Up to now, the research on the function of plant nucleoporin is mainly concentrated in Arabidopsis (Lee and Seo, 2015; Zhu et al., 2017; Zhang et al., 2020), and our knowledge on the functions of rice nucleoporins remains poor. In this study, the nucleoporin-encoding gene *OsSEH1* play a positive role in cold stress of rice as *osseh1* knock-out lines showed significant decreased survival rate compared with that of WT plants after cold treatment (Figure 1A). This study advances our understanding of the function of plant nucleoporins.

Multiple components of physiology and biochemistry, such as photosynthesis, respiration, enzymatic reactions, osmotic potential, secondary metabolism, and nutrient absorption are negatively impacted by cold stress on plants (Balabusta et al., 2016; Wang et al., 2021). As ROS are very sensitive to ambient temperature changes, cold stress usually causes rapid and excessive accumulation of ROS in the cells (Noctor and Foyer, 1998; Xia et al., 2015; Choudhury et al., 2017). To protect the plant cells from oxidative stress and maintain normal cell functions, plants scavenge the excess ROS through diverse antioxidant enzymes, such as SOD, POD, CAT and APX. Interestingly, we noticed that the soluble sugar content, ROS content, CAT activity and APX activity of WT were decreased after cold stress in this study. Further, we found similar results of soluble sugar content (Wang et al., 2022; Xu et al., 2023), ROS

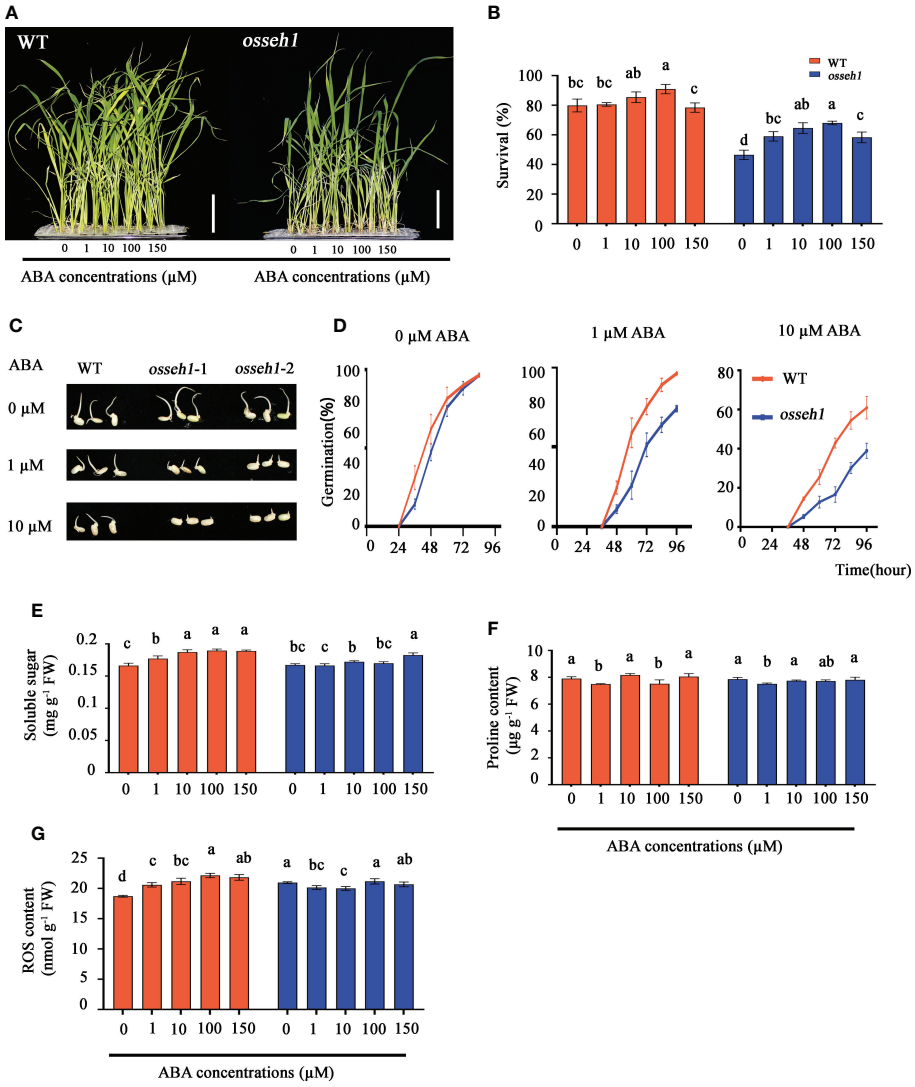


FIGURE 8
Responses of *osseh1* knock-out lines and WT plants to different concentration ABA under cold stress. **(A)** Phenotypes of *osseh1* knock-out lines and WT plants sprayed with different concentration ABA under cold stress. **(B)** Survival rates of *osseh1* knock-out lines and WT plants sprayed with different concentration ABA after cold treatment. **(C)** Germination phenotype of seeds from *osseh1* mutants and WT plants grown on 0, 1 or 10 μM ABA for 4 days after imbibition. **(D)** Germination rates corresponding to **(C)**. Statistical analysis of **(E)** soluble sugar, **(F)** proline content, **(G)** ROS content. Data represents means ± SEM (n = 3). Scale bars, 5cm.

content (Wang et al., 2022; Shu et al., 2023) and antioxidative enzyme activity (Wang et al., 2022, Liu et al., Hao et al., 2022; Liu et al., 2022) have been reported in previous studies. This results probably due to the impairment of the physiological metabolic sites of soluble sugar, ROS, CAT and APX by cold stress (Hao et al., 2022). In addition, the soluble sugar content, ROS content, CAT activity and APX activity of plants fluctuated under cold stress (Wang et al., 2022; Xu et al., 2023; Shu et al., 2023), rather than continuous increasing or decreasing, resulting in decreased content or activity of the physiological characteristics in a period of time after cold stress.

Numerous studies have demonstrated that plant response to abiotic stresses by alleviating oxidative stress (Ning et al., 2010; Fang et al., 2015; Zhou et al., 2018; Xiong et al., 2018; Liu et al., 2018; Zhao et al., 2020). For example, overexpression of an *ERF* family transcription factor (TF), *OsLG3*, increases drought tolerance by participating in H_2O_2 homeostasis (Xiong et al., 2018). Increasing the expression of *OsLPTL159* enhances rice cold tolerance by minimizing the toxic effects of ROS (Zhao et al., 2020). In this study, the activity of SOD and APX showed a significant difference between *osseh1* knock-out lines and WT plants under cold stress (Figures 1F, I). In addition, RNA-seq

data analysis showed multiple genes involved in oxidation-reduction process showed different expression levels between *osseh1* knock-out lines and wild type under cold stress (Figure 5A). Finally, the accumulation of amino acids, alkaloids, organic acids and lipids showed significant differences between the WT plants and *osseh1* mutants, suggesting an imbalance of antioxidation-related compounds metabolism in *osseh1* mutants (Figures 3A, C). These results demonstrated that *OsSEH1* improve cold tolerance may associated with reducing oxidative stress in cells by regulating the levels of redox genes and effectively scavenging ROS.

In plants, the content of phenylpropanoid and flavonoid metabolite are closely related to the ability to scavenge ROS under adverse environment (Agati et al., 2012). In this study, the results of integration of metabolomic and transcriptomic revealed that the phenylpropanoid and flavonoid biosynthetic pathway were significantly enriched (Figure 6A). Metabolome analysis suggested lower accumulation of phenylpropanoid metabolites was discovered in the leaves of *osseh1* knock-out lines compared with that of wild type plants after cold stress, such as phenylalanine, L-tyrosine, caffeoylshikimic acid, luteolin and vitexin (Figure 7). Phenylalanine, the starting component in the phenylpropyl biosynthesis pathway, is essential for all subsequent metabolic processes. Phenylalanine is transformed to t-cinnamic acid by PAL which is an important branch point enzyme regulated at the transcriptional level (Weitzel and Petersen, 2010). The biosynthesis of downstream metabolites, such as phenylpropanoid and flavonoid molecules, is impacted by the decreasing phenylalanine concentration. Some studies have demonstrated that the content of phenylpropanoid metabolites is mainly regulated at the transcriptional level (Liu et al., 2015; Dong and Lin, 2021). Our RNA-Seq data revealed that many genes involved in the phenylpropanoid biosynthesis pathway, including *PAL, ANS, 4CL, prx30, prx38, prx45, prx58, prx72, prx115, prx117* and *prx137*, showed different expression levels between *osseh1* knock-out lines and wild type plants at transcriptional level (Figure 7). These transcriptional and metabolic changes might indicate *OsSEH1* plays a role in the phenylpropanoid biosynthesis pathway to response to cold stress.

Plant hormones play important roles in the plant responses and resistance to multiple abiotic stresses. As a signal molecule against abiotic stress, ABA plays an important role in regulating multiple stress responses in plants (Li et al., 2020; Takahashi et al., 2020; Wang et al., 2020). Accumulated ABA increases the tolerance of drought stress by inducing closing of leaf stomata to reduce water loss from plants (Guajardo et al., 2016). ABA also increase the content of carbohydrates, ATP, NAD (H), and heat shock proteins to regulate heat stress response (Li et al., 2020). Previous studies indicated that an appropriate increased levels of ABA may be beneficial to improve cold tolerance of plants (Mega et al., 2015; Huang et al., 2016). Consistent with the previous studies, we determined in this study that low concentration of exogenous ABA did increase the cold tolerance of both *osseh1* knock-out lines and WT plants, while *osseh1* lines had more sensitive phenotypes than WT plants (Figure 8). However, the underlying mechanism of *OsSEH1* response to ABA still remains unclear.

In summary, we characterized a function of *OsSEH1* as a positive regulator of cold stress. Further, transcriptomic and metabolic profiling revealed that *OsSEH1* plays a role in the oxidation-reduction process by coordinately regulating genes expression and metabolite accumulation involved in phenylpropanoid and flavonoid biosynthetic pathway. In addition, *osseh1* lines had hypersensitive phenotypes to exogenous ABA compared with WT plants, suggesting that *OsSEH1* may mediate cold tolerance by regulating ABA levels. Considering the positive regulation of cold stress by *OsSEH1*, the manipulation of *OsSEH1* expression levels may be a powerful strategy to improve the tolerance to cold stress of plants.

Data availability statement

The datasets presented in this study can be found in online repositories. The names of the repository/repositories and accession number(s) can be found below: https://ngdc.cncb.ac.cn/gsa/, CRA008530.

Author contributions

MZ and DM conceived and designed the experiments. SG performed most of the experiments, analyzed the data and wrote the manuscript. JZ performed the physiology experiments. ZZ and WC performed the functional tests and RT-qPCR. HX analyzed the data. All authors contributed to the article and approved the submitted version.

Funding

his work was supported by the Liaoning Revitalization Talents Program (XLYC2008025), Shenyang Agricultural University Postgraduate Innovation Incubation Program (2021YCXB14), Special Fund for Local Science and Technology Development of Liaoning Province Guided by Central Authorities, Shenyang Seed Industry Innovation and Technology Project (21-110-3-08) and China Agriculture Research System (CARS-01-13).

Conflict of interest

The authors declare that the research was conducted in the absence of any commercial or financial relationships that could be construed as a potential conflict of interest.

Publisher's note

All claims expressed in this article are solely those of the authors and do not necessarily represent those of their affiliated organizations, or those of the publisher, the editors and the reviewers. Any product that may be evaluated in this article, or claim that may be made by its manufacturer, is not guaranteed or endorsed by the publisher.

Supplementary material

The Supplementary Material for this article can be found online at: https://www.frontiersin.org/articles/10.3389/fpls.2022.1110724/full#supplementary-material

References

Agati, G., Azzarello, E., Pollastri, S., and Tattini, M. (2012). Flavonoids as antioxidants in plants: Location and functional significance. *Plant Sci.* 196, 67–76. doi: 10.1016/j.plantsci.2012.07.014

Agati, G., Brunetti, C., Di Ferdinando, M., Ferrini, F., Pollastri, S., and Tattini, M. (2013). Functional roles of flavonoids in photoprotection: New evidence, lessons from the past. *Plant Physiol. And Biochem.* 72, 35–45. doi: 10.1016/j.plaphy.2013.03.014

Balabusta, M., Szafranska, K., and Posmyk, M. M. (2016). Exogenous melatonin improves antioxidant defensein cucumber seeds (*Cucumis sativus* l.) germinated under chilling stress. *Front. In Plant Sci.* 7. doi: 10.3389/fpls.2016.00575

Bates, L. S., Waldren, R. P., and Teare, I. D. (1973). Rapid determination of proline for water stress studies. *Plant Soil* 39, 305–307. doi: 10.1007/BF00018060

Boerjan, W., Ralph, J., and Baucher, M. (2003). Lignin biosynthesis. *Annu. Rev. Plant Biol.* 54, 519–546. doi: 10.1146/annurev.arplant.54.031902.134938

Choudhury, F. K., Rivero, R. M., Blumwald, E., and Mittler, R. (2017). Reactive oxygen species, abiotic stress and stress combination. *Plant J.* 90, 856–867. doi: 10.1111/tpj.13299

Dong, C.-H., Agarwal, M., Zhang, Y., Xie, Q., and Zhu, J.-K. (2006a). The negative regulator of plant cold responses, HOS1, is a RING E3 ligase that mediates the ubiquitination and degradation of ICE1. *Proc. Natl. Acad. Sci. United States America* 103, 8281–8286. doi: 10.1073/pnas.0602874103

Dong, C.-H., Hu, X., Tang, W., Zheng, X., Kim, Y. S., Lee, B.-H., et al. (2006b). A putative arabidopsis nucleoporin, AtNUP160, is critical for RNA export and required for plant tolerance to cold stress. *Mol. Cell. Biol.* 26, 9533–9543. doi: 10.1128/MCB.01063-06

Dong, N. Q., and Lin, H. X. (2021). Contribution of phenylpropanoid metabolism to plant development and plant-environment interactions. *J. Of Integr. Plant Biol.* 63, 180–209. doi: 10.1111/jipb.13054

Fang, Y. J., Liao, K. F., Du, H., Xu, Y., Song, H. Z., Li, X. H., et al. (2015). A stress-responsive NAC transcription factor SNAC3 confers heat and drought tolerance through modulation of reactive oxygen species in rice. *J. Of Exp. Bot.* 66, 6803–6817. doi: 10.1093/jxb/erv386

Fecht-Christoffers, M. M., Fuhrs, H., Braun, H.-P., and Horst, W. J. (2006). The role of hydrogen peroxide-producing and hydrogen peroxide-consuming peroxidases in the leaf apoplast of cowpea in manganese tolerance. *Plant Physiol.* 140, 1451–1463. doi: 10.1104/pp.105.070474

Fujino, K., Sekiguchi, H., Matsuda, Y., Sugimoto, K., Ono, K., and Yano, M. (2008). Molecular identification of a major quantitative trait locus, qLTG3-1, controlling low-temperature germinability in rice. *Proc. Natl. Acad. Sci. United States America* 105, 12623–12628. doi: 10.1073/pnas.0805303105

Gaveliene, V., Pakalniskyte, L., and Novickiene, L. (2014). Regulation of proline and ethylene levels in rape seedlings for freezing tolerance. *Cent. Eur. J. Of Biol.* 9, 1099–1107. doi: 10.2478/s11535-014-0340-z

Guajardo, E., Correa, J. A., and Contreras-Porcia, L. (2016). Role of abscisic acid (ABA) in activating antioxidant tolerance responses to desiccation stress in intertidal seaweed species. *Planta* 243, 767–781. doi: 10.1007/s00425-015-2438-6

Guo, X. Y., Liu, D. F., and Chong, K. (2018). Cold signaling in plants: Insights into mechanisms and regulation. *J. Of Integr. Plant Biol.* 60, 745–756. doi: 10.1111/jipb.12706

Han, Q.-H., Huang, B., Ding, C.-B., Zhang, Z.-W., Chen, Y.-E., Hu, C., et al. (2017). Effects of melatonin on anti-oxidative systems and photosystem II in cold-stressed rice seedlings. *Front. Plant Sci.* 8. doi: 10.3389/fpls.2017.00785

Han, B., Ma, X. D., Cui, D., Wang, Y. J., Geng, L. Y., Cao, G. L., et al. (2020). Comprehensive evaluation and analysis of the mechanism of cold tolerance based on the transcriptome of weedy rice seedlings. *Rice* 13, 14. doi: 10.1186/s12284-019-0363-1

Hao, L. L., Zhang, Y., Li, Y., Bai, L. X., Yue, D. F., Zhang, H. Y., et al. (2022). Comprehensive comparative analysis and expression profiles and effects on physiological response of DEAD-box RNA helicase genes in lumnitzera littorea (Jack) voigt under cold stress. *J. Of Plant Interact.* 17, 595–607. doi: 10.1080/17429145.2022.2074158

Hassan, S., and Mathesius, U. (2012). The role of flavonoids in root-rhizosphere signalling: opportunities and challenges for improving plant-microbe interactions. *J. Of Exp. Bot.* 63, 3429–3444. doi: 10.1093/jxb/err430

Huang, L., Hong, Y. B., Zhang, H. J., Li, D. Y., and Song, F. M. (2016). Rice NAC transcription factor ONAC095 plays opposite roles in drought and cold stress tolerance. *BMC Plant Biol.* 16. doi: 10.1186/s12870-016-0897-y

Ishitani, M., Xiong, L., Lee, H., Stevenson, B., and Zhu, J. K. (1998). HOS1, a genetic locus involved in cold-responsive gene expression in arabidopsis. *Plant Cell* 10, 1151–1161. doi: 10.1105/tpc.10.7.1151

Lee, K., and Seo, P. J. (2015). The E3 ubiquitin ligase HOS1 is involved in ethylene regulation of leaf expansion in arabidopsis. *Plant Signaling Behav.* 10. doi: 10.1080/15592324.2014.1003755

Lee, H., Xiong, L., Gong, Z., Ishitani, M., Stevenson, B., and Zhu, J. K. (2001). The arabidopsis HOS1 gene negatively regulates cold signal transduction and encodes a RING finger protein that displays cold-regulated nucleo–cytoplasmic partitioning. *Genes Dev.* 15, 912–924. doi: 10.1101/gad.866801

Li, P., He, Q., Jin, J., Liu, Y., Wen, Y., Zhao, K., et al. (2022b). Tomato oxalyl-CoA synthetase degrades oxalate and affects fruit quality. *Front. Plant Sci.* 13. doi: 10.3389/fpls.2022.951386

Liu, G. C., Liu, F. X., Wang, Y., and Liu, X. (2022). A novel long noncoding RNA CIL1 enhances cold stress tolerance in arabidopsis. *Plant Sci.* 323. doi: 10.1016/j.plantsci.2022.111370

Liu, J. Y., Osbourn, A., and Ma, P. D. (2015). MYB transcription factors as regulators of phenylpropanoid metabolism in plants. *Mol. Plant* 8, 689–708. doi: 10.1016/j.molp.2015.03.012

Liu, C. T., Ou, S. J., Mao, B. G., Tang, J. Y., Wang, W., Wang, H. R., et al. (2018). Early selection of bZIP73 facilitated adaptation of japonica rice to cold climates. *Nat. Commun.* 9, 12. doi: 10.1038/s41467-018-05753-w

Liu, C., Schlaeppi, M. R., Mao, B., Wang, W., Wang, A., and Chu, C. (2019). The bZIP73 transcription factor controls rice cold tolerance at the reproductive stage. *Plant Biotechnol. J.* 17, 1834–1849. doi: 10.1111/pbi.13104

Livak, K. J., and Schmittgen, T. D. (2001). Analysis of relative gene expression data using real-time quantitative PCR and the 2(-delta delta C(T)) method. *Methods (San Diego Calif.)* 25, 402–408. doi: 10.1006/meth.2001.1262

Li, C., Xu, Y., Li, Z., Cheng, P., and Yu, G. (2022a). Transcriptomic and metabolomic analysis reveals the potential mechanisms underlying the improvement of β-carotene and torulene production in rhodosporidiobolus

colostri under low temperature treatment. *Food Res. Int.* 156, 111158. doi: 10.1016/j.foodres.2022.111158

Li, G. Y., Zhang, C. X., Zhang, G. H., Fu, W. M., Feng, B. H., Chen, T. T., et al. (2020b). Abscisic acid negatively modulates heat tolerance in rolled leaf rice by increasing leaf temperature and regulating energy homeostasis. *Rice* 13, 16. doi: 10.1186/s12284-020-00379-3

Lu, G., Wu, F.-Q., Wu, W., Wang, H.-J., Zheng, X.-M., Zhang, Y., et al. (2014). Rice LTG1 is involved in adaptive growth and fitness under low ambient temperature. *Plant J.* 78, 468–480. doi: 10.1111/tpj.12487

Ma, Y., Dai, X. Y., Xu, Y. Y., Luo, W., Zheng, X. M., Zeng, D. L., et al. (2015). COLD1 confers chilling tolerance in rice (vol 160, pg 1209, 2015). *Cell* 162, 222–222. doi: 10.1016/j.cell.2015.06.046

Mao, D. H., Xin, Y. Y., Tan, Y. J., Hu, X. J., Bai, J. J., Liu, Z. Y., et al. (2019). Natural variation in the HAN1 gene confers chilling tolerance in rice and allowed adaptation to a temperate climate. *Proc. Of Natl. Acad. Of Sci. Of United States Of America* 116, 3494–3501. doi: 10.1073/pnas.1819769116

Ma, Y. Y., Zhang, Y. L., Lu, J., and Shao, H. B. (2009). Roles of plant soluble sugars and their responses to plant cold stress. *Afr. J. Of Biotechnol.* 8, 2004–2010.

Mega, R., Meguro-Maoka, A., Endo, A., Shimosaka, E., Murayama, S., Nambara, E., et al. (2015). Sustained low abscisic acid levels increase seedling vigor under cold stress in rice (*Oryza sativa* l.). *Sci. Rep.* 5. doi: 10.1038/srep13819

Meier, I., and Brkljacic, J. (2009). The nuclear pore and plant development. *Curr. Opin. In Plant Biol.* 12, 87–95. doi: 10.1016/j.pbi.2008.09.001

Mittler, R. (2017). ROS are good. *Trends In Plant Sci.* 22, 11–19. doi: 10.1016/j.tplants.2016.08.002

Moura, J., Bonine, C. A. V., Viana, J. D. F., Dornelas, M. C., and Mazzafera, P. (2010). Abiotic and biotic stresses and changes in the lignin content and composition in plants. *J. Of Integr. Plant Biol.* 52, 360–376. doi: 10.1111/j.1744-7909.2010.00892.x

Nakabayashi, R., Yonekura-Sakakibara, K., Urano, K., Suzuki, M., Yamada, Y., Nishizawa, T., et al. (2014). Enhancement of oxidative and drought tolerance in arabidopsis by overaccumulation of antioxidant flavonoids. *Plant J.* 77, 367–379. doi: 10.1111/tpj.12388

Ning, J., Li, X. H., Hicks, L. M., and Xiong, L. Z. (2010). A raf-like MAPKKK gene DSM1 mediates drought resistance through reactive oxygen species scavenging in rice. *Plant Physiol.* 152, 876–890. doi: 10.1104/pp.109.149856

Noctor, G., and Foyer, C. H. (1998). ASCORBATE AND GLUTATHIONE: Keeping active oxygen under control. *Annu. Rev. Plant Physiol. Plant Mol. Biol.* 49, 249–279. doi: 10.1146/annurev.arplant.49.1.249

Parry, G. (2015). The plant nuclear envelope and regulation of gene expression. *J. Of Exp. Bot.* 66, 1673–1685. doi: 10.1093/jxb/erv023

Polle, A., Krings, B., and Rennenberg, H. (1989). Superoxide dismutase activity in needles of Norwegian spruce trees (*Picea abies* L.)1. *Plant Physiol* 90, 1310–1315. doi: 10.1104/pp.90.4.1310

Rout, M. P., Aitchison, J. D., Suprapto, A., Hjertaas, K., Zhao, Y., and Chait, B. T. (2000). The yeast nuclear pore complex: composition, architecture, and transport mechanism. *J. Cell Biol.* 148, 635–651. doi: 10.1083/jcb.148.4.635

Sasaki, T., and Burr, B. (2000). International rice genome sequencing project: the effort to completely sequence the rice genome. *Curr. Opin. Plant Biol.* 3, 138–141. doi: 10.1016/S1369-5266(99)00047-3

Shi, Y. T., Ding, Y. L., and Yang, S. H. (2018). Molecular reculation of CBF sicnalinc in colc acclimation. *Trends In Plant Sci.* 23, 623–637. doi: 10.1016/j.tplants.2018.04.002

Shu, P., Li, Y., Xiang, L., Sheng, J., and Shen, L. (2023). SlNPR1 modulates chilling stress resistance in tomato plant by alleviating oxidative damage and affecting the synthesis of ferulic acid. *Scientia Hortic.* 307, 111486. doi: 10.1016/j.scienta.2022.111486

Song, J. Y., Li, J. Q., Sun, J., Hu, T., Wu, A. T., Liu, S. T., et al. (2018). Genome-wide association mapping for cold tolerance in a core collection of rice (*Oryza sativa* l.) landraces by using high-density single nucleotide polymorphism markers from specific-locus amplified fragment sequencing. *Front. In Plant Sci.* 9. doi: 10.3389/fpls.2018.00875

Sperotto, R. A., De Araujo, A. T., Adamski, J. M., Cargnelutti, D., Ricachenevsky, F. K., De Oliveira, B. H. N., et al. (2018). Deep RNAseq indicates protective mechanisms of cold-tolerant indica rice plants during early vegetative stage. *Plant Cell Rep.* 37, 347–375. doi: 10.1007/s00299-017-2234-9

Sudheeran, P. K., Feygenberg, O., Maurer, D., and Alkan, N. (2018). Improved cold tolerance of mango fruit with enhanced anthocyanin and flavonoid contents. *Molecules* 23. doi: 10.3390/molecules23071832

Sun, M., Shen, Y., Chen, Y., Wang, Y., Cai, X., Yang, J., et al. (2022). Osa-miR1320 targets the ERF transcription factor OsERF096 to regulate cold tolerance *via* JA-mediated signaling. *Plant Physiol* 189, 2500–2516. doi: 10.1093/plphys/kiac208

Takahashi, Y., Zhang, J., Hsu, P.-K., Ceciliato, P. H. O., Zhang, L., Dubeaux, G., et al. (2020). MAP3Kinase-dependent SnRK2-kinase activation is required for abscisic acid signal transduction and rapid osmotic stress response. *Nat. Commun.* 11. doi: 10.1038/s41467-019-13875-y

Treutter, D. (2005). Significance of flavonoids in plant resistance and enhancement of their biosynthesis. *Plant Biol. (Stuttgart Germany)* 7, 581–591. doi: 10.1055/s-2005-873009

Vanacker,, Carver,, and Foyer, (1998). Pathogen-induced changes in the antioxidant status of the apoplast in barley leaves. *Plant Physiol.* 117, 1103–1114. doi: 10.1104/pp.117.3.1103

Vanholme, R., De Meester, B., Ralph, J., and Boerjan, W. (2019). Lignin biosynthesis and its integration into metabolism. *Curr. Opin. In Biotechnol.* 56, 230–239. doi: 10.1016/j.copbio.2019.02.018

Verma, S., and Dubey, R. S. (2003). Lead toxicity induces lipid peroxidation and alters the activities of antioxidant enzymes in growing rice plants. *Plant Sci.* 164, 645–655. doi: 10.1016/S0168-9452(03)00022-0

Vogt, T. (2010). Phenylpropanoid biosynthesis. *Mol. Plant* 3, 2–20. doi: 10.1093/mp/ssp106

Wang, W. X., Du, J., Chen, L. M., Zeng, Y. J., Tan, X. M., Shi, Q. H., et al. (2021). Transcriptomic, proteomic, and physiological comparative analyses of flooding mitigation of the damage induced by low-temperature stress in direct seeded early indica rice at the seedling stage. *BMC Genomics* 22. doi: 10.1186/s12864-021-07458-9

Wang, Q., Yu, F., and Xie, Q. (2020). Balancing growth and adaptation to stress: crosstalk between brassinosteroid and abscisic acid signaling. *Plant Cell Environment* 43, 2325–2335. doi: 10.1111/pce.13846

Wang, H., Zhong, L., Fu, X., Huang, S., Fu, H., Shi, X., et al. (2022). Physiological and transcriptomic analyses reveal the mechanisms of compensatory growth ability for early rice after low temperature and weak light stress. *Plants* 11, 2523. doi: 10.3390/plants11192523

Weitzel, C., and Petersen, M. (2010). Enzymes of phenylpropanoid metabolism in the important medicinal plant Melissa officinalis l. *Planta* 232, 731–742. doi: 10.1007/s00425-010-1206-x

Xia, X.-J., Zhou, Y.-H., Shi, K., Zhou, J., Foyer, C. H., and Yu, J.-Q. (2015). Interplay between reactive oxygen species and hormones in the control of plant development and stress tolerance. *J. Of Exp. Bot.* 66, 2839–2856. doi: 10.1093/jxb/erv089

Xiong, H. Y., Yu, J. P., Miao, J. L., Li, J. J., Zhang, H. L., Wang, X., et al. (2018). Natural variation in OsLG3 increases drought tolerance in rice by inducing ROS scavenging. *Plant Physiol.* 178, 451–467. doi: 10.1104/pp.17.01492

Xu, H., Li, J., Wang, L., Li, X., Liu, Y., Wang, X., et al. (2023). Integrated transcriptomic and metabolomics analysis reveals abscisic acid signal transduction and sugar metabolism pathways as defense responses to cold stress in argyranthemum frutescens. *Environ. Exp. Bot.* 205, 105115. doi: 10.1016/j.envexpbot.2022.105115

Yang, Y., Wang, W., Chu, Z. Q., Zhu, J. K., and Zhang, H. M. (2017b). Roles of nuclear pores and nucleo-cytoplasmic trafficking in plant stress responses. *Front. In Plant Sci.* 8. doi: 10.3389/fpls.2017.00574

Yang, F. Y., Zhang, Y. S., Wen-Ke, L. I., Hou-Quan, L., and Luo, J. M. (2017a). Chilling damage comprehensive assessment methods for rice. *Chin. J. Appl. Ecol.*. 28, 3281–3288. doi: 10.13287/j.1001-9332.201710.021

Yan, H., Zheng, W., Wang, Y., Wu, Y., Yu, J., and Xia, P. (2022). Integrative metabolome and transcriptome analysis reveals the regulatory network of flavonoid biosynthesis in response to MeJA in camelliavietnamensis Huang. *Int. J. Mol. Sci.* 23, 9370. doi: 10.3390/ijms23169370

Yoshida, S., Forno, D. A., Cock, J. H., and Gomez, K. A. (1971). Laboratory manual for physiological studies of rice. *Int. Rice Res. Institute*.

Zhang, Z. Y., Li, J. J., Pan, Y. H., Li, J. L., Zhou, L., Shi, H. L., et al. (2017). Natural variation in CTB4a enhances rice adaptation to cold habitats. *Nat. Commun.* 8, 13. doi: 10.1038/ncomms14788

Zhang, J. Y., Luo, W., Zhao, Y., Xu, Y. Y., Song, S. H., and Chong, K. (2016). Comparative metabolomic analysis reveals a reactive oxygen species-dominated dynamic model underlying chilling environment adaptation and tolerance in rice. *New Phytol.* 211, 1295–1310. doi: 10.1111/nph.14011

Zhang, A. Q., Wang, S., Kim, J., Yan, J. P., Yan, X. F., Pang, Q. Y., et al. (2020). Nuclear pore complex components have temperature-influenced roles in plant growth and immunity. *Plant Cell And Environ.* 43, 1452–1466. doi: 10.1111/pce.13741

Zhang, Y. T., Yang, L. W., Hu, H. L., Yang, J. J., Cui, J. B., Wei, G. Q., et al. (2022). Transcriptome and metabolome changes in Chinese cedar during cold acclimation reveal the roles of flavonoids in needle discoloration and cold resistance. *Tree Physiol.* 42, 1858–1875. doi: 10.1093/treephys/tpac046

Zhao, J., Wang, S. S., Qin, J. J., Sun, C. Q., and Liu, F. X. (2020). The lipid transfer protein OsLTPL159 is involved in cold tolerance at the early seedling stage in rice. *Plant Biotechnol. J.* 18, 756–769. doi: 10.1111/pbi.13243

Zhou, Y. B., Liu, C., Tang, D. Y., Yan, L., Wang, D., Yang, Y. Z., et al. (2018). The receptor-like cytoplasmic kinase STRK1 phosphorylates and activates CatC, thereby regulating H2O2 homeostasis and improving salt tolerance in rice. *Plant Cell* 30, 1100–1118. doi: 10.1105/tpc.17.01000

Zhu, Y. F., Wang, B. S., Tang, K., Hsu, C. C., Xie, S. J., Du, H., et al. (2017). An arabidopsis nucleoporin NUP85 modulates plant responses to ABA and salt stress. *PloS Genet.* 13. doi: 10.1371/journal.pgen.1007124

Zimmerli, C. E., Allegretti, M., Rantos, V., Goetz, S. K., Obarska-Kosinska, A., Zagoriy, I., et al. (2021). Nuclear pores dilate and constrict in cellulo. *Science* 374, 1341–134+. doi: 10.1126/science.abd9776

frontiers | Frontiers in Plant Science

TYPE Original Research
PUBLISHED 15 February 2023
DOI 10.3389/fpls.2023.1119162

Check for updates

OPEN ACCESS

EDITED BY
Xinyang Wu,
China Jiliang University, China

REVIEWED BY
Xuan Chen,
Xi'an University of Technology, China
Qinsong Yang,
Beijing Forestry University, China

*CORRESPONDENCE
Peisen Su
pssu2014@163.com
Shangjing Guo
guoshangjing@lcu.edu.cn
Jun Yan
xinsinian2006@163.com

SPECIALTY SECTION
This article was submitted to Plant Abiotic Stress, a section of the journal Frontiers in Plant Science

RECEIVED 08 December 2022
ACCEPTED 30 January 2023
PUBLISHED 15 February 2023

CITATION
Su P, Sui C, Niu Y, Li J, Wang S, Sun F, Yan J and Guo S (2023) Comparative transcriptomic analysis and functional characterization reveals that the class III peroxidase gene *TaPRX-2A* regulates drought stress tolerance in transgenic wheat. *Front. Plant Sci.* 14:1119162. doi: 10.3389/fpls.2023.1119162

COPYRIGHT
© 2023 Su, Sui, Niu, Li, Wang, Sun, Yan and Guo. This is an open-access article distributed under the terms of the Creative Commons Attribution License (CC BY). The use, distribution or reproduction in other forums is permitted, provided the original author(s) and the copyright owner(s) are credited and that the original publication in this journal is cited, in accordance with accepted academic practice. No use, distribution or reproduction is permitted which does not comply with these terms.

Comparative transcriptomic analysis and functional characterization reveals that the class III peroxidase gene *TaPRX-2A* regulates drought stress tolerance in transgenic wheat

Peisen Su[1*], Chao Sui[1], Yufei Niu[1], Jingyu Li[1], Shuhan Wang[1], Fanting Sun[1], Jun Yan[2*] and Shangjing Guo[1*]

[1]College of Agronomy, Liaocheng University, Liaocheng, China, [2]Key Laboratory of Huang-Huai-Hai Smart Agricultural Technology of the Ministry of Agriculture and Rural Affairs, College of Information Science and Engineering, Shandong Agricultural University, Tai'an, Shandong, China

Drought is a major abiotic stress that reduces crop yields and quality worldwide. Although some genes involved in the response to drought stress have been identified, a more in-depth understanding of the mechanisms underlying wheat tolerance to drought is needed for the control of drought tolerance. Here, we evaluated the drought tolerance of 15 wheat cultivars and measured their physiological–biochemical parameters. Our data showed that the drought tolerance of the resistant wheat cultivars was significantly higher than that of drought-sensitive cultivars, which was associated with a greater antioxidant capacity of the former. Transcriptomic analysis revealed that different mechanisms of drought tolerance exist between the wheat cultivars Ziyou 5 and Liangxing 66. Transcriptomic analysis also revealed a large number of DEGs, including those involved in flavonoid biosynthesis, phytohormone signalling, phenolamides and antioxidants. qRT–PCR was performed, and the results showed that the expression levels of *TaPRX-2A* were significantly different among the various wheat cultivars under drought stress. Further study revealed that overexpression of *TaPRX-2A* enhanced tolerance to drought stress through the maintenance of increased antioxidase activities and reductions in ROS contents. Overexpression of *TaPRX-2A* also increased the expression levels of stress-related genes and ABA-related genes. Taken together, our findings show that flavonoids, phytohormones, phenolamides and antioxidants are involved in the plant response to drought stress and that *TaPRX-2A* is a positive regulator of this response. Our study provides insights into tolerance mechanisms and highlights the potential of *TaPRX-2A* overexpression in enhancing drought tolerance in crop improvement programmes.

KEYWORDS

transcriptomics, drought tolerance, class III peroxidase, TaPRX-2A, ROS

Introduction

Environmental stresses severely impact plant growth, development and productivity. Drought is a major abiotic stress that reduces crop yields and quality worldwide and is occurring more frequently due to climate change and water scarcity (Mahajan and Tuteja, 2005; Zampieri et al., 2017). When persistently exposed to drought stress, plants can experience multiple types of damage (including oxidative injury) (Joshi et al., 2016). Reactive oxygen species (ROS), including superoxide radicals (O_2^-), hydrogen peroxide (H_2O_2), and hydroxyl radicals (OH^-), constitute the primary cause of oxidative damage, which damages cells by destroying membrane lipids (McCord, 2000). To counter environmental stresses, plants have evolved sophisticated molecular mechanisms, such as ROS scavenging, phytohormone signalling pathway (those of abscisic acid (ABA)) activation, and secondary metabolism (including that involving flavonoids, melatonin, and secoisolariciresinol) (Campo et al., 2014; Zhu, 2016; Meng et al., 2021; Feng et al., 2022; Song et al., 2022). Moreover, the antioxidant system plays important roles in reducing ROS levels by the action of several endogenous antioxidant enzymes (catalase (CAT), ascorbate peroxidase (APX), and superoxide dismutase (SOD)) (Mittler, 2002). In addition, by catalysing redox reactions, peroxidases (PRXs) protect cells from ROS damage (Wood et al., 2003).

PRXs are antioxidant enzymes that are widely distributed in living organisms, including plants, microorganisms, and animals. The members of the PRX superfamily are categorized into haem (animal and nonanimal) and nonheme PRXs based on their structure (Welinder, 1992; Taurog, 1999). In plants, PRXs can be divided into three classes (class I, class II, and class III) based on their functions. Class I PRXs include APXs, class II subgroups include lignin PRXs, and class III subgroups (guaiacol PRXs, EC1.11.17) include secretory PRXs that are plant specific (Bhatt and Tripathi, 2011). Currently, a large number of class III PRX families have been identified as multigenic families in plants. For example, there are 155 members of the class III PRX gene family in rice. *Arabidopsis thaliana* class III PRXs comprise 75 isoenzymes, and *Brachypodium distachyon* class III PRXs comprise 151 isoenzymes (Fawal et al., 2013). Maize class III PRXs comprise 119 members (Wang et al., 2015). In addition, 374, 159 and 169 PRX members have been identified in *Triticum aestivum*, *Triticum urartu* and *Aegilops tauschii*, respectively (Yan et al., 2019).

Class III subgroups comprise large multigene families in the plant kingdom, and these members are involved in various biophysiological processes, such as lignin biosynthesis, cell wall hardening, defence against pathogens, H2O2 removal, and tolerance to abiotic stresses (Cosio and Dunand, 2009; Wang et al., 2015). In plants, class III PRXs can oxidize phenolic compounds, thereby reducing the level of H2O2, which makes these enzymes efficient components of the antioxidant system against stresses. The function of members of the class III PRX gene family has been widely studied and demonstrated. In *A. thaliana*, *AtPrx71* is involved in cell growth, cell wall damage, and inhibition of cell expansion through accumulation of H_2O_2 (Raggi et al., 2015). At low temperature, the class III PRXs *PRX62* and *PRX69* promote root hair growth in *Arabidopsis* by modulating ROS homeostasis (Pacheco et al., 2022). It was reported that wheat PRX-1 is a specific wheat allergen that causes grass pollen-related wheat allergies (Ogino et al., 2021). Additionally, some class III PRXs respond to biotic and abiotic stresses. For example, *T. aestivum PRX111*, *PRX112* and *PRX113* respond to nematode infection (Simonetti et al., 2009). The French bean (*Phaseolus vulgaris*) PRX gene (*FBP1*) can cause oxidative burst impairments to increase *Arabidopsis* susceptibility to fungi and bacteria through the downregulation of *AtPrx33* and *AtPrx34* transcription (Daudi et al., 2012). In tomato, APX is phosphorylated by the protein kinase CPK28, which enhances thermotolerance (Hu et al., 2021). *OsPrx30* transcription is modulated by the AT-hook protein *OsATH1*, and its overexpression enhances rice susceptibility to rice bacterial blight through the maintenance of increased PRX activity and reductions of H_2O_2 contents (Liu et al., 2021). Overexpression of *AtPrx64* was shown to improve tolerance to aluminium stress through a reduction in ROS accumulation and increase in lignin content (Wu et al., 2017), and by mediating the IbBBX24-IbTOE3-IbPRX17 module, *IbPRX17* overexpression was shown to enhance abiotic stress tolerance (Zhang et al., 2022). Some studies have demonstrated that wheat glutathione peroxidase (GPXs) can improve salt tolerance in transgenic *Arabidopsis* (Zhai et al., 2013). Our previous study showed that, by scavenging ROS and regulating stress-related genes, *TaPRX-2A* can improve wheat salt tolerance (Su et al., 2020).

Wheat, an important commercial crop species, yields are often restricted by abiotic stresses. In this study, we evaluated the drought tolerance of various wheat cultivars and performed a transcriptomic analysis between Ziyou 5 (a drought-resistant line) and Liangxing 66 (a drought-sensitive line). Our results showed that drought stress altered several metabolic pathways, including those involving flavonoids, phytohormones, phenolamides and antioxidants. Furthermore, we functionally characterized the class III PRX gene *TaPRX-2A*. Overexpression of *TaPRX-2A* enhanced the tolerance to drought stress of the transgenic lines, which occurred through the scavenging of ROS and increase in stress-responsive gene transcription. This work provides researchers with new insights into the class III PRXs molecular mechanisms underlying drought stress tolerance of wheat.

Materials and methods

Plant materials and abiotic stress treatments

"Nonglin20", "Shanrong 3", "Jimai 22", "Liangxing 66", "Xiaoyan 6", "Haomai 1", "Ailiduo", "Pubing 51", "Qunzhong 10", "Liangmai 2", "LS117TL", "Ziyou 5", "Baokemai 1330", "NSA98-1018" and "Pubing 9946" wheat (*T. aestivum*) seedlings were used in this study and obtained from Shandong Agricultural University. The seedlings were grown at 25°C under a photoperiod of 16/8 hours (h). The seedlings of the various wheat (*T. aestivum*) cultivars were subjected to drought stress when the plants produced one leaf and one heart. Concerning the drought stress treatment, the seedlings were not watered for 21 days (d) and then rewatered for 7 days.

Transcriptional profiling

Ziyou 5 and Liangxing 66 wheat (*T. aestivum*) seedlings were treated with 20% PEG6000, and the leaves were harvested at 48 h after treatment. The RNA of the samples was extracted using an RNAprep Pure Plant Kit (TIANGEN) and sent to Metware Corporation (Wuhan) for RNA sequencing (RNA-seq), which was performed using an Illumina HiSeq™ 2000 instrument. The clean RNA-seq reads were subsequently mapped to the wheat reference genome (http://plants.ensembl.org/Triticum_aestivum/Info/Index). Then, the transcripts were assembled, and the differentially expressed genes (DEGs) were analyzed using the DEGseq R package with the default parameters ($|\log_2$(fold-change)| >= 1, false discovery rate (FDR) < 0.05) (Mortazavi et al., 2008).

Isolation and cloning of *TaPRX-2A* and transgenic plant generation

We cloned the *TaPRX-2A* gene from the wheat cultivar Sumai 3. The wheat leaves were harvested from three-week-old plants and the RNA was extracted with TRIzol reagent (TransGen). The open reading frame (ORF) of *TaPRX-2A* (Ensembl ID: TraesCS2A02G573900) was obtained from the NCBI database (https://www.ncbi.nlm.nih.gov/). Specific primers were designed according to the *TaPRX-2A* sequence, and the primer sequences are listed in Table S3. Subsequently, the *TaPRX-2A* clone was ligated into the overexpression (OE) vector PC186 (pUbi::GWOE::Nos), after which the vector was transformed into the wheat KN199 background using particle gun-mediated gene transformation (Yao et al., 2006).

Measurements of physiological–biochemical parameters

The leaves of various wheat cultivars were collected under control and drought stress treatment after 21 days. The all samples were used to measure physiological parameters related to drought stress, such as relative water content (RWC), malondialdehyde (MDA), ROS, and antioxidant enzymes. The following formula was used to measure the leaf RWC: RWC = (FW − DW)/(TW − DW) × 100% (FW, fresh weight; DW, dry weight; TW, turgid fresh weight) (Zhou et al., 2014). We used the thiobarbituric acid method to measure the MDA content (Heath and Packer, 1968), and we used the ninhydrin reaction method to measure the proline content and the anthrone method to measure the total soluble sugar content (Spiro, 1966; Bates et al., 1973). The ROS (H_2O_2, O_2^-) levels were visualized using 3,3'-diaminobenzidine (DAB) and nitroblue tetrazolium (NBT) staining (Gay et al., 1999; Tian et al., 2013). The activity of antioxidant enzymes (SOD, CAT, PRX) was measured using a previously described method (Chance and Maehly, 1955; Dhindsa et al., 1981; Aebi, 1984).

Total RNA extraction and expression pattern analysis of stress-related genes

The RNA of leaves of various wheat cultivars, namely, "Shanrong 3", "Liangxing 66", "Xiaoyan 6", "Ailiduo", "Ziyou 5", "Baokemai 1330", "Shannong 41", "JM22", "Guomai 115", "Taimai 198", "Huaimai 33", "NSA98-1018", and "Pubing 9946", *TaPRX-2A* transgenic lines and wild-type (WT) plants was extracted with TRIzol reagent (TransGen). Then, the mRNAs were reverse transcribed into first-strand cDNAs. The expression patterns of stress-related genes were determined using qRT–PCR (Roche LightCycler® 480 system). The *18S rRNA* gene of wheat was used as an endogenous control, and the relative expression of the stress-related genes was calculated using the $2^{-\Delta\Delta CT}$ method. All the qRT–PCR primers used in this study are listed in Table S3.

Results

Drought tolerance of different wheat cultivars

To comprehensively evaluate the drought tolerance of the different wheat cultivars, we assessed the drought tolerance of 15 different wheat cultivars. The seedlings of all the different wheat cultivars were subjected to drought stress for 21 days. Then, we measured their physiological–biochemical indices. The results showed that different wheat cultivars had different drought tolerances. Some wheat cultivars (Liangmai 2, LS117TL, Ziyou 5, Baokemai 1330, and NSA98-1018) were drought-tolerant and had high survival rates, while others (Nonglin 20, Shanrong 3, Jimai 22, Liangxing 66, Xiaoyan 6, Haomai 1 and Ailiduo) were drought-sensitive and had low survival rates. Similarly, several wheat cultivars (Qunzhong 10, Pubing 51, and Pubing 9946) were moderately drought tolerant. After drought stress for 21 days, the leaves of the drought-tolerant cultivars were slightly wilted compared with those of the drought-sensitive cultivars. The phenotypic changes and survival rates of different the wheat cultivars under both the control and the drought stress treatments were recorded (Figure S1).

ROS constitute the main cause of oxidative damage, which is associated with the physiological response to abiotic stresses in plants. To gain further insight into the differences in drought tolerance between different wheat cultivars, we measured several important physiological–biochemical properties associated with oxidation resistance. First, we measured the levels of ROS accumulation and the activities of antioxidant enzymes under drought stress. Under drought stress, we observed that the O^{2-} and H_2O_2 contents in the drought-tolerant wheat cultivars (Qunzhong 10, Liangmai 2, LS117TL, and Ziyou 5) were significantly lower than those in the drought-sensitive cultivars (Nonglin 20, Shanrong 3, Jimai 22, Liangxing 66, and Ailiduo) (Figures 1A, B). The activities of antioxidant enzymes (PRX, CAT) in the different wheat cultivars were subsequently measured. The results showed that the activities of PRX and CAT were higher in the drought-tolerant and drought-sensitive wheat cultivars under drought stress than in the controls. Specifically, the PRX activity in the drought-tolerant wheat cultivar Baokemai 1330 was significantly higher than that in the drought-sensitive cultivars (Figures 1C, D).

Transcriptome sequencing analysis

To study the mechanism of drought tolerance between different wheat cultivars, we sequenced the transcriptome of a drought-tolerant

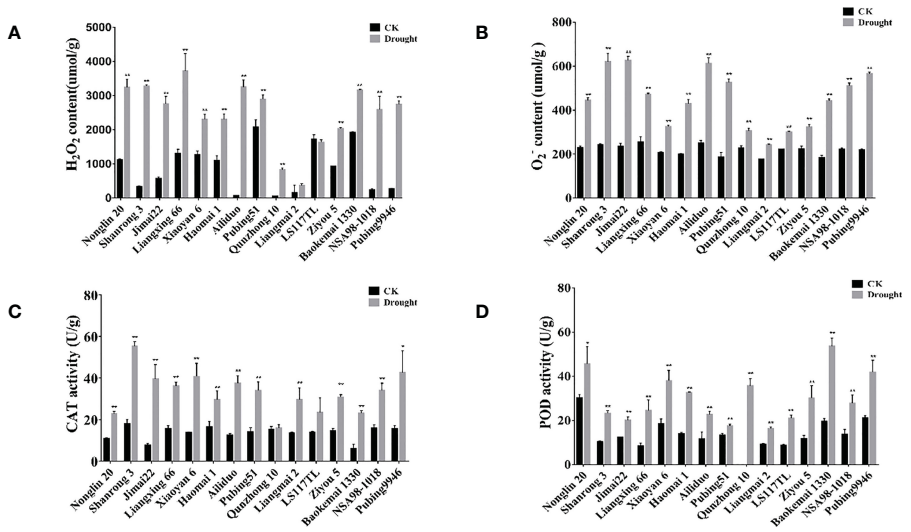


FIGURE 1
Analysis of ROS scavenging capacity and antioxidant enzymes activity. **(A)** H_2O_2 content for different wheat cultivars under control and drought treatment. **(B)** O_2^- content for different wheat cultivars under control and drought treatment. **(C)** Detection of CAT activity for different wheat cultivars under control and drought treatment. **(D)** Detection of POD activity for different wheat cultivars under control and drought treatment. All experiments included three replicates and the data present the mean ± SD. *P < 0.05 and **P < 0.01 indicate a significant difference compared with WT.

wheat cultivar (Ziyou 5) and a drought-sensitive cultivar (Liangxing 66). The genes that were differentially between the control and treated samples were analysed. The results showed that 20663 (down, 8635; up, 12028) and 23775 (down, 12170; up, 11605) genes were differentially expressed in Liangxing 66 and Ziyou 5 (control vs. drought), respectively (Figure S2A–C and Table S1). According to our constructed Venn diagram, we focused on the 734 DEGs that cover 4 different combinations and found that these genes were mainly involved in the flavonoid, plant hormone, MAPK signalling, phenolamide and antioxidant pathways (Figure S2C; Table S1). Based on the DEG expression levels, principal component analysis (PCA) was performed on the samples (three biological replicates) (Figure S2D). According to the PCA score plot, the first principal components (PCs) accounted for 41.36% and the second PCs accounted for 18.47% of the total variance among the four sample groups. The four sample groups (i.e., Liangxing 66-CK, Liangxing 66-D, Ziyou 5-CK, Ziyou 5-D) could be easily distinguished from each other, since they were clustered into four distinct areas in the PCA score plot, indicating that each of the sample groups exhibited distinct expression profiles.

To determine the potential functions, all the DEGs were annotated by Gene Ontology (GO) enrichment analysis. The results showed that most DEGs were enriched in biological processes, including cellular processes (9319, 10610), metabolic processes (7824, 8884), responses to stimulus (5026, 5363), biological regulation (3623, 4040), and developmental processes (1930, 2099) in Liangxing 66 and Ziyou 5, respectively (control vs. drought). In the cellular component category, the top two categories were cellular anatomical entity (13490, 15364) and protein-containing complex (1239, 1603). In the molecular function category, the top four terms were binding (8968, 10076), catalytic activity (8639, 9664), transporter activity (1200, 1335), and transcription regulator activity (850, 917) (Figures S3A, B; Table S1).

To better understand the interactions of the DEGs, we performed a Kyoto Encyclopedia of Genes and Genomes (KEGG) (https://www.genome.jp/kegg) functional enrichment analysis of the DEGs (control vs. drought). The results showed that the related KEGG pathways were mostly enriched in metabolic pathways (3615, 4066), biosynthesis of secondary metabolites (2271, 2557), plant–pathogen interactions (962, 942), the MAPK signalling pathway (507, 517), plant hormone signal transduction (541, 570), starch and sucrose metabolism (346, 361), phenylpropanoid biosynthesis (319, 351), oxidative phosphorylation (164, 193), flavonoid biosynthesis (161, 179), glutathione metabolism (157, 189), peroxisomes (155, 182), tryptophan metabolism (106, 136), arginine and proline metabolism (92, 114), and flavone and flavonol biosynthesis (40, 55) in Liangxing 66 and Ziyou 5, respectively (control vs. drought) (Figures S3C, D; Table S1).

Drought stress alters the expression profiles of genes involved in the flavonoid biosynthesis pathway

To better understand the influence of drought stress on the expression profiles of genes involved in the flavonoid biosynthesis pathway, we analysed the transcriptomic data of the drought-stressed wheat cultivars (Ziyou 5 and Liangxing 66). Based on the transcript levels, we constructed a network involving all the relationships of genes involved in the flavonoid biosynthesis pathway (Figure 2). The analysis showed that the expression levels of 372 (Liangxing 66-CK vs. Liangxing 66-D) and 405 (Ziyou 5-CK vs. Ziyou 5-D) genes in the

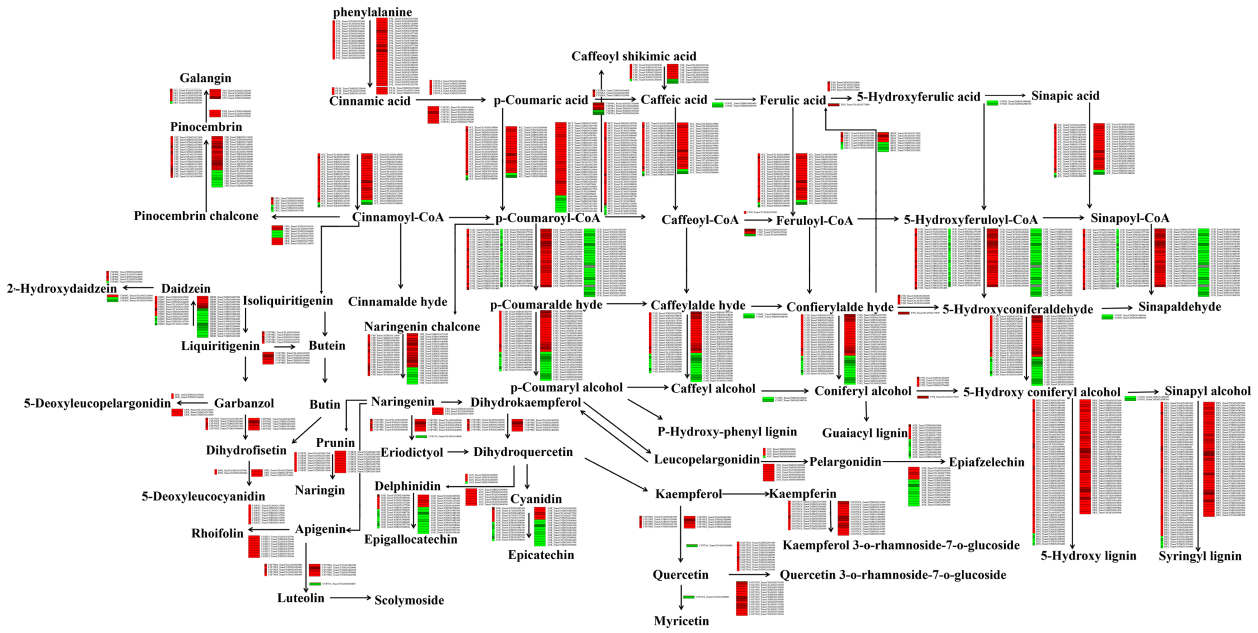


FIGURE 2
Effects of drought stress on flavonoid biosynthesis-related genes. Regulatory network for the flavonoid metabolites, selected integrated expression levels of known genes involved in flavonoid biosynthetic pathway for wheat leaves treated with drought stress. The green and red represent doen-regulated and up-regulated gene expression under drought stress. *PAL*, phenylalanine ammonia-lyase; *PTAL*, phenylalanine/tyrosine ammonia-lyase; *CYP73A*, trans-cinnamate 4-monooxygenase; *COMT*, caffeic acid 3-O-methyltransferase; *CMT*, caffeoyl-CoA O-methyltransferase; *HCT*, shikimate O-hydroxycinnamoyltransferase; *CYP98A*, 5-O-(4-coumaroyl)-D-quinate 3'-monooxygenase; *CSE*, caffeoylshikimate esterase; *REF1*, coniferyl-aldehyde dehydrogenase; *DFR*, flavanone 4-reductase; *CYP75A*, flavonoid 3',5'-hydroxylase; *PRX*, peroxidase; *4CL*, 4-coumarate–CoA ligase; *CCR*, cinnamoyl-CoA reductase; *HCT*, shikimate O-hydroxycinnamoyl transferase; *CYP98A*, 5-O-(4-coumaroyl)-D-quinate 3'-monooxygenase; *F5H*, ferulate-5-hydroxylase; *CAD*, cinnamyl-alcohol dehydrogenase; *CHS*, chalcone synthase; *CHI*, chalcone isomerase; *FLS*, flavonol synthase; *CYP75B1*, flavonoid 3'-monooxygenase; *ANS*, anthocyanidin synthase; *ANR*, anthocyanidin reductase; *HIDH*, 2-hydroxyisoflavanone dehydratase; *UGT73C6*, flavonol-3-O-L-rhamnoside-7-O-glucosyltransferase; *CYP81E*, 4'-methoxyisoflavone 2'-hydroxylase; *F3H*, naringenin 3-dioxygenase; *C12RT1*, flavanone 7-O-glucoside 2''-O-beta-L-rhamnosyltransferase.

flavonoid biosynthesis pathway changed. When combining data obtained from each group, we found that most expression levels of these genes increased between the two groups, as was the case for phenylalanine ammonia lyase (*PAL*), phenylalanine/tyrosine ammonia-lyase (*PTAL*), trans-cinnamate 4-monooxygenase (*CYP73A*), ferulate-5-hydroxylase (*F5H*), caffeoyl-CoA O-methyltransferase (*CMT*), 5-O-(4-coumaroyl)-D-quinate 3'-monooxygenase (*CYP98A*), flavanone 4-reductase (*DFR*), flavonoid 3'-monooxygenase (*CYP75B1*), and flavanone 7-O-glucoside 2'-O-beta-L-rhamnosyltransferase (*C12RT1*). However, the expression level of flavonoid 3',5'-hydroxylase (*CYP75A*) decreased. In addition, the expression levels of 4-coumarate-CoA ligase (*4CL*), shikimate O-hydroxycinnamoyl transferase (*HCT*), cinnamoyl-CoA reductase (*CCR*), chalcone synthase (*CHS*), chalcone isomerase (*CHI*), anthocyanidin reductase (*ANR*), anthocyanidin synthase (*ANS*), *PRX*, and flavonol synthase (*FLS*) were different, with some increasing and some decreasing (Table S2). Considering that data are from the two different individual groups, the results of our transcriptomic analysis revealed specific increases in naringenin 3-dioxygenase (*F3H*) expression (Ziyou 5-CK vs. Ziyou 5-D) (Figure 2, Table S2). These results suggested that the flavonoid biosynthesis pathway in wheat plays a major role in the response to drought stress. Moreover, these results highlight that treatment of distinct wheat cultivars can consistently elicit discrete profiles of specific genes. In addition, the RNA-seq-based transcript levels of these genes involved in the flavonoid biosynthesis pathway were also verified *via* qRT-PCR. The expression trends according to the qRT-PCR data were consistent with the trends according to the transcriptomic data (Figure S4).

Plant hormone signalling pathway activity is induced by drought stress

Our transcriptome analysis also indicated that, in addition to the flavonoid biosynthesis pathway, the ABA (a plant hormone) pathway is involved in the response to drought stress. Therefore, we generated a network to explore the relationships between drought stress and ABA signalling pathways. Under drought stress, 148 (Liangxing 66-CK vs. Liangxing 66-D) and 166 (Ziyou 5-CK vs. Ziyou 5-D) ABA-related genes were enriched in plant hormone pathways. The expression levels of beta-carotene 3-hydroxylase (*crtZ*), xanthoxin dehydrogenase (*ABA2*), and abscisic-aldehyde oxidase (*AAO3*) increased, while those of prolycopene isomerase (*crtISO*), violaxanthin de-epoxidase (*VDE*), and PYR/PYL decreased. Moreover, we found that carotenoid epsilon hydroxylase (*CYP97C1*) was specifically expressed in the samples (Ziyou 5-CK vs. Ziyou 5-D) (Figure 3; Table S2). Similarly, the expression trends of genes involved in the ABA pathway according to the qRT-PCR data were consistent with the trends according to the transcriptomic data (Figure S5).

We also generated networks about auxin, SA and JA pathways. (1) auxin: Under drought stress, 171 (Liangxing 66-CK vs Liangxing 66-

10.3389/fpls.2023.1119162

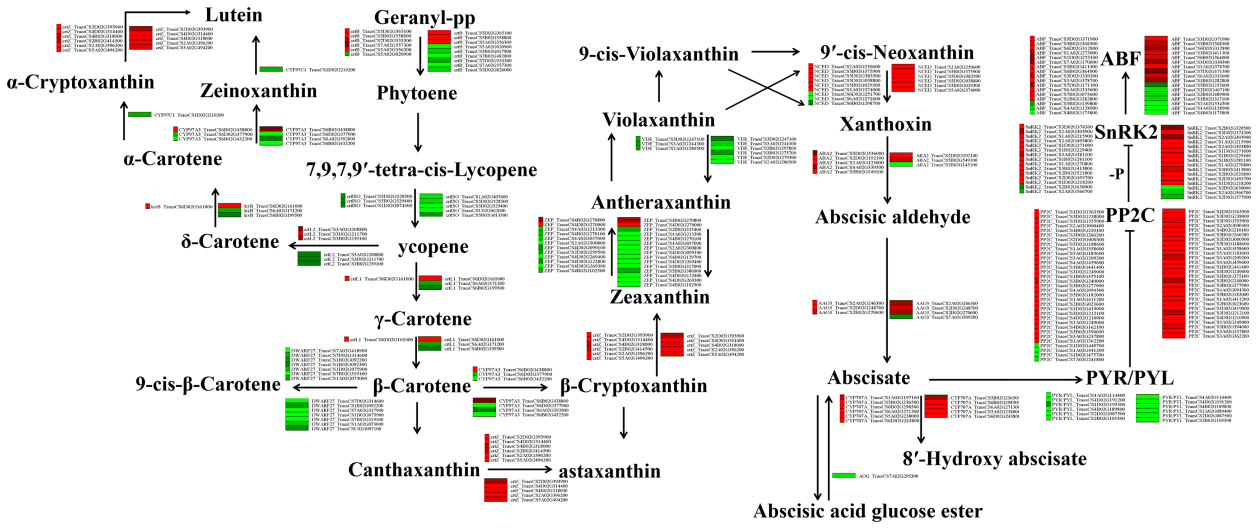


FIGURE 3
Effects of drought stress on ABA biosynthesis and signal transduction in wheat. Overview of ABA biosynthesis and signal transduction. The green and red represent down-regulated and up-regulated gene expression under drought stress. *ctrB*, 15-cis-phytoene synthase; *ctrZ*, beta-carotene 3-hydroxylase; *ZEP*, zeaxanthin epoxidase; *crtISO*, prolycopene isomerase; *crtL2*, lycopene epsilon-cyclase; *lcyB*, lycopene beta-cyclase; *CYP97A3*, beta-ring hydroxylase; *crtZ*, beta-carotene 3-hydroxylase; *CYP97C1*, carotenoid epsilon hydroxylase; *crtL1*, lycopene beta-cyclase; *DWARF27*, beta-carotene isomerase; *VDE*, violaxanthin de-epoxidase; *NCED*, 9-cis-epoxycarotenoid dioxygenase; *ABA2*, xanthoxin dehydrogenase; *AAO3*, abscisic-aldehyde oxidase; *AOG*, abscisate beta-glucosyltransferase; *PP2C*, protein phosphatase 2C; *CYP707A*, (+)-abscisic acid 8′-hydroxylase. *ABF*, ABA responsive element binding factor; *PYL*, abscisic acid receptor PYR/PYL family; *SnRK2*, serine/threonine-protein kinase SRK2.

D) and 210 (Ziyou 5-CK vs Ziyou 5-D) auxin-related genes were enriched in plant hormone pathways. Among them, the expression levels of 3-phosphoshikimate 1-carboxyvinyltransferase (*AROA*), chorismate synthase (*AROC*), anthranilate phosphoribosyl transferase (*TRPD*), aromatic aminotransferase (*ISS1*), and transport inhibitor response 1 (*TIR1*), exhibited upregulation, while arylalkylamine N-acetyltransferase (*AANAT*), indole-3-acetaldehyde oxidase (*AAO*) exhibited downregulation. Indole-3-pyruvate monooxygenase (*YUCCA*), amidase (*AMI*), L-tryptophan—pyruvate aminotransferase (*TAA1*), auxin-responsive protein (*AUX/IAA*), auxin response factor (*ARF*), auxin responsive GH3 gene family (*GH3*), SAUR family protein (*SAUR*) were different expression trends (upregulations, or downregulations). (2) SA: Under drought stress, 46 (Liangxing 66-CK vs Liangxing 66-D) and 59 (Ziyou 5-CK vs Ziyou 5-D) genes in SA pathways were enriched in plant hormone pathways. Among them, the expression levels of *PAL*, *PTAL*, and *PR1* were significantly upregulated, whereas *ICS* and *NPR1* were significantly downregulated. (3) JA: Under drought stress, 179 (Liangxing 66-CK vs Liangxing 66-D) and 168 (Ziyou 5-CK vs Ziyou 5-D) genes in JA pathway were enriched in plant hormone pathways. Among them, the expression levels of hydroperoxide dehydratase (*AOS*), allene oxide cyclase (*AOC*), and acetyl-CoA acyltransferase (*FAD*) were upregulated, whereas hydroperoxide lyase (*HPL*) was significantly downregulated. Fatty acid alpha-dioxygenase (*DOX*) was significantly upregulated in "Liangxing 66" (control vs. drought treated), while *DOX* was significantly downregulated in "Ziyou 5" (control vs. drought treated). OPC-8:0 CoA ligase 1 (*OPCL1*) and jasmonate O-methyltransferase (*JAM*) specially expressed in "Liangxing 66" (control vs. drought treated), while *COI1* specially expressed in "Ziyou 5" (control vs. drought treated) (Figure S6, Table S2). In addition, qRT-PCR analysis confirmed the significantly differential gene expression trends detected in transcriptome data (Figure S7).

Phenolamides and antioxidant pathway activity in response to drought stress

We found that drought stress modulates the phenolamide and antioxidant pathways. The transcriptomic data revealed significant differences in the expression of many phenolamide-related and antioxidant pathway-related genes. Among them, arginase (*ARG*), agmatine coumaroyl transferase (*ACT*), glutamate 5-kinase (*proB*), pyrroline-5-carboxylate reductase (*proC*), ornithine–oxo-acid transaminase (*ROCD*), prolyl 4-hydroxylase (*P4HA*), aspartate aminotransferase (*GOT1*), ornithine decarboxylase (*ODC1*), spermidine synthase (*SPE*), polyamine oxidase (*PAO*), phosphomannomutase (*PMM*), and mannose-1-phosphate guanylyltransferase (*GMPP*) were upregulated in response to drought stress. In contrast, ribonucleoside-diphosphate reductase subunit M1 (*RRM1*) was significantly downregulated under drought stress. Moreover, the expression trends of genes involved in the antioxidant pathway, such as *GPX*, L-*APX*, peroxiredoxin (*PRDX6*), glutathione reductase (*GSR*), gamma-glutamyltranspeptidase (*GGT*), glutathione S-transferase (*GST*), L-ascorbate oxidase (*AOX*), monodehydroascorbate reductase

10.3389/fpls.2023.1119162

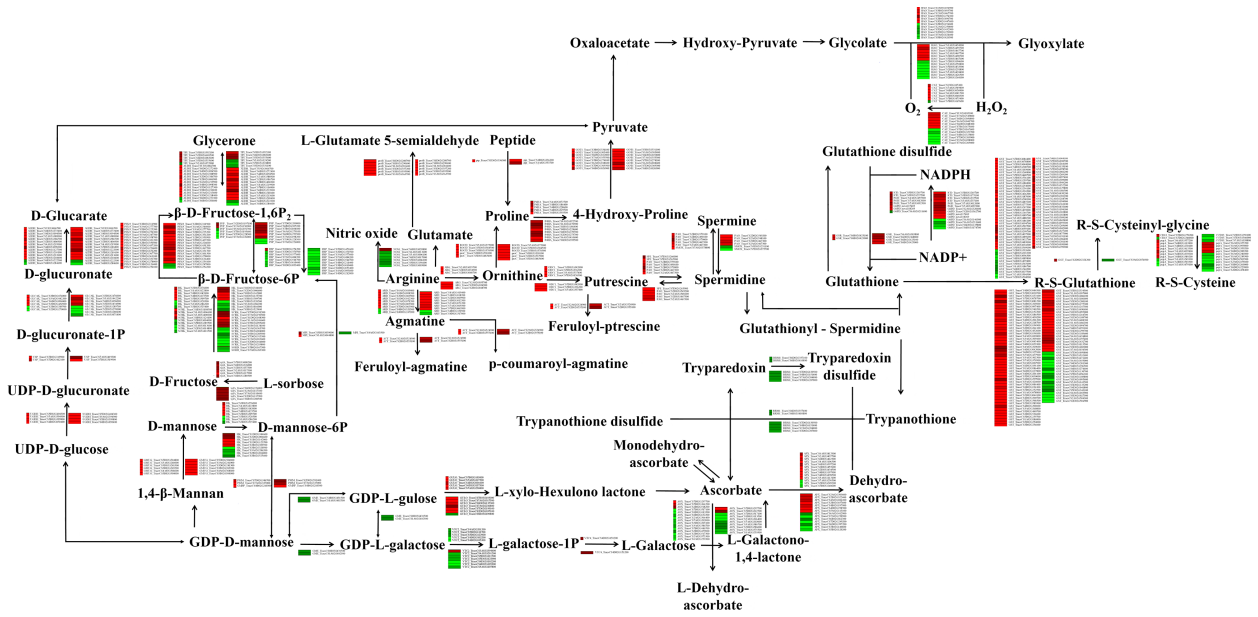


FIGURE 4
Effects of drought stress on phenolamides and antioxidant biosynthesis-related genes in wheat. Overview of phenolamides and antioxidant biosynthesis. The green and red represent doen-regulated and up-regulated gene expression under drought stress. *ALDH*, aldehyde dehydrogenase (NAD+); *SMOX*, spermine oxidase; *ROCD*, ornithine−oxo-acid transaminase; *ACT*, agmatine coumaroyltransferase; *PRDX6*, peroxiredoxin 6; *G6PD*, glucose-6-phosphate 1-dehydrogenase; *GPX*, glutathione peroxidase; *APX*, L-ascorbate peroxidase; *RRM1*, ribonucleoside-diphosphate reductase subunit M1; *NOS1*, nitric-oxide synthase; *proB*, glutamate 5-kinase; *proC*, pyrroline-5-carboxylate reductase; *pip*, proline iminopeptidase; *P4HA*, prolyl 4-hydroxylase; *GOT1*, aspartate aminotransferas; *ODC1*, ornithine decarboxylase; *GLDH*, L-galactono-1,4-lactone dehydrogenase; *SPE*, spermidine synthase; *GSR*, glutathione reductase (NADPH); *PGD*, 6-phosphogluconate dehydrogenase; *ICD*, isocitrate dehydrogenase; *GGT*, gamma-glutamyltranspeptidase/glutathione hydrolase; *UGDH*, UDP glucose 6-dehydrogenase; *GMPP*, mannose-1-phosphate guanylyltransferase; *SORD*, L-iditol 2-dehydrogenase; *xylA*, xylose isomerase; *RRM1*, ribonucleoside-diphosphate reductase subunit M1; *GST*, glutathione S-transferase; *CD13*, aminopeptidase N; *pepA*, leucyl aminopeptidase; *GME*, GDP-D-mannose 3′, 5′-epimerase; *VTC2*, GDP-L-galactose phosphorylase; *VTC4*, inositol-phosphate phosphatase; *GULO*, L-gulonolactone oxidase; *AOX*, L-ascorbate oxidase; *NADH*, monodehydroascorbate reductase; *HK*, hexokinase; *scrK*, fructokinase; *PFP*, diphosphate-dependent phosphofructokinase; *PFK9*, 6-phosphofructokinase; *FBP*, fructose-1,6-bisphosphatase I; *ALDO*, fructose-bisphosphate aldolase; *TPI*, triosephosphate isomerase; *PMM*, phosphomannomutase; *GMUG*, mannan endo-1,4-beta-mannosidase; *MPI*, mannose-6-phosphate isomerase; *USP*, UDP-sugar pyrophosphorylase; *GLCAK*, glucuronokinase; *HAO*, (S)-2-hydroxy-acid oxidase; *CAT*, catalase.

(*NADH*), (S)-2-hydroxy-acid oxidase (*HAO*), and *CAT*, were different, with the expression of some increasing and some decreasing, in the Liangxing 66-CK vs. Liangxing 66-D and Ziyou 5-CK vs. Ziyou 5-D comparison groups. GDP-D-mannose 3',5'-epimerase (*GME*) was expressed specifically in Ziyou 5 (control vs. drought stressed) (Figure 4; Table S2). We also compared the expression levels of the genes involved in the phenolamide and the antioxidant pathways between the qRT-PCR data and the transcriptomic data, and the we found that the expression trends were also the same (Figure S8).

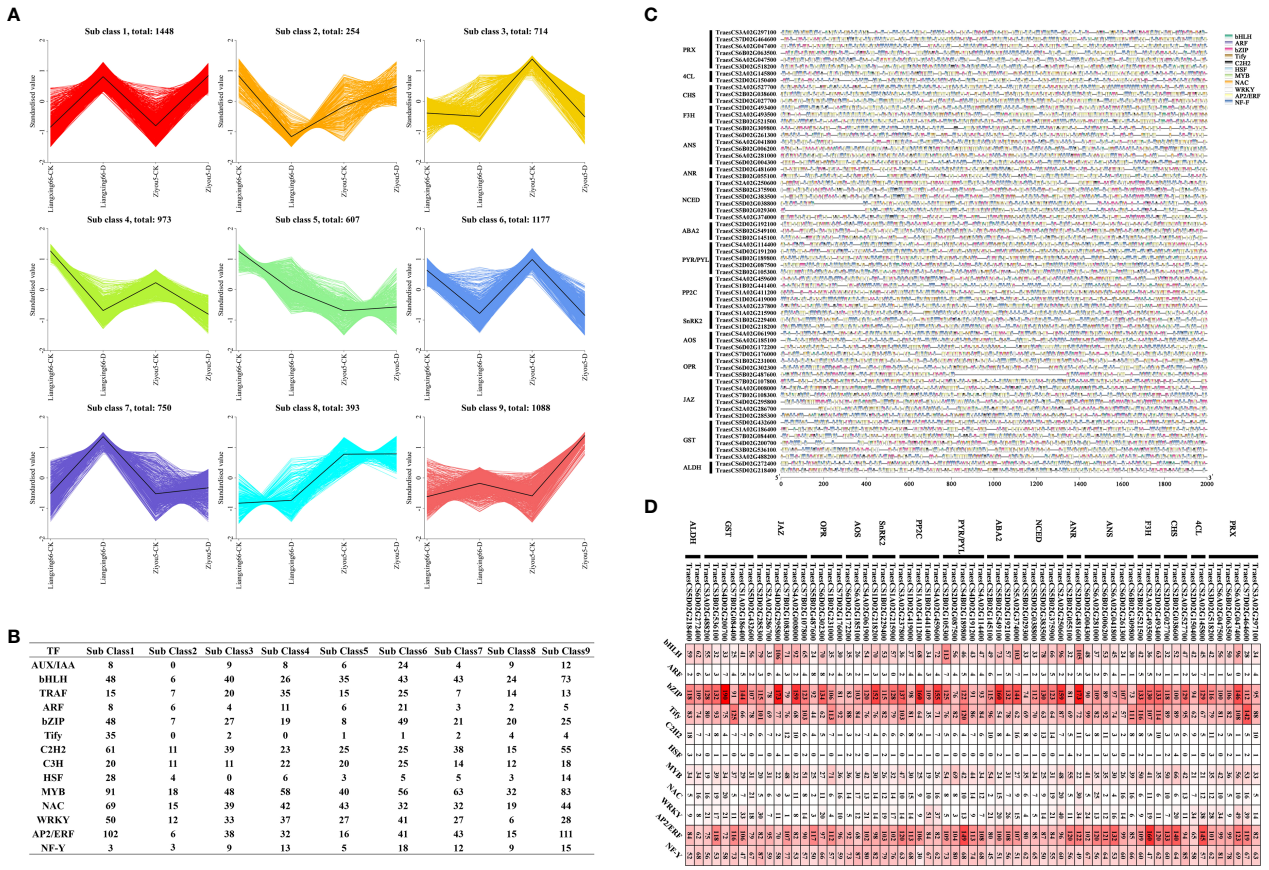
Coexpression analysis

To explore the regulatory mechanisms of genes involved in different metabolic pathways, we performed a coexpression cluster analysis of these genes involved in different metabolic pathways and all differentially expressed transcription factor (TF)-encoding genes. We found that these DEGs could be divided into 9 clusters: subclass 1-subclass 9 (Figure 5A). We performed an additional analysis to explore which types of TFs have regulatory functions with respect to these genes among various metabolic pathways and counted the number of TF-encoding genes in the 9 clusters. The results showed that bHLH, bZIP, NAC, C2H2, MYB and AP2/ERF TFs were the most abundant (Figure 5B). We analysed the TF-binding sites of these gene promoters in the 2000 bp upstream sequences, and the results showed that the binding sites of bHLH, bZIP, Tify, MYB, ERF, and NF-Y TFs throughout the promoter regions of these genes were the most abundant, including in the *ALDH*, *GST*, *JAZ*, *OPR*, *AOS*, *SnRK2*, *PP2C*, *PYL*, *ABA2*, *NCED*, *ANR*, *ANS*, *F3H*, *CHS*, *4CL* and *PRX* genes (Figures 5C, D). Taken together, these results suggested that the regulation of TFs and pathway genes affects the response to drought stress in wheat.

TaPRX-2A enhances the drought tolerance of transgenic wheat

PRXs have been shown to be involved in plant tolerance to abiotic stresses. Our RNA-seq data indicated that the expression levels of many PRXs changed after drought stress treatment. In our previous study, we confirmed that a PRX gene, *TaPRX-2A*, responded to various abiotic stresses (salt and drought), and *TaPRX-2A* overexpression was shown to enhance the salt tolerance of wheat significantly (Su et al., 2020). However, what's interesting is

10.3389/fpls.2023.1119162



TF	Sub Class1	Sub Class2	Sub Class3	Sub Class4	Sub Class5	Sub Class6	Sub Class7	Sub Class8	Sub Class9
AUX/IAA	8	0	9	8	6	24	4	9	12
bHLH	48	6	40	26	35	43	43	24	73
TRAF	15	7	20	35	15	25	7	14	13
ARF	8	6	4	11	6	21	3	2	5
bZIP	48	7	27	19	8	49	21	20	25
Tify	35	0	2	0	1	1	2	4	4
C2H2	61	11	39	23	25	25	38	15	55
C3H	20	11	11	22	20	25	14	12	18
HSF	28	4	0	6	3	5	5	3	14
MYB	91	18	48	58	40	56	63	32	83
NAC	69	15	39	42	43	32	32	19	44
WRKY	50	12	33	37	27	41	27	6	28
AP2/ERF	102	6	38	32	16	41	43	15	111
NF-Y	3	3	9	13	5	18	12	9	15

FIGURE 5
(A) Cluster analysis of co-expression patterns of genes associated with flavonoid, phytohormone, phenolamides and antioxidant metabolic pathways and all differentially expressed transcription factors. **(B)** Quantity statistics of the transcription factors in different sub clusters. **(C)** The promoter binding sites analysis of genes associated with different pathways. **(D)** The cis-elements distribution. We analyzed transcription factor binding site based on the 2000 bp DNA sequence upstream of the gene.

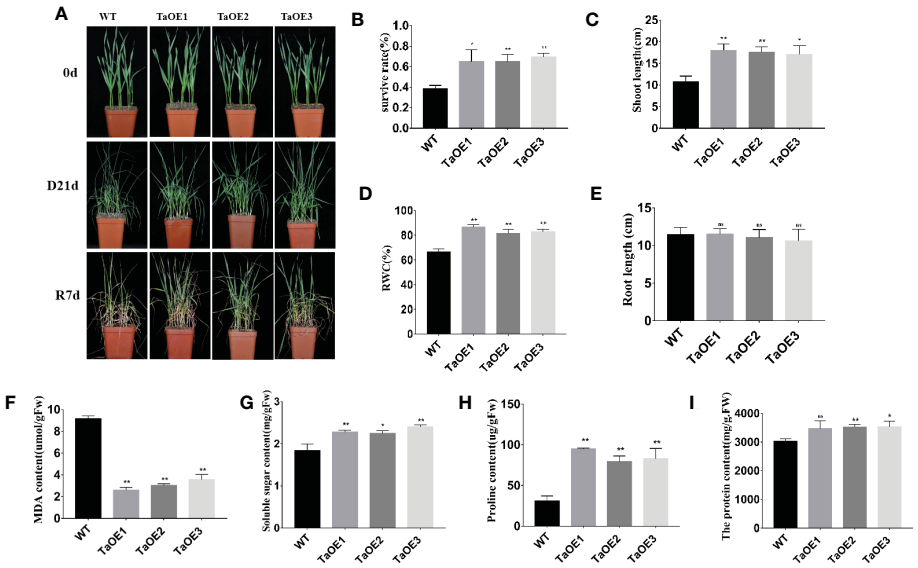


FIGURE 6
TaPRX-2A overexpression increased the drought tolerance. **(A)** Phenotype of *TaPRX-2A*-overexpressing transgenic and WT wheat (the cultivar "KN199") with drought treatment. **(B)** Survival rates of *TaPRX-2A*-overexpressing transgenic lines and WT wheat. **(C)** shoot length of *TaPRX-2A*-overexpressing transgenic lines and WT wheat. **(D)** Relative water content (RWC), and **(E)** root length. **(F)** MDA content of *TaPRX-2A*-overexpressing transgenic lines and WT wheat. **(G)** soluble sugar content of *TaPRX-2A*-overexpressing transgenic lines and WT wheat. **(H)** proline content, and **(I)** soluble protein content of *TaPRX-2A*-overexpressing and WT plants. All experiments included three replicates and the data present the mean ± SD. *P < 0.05 and **P < 0.01 indicate a significant difference compared with WT. The "ns" presents "no differences".

that this gene *TaPRX-2A* is not found in our transcriptome. To further explore the detailed temporal and spatial expression patterns of *TaPRX-2A* at different time after drought treatment, we measured the expression levels of *TaPRX-2A* in the wheat cultivars with varying degrees of drought tolerance at 24h and 48h after drought treatment. Compared with that of "Liangxing 66", the expression profile of *TaPRX-2A* was significantly different in several wheat cultivars with different drought tolerances, such as "Ziyou 5", "Xiaoyan 6", "Guomai 115", and "Baokemai 1330", at 24 h after treatment (Figure S9). Thus, we grew three independent *TaPRX-2A* overexpression transgenic lines (TaOE1, TaOE2, and TaOE3) and WT wheat plants under natural drought-stress conditions for 21 days, followed by rewatering for 7 days. Under nonstress conditions, we observed no significant differences in phenotypic characteristics between the *TaPRX-2A* transgenic lines and WT wheat plants. However, the *TaPRX-2A* transgenic lines grew more robustly than did the WT plants. The WT plants were more withered after drought stress treatment for 21 days. After being rewatered for 7 days, the *TaPRX-2A* transgenic lines presented higher survival percentages (65%, 65.2, 69.3%) than did the WT plants (38.7%) (Figures 6A, B). Then, the shoot length, RWC, and root length of the TaOE and WT plants were compared between the normal and drought-stress conditions. Compared with the WT plants, the TaOE plants had longer shoots and a higher RWC (Figures 6C, D). Interestingly, the lengths of the roots of the TaOE plants were not significantly different from those of the WT plants (Figure 6E). Taken together, these results indicated that *TaPRX-2A* overexpression drastically enhanced wheat drought tolerance.

TaPRX-2A overexpression influences physiological-biochemical indices related to osmotic and oxidative stress

We further measured physiological–biochemical indices, including MDA, soluble sugar, proline, and soluble protein contents, to explore the mechanism of *TaPRX-2A*-mediated drought resistance. The results showed that the MDA, soluble sugar, proline, and soluble protein contents in the WT were not significantly different from those of the TaOE lines under normal conditions. However, the MDA content in the WT was significantly higher than that in the TaOE lines under drought stress (Figure 6F). The soluble sugar, proline, and soluble protein contents in the WT were significantly lower than those in the TaOE lines (Figures 6G–I). These results demonstrated that *TaPRX-2A* overexpression improved transgenic plant tolerance to drought stress through changes to metabolite (MDA, soluble sugar, proline, and soluble protein) contents (Figure 6).

TaPRX-2A regulates ROS scavenging in transgenic wheat

PRXs can scavenge ROS to maintain steady-state levels of ROS when plants experience stress conditions. Therefore, the ROS levels of the TaOE and WT lines under drought stress were assessed. The levels of O_2^- and H_2O_2 were major indicators of the ROS level. Therefore, the accumulation of O_2^- and H_2O_2 was measured in both the TaOE and the WT lines. The accumulation of O_2^- and H_2O_2 was determined by NBT staining and DAB staining. The results showed that the levels of O_2^- (stained blue with NBT) and H_2O_2 (stained brown by DAB) were significantly higher in the WT plants than in the transgenic lines under drought stress (Figures 7A–D). In addition, we measured the activities of antioxidant enzymes (SOD, PRX, and CAT). The results showed that the SOD, CAT, and PRX activities in the transgenic plants were significantly higher than those in the WT plants (Figures 7E–G).

TaPRX-2A regulates the expression of stress-related genes

To determine whether *TaPRX-2A* affects the expression of stress-related genes that contribute to drought tolerance, the expression patterns of various stress-related genes were determined in the transgenic lines and WT plants (Figure S10). These stress-related genes were selected on the basis of their purported involvement in the response to various abiotic stresses. These genes include *TLP4*, which encodes a thaumatin-like protein; *DE6*, which encodes dehydrin 6; *RD22*, which encodes a dehydration-responsive protein; ABA-related genes including *CRTB*, *ZEP*, *PYR*, *PP2c*, and *SnRK2*; *ABAI*, which encodes an ABA-inducing protein; *GLP4*, which encodes a germin-like protein; *GST22*, which encodes glutathione S-transferase; and *FeSOD*, *CuSOD*, *APX*, and *CAT*, which encode ROS-scavenging enzymes. We found that several of these genes (*RD22*, *ABAI, CAT* and *APX*) were highly expressed in the transgenic lines and in the WT plants under both nonstress and drought-stress conditions. In addition, the expression of several stress-related genes (*TLP4*, *GLP4*, *GST22*, *FeSOD*, *CuSOD*) was higher in the transgenic lines than in the WT plants under drought stress. Nevertheless, the expression of the *DE6* gene was not significantly different between the transgenic lines and the WT plants (Figure S10A). In addition, we identified ABA-related genes, including *CRTB*, *ZEP*, *PYR*, *PP2c*, and *SnRK2*, in the transgenic lines and WT plants, and the results showed that the expression levels of these ABA-related genes were higher in the transgenic lines than in the WT plants under drought stress. Other genes (*ZEP*, *PYR*) were expressed as low levels in both the transgenic lines and in the WT plants under drought stress (Figure S10B). Taken together, these results suggested that the overexpression of *TaPRX-2A* improved drought tolerance by the control of stress-responsive and ABA-related gene expression.

Discussion

Drought stress is a widespread abiotic stress that causes major crop yield and economic losses (Mahajan and Tuteja, 2005; Zampieri et al., 2017). The molecular mechanisms through which plants respond to drought conditions have been extensively reported. Plants increase their tolerance to drought stress by activating signalling pathways that drive biochemical and physiological responses. Secondary metabolism, including the production of flavonoids, melatonin, secoisolariciresinol and plant hormones (ABA), is a major signalling event (Campo et al., 2014; Zhu, 2016;

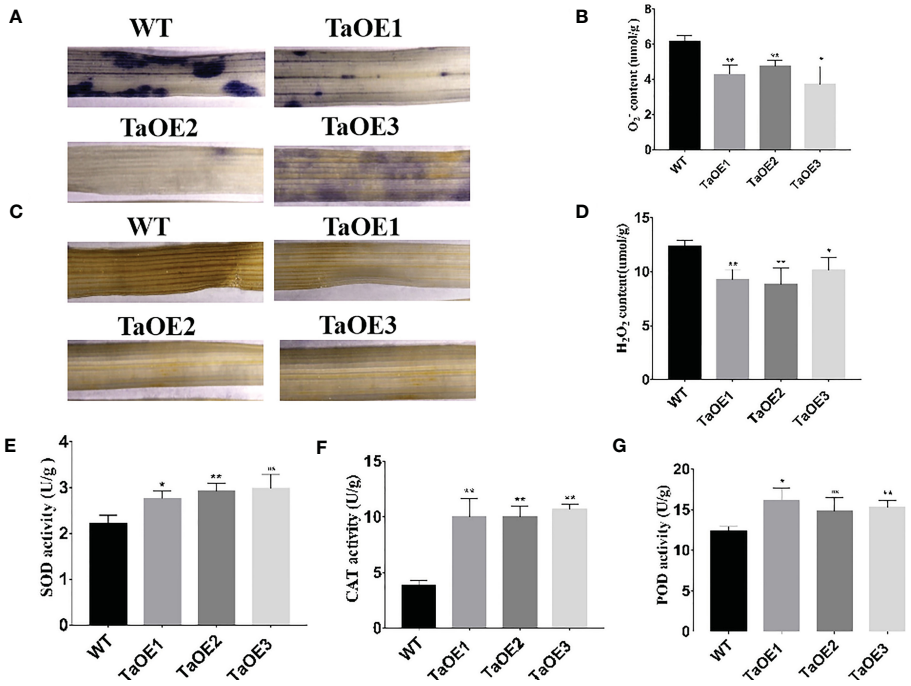


FIGURE 7
Analysis of ROS scavenging capacity andantioxidant enzymes activity in transgenic wheat lines. **(A)** Detection of O_2^- generation by NBT staining and O_2^- content **(B)**. **(C)** Detection of H_2O_2 accumulation by DAB staining and H_2O_2 content **(D)**. **(E)** Detection of SOD activity in *TaPRX-2A*-overexpressing transgenic lines and WT wheat. **(F)** Detection of CAT activity in *TaPRX-2A*-overexpressing transgenic lines and WT wheat. **(G)** Detection of POD activity in *TaPRX-2A*-overexpressing transgenic lines and WT wheat. All experiments included three replicates and the data present the mean ± SD. *P < 0.05 and **P < 0.01 indicate a significant difference compared with WT. The "ns" presents "no differences".

Meng et al., 2021; Feng et al., 2022; Song et al., 2022). Class III PRXs compose a large gene family with multiple genes in higher plants. It has been reported that class III PRXs respond to abiotic stresses. However, information regarding class III PRX resistance mechanisms used by wheat to combat drought stress is limited. Here, we revealed that, by scavenging ROS and enhancing stress-responsive gene expression, *TaPRX-2A* enhanced wheat tolerance to drought conditions.

Many studies have revealed that integrated analysis of transcriptomic data can yield functional insights into various biological processes (Hoefgen and Nikiforova, 2008). It is also known that flavonoid biosynthesis, plant hormonal signalling, and peroxidases play an important role in plant against abiotic stresses (Ma et al., 2014; Guo et al., 2020). Like these studies, our study revealed changes in flavonoids, plant hormones, phenolamides and activity of antioxidant signalling pathways, thereby expanding the scope of known drought tolerance-related DEGs. The previous study showed that PRXs enhanced wheat tolerance against salt stress through ABA signalling (Su et al., 2020). As components with antioxidant properties, the flavonoids and peroxidases has been widely reported to be involved in plant resistance to abiotic stress, respectively. But, little information has been showed about the regulatory relationship between flavonoid biosynthesis and peroxidases in plant resistance to abiotic stress. Therefore, the regulatory relationship in wheat against abiotic stresses between different metabolic pathways and peroxidases still needs further study in future.

When plants experience drought for an extended period, a large number of ROS are induced. ROS exist in many forms, such as O_2^-, H_2O_2, and OH^- in plants (McCord, 2000; Joshi et al., 2016). The class III PRXs catalyse H_2O_2 reduction in the peroxidative cycle through the transfer of electrons from different donors (Hiraga et al., 2001; Gill and Tuteja, 2010). Some studies have revealed that class III PRXs play an important role in enhancing tolerance to stresses through the regulation of ROS balance in plants. For example, the *Oryza sativa* class III PRX gene *OsPRX38* activates the antioxidant system and scavenges H_2O_2 to enhance arsenic (As) tolerance (Maria et al., 2019). Furthermore, plants have evolved a complex antioxidant system (involving SOD, CAT, and PRX) to protect cells from damage by maintaining the balance of ROS levels (Dat et al., 2000; Gill and Tuteja, 2010). Our results showed that *TaPRX-2A* enhanced transgenic plant tolerance to drought stress by increasing antioxidant enzyme activity, thereby reducing O_2^- and H_2O_2 levels. Moreover, *TaPRX-2A* also increased the expression of antioxidant-related genes, such as *CuSOD*, *FeSOD*, *CAT*, and *APX*. Therefore, these results showed that *TaPRX-2A* enhanced drought tolerance by regulating the expression of antioxidant genes that affect enzyme activity. In rice, the class III PRX gene *OsPrx30* mediates rice bacterial blight (*Xanthomonas oryzae* pv. *oryzae*)-induced ROS accumulation by the AT-hook protein *OsATH1* (Liu et al., 2021). Do wheat class III PRXs also respond to environmental stresses in this way? Future research will explore the mechanisms through which transcription factors regulate *TaPRX-2A* and regulate other antioxidant-encoding genes.

The signalling pathway of the plant hormone ABA is central to abiotic stress responses, and ABA is involved in a variety of cross-regulatory networks in response to stresses. For example, the transcription of the *Arabidopsis* dehydration-responsive gene *RD22* may be induced by ABA (Shinozaki et al., 2003). In addition, it was reported that ABA can induce the expression of dehydrin (DE)- and thaumatin-like protein (*TLP*)-encoding genes, which are essential for tolerance to abiotic stresses (Jung et al., 2005; Seo and Park, 2016). It has also been reported that ABA is involved in the PRX-mediated stress response. For example, the ABA signalling pathway controls the expression of class III PRX genes in *Tamarix hispida* (Gao et al., 2012). We previously identified that *TaPRX-2A* enhanced wheat tolerance to salt stress through activation of the ABA signalling pathway and expression of stress-related genes. Similar to the function of *TaPRX-2A* in response to salt stress, *TaPRX-2A* also improved transgenic wheat drought tolerance by altering the expression of genes involved in the ABA signalling pathway and stress-related genes, including *RD22*, *TLP4*, *GLP4*, and *GST22*, in our work. Further study is needed to explore the cross-talk regulatory mechanisms through which *TaPRX-2A* regulates the ABA signalling pathway and stress-related genes under various stresses.

Finally, we also preliminarily explore the SNP distributions of *TaPRX-2A* in different wheat cultivars and found 23 SNPs (16 in the promoter, 7 in the coding DNA sequence (CDS), and 3 in the 5'-untranslated region (UTR)) in the *TaPRX-2A* sequences. Among the 7 SNPs in the CDS, we diagrammed the four SNPs that cause changes in amino acids. The 16 SNPs in promoter influenced only a few *cis*-acting elements. Therefore, it will be interesting to explore the question about what kind of variations caused the different expression patterns of *TaPRX-2A* in different cultivars merits further consideration in subsequent investigations. In the future, *TaPRX-2A* can be used to develop SNP markers or GWAS for screening drought-resistant wheat varieties. This work will have strong application value for the cultivation of the drought-tolerant wheat varieties in the future, which is especially relevant given the anticipated hydrodynamics changes associated with ongoing climate change.

Conclusion

In this study, we evaluated drought tolerance of various wheat cultivars and identified a class III PRXs gene *TaPRX-2A* in response to drought stress by RNA-Seq analysis in wheat. The overexpression of *TaPRX-2A* enhanced transgenic wheat tolerance against drought stress through improving antioxidant enzymes activity, activating ABA signaling pathway, and regulating stress-related genes expression, resulting in lower ROS accumulation. This work and its findings have strong future application value in the cultivation of drought-tolerant wheat varieties, which is especially relevant given the anticipated crop losses associated with the future impacts of climate change.

Data availability statement

The datasets presented in this study can be found in online repositories. The names of the repository/repositories and accession number(s) can be found below: https://www.ncbi.nlm.nih.gov/search/all/?term=PRJNA914511. The accession number of the raw data is PRJNA914511.

Author contributions

PS and SG conceived and designed the experiments. PS performed most experiments. JY performed the bioinformatics analysis of *TaPRX-2A*, and revised the manuscript. CS,YN, SW, FS, and JL performed the transcriptome sequencing analysis, physiological-biochemical indices measures, and expression analysis. PS wrote and revised the manuscript. All authors contributed to the article and approved the submitted version.

Funding

This work was funded by Natural Science Foundation of Shandong Province (ZR2022QC129); Doctoral research start-up funds, Liaocheng University (318052018); State Key Laboratory of Crop Biology, Shandong Agricultural University (2021KF03); Industrial Promotion Project of Shandong Agricultural Science and Technology Park (2019YQ035), and Shandong Province Higher Educational Program for Introduction and Cultivation of Young Innovative Talents in 2021.

Conflict of interest

The authors declare that the research was conducted in the absence of any commercial or financial relationships that could be construed as a potential conflict of interest.

Publisher's note

All claims expressed in this article are solely those of the authors and do not necessarily represent those of their affiliated organizations, or those of the publisher, the editors and the reviewers. Any product that may be evaluated in this article, or claim that may be made by its manufacturer, is not guaranteed or endorsed by the publisher.

Supplementary material

The Supplementary Material for this article can be found online at: https://www.frontiersin.org/articles/10.3389/fpls.2023.1119162/full#supplementary-material

SUPPLEMENTARY FIGURE 1
The comparison of drought tolerance in 15 different wheat cultivars. **(A)** The phenotype of drought tolerance in different wheat cultivars was observed at 21 days after drought stress treatments. **(B)** The survive rate. Each treatment included at least 15 plants.

SUPPLEMENTARY FIGURE 2
Overview of transcriptome changes in wheat treated with drought stress. **(A)** Hierarchical clustering of DEGs in drought-treated and control wheat. FPKM expression values were used to create the heatmap. **(B)** Number of DEGs of Liangxing 66-CK vs Liangxing 66-D, Liangxing 66-CK vs Ziyou 5-CK, Ziyou 5-

CK vs Ziyou 5-D and Liangxing 66-D vs Ziyou 5-D between control and drought treatment, respectively. **(C)** Venn diagram among Liangxing 66-CK vs Liangxing 66-D, Liangxing 66-CK vs Ziyou 5-CK, Ziyou 5-CK vs Ziyou 5-D and Liangxing 66-D vs Ziyou 5-D. **(D)** Principal component analysis (PCA) of transcriptomedata obtained from drought-treated and control wheat. Each sample included three biological replicates.

SUPPLEMENTARY FIGURE 3

Transcriptomic analysis reveals the effect of drought stress in wheat. **(A)** GO classification diagram of DEGs of Liangxing 66-CK vs Liangxing 66-D in biological process (BP), cellular component (CC) and molecular function (MF). **(B)** GO classification diagram of DEGs of Ziyou 5-CK vs Ziyou 5-D in BP, CC and MF. **(C)** KEGG enrichment dotplot of DEGs of Liangxing 66-CK vs Liangxing 66-D. **(D)** KEGG enrichment dotplot of DEGs of Ziyou 5-CK vs Ziyou 5-D.

SUPPLEMENTARY FIGURE 4

The relative expression of flavonoid biosynthesis genes. *18SrRNA* was as an endogenous control. The gene relative expression was calculated by the cycle threshold (Ct) values using formula $2^{-\Delta\Delta CT}$. All experiments included three replicates and the data present the mean ± SD.

SUPPLEMENTARY FIGURE 5

Expression levels of ABA biosynthesis and signal genes. *18SrRNA* was as an endogenous control. The gene relative expression was calculated by the cycle threshold (Ct) values using formula $2^{-\Delta\Delta CT}$. All experiments included three replicates and the data present the mean ± SD.

SUPPLEMENTARY FIGURE 6

Effects of drought stress on SA, JA, and IAA biosynthesis and signal transduction in wheat. Overview of SA, JA, and IAA biosynthesis and signal transduction. The green and red represent doen-regulated and up-regulated gene expression under drought stress. *AROK*, shikimate kinase; *AROA*, 3-phosphoshikimate 1-carboxyvinyltransferase; *AROC*, chorismate synthase; *TPR3*, anthranilate synthase; *TRPA*, tryptophan synthase alpha chain; *TRPB*, tryptophan synthase beta chain; *DDC*, aromatic-L-amino-acid; *AAO*, indole-3-acetaldehyde oxidase; *YUCCA*, indole-3-pyruvate monooxygenase; *trpD*, anthranilate phosphoribosyltransferase; *TRP1*, anthranilate synthase; *DDC*, L-tryptophan decarboxylase; *TAA1*, L-tryptophan—pyruvate aminotransferase; *ISS1*, aromatic aminotransferase; *ALDH*, aldehyde dehydrogenase (NAD+); *AANAT*, arylalkylamine N-acetyltransferase; *ASMT*, acetylserotonin O-methyltransferase, *AMI*, amidase; *PLA2G16*, HRAS-like suppressor 3; *ISS1*, aromatic aminotransferase; *LOX*, lipoxygenase; *AOS*, hydroperoxide dehydratase; *AOC*, allene oxide cyclase; *OPR*, 12-oxophytodienoic acid reductase; *PLA2G*, secretory phospholipase A2; *HPL*, hydroperoxide lyase; *DOX*, fatty acid alpha-dioxygenase; *OPCL1*, OPC-8:0 CoA ligase 1; *ACOX*, acyl-CoA oxidaseL; *MFP2*, enoyl-CoA hydratase/3-hydroxyacyl-CoA dehydrogenase; *FAD*, acetyl-CoA acyltransferase; *JAM*, jasmonate O-methyltransferase; *JAZ*, jasmonate ZIM domain-containing protein; *aroC*, chorismate synthase; *aroA*, 3-phosphoshikimate 1-carboxyvinyltransferase; *AUX1*, auxin influx carrier; *TIR1*, transport inhibitor response 1; *AUX/IAA*, auxin-responsive protein; *ARF*, auxin response factor; *GH3*, auxin responsive GH3 gene family; *SAUR*, SAUR family protein; *PR1*, pathogenesis-related protein 1.

SUPPLEMENTARY FIGURE 7

The relative expression of genes involved in phytohormones (SA, IAA, and JA) pathways. *18SrRNA* was as an endogenous control. The gene relative expression was calculated by the cycle threshold (Ct) values using formula $2^{-\Delta\Delta CT}$. All experiments included three replicates and the data present the mean ± SD.

SUPPLEMENTARY FIGURE 8

The relative expression of genes involved in phenolamides and antioxidant pathway. *18SrRNA* was as an endogenous control. The gene relative expression was calculated by the cycle threshold (Ct) values using formula $2^{-\Delta\Delta CT}$. All experiments included three replicates and the data present the mean ± SD.

SUPPLEMENTARY FIGURE 9

The expression profile of *TaPRX-2A* among wheat cultivars with different levels of drought tolerance. *18SrRNA* was as an endogenous control. The gene relative expression was calculated by the cycle threshold (Ct) values using formula $2^{-\Delta\Delta CT}$. All experiments included three replicates and the data present the mean ± SD.

SUPPLEMENTARY FIGURE 10

The expression profile of stress-related genes in *TaPRX-2A*-overexpressing transgenic lines and WT plants under drought stress. (A) The expression levels of stress-related genes in transgenic lines and WT plants under drought stress. (B) The expression levels of ABA-related genes in transgenic lines and WT plants. *18SrRNA* was as an endogenous control. The gene relative expression was calculated by the cycle threshold (Ct) values using formula $2^{-\Delta\Delta CT}$. All experiments included three replicates and the data present the mean ± SD.

SUPPLEMENTARY TABLE 1

EXECL file with RNA-Seq data.

SUPPLEMENTARY TABLE 2

DEGs involved in flavonoid biosynthesis pathway, phytohormones, and phenolamides and antioxidant biosynthesis pathways.

SUPPLEMENTARY TABLE 3

Primers used for analysis.

References

Aebi, H. (1984). Catalase *in vitro*. *Methods Enzymol.* 105, 121–126. doi: 10.1016/S0076-6879(84)05016-3

Bates, L. S., Waldren, P. R., and Teare, I. D. (1973). Rapid determination of free proline for water-stress studies. *Plant Soil.* 39, 205–207. doi: 10.1007/BF00018060

Bhatt, I., and Tripathi, B. N. (2011). Plant peroxiredoxins: catalytic mechanisms, functional significance and future perspectives. *Biotechnol. Adv.* 29, 850–859. doi: 10.1016/j.biotechadv.2011.07.002

Campo, S., Baldrich, P., Messeguer, J., Lalanne, E., Coca, M., and San, S. B. (2014). Overexpression of a calcium-dependent protein kinase confers salt and drought tolerance in rice by preventing membrane lipid peroxidation. *Plant Physiol.* 165, 688–704. doi: 10.1104/pp.113.230268

Chance, B., and Maehly, A. (1955). Assay of catalases and peroxidases. *Methods Enzymol.* 2, 764–775. doi: 10.1016/S0076-6879(55)02300-8

Cosio, C., and Dunand, C. (2009). Specific functions of individual class III peroxidase genes. *J. Exp. Bot.* 60, 391–408. doi: 10.1093/jxb/ern318

Dat, J., Vandenabeele, S., Vranová, E., Van, M. M., Inzé, D., and Van, B. F. (2000). Dual action of the active oxygen species during plant stress responses. *Cell Mol. Life Sci.* 57, 779–795. doi: 10.1007/s000180050041

Daudi, A., Cheng, Z., O'Brien, J. A., Mammarella, N., Khan, S., Ausubel, F. M., et al. (2012). The apoplastic oxidative burst peroxidase in *Arabidopsis* is a major component of pattern-triggered immunity. *Plant Cell.* 24, 275–287. doi: 10.1105/tpc.111.093039

Dhindsa, R. A., Plumb-Dhindsa, P., and Thorpe, T. A. (1981). Leaf senescence: correlated with increased permeability and lipid peroxidation, and decreased levels of superoxide dismutase and catalase. *J. Exp. Bot.* 126, 93–101. doi: 10.1093/jxb/32.1.93

Fawal, N., Li, Q., Savelli, B., Brette, M., Passaia, G., Fabre, M., et al. (2013). PeroxiBase: a database for large-scale evolutionary analysis of peroxidases. *Nucleic Acids Res.* 41, D441–D444. doi: 10.1093/nar/gks1083

Feng, X., Peng, F., Yin, Z., Wang, J., Zhang, Y., Zhang, H., et al. (2022). Secondary metabolite pathway of SDG (secoisolariciresinol) was observed to trigger ROS scavenging system in response to Ca^{2+} stress in cotton. *Genomics* 114 (4), 110398. doi: 10.1016/j.ygeno.2022.110398

Gao, C., Zhang, K., Yang, G., and Wang, Y. (2012). Expression analysis of four peroxiredoxin genes from Tamarix hispida in response to different abiotic stresses and Exogenous Abscisic Acid (ABA). *Int J Mol Sci.* 13, 3751–3764. doi: 10.3390/ijms13033751.

Gay, C., Collins, J., and Gebicki, J. M. (1999). Hydroperoxide assay with the ferric-xylenol orange complex. *Anal. Biochem.* 273, 149–155. doi: 10.1006/abio.1999.4208

Gill, S. S., and Tuteja, N. (2010). Reactive oxygen species and antioxidant machinery in abiotic stress tolerance in crop plants. *Plant Physiol. Biochem.* 48, 909–930. doi: 10.1016/j.plaphy.2010.08.016

Guo, X., Xin, Z., Yang, T., Ma, X., Zhang, Y., Wang, Z., et al. (2020). Metabolomics response for drought stress tolerance in chinese wheat genotypes (*Triticum aestivum*). *Plants (Basel)* 9 (4), 520. doi: 10.3390/plants9040520

Heath, R., and Packer, L. (1968). Photoperoxidation in isolated chloroplasts: I. kinetics and stoichiometry of fatty acid peroxidation. *Arch. Biochem. Biophys.* 125, 189–198. doi: 10.1016/0003-9861(68)90654-1

Hiraga, S., Sasaki, K., Ito, H., Ohashi, Y., and Matsui, H. (2001). A large family of class III plant peroxidases. *Plant Cell Physiol.* 42, 462–468. doi: 10.1093/pcp/pce061

Hoefgen, R., and Nikiforova, V. J. (2008). Metabolomics integrated with transcriptomics:Assessing systems response to sulfur-deficiency stress. *Physiol. Plant* 132, 190–198. doi: 10.1111/j.1399-3054.2007.01012.x

Hu, Z., Li, J., Ding, S., Cheng, F., Li, X., Jiang, Y., et al. (2021). The protein kinase CPK28 phosphorylates ascorbate peroxidase and enhances thermotolerance in tomato. *Plant Physiol.* 186 (2), 1302–1317. doi: 10.1093/plphys/kiab120

Joshi, R., Wani, S. H., Singh, B., Bohra, A., Dar, Z. A., Lone, A. A., et al. (2016). Transcription factors and plants response to drought stress: Current understanding and future directions. *Front. Plant Sci.* 7 1029. doi: 10.3389/fpls.2016.01029

Jung, Y. C., Lee, H. J., Yum, S. S., Soh, W. Y., Cho, D. Y., Auh, C. K., et al. (2005). Drought-inducible-but ABA-independent-thaumatin-like protein from carrot (*Daucus carota* l.). *Plant Cell Rep.* 24, 366–373. doi: 10.1007/s00299-005-0944-x

Liu, H., Dong, S. Y., Li, M., Gu, F. W., Yang, G. L., Guo, T., et al. (2021). The class III peroxidase gene OsPrx30, transcriptionally modulated by the AT-hook protein OsATH1, mediates rice bacterial blight-induced ROS accumulation. *J. Integr. Plant Biol.* 63 (2), 393–408. doi: 10.1111/jipb.13040

Ma, D., Sun, D., Wang, C., Li, Y., and Guo, T. (2014). Expression of flavonoid biosynthesis genes and accumulation of flavonoid in wheat leaves in response to drought stress. *Plant Physiol. Biochem.* 80, 60–66. doi: 10.1016/j.plaphy.2014.03.024

Mahajan, S., and Tuteja, N. (2005). Cold, salinity and drought stresses: an overview. *Arch. Biochem. Biophys.* 444, 139–158. doi: 10.1016/j.abb.2005.10.018

Maria, K., Yogeshwar, V. D., Neelam, G., Madhu, T., Iffat, Z. A., Mehar, H. A., et al. (2019). *Oryza sativa* class III peroxidase (*Osprx38*) overexpression in *Arabidopsis thaliana* reduces arsenic accumulation due to apoplastic lignification. *J. Hazard Mater.* 362, 383–393. doi: 10.1016/j.jhazmat.2018.09.029

McCord, J. M. (2000). The evolution of free radicals and oxidative stress. *Am. J. Med.* 108, 652–659. doi: 10.1016/S0002-9343(00)00412-5

Meng, D., Dong, B., Niu, L., Song, Z., Wang, L., Amin, R., et al. (2021). The pigeon pea CcCIPK14-CcCBL1 pair positively modulates drought tolerance by enhancing flavonoid biosynthesis. *Plant J.* 106 (5), 1278–1297. doi: 10.1111/tpj.15234

Mittler, R. (2002). Oxidative stress, antioxidants and stress tolerance. *Trends Plant Sci.* 7, 405–410. doi: 10.1016/S1360-1385(02)02312-9

Mortazavi, A., Williams, B. A., McCue, K., Schaeffer, L., and Wold, B. (2008). Mappingand quantifying mammalian transcriptomes by RNA-seq. *NatMethods* 5, 621–628. doi: 10.1038/nmeth.1226

Ogino, R., Chinuki, Y., Yokooji, T., Takizawa, D., Matsuo, H., and Morita, E. (2021). Identification of peroxidase-1 and beta-glucosidase as cross-reactive wheat allergens in grass pollen-related wheat allergy. *Allergol. Int.* 70 (2), 215–222. doi: 10.1016/j.alit.2020.09.005

Pacheco, J. M., Ranocha, P., Kasulin, L., Fusari, C. M., Servi, L., Aptekmann, A. A., et al. (2022). Apoplastic class III peroxidases *PRX62* and *PRX69* promote *Arabidopsis* root hair growth at low temperature. *Nat. Commun.* 13 (1), 1310. doi: 10.1038/s41467-022-28833-4

Raggi, S., Ferrarini, A., Delledonne, M., Dunand, C., Ranocha, P., De Lorenzo, G., et al. (2015). The *Arabidopsis* class III peroxidase *AtPRX71* negatively regulates growth under physiological conditions and in response to cell wall damage. *Plant Physiol.* 169, 2513–2525. doi: 10.1104/pp.15.01464

Seo, P. J., and Park, C. M. (2016). MYB96-mediated abscisic acid signals induce pathogen resistance response by promoting salicylic acid biosynthesis in *Arabidopsis*. *New Phytol.* 186, 471–483. doi: 10.1111/j.1469-8137.2010.03183.x

Shinozaki, K., Yamaguchi-Shinozaki, K., and Seki, M. (2003). Regulatory network of gene expression in the drought and cold stress responses. *Curr. Opin. Plant Biol.* 6, 410–417. doi: 10.1016/S1369-5266(03)00092-X

Simonetti, E., Veronico, P., Melillo, M. T., Delibes, Á., Andrés, M. F., and López-Braña, I. (2009). Analysis of class III peroxidase genes expressed in roots of resistant and susceptible wheat lines infected by heterodera avenae. *Mol. Plant-Microbe Interact.* 22, 1081–1092. doi: 10.1094/MPMI-22-9-1081

Song, Z., Yang, Q., Dong, B., Li, N., Wang, M., and Du, T. (2022). Melatonin enhances plant stress tolerance by promoting flavonoid enrichment, focusing on luteolin for salt stress. *J. Exp. Bot.* 73, 5992–6008. doi: 10.1093/jxb/erac276

Spiro, R. G. (1966). Analysis of sugars found in glycoprotein. *Method enzymol.* 8, 3–26. doi: 10.1016/0076-6879(66)08005-4

Su, P. S., Yan, J., Li, W., Wang, L., Zhao, J. X., Ma, X., et al. (2020). A member of wheat class III peroxidase gene family, TaPRX-2A, enhanced the tolerance of salt stress. *BMC Plant Biol.* 20, 392. doi: 10.1186/s12870-020-02602-1

Taurog, A. (1999). Molecular evolution of thyroid peroxidase. *Biochimie* 81, 557–562. doi: 10.1016/S0300-9084(99)80110-2

Tian, F., Gong, J., Zhang, J., Zhang, M., Wang, G., Li, A., et al. (2013). Enhanced stability of thylakoid membrane proteins and antioxidant competence contribute to drought stress resistance in the *tasg1* wheat stay-green mutant. *J. Exp. Bot.* 64, 1509–1520. doi: 10.1093/jxb/ert004

Wang, Y., Wang, Q., Zhao, Y., Han, G., and Zhu, S. (2015). Systematic analysis of maize class III peroxidase gene family reveals a conserved subfamily involved in abiotic stress response. *Gene* 566, 95–108. doi: 10.1016/j.gene.2015.04.041

Welinder, K. G. (1992). Superfamily of plant, fungal and bacterial peroxidases. *Curr. Opin. Struct. Biol.* 2, 388–393. doi: 10.1016/0959-440X(92)90230-5

Wood, Z. A., Schröder, E., Robin Harris, J., and Poole, L. B. (2003). Structure, mechanism and regulation of peroxiredoxins. *Trends Biochem. Sci.* 28, 32–40. doi: 10.1016/S0968-0004(02)00003-8

Wu, Y., Yang, Z., How, J., Xu, H., Chen, L., and Li, K. (2017). Overexpression ofa peroxidase gene (*AtPrx64*) of arabidopsis thaliana in tobaccoimproves plant's tolerance to aluminum stress. *Plant Molec. Biol.* 95, 157–168. doi: 10.1007/s11103-017-0644-2

Yan, J., Su, P. S., Li, W., Xiao, G. L., Zhao, Y., Ma, X., et al. (2019). Genome-wide and evolutionary analysis of the class III peroxidase gene family in wheat and aegilops tauschii reveals that some members are involved in stress responses. *BMC Genomics* 20, 666. doi: 10.1186/s12864-019-6006-5

Yao, Q., Cong, L., Chang, J. L., Li, K. X., Yang, G. X., and He, G. Y. (2006). Low copy number gene transfer and stable expression in a commercial wheat cultivar *via* particle bombardment. *J. Exp. Bot.* 57, 3737–3746. doi: 10.1093/jxb/erl145

Zampieri, M., Ceglar, A., Dentener, F., and Toreti, A. (2017). Wheat yield loss attributable to heat waves, drought and water excess at the global, national and subnational scales. *Environ. Res. Lett.* 12, 064008. doi: 10.1088/1748-9326/aa723b

Zhai, C. Z., Zhao, L., Yin, L. J., Chen, M., Wang, Q. Y., Li, L. C., et al. (2013). Two wheat glutathione peroxidase genes whose products are located in chloroplasts improve salt and H_2O_2tolerances in *Arabidopsis*. *PloS One* 8, e73989. doi: 10.1371/journal.pone.0073989

Zhang, H., Wang, Z., Li, X., Gao, X., Dai, Z., Cui, Y., et al. (2022). The IbBBX24-IbTOE3-IbPRX17 module enhances abiotic stress tolerance by scavenging reactive oxygen species in sweet potato. *New Phytol.* 233 (3), 1133–1152. doi: 10.1111/nph.17860

Zhou, S. M., Sun, X. D., Yin, S. H., Kong, X. Z., Zhou, S., Xu, Y., et al. (2014). The role of the f-box gene TaFBA1 from wheat (*Triticum aestivum* l.) in drought tolerance. *Plant Physiol. Biochem.* 84, 213–223. doi: 10.1016/j.plaphy.2014.09.017

Zhu, J. K. (2016). Abiotic stress signaling and responses in plants. *Cell* 167 (2), 313–324. doi: 10.1016/j.cell.2016.08.029

frontiers | Frontiers in Plant Science

TYPE Original Research
PUBLISHED 17 February 2023
DOI 10.3389/fpls.2022.1128007

Check for updates

OPEN ACCESS

EDITED BY
Meng Jiang,
Zhejiang University, China

REVIEWED BY
Chong Yang,
Guangdong Academy of Science (CAS), China
Ling Xu,
Zhejiang Sci-Tech University, China
Muhammad Awais Ghani,
University of Agriculture, Faisalabad, Pakistan

*CORRESPONDENCE
Xiaohua Wu
wuxiaohua2001@126.com

SPECIALTY SECTION
This article was submitted to Plant Abiotic Stress, a section of the journal Frontiers in Plant Science

RECEIVED 20 December 2022
ACCEPTED 30 December 2022
PUBLISHED 17 February 2023

CITATION
Wang J, Wang Y, Wu X, Wang B, Lu Z, Zhong L, Li G, and Wu X (2023) Insight into the bZIP gene family in *Lagenaria siceraria*: Genome and transcriptome analysis to understand gene diversification in Cucurbitaceae and the roles of *LsbZIP* gene expression and function under cold stress.
Front. Plant Sci. 13:1128007.
doi: 10.3389/fpls.2022.1128007

COPYRIGHT
© 2023 Wang, Wang, Wu, Wang, Lu, Zhong, Li and Wu. This is an open-access article distributed under the terms of the Creative Commons Attribution License (CC BY). The use, distribution or reproduction in other forums is permitted, provided the original author(s) and the copyright owner(s) are credited and that the original publication in this journal is cited, in accordance with accepted academic practice. No use, distribution or reproduction is permitted which does not comply with these terms.

Insight into the bZIP gene family in *Lagenaria siceraria*: Genome and transcriptome analysis to understand gene diversification in Cucurbitaceae and the roles of *LsbZIP* gene expression and function under cold stress

Jian Wang[1], Ying Wang[1], Xinyi Wu[1], Baogen Wang[1], Zhongfu Lu[1], Liping Zhong[2], Guojing Li[1,3] and Xiaohua Wu[1]*

[1]Institute of Vegetables, Zhejiang Academy of Agricultural Sciences, Hangzhou, China, [2]College of Horticulture Science, Zhejiang Agriculture and Forestry (A&F) University, Hangzhou, China, [3]State Key Laboratory for Managing Biotic and Chemical Threats to the Quality and Safety of Agro-Products, Zhejiang Academy of Agricultural Sciences, Hangzhou, China

The basic leucine zipper (bZIP) as a well-known transcription factor family, figures prominently in diverse biological and developmental processes and response to abiotic/biotic stresses. However, no knowledge of the bZIP family is available for the important edible Cucurbitaceae crop bottle gourd. Herein, we identified 65 putative *LsbZIP* genes and characterized their gene structure, phylogenetic and orthologous relationships, gene expression profiles in different tissues and cultivars, and responsive genes under cold stress. The phylogenetic tree of 16 released Cucurbitaceae plant genomes revealed the evolutionary convergence and divergence of bZIP family. Based on the specific domains, *LsbZIP* family were classified into 12 clades (A–K, S) with similar motifs and exon-intron distribution. 65 *LsbZIP* genes have undergone 19 segmental and two tandem duplication events with purifying selection. The expression profiling of *LsbZIP* genes showed tissue-specific but no cultivar-specific pattern. The cold stress-responsive candidate *LsbZIP* genes were analyzed and validated by RNA-Seq and RT-PCR, providing new insights of transcriptional regulation of bZIP family genes in bottle gourd and their potential functions in cold-tolerant variety breeding.

KEYWORDS

***Lagenaria siceraria*, bZIP transcription factor, Cucurbitaceae evolution, expression pattern, cold stress**

Introduction

Plants are subjected to various abiotic stresses such as drought, chilling, salinity and high temperature with the increasing environmental degradation and changing weather, which extremely limits the growth and production of crops. Therefore, plants have evolved complicated stress-responsive defense tactics involving in a number of proteins, containing phosphatase, protein kinase and transcription factors (TFs), to adapt, survive and reproduce in harsh environment (Sornaraj et al., 2016). TFs, as the primary modulators in stress response, bind specific promoter regions of downstream target genes to alter transcription activity and stimulate or suppress gene expressions (Kong et al., 2015). Among more than 80 TF families, the basic leucine zipper (bZIP) family is one of the largest and diverse groups (Llorca et al., 2014; Yin et al., 2017). The bZIP domain is consist of two functional regions, the basic area for DNA binding and the leucine zipper for protein dimerization (Li et al., 2019). The basic region is highly conserved with 16 amino acid residues, including a specific motif of N-X7-R/K for nuclear localization signal and sequence-specific binding, while the leucine zipper motif is predisposed to form an alpha helical loop with dimerization specificity (Wang et al., 2011).

The bZIP TFs with plenty of diverse members have been found to be involved in the regulation of multiple biological processes, namely flower and seed development (Zhang et al., 2016; Jain et al., 2017), hormone signal transduction (Sirichandra et al., 2010), energy metabolism (Weiste et al., 2017), embryogenesis (Huang et al., 2012), photomorphogenesis (Lindemose et al., 2013), lateral root development and leaf senescence (Dankov et al., 2009). Additionally, bZIP TFs play vital roles in response to abiotic/biotic stresses including extreme temperatures, water shortage, high salinity and hormone-induced defense from pathogens (Zander et al., 2010; Lindemose et al., 2013; Sornaraj et al., 2016; Wang et al., 2020). The regulatory network of downstream genes can be controlled by the combination of bZIPs and corresponding cis-elements such as A-box (TACGTA), C-box (GACGTC), G-box (CACGTG) and abscisic acid (ABA)-responsive elements (ABRE) (CCACGTGG) (Foster et al., 1994; Zhang et al., 2008; Tang et al., 2015). In *Arabidopsis*, four bZIP factors *ABF1* (*AtbZIP35*), *ABF2* (*AtbZIP36*), *ABF3* (*AtbZIP37*) and *ABF4* (*AtbZIP38*) are predominant in regulating downstream gene expression of ABA signaling in response to osmotic stresses like drought and salt (Jakoby et al., 2002; Yoshida et al., 2015). And *TGA2* (*AtbZIP20*), *TGA5* (*AtbZIP26*) and *TGA6* (*AtbZIP45*) mediate salicylic acid (SA)-dependent pathway and meanwhile trigger ethylene and jasmonic acid (JA) pathways under abiotic stress (Zander et al., 2010). *OsbZIP1* increases pathogen resistance to *Magnaporthe grisea* in rice through SA, JA and ABA signal transduction pathway (Meng et al., 2005). *ZmbZIP17* is capable of binding ABREs and transduces stress signals through ABA pathway during germination and post-germination seedling establishment (Yang et al., 2013). Likewise, *LIP19* acts as a molecular switch for low-temperature signal transduction in rice (Shimizu et al., 2005), while *OsBZ8* positively regulates salt tolerance with ABA pathway (Mukherjee et al., 2006). With respect to number of bZIPs, 78 bZIP genes have been identified in *Arabidopsis* and classified into 13 groups (Jakoby et al., 2002; Dröge-Laser et al., 2018). So far, the genome-wide characterization of bZIP genes from many plant species have been reported, including 89 in rice (Nijhawan et al., 2008), 125 in maize (Wei et al., 2012), 247 in rapeseed (Zhou et al., 2017), 89 in barely (Pourabed et al., 2015), 92 in sorghum (Wang et al., 2011), 131 in soybean (Liao et al., 2008), 99 in poplar (Zhao et al., 2021), 56 in potato (Mirzaei et al., 2020) and 227 in wheat (Liang et al., 2022). The diversity and expansion of bZIP gene members is attributed to the whole genome, tandem and segmental duplication events (Panchy et al., 2016; Qiao et al., 2019). It's one of the evolutionary strategies to adapt various stresses by expanding TFs family members like bZIP to achieve targeted regulation and control of complex gene expression.

Cucurbitaceae is one of the most important edible plant family in the world and encompasses nearly 1000 species from 115 genera (Schaefer et al., 2009). Bottle gourd [*Lagenaria siceraria* (Molina) Standl.], known as calabash or white-flowered gourd, is an annual Cucurbitaceae plant grown for its fruit. It is one of the world's first cultivated plants not primarily for food, but also for use as containers, decorations, musical instruments and so on (Schlumbaum and Vandorpe, 2012). Bottle gourd is planted all over China and widely cultivated in tropical to temperate regions of the world. It is suitable to grow in conditions with moderate temperature and sufficient sunlight. However, cold stress owing to early-spring low temperature is a major abiotic stress and limiting factor for its industry (Chimonyo and Modi, 2013). Low temperature can influence many physiological and biochemical metabolisms like photosynthesis, osmotic regulation, the activity of antioxidants and so on. Breeding new bottle gourd varieties with low temperature resistance is necessary to elevate its production and quality. To accelerate the breeding process, the landscape of gene families which influence growth, development and stress response should also be comprehensively studied. As the release of our recently assembly high quality genome of bottle gourd variety "HZCG" (Xu et al., 2021), it allows us to carry out a genome-wide identification and analysis of *LsbZIP* gene family and its expression pattern under cold stress. The comparison of all bZIPs from present available Cucurbitaceae genomes in this research aims to reveal the evolution and selection in Cucurbitaceae species differentiation. This study provides the full-scale description of *LsbZIP* genes involved in response to cold stress, and lays a foundation for further molecular breeding in bottle gourd.

Materials and methods

Sequence retrieval and domain identification

The reference genome of bottle gourd (genome assembly ZAAS_Lsic_2.0) was obtained from our previous study (Xu et al., 2021), the query sequences 78 *AtbZIPs* (genome assembly TAIR10) from the *Arabidopsis* information resource (TAIR) (https://www.arabidopsis.org/index.jsp) were retrieved (Jakoby et al., 2002; Dröge-Laser et al., 2018), and the other genomes of selected 15 Cucurbitaceae species were downloaded from Cucurbit Genomics Database (CuGenDBv2, http://cucurbitgenomics.org/v2/) (Wang et al., 2020). A local protein database was created by TBtools v1.098769 to blast the underlying Cucurbitaceae bZIP sequences using an e value cut-off of $1e^{-5}$ (Chen et al., 2020). To avoid missing potential bZIPs, a hidden Markov model (HMM) file of the bZIP domain (PF00170 and PF07716) was downloaded (https://pfam.

xfam.org/) and used as the template to identify bZIP sequences in the respective genome. The primary candidate sequences were further submitted in the Plant Transcription Factor Database (http://planttfdb.gao-lab.org/), SMART database (http://smart.embl.de/), NCBI CDD (https://www.ncbi.nlm.nih.gov/cdd/) for confirmation. The physicochemical properties were calculated based on the high confidence bZIPs by ProtParam (https://web.expasy.org/protparam/) (Gasteiger et al., 2003).

Multiple alignments and phylogenetic tree construction

All *bZIP* sequences from *Arabidopsis* and 15 Cucurbitaceae were screened and aligned by Muscle algorithm (Edgar, 2004). TrimAl v1.2 was invoked to remove the unambiguous aligments using gappyout trimming mode (Capella-Gutiérrez et al., 2009). The construction of phylogenetic trees was executed with IQ-tree software, using a maximal likelihood (ML) method with 1,000 bootstrap replications (Nguyen et al., 2015). Amino acid sequences from bottle gourd, as well as 78 *AtbZIPs* were completely aligned by Clustal X2.1 and converted ALN file into MEGA 7.0.14 to build a neighbor-joining (NJ) phylogenetic tree with following parameters: poission model, and pairwise deletion for the reliability of interior branches.

Gene distribution and duplication visualization

The chromosomal locations of *LsbZIP* genes and their tandem duplications were represented according to previous studies (Wang et al., 2022). Gene duplication events were predicted by multiple collinearity scan toolkit (MCScanX) (Wang et al., 2012). The Ka and Ks were calculated using MCScanX package to assess the selection history and divergence time of *LsbZIP* gene families. The distribution and collinearity relationships were displayed with Advanced Circos function in Tbtools.

Prediction of conserved motifs and exon/intron structure

To better decipher the structure diversity of *LsbZIP* genes, motifs were detected using the Multiple Expectation Maximization for Motif Elicitation (MEME)/Motif Alignment and Search Tool (MAST) system (http://meme-suite.org/) with default set (Bailey et al., 2009). The exon-intron structure and the intron phases of *bZIP* gene family were visualized by the online program Gene Structure Display Server 2.0(GSDS, http://gsds.gao-lab.org/) (Hu et al., 2015).

Orthologous gene clusters analysis of eight selected species

Eight common and important species genomes namely *Arabidopsis thaliana*, *Brassica napus*, *Cucumis sativus*, *Glycine max*, *Oryza sativa*, *Solanum lycopersicum*, *Vitis vinifera* and *Lagenaria siceraria* were blasted through Ortho Venn 2.0 web server (https://orthovenn2.bioinfotoolkits.net/home). 65 *LsbZIP* protein sequences were uploaded and analyzed with e-value 1e-5 and inflation value of 1.5 (Wang et al., 2022).

Ab initio prediction of the core promoter in *LsbZIPs*

The putative promoter sequences were extracted from 2000 base pair (bp) upstream of the transcriptional starting site (ATG) of genomic DNA sequences. The cis-regulatory elements (CREs) were obtained by introducing promoter sequences into the PlantCARE database (http://bioinformatics.psb.ugent.be/webtools/plantcare/html/).

The expression patterns analysis of *LsbZIP* genes in different tissues and varieties

To determine the gene expression profiles of bZIP family, RNA-Seq data of various tissues including leaf, root, stem, flower and fruit were downloaded from NCBI sequence read archive (SRA) with accession SRP107894 (Wu et al., 2017). A collection of re-sequencing data of 5 bottle gourd accessions were also downloaded from SRP095913 (Xu et al., 2021). The expression of each *LsbZIP* gene was quantified with transcripts per million (TPM). The transcript abundances were output by kallisto in TPM units. Normalization (log_2) and heat-maps were generated using Tbtools software.

Plant materials and treatments

'YZ', a bottle gourd variety of rootstock type tolerance to low temperature, was used in this experiment. Healthy and sterilized seeds were germinated and sown in plastic pots. The seedings were placed in growth chamber at 28°C/22°C (16 h/8 h) day/night temperatures with a relative humidity of 75%. At 2~3 leaf stage, uniform seedlings were divided into two groups for room temperature (24°C) or cold treatment (4°C). The leaf samples were harvested for gene expression validation at 0, 1, 6, 12, 24 h after cold treatment. And three biological replications were used in this study.

Transcriptome and qRT-PCR analysis

The transcriptional profile of bZIP genes of bottle gourd under cold stress were downloaded under accession PRJNA553072 from our previous study (Wang et al., 2020). The differentially expressed genes (DEGs) of *LsbZIPs* were quantified with fragments per kilobase of transcript per million mapped fragments (FPKM) method between control and cold treatment. DEGs were screened according the criteria (false discovery rate <0.5 and absolute fold change ≥2). For cold-induced *LsbZIPs* expression, total RNA was extracted from RNAprep Pure Plant Kit (Tiangen, China). *TuB-α* gene (BG_GLEAN_10019523) was used as the internal control gene in bottle gourd (Li et al., 2021). qRT-PCR was performed on a Bio-Rad

CFX96 (BIO RAD, USA) with SuperReal PreMix Plus/SYBR Green (Tiangen, China). Triplicate replications were performed for analysis. The gene relative expression level was calculated by the $2^{-\Delta\Delta Ct}$ method. All primers used for qRT-PCR are listed in Supplementary Table S1.

Results and discussions

Systematic identification and classification of *bZIPs*

So far two genomes of bottle gourd inbred lines, HZCG (food-type, China) assembled with Illumina paired-end and USVL1VR-Ls (rootstock-type, India) assembled with PacBio and BioNano, have been released (Wu et al., 2017; Xu et al., 2021). Based on the specificity of bZIP family domain, 65 and 60 bZIP genes were identified in HZCG and USVL1VR-Ls, respectively (Table S2, Figure S1). The comparison of bZIP genes in two bottle gourd reference genomes showed that each bZIP in USVL1VR-Ls was able to find its homolog in HZCG (Supplementary Figure S1). Thus, we selected 65 bZIPs in HZCG genome for our subsequent analysis and named them as *LsbZIP1~LsbZIP65* according to their location (Table S2). Generally, 65 *LsbZIPs* were roughly spread equally across 11 all chromosomes (Chr) while only Chr 6 contained one bZIP gene and Chr 10 contained two bZIP genes (Figure 1). The physicochemical parameters showed that the length of amino acid (AA) residues ranged from 129 AA (*LsbZIP36*) to 1225 AA (*LsbZIP8*), with isoelectric point (pI) ranging from 4.55 (*LsbZIP6*) to 9.89 (*LsbZIP33*) (Supplementary Table S2). The molecular weight (MW) ranged from 15.14 kDa (*LsbZIP36*) to 135.15 kDa (*LsbZIP8*) with average 39.74 kDa. In addition, the prediction of subcellular localization of all *LsbZIP* proteins were distributed in nucleus except *LsbZIP8* locating on plasma membrane and *LsbZIP34* locating in cytoplasmic zone.

For the gene duplication events, 19 gene pairs were segmentally duplicated on all chromosomes except Chr 10 (Figure 2; Table 1). There were only two tandem duplication events with gene pairs (*LsbZIP40*/*LsbZIP41*, *HG_GLEAN_10002003*/*LsbZIP62*) in bottle gourd. To estimate the selective pattern, Ka/Ks is calculated to uncover the diversity of duplicated gene pairs in the evolution. In this study, all duplicated gene pairs were subjected to strong purifying selection for the purpose of eliminating detrimental mutations as Ka/Ks<1 while 8 duplicated gene pairs showed NaN caused by high sequence divergence value (Table 1).

Phylogenetic analysis of Cucurbitaceae species

Based on the specific domains bZIP_1 (PF00170) and bZIP_2 (PF07716), we finally identified and confirmed 1510 sequences from 17 Cucurbitaceae species including two different bottle gourd genomes (Tables 2, S3, S4; Figure 3). Apart from the splicing variants found in *Sechium edule* and *Trichosanthes anguina*, only 1235 unique *bZIP* sequences were retrieved and grouped into 13 subfamilies in Cucurbit genomes. Generally, clade A, D, E, I and S occupied the numerous bZIP members exceeding 100 while other clades B, J, K contained limited numbers of bZIP homologs less than 20 (Table 2). 11 of 13 clades were existed in all selected cucurbit crops except clades B, K and M. Clade B and K usually owned 1~3 and only one bZIP gene in 15 species (not found in cushaw pumpkin and ridge gourd) respectively, and clade M was consist of 1~ 3 bZIP members in 12 species (not identified in wax, cucumber, bottle gourd and bitter gourd). The number showed diverse distribution not only in different clades, but also in different species. The total number of bZIPs in 16 species could be divided into two categories. One type mostly belonged to Cucurbita genera including *C. argyosperma*, *C. maxima*, *C. moschata* and *C. pepo* besides *S. edule*. The gene family number in this class was approximately two-fold than it in another class reaching the amount of average 65 members (Table 2). The majority of all clades were quite distinct from each other, but clade F was sandwiched between two separated clades S.

Gene structure and motif analysis

According to the classification criterion of *AtbZIPs* by Dröge-Laser et al. (2018), 65 *LsbZIPs* were divided into 12 clades (LsbZIP-A, LsbZIP-B, LsbZIP-C, LsbZIP-D, LsbZIP-E, LsbZIP-F, LsbZIP-G, LsbZIP-H, LsbZIP-I, LsbZIP-J, LsbZIP-K and LsbZIP-S) based on their characterized domains (Figure 4). To recapitulate briefly, different clades had diverse phylogenetic clustering. For the relatively small clade like clade J, H and K, bZIPs from two species

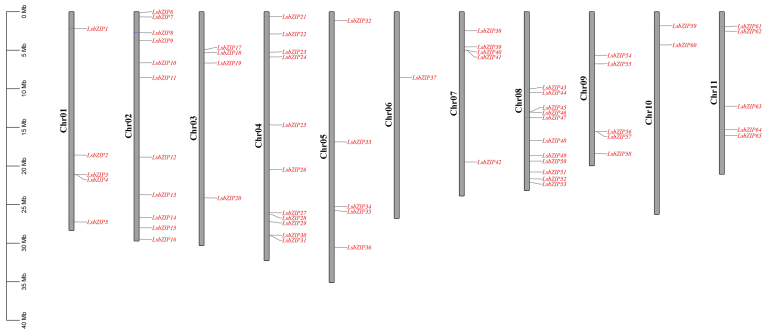


FIGURE 1
The distribution of bZIP genes on the bottle gourd chromosomes.

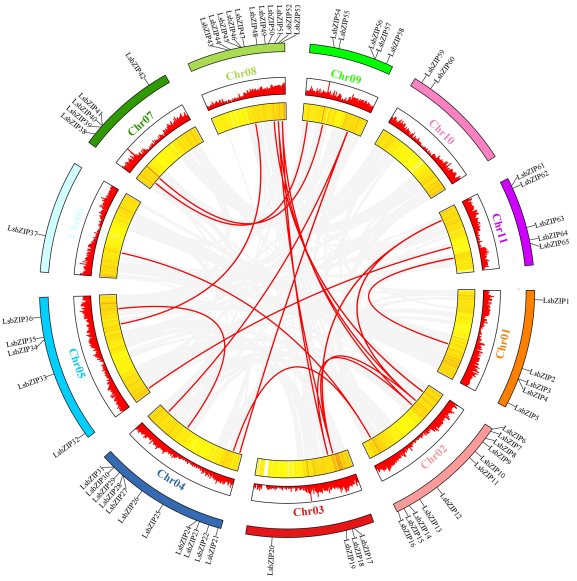


FIGURE 2
Interchromosomal synteny of linked *LsbZIP* genes. The red bars and yellow color strips indicated the gene density in the chromosomes.

showed highly homologous with nearly 100 bootstrap value. In some clades like clade B, I and S, the whole clade can be further separated into two or three subfamilies because of the dissimilar divergences. On the other hand, *LsbZIPs* didn't present one to one mapping relationship with *AtbZIPs*, indicating the selective evolution from gene duplication.

To better depict the specific domain, the phylogeny, exon/intron structure and conserved motifs distribution were integrated in Figure 5. The phylogenetic classification was consistent with previous results. According to MEME analysis, 10 highly conserved motifs were identified in *LsbZIPs*. And all 65 *bZIPs* roughly split into 7 types in consideration of the number and order of motifs. Four clades (B, J, H and K) shared the same distribution pattern with motif 1 and motif 3. *LsbZIPs* containing motif 9 at the C-terminal end were found in type C, S, F while clade A had motif 10 at the N-terminal end. Motifs 5 and 8 can be detected only in clade I, and then 4 motifs (7, 2, 6, 4) can be identified only in clade D. In addition, Clade G owned a replication with motif 3. The results indicated that members classified into the same clade mostly shared the same or similar conserved motifs (Figure 5 and Table S5). The distributed positions of exons/introns on *LsbZIP* genes were investigated by GSDS, to gain further insight into the structure diversity in bottle gourd. The number of

TABLE 1 Ka/Ks calculation for the duplication of bZIP gene pairs in bottle gourd.

Duplicated gene 1	Duplicated gene 2	Ka	Ks	Ka/Ks	Duplication type
LsbZIP40	*LsbZIP41*	0.095567774	0.46292708	0.206442393	Tandem
HG_GLEAN_10002003	*LsbZIP62*	0.20465024	0.746788399	0.274040465	Tandem
LsbZIP2	*LsbZIP65*	0.173528729	1.118537237	0.155138983	Segmental
LsbZIP8	*LsbZIP50*	0.205161542	3.729959631	0.05500369	Segmental
LsbZIP10	*LsbZIP17*	0.398267583	NaN	NaN	Segmental
LsbZIP10	*LsbZIP51*	0.309843954	NaN	NaN	Segmental
LsbZIP10	*LsbZIP62*	0.384704842	2.136583395	0.180056085	Segmental
LsbZIP11	*LsbZIP19*	0.669456185	NaN	NaN	Segmental
LsbZIP11	*LsbZIP53*	0.457676449	2.188328049	0.209144351	Segmental
LsbZIP14	*LsbZIP22*	0.342001797	NaN	NaN	Segmental
LsbZIP14	*LsbZIP37*	0.304349709	1.27762649	0.238214933	Segmental
LsbZIP17	*LsbZIP51*	0.412887924	1.819003474	0.226985781	Segmental
LsbZIP17	*LsbZIP62*	0.37037958	1.513609512	0.244699559	Segmental
LsbZIP19	*LsbZIP53*	0.664505207	NaN	NaN	Segmental
LsbZIP21	*LsbZIP57*	0.290708373	1.870059385	0.155454086	Segmental
LsbZIP26	*LsbZIP36*	0.264737608	NaN	NaN	Segmental
LsbZIP30	*LsbZIP56*	0.547629151	NaN	NaN	Segmental
LsbZIP32	*LsbZIP63*	0.696047991	NaN	NaN	Segmental
LsbZIP34	*LsbZIP46*	0.307254005	1.778039766	0.172804912	Segmental
LsbZIP38	*HG_GLEAN_10000143*	0.423630263	3.164151086	0.133884335	Segmental
LsbZIP39	*LsbZIP55*	0.135245327	1.184936605	0.114137184	Segmental

NaN means high sequence divergence value (pS ≥ 0.75).

10.3389/fpls.2022.1128007

TABLE 2 bZIP family members of 16 Cucurbitaceae plant species and their phylogenetic classifications.

Plant species	Common name	Number of *bZIP* genes	Group classfication													Reference
			A	B	C	D	E	F	G	H	I	J	K	M	S	
Benincasa hispida	Wax gourd	62	9	1	4	9	5	2	4	2	8	1	1	–	16	In this study
Citrullus lanatus	Watermelon	66	11[c]	1	4	9[c]	5	2	4	2	8	1	1	2[c]	16[c]	Yang et al. (2019)
Cucumis hystrix	Wild cucumber	62	9	1	4	8	7	1	5	3	7	1	1	1	14	In this study
Cucumis melo	Melon	62	9	1	4	9	5	2	3	2	8	1	1	1	16	In this study
Cucumis sativus	Cucumber	65[c]	10	1	4	10	6	2	4	2	9	1	1	–	15	Baloglu et al. (2014)
Cucurbita argyrosperma	Cushaw pumpkin	101	17	–	7	14	9	4	7	3	9	1	1	3	26	In this study
Cucurbita maxima	Winter squash	109	16	2	6	17	10	4	8	3	15	1	1	3	23	In this study
Cucurbita moschata	Pumpkin	108	17	2	6	16	8	4	7	4	14	2	1	3	24	In this study
Cucurbita pepo	Zucchini	93	8	3	7	14	8	4	8	3	11	1	1	2	23	In this study
Lagenaria siceraria	Bottle gourd	65	10	1	3	9	5	3	4	2	9	1	1	–	17	In this study
Luffa acutangula	Ridge gourd	68	10	1	4	10	6	2	4	2	9	1	–	2	17	In this study
Luffa cylindrica	Sponge gourd	68	11	1	4	9	6	2	4	2	8	1	1	2	17	In this study
Momordica charantia	Bitter gourd	63	9	1	4	9	7	2	6	2	8	1	1	–	13	In this study
Sechium edule	Chayote	102[a]	15	2	7	14	9	4	8	2	15	1	1	2	22	In this study
Siraitia grosvenorii	Monkfruit	75	11	1	6	12	4	1	5	2	9	1	1	2	20	In this study
Trichosanthes anguina	Snake gourd	66[a]	11[b]	1	4	9	6	2	3	2	8	1[b]	1	2	16	In this study
Total		1235	183	20	78	178	106	41	84	38	155	17	15	25	295	

[a]: the occurrence of additional splicing variants; [b]: splicing variants belong to different clades of bZIPs; [c]: values differ from previously published numbers.

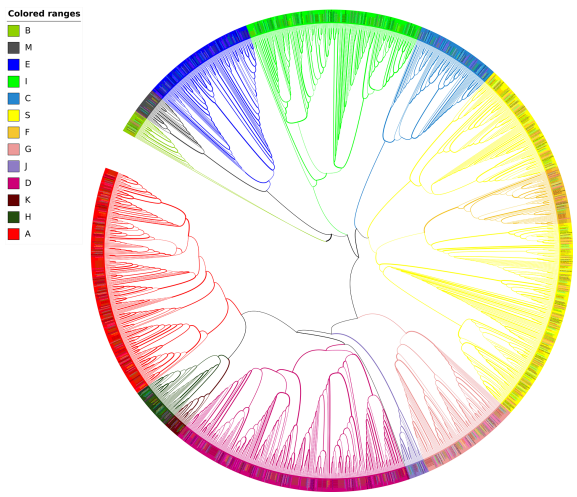


FIGURE 3
Unrooted Maximum likelihood phylogenetic tree of bZIP genes in 16 Cucurbitaceae species. Different colors represent bZIPs in different clades according to Dröge-Laser et al. (2018).

exons ranged from 1 to 22, and clade G and D had relative more exons than other clades. The phylogenetic classification of *LsbZIPs* was not obviously consistent with exon/intron distribution. However, some genes in the same type shared similar structures, such clade C possessed six exons and five introns.

Orthologous clusters comparisons in different species

The comparison and annotation of orthologous gene clusters among multiple species were displayed in Figure 6A (https://orthovenn2.bioinfotoolkits.net/task/result/3515a11fe06d38df8aca0e62cc1739d9). The number of orthologous proteins in each cluster varied from 4 to 352. In summary, a total of 60 orthologous proteins in *C. sativus* were predicted to have similar conserved domain with *LsbZIPs*. *O. sativa* had the lowest homology with 30 proteins while the orthologous proteins in the rest species varied from 37 (*S. lycopersicum*) to 42 (*G. max*). 8 *LsbZIPs* were only orthologous in *C. sativus*, *LsbZIP33* and *LsbZIP34* was only orthologous in *G. max* and *B. napus*, respectively (Figure 6B, Table S6). 20 *LsbZIP* proteins were able to find their orthologous proteins in each

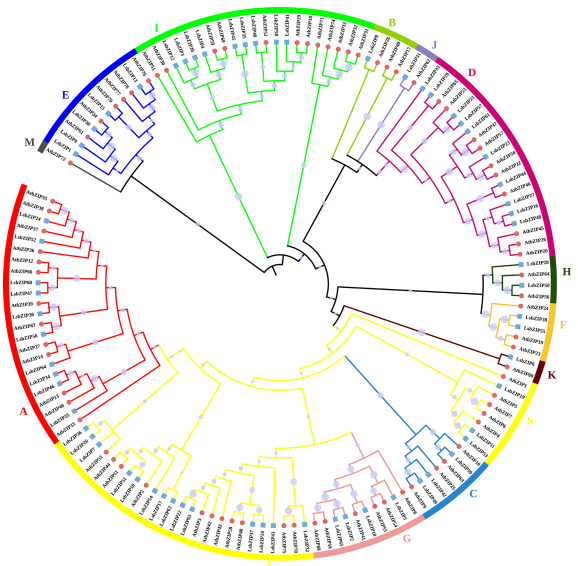


FIGURE 4
Phylogenetic tree of bZIP genes from *Arabidopsis* and bottle gourd. The tree is constructed by Neighbor-Joining method with bootstrap values of 1000 replicates. Different colored branches and stripes indicate different subgroups. The red circles and blue squares represent bZIP genes from *Arabidopsis* and bottle gourd, respectively.

species. 26 clusters including 352 proteins were overlapped in all 8 species and 26 proteins belonged to *L. siceraria* were corresponding to orthologous proteins, respectively (Figure 6A). 3 singleton proteins (*LsbZIP43*, *LsbZIP20*, *LsbZIP40*) were identified to have no orthologs in any of these species.

Cis-regulatory elements analysis of *LsbZIP* genes

To further understand the transcriptional regulation of bZIP genes in bottle gourd, 2000 bp sequences upstream of the translation initiation site (ATG) were extracted to predict cis-elements by PlantCARE database. In a summary, we identified 64 cis-acting elements which can be grouped into 9 different responsive processes based on the diverse functions (Table S7, Figure 7). Besides the core promoter elements (CAAT-box and TATA-box) found in all 65 *bZIP* genes, the column clustering had a certain degree of preferences. CREs involved in light responsiveness, hormone responsiveness and stress responsive were ubiquitous in each *LsbZIP*, accounting for the majority of putative promoters. Three genes (*LsbZIP11*, *LsbZIP43*, *LsbZIP48*) had more than 10 different light-responsive CREs. The numbers of concerned CREs in stress responsiveness contained low-temperature responsive elements (LTR) in 20 *LsbZIPs*, anaerobic-responsive element (ARE) in 57 *LsbZIPs*, wound-responsive element (WUN-motif) in 7 *LsbZIPs*. Twelve hormone responsive elements were found, in which included abscisic acid responsiveness element (ABRE) in 41 *LsbZIPs*, auxin-responsive element (AuxRR-core, TGA-element) in 6 *LsbZIPs*, gibberellin-responsive element (GARE-motif, P-box, and TATC-box) in 31 *LsbZIPs*, salicylic acid responsiveness (SARE, TCA-element) and MeJA-responsiveness (CGTCA-motif and TGACG-motif) in 35 and 41 *LsbZIPs*, respectively (Table S7). Moreover, circadian control was found in 6 *LsbZIPs* as well as zein metabolism regulation (O2-site) and flavonoid biosynthetic gene regulation (MBSI) were found in 15 and 4 *LsbZIPs*, respectively. The results demonstrated that bZIP TFs acted as an important role not only in the regulation of multiple biological processes, but also in response to many abiotic stresses.

Expression patterns of *LsbZIPs* in various tissues and cultivars

To dissect the tissue-specific expression of *LsbZIP* genes, the expression of 65 *LsbZIPs* were determined in five tissues (root, leaf, flower, fruit and stem) from RNA-Seq data SRP107894 (Wu et al., 2017). As shown in Figure 8A, four genes (*LsbZIP29, LsbZIP56, LsbZIP7, LsbZIP33*) were found not totally expressed in all tissues under normal conditions, indicating that they may be pseudogenes or act in response to abiotic/biotic stresses. And 17 genes were expressed

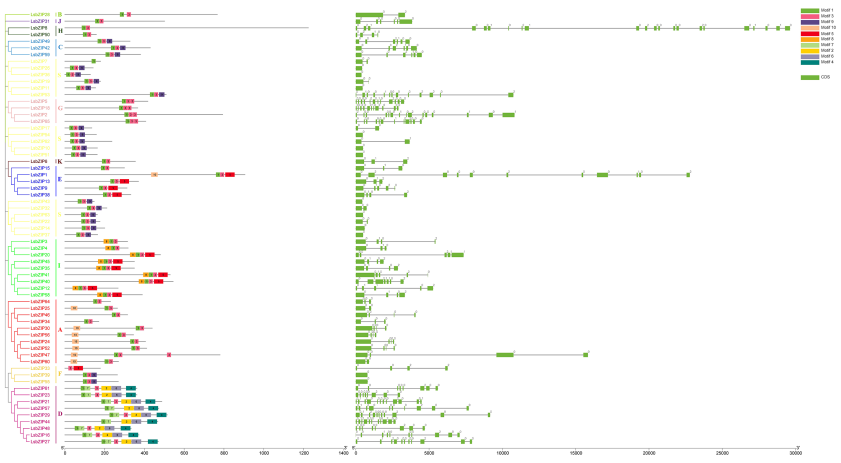


FIGURE 5
Conserved motifs and gene structures of *LsbZIP* genes in the bottle gourd. Left: 10 Motifs are indicated by different colored boxes. Right: Green boxes indicate the exons, and grey lines indicate the introns. Different numbers indicate the phase of introns.

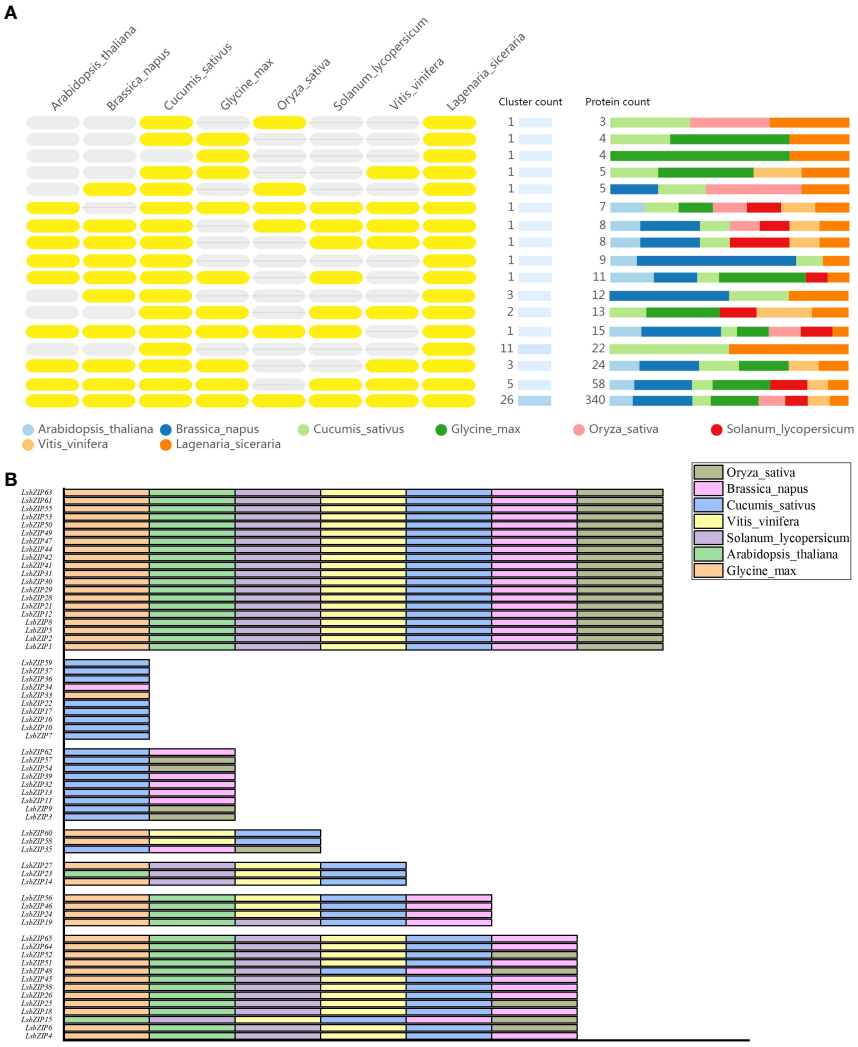


FIGURE 6
Comparative analysis of orthologous gene clusters among multiple species. **(A)** Yellow ovals on the left side represent the presence of orthologous genes while grey ovals represent the absence of orthologous genes. Different colors bars on the right side indicate the number and ratio of orthologous proteins in 8 plant species. **(B)** Layout of the different orthologous gene pairs. Each species was marked with different color.

at a low level (log_2(TPM+1)<3), especially in roots and leaves. Meanwhile, 6 genes (*LsbZIP10, LsbZIP51, LsbZIP26, LsbZIP39, LsbZIP50, LsbZIP54*) were highly expressed in leaves, flowers, fruits and stems except in roots. These genes may be involved in the development process of various organs. In roots, 44 of 65 identified *LsbZIP* genes were regarded as silent while 11 *LsbZIP* genes exhibited high transcript expression level (Table S8). Three genes (*LsbZIP17, LsbZIP43, LsbZIP63*) were root-specific expressed while four genes (*LsbZIP36, LsbZIP45, LsbZIP14 and LsbZIP37*) were relatively high induced in flowers and stems. To sum it up, tissue-specific genes with high expressions might be involved in corresponding tissue defense system. And the illustrated heatmap showed that *LsbZIPs* were most active in flower and not relatively active in leaves. To further discuss the expression patterns in different varieties, our previous RNA-Seq data with five bottle gourd accession were used in this study (Xu et al., 2021). The results showed that 5 genes (*LsbZIP21*, *LsbZIP56, LsbZIP29, LsbZIP33, LsbZIP43*) were rarely expressed in all cultivars, similar to the tendency in Figure 8B. The genes with high expression level in different cultivars were exactly same in different tissues, demonstrating these genes played important roles in manipulating normal growth and development in plants. However, three genes (*LsbZIP36, LsbZIP50, LsbZIP63*) were highly expressed in variety HZ and YD-4 whilst low expression in G22, J104 and J129. And *LsbZIP37* had relative high transcript abundance in J104 and J129 than in other 3 cultivars (Table S9). It revealed that a few *LsbZIP* genes had cultivar-specific expression, to a certain extent.

Expression of *LsbZIP* genes under cold stress

To investigate early changes in gene expression, we retrieved the transcriptional data under the accession number PRJNA553072 in the bottle gourd cultivar "YZ", which is a rootstock type showing high tolerance to low temperature (Wang et al., 2020). The differentially expressed genes (DEGs) in accordance with false discovery rate <0.5 and absolute fold change ≥2 were selected and shown in Figure 9A. In general, 19 *LsbZIPs* were detected in YZ under low temperature

10.3389/fpls.2022.1128007

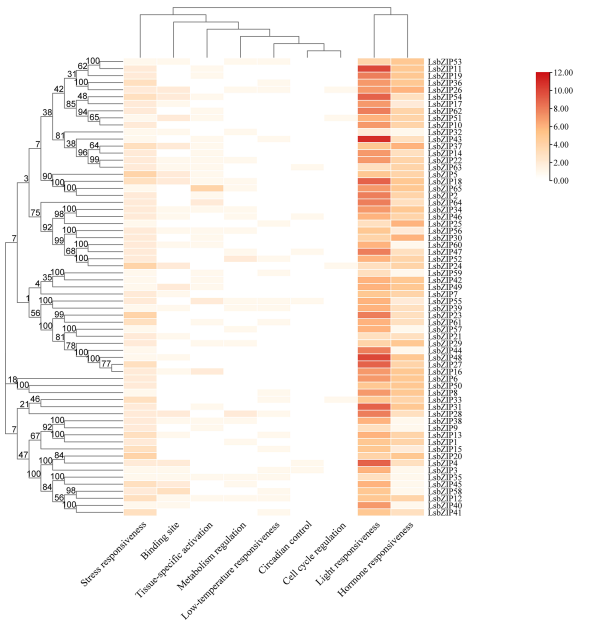


FIGURE 7
Cis-acting regulatory elements in the promoters of *LsbZIPs*.

treatment for 2 days. 7 genes were significantly down-regulated and 10 genes were up-regulated remarkably (Figure 9A and Table S10). Intriguingly, two genes (*LsbZIP7* and *LsbZIP62*) were not expressed at room temperature similar to the results found in Figure 8A. And *LsbZIP7* was highly induced after low temperature treatment while *LsbZIP62* was slightly induced, as well. Three genes *LsbZIP55*, *LsbZIP37*, and *LsbZIP24* which kept relative high gene expression exhibited opposite expression patterns. The expression of *LsbZIP55* cut in half, but the expression level of *LsbZIP37* and *LsbZIP24* increased 2-3 folds compared to respective control (Table S10). In addition, another three genes namely *LsbZIP28*, *LsbZIP61*, *LsbZIP6* increased their expression up to 5, 7, 30 times respectively in response to cold stress. Five genes (*LsbZIP56*, *LsbZIP40*, *LsbZIP16*, *LsbZIP31* and *LsbZIP22*) were dramatically down-regulated by low temperature. To gain insight into the changing trends in response to cold stress, 10 selected *LsbZIP* genes were determined by qRT-PCR to validate the RNA-Seq data (Figure 9B). The leaves were harvested at 5 different time-points (0h, 1h, 6h, 12h, 24h) after cold treatment at 4°C. The plants without 0 h cold treatment were considered as control. The relative expression level of selected *LsbZIP* genes was evaluated by the $2^{-\Delta\Delta Ct}$ method. Statistical significance was detected by LSD test using SPSS v16.0 (SPSS, Inc., Chicago, IL, USA). 8 genes were activated fast within one hour cold stress, indicating the responsive rate varied in different gene expression. *LsbZIP6* was quickly induced to be remarkably expressed at 1 hour after treatment (HAT) and continuously rise up to 20 folds than 0 HAT. The parallel increasing pattern was observed in *LsbZIP61* and *LsbZIP28*, but the expression of these two genes were initiated to ascend 12 HAT. Three genes (*LsbZIP16*, *LsbZIP22* and *LsbZIP31*) presented earlier increase and later decrease trend. On the other hand, three genes including *LsbZIP40*, *LsbZIP56*, *LsbZIP65* were down-regulated within 1 HAT and subsequently inhibited all the time till 24 HAT. In addition, only one gene *LsbZIP44* showed a distinct expression pattern. It was highly expressed within 1 HAT, then suppressed after 6 h cold treatment. Interestingly, *LsbZIP44* was again induced, followed by gradual increase at 12 and 24 h.

Discussion

Increasing evidences have suggested that bZIP TFs play vital roles in many biological and physiological processes and regulating signal transductions in response to various abiotic and biotic stresses, such as seed germination (Toh et al., 2012), flower development (Strathmann et al., 2001), cold tolerance (Ritonga and Chen, 2020), salt stress (Wang et al., 2010) and pathogen defense (Thurow et al., 2005), etc. So far, a number of plant species have systematically analyzed bZIP family genes in the genome-wide scale, including some crucial crops like *A. thaliana* (78) (Dröge-Laser et al., 2018), *O. sativa*



FIGURE 8
Heatmaps of *LsbZIP* genes displaying tissue-specific and cultivar-specific expression. **(A)** Hierarchical clustering of expression profile of bZIP genes in different tissues (root, leaf, flower, fruit, stem) of bottle gourd under normal condition. **(B)** The expression profile of bZIP genes in 5 bottle gourd varieties (G22, HZ, J104, J129, YD-4) under normal condition. Data were transformed with a $\log_2$(TPM+1) transformation.

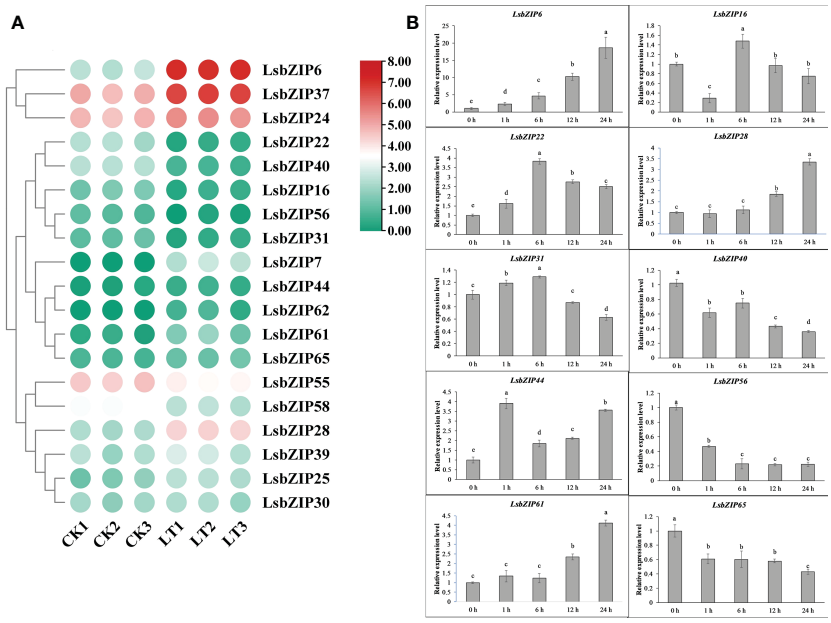


FIGURE 9
Expression profile of *LsbZIP* genes in leaves under cold stress. **(A)** The expression levels of DEGs in leaves under cold stress. **(B)** Relative expression of selected 10 *LsbZIP* genes in response to cold stress at 5 time points. Mean ± SE of three replicates represent the significant difference with LSD test. The data followed by the different letter in the graph are significant at P≥0.05.

(89) (Nijhawan et al., 2008), *Z. mays* (125) (Wei et al., 2012) and a few cucurbit vegetables cucumber (64) (Baloglu et al., 2014) and watermelon (62) (Yang et al., 2019). However, the genome-wide characterization of bZIP family genes in *Lagenaria siceraria* has not been reported. In this study, we compared the former published bottle gourd genome to our newly assembled genome and finally identified 65 unique *LsbZIP* sequences.

Cucurbitaceous plants, also known as the gourd family, are one of the most important edible plant families and have great economic value. Currently, at least 16 genomes of Cucurbitaceae species including diverse varieties in each species have been released (Wang et al., 2020). To dig deeply into the evolution and divergence in Cucurbit, the available known cucurbit genomes were collected and exhaustively searched for the putative bZIP genes. A total number of 1235 non-redundant protein sequences from 16 Cucurbitaceae species were subdivided into 13 clades with well-supported bootstrap values (Figure 3, Table S4). In clade B, three *AtbZIPs* (*AtbZIP17*, *AtbZIP49*, *AtbZIP28*) formed a small unique cluster independent from other Cucurbitaceae bZIPs. This scenario also emerged in clade A, F, I, suggesting that these group-specific sequence characteristics of the bZIP members may form before the divergence of *Arabidopsis* and Cucurbitaceae since conserved domains were homologous in the same clade containing both *Arabidopsis* and Cucurbitaceae bZIP genes. However, it seemed that intraspecific duplication and parallel evolution of the bZIP family in each Cucurbitaceae has occurred afterward and led to the member variation in each clade. The majority of *bZIPs* in other clades originated from the whole genome duplication to evolve both generically and specifically in Cucurbitaceae. The results were in consistent with the conclusion in legumes (Wang et al., 2020).

In bottle gourd, 65 *LsbZIP* genes were undoubtably grouped into 12 subfamilies except clade M (Table S2, Figure 4). The general idea is that *bZIP* proteins in plant had extra functional conserved domains, in addition to specific *bZIP1* (PF00170) and *bZIP2* (PF07716) domains, participating in various biological processes (Jin et al., 2014). The domain basic leucine-zipper C terminal (bZIP_C) was identified only in clade C. Similar phenomena happened in clade G with G-box binding protein MFMR, and in clade D with seed dormancy control protein DOG1 as well (Table S2). The structure of motifs and exon-intron composition followed the classification pattern of phylogeny (Figure 5). Motif 2 and 6 were characteristic in clade D, composing DOG1 domain found in *Arabidopsis* (Dröge-Laser et al., 2018). The number of introns in *LsbZIPs* varied from 0 to 14, besides *LsbZIP8* owning incredible 21 introns (Figure 5). It was basically coincident with the results in *V. vinifera*, *Brachypodium distachyon*, *S. lycopersicum*, cassava and potato (Li et al., 2015a; Liu and Chu, 2015; Hu et al., 2016b; Mirzaei et al., 2020; Wang et al., 2020). Furthermore, most *bZIP* genes in clade F and S were prevalently intronless (Figure 5). It has been demonstrated that lack of introns contribute to accelerating the post-transcription in response to abiotic stresses (Zhou et al., 2018). And similar findings were observed in soybean and watermelon, revealing evolutionary imprint and functional divergence (Li et al., 2015b; Liu et al., 2017; Zhang et al., 2018; Yang et al., 2019). Compared to the intronless phenomenon, majority of clade D and G obviously possessed more introns (Figure 5). Previous researches suggested that the rate of evolution in genes without introns would increase after gene

duplication (Lecharny et al., 2003; Lurin, 2004; Jain et al., 2006). It is deduced that *bZIPs* in clade D and G might derive earliest than other clades (Hu et al., 2016b). The orthologous genes in clade D and G shared overlaps in seven or eight species while genes in clade F shared overlaps in one or two species (Figure 6A, Table S6). It verified the speculation on the other side. Gene duplication is the main reason of genome evolution and expansion in multigene family (Si et al., 2019). In this study, 19 segmental duplication events in bottle gourd genome led to the expansion of bZIP family genes as in rice (Nijhawan et al., 2008), sorghum (Wang et al., 2011), maize (Wei et al., 2012), tomato (Li et al., 2015a) and peanut (Wang et al., 2019).

The genome-wide expression pattern of *LsbZIPs* exhibited tissue-specific trait in various organs in Figure 8A. For example, three genes including *LsbZIP17*, *LsbZIP43* and *LsbZIP63* were highly expressed and preferentially enriched in roots, indicating that they might play roles in root development. Similar tissue-specific pattern were obtained in many species such as apple (Li et al., 2016), grape (Liu et al., 2014), banana (Hu et al., 2016a), watermelon (Yang et al., 2019) and *Prunus mume* (Li et al., 2022). *LsbZIP50* and *LsbZIP24*, which were found to be highly expressed in all tissues except root, were orthologous of HY5 (At5g11260) and abscisic acid responsive elements-binding factor (ABF3, At4g34000), respectively (Figure 7; Table S6). The function of HY5 in numerous developmental processes has been well-established, like photomorphogenesis generation, chloroplast development and pigment accumulation (Gangappa and Botto, 2016; Yang et al., 2018). Likewise, *LsbZIPs* of clade A (52, 30), clade D (48, 61) and clade G (18, 5, 65) with high expression in all tissues were homologous to ABFs, TGA factors (TGAs) and G-box-binding factors (GBFs) in *Arabidopsis*. The ABFs have been found to act as the core of ABA signaling which counteract abiotic stresses (Banerjee and Roychoudhury, 2017). TGAs redundantly are regarded as vital transcriptional regulators by triggering systemic acquired resistance to interact with nonexpressor of pathogenesis-related genes 1 (NPR1), which is key gene in plant pathogen response (Fu and Dong, 2013). In addition, *LsbZIP37* showed cultivar-specific expression pattern in J104 and J129 which are relative resistant to cold stress, implying that *LsbZIP37* might participate in the regulation of cold stress response (Figure 8B).

Although bottle gourd is routinely used as a rootstock of other Cucurbitaceae crops due to its climate resiliency and high resistance to biotic stresses (Wang et al., 2020), the mechanism of which bottle gourd respond to cold stress has not been clearly understood. And plants have been found to evolve different strategies to adapt environmental stresses like cold (Xi et al; Wu et al., 2016; Xu et al., 2022). In the previous reports, a number of bZIPs including *OsbZIP73*, *OsbZIP52/RISBZ5*, *MdHY5* acts as positive or negative roles in response to cold stress (Liu et al., 2012; An et al., 2017; Liu et al., 2018). Based on the previous transcriptome profile, 19 *LsbZIP* genes were differentially expressed (12 up-regulated, 7 down-regulated) under cold stress (Figure 9A). Subsequently, 10 selected *LsbZIPs* were validated through RT-PCR at different time points after cold treatment (Figure 9B). *LsbZIP6* (clade K), *LsbZIP28* (clade B) and *LsbZIP61* (clade D) were quickly activated in response to cold stress. Their homologous genes in *Arabidopsis* contain three members of group B (*AtbZIP17*, *AtbZIP28*, *AtbZIP49*) and one member of group K (*AtbZIP60*), and have important effects on evolutionary conserved endoplasmic reticulum (ER) stress response (Howell, 2013). Transgenic plants overexpressed *AtbZIP17* showed salt tolerance and truncated *AtbZIP60* actively moved to the nucleus to regulate ER stress-genes (Iwata and Koizumi, 2005; Iwata et al., 2008; Liu et al., 2010). Therefore, B-bZIP *LsbZIP6* and K-bZIP *LsbZIP28* might converge on ER-stress pathways targeting specific gene sets like *AtbZIP60* and *AtbZIP28/bZIP17* were existed in heterodimer (Kim et al., 2018). *LsbZIP61* had orthologous relationship with TGA1, which interacts with NPR1 and induces apoplastic defense and ER stress response (Shearer et al., 2012; Wang and Fobert, 2013). G-bZIP *LsbZIP65*, which was orthologous to GBF1, exhibited a decline expression trend after cold treatment (Figure 9B). GBF1 is a well-known negative regulator of hypocotyl expansion (Gangappa et al., 2013), and can bind to the catalase2 promoter to inhibit the H_2O_2-scavenging activity, leading to ROS accumulation (Giri et al., 2017). The down-regulated expression of *LsbZIP65* might decrease the accumulation of H_2O_2 through less binding catalase2 promoter in order to endure cold stress in bottle gourd.

Conclusion

In this study, we firstly identified and characterized 65 non-duplicated *bZIP* genes in *L. siceraria* and divided into 12 subfamilies at a genome-wide scale. The phylogenetic analysis based on 1235 *bZIP* sequences from 16 Cucurbitaceae revealed evolutionary convergence and divergence of *bZIP* gene family. The analysis of *LsbZIPs* domain, structure and orthologous relationships were consistent with the classification. The tissue-specific expression pattern of *LsbZIPs* indicated the pivotal roles in various physiological and biological processes. We elaborated the expression profiles of *LsbZIPs* in response to low-temperature stress, which provide valuable information of bZIPs under cold condition and strategies to breed cultivars conferred cold tolerance.

Data availability statement

The datasets presented in this study can be found in online repositories. The names of the repository/repositories and accession number(s) can be found in the article/Supplementary Material.

Author contributions

JW analyzed the data. YW and XinW conducted the qPCR analysis. JW drew the figures and edited the manuscript. BW, ZL and LZ contributed regents/materials/analysis tool. JW, GL and XiaW conceived and designed the study, obtained funds, and critically revised the manuscript. All authors contributed to the article and approved the submitted version.

Funding

This study was mainly supported by Key Research and Development Programs of Zhejiang Province (Grant No. 2021C02052 and 2021C02042), the Key Science Project of Vegetable Breeding in Zhejiang (14th Five-Year Plan) (2021C02065).

Conflict of interest

The authors declare that the research was conducted in the absence of any commercial or financial relationships that could be construed as a potential conflict of interest.

Publisher's note

All claims expressed in this article are solely those of the authors and do not necessarily represent those of their affiliated organizations, or those of the publisher, the editors and the reviewers. Any product that may be evaluated in this article, or claim that may be made by its manufacturer, is not guaranteed or endorsed by the publisher.

Supplementary material

The Supplementary Material for this article can be found online at: https://www.frontiersin.org/articles/10.3389/fpls.2022.1128007/full#supplementary-material

SUPPLEMENTARY FIGURE 1
Phylogenetic analysis of bZIPs between two bottle gourd genomes ('USVL1VR-Ls' and 'HZCG').

References

An, J. P., Qu, F. J., Yao, J. F., Wang, X. N., You, C. X., Wang, X. F., et al. (2017). The bZIP transcription factor MdHY5 regulates anthocyanin accumulation and nitrate assimilation in apple. *Horticult. Res.* 4, 17023. doi: 10.1038/hortres.2017.23

Bailey, T. L., Boden, M., Buske, F. A., Frith, M., Grant, C. E., Clementi, L., et al. (2009). MEME SUITE: tools for motif discovery and searching. *Nucleic Acids Res.* 37, W202–W208. doi: 10.1093/nar/gkp335

Baloglu, M. C., Eldem, V., Hajyzadeh, M., and Unver, T. (2014). Genome-wide analysis of the bZIP transcription factors in cucumber. *PLoS One* 9, e96014. doi: 10.1371/journal.pone.0096014

Banerjee, A., and Roychoudhury, A. (2017). Abscisic-acid-dependent basic leucine zipper (bZIP) transcription factors in plant abiotic stress. *Protoplasma* 254, 3–16. doi: 10.1007/s00709-015-0920-4

Capella-Gutiérrez, S., Silla-Martínez, J. M., and Gabaldón, T. (2009). trimAl: a tool for automated alignment trimming in large-scale phylogenetic analyses. *Bioinformatics* 25, 1972–1973. doi: 10.1093/bioinformatics/btp348

Chen, C., Chen, H., Zhang, Y., Thomas, H. R., Frank, M. H., He, Y., et al. (2020). TBtools: An integrative toolkit developed for interactive analyses of big biological data. *Mol. Plant* 13, 1194–1202. doi: 10.1016/j.molp.2020.06.009

Chimonyo, V. G. P., and Modi, A. T. (2013). Seed performance of selected bottle gourd (Lagenaria siceraria (Molina) standl.). *Am. J. Exp. Agric.* 3, 740. doi: 10.9734/ajea/2013/4114

Dankov, K., Dobrikova, A., Bogos, B., Gombos, Z., and Apostolova, E. (2009). The role of anionic lipids in LHCII organization and in photoinhibition of photosynthetic apparatus. *Comptes rendus l'Académie bulgare Des. Sci.* 62, 941–948.

Dröge-Laser, W., Snoek, B. L., Snel, B., and Weiste, C. (2018). The arabidopsis bZIP transcription factor family–an update. *Curr. Opin. Plant Biol.* 45, 36–49. doi: 10.1016/j.pbi.2018.05.001

Edgar, R. C. (2004). MUSCLE: multiple sequence alignment with high accuracy and high throughput. *Nucleic Acids Res.* 32, 1792–1797. doi: 10.1093/nar/gkh340

Foster, R., Izawa, T., and Chua, N.-H. (1994). Plant bZIP proteins gather at ACGT elements. *FASEB J.* 8, 192–200. doi: 10.1096/fasebj.8.2.8119490

Fu, Z. Q., and Dong, X. (2013). Systemic acquired resistance: Turning local infection into global defense. *Annu. Rev. Plant Biol.* 64, 839–863. doi: 10.1146/annurev-arplant-042811-105606

Gangappa, S. N., and Botto, J. F. (2016). The multifaceted roles of HY5 in plant growth and development. *Mol. Plant*. 9, 1353–1365. doi: 10.1016/j.molp.2016.07.002

Gangappa, S. N., Srivastava, A. K., Maurya, J. P., Ram, H., and Chattopadhyay, S. (2013). Z-box binding transcription factors (ZBFs): A new class of transcription factors in arabidopsis seedling development. *Mol. Plant* 6, 1758–1768. doi: 10.1093/mp/sst140

Gasteiger, E., Gattiker, A., Hoogland, C., Ivanyi, I., Appel, R. D., and Bairoch, A. (2003). ExPASy: the proteomics server for in-depth protein knowledge and analysis. *Nucleic Acids Res.* 31, 3784–3788. doi: 10.1093/nar/gkg563

Giri, M. K., Singh, N., Banday, Z. Z., Singh, V., Ram, H., Singh, D., et al. (2017). GBF1 differentially regulates CAT2 and PAD4 transcription to promote pathogen defense in arabidopsis thaliana. *Plant J.* 91, 802–815. doi: 10.1111/tpj.13608

Howell, S. H. (2013). Endoplasmic reticulum stress responses in plants *Annu. Rev. Plant Biol.* 64, 477–499. doi: 10.1146/annurev-arplant-050312-120053

Huang, X., Ouyang, X., Yang, P., Lau, O. S., Li, G., Li, J., et al. (2012). Arabidopsis FHY3 and HY5 positively mediate induction of COP1 transcription in response to photomorphogenic UV-b light. *Plant Cell* 24, 4590–4606. doi: 10.1105/tpc.112.103994

Hu, B., Jin, J., Guo, A.-Y., Zhang, H., Luo, J., and Gao, G. (2015). GSDS 2.0: an upgraded gene feature visualization server. *Bioinformatics* 31, 1296–1297. doi: 10.1093/bioinformatics/btu817

Hu, W., Wang, L., Tie, W., Yan, Y., Ding, Z., Liu, J., et al. (2016a). Genome-wide analyses of the bZIP family reveal their involvement in the development, ripening and abiotic stress response in banana. *Sci. Rep.* 6, 30203. doi: 10.1038/srep30203

Hu, W., Yang, H., Yan, Y., Wei, Y., Tie, W., Ding, Z., et al. (2016b). Genome-wide characterization and analysis of bZIP transcription factor gene family related to abiotic stress in cassava. *Sci. Rep.* 6, 1–12. doi: 10.1038/srep22783

Iwata, Y., F., N. V., and Koizumi, N. (2008). Arabidopsis bZIP60 is a proteolysis-activated transcription factor involved in the endoplasmic reticulum stress response. *Plant Cell* 20, 3107–3121. doi: 10.1105/tpc.108.061002

Iwata, Y., and Koizumi, N. (2005). An arabidopsis transcription factor, AtbZIP60, regulates the endoplasmic reticulum stress response in a manner unique to plants. *Proc. Natl. Acad. Sci. United States America* 102, 5280–5285. doi: 10.1073/pnas.0408941102

Jain, P., Shah, K., Sharma, N., Kaur, R., Singh, J., Vinson, C., et al. (2017). A-ZIP53, a dominant negative reveals the molecular mechanism of heterodimerization between bZIP53, bZIP10 and bZIP25 involved in arabidopsis seed maturation. *Sci. Rep.* 7, 1–17. doi: 10.1038/s41598-017-14167-5

Jain, M., Tyagi, A. K., and Khurana, J. P. (2006). Genome-wide analysis, evolutionary expansion, and expression of early auxin-responsive SAUR gene family in rice (Oryza sativa). *Genomics* 88, 360–371. doi: 10.1016/j.ygeno.2006.04.008

Jakoby, M., Weisshaar, B., Dröge-Laser, W., Vicente-Carbajosa, J., Tiedemann, J., Kroj, T., et al. (2002). bZIP transcription factors in arabidopsis. *Trends Plant Sci.* 7, 106–111. doi: 10.1016/S1360-1385(01)02223-3

Jin, Z., Xu, W., and Liu, A. (2014). Genomic surveys and expression analysis of bZIP gene family in castor bean (Ricinus communis l.). *Planta* 239, 299–312. doi: 10.1007/s00425-013-1979-9

Kim, J.-S., Yamaguchi-Shinozaki, K., and Shinozaki, K. (2018). ER-anchored transcription factors bZIP17 and bZIP28 regulate root elongation. *Plant Physiol.* 176, 2221–2230. doi: 10.1104/pp.17.01414

Kong, S., Park, S.-Y., and Lee, Y.-H. (2015). Systematic characterization of the bZIP transcription factor gene family in the rice blast fungus, m agnaporthe oryzae. *Environ. Microbiol.* 17, 1425–1443. doi: 10.1111/1462-2920.12633

Lecharny, A., Boudet, N., Gy, I., Aubourg, S., and Kreis, M. (2003). Introns in, introns out in plant gene families: a genomic approach of the dynamics of gene structure. *J. Struct. Funct. Genomics* 3, 111–116. doi: 10.1023/A:1022614001371

Liang, Y., Xia, J., Jiang, Y., Bao, Y., Chen, H., Wang, D., et al. (2022). Genome-wide identification and analysis of bZIP gene family and resistance of TaABI5 (TabZIP96) under freezing stress in wheat (Triticum aestivum). *Int. J. Mol. Sci.* 23, 2351. doi: 10.3390/ijms23042351

Liao, Y., Zou, H.-F., Wei, W., Hao, Y.-J., Tian, A.-G., Huang, J., et al. (2008). Soybean GmbZIP44, GmbZIP62 and GmbZIP78 genes function as negative regulator of ABA signaling and confer salt and freezing tolerance in transgenic arabidopsis. *Planta* 228, 225–240. doi: 10.1007/s00425-008-0731-3

Li, D., Fu, F., Zhang, H., and Song, F. (2015a). Genome-wide systematic characterization of the bZIP transcriptional factor family in tomato (Solanum lycopersicum l.). *BMC Genomics* 16, 771. doi: 10.1186/s12864-015-1990-6

Li, X., Gao, S., Tang, Y., Li, L., Zhang, F., Feng, B., et al. (2015b). Genome-wide identification and evolutionary analyses of bZIP transcription factors in wheat and its relatives and expression profiles of anther development related TabZIP genes. *BMC Genomics*. 16, 976. doi: 10.1186/s12864-015-2196-7

Li, Y.-Y., Meng, D., Li, M., and Cheng, L. (2016). Genome-wide identification and expression analysis of the bZIP gene family in apple (Malus domestica). *Tree Genet. Genomes* 12, 1–17. doi: 10.1007/s11295-016-1043-6

Lindemose, S., O'Shea, C., Jensen, M. K., and Skriver, K. (2013). Structure, function and networks of transcription factors involved in abiotic stress responses. *Int. J. Mol. Sci.* 14, 5842–5878. doi: 10.3390/ijms14035842

Liu, J., Chen, N., Chen, F., Cai, B., Dal Santo, S., Tornielli, G. B., et al. (2014). Genome-wide analysis and expression profile of the bZIP transcription factor gene family in grapevine (Vitis vinifera). *BMC Genomics* 15, 281. doi: 10.1186/1471-2164-15-281

Liu, X., and Chu, Z. (2015). Genome-wide evolutionary characterization and analysis of bZIP transcription factors and their expression profiles in response to multiple abiotic stresses in brachypodium distachyon. *BMC Genomics* 16, 227. doi: 10.1186/s12864-015-1457-9

Liu, C., Ou, S., Mao, B., Tang, J., Wang, W., Wang, H., et al. (2018). Early selection of bZIP73 facilitated adaptation of japonica rice to cold climates. *Nat. Commun.* 9, 3302. doi: 10.1038/s41467-018-05753-w

Liu, J. X., Srivastava, R., and Howell, S. H. (2010). Stress-induced expression of an activated form of AtbZIP17 provides protection from salt stress in arabidopsis. *Plant Cell Environ.* 31, 1735–1743. doi: 10.1111/j.1365-3040.2008.01873.x

Liu, C., Wu, Y., and Wang, X. (2012). bZIP transcription factor OsbZIP52/RISBZ5: a potential negative regulator of cold and drought stress response in rice. *Planta* 235, 1157–1169. doi: 10.1007/s00425-011-1564-z

Liu, H., Zhong, Y., Guo, C., Wang, X. L., Xiong, J., Cheng, Q., et al. (2017). Genome-wide analysis and evolution of the bZIP transcription factor gene family in six fragaria species. *Plant Systematics Evol.* 303, 1225–1237. doi: 10.1007/s00606-017-1433-8

Li, Y., Wang, Y., Wu, X., Wang, J., Wu, X., Wang, B., et al. (2021). Novel genomic regions of fusarium wilt resistance in bottle gourd [Lagenaria siceraria (Mol.) standl.] discovered in genome-wide association study. *Front. Plant Sci.* 12, 715. doi: 10.3389/fpls.2021.650157

Li, Q., Xiong, L., Gao, J., and Zhang, H.-Y. (2019). Molecular mechanisms of the protein-protein interaction–regulated binding specificity of basic-region leucine zipper transcription factors. *J. Mol. Modeling* 25, 1–11. doi: 10.1007/s00894-019-4138-9

Li, P., Zheng, T., Li, L., Wang, J., Cheng, T., and Zhang, Q. (2022). Genome-wide investigation of the bZIP transcription factor gene family in prunus mume: classification, evolution, expression profile and low-temperature stress responses. *Hortic. Plant J.* 8, 230–242. doi: 10.1016/j.hpj.2021.01.009

Llorca, C. M., Potschin, M., and Zentgraf, U. (2014). bZIPs and WRKYs: two large transcription factor families executing two different functional strategies. *Front. Plant Sci.* 5. doi: 10.3389/fpls.2014.00169

Lurin, C. (2004). Genome-wide analysis of arabidopsis pentatricopeptide repeat proteins reveals their essential role in organelle biogenesis. *Plant Cell* 16, 2089–2103. doi: 10.1105/tpc.104.022236

Meng, X.-B., Zhao, W.-S., Lin, R.-M., Wang, M., and Peng, Y.-L. (2005). Identification of a novel rice bzip-type transcription factor gene, osbzip1, involved in response to infection ofmagnaporthe grisea. *Plant Mol. Biol. Rep.* 23, 301–302. doi: 10.1007/BF02772762

Mirzaei, K., Bahramnejad, B., and Fatemi, S. (2020). Genome-wide identification and characterization of the bZIP gene family in potato (Solanum tuberosum). *Plant Gene* 24, 100257. doi: 10.1016/j.plgene.2020.100257

Mukherjee, K., Choudhury, A. R., Gupta, B., Gupta, S., and Sengupta, D. N. (2006). An ABRE-binding factor, OSBZ8, is highly expressed in salt tolerant cultivars than in salt sensitive cultivars of indica rice. *BMC Plant Biol.* 6, 1–14. doi: 10.1186/1471-2229-6-18

Nguyen, L.-T., Schmidt, H. A., Von Haeseler, A., and Minh, B. Q. (2015). IQ-TREE: A fast and effective stochastic algorithm for estimating maximum-likelihood phylogenies. *Mol. Biol. Evol.* 32, 268–274. doi: 10.1093/molbev/msu300

Nijhawan, A., Jain, M., Tyagi, A. K., and Khurana, J. P. (2008). Genomic survey and gene expression analysis of the basic leucine zipper transcription factor family in rice. *Plant Physiol.* 146, 333. doi: 10.1104/pp.107.112821

Panchy, N., Lehti-Shiu, M., and Shiu, S.-H. (2016). Evolution of gene duplication in plants. *Plant Physiol.* 171, 2294–2316. doi: 10.1104/pp.16.00523

Pourabed, E., Ghane Golmohamadi, F., Soleymani Monfared, P., Razavi, S. M., and Shobbar, Z.-S. (2015). Basic leucine zipper family in barley: genome-wide characterization of members and expression analysis. *Mol. Biotechnol.* 57, 12–26. doi: 10.1007/s12033-014-9797-2

Qiao, X., Li, Q., Yin, H., Qi, K., Li, L., Wang, R., et al. (2019). Gene duplication and evolution in recurring polyploidization–diploidization cycles in plants. *Genome Biol.* 20, 1–23. doi: 10.1186/s13059-019-1650-2

Ritonga, F. N., and Chen, S. (2020). Physiological and molecular mechanism involved in cold stress tolerance in plants. *Plants* 9, 560. doi: 10.3390/plants9050560

Schaefer, H., Heibl, C., and Renner, S. S. (2009). Gourds afloat: a dated phylogeny reveals an Asian origin of the gourd family (Cucurbitaceae) and numerous oversea dispersal events. *Proc. R. Soc. B: Biol. Sci.* 276, 843–851. doi: 10.1098/rspb.2008.1447

Schlumbaum, A., and Vandorpe, P. (2012). A short history of lagenaria siceraria (bottle gourd) in the Roman provinces: morphotypes and archaeogenetics. *Vegetation history archaeobotany* 21, 499–509. doi: 10.1007/s00334-011-0343-x

Shearer, H. L., Cheng, Y. T., Wang, L., Liu, J., Boyle, P., Després, C., et al. (2012). Arabidopsis clade I TGA transcription factors regulate plant defenses in an NPR1-independent fashion. *Mol. Plant Microbe Interact.* 25, 1459–1468. doi: 10.1094/MPMI-09-11-0256

Shimizu, H., Sato, K., Berberich, T., Miyazaki, A., Ozaki, R., Imai, R., et al. (2005). LIP19, a basic region leucine zipper protein, is a fos-like molecular switch in the cold signaling of rice plants. *Plant Cell Physiol.* 46, 1623–1634. doi: 10.1093/pcp/pci178

Si, W., Hang, T., Guo, M., Chen, Z., and Ding, T. (2019). Whole-genome and transposed duplication contributes to the expansion and diversification of TLC genes in maize. *Int. J. Mol. Sci.* 20, 5484. doi: 10.3390/ijms20215484

Sirichandra, C., Davanture, M., Turk, B. E., Zivy, M., Valot, B., Leung, J., et al. (2010). The arabidopsis ABA-activated kinase OST1 phosphorylates the bZIP transcription factor ABF3 and creates a 14-3-3 binding site involved in its turnover. *PloS One* 5, e13935. doi: 10.1371/journal.pone.0013935

Sornaraj, P., Luang, S., Lopato, S., and Hrmova, M. (2016). Basic leucine zipper (bZIP) transcription factors involved in abiotic stresses: a molecular model of a wheat bZIP factor and implications of its structure in function. *Biochim. Biophys. Acta (BBA)-General Subj.* 1860, 46–56. doi: 10.1016/j.bbagen.2015.10.014

Strathmann, A., Kuhlmann, M., Heinekamp, T., and Dröge-Laser, W. (2001). BZI-1 specifically heterodimerises with the tobacco bZIP transcription factors BZI-2, BZI-3/TBZF and BZI-4, and is functionally involved in flower development. *Plant J.* 28, 397–408. doi: 10.1046/j.1365-313X.2001.01164.x

Tang, W., Ru, Y., Hong, L., Zhu, Q., Zuo, R., Guo, X., et al. (2015). System-wide characterization of bZIP transcription factor proteins involved in infection-related morphogenesis of m agnaporthe oryzae. *Environ. Microbiol.* 17, 1377–1396. doi: 10.1111/1462-2920.12618

Thurow, C., Schiermeyer, A., Krawczyk, S., Butterbrodt, T., Nickolov, K., and Gatz, C. (2005). Tobacco bZIP transcription factor TGA2. 2 and related factor TGA2. 1 have distinct roles in plant defense responses and plant development. *Plant J.* 44, 100–113. doi: 10.1111/j.1365-313X.2005.02513.x

Toh, S., McCourt, P., and Tsuchiya, Y. (2012). HY5 is involved in strigolactone-dependent seed germination in arabidopsis. *Plant Signaling Behav.* 7, 556–558. doi: 10.4161/psb.19839

Wang, L., and Fobert, P. R. (2013). Arabidopsis clade I TGA factors regulate apoplastic defences against the bacterial pathogen pseudomonas syringae through endoplasmic reticulum-based processes. *PLoS One* 8, e77378. doi: 10.1371/journal.pone.0077378

Wang, Y., Gao, C., Liang, Y., Wang, C., Yang, C., and Liu, G. (2010). A novel bZIP gene from tamarix hispida mediates physiological responses to salt stress in tobacco plants. *J. Plant Physiol.* 167, 222–230. doi: 10.1016/j.jplph.2009.09.008

Wang, Y., Tang, H., DeBarry, J. D., Tan, X., Li, J., Wang, X., et al. (2012). MCScanX: a toolkit for detection and evolutionary analysis of gene synteny and collinearity. *Nucleic Acids Res.* 40, e49–e49. doi: 10.1093/nar/gkr1293

Wang, Y., Wang, L., Xing, N., Wu, X., Wu, X., Wang, B., et al. (2020). A universal pipeline for mobile mRNA detection and insights into heterografting advantages under chilling stress. *Horticult. Res.* 7, 13. doi: 10.1038/s41438-019-0236-1.

Wang, J., Yang, C., Wu, X., Wang, Y., Wang, B., Wu, X., et al. (2022). Genome-wide characterization of NBS-LRR family genes and expression analysis under powdery mildew stress in lagenaria siceraria. *Physiol. Mol. Plant Pathol.* 118, 101798. doi: 10.1016/j.pmpp.2022.101798

Wang, Z., Yan, L., Wan, L., Huai, D., Kang, Y., Shi, L., et al. (2019). Genome-wide systematic characterization of bZIP transcription factors and their expression profiles during seed development and in response to salt stress in peanut. *BMC Genomics* 20, 51. doi: 10.1186/s12864-019-5434-6

Wang, J., Zhou, J., Zhang, B., Vanitha, J., Ramachandran, S., and Jiang, S.-Y. (2011). Genome-wide expansion and expression divergence of the basic leucine zipper transcription factors in higher plants with an emphasis on sorghum f. *J. Integr. Plant Biol.* 53, 212–231. doi: 10.1111/j.1744-7909.2010.01017.x

Wei, K., Chen, J., Wang, Y., Chen, Y., Chen, S., Lin, Y., et al. (2012). Genome-wide analysis of bZIP-encoding genes in maize. *DNA Res.* 19, 463–476. doi: 10.1093/dnares/dss026

Weiste, C., Pedrotti, L., Selvanayagam, J., Muralidhara, P., Fröschel, C., Novák, O., et al. (2017). The arabidopsis bZIP11 transcription factor links low-energy signalling to auxin-mediated control of primary root growth. *PloS Genet.* 13, e1006607. doi: 10.1371/journal.pgen.1006607

Wu, S., Shamimuzzaman, M., Sun, H., Salse, J., Sui, X., Wilder, A., et al. (2017). The bottle gourd genome provides insights into cucurbitaceae evolution and facilitates mapping of a papaya ring-spot virus resistance locus. *Plant J.* 92, 963–975. doi: 10.1111/tpj.13722

Wu, L., Wu, J., Liu, Y., Gong, X., Xu, J., Lin, D., et al. (2016). The rice pentatricopeptide repeat gene TCD10 is needed for chloroplast development under cold stress. *Rice* 9, 67. doi: 10.1186/s12284-016-0134-1

Xi, L., Jie, L., Yunshuai, H., Penghui, C., Chunlei, Z., Yaken, R., et al. (2018). WSL5, a pentatricopeptide repeat protein, is essential for chloroplast biogenesis in rice under cold stress. *J. Exp. Bot.* 69, 3949–3961. doi: 10.1093/jxb/ery214

Xu, L., Cao, M., Wang, Q., Xu, J., Liu, C., Ullah, N., et al. (2022). Insights into the plateau adaptation of salvia castanea by comparative genomic and WGCNA analyses. *J. Advanced Res.* 42, 221–235. doi: 10.1016/j.jare.2022.02.004

Xu, P., Wang, Y., Sun, F., Wu, R., Du, H., Wang, Y., et al. (2021). Long-read genome assembly and genetic architecture of fruit shape in the bottle gourd. *Plant J.* 107, 956–968. doi: 10.1111/tpj.15358

Yang, Y., Liang, T., Zhang, L., Shao, K., Gu, X., Shang, R., et al. (2018). UVR8 interacts with WRKY36 to regulate HY5 transcription and hypocotyl elongation in arabidopsis. *Nat. Plants* 4, 98–107. doi: 10.1038/s41477-017-0099-0

Yang, Y., Li, J., Li, H., Yang, Y., Guang, Y., and Zhou, Y. (2019). The bZIP gene family in watermelon: genome-wide identification and expression analysis under cold stress and root-knot nematode infection. *PeerJ* 7, e7878. doi: 10.7717/peerj.7878

Yang, Y.-G., Lv, W.-T., Li, M.-J., Wang, B., Sun, D.-M., and Deng, X. (2013). Maize membrane-bound transcription factor Zmbzip17 is a key regulator in the cross-talk of ER quality control and ABA signaling. *Plant Cell Physiol.* 54, 2020–2033. doi: 10.1093/pcp/pct142

Yin, W., Cui, P., Wei, W., Lin, Y., and Luo, C. (2017). Genome-wide identification and analysis of the basic leucine zipper (bZIP) transcription factor gene family in ustilaginoidea virens. *Genome* 60, 1051–1059. doi: 10.1139/gen-2017-0089

Yoshida, T., Fujita, Y., Maruyama, K., Mogami, J., Todaka, D., Shinozaki, K., et al. (2015). Four a rabidopsis AREB/ABF transcription factors function predominantly in gene expression downstream of SnRK2 kinases in abscisic acid signalling in response to osmotic stress. *Plant Cell Environ.* 38, 35–49. doi: 10.1111/pce.12351

Zander, M., La Camera, S., Lamotte, O., Métraux, J.-P., and Gatz, C. (2010). Arabidopsis thaliana class-II TGA transcription factors are essential activators of jasmonic acid/ethylene-induced defense responses. *Plant J.* 61, 200–210. doi: 10.1111/j.1365-313X.2009.04044.x

Zhang, M., Liu, Y. H., Shi, Y. H., Guo, M. L., Chai, M. N., He, Q., et al. (2018). Evolutionary and expression analyses of soybean basic leucine zipper transcription factor family. *BMC Genomics*. 19, 159. doi: 10.1186/s12864-018-4511-6

Zhang, L., Yu, H., Lin, S., and Gao, Y. (2016). Molecular characterization of FT and FD homologs from eriobotrya deflexa nakai forma koshunensis. *Front. Plant Sci.* 7, 8. doi: 10.3389/fpls.2016.00008

Zhang, Y., Zhang, G., Xia, N., Wang, X.-J., Huang, L.-L., and Kang, Z.-S. (2008). Cloning and characterization of a bZIP transcription factor gene in wheat and its expression in response to stripe rust pathogen infection and abiotic stresses. *Physiol. Mol. Plant Pathol.* 73, 88–94. doi: 10.1016/j.pmpp.2009.02.002

Zhao, K., Chen, S., Yao, W., Cheng, Z., Zhou, B., and Jiang, T. (2021). Genome-wide analysis and expression profile of the bZIP gene family in poplar. *BMC Plant Biol.* 21, 1–16. doi: 10.1186/s12870-021-02879-w

Zhou, Y., Xu, D., Jia, L., Huang, X., Ma, G., Wang, S., et al. (2017). Genome-wide identification and structural analysis of bZIP transcription factor genes in brassica napus. *Genes* 8, 288. doi: 10.3390/genes8100288

Zhou, Y., Zeng, L., Chen, R., Wang, Y., and Song, J. (2018). Genome-wide identification and characterization of stress-associated protein (SAP) gene family encoding A20/AN1 zinc-finger proteins in medicago truncatula. *Arch. Biol. Sci.* 70, 087–098. doi: 10.2298/ABS170529028Z

frontiers | Frontiers in Plant Science

TYPE Original Research
PUBLISHED 31 March 2023
DOI 10.3389/fpls.2023.1134209

Check for updates

OPEN ACCESS

EDITED BY
Tianlun Zhao,
Zhejiang University, China

REVIEWED BY
Yanpeng Wang,
Institute of Genetics and Developmental Biology (CAS), China
Jitesh Kumar,
University of Minnesota Twin Cities, United States

*CORRESPONDENCE
Yuming Lu
luymin@sjtu.edu.cn
Jian-Kang Zhu
zhujk@sustech.edu.cn
Yifu Tian
tianyifu@caas.cn

†These authors have contributed equally to this work and share first authorship

SPECIALTY SECTION
This article was submitted to Plant Abiotic Stress, a section of the journal Frontiers in Plant Science

RECEIVED 30 December 2022
ACCEPTED 13 March 2023
PUBLISHED 31 March 2023

CITATION
Shen R, Yao Q, Zhong D, Zhang X, Li X, Cao X, Dong C, Tian Y, Zhu J-K and Lu Y (2023) Targeted insertion of regulatory elements enables translational enhancement in rice.
Front. Plant Sci. 14:1134209.
doi: 10.3389/fpls.2023.1134209

COPYRIGHT
© 2023 Shen, Yao, Zhong, Zhang, Li, Cao, Dong, Tian, Zhu and Lu. This is an open-access article distributed under the terms of the Creative Commons Attribution License (CC BY). The use, distribution or reproduction in other forums is permitted, provided the original author(s) and the copyright owner(s) are credited and that the original publication in this journal is cited, in accordance with accepted academic practice. No use, distribution or reproduction is permitted which does not comply with these terms.

Targeted insertion of regulatory elements enables translational enhancement in rice

Rundong Shen[1,2,3†], Qi Yao[1,4†], Dating Zhong[1,4†], Xuening Zhang[1,4], Xinbo Li[1,2,3], Xuesong Cao[1], Chao Dong[2,3], Yifu Tian[1,2,3*], Jian-Kang Zhu[2,5*] and Yuming Lu[1,4*]

[1]Shanghai Center for Plant Stress Biology, Center for Excellence in Molecular Plant Sciences, Chinese Academy of Sciences, Shanghai, China, [2]Center for Advanced Bioindustry Technologies, and Institute of Crop Sciences, Chinese Academy of Agricultural Sciences, Beijing, China, [3]Hainan Yazhou Bay Seed Lab, Sanya, Hainan, China, [4]Shanghai Collaborative Innovation Center of Agri-Seeds, Joint Center for Single Cell Biology, School of Agriculture and Biology, Shanghai Jiao Tong University, Shanghai, China, [5]Institute of Advanced Biotechnology, and School of Life Sciences, Southern University of Science and Technology, Shenzhen, China

In-locus editing of agronomically-important genes to optimize their spatiotemporal expression is becoming an important breeding approach. Compared to intensive studies on mRNA transcription, manipulating protein translation by genome editing has not been well exploited. Here, we found that precise knock-in of a regulating element into the 5'UTR of a target gene could efficiently increase its protein abundance in rice. We firstly screened a translational enhancer (AMVE) from alfalfa mosaic virus using protoplast-based luciferase assays with an 8.5-folds enhancement. Then the chemically modified donor of AMVE was synthesized and targeted inserted into the 5'UTRs of two genes (*WRKY71* and *SKC1*) using CRISPR/Cas9. Following the *in-locus* AMVE knock-in, we observed up to a 2.8-fold increase in the amount of WRKY71 protein. Notably, editing of *SKC1*, a sodium transporter, significantly increased salt tolerance in T2 seedlings, indicating the expected regulation of AMVE knock-in. These data demonstrated the feasibility of such *in-locus* editing to enhance protein expression, providing a new approach to manipulating protein translation for crop breeding.

KEYWORDS

translational regulation, enhancer, knock-in, rice, breeding

Introduction

Over the past decades, transgene is one of the most important technologies to modify gene expression and has been widely used in countless research and breeding applications. With the development of CRISPR/Cas technology, optimizing the spatiotemporal expression of agronomically important genes through genome editing is gradually

becoming a trend in molecular breeding. Currently, it is mainly achieved by large-scale editing of promoters to randomly alter the transcript level of target genes, and there have been several very promising application studies (Rodriguez-Leal et al., 2017; Shi et al., 2017; Zeng et al., 2020; Wang et al., 2021; Liu et al., 2021a; Song et al., 2022). It is well known that gene expression consists of two parts, transcription and translation. And current research shows that protein translation can also violently regulate protein abundance (Leppek et al., 2018). However, there are few studies on translational regulation in plants, and the use of genome editing to *in-locus* modify gene sequences for translational regulation is rarely reported.

Similar to cis-elements in promoters that regulate transcription, UTRs (untranslated regions) have been proven to greatly affect protein translation (Leppek et al., 2018). For example, upstream open reading frames (uORFs) are typical translational elements that are thought to potentially inhibit the translation of main ORFs. And by editing of uORFs, several studies have successfully increased the protein abundance of target genes without transcriptional perturbation (Xu et al., 2017; Zhang et al., 2018; Liu et al., 2021b). In addition to uORF, many cis-acting RNA elements within the 5'UTR, known as translational enhancers, also contribute to the translational regulation of mRNAs (Leppek et al., 2018). The most extensively used enhancer is the Omega element from the tobacco mosaic virus (TMV). It was widely used to increase protein expression in many transgenic vectors by inserting it into the 5'UTR of target genes (Gallie and Walbot, 1992; Gallie, 2002). And another leading sequence from alfalfa mosaic virus (AMV) has also been used to facilitate protein translation (named AMVE) (Jobling and Gehrke, 1987). In addition, some endogenous sequences of 5'UTRs in plants also could enhance gene expression, such as the 5'UTR of the rice *ADH1* (named ADHE) (Sugio et al., 2008). Apart from the native sequences, some synthetic 5'UTRs (e.g. SynJ, SynM, MsynJ and pSTART) were able to promote transgene expression as enhancers (De Amicis et al., 2007; Kanoria and Burma, 2012). Even under a strong promoter like CaMV 35S, these translational enhancers can improve the transgene expression significantly. Based on the fact of such translational regulations, we hypothesized that targeted knock-in of translational enhancers into the 5'UTR of endogenous genes could increase protein translation, thus providing a new strategy of gene activation with important application value. However, targeted sequence knock-in in plants has been a huge challenge, severely limiting such attempts.

With the development of CRISPR/Cas, the sequence knock-in technologies have made great progresses in plants (Li et al., 2016; Li et al., 2018; Li et al., 2019; Dong et al., 2020; Lu et al., 2020a; Lu et al., 2020b). And we have recently developed an efficient sequence knock-in method in rice using chemically modify donor DNA with frequencies of up to 50% (Lu et al., 2020b). This technological breakthrough makes it possible to knock-in translational enhancers into 5'UTRs. Here, we screened a functional enhancer AMVE and evaluated its feasibility of *in-locus* activation by targeted inserting into 5'UTRs of two genes.

Materials and methods

Plant materials and growth condition

The plant materials used in the study were Nipponbare (*Oryza sativa* L. ssp. *Japonica* cv. Nipponbare). The seeds were firstly germinated in Hoagland's solution and rice seedlings were grown in a growth chamber at 30°C for a 12-hours light period and 28°C for a 12-hours dark period. Two-week-old rice plants were transplanted to the fresh Hoagland's solution for subsequent treatment. Morphological characteristics were recorded within seven days.

Plasmid construction

The pDLUC01 and pCBSG032 vectors were stored in our laboratory. The translational enhancer sequences were synthesized and cloned into the digested pDLUC01 vector for protoplast transfection. The target sequences of sgRNA for rice genes were designed using CRISPR-GE and/or CRISPR-P (Liu et al., 2017; Xie et al., 2017) and cloned into the *Bsa*I-digested pCBSG032 vector to construct CRISPR/Cas9 plasmids as previously reported (Lu et al., 2017). Primers used for plasmid construction were listed in Supplementary Table 3.

Protoplast transformation

Rice seedlings grown on MS medium (1/2x, 28°C for 7-10 days) were used for protoplast preparation. The dual-luciferase reporter plasmids with different translational enhancer sequences were transformed into protoplasts, respectively. According to previous described methods, 10 μg of plasmid DNA were transfected into approximately 5×10^5 protoplasts. After a 12-hours incubation at 25°C in dark, protoplasts were harvested by brief centrifugation (100 g for 3 minutes) for subsequent experiments. FLuc/RLuc activity was measured using a Dual-Luciferase Reporter Assay Kit (Vazyme Biotech Co. Ltd, Nanjing, China).

Generation of knock-in rice

Sequence knock-in rice was produced according to a previous study with some minor modifications (Lu et al., 2020b). Briefly, CRISPR/Cas9 plasmids were firstly prepared using a plasmid Midi-preparation Kit (Tiangen Biotech Co. Ltd, Beijing, China) and diluted to 1 μg/μl. Then, 0.1 pmol CRISPR/Cas9 plasmids were mixed with 2 pmol donor DNA and coated to 3 mg golden particles. Bombardment-mediated transformations were conducted on one-month-old rice calli of Nipponbare with the PDS1000/He particle bombardment system (Bio-Rad, California, USA). The transformed calli were then cultured at 28°C in the dark for 16 hours and transferred onto the selection medium with hygromycin (50 mg/L) for plantlets regeneration (Lu et al., 2017).

Genotyping

Genomic DNA of the regenerated rice was extracted by CTAB method. Forward and reverse primers were designed within 200 bp of the target site, respectively. The PCR product containing the inserted sequence was larger than that of the wild type. The amplified PCR products were cloned into TA cloning vector pCE2-TA/Blunt-Zero (Vazyme Biotech Co. Ltd, Nanjing, China) for Sanger sequencing and/or directly sequenced using the Hi-TOM method. The PCR primers used for genotyping are listed in Supplementary Table 3.

RNA extraction and qRT-PCR

Total RNA was extracted from the rice protoplasts or young leaves using the Plant Total RNA Extraction Kit (Sango Biotech Co. Ltd, Shanghai, China). Reverse transcription was performed with 1 μg using HiScript cDNA Synthesis Kit (Vazyme Biotech Co. Ltd, Nanjing, China) according to the manufacturer's instruction. Quantitative PCR (qPCR) was performed using ChamQ SYBR Master Mix (Vazyme Biotech Co. Ltd, Nanjing, China). Each qPCR assay was replicated at least three times. The *RLuc* gene was used as an internal control for rice protoplasts and the rice *Actin1* gene was used as the housekeeping gene for plant samples. The primers were listed in Supplementary Table 3.

Protein extraction and immunoblot analysis

Total proteins were extracted from rice leaves using 2×SDS loading buffer. The protein samples were separated using a 12% SDS-PAGE gel and transferred onto PVDF membranes. Membranes were blocked with 5% skim milk for 1 hour and incubated overnight at 4°C with primary antibodies of rabbit anti-Actin antibody (Sango Biotech Co. Ltd, Shanghai, China, 1:1,000 dilution) or anti-OsWRKY71 antibody (Beijing Protein Innovation Co. Ltd, Beijing, China, 1:1,000 dilution). The membranes were washed three times with TBST and incubated with secondary antibodies for 1 hour at room temperature. The secondary antibody was a goat anti-rabbit antibody conjugated to horseradish peroxidase (Sango Biotech Co. Ltd, Shanghai, China). Protein signals were detected with Clarity Western ECL Substrate (Bio-Rad, California, USA) using ChemiDocXRS imaging system (Bio-Rad, California, USA).

Bacteria strains and inoculation

Xoo strain (PXO99) was grown on PSA plates (10 g/l peptone, 10 g/l sucrose, 1 g/l glutamic acid, 16 g/l bacto-agar, pH 7.0) at 28 °C for 2 days. The bacterial cells were suspended in sterile water to an OD600 0.6 for inoculation. Leaves of rice plants (6-8 weeks old) were inoculated using a leaf-clipping method as previously described. Disease symptoms were assessed 14 days after inoculation by measuring the lesion length.

Off-target analysis

The CRISPR-P (v.2.0) program was used to predict the potential off-target sites for sgRNAs in rice genome (Liu et al., 2017). Potential off-target sites were PCR amplified from the edited lines and subjected to Sanger sequencing. The PCR primers used for off-target analysis are listed in Supplementary Table 3.

Results

Screening of translational enhancers for rice

According to previous studies on translational enhancers, twelve candidates were selected, including the virus-derived Omega and AMVE (Jobling and Gehrke, 1987; Gallie and Walbot, 1992; Gallie, 2002), plant-derived ADHE, OspsbA and NtpsbA (Zou et al., 2003; Sugio et al., 2008), and synthetic sequences SynM, SynJ, MsynJ and pSTART (De Amicis et al., 2007; Kanoria and Burma, 2012) (Supplementary Figure 1B). To conduct a quick evaluation in rice, a protoplasts-based transient assay was developed. A dual-luciferase reporter (pDLUC01) was constructed to access the effects of these translational enhancers (Figure 1A). The firefly luciferase (*FLuc*) was used as the reporter and the *R. reniformis* luciferase (*RLuc*) was used as the internal control. Enhancer sequences were inserted into the 5'UTR of *FLuc* driven by a truncated 35S promoter (35Smini, Supplementary Figure 1A). Enhancers were then parallelly assessed in rice protoplasts. The results showed that six of them had enhancement effect, especially AMVE and ADHE, which remarkably increased 8.5 times and 4.3 times on FLuc expression, respectively (Figure 1B). As expected, quantitative RT-PCR (qRT-PCR) analysis showed that there was no significant difference in the transcript level of FLuc/RLuc, suggesting that such regulation possibly happened at the translational level without altering mRNA abundance (Figure 1C). It could be noticed that the Omega enhancer derived from TMV that was widely used in dicots did not function in rice, indicating a possible specificity of species requirement for such translational enhancers. Accordingly, we chose AMVE and ADHE for subsequent tests.

Translational enhancement of *WRKY71*

Unlike the transcriptional regulation that could be easily quantified using qRT-PCR, assessment of translational regulation usually requires antibodies corresponding to the target genes for immunoblot assays. Thus we chose *WRKY71* as the target gene for its commercially available antibody and proven functions in bacterial resistance (Liu et al., 2007; Liu et al., 2016). To do a quick evaluation of AMVE and ADHE on *WRKY71*, the promoter

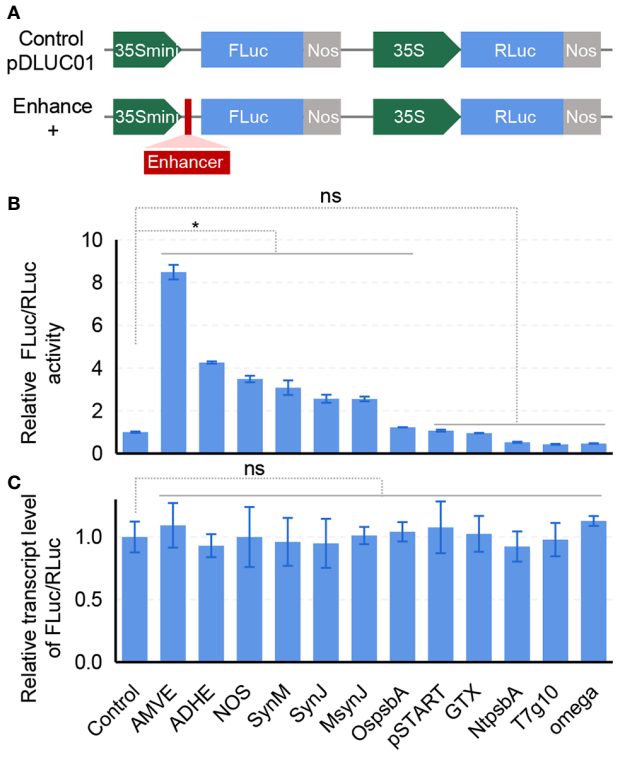


FIGURE 1
Screening of translational enhancers in rice protoplasts. **(A)** Diagram of the dual-luciferase plasmid pDLUC01. FLuc, firefly luciferase. RLuc, *R. reniformis* luciferase. The insertion site for enhancer sequences was marked as a red box. **(B)** Assessment of enhancers in protoplast-based dual-luciferase assays. RLuc was used as an internal control. **(C)** Transcript levels of FLuc/RLuc in rice protoplasts. **(B, C)** All values represent means ± s.d. of three independent experiments (n = 3). *$P < 0.05$; ns, no significant difference (two-tailed Student' s *t* test).

and 5'UTR sequence of *WRKY71* were cloned into pDLUC01 reporter to replace the 35Smin promoter (pDLUC02-WRKY71), and AMVE and ADHE were then inserted into its 5'UTR (Figure 2A). Protoplast-based assay indicated that both AMVE and ADHE could increase the FLuc/RLuc activity by 5.8 and 2.9 times, respectively (Figure 2B). Thus, AMVE was selected for knock-in.

To generate AMVE knock-in rice, chemically modified donor DNA of AMVE was synthesized according to our previous studies (Figure 2C). A sgRNA target within the 5'UTR of *WRKY71* was designed (Figure 2D) and a total of 60 T0 rice plants were generated using bombardment-mediated transformation. Among the 11 knock-in plantlets, three T0 plants had a precisely forward and seamless insertion of AMVE and their T1 homozygous were identified and used for evaluations (Figures 2E, F; Supplementary Tables 1, 4). Similar to the results in protoplasts, the transcript levels of *WRKY71* in knock-in mutants (WRKY71#04, #07 and #14) remained unchanged (Figure 2G), while its protein abundance was increased obviously by about 2.8 times identified with immunoblot assays (Figure 2H). Consistent with previous studies (Liu et al., 2007; Liu et al., 2016), up-regulation of *WRKY71* improved the resistance to *Xanthomonas oryzae* (*Xoo*) of bacterial blight (Figure 2I). These results demonstrated the feasibility of such translational manipulations *via in-locus* editing.

Knock-in of AMVE to improve salt tolerance of rice

To further validate the strategy, we selected another important gene *SKC1* that encodes a Na^+-selective transporter (Ren et al., 2005; Kobayashi et al., 2017; Quan et al., 2017). *In vitro* assays using protoplasts as described above demonstrated that inserting AMVE into 5'UTR of *SKC1* in the luciferase reporter pDLUC02 resulted in a 10.4-folds enhancement (Figure 3A), which convinced us to do subsequent gene editing. A sgRNA target of CRISPR/Cas9 was designed in the 5'UTR of *SKC1* (Figure 3B) and a total of 119 T0 plants were regenerated *via* biolistic-mediated transformation. We identified 32 targeted insertion mutants from these transgenic lines. Six precise knock-in mutants containing a forward AMVE insert were identified by Sanger sequencing (Figure 3C and Supplementary Table 1). Unfortunately, our efforts to make SKC1 antibodies failed (Supplementary Figure 3). Since previous studies demonstrated that up-regulation of *SKC1 via* transgene can increase the salinity tolerance of rice mutants (Farquharson, 2009), three lines of them (SKC1#49, #52 and #57) were selected directly for salinity-tolerance evaluations.

A population of T2 mutants was generated from homozygotes of their T1 lines. qRT-PCR results showed that the transcript levels of *SKC1* in the three AMVE knock-in mutants were comparable to those in WT (Figure 3D). Two-week-old seedlings grown in liquid Hoagland's solution were then treated with 150 mM NaCl. After 7-days treatment, the three edited mutant lines showed more tolerance to salt stress than WT plants (Figure 3E) and gave a much more survival rate (45% vs. 65%, Figure 3F). These results were consistent with previous findings (Farquharson, 2009), indicating an up-regulation of *SKC1*. Because the transcript level of *SKC1* remained unchanged, we believed that such an AMVE-mediated up-regulation happened at the translational level, consistent with the results of *WRKY71*. In addition, we observed a genetic segregation of a 1:2:1 for these T1 heterozygotes that followed the Mendel's law (Supplementary Table 2), indicating that both the genotype and phenotype may be passed on to offspring. These results demonstrated that the knock-in of enhancers into 5'UTRs could be useful for plant breeding.

Discussion and conclusions

Transgene-mediated up-regulation of a target gene is widely used in plant research and breeding that usually driven by a constitutive promoter. Such transcriptional manipulation is currently the main method of gene expression regulation. Now we have entered the era of gene editing, and sequence modification in promoters *via* CRISPR/Cas have successfully altered the transcription of mRNAs in several studies (Rodriguez-Leal et al., 2017; Shi et al., 2017; Zeng et al., 2020; Wang et al., 2021; Liu et al., 2021a; Song et al., 2022), providing a useful strategy. Unlike the extensive studies on transcriptional regulations, the mechanism of

10.3389/fpls.2023.1134209

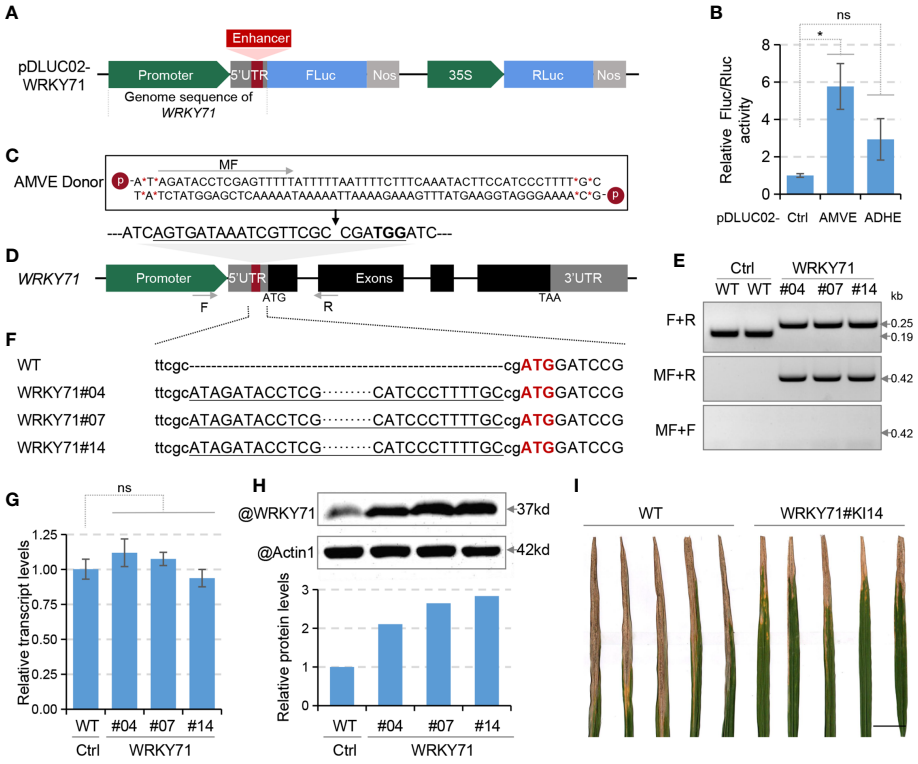


FIGURE 2
Translational enhancement of *WRKY71*. **(A)** Schematic diagram of dual-luciferase plasmid for *WRKY71* (pDLUC02-WRKY71). **(B)** Assessment of enhancers ADHE and AMVE in protoplast-based dual-luciferase assays. Plasmids pDLUC02-WRKY71 with or without (Ctrl) enhancer sequences were used as reporters. **(C)** The chemically modified donor sequence of AMVE. **(D)** Schematic diagram of *WRKY71* for AMVE knock-in. The sgRNA target of Cas9 is underlined with the protospacer-adjacent motif (PAM) in bold. **(E)** Genotyping of AMVE knock-in mutants on *WRKY71* with PCR. Genomic DNA was amplified using primers flanking target sites (F+R). Forward (middle) and reverse (lower) insertion mutants were identified using primers F +MR and F+MF, respectively. Positions of primers are indicated as arrows in **(C, D)**. **(F)** Sequencing results of AMVE knock-in mutants. Sequences of AMVE were underlined and the start codon of *WRKY71* is in red. **(G)** Transcription levels of *WRKY71* in WT (Ctrl) and T1 mutants were determined using qRT-PCR. The rice *Actin1* gene was used as the internal control. **(H)** Comparison of the protein level of WRKY71 between the WT (Ctrl) and T1 mutants. Actin1 was used as the loading control in the immunoblot assay. The ratio of the gray value (WRKY71/Actin1) was calculated using ImageJ. **(I)** Representative results of lesion length symptoms caused by *Xoo* strains in rice leaves. Photograph was taken two weeks after inoculation with PXO99. Bar, 2 cm. **(B, G)** All values represent means ± s.d. of three independent experiments (n = 3). $*P < 0.05$; ns, no significant difference (two-tailed Student' s *t* test).

protein translation has been less studied. Although translational enhancers have been discovered for decades and successfully applied to many transgene studies, the underlying mechanisms are still not well understood that greatly hinders their applications with genome editing. Nevertheless, numerous studies have shown that the inserting of such enhancers into the 5'UTR of transgenic vectors can greatly increase the expression of target proteins (Gallie, 2002; Zou et al., 2003; De Amicis et al., 2007; Sugio et al., 2008; Kanoria and Burma, 2012). And our study here demonstrated that they could also enhance the expression of endogenous genes when precise knock-in to the 5'UTRs, providing a new approach for the up-regulation of target genes.

When we screened the enhancers using rice protoplasts, we found that AMVE has the strongest enhancement effect, and the rice-derived ADHE1 also functions well. However, the ones previously reported to work well in dicots (e.g. Omega) had a much weaker effect, indicating that translational enhancers may have different effects among species. And we may be able to find better enhancers from endogenous UTRs in the future. We also proved that *in-locus* inserting enhancer sequences into 5'UTRs would not affect the transcription of target genes. We think that the enhancement effect is caused by a post-transcriptional mechanism, such as facilitating the initiation of translation or stabilizing post-transcriptional mRNA. And it would be interesting to conduct an in-depth study of this mechanism.

Compared with transcriptional regulations, such translational enhancement has several drawbacks. First, due to the lack of antibodies, it is difficult to quantify the protein level for many genes (e.g. *SKC1*). It would be a big problem if one cannot evaluate the consequence of genome editing. Second, AMVE is the strongest enhancer among the 12 candidates, and up to 10.4-times improvement was found for *SKC1*. However, sometimes we may need a stronger enhancement for breeding, and further screening for better enhancers is recommended in the future. However, we found that the effects of translation enhancers in protoplast-based luciferase reporter were not exactly the same as those of endogenous genes in rice plant. We believe that the flanking sequence of the target gene may also have an impact on protein translation, and that future optimization of reporting systems is needed to accurately evaluate translation regulation. Lastly, it could be found that the

10.3389/fpls.2023.1134209

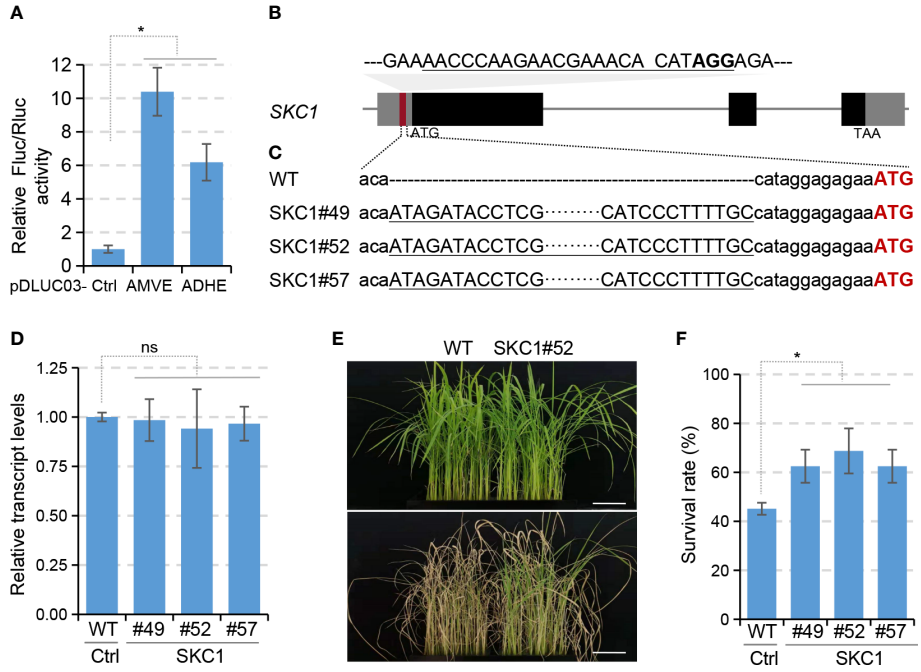


FIGURE 3
Knock-in of AMVE to improve salt tolerance of rice. **(A)** Assessment of enhancers ADHE and AMVE in protoplast-based dual-luciferase assays. Plasmids pDLUC02-SKC1 with or without (Ctrl) enhancer sequences were used as reporters. **(B)** Schematic diagram of *SKC1* for AMVE knock-in. The sgRNA target of Cas9 is underlined with the PAM in bold. **(C)** Sequencing results of AMVE knock-in mutants. Sequences of AMVE were underlined and the start codon of *SKC1* is in red. **(D)** Transcription levels of *SKC1* in WT (Ctrl) and T2 mutants were determined using qRT-PCR. The rice *Actin1* gene was used as the internal control. **(E, F)** Morphological and survival comparisons of the WT plants and T2 mutants in salt-stress treatment. Four-week-old rice seedlings (upper) were treated with 150 mM NaCl for 7 days (lower). Bar, 5 cm. **(A, D, F)** All values represent means ± s.d. of three independent experiments (n = 3). *$P < 0.05$; ns, no significant difference (two-tailed Student' s *t* test).

translational enhancement differs to some extent among genes. We speculate that this may be affected by the original translation efficiency or expression level of the gene like the cis-elements for transcription regulation. For genes that do not have room for translational optimization, the enhancement may be limited. Despite the success of the two cases on *WRKY71* and *SKC1*, evaluations on other genes would provide more information in the future. Off-target editing is another concern for plant breeding. We tested whether this insertion strategy could induce off-target editing at these predicted off-target sites and no mutation was detected (Supplementary Table 5).

In conclusion, we screened a functional enhancer AMVE for translational regulation in rice. Targeted knock-in of AMVE into the 5'UTRs of *WRKY71* and *SKC1* successfully improved the protein abundance, resulted in expected trait improvement. It is the first study that using translational enhancer for such *in-locus* activation of target genes, providing a new strategy to manipulate protein translation. With the development of genome editing technologies, *in-locus* gene activation mediated by editing of regulatory elements will become easier over time, making this strategy a useful method for breeding.

Data availability statement

The raw data supporting the conclusions of this article will be made available by the authors, without undue reservation.

Author contributions

YL and RS designed the study. RS, YT, and QY performed the most experiments. QY, DZ, XZ, and XL performed rice transformation. CD and XC genotyped the transgenic lines. RS, YL, YT, and J-KZ wrote and revised the manuscript. All authors contributed to the article and approved the submitted version.

Funding

This study was supported by the National Natural Science Foundation of China (No. 32070396) and the National Key R&D Program of China (No. 2021YFD1201300).

Conflict of interest

The authors declare that the research was conducted in the absence of any commercial or financial relationships that could be construed as a potential conflict of interest.

Publisher's note

All claims expressed in this article are solely those of the authors and do not necessarily represent those of their affiliated organizations, or those of the publisher, the editors and the reviewers. Any product that may be evaluated in this article, or claim that may be made by its manufacturer, is not guaranteed or endorsed by the publisher.

Supplementary material

The Supplementary Material for this article can be found online at: https://www.frontiersin.org/articles/10.3389/fpls.2023.1134209/full#supplementary-material

References

De Amicis, F., Patti, T., and Marchetti, S. (2007). Improvement of the pBI121 plant expression vector by leader replacement with a sequence combining a poly(CAA) and a CT motif. *Transgenic Res.* 16, 731–738. doi: 10.1007/s11248-006-9063-x

Dong, O. X., Yu, S., Jain, R., Zhang, N., Duong, P. Q., Butler, C., et al. (2020). Marker-free carotenoid-enriched rice generated through targeted gene insertion using CRISPR-Cas9. *Nat. Commun.* 11, 1178. doi: 10.1038/s41467-020-14981-y

Farquharson, K. L. (2009). Targeted overexpression of a sodium transporter in the root stele increases salinity tolerance. *Plant Cell* 21, 1875. doi: 10.1105/tpc.109.210710

Gallie, D. R. (2002). The 5'-leader of tobacco mosaic virus promotes translation through enhanced recruitment of eIF4F. *Nucleic Acids Res.* 30, 3401–3411. doi: 10.1093/nar/gkf457

Gallie, D. R., and Walbot, V. (1992). Identification of the motifs within the tobacco mosaic virus 5'-leader responsible for enhancing translation. *Nucleic Acids Res.* 20, 4631–4638. doi: 10.1093/nar/20.17.4631

Jobling, S. A., and Gehrke, L. (1987). Enhanced translation of chimaeric messenger RNAs containing a plant viral untranslated leader sequence. *Nature* 325, 622–625. doi: 10.1038/325622a0

Kanoria, S., and Burma, P. K. (2012). A 28 nt long synthetic 5'UTR (synJ) as an enhancer of transgene expression in dicotyledonous plants. *BMC Biotechnol.* 12, 85. doi: 10.1186/1472-6750-12-85

Kobayashi, N. I., Yamaji, N., Yamamoto, H., Okubo, K., Ueno, H., Costa, A., et al. (2017). OsHKT1;5 mediates na(+) exclusion in the vasculature to protect leaf blades and reproductive tissues from salt toxicity in rice. *Plant J.* 91, 657–670. doi: 10.1111/tpj.13595

Leppek, K., Das, R., and Barna, M. (2018). Functional 5' UTR mRNA structures in eukaryotic translation regulation and how to find them. *Nat. Rev. Mol. Cell Biol.* 19, 158–174. doi: 10.1038/nrm.2017.103

Li, S., Li, J., He, Y., Xu, M., Zhang, J., Du, W., et al. (2019). Precise gene replacement in rice by RNA transcript-templated homologous recombination. *Nat. Biotechnol.* 37, 445–450. doi: 10.1038/s41587-019-0065-7

Li, J., Meng, X., Zong, Y., Chen, K., Zhang, H., Liu, J., et al. (2016). Gene replacements and insertions in rice by intron targeting using CRISPR-Cas9. *Nat. Plants* 2, 16139. doi: 10.1038/nplants.2016.139

Li, J., Zhang, X., Sun, Y., Zhang, J., Du, W., Guo, X., et al. (2018). Efficient allelic replacement in rice by gene editing: A case study of the NRT1.1B gene. *J. Integr. Plant Biol.* 60, 536–540. doi: 10.1111/jipb.12650

Liu, X., Bai, X., Wang, X., and Chu, C. (2007). OsWRKY71, a rice transcription factor, is involved in rice defense response. *J. Plant Physiol.* 164, 969–979. doi: 10.1016/j.jplph.2006.07.006

Liu, H., Ding, Y., Zhou, Y., Jin, W., Xie, K., and Chen, L. L. (2017). CRISPR-p 2.0: An improved CRISPR-Cas9 tool for genome editing in plants. *Mol. Plant* 10, 530–532. doi: 10.1016/j.molp.2017.01.003

Liu, L., Gallagher, J., Arevalo, E. D., Chen, R., Skopelitis, T., Wu, Q., et al. (2021a). Enhancing grain-yield-related traits by CRISPR-Cas9 promoter editing of maize CLE genes. *Nat. Plants* 7, 287–294. doi: 10.1038/s41477-021-00858-5

Liu, X., Liu, H., Zhang, Y., He, M., Li, R., Meng, W., et al. (2021b). Fine-tuning flowering time *via* genome editing of upstream open reading frames of heading date 2 in rice. *Rice (N Y)* 14, 59. doi: 10.1186/s12284-021-00504-w

Liu, Q., Yang, J., Zhang, S., Zhao, J., Feng, A., Yang, T., et al. (2016). OsGF14b positively regulates panicle blast resistance but negatively regulates leaf blast resistance in rice. *Mol. Plant Microbe Interact.* 29, 46–56. doi: 10.1094/MPMI-03-15-0047-R

Lu, Y., Ronald, P. C., Han, B., Li, J., and Zhu, J. K. (2020a). Rice protein tagging project: A call for international collaborations on genome-wide in-locus tagging of rice proteins. *Mol. Plant* 13, 1663–1665. doi: 10.1016/j.molp.2020.11.006

Lu, Y., Tian, Y., Shen, R., Yao, Q., Wang, M., Chen, M., et al. (2020b). Targeted, efficient sequence insertion and replacement in rice. *Nat. Biotechnol.* 38, 1402–1407. doi: 10.1038/s41587-020-0581-5

Lu, Y., Ye, X., Guo, R., Huang, J., Wang, W., Tang, J., et al. (2017). Genome-wide targeted mutagenesis in rice using the CRISPR/Cas9 system. *Mol. Plant* 10, 1242–1245. doi: 10.1016/j.molp.2017.06.007

Quan, R., Wang, J., Hui, J., Bai, H., Lyu, X., Zhu, Y., et al. (2017). Improvement of salt tolerance using wild rice genes. *Front. Plant Sci.* 8, 2269. doi: 10.3389/fpls.2017.02269

Ren, Z. H., Gao, J. P., Li, L. G., Cai, X. L., Huang, W., Chao, D. Y., et al. (2005). A rice quantitative trait locus for salt tolerance encodes a sodium transporter. *Nat. Genet.* 37, 1141–1146. doi: 10.1038/ng1643

Rodriguez-Leal, D., Lemmon, Z. H., Man, J., Bartlett, M. E., and Lippman, Z. B. (2017). Engineering quantitative trait variation for crop improvement by genome editing. *Cell* 171, 470–480. doi: 10.1016/j.cell.2017.08.030

Shi, J., Gao, H., Wang, H., Lafitte, H. R., Archibald, R. L., Yang, M., et al. (2017). ARGOS8 variants generated by CRISPR-Cas9 improve maize grain yield under field drought stress conditions. *Plant Biotechnol. J.* 15, 207–216. doi: 10.1111/pbi.12603

Song, X., Meng, X., Guo, H., Cheng, Q., Jing, Y., Chen, M., et al. (2022). Targeting a gene regulatory element enhances rice grain yield by decoupling panicle number and size. *Nat. Biotechnol.* 40, 1403–1411. doi: 10.1038/s41587-022-01281-7

Sugio, T., Satoh, J., Matsuura, H., Shinmyo, A., and Kato, K. (2008). The 5'-untranslated region of the oryza sativa alcohol dehydrogenase gene functions as a translational enhancer in monocotyledonous plant cells. *J. Biosci. Bioeng* 105, 300–302. doi: 10.1263/jbb.105.300

Wang, X., Aguirre, L., Rodriguez-Leal, D., Hendelman, A., Benoit, M., and Lippman, Z. B. (2021). Dissecting cis-regulatory control of quantitative trait variation in a plant stem cell circuit. *Nat. Plants* 7, 419–427. doi: 10.1038/s41477-021-00898-x

Xie, X., Ma, X., Zhu, Q., Zeng, D., Li, G., and Liu, Y. G. (2017). CRISPR-GE: A convenient software toolkit for CRISPR-based genome editing. *Mol. Plant* 10, 1246–1249. doi: 10.1016/j.molp.2017.06.004

Xu, G., Yuan, M., Ai, C., Liu, L., Zhuang, E., Karapetyan, S., et al. (2017). uORF-mediated translation allows engineered plant disease resistance without fitness costs. *Nature* 545, 491–494. doi: 10.1038/nature22372

Zeng, D., Liu, T., Ma, X., Wang, B., Zheng, Z., Zhang, Y., et al. (2020). Quantitative regulation of waxy expression by CRISPR/Cas9-based promoter and 5'UTR-intron editing improves grain quality in rice. *Plant Biotechnol. J.* 18, 2385–2387. doi: 10.1111/pbi.13427

Zhang, H., Si, X., Ji, X., Fan, R., Liu, J., Chen, K., et al. (2018). Genome editing of upstream open reading frames enables translational control in plants. *Nat. Biotechnol.* 36, 894–898. doi: 10.1038/nbt.4202

Zou, Z., Eibl, C., and Koop, H. U. (2003). The stem-loop region of the tobacco psbA 5'UTR is an important determinant of mRNA stability and translation efficiency. *Mol. Genet. Genomics MGG* 269, 340–349. doi: 10.1007/s00438-003-0842-2

frontiers | Frontiers in Plant Science

TYPE Original Research
PUBLISHED 04 April 2023
DOI 10.3389/fpls.2023.1120584

Check for updates

OPEN ACCESS

EDITED BY
Tianlun Zhao,
Zhejiang University, China

REVIEWED BY
Chenchen Zhao,
University of Tasmania, Australia
Rui-Qing Li,
Anhui Agricultural University, China

*CORRESPONDENCE
Qiangqiang Xiong
qqxiong@yzu.edu.cn

SPECIALTY SECTION
This article was submitted to Plant Abiotic Stress, a section of the journal Frontiers in Plant Science

RECEIVED 10 December 2022
ACCEPTED 20 March 2023
PUBLISHED 04 April 2023

CITATION
Sun C, Wang R, Tang G, Cai S, Shi H, Liu F, Xie H, Zhu J and Xiong Q (2023) Integrated 16S and metabolomics revealed the mechanism of drought resistance and nitrogen uptake in rice at the heading stage under different nitrogen levels. *Front. Plant Sci.* 14:1120584. doi: 10.3389/fpls.2023.1120584

COPYRIGHT
© 2023 Sun, Wang, Tang, Cai, Shi, Liu, Xie, Zhu and Xiong. This is an open-access article distributed under the terms of the Creative Commons Attribution License (CC BY). The use, distribution or reproduction in other forums is permitted, provided the original author(s) and the copyright owner(s) are credited and that the original publication in this journal is cited, in accordance with accepted academic practice. No use, distribution or reproduction is permitted which does not comply with these terms.

Integrated 16S and metabolomics revealed the mechanism of drought resistance and nitrogen uptake in rice at the heading stage under different nitrogen levels

Changhui Sun[1,2], Runnan Wang[1,2], Guoping Tang[3], Shuo Cai[4], Hong Shi[4], Fangping Liu[4], Hengwang Xie[4], Jinyan Zhu[1,2,5] and Qiangqiang Xiong[1,2,4,5]*

[1]Jiangsu Key Laboratory of Crop Genetics and Physiology, Agricultural College of Yangzhou University, Yangzhou, China, [2]Jiangsu Key Laboratory of Crop Cultivation and Physiology, Agricultural College of Yangzhou University, Yangzhou, China, [3]Jiangxi Academy of Agricultural Sciences Rice Research Institute, Nanchang, China, [4]Jiangxi Irrigation Experiment Central Station, Nanchang, China, [5]Jiangsu Co-Innovation Center for Modern Production Technology of Grain Crops, Yangzhou University, Yangzhou, China

The normal methods of agricultural production worldwide have been strongly affected by the frequent occurrence of drought. Rice rhizosphere microorganisms have been significantly affected by drought stress. To provide a hypothetical basis for improving the drought resistance and N utilization efficiency of rice, the study adopted a barrel planting method at the heading stage, treating rice with no drought or drought stress and three different nitrogen (N) levels. Untargeted metabolomics and 16S rRNA gene sequencing technology were used to study the changes in microorganisms in roots and the differential metabolites (DMs) in rhizosphere soil. The results showed that under the same N application rate, the dry matter mass, N content and N accumulation in rice plants increased to different degrees under drought stress. The root soluble protein, nitrate reductase and soil urease activities were improved over those of the no-drought treatment. Proteobacteria, Bacteroidota, Nitrospirota and Zixibacteria were the dominant flora related to N absorption. A total of 184 DMs (98 upregulated and 86 downregulated) were identified between low N with no drought (LN) and normal N with no drought (NN); 139 DMs (83 upregulated and 56 downregulated) were identified between high N with no drought (HN) and NN; 166 DMs (103 upregulated and 63 downregulated) were identified between low N with drought stress (LND) and normal N with drought stress (NND); and 124 DMs (71 upregulated and 53 downregulated) were identified between high N with drought stress (HND) and NND. Fatty acyl was the metabolite with the highest proportion. KEGG analysis showed that energy metabolism pathways, such as D-alanine metabolism and the phosphotransferase system (PTS), were enriched. We conclude that N-metabolism enzymes with higher activity and higher bacterial diversity have a significant effect on drought tolerance and nitrogen uptake in rice.

KEYWORDS

rice, heading date, nitrogen, drought, 16S rRNA, metabolomics

Introduction

Dramatic changes in global climate will increase the intensity and frequency of drought events. The phenomenon of persistent drought has become more frequent in the southern region of China (Xiong et al., 2020). A record-breaking heat wave hit the Yangtze River valley during the boreal summer of 2022 (Zhang et al., 2023). Meteorological drought in the Yangtze River Basin has continued to develop, and the situation of rice production has been relatively severe. The lack of water not only inhibits the growth and development of crops but also affects the absorption, utilization and distribution of nutrients in crops, resulting in changes in the accumulation of dry matter and nutrients in various organs (Li and Yang, 2017; Asadi and Eshghizadeh, 2021). When encountering drought stress, it is generally believed that drought first acts on the root system, affecting the morphological structure and physiological activity of the root system and changing its ability to absorb water and nutrients (Steinemann et al., 2015; Li et al., 2020). At the same time, there are certain effects on the root microbial community and metabolites. Due to the reduced cost and increasing throughput of next-generation sequencing, major advances in characterizing these communities have recently been achieved, mainly through the use of amplicon sequencing of the 16SrRNA gene. Compositional analysis of these communities is important to develop tools that will let us manipulate root-associated microbiota for increased crop productivity (Edwards et al., 2018). Studies have shown that the overall response of the bacterial microbiota to drought stress is taxonomically consistent across soils and cultivars and is primarily driven by an enrichment of multiple Actinobacteria and Chloroflexi, as well as a depletion of several Acidobacteria and Deltaproteobacteria (Santos-Medellín et al., 2017). The energy metabolism pathway, carbon fixation in the photosynthetic organism pathway, carbohydrate metabolic process, and reactive oxygen species metabolic process functions have a certain correlation with drought stress (Xiong et al., 2019a).

Water and fertilizer are the two main factors that limit agricultural production. The mutual restriction of water and fertilizer affects the growth of crop roots (Gu et al., 2016). Therefore, when crops encounter arid environments, the growth and metabolism of crops are also limited by nutrients. Soil moisture affects not only the transformation and migration of nutrients in the soil but also the absorption, transport and distribution of nutrients by the plant by affecting the metabolic process of the plant. Nutrients also affect plant water status and the progression of drought stress (Gonzalez-Dugo et al., 2010; Shao et al., 2019). Among them, nitrogen (N) is one of the main elements of amino acids, chlorophyll, nucleic acids, lipids and many intermediate metabolites. N plays an important role in plant growth and agricultural production (Xiong et al., 2019c), further affecting the enrichment of root microorganisms. Studies have shown that compared with no N fertilizer treatment, N application causes the N-fixing bacterial community in rice roots to aggregate and significantly increases the relative abundance of Methylosinus in rice roots (Liu et al., 2021). Appropriate coupled regulation of water and N can create a good rhizosphere environment for rice growth (Xu et al., 2017a), and mild dry-wet alternating irrigation and moderate N increase the enzyme activity in rice rhizosphere soil and increase the number of microorganisms in the soil (Xu et al., 2017b). N deficiency at the tillering stage and N compensation at the young panicle differentiation stage increase the activities of nitrate reductase and glutamine synthase (Xiong et al., 2018). In this study, Yangda 3 (late-maturing medium *japonica*) was used as the experimental material. The barrel cultivation method was used to apply no drought and drought stress at the heading stage. Three different N application levels were set. The study aimed to explore the effect of different water and N applications on the effects of the SPAD value of rice leaves, dry matter mass of rice organs, N content of rice organs and soil, N accumulation of rice organs, N-metabolic enzyme activities of roots and soil urease activities. Furthermore, integrated microbiology and liquid chromatography-mass spectrometry (LC-MS) metabolomics analysis was used to reveal the N uptake mechanism of rice in response to drought stress under different N levels. This study provides a theoretical reference for improving rice drought resistance and N utilization efficiency.

Abbreviations: N, nitrogen; DMs, differential metabolites; LN, low N with no drought; NN, normal N with no drought; HN, high N with no drought; LND, low N with drought stress; NND, normal N with drought stress; HND, high N with drought stress; PTS, phosphotransferase system; LC-MS, liquid chromatography-mass spectrometry; NR, nitrate reductase; GS, glutamine synthetase; PCA, principal component analysis; OPLS-DA, orthogonal partial least-squares-discriminant analysis; VIP, variable importance of projection; PCoA, principal coordinate analysis; KEGG, Kyoto Encyclopedia of Genes and Genomes.

Materials and methods

Experimental material

The late-maturing medium *japonica* conventional *japonica* rice variety Yangda 3 (Rice No.20210062, Nanjing 46 irradiated early-maturing line/Suxiangjing 3) was used as the experimental material. The rice seeds were provided by the College of Agriculture, Yangzhou University.

Cultivation method

The experiment was carried out in 2021 in the on-campus potting field of the College of Agriculture, Yangzhou University. The barrel planting method was adopted. The height of each barrel was 25 cm, the outer diameter of the upper part of the barrel was 28 cm, and the inner diameter of the bottom of the barrel was 20 cm. The seeds were subjected to a sterilization treatment and sown on May 26, 2021, then the rice plants were transplanted on June 18. Seedlings with good and consistent growth were selected for transplanting, with 3 holes per barrel, 2 seedlings per hole, and 15 kg of air-dried soil per pot. After transplanting, water, disease and pest management were carried out according to high-yield cultivation methods.

Experimental design

A one-time basic application of phosphate fertilizer (6.0 g of calcium magnesium phosphate rock powder) was utilized. At the tillering stage and heading stage, 1.5 g of potassium chloride was applied to each barrel, and N fertilizer application was based on basal fertilizer:tiller fertilizer:panicle fertilizer = 5:3:2. The experiment was designed with three N application levels: low N (2 g according to pure N, 100 kg·hm^{-2}), normal N (control, 4.5 g according to pure N, 225 kg·hm^{-2}), and high N (7.5 g according to pure N, 375 kg·hm^{-2}), and the source of N was urea. Drought stress and no drought were carried out for each N application level. The no-drought treatment: The rice was kept in a 2 cm water layer after transplanting. Drought stress: In the early stage of the no-drought treatment, from August 28 to September 3, the barrels were transported to the net room to dry naturally to approximately 10% of the soil moisture. A soil moisture meter was installed to monitor the soil moisture (measuring range 0 ~ 100%, WKT-M3, Jiangsu VicoMeter Instrumentation Co., Ltd., China), at this time the rice was at the heading stage. On September 3, the drought ended, and rehydration treatment (keeping the rice in a 2 cm water layer) was carried out. According to drought and different nitrogen levels, six treatments were set in the experiment: low N with no drought (LN), normal N with no drought (NN), high N with no drought (HN), low N with drought stress (LND), normal N with drought stress (NND), and high N with drought stress (HND). Each treatment was replicated three times, and 10 plastic barrels were used per replication. Overall, there were 30 parallel barrels with consistent growth conditions per treatment available for sampling. Thus, the 6 treatments had a total of 180 barrels.

Determination of the SPAD value, dry matter, N content, and enzymatic activity

On the first day after the drought treatment, a SPAD-502 chlorophyll analyser (Zhejiang, China) was used to measure the SPAD value of the second bottom leaf of rice. Six rice plants with good and consistent growth were selected to measure the SPAD value of the base, middle and top of the leaf, and the average value was taken. At the heading stage, three rice plant samples were taken from each treatment and separated into the roots, stem sheaths, leaves and panicles. The dry matter samples were placed at 105°C for 30 min, dried to constant weight in an 80°C oven, and then weighed. The N content was determined by the Kjeldahl method (Sihite, 2022). The soluble protein content and nitrate reductase (NR), glutamine synthetase (GS) and soil urease activities were determined using kits from Suzhou Michy Biomedical Technology Co., Ltd. (Suzhou, China).

Sample collection

Rice rhizosphere soil sampling: The entire rice root system and soil as a whole were excavated, the soil around the roots was removed, and only the soil on the roots was retained. A total of 10 g soil was obtained from each treatment, and three biological replicates were obtained from each treatment. Each sample was mixed.

Nonrhizosphere soil sampling: In the barrels from which the rice rhizosphere soil samples were taken, the soil was collected 10 cm from the plant to a depth of about 20 cm and put into a sampling tube. A total of 10 g soil was obtained from each treatment, and three biological replicates were obtained from each treatment. Each sample was mixed.

Rice root sampling: The whole rice plant was dug out with a shovel, the soil was washed with tap water, and root tips with a length of approximately 5 cm were taken. Three biological replicates were taken from each treatment.

All samples were first frozen in liquid N, transported to the laboratory and stored in a -80°C ultralow-temperature freezer until measurement.

High-throughput sequencing

In this study, the V3-V4 region of the bacterial 16S rRNA (16S) gene was used as the target DNA sequence for PCR amplification. The V3-V4 region of 16S rDNA was amplified with the forward primer 343F (5'-TACGGRAGGCAGCAG-3') and the reverse primer 798R (5'-AGGGTATCTAATCCT-3'). The PCR conditions were as follows: predenaturation at 95°C for 3 min; denaturation at 95°C for 30 s, annealing at 55°C for 30 s, and extension at 72°C for 45 s for 25 cycles, followed by extension at 72°C for 20 min. After amplification, the PCR amplification products were subjected to gel electrophoresis using 2% agarose to check the amplification effect. The PCR products of the samples were subjected to high-throughput sequencing on the Illumina MiSeq platform. The DNA extracting and 16S sequencing was performed according to the method of Zhu et al. (2022). 16S sequencing and analysis were conducted by OE Biotech Co., Ltd. (Shanghai, China). The 16S rRNA gene raw sequencing data from this study have been deposited in the Genome Sequence Archive in BIG Data Center (http://bigd.big.ac.cn/), Beijing Institute of Genomics (BIG) Chinese Academy of Sciences, under the accession number: CRA005709.

Determination of rhizosphere soil metabolites

To determine the rhizosphere soil metabolites, 20 μL of an internal standard (L-2-chlorophenylalanine, 0.06 mg·mL^{-1}; methanol configuration) and 1 mL methanol-water (V:V=1:1) were added to a 500 mg soil sample. Two small steel balls were added, placed at -20°C for 2 min to precool, and added to a grinder for grinding (60 Hz, 2 min), and the homogenized sample was transferred into a 15 mL centrifuge tube with 1 mL methanol-water (V:V=1:1). If the transfer tube wall remained, the above operation was repeated once. After centrifugation for 10 min (7700 rpm, 4°C), 2.5 mL of supernatant was placed in a 5 mL centrifuge

tube, lyophilized, reconstituted with 400 µL methanol-water (V: V=1:4), vortexed for 60 s, sonicated for 30 s, and centrifuged for 10 min (12000 rpm, 4°C). A total of 150 µL of the supernatant was aspirated with a syringe, filtered with a 0.22 µm organic phase pinhole filter, transferred to an LC injection vial, and stored at -80°C.

The analytical instrument in this experiment was an LC-MS system composed of an ACQUITY UPLC I-Class plus ultrahigh-performance liquid phase tandem QE high-resolution mass spectrometer. Chromatographic conditions: column: ACQUITY UPLC HSS T3 (100 mm×2.1 mm, 1.8 um); column temperature: 45°C; mobile phase: mobile phase: A-water (containing 0.1% formic acid), B-acetonitrile (containing 0.1% Formic acid); flow rate: 0.35 $mL{\cdot}min^{-1}$; injection volume: 2 µL. Mass spectrometry conditions: ion source: electron spray ionization; sample mass spectrometry signals were collected in positive and negative ion scanning modes.

16S and metabolome analysis

16S analysis was performed according to the method of Zhu et al. (2022). Metabolome analysis was conducted by OE Biotech Co., Ltd. (Shanghai, China). The original LC-MS data were processed by Progenesis QI V2.3 software (Nonlinear Dynamics, Newcastle, UK) for baseline filtering, peak identification, integral, retention time correction, peak alignment, and normalization. The main parameters of 5 ppm precursor tolerance, 10 ppm product tolerance, and 5% product ion threshold were applied. Compound identification was based on the precise mass-to-charge ratio (M/z), secondary fragments, and isotopic distribution using the human metabolome database, lipid maps (V2.3), metlin, electron microscopy data bank, plant metabolome data bank, and self-built databases to perform qualitative analysis.

The extracted data were then further processed by removing any peaks with a missing value (ion intensity = 0) in more than 50% of groups, by replacing the zero value by half of the minimum value, and by screening according to the qualitative results of the compound. Compounds with resulting scores less than 36 (out of 60) were also deemed to be inaccurate and were removed. A data matrix was combined from the positive and negative ion data.

The matrix was imported into R to carry out principal component analysis (PCA) to observe the overall distribution among the samples and the stability of the whole analysis process. Orthogonal partial least-squares-discriminant analysis (OPLS-DA) and partial least-squares-discriminant analysis were utilized to distinguish the metabolites that differed between groups. To prevent overfitting, 7-fold cross-validation and 200-response permutation testing were used to evaluate the quality of the model.

Variable importance of projection (VIP) values obtained from the OPLS-DA model were used to rank the overall contribution of each variable to group discrimination. A two-tailed Student's t test was further used to verify whether the differences in metabolites between groups were significant. Differential metabolites were selected with VIP values > 1.0 and P values < 0.05.

Data analysis

Excel 2019 was used for data organization, Adobe Illustrator 2022 was used to integrate all figures. PCA and correlation heatmaps were drawn in the R language. SPAD, plant biomass, N content and accumulation, N-metabolism enzymes activity data were subjected to multivariate statistical Tukey's test analysis with SPSS 18.0 software. In the multivariate analysis of microbial communities, ANOVA was used to compare the composition of microbial communities among treatments. The Chao1 index, Shannon index, Simpson index, 16S rRNA and environmental factor data were tested with Kruskal–Wallis statistical tests.

Results

Effects of different water and N conditions on the SPAD value of rice leaves

Under no drought and drought stress, the SPAD value of rice leaves increased with increasing N application rate (Figure 1A). Under no drought stress, the SPAD value of HN was increased by 13.64% compared with that of LN, and there was a significant difference. Under drought stress, the SPAD value of NND was 8.18% higher than that of LND and reached a significant level. The SPAD value of HND was 12.97% higher than that of NND, and the difference was significant. The SPAD value of HND was 22.21% higher than that of LND, and the difference was significant.

Effects of different water and N conditions on the dry matter mass of rice

There were differences in the dry matter mass of various organs of rice under different water and N conditions (Table 1 and Supplementary Figure 1). Under no drought stress, the root dry matter mass of LN was 76.11% lower than that of NN. The root dry matter mass of HN was 27.99% lower than that of NN, and there was a significant difference. The stem sheath dry matter mass of NN was 61.52% higher than that of LN. The dry matter mass of leaves under NN increased by 109.88% compared with that under LN. The dry matter mass of leaves in HN increased by 43.92% compared with NN, and the difference was significant. Compared with LN, the panicle dry matter mass of NN increased by 122.78% and reached a significant level.

Under drought stress, the dry matter mass of roots under LND decreased by 67.16% compared with that under NND, and the difference was significant. The dry matter mass of the stem sheaths in the LND treatment decreased by 64.81% compared with that in the NND treatment. The dry matter mass of leaves under LND decreased by 76.92% compared with that under NND, and the difference was significant. Under LND, the panicle dry matter mass decreased by 62.37% compared with that under NND.

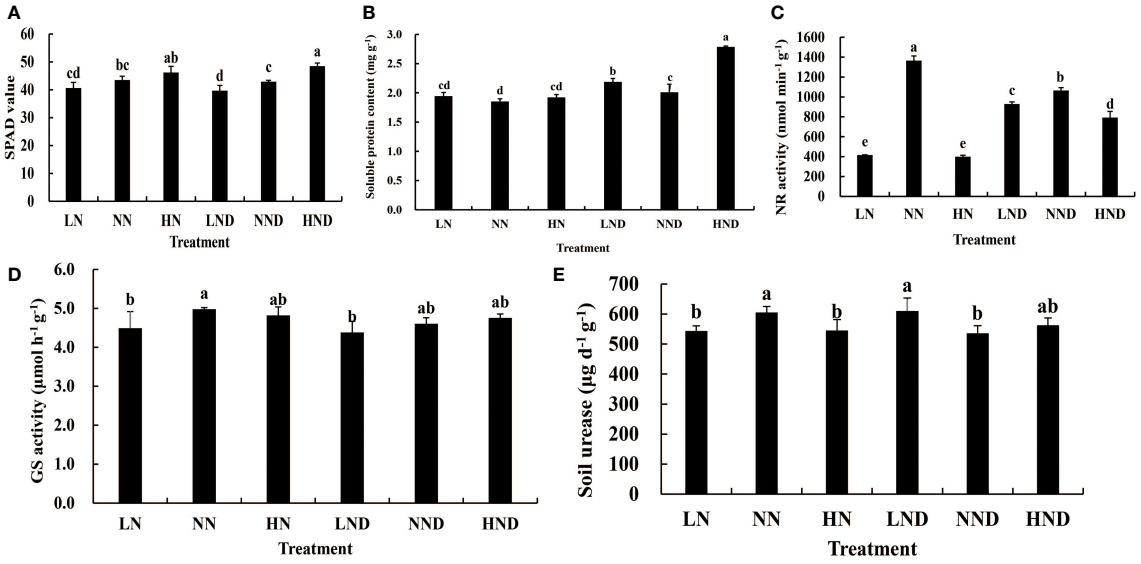


FIGURE 1
Effects of different water and N conditions on the rice leaf SPAD value and N-metabolism enzyme activities. **(A)** SPAD value; **(B)** soluble protein content; **(C)** NR activity; **(D)** GS activity; **(E)** soil urease activity. Lower-case letters represent the significance of the p-value at the 0.05 level.

Effects of different water and N conditions on the N content of rice organs and soil

The N content of each organ of rice increased with increasing N application rate (Table 2 and Supplementary Figure 1). In the no-drought treatment, the root N content of NN increased by 41.06% compared with that of LN. The root N content of HN increased by 54.18% compared with that of NN, and the difference reached a significant level. Compared with NN, the N content of the stem sheaths in HN increased by 44.18%, and there was a significant difference. The N content of leaves under NN increased by 15.56% compared with that under LN. The N content of leaves in HN increased by 20.99% compared with that in NN, and there was a significant difference. Compared with LN, the panicle N content under NN increased by 4.3%, and the difference reached a significant level.

Under drought stress, the N content of roots under NND increased by 14.73% compared with that under LND. The N content of roots under HND increased by 31.68% compared with that under NND, and the difference reached a significant level. The N content of the stem sheaths under NND increased by 18.49% compared with that under LND. Compared with NND, the N content of the stem sheaths in HND increased by 52.63%, and the difference reached a significant level. The N content of leaves under NND increased by 12.76% compared with that under LND. The N content of leaves under HND increased by 18.89% compared with that under NND, and there was a significant difference. Compared with that under LND, the panicle N content under NND increased by 13.46%, which was a significant difference.

Under different water and N conditions, the N contents of the rhizosphere soil and nonrhizosphere soil were also different (Table 2). Under the no-drought treatment, the N content of the nonrhizosphere soil decreased gradually with increasing N application rate. The N content of the nonrhizosphere soil under NN decreased by 3.45% compared with that under LN. The N content of the nonrhizosphere soil in HN was decreased by 10.71% compared with NN, and there was a significant difference. The N content of rhizosphere soil in HN was 5.88% higher than that in NN, a significant difference. Under drought stress, with the increase in the N application rate, the N content of the nonrhizosphere soil first decreased and then increased. The N content of nonrhizosphere soil in NND was 6.17% lower than

TABLE 1 Effects of different water and N conditions on the dry mass of various organs in rice.

Treatment	Root (g·plant-1)	Stem-sheath (g·plant^{-1})	Leaf (g·plant^{-1})	Panicle (g·plant^{-1})
LN	1.40c	9.85c	2.43d	3.38b
NN	5.86a	15.91b	5.10c	7.53a
HN	4.22b	20.51ab	7.34a	8.16a
LND	1.10c	6.39c	1.35d	2.54b
NND	3.35b	18.16ab	5.85bc	6.75a
HND	4.14b	21.97a	6.95ab	8.15a

Different lowercase letters indicate significant differences at $P < 0.05$. The same applies below.

10.3389/fpls.2023.1120584

TABLE 2 Effects of different water and N conditions on the N contents of rice organs and soil.

Treatment	Root (g·kg^{-1})	Stem-sheath (g·kg^{-1})	Leaf (g·kg^{-1})	Panicle (g·kg^{-1})	Soil (g·kg^{-1})	Rhizosphere soil (g·kg^{-1})
LN	2.63f	4.27c	16.90c	10.23cd	0.87a	0.83c
NN	3.71e	5.50b	19.53b	10.67bc	0.84b	0.85c
HN	5.72b	7.93a	23.63a	11.13ab	0.75d	0.90ab
LND	4.21d	4.49c	18.03c	9.81d	0.81c	0.86bc
NND	4.83c	5.32b	20.33b	11.13ab	0.75d	0.91a
HND	6.36a	8.12a	24.17a	11.83a	0.80c	0.83c

Lower-case letters represent the significance of the p-value at the 0.05 level.

that in LND. The N content in the nonrhizosphere soil under HND decreased by 6.67% compared with that under NND. The N content of the rhizosphere soil first increased and then decreased with increasing N application rate. The N content of rhizosphere soil in NND increased by 5.81% compared with that in LND. The N content of rhizosphere soil under HND decreased by 8.79% compared with that under NND, and the difference was significant.

Under the same N application rate, the N content of roots and leaves under drought stress was higher than that under the no-drought treatment.

Effects of different water and N conditions on N accumulation in various organs of rice

Accumulated N is the product of dry matter mass and N content, and a certain differences in N accumulation also occur due to changes in the N content and dry matter mass in various organs of rice under different water and N conditions (Table 3 and Supplementary Figure 1). In the no-drought treatment, the N accumulation of roots in LN decreased by 83.03% compared with that in NN, and the difference reached a significant level. The N accumulation of roots in HN increased by 10.09% compared with that in NN, although the difference was not significant. Compared with that under LN, the N accumulation in the stem sheaths under NN increased by 108.1%. The N accumulation of the stem sheaths in HN increased by 86.61% compared with that in NN, and there was a significant difference. The N accumulation in leaves under LN was 58.69% lower than that under NN. Compared with NN, the N accumulation of leaves in HN increased by 74.17%, and there was a significant difference. The N accumulation of the panicle under LN decreased by 56.98% compared with that under NN, and the difference reached a significant level.

Under drought stress, the N accumulation of roots in LND decreased by 70.99% compared with that in NND. The root N accumulation under HND increased by 61.73% compared with that under NND, and the difference reached a significant level. Compared with NND, the N accumulation of the stem sheaths in LND decreased by 70.14%. The N accumulation in the stem sheaths under HND increased by 85.64% compared with that under NND, and there was a significant difference. Compared with NND, the HND plants accumulated 41.33% more leaves, and the difference reached significance. The N accumulation of the panicle in LND decreased by 66.8% compared with that in NND, and the difference was significant.

Under the same N application rate, the effects of drought stress on N accumulation in various organs of rice were different. Compared with the no-drought treatment, the N accumulation of roots in LND and HND increased by 27.03% and 9.17%, respectively.

Effects of different water and N conditions on the activity of N-metabolism enzymes

Under different N application rates, the soluble protein content of roots under drought stress was higher than that under no drought

TABLE 3 Effects of different water and N conditions on N accumulation in various organs of rice.

Treatment	Root (g·plant^{-1})	Stem-sheath (g·plant^{-1})	Leaf (g·plant^{-1})	Panicle (g·plant^{-1})
LN	0.37c	4.2c	4.11c	3.45b
NN	2.18ab	8.74b	9.95b	8.02a
HN	2.4a	16.31a	17.33a	9.07a
LND	0.47c	2.87c	2.41c	2.49b
NND	1.62b	9.61b	11.88b	7.5a
HND	2.62a	17.84a	16.79a	9.69a

Lower-case letters represent the significance of the p-value at the 0.05 level.

stress to varying degrees (Figure 1B). The root soluble protein content of LND was 12.89% higher than that of LN. The root soluble protein content of NND was 8.65% higher than that of NN. The soluble protein content of HND was 45.31% higher than that of HN. Under the same N application rate, the root NR activity under drought stress was significantly different from that under no-drought treatment (Figure 1C). The root NR activity of HND was 99.12% higher than that of HN. The root NR activity of LND was 123.79% higher than that of LN. Under both drought stress and no-drought treatment, the NR activity of roots in NN was the highest, indicating that moderate N fertilizer can maintain higher NR activity. Compared with LN, the root GS activity of LND decreased by 2.45%. The root GS activity under NND was 7.63% lower than that under NN. The root GS activity of HND decreased by 1.45% compared with that of HN, although the difference was not significant (Figure 1D). The urease activity in the rhizosphere soil after drought stress was different from that under the no-drought treatment (Figure 1E). The rhizosphere soil urease activity of LND increased by 12.17% compared with that of LN, and there was a significant difference. The rhizosphere soil urease activity of HND increased by 3.35% compared with that of HN, although the difference was not significant. Compared with NN, the rhizosphere soil urease activity of NND decreased by 11.53%, and there was a significant difference.

16S analysis

A petal diagram was drawn based on the overlap of sample OTUs for the analysis of shared and unique OTUs between different samples (Figure 2A). As seen from the figure, LN contained 1802 OTUs, including 368 unique OTUs; LND contained 1810 OTUs, including 376 unique OTUs. NN contained 1840 OTUs, including 406 unique OTUs; NND contained 1814 OTUs, including 380 unique OTUs. HN contained 1825 OTUs, including 391 unique OTUs. HND contained 1674 OTUs, including 240 unique OTUs.

The root microbial community composition was similar under different water and N conditions, but the proportion of various microorganisms was different. At the phylum level, Proteobacteria, Bacteroidota and Nitrospirota were the dominant groups, with HN accounting for 37.49%, 13.28%, and 2.40%, HND accounting for 38.88%, 17.17%, and 1.16%, LN accounting for 44.95%, 10.84%, and 3.03%, LND accounting for 49.03%, 10.24%, and 2.71%, NN accounting for 43.69%, 15.02%, and 1.92%, and NND accounting for 50.18%, 11.49%, and 1.52%, respectively (Figures 2B, C). Compared with the no-drought treatment, under the same N application rate, the proportion of Proteobacteria in LND was higher than that in LN. The proportion of Proteobacteria in NND was higher than that in NN. The proportion of Proteobacteria in HND was higher than that in HN, indicating that under the same N application rate, drought stress had a higher proportion. Drought stress was beneficial for increasing the abundance of Proteobacteria in the roots. Under the no-drought treatment, the proportion of Bacteroidota in NN was higher than that in LN and HN, indicating that the appropriate amount of N applied increased the abundance of Bacteroidota in the roots.

We assessed alpha diversity between treatments using Chao1, Shannon and Simpson indices (Figures 3A-C). The results showed that there was no significant difference in the Chao1 index between LND and LN, NND and NN, and HND and HN under the same N application rate. The Shannon and Simpson indices of HND were significantly lower than those of HN, indicating that compared with the no-drought treatment, the high N treatment significantly reduced the microbial diversity of roots under drought stress.

We performed PCoA (principal coordinate analysis) on the samples (Figure 3D), and two principal components (PC1 and PC2) were extracted, i.e., 53.3% and 14.77%, respectively. The results showed that there were some differences among the samples. The closer the sample distance, the more similar the species composition. The farther the sample distance, the more different the species composition. Under the same N application rate, compared with the no-drought treatment, the distance between the samples in the HND was farther than that in HN, indicating that compared with the no-drought treatment, the high N treatment under drought stress had the most significant effect on the changes in the composition and structure of root microbial species.

Metabolic profiling

Multivariate statistical analysis was performed on 18 rhizosphere soil samples by the PCA method, and the 18 samples were all within the 95% confidence interval. In the PCA score plot, two principal components (PC1 and PC2) were extracted, i.e., 21.1% and 14.9%, respectively (Figure 3E). The results showed that under different water and N conditions, there were certain differences between treatments. The drought treatments clustered at the left side but the N levels were not clearly separated. For the water treatments, the differences between nitrogen rates were much greater when the data points from HN and NN are mixed.

A total of 184 DMs (98 upregulated and 86 downregulated) were identified between LN and NN (Supplementary Figure 2A and Figure 3F). Among them were 29 fatty acyls, accounting for 15.76% (Supplementary Table 1). A total of 139 DMs (83 upregulated and 56 downregulated) were identified between HN and NN (Supplementary Figure 2B and Figure 3F). There were 29 fatty acyls, accounting for 10.79% (Supplementary Table 2). A total of 166 DMs (103 upregulated and 63 downregulated) were identified between LND and NND (Supplementary Figure 2C and Figure 3F). There were 15 fatty acyls, accounting for 9.04% (Supplementary Table 3). A total of 124 DMs (71 upregulated and 53 downregulated) were identified between HND and NND (Supplementary Figure 2D and Figure 3F). Among them were 14 fatty acyls, accounting for 11.29% (Supplementary Table 4).

KEGG analysis

The Kyoto Encyclopedia of Genes and Genomes (KEGG) database is the main public database of metabolic pathways and can be used in studies of metabolite accumulation in a general

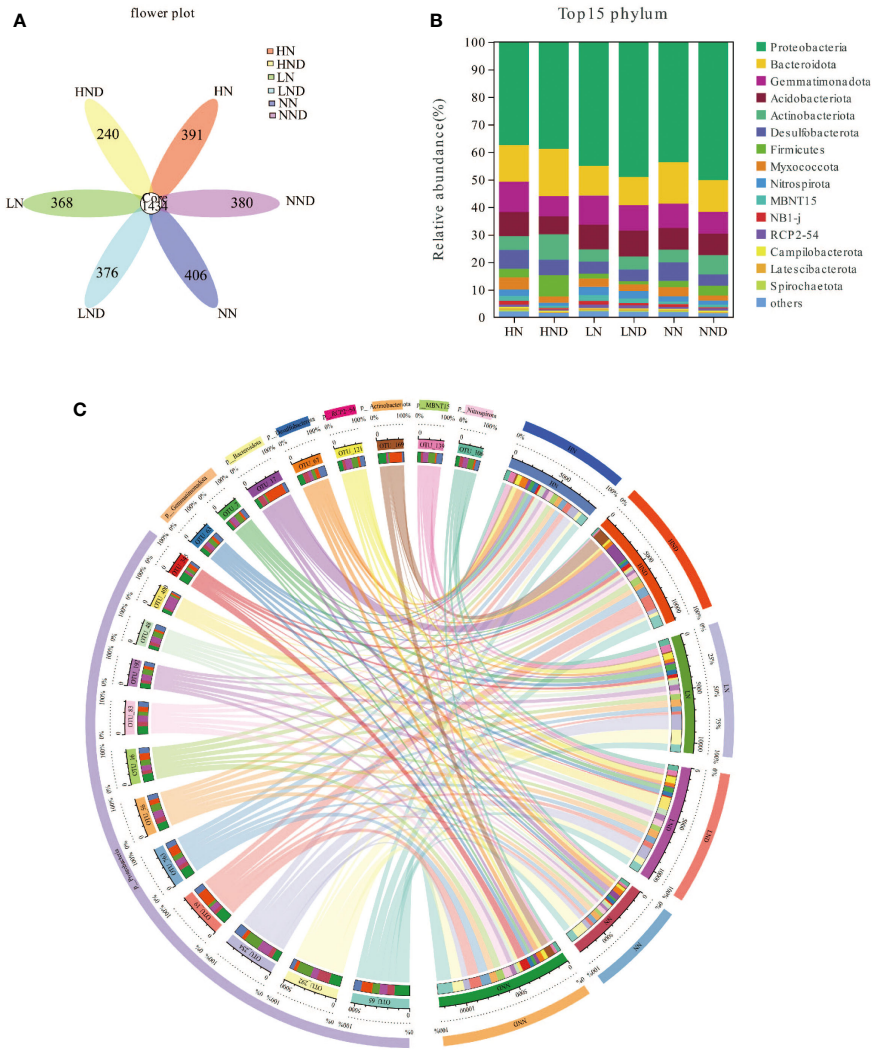


FIGURE 2
Root microbial community structure composition and diversity analysis. **(A)** Petal map of root microbial OTUs; **(B)** Bar plot of root microbial species composition changes at the phylum level; **(C)** Circos plot of root microbial species composition changes at the phylum level.

network. In this study, we enriched the differential metabolites of each comparison group and classified them into different pathways (Supplementary Table 5). We found that arginine and proline metabolism were enriched in the LN and NN comparison groups. Amino sugar and nucleotide sugar metabolism were enriched in the LN and NN comparison groups and the LND and NND comparison groups. The phosphotransferase system (PTS) was enriched in the HN and NN comparison groups and the HND and NND comparison groups.

D-Alanine metabolism and phenylalanine, tyrosine and tryptophan biosynthesis were enriched in the HN and HND comparison groups, NN and NND comparison groups, and LN and LND comparison groups. This indicated that under the same N application rate, drought stress treatment had a certain degree of influence on D-alanine metabolism and phenylalanine, tyrosine and tryptophan biosynthesis in rhizosphere soil.

Correlation analysis

We conducted a correlation analysis between environmental factors, N content, accumulation, dry matter mass and 16S rRNA. Root NR activity was significantly positively correlated with Proteobacteria ($P < 0.05$) (Figure 4A). The leaf N content, panicle N content, stem sheath N content, root N content, leaf N accumulation, panicle N accumulation, stem sheath N accumulation, and root N accumulation were significantly negatively correlated with Nitrospirota and Zixibacteria (Figure 4B). The N accumulation, panicle N accumulation, stem sheath N accumulation, and root N accumulation in leaves were significantly negatively correlated with Proteobacteria (Figure 4C). The correlation between N content, accumulation, N-metabolism enzyme activities and 16S rRNA is visualized more intuitively in Figure 5.

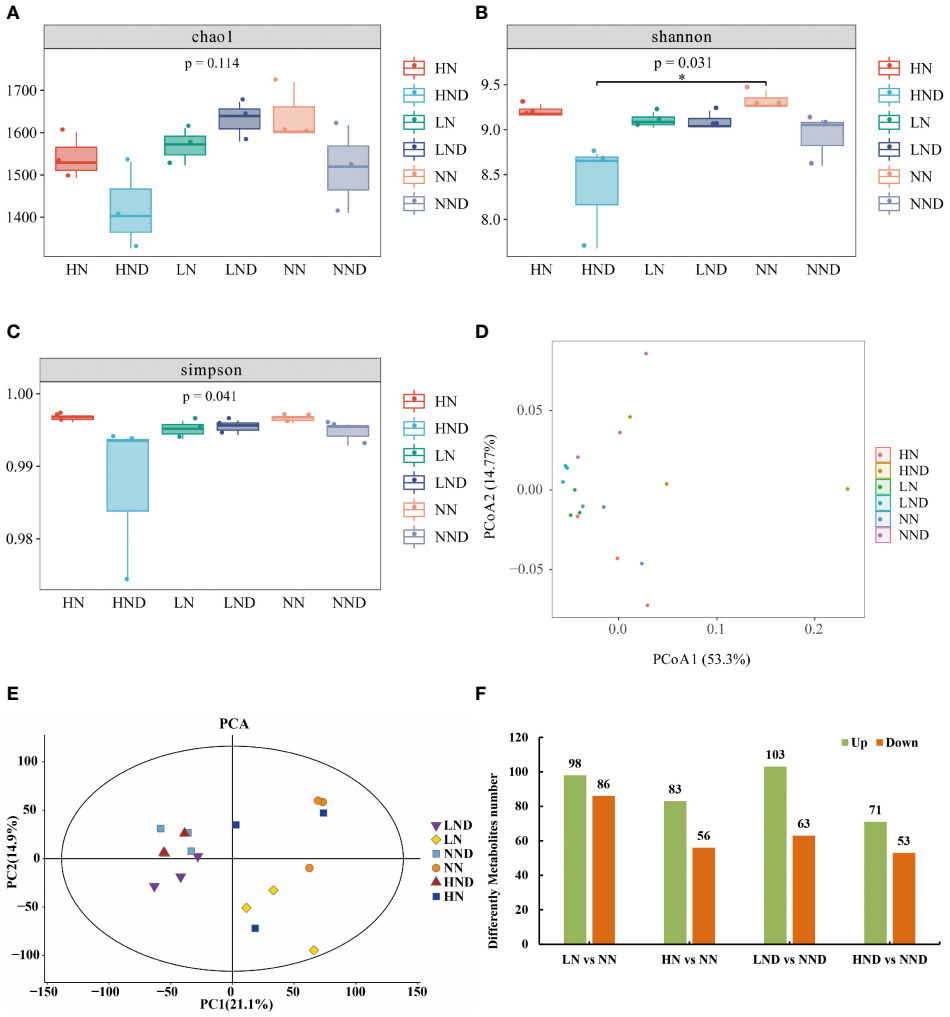


FIGURE 3
Root microbial diversity analysis, beta diversity analysis and up-and-downregulated DMs. **(A)** Chao1 index of the root microbial community; **(B)** Shannon index; **(C)** Simpson index; **(D)** PCoA of the root microbial community; **(E)** PCA of rhizosphere soil samples; **(F)** Up- and downregulated DMs. *p < 0.05.

Discussion

Analysis of nitrogen uptake and 16S

Under the same N fertilizer level, the leaf SPAD value decreased with the decrease in soil water potential. Under the same soil water potential, the leaf SPAD value increased with the increase in N fertilizer level (Cheng et al., 2007). This study also showed that the SPAD value of rice leaves increased with the increase in N application under no drought and drought stress (Figure 1A). Dry matter is an important indicator for measuring crop yield, and moderate drought is beneficial to the increase in dry matter accumulation in rice (Yi et al., 2020) and the operation of dry matter in rice (Li et al., 2008). This study showed that the dry matter content of stem sheaths and leaves under NND increased to a certain extent compared with that under NN (Table 1). Water deficit can increase the air content in the plough layer soil, thereby increasing the soil redox potential, reducing the toxic substances, enhancing the root vigour, and enhancing the absorption of N by the roots (Liu, 2009). Mild water stress enhanced the ability of N redistribution and reuse in leaves and stem sheaths before heading, and it reduced N retention in stems and leaves, thereby improving N use efficiency and export efficiency (Wang et al., 2004). In this study, compared with the no-drought treatment, under the same N application rate, drought stress increased the N content of rice roots and leaves to a certain extent, and N accumulation in the stem sheaths of NND and HND increased to a certain extent (Tables 2 and 3). Nitrospirota is a key taxon that regulates N uptake by rice roots after abrupt drought-flood transitions (Zhu et al., 2022). One study found that the relative abundance of the phylum Zixibacteria was positively correlated with soil mineral N (Ihsan et al., 2022). The results of 16S analysis in this study showed that Nitrospirota was the dominant bacterium related to N absorption. The correlation analysis further showed that leaves N content, panicle N content, stem sheath N content, root N content, leaf N accumulation, panicle N accumulation, stem sheath N accumulation, and root N accumulation were significantly

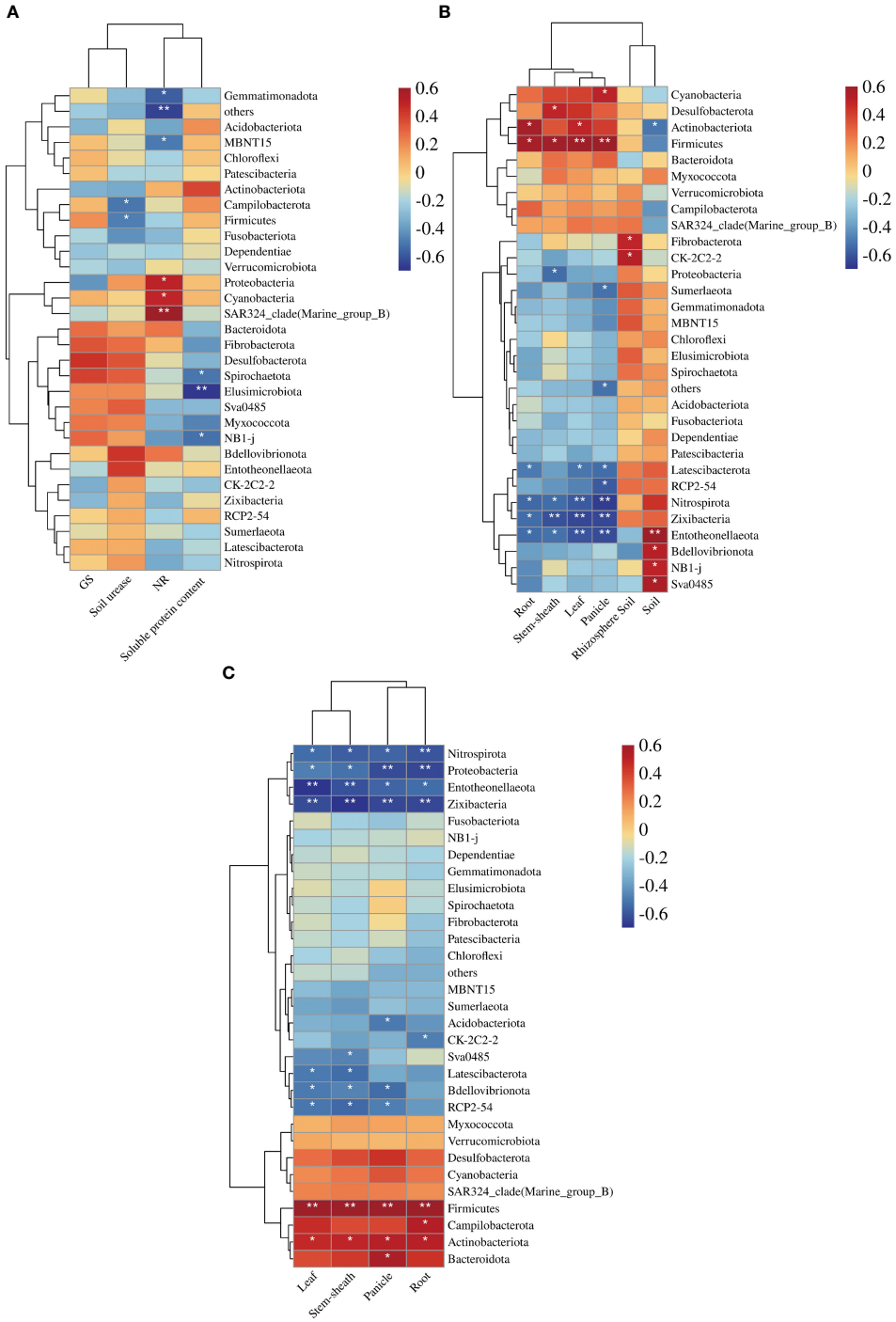


FIGURE 4
Correlation analysis between the environmental factors, N content, accumulation, dry matter mass and 16S rRNA. **(A)** Heat map of the correlation between 16S and N-metabolism enzyme activity; **(B)** Heat map of the correlation between 16S and N content; **(C)** Heat map of the correlation between 16S and N accumulation. Each grid represents the correlation between the two attributes, and different colors represent the size of the correlation coefficient between the attributes. *p < 0.05; **p < 0.01.

negatively correlated with Nitrospirota and Zixibacteria (Figures 2B, C and 4B, C), which indicates that Nitrospirota and Zixibacteria had an important effect on N uptake in rice plants. Under drought stress, the content of soluble protein in the roots of rice seedlings increased rapidly and showed an upwards trend with increasing stress duration (Feng et al., 2020). The root NR activity of maize seedlings under drought stress was higher than that of the control (Si and Wu, 2001). A certain degree of drought stress enhanced root vigour, resulting in rapid root growth and increased secretions, which worked together with soil microorganisms to increase urease activity (Wang et al., 2020). In this study, under drought stress, root soluble protein, NR and soil urease activities increased to a certain extent (Figures 1B, C,

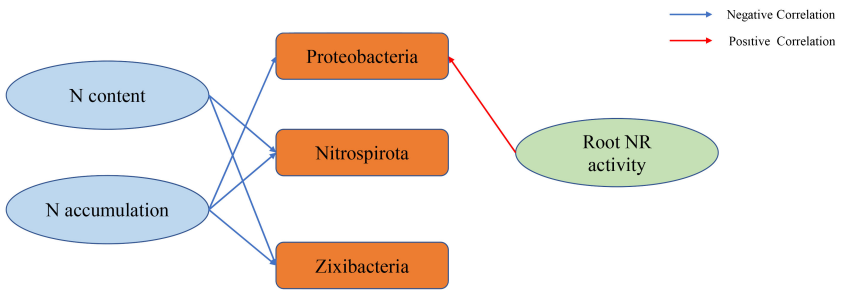


FIGURE 5
Flow chart visualizing the correlations between the N-metabolism enzyme activities, N content, accumulation and 16S.

E). At the same time, the results of 16S analysis showed that under the same N application rate, drought stress increased the root Proteobacteria abundance (Figures 2B, C). Proteobacteria have better drought resistance, especially with thicker cell walls, which are more resistant to water stress, explaining their obvious enrichment after drought stress (Wang et al., 2021). The correlation analysis also showed that root NR activity was significantly positively correlated with Proteobacteria (Figure 4A). Bacteroidota in the rhizosphere soil are easily enriched at the heading stage of rice (Chen et al., 2022). Appropriate N application can increase the abundance of Bacteroidota in rhizosphere soil. At the same time, Bacteroidota has also been identified as a highly N-sensitive bacterial group and a dominant phylum related to N absorption (Wang et al., 2022). Nitrogen addition usually inhibits microbial biomass, alleviating the effect of nitrogen limitation on some microorganisms, especially nitrifiers and denitrifiers that use inorganic nitrogen for energy or as an electron acceptor. A high level of N fertilizer can have a negative effect on the root microbial community (Liu et al., 2023). With the increase in nitrogen, some microorganisms with weak tolerance to high permeability potential may be killed, resulting in a decrease in microbial diversity (Xiong et al., 2021). This study also found that moderate N application was beneficial to the enhancement of Bacteroidota abundance in roots (Figures 2B, C). Therefore, moderate N application increased the bacterial diversity, and root bacterial abundance was increased under drought stress. This could provide a new idea for improving rice drought resistance.

Analysis of metabolites and enrichment pathways

The LN and NN comparison group, HN and NN comparison group, LND and NND comparison group, and HND and NND comparison group had the most different metabolites in fatty acyls (Supplementary Tables 1-4), indicating that N application had a more significant effect on fatty acyls. Increasing the N supply can effectively increase the level of N-containing phospholipids, which in turn leads to the decomposition of diacylglycerols and triglycerides, thereby releasing more fatty acyl groups (Allwood et al., 2019). Amino acids, nitrogenous compounds and fatty acids were observed to be significantly different under different N supply levels. Most of them were increased by high N and decreased by low N (Xin et al., 2019). Arginine and proline metabolism and a one-carbon pool supplied by folate have been enriched after the addition of N fertilizer. Anthocyanin and flavonoid biosynthesis have also been enriched, meaning that N application was highly correlated with the synthesis of nutrients (Zhao et al., 2023). Low-N stress influenced the metabolism of arginine and proline (Hou et al., 2021). Rice N deficiency enrichment pathways are mainly associated with amino sugar and nucleotide sugar metabolism (Shen et al., 2019). In this study, arginine and proline metabolism were enriched in the LN and NN comparison groups. Amino sugar and nucleotide sugar metabolism were enriched in the LN and NN comparison groups and the LND and NND comparison groups (Supplementary Table 5). The phosphotransferase system (PTS) regulates N and carbon pools to maintain balance. For example, when N is limiting, the PTS system will work with the nitrogen stress response to enhance N uptake and metabolism (Hagberg et al., 2022). In this study, the HN and NN comparison groups and the HND and NND comparison groups were enriched with respect to the PTS (Supplementary Table 5). Amino acid sugars and nucleotide sugars are often used as glucose donors in the biosynthesis of various oligosaccharides and polysaccharides and are active forms of sugar synthesis or interconversion. Phosphoenolpyruvate: sugar PTS plays an important role in phosphorylating and transporting glucose in *Escherichia coli* (Zhou, 2010). This study found that under the same N application rate, drought treatment had a significant effect on D-alanine metabolism in rhizosphere soils and on phenylalanine, tyrosine and tryptophan biosynthesis (Supplementary Table 5). D-Alanine metabolism was highly enriched in the leaves of Camellia Tieguanyin plants under drought stress (Guo et al., 2017). Differentially expressed genes involved in phenylalanine, tyrosine and tryptophan biosynthesis were all upregulated specifically in a drought-tolerant Eruca line under drought stress (Huang et al., 2019). Energy metabolism pathways change strongly under abrupt drought–flood alteration stress (Xiong et al., 2019b). This study also showed that under drought stress and N application, the rhizosphere soil was mainly enriched in the energy metabolism pathway. Drought stress has a certain effect on the activity of N-metabolism enzymes in roots. The changes in the activities of N-metabolism enzymes further affected root microbial diversity and N absorption and utilization, thereby affecting the adaptability of rice to drought stress, which is of great significance for rice microbial drought resistance breeding.

Conclusions

In this study, under the no-drought treatment and drought stress, the SPAD values of the rice leaves, dry matter mass of each organ, N content and N accumulation in each organ were positively correlated with the N application rate. Proteobacteria, Bacteroidota and Nitrospirota were the dominant flora related to root N uptake. There was a correlation between Proteobacteria and root NR activity and between Nitrospirota, Zixibacteria and the rice plant N content and N accumulation. Compared with the no-drought treatment, a certain degree of drought stress enhanced the N uptake and utilization capacity of the rice roots and stem sheaths. The activities of N-metabolism enzymes in roots also increased to varying degrees. Metabolites related to N uptake in rhizosphere soils were mainly fatty acyls. The results of KEGG analysis showed that energy metabolism pathways such as D-alanine metabolism, phenylalanine, tyrosine and tryptophan biosynthesis, arginine and proline metabolism, amino sugar and nucleotide sugar metabolism, and PTS were enriched in the rhizosphere soil under different water and N conditions. The comprehensive analysis of root N-metabolizing enzyme activities, microbial diversity and rhizosphere soil metabolites provides a new perspective on water and N regulation in rice breeding for drought resistance.

Data availability statement

The original contributions presented in the study are publicly available. This data can be found here: NGDC, CRA005709.

Author contributions

QX conceived and designed the experiment. GT, SC, HS, FL and JZ performed the data analysis. CS, HX and RW executed the experiment, analysed the data and interpreted the results. QX and CS wrote the manuscript. All authors contributed to the article and approved the submitted version.

Funding

We are grateful for financial support from the National Natural Science Foundation of China (32101816), Postgraduate Research & Practice Innovation Program of Jiangsu Province (SJCX22_1782), the Project funded by China Postdoctoral Science Foundation (2021M702768), Jiangsu Province Postdoctoral Research Funding (2021K292B), Jixi Province Postdoctoral Scientific Research Funding (2021KY47) and the Priority Academic Program Development of Jiangsu Higher Education Institutions (PAPD).

Conflict of interest

The authors declare that the research was conducted in the absence of any commercial or financial relationships that could be construed as a potential conflict of interest.

Publisher's note

All claims expressed in this article are solely those of the authors and do not necessarily represent those of their affiliated organizations, or those of the publisher, the editors and the reviewers. Any product that may be evaluated in this article, or claim that may be made by its manufacturer, is not guaranteed or endorsed by the publisher.

Supplementary material

The Supplementary Material for this article can be found online at: https://www.frontiersin.org/articles/10.3389/fpls.2023.1120584/full#supplementary-material

SUPPLEMENTARY FIGURE 1
Phenotypic figures of 6 treatments at the heading stage. **(A)** LN; **(B)** LND; **(C)** NN; **(D)** NND; **(E)** HN; **(F)** HND.

SUPPLEMENTARY FIGURE 2
Rhizosphere soil differential metabolite volcano maps.

SUPPLEMENTARY TABLE 1
Identification information for DMs between the LN and NN treatments.

SUPPLEMENTARY TABLE 2
Identification information for DMs between the HN and NN treatments.

SUPPLEMENTARY TABLE 3
Identification information for DMs between the LND and NND treatments.

SUPPLEMENTARY TABLE 4
Identification information for DMs between the HND and NND treatments.

SUPPLEMENTARY TABLE 5
Enriched KEGG pathways associated with DMs.

References

Allwood, J. W., Xu, Y., Martinez-Martin, P., Palau, R., Cowan, A., Goodacre, R., et al. (2019). Rapid UHPLC-MS metabolite profiling and phenotypic assays reveal genotypic impacts of nitrogen supplementation in oats. *Metabolomics* 15, 1–19.

Asadi, M., and Eshghizadeh, H. R. (2021). Response of sorghum genotypes to water deficit stress under different CO_2 and nitrogen levels. *Plant Physiol. Bioch.* 158, 255–264.

Chen, C., Song, W., Sun, L., Qin, S., Ren, C., Yang, J., et al. (2022). Effect of seaweed extract supplement on rice rhizosphere bacterial community in tillering and heading stages. *Agronomy* 12, 342.

Cheng, J., Cao, C., Cai, M., Yuan, B., and Zhai, J. (2007). Physiological characteristics of rice under water stress and nitrogen nutrition. the crop science society of china.

proceedings of the 2007 annual academic conference of the crop science society of China. *Crop Sci. Soc. China*, 155–160.

Edwards, J., Santos-Medellín, C., and Sundaresan, V. (2018). Extraction and 16S rRNA sequence analysis of microbiomes associated with rice roots. *Bio-protocol* 8, e2884–e2884.

Feng, H., Zhang, L., and Chen, H. (2020). Effect of exogenous acetic acid on alleviating drought stress in the roots of rice seedlings. *Plant Physiol. J.* 56, 209–218.

Gonzalez-Dugo, V., Durand, J. L., and Gastal, F. (2010). Water deficit and nitrogen nutrition of crops. *A Rev. Agron. Sustain Dev.* 30, 529–544.

Gu, J., Dong, M., Zhao, B., Chen, P., Ji, H., and Han, L. (2016). Effects of dry matter accumulation and photosynthate transporation of stem and sheath and grain production under different water and nitrogen management in rice. *J. Nucl. Agric. Sci.* 30, 347–354.

Guo, Y., Zhao, S., Zhu, C., Chang, X., Yue, C., Wang, Z., et al. (2017). Identification of drought-responsive miRNAs and physiological characterization of tea plant (Camellia sinensis l.) under drought stress. *BMC Plant Biol.* 17, 1–20.

Hagberg, K. L., Price, J. P., Yurgel, S. N., and Kahn, M. L. (2022). The sinorhizobium meliloti nitrogen stress response changes radically in the face of concurrent phosphate stress. *Front. Microbiol.* 13.

Hou, W., Wang, J., Christensen, M. J., Liu, J., Zhang, Y., Liu, Y., et al. (2021). Metabolomics insights into the mechanism by which epichloë gansuensis endophyte increased achnatherum inebrians tolerance to low nitrogen stress. *Plant Soil* 463, 487–508.

Huang, B. L., Li, X., Liu, P., Ma, L., Wu, W., Zhang, X., et al. (2019). Transcriptomic analysis of eruca vesicaria subs. sativa lines with contrasting tolerance to polyethylene glycol-simulated drought stress. *BMC Plant Biol.* 19, 1–11.

Ihsan, M., Li, Y., Shakeel, A., Muhammad, Z., Saqib, F., Izhar, A., et al. (2022). Irrigation and nitrogen fertilization alter soil bacterial communities, soil enzyme activities, and nutrient availability in maize crop. *Front. Microbiol.* 13, 105.

Li, G., Tang, X., Cheng, Y., Li, Z., Cai, K., and Huang, Y. (2008). Compensatory reponse of rice yield and its modules to durative water stress. *Acta Scientiarum Naturalium Universitatis Sunyatseni* 3, 94–99.

Li, S., Wan, L., Nie, Z., and Li, X. (2020). Fractal and topological analyses and antioxidant defense systems of alfalfa (Medicago sativa l.) root system under drought and rehydration regimes. *Agronomy* 10, 805.

Li, J., and Yang, J. (2017). Research advances in the effects of water, nitrogen and their interaction on the yield, water and nitrogen use efficiencies of rice. *Chin. J. Rice Sci.* 31, 327–334.

Liu, H. (2009). Effect of water-saving irrigation on dry matter and nitrogen content of rice root. *Shandong Agric. Sci.* 3, 19–21.

Liu, Y., Chu, G., Stirling, E., Zhang, H., Chen, S., Xu, C., et al. (2023). Nitrogen fertilization modulates rice seed endophytic microbiomes and grain quality. *Sci. Total Environ.* 857, 159181.

Liu, J., Han, J., Zhu, C., Cao, W., Luo, Y., Zhang, M., et al. (2021). Elevated atmospheric CO_2 and nitrogen fertilization affect the abundance and community structure of rice root-associated nitrogen-fixing bacteria. *Front. Microbiol.* 12, 628108.

Santos-Medellín, C., Edwards, J., Liechty, Z., Nguyen, B., and Sundaresan, V. (2017). Drought stress results in a compartment-specific restructuring of the rice root-associated microbiomes. *MBio* 8, e00764–e00717.

Shao, S., Ma, B., Chang, Y., Jing, W., Hou, D., Zhao, B., et al. (2019). Research progress on effects of interactions between water and nitrogen on yield formation in rice. *China Rice* 25, 21–25.

Shen, T., Xiong, Q., Zhong, L., Shi, X., Cao, C., He, H., et al. (2019). Analysis of main metabolisms during nitrogen deficiency and compensation in rice. *Acta Physiol. Plant* 41, 1–14.

Si, Q., and Wu, H. (2001). Effect of different stress on roots activity and nitrate reductase activity in zea mays l. *Agric. Res. Arid Areas* 2, 67–70.

Sihite, W. (2022). Penentuan kadar air, nitrogen (N) pada pupuk npk dengan menggunakan metode gravimetri dan kjeldahl. *Universitas Sumatera Utara*.

Steinemann, S., Zeng, Z., McKay, A., Heuer, S., Langridge, P., and Huang, C. Y. (2015). Dynamic root responses to drought and rewatering in two wheat (Triticum aestivum) genotypes. *Plant Soil* 391, 139–152.

Wang, S., Cao, W., Ding, Y., Tian, Y., and Jiang, D. (2004). Interactions of water management and nitrogen fertilizer on nitrogen absorption and utilization in rice. *Scientia Agricultura Sin.* 4, 497–501.

Wang, H., Li, X., and Chen, M. (2020). Effects of water-nitrogen coupling on enzyme activities in rhizosphere soil of adzuki bean with different drought tolerance. *J. Shanxi Agric. Sci.* 48, 1812–1815+1819.

Wang, J., Liao, L., Ye, Z., Liu, H., Zhang, C., Zhang, L., et al. (2022). Different bacterial co-occurrence patterns and community assembly between rhizosphere and bulk soils under n addition in the plant–soil system. *Plant Soil* 471, 697–713.

Wang, K., Nan, L., Shi, S., and Guo, Q. (2021). Influence of root growth and bacterial community in the rhizosphere of different root types of alfalfa under drought stress. *Acta Ecol. Sin.* 41, 7735–7742.

Xin, W., Zhang, L., Zhang, W., Gao, J., Yi, J., Zhen, X., et al. (2019). An integrated analysis of the rice transcriptome and metabolome reveals root growth regulation mechanisms in response to nitrogen availability. *Int. J. Mol. Sci.* 20, 5893.

Xiong, Q., Cao, C., Shen, T., Zhong, L., He, H., and Chen, X. (2019a). Comprehensive metabolomic and proteomic analysis in biochemical metabolic pathways of rice spikes under drought and submergence stress. *BBA Proteins Proteom* 1867, 237–247.

Xiong, Q., Hu, J., Wei, H., Zhang, H., and Zhu, J. (2021). Relationship between plant roots, rhizosphere microorganisms, and nitrogen and its special focus on rice. *Agriculture* 11, 234.

Xiong, Q., Shen, T., Zhong, L., Zhu, C., Peng, X., He, X., et al. (2019b). Comprehensive metabolomic, proteomic and physiological analyses of grain yield reduction in rice under abrupt drought–flood alternation stress. *Physiol. Plantarum* 167, 564–584.

Xiong, Q., Tang, G., Zhong, L., He, H., and Chen, X. (2018). Response to nitrogen deficiency and compensation on physiological characteristics, yield formation, and nitrogen utilization of rice. *Front. Plant Sci.* 9, 1075.

Xiong, Q., Zhong, L., Du, J., Zhu, C., Peng, X., He, X., et al. (2020). Ribosome profiling reveals the effects of nitrogen application translational regulation of yield recovery after abrupt drought-flood alternation in rice. *Plant Physiol. Bioch.* 155, 42–58.

Xiong, Q., Zhong, L., Shen, T., Cao, C., He, H., and Chen, X. (2019c). iTRAQ-based quantitative proteomic and physiological analysis of the response to n deficiency and the compensation effect in rice. *BMC Genomics* 20, 1–16.

Xu, G., Lu, D., Sun, H., Wang, H., and Li, Y. (2017a). Alternative wetting and drying irrigation and nitrogen coupling on rhizosphere environment of rice. *Trans. Chin. Soc. Agric. Eng.* 33, 186–194.

Xu, G., Sun, H., Lu, D., Wang, H., and Li, Y. (2017b). Differences in ultrastructure and activity of rice roots under different irrigation and nitrogen supply levels. *J. Plant Nutr. Fertilizers* 23, 811–820.

Yi, Z., Zhu, D., Wang, Y., Hu, G., Zhang, Y., Xiang, J., et al. (2020). Effects of water deficit on rice seedling quality and its regulation. *China Rice* 26, 32–36.

Zhang, D., Chen, L., Yuan, Y., Zuo, J., and Ke, Z. (2023). Why was the heat wave in the Yangtze river valley abnormally intensified in late summer 2022. *Environ. Res. Lett.* 18, 034014.

Zhao, F., Wang, Y., Hu, J., Shi, S., Zhang, H., Wang, Y., et al. (2023). Metabolite profiling of wheat response to cultivar improvement and nitrogen fertilizer. *Metabolites* 13, 107.

Zhou, J. (2010). Modification of phosphoenolpyruvate: carbohydrate phosphotransferase system of escherichia coli by genetic engineering and characterization of mutants. *Anhui Normal Univ.*

Zhu, J., Li, A., Zhang, J., Sun, C., Tang, G., Chen, L., et al. (2022). Effects of nitrogen application after abrupt drought-flood alternation on rice root nitrogen uptake and rhizosphere soil microbial diversity. *Environ. Exp. Bot.* 201, 105007.

frontiers | Frontiers in Plant Science

TYPE Original Research
PUBLISHED 05 April 2023
DOI 10.3389/fpls.2023.1168723

Check for updates

OPEN ACCESS

EDITED BY
Meng Jiang,
Zhejiang University, China

REVIEWED BY
Guanfu Fu,
China National Rice Research Institute (CAAS), China
Yunlong Wang,
Nanjing Agricultural University, China
Qingyun Bu,
Chinese Academy of Sciences (CAS), China

*CORRESPONDENCE
Tao Wu
jidawt@163.com
Xinglin Du
duxinglin2004@163.com

SPECIALTY SECTION
This article was submitted to Plant Abiotic Stress, a section of the journal Frontiers in Plant Science

RECEIVED 18 February 2023
ACCEPTED 22 March 2023
PUBLISHED 05 April 2023

CITATION
Zhang M, Zhao R, Huang K, Wei Z, Guo B, Huang S, Li Z, Jiang W, Wu T and Du X (2023) OsWRKY76 positively regulates drought stress *via* OsbHLH148-mediated jasmonate signaling in rice. *Front. Plant Sci.* 14:1168723. doi: 10.3389/fpls.2023.1168723

COPYRIGHT
© 2023 Zhang, Zhao, Huang, Wei, Guo, Huang, Li, Jiang, Wu and Du. This is an open-access article distributed under the terms of the Creative Commons Attribution License (CC BY). The use, distribution or reproduction in other forums is permitted, provided the original author(s) and the copyright owner(s) are credited and that the original publication in this journal is cited, in accordance with accepted academic practice. No use, distribution or reproduction is permitted which does not comply with these terms.

OsWRKY76 positively regulates drought stress *via* OsbHLH148-mediated jasmonate signaling in rice

Mingxing Zhang, Ranran Zhao, Kai Huang, Zhiqi Wei, Boya Guo, Shuangzhan Huang, Zhao Li, Wenzhu Jiang, Tao Wu* and Xinglin Du*

Jilin Province Engineering Laboratory of Plant Genetic Improvement, College of Plant Science, Jilin University, Changchun, China

Drought stress is a major environmental threat that limits plant growth and crop productivity. Therefore, it is necessary to uncover the molecular mechanisms behind drought tolerance in crops. Here, OsWRKY76 positively regulated drought stress in rice. *OsWRKY76* expression was induced by PEG treatment, dehydration stress, and exogenous MeJA rather than by no treatment. Notably, *OsWRKY76* knockout weakened drought tolerance at the seedling stage and decreased MeJA sensitivity. *OsJAZ12* was significantly induced by drought stress, and its expression was significantly higher in *OsWRKY76*-knockout mutants than in wild-type ZH11 under drought stress. Yeast two-hybrid and bimolecular fluorescence complementation assays showed that OsWRKY76 interacted with OsJAZ12. OsWRKY76 weakened the interaction between OsbHLH148 and OsJAZ12 in yeast cells. The OsJAZ12 protein repressed the transactivation activity of OsbHLH148, and this repression was partly restored by OsWRKY76 in rice protoplasts. Moreover, *OsDREB1E* expression was lower in *OsWRKY76*-knockout mutants than in wild-type ZH11 under drought stress, but it was upregulated under normal growth conditions. Yeast one-hybrid, electrophoretic mobility shift, and dual-luciferase assays showed that OsWRKY76 and OsbHLH148 bound directly to the *OsDREB1E* promoter and activated *OsDREB1E* expression in response to drought stress. These results suggest that OsWRKY76 confers drought tolerance through OsbHLH148-mediated jasmonate signaling in rice, offering a new clue to uncover the mechanisms behind drought tolerance.

KEYWORDS

drought stress, jasmonate signaling, OsWRKY76, OsbHLH148, rice (*Oryza sativa*)

Introduction

Drought is one of the most serious environmental stressors in crops (Sinclair, 2011). Rice (*Oryza sativa*) is a staple crop that feeds over half of the world's population (Seck et al., 2012). Since the rice cultivation process relies heavily on fresh water resources, shortages of fresh water availability and adverse climate change threaten rice growth and productivity (Hu and Xiong, 2014). This necessitates the identification of drought-resistance genes to create drought-tolerant rice varieties.

Plants have developed complex strategies against drought stress, such as modifying root growth, regulating osmotic substances to maintain intracellular water content, and scavenging excessive reactive oxygen species (ROS) to prevent ROS toxicity caused by drought stress (Rodrigues et al., 2019; Gupta et al., 2020). Numerous rice genes have been reported to play vital roles in drought stress. HDG11 confers drought tolerance and increases grain yield in rice by improving levels of soluble sugar and proline, and ROS-scavenging enzyme activities (Yu et al., 2013). OsTF1L enhances stomatal closure and lignin biosynthesis and positively regulates drought tolerance in rice (Bang et al., 2019). *AtNOG1-1* or *AtNOG1-2* overexpression in rice increases drought tolerance without affecting grain yield, whereas *OsNOG1-RNAi* rice plants are more sensitive to drought stress than wild-type plants (Pant et al., 2022). Moreover, the primary signal caused by drought is a water deficit, leading to osmotic stress. Under osmotic stress created by PEG treatment, the shoots and roots of *OsWIH2*-overexpressing rice plants are longer than those of wild-type rice plants (Gu et al., 2021). *OsWIH2*-overexpressing rice plants have a significantly higher survival rate and a lower water loss rate compared with wild-type rice plants (Gu et al., 2021). Glutathione peroxidase 1 (GPX1) acts as a redox transducer and confers osmotic stress tolerance in rice by interacting with bZIP68 and promoting the oxidation of bZIP68 (Zhou et al., 2022).

Phytohormones, such as jasmonates (JAs), play a crucial role in responding to stress (Y. Wang et al., 2021). JAs are a general term for JA and its active derivatives, which comprise its isoleucine conjugate (JA-Ile) and its methyl ester (MeJA). JAs participate in plant growth and development, such as stomatal opening, root formation, and leaf senescence (H. Huang et al., 2017). Furthermore, a number of recent reports have revealed that JAs can increase plant stress tolerance through the JA signaling pathway. The core component of the JA signaling pathway is JA-Ile (Marquis et al., 2020). Under normal growth conditions, intracellular JA-Ile levels are very low, and JA signaling occurs during the inhibition state. JAZ proteins that feature the jasmonate zinc-finger inflorescence meristem domain interact with various transcription factors (TFs) participating in the JA signaling pathway. JAZ proteins can suppress this TF activity by recruiting the co-repressor topless (TPL) and the adaptor protein of JAZ (NINJA) to form a JAZ–NINJA–TPL complex or histone-modifying proteins HDA6 and HDA19 (Pauwels et al., 2010; Zhu et al., 2011; Ke et al., 2015). When plants suffer from stress, JA-Ile levels are elevated in the cytosol, and JA-Ile is transported into the nucleus and promotes the interaction of JAZ proteins with the F-box protein COI1 within a kinetochore protein 1–cullin 1–F-box protein COI1 (SCF^{COI1}) complex, which leads to JAZ protein degradation *via* the 26S proteasome and activation of various JA- and stress-responsive genes (Mosblech et al., 2011; Wasternack and Hause, 2013; Wasternack and Song, 2017).

Basic helix–loop–helix (bHLH) TFs play a vital role in the JA signaling pathway. In *Arabidopsis thaliana*, the expression of the bHLH family *MYC2* is rapidly upregulated by JA (Lorenzo et al., 2004). MYC2 and its paralogs MYC3 and MYC4 interact with JAZ proteins, are directly repressed by JAZ proteins, and positively regulate JA-dependent plant defense (Fernández-Calvo et al., 2011; Schweizer et al., 2013). *OsbHLH148*, whose expression is rapidly increased under dehydration stress and MeJA treatment, confers drought tolerance in rice and regulates the JA signaling pathway (Seo et al., 2011). OsbHLH148 interacts with some OsJAZ proteins, including OsJAZ7, OsJAZ8, OsJAZ11, and OsJAZ12, but OsJAZ12 interacts with OsCOI1 only in the presence of coronatine, causing OsJAZ12 degradation (Seo et al., 2011). In addition, OsJAZ1 attenuates drought tolerance in rice and negatively regulates the JA signaling pathway (Fu et al., 2017). OsbHLH148–OsJAZ model could act as a key regulator in drought stress and jasmonate signaling.

Studies have identified that some WRKY TFs participate in drought stress in rice. OsWRKY47 positively regulates tolerance to water deficit stress (Raineri et al., 2015). OsWRKY11 activates the transcription of the drought-responsive gene *RAB21* and enhances drought stress tolerance (Lee et al., 2018). However, OsWRKY55 positively regulates *OsAP2-39* expression and negatively regulates drought stress (K. Huang et al., 2021). OsWRKY5 represses ABA-induced stomatal closure and weakens drought tolerance in rice (Lim et al., 2022). Furthermore, WRKY proteins interact with other proteins, such as kinases and TFs, regulate their downstream target genes, and then form complex regulatory networks. OsMPK3, OsMPK4, and OsMPK7 interact with OsWRKY30 and phosphorylate OsWRKY30, which is essential for OsWRKY30 to confer drought tolerance in rice (Shen et al., 2012). OsWRKY87 interacts with SAPK10 and is phosphorylated by it. OsWRKY87 can activate *ABF1* transcription and enhance rice drought tolerance (Yan et al., 2021). However, the underlying molecular mechanisms by which other OsWRKY TFs participate in drought stress have not been fully understood.

Our previous data showed that OsWRKY76 interacts with OsbHLH148 and coordinately plays a positive role in cold tolerance in rice (Zhang et al., 2022). Moreover, OsbHLH148 confers drought tolerance in rice and regulates the JA signaling pathway (Seo et al., 2011). However, whether and how OsWRKY76 mediates the drought stress response and the JA signaling pathway in rice is unknown. In this study, we proposed that OsWRKY76 plays a crucial role in regulating drought stress and jasmonate signaling in rice. *OsWRKY76* knockout weakened drought tolerance at the seedling stage and decreased MeJA sensitivity. OsWRKY76 interacted with OsJAZ proteins and activated OsbHLH148

transcriptional activity by interfering with the association of OsJAZ12 with OsbHLH148. OsWRKY76 and OsbHLH148 directly activated the transcription of *OsDREB1E* under drought stress.

Materials and methods

Plant materials and growth conditions

The *OsWRKY76*-knockout mutants and *OsbHLH148*-knockout mutants in the background of rice variety ZH11 (*Oryza sativa* L. ssp. *japonica*) were obtained from a mutant library (BIOGLE, Changzhou, Jiangsu, China) using a CRISPR/Cas9 genome editing approach. All homozygous T_3 seedlings (*w76-1*, *w76-2*, *b148-1*, and *b148-2*) were used for this study. All rice seedlings were planted in a growth room (80% relative humidity and PPFD 75 μmol/m^2s) with a cycle of 14 h light at 30°C and 10 h dark at 26°C.

Drought-tolerance assays and treatments

For analysis of drought stress tolerance, 2-week-old seedlings of wild-type ZH11 rice and *OsWRKY76*-knockout mutants (*w76-1* and *w76-2*) were transferred to the hydroponic culture medium with or without 20% PEG 6000 for 10 days, and their survival rates were counted after recovery for 10 days. To further test the effect of OsWRKY76 on drought tolerance, 10-day-old seedlings of wild-type ZH11 rice and *OsWRKY76*-knockout mutants (*w76-1* and *w76-2*) grown in soil suffered from drought stress for one week by stopping irrigation until the leaves of wild-type ZH11 were completely wilted. After recovery with rewatering for one week, the survival rates of the plants were counted visually.

For drought stress and MeJA treatments, two-week-old ZH11 seedlings were treated under dehydration stress (air-dried), 20% PEG 6000 treatment, and MeJA (100 μM) treatment (Fu et al., 2017). The leaves of the ZH11 seedlings were harvested at different time points after treatment.

For the analysis of MeJA on seed germination, seeds of wild-type ZH11 rice and *OsWRKY76*-knockout mutants (*w76-1* and *w76-2*) were germinated on 1/2 MS medium containing 0, 5, or 50 μM MeJA for 3 days, and then germination was scored. To determine the effect of MeJA on seedling development, 1-d-old seedlings of wild-type ZH11 rice and *OsWRKY76*-knockout mutants (*w76-1* and *w76-2*) were transferred to 1/2 MS medium containing 0, 5, or 50 μM MeJA for 5 days, and then shoot length and root length were measured.

Reverse transcription quantitative PCR analysis

Total RNA was extracted from rice leaves using TRIzol reagent (Tiangen, Beijing, China), and then reverse transcription was performed using a StarScript II RT Kit with gDNA Remover (Genstar, Beijing, China). Reverse transcription quantitative PCR (RT-qPCR) was performed with the SYBR Green-based Fast Mixture (Genstar, Beijing, China) using an Mx3005P instrument (Stratagene, La Jolla, CA, USA). Relative expression levels of genes were calculated by normalization to *OsActin* and *Ubiquitin5* genes (Mao et al., 2019).

3, 3′-diaminobenzidine staining

To determine the presence of hydrogen peroxide (H_2O_2) in the rice leaves, 3, 3′-diaminobenzidine (DAB) staining (Wang et al., 2021) was performed using two-week-old rice seedlings of wild-type ZH11 rice and *OsWRKY76*-knockout mutants (*w76-1* and *w76-2*) with or without dehydration treatment. The rice leaves were cut into 2-cm pieces, immersed in 1 mg ml^{-1} DAB in 50 mM Tris–acetate buffer (pH 5.0), and then vacuum infiltrated for 40 min. After incubation at 30°C for 3 h in the dark, the rice leaves were immersed in 95% ethanol until the chlorophyll was completely removed.

Yeast two- and three-hybrid assays

For the yeast two-hybrid assay, according to the Yeast Protocol Handbook of Clontech, the full-length coding sequences (CDSs) of *OsbHLH148*, *OsJAZ7*, *OsJAZ8*, *OsJAZ11*, and *OsJAZ12* were cloned and fused into the vector pGADT7 (AD) to generate AD-OsbHLH148, AD-OsJAZ7, AD-OsJAZ8, AD-OsJAZ11, and AD-OsJAZ12, respectively, as prey. The full-length CDSs of *OsWRKY76* and *OsbHLH148* were inserted into the vector pbridge (BD) to form BD-OsWRKY76 and BD-OsbHLH148, respectively, as bait. In the yeast three-hybrid assay, according to the Yeast Protocol Handbook of Clontech, the full-length CDSs of *OsWRKY76* were inserted into the BD-OsbHLH148 vector to form BD-OsbHLH148-OsWRKY76 in which *OsWRKY76* driven by the Met25 promoter was expressed in the absence of methionine. These prey and bait vectors were transformed into Y2HGold cells grown on SD/-Trp-Leu dropout plates for the yeast two-hybrid assay and into Y190 cells grown on SD/-Trp-Leu-Met dropout plates for the yeast three-hybrid assay. The positive transformants were grown on SD/-Trp-Leu and SD/-Trp-Leu-His dropout plates for the yeast two-hybrid assay, and β-galactosidase activity levels were detected for the yeast three-hybrid assay.

Bimolecular fluorescence complementation

To confirm the *in vivo* interaction between OsWRKY76 and OsJAZ12, a bimolecular fluorescence complementation (BiFC) assay was performed. The CDSs of *OsWRKY76* and *OsJAZ12* were amplified and fused into the pxy103 (nYFP) and apXY105 (cYFP) vectors, respectively. Thus, *OsWRKY76-nYFP* and *cYFP-OsJAZ12* fusion constructs were obtained. cYFP or cYFP-OsJAZ12 and nYFP or OsWRKY76-nYFP were transformed into *Arabidopsis* protoplasts (S. C. Wang et al., 2005). Fluorescence signals were analyzed using a Zeiss Axio Observer A1 (Carl Zeiss, Jena, Germany).

Gal4-dependent chimeric transactivation assay

To determine OsbHLH148 transcriptional activity, the full-length CDS of *OsbHLH148* was amplified and fused into the Gal4 DNA-binding domain (GD), creating the GD-b148 effector vector. Moreover, the full-length CDSs of OsWRKY76 and OsJAZ12 were cloned into the effector vector without GD. Combinations of these effector vectors, reporter vector (*35S-Gal4:FLUC*) (firefly luciferase, FLUC), and internal control (*35S:RLUC*) (Renilla luciferase, RLUC) were transformed into rice protoplasts followed by incubation at 30°C for 15 h in the dark to allow transient expression. FLUC and RLUC activities were measured using a Dual-Luciferase reporter assay system (Promega, Madison, Wisconsin, USA).

Yeast one-hybrid assay

The yeast one-hybrid assay was performed as previously described (Lin et al., 2007). An upstream 2000-bp sequence of *OsDREB1E*'s start codon as a promoter sequence of *OsDREB1E* was cloned and fused into the pLacZi2μ vector to generate *OsDREB1Epro : LacZ*. The full-length CDSs of *OsWRKY76* and *OsbHLH148* were ligated into the pJG4-5 (GAD) vector to form GAD-OsWRKY76 (GAD-W76) and GAD-OsbHLH148 (GAD-b148), respectively. The GAD, GAD-W76, and GAD-b148 constructs were separately co-transformed with the *OsDREB1Epro : LacZ* vector into the yeast strain EGY48. The positive transformants were identified using SD/-Trp-Ura dropout plates containing X-Gluc for blue color development.

Electrophoretic mobility shift assay

Electrophoretic mobility shift assay (EMSA) was conducted as previously described (Gao et al., 2019). The full-length CDS of OsWRKY76 was inserted into the pGEX-4T-3 vector to fuse it to the glutathione S-transferase (GST) coding region and to create a recombinant vector encoding a GST-WRKY76 fusion protein. The recombinant vector and empty GST vector were then transformed into the *E. coli* strain BL21 (DE3), which was purified using GST Resin. The 6-FAM 5' end-labeled and unlabeled *OsDREB1E* probe was synthesized by a Bio-Tech Company (Sangon, Shanghai, China). Fluorescence signals in the gel were detected using a Tanon 5200 Multi imaging system (Tanon, Shanghai, China).

Dual-luciferase assay

The *OsDREB1E* promoter was cloned into the double vector pGreenII 0800-LUC, in which the *OsDREB1E* promoter was fused with the *FLUC* reporter gene, and the *Renilla luciferase* gene was driven by the 35S promoter as an internal control. The full-length CDSs of *OsWRKY76* and *OsbHLH148* were inserted into pCAMBIA1300 as the effector vector. The effector vectors were co-transformed with the double vector into rice protoplasts, followed by incubation at 30°C for 15 h in the dark to allow transient expression. The transformed protoplasts were treated with and without 10% PEG 6000 treatment for 20 min. The FLUC and RLUC activities were measured with a Dual-Luciferase reporter assay system (Promega, Madison, Wisconsin, USA).

Statistical analysis

Based on no fewer than three independent experiments ($n \geq 3$), results are presented as the mean ± SD. Mean differences between two groups were compared using Student's *t*-test and between three or more groups using one-way ANOVA. For Student's *t*-test, asterisks represent the *P*-values (*, $P < 0.05$; **, $P < 0.01$). For ANOVA, different letters represent significant mean differences ($P < 0.05$) measured using Duncan's multiple range test (DMRT).

Primers and accession numbers

The sequences of all primers used for this study are listed in Table S1. The sequence data from this study can be found in the Rice Genome Annotation Project Database (http://rice.uga.edu./), and the accession numbers of genes are listed in Table S2.

Results

Expression of the *OsWRKY76* gene in response to drought stress and MeJA treatment

To investigate the responses of *OsWRKY76* to drought stress and MeJA treatment, we examined the expression of *OsWRKY76* under PEG treatment, dehydration stress, and exogenous MeJA in two-week-old seedlings of wild-type rice using reverse RT-qPCR analysis. *OsWRKY76* expression was induced rapidly within 30 min of exposure to dehydration stress, showing an 8-fold increase over that in control plants and then showing a gradual descent over a period of 6 h (Figure 1A). *OsWRKY76* was strongly upregulated by PEG treatment and exogenous MeJA (Figures 1B, C). By contrast, *OsWRKY76* expression showed no significant differences under no treatment (Figure 1D). These results suggest that *OsWRKY76* can respond to drought stress and MeJA treatment and may play an important role in the drought tolerance of rice and the JA signaling pathway.

OsWRKY76 confers drought tolerance in rice

To test the effect of OsWRKY76 on the drought tolerance of rice, *OsWRKY76*-knockout mutants (*w76-1* and *w76-2*) were

10.3389/fpls.2023.1168723

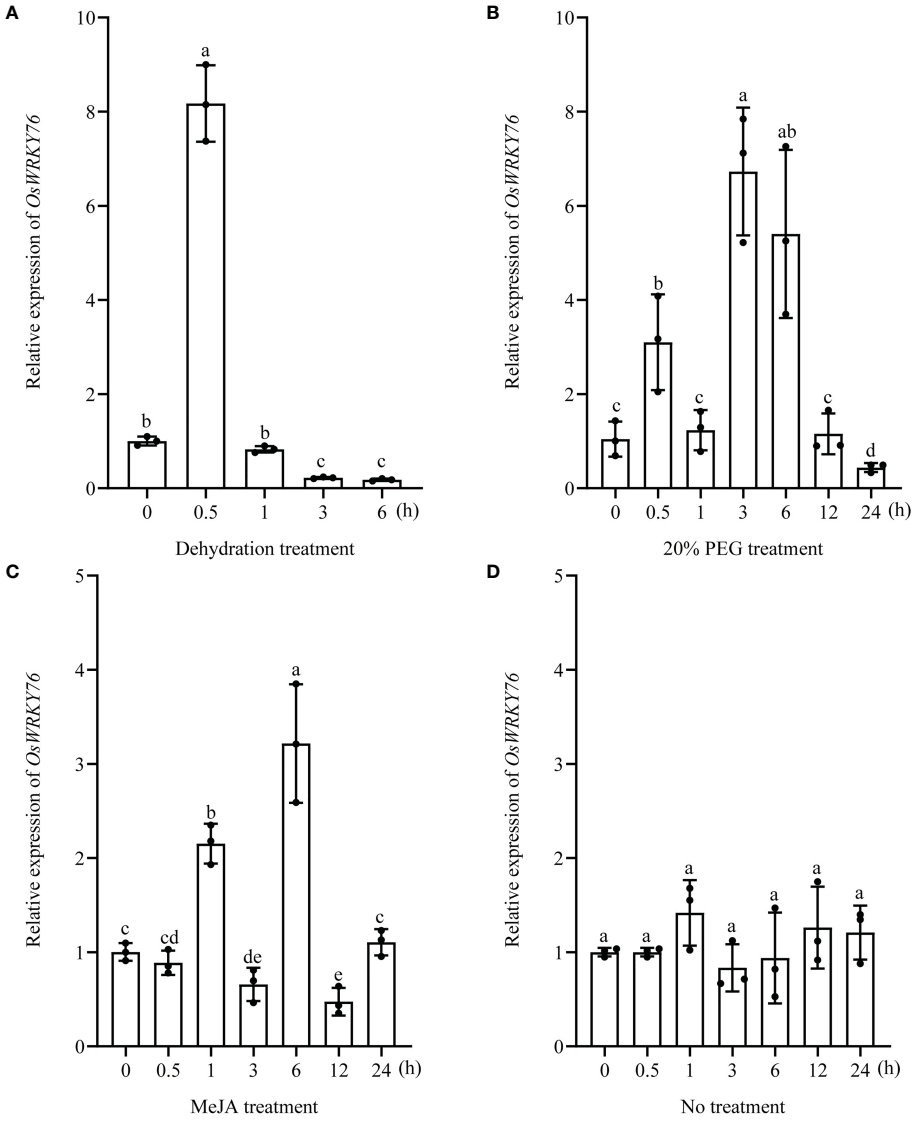


FIGURE 1
OsWRKY76 responds to drought stress and MeJA treatment. **(A–D)** Reverse transcription quantitative PCR (RT-qPCR) analysis showing the expression levels of *OsWRKY76* under dehydration stress **(A)**, 20% PEG treatment **(B)**, 100 μM exogenous MeJA treatment **(C)**, and no treatment **(D)** in two-week-old seedlings of wild-type rice (n = 3; $P < 0.05$; one-way ANOVA).

obtained using a CRISPR/Cas9 genome editing approach in the *japonica* rice accession 'ZH11' background, resulting in frameshift mutations (Zhang et al., 2022). Analysis of drought stress tolerance showed no significant differences in two-week-old rice seedling growth between wild-type ZH11 and *OsWRKY76*-knockout mutants (*w76-1* and *w76-2*) under normal conditions (Figures 2A, F). By contrast, *w76-1* and *w76-2* plants treated with 20% PEG showed more severe wilting, chlorosis, electrolyte leakage, and water loss than wild-type ZH11 (Figures 2B–D and S1), together with lower survival rates after 10 days of recovery (Figure 2E). We further investigated drought stress conditions. When watering was stopped for 7 days and then resumed for 7 days, *OsWRKY76*-knockout mutants (*w76-1* and *w76-2*) showed more severe wilting and lower survival rates than wild-type ZH11 (Figures 2G, H). These observations suggest that loss of OsWRKY76 function renders rice more sensitive to drought stress than the wild type.

Drought stress triggers ROS accumulation in rice cells, and ROS are biomarkers of rice drought tolerance (Li et al., 2021). Using DAB staining, we determined the presence of H_2O_2 in rice leaves. DAB staining was light in wild-type ZH11 and *OsWRKY76*-knockout mutants (*w76-1* and *w76-2*) under normal conditions (Figure 2I). However, DAB staining was stronger in *OsWRKY76*-knockout mutants (*w76-1* and *w76-2*) than in wild-type ZH11 after 6 h of dehydration treatment (Figure 2I). These leaf phenotypes demonstrated that more H_2O_2 accumulated in *OsWRKY76*-knockout mutants (*w76-1* and *w76-2*) than in wild-type ZH11 after drought stress. Taken together, these results suggest that OsWRKY76 positively regulates drought tolerance by repressing ROS accumulation.

10.3389/fpls.2023.1168723

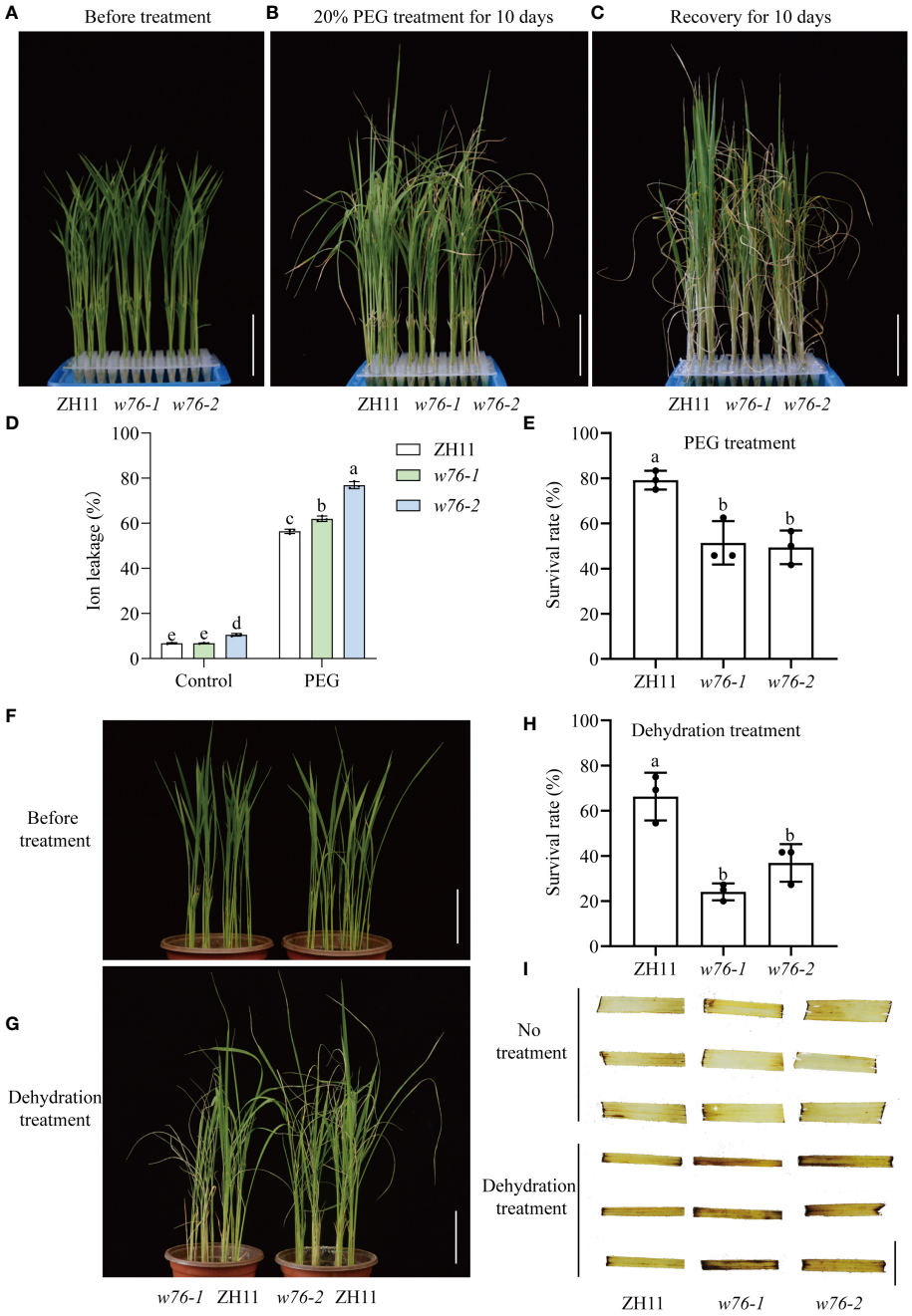


FIGURE 2
OsWRKY76 confers drought tolerance in rice. **(A–C)** Phenotypes of wild-type ZH11 and *OsWRKY76*-knockout mutants (*w76-1* and *w76-2*) before treatment **(A)**, with 20% PEG treatment for 10 days **(B)**, and after recovery for 10 days **(C)**. Scale bars, 5 cm. **(D)** Ion leakage rate in leaf cells of ZH11 and *OsWRKY76*-knockout mutants (*w76-1* and *w76-2*) under no treatment and 10 days of 20% PEG treatment. **(E)** Survival rates of ZH11 and *OsWRKY76*-knockout mutants (*w76-1* and *w76-2*) after 10 days of recovery. **(F, G)** Phenotypes of wild-type ZH11 and *OsWRKY76*-knockout mutants (*w76-1* and *w76-2*) under normal conditions **(F)** and after 7 days of rewatering **(G)**. Scale bars, 5 cm. **(H)** Survival rates of ZH11 and *OsWRKY76*-knockout mutants (*w76-1* and *w76-2*) after 7 days of rewatering. **(I)** 3, 3′-diaminobenzidine (DAB) staining in wild-type ZH11 and *OsWRKY76*-knockout mutants (*w76-1* and *w76-2*) under normal conditions and 6-h dehydration treatment. Scale bars, 1 cm. (n = 3; $P < 0.05$; one-way ANOVA).

OsWRKY76 positively regulates JA signaling

Given that *OsWRKY76* expression levels were induced by MeJA treatment, we hypothesized that *OsWRKY76* is involved in the JA signaling pathway. To test whether *OsWRKY76* knockout affected sensitivity to MeJA, we performed the effects of MeJA on seed germination or seedling development among the wild-type ZH11 plants and the *OsWRKY76* mutants. As shown in Figures 3A, B, *OsWRKY76*-knockout mutants (*w76-1* and *w76-2*) showed hyposensitivity to exogenous MeJA compared to wild-type ZH11 during seed germination. Furthermore, MeJA treatment significantly inhibited shoot and root growth in wild-type ZH11 compared with *OsWRKY76*-knockout mutants (*w76-1* and *w76-2*)

10.3389/fpls.2023.1168723

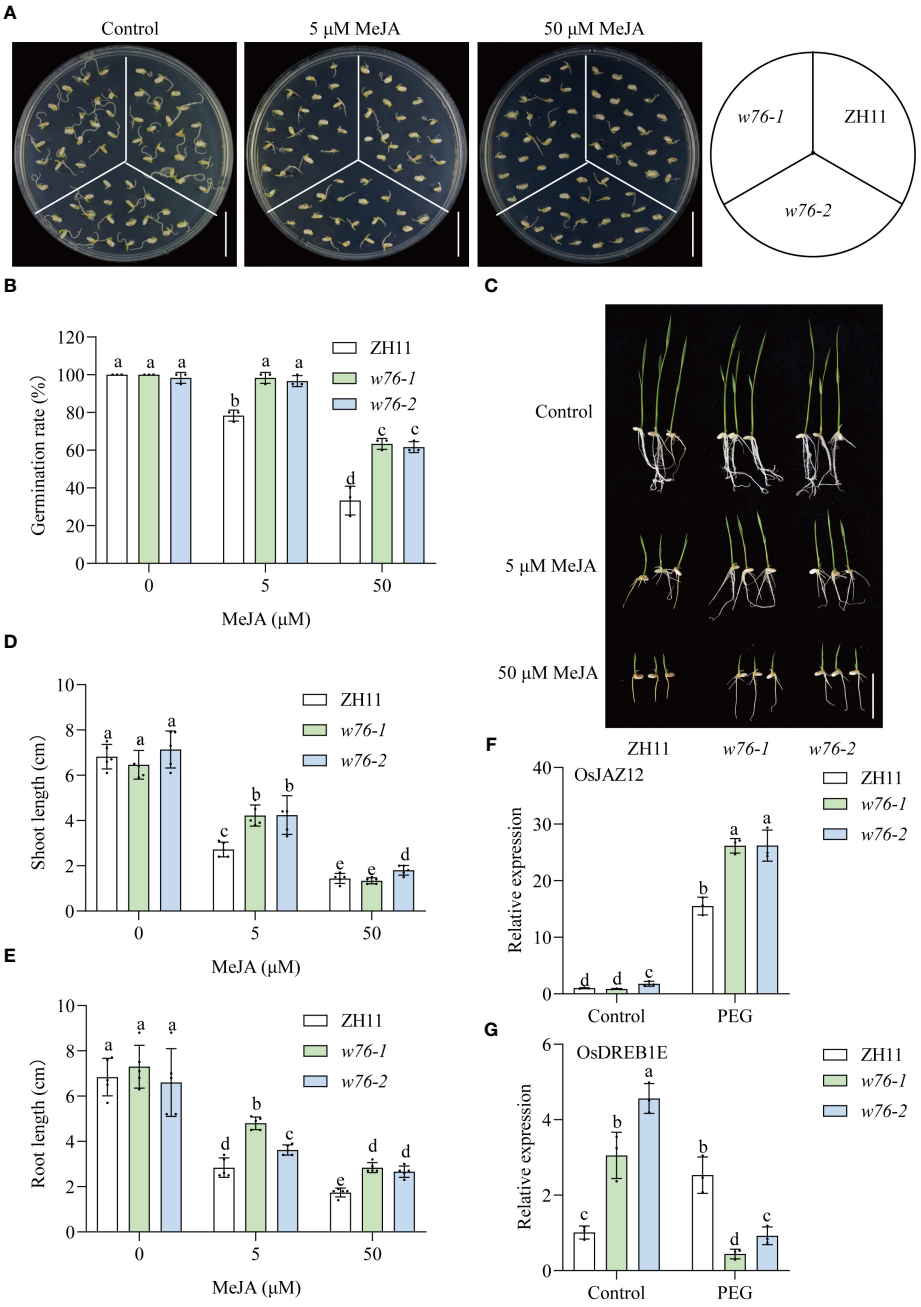


FIGURE 3
OsWRKY76 positively regulates JA signaling. **(A, B)** Germination phenotypes **(A)** and seed germination rates **(B)** of wild-type ZH11 and *OsWRKY76*-knockout mutant (*w76-1* and *w76-2*) seeds treated with MeJA for 3 days. ZH11, *w76-1*, and *w76-2* seeds were germinated on 1/2 MS medium containing 0, 5, or 50 μM MeJA. Scale bars, 5 cm. **(C–E)** Seedling phenotypes **(C)**, shoot length **(D)**, and root length **(E)** of wild-type ZH11 and *OsWRKY76*-knockout mutant (*w76-1* and *w76-2*) plants treated with MeJA for 5 days. One-day-old seedlings were transferred to 1/2 MS medium containing 0, 5, or 50 μM MeJA. Scale bars, 5 cm. **(F, G)** Reverse transcription quantitative PCR (RT-qPCR) analysis showing the expression levels of *OsJAZ12* **(F)** and *OsDREB1E* **(G)** in the *OsWRKY76*-knockout mutants (*w76-1* and *w76-2*) treated with or without 20% PEG 6000 for 3 h (n = 3; $P < 0.05$; one-way ANOVA).

(Figures 3C–E). These results suggest that the loss of the OsWRKY76 function decreases MeJA sensitivity.

To further confirm this speculation, we performed RT-qPCR to examine the expression of JA signaling and drought-responsive genes under drought stress in *OsWRKY76*-knockout mutants. The expression of *OsJAZ12* (related to JA signaling) was significantly induced at 3 h of exposure to 20% PEG treatment, showing a 15-fold increase over that in wild-type ZH11 (Figure 3F). *OsJAZ12* expression was notably higher in *OsWRKY76*-knockout mutants (*w76-1* and *w76-2*) than in wild-type ZH11 under PEG treatment (Figure 3F). OsDREB1E positively regulates tolerance to drought stress (Chen et al., 2008). *OsDREB1E* expression was lower in *OsWRKY76*-knockout mutants (*w76-1* and *w76-2*) than in wild-type ZH11 subjected to drought stress, but it was upregulated under

normal growth conditions (Figure 3G). These results indicate that the JA signaling pathway is attenuated in the *OsWRKY76*-knockout mutants under drought stress. The expression level of the drought-tolerance gene *OsDREB1E* was also repressed under drought stress. Taken together, these results suggest that OsWRKY76 positively regulates JA signaling under drought stress.

OsWRKY76 interacts with OsJAZ12

OsbHLH148 interacted with some OsJAZ proteins. The interaction between OsbHLH148 and OsJAZ12 was relatively strong, and the interaction with OsJAZ7, 8, and 11 was relatively weak (Seo et al., 2011). Our previous data showed that OsWRKY76 interacts with OsbHLH148 *in vitro* and *in vivo* (Zhang et al., 2022). To investigate whether OsWRKY76 interacted with these OsJAZ proteins, we performed a yeast two-hybrid assay. In yeast cells, OsWRKY76 interacted with OsJAZ8, 11, and 12 but not with OsJAZ7 (Figure 4A). The interaction between OsWRKY76 and OsJAZ12 was further confirmed using a BiFC assay in rice protoplasts (Figure 4B). These results indicate that OsWRKY76, OsbHLH148, and OsJAZ12 form a heterotrimer.

OsWRKY76 competes with OsJAZ12 to bind OsbHLH148

To test the effect of OsWRKY76 on the interaction between OsbHLH148 and OsJAZ12, we performed a yeast three-hybrid assay. When co-transformed with pGADT7 (AD) and pbridge-

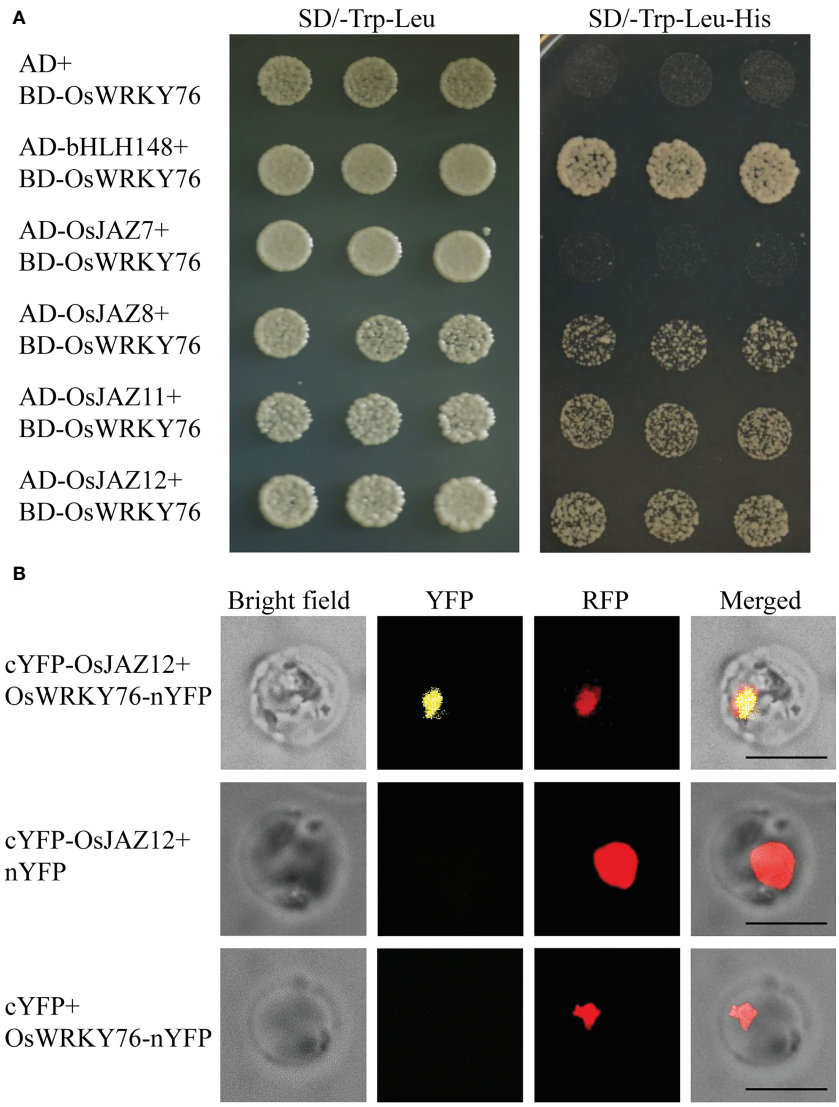


FIGURE 4
OsWRKY76 interacts with OsJAZ12. **(A)** Yeast two-hybrid assay. The pbridge-OsWRKY76 (BD-W76) bait vector was co-transformed with pGADT7 (AD), AD-OsbHLH148, AD-OsJAZ7, AD-OsJAZ8, AD-OsJAZ11, or AD-OsJAZ12 prey vector into the yeast strain Y2HGold. The positive transformants were grown on SD/-Trp-Leu and SD/-Trp-Leu-His dropout plates to identify protein–protein interactions. **(B)** Bimolecular fluorescence complementation (BiFC) assay of OsWRKY76 and OsJAZ12 interactions. cYFP or cYFP-OsJAZ12 and nYFP or OsWRKY76-nYFP were transformed into *Arabidopsis* protoplasts. Scale bars, 20 μm.

OsbHLH148 (BD-b148), β-galactosidase activity was significantly higher than that of the empty vector, indicating that OsbHLH148 has transcriptional activation activity in yeast cells (Figures 5A, B). When co-transformed with pGADT7-OsJAZ12 (AD-JAZ12) and BD-b148, β-galactosidase activity was significantly higher than when co-transformed with AD and BD-b148, and it was also significantly higher than when co-transformed with AD-JAZ12 and pbridge-OsbHLH148-OsWRKY76 (BD-b148-W76), indicating that OsWRKY76 weakens the interaction between OsbHLH148 and OsJAZ12 in yeast cells (Figures 5A, B).

To analyze the effect of OsWRKY76 and OsJAZ12 proteins on OsbHLH148 transcriptional activity, we performed a Gal4-dependent chimeric transactivation assay. The full-length CDS of *OsbHLH148* was amplified and fused into the GD, creating the GD-b148 effector vector (Figure 5C). The Gal4-dependent chimeric transactivation assay showed that the FLUC activity of the GD-b148 vector was 6-fold higher than that of the GD vector, indicating that OsbHLH148 is a transcriptional activator in rice protoplasts (Figure 5D). The OsWRKY76 protein activated the transactivation activity of OsbHLH148. However, the OsJAZ12 protein repressed the transactivation activity of OsbHLH148, and this repression was partly restored by OsWRKY76 (Figure 5D). Taken together, these results indicate that OsWRKY76 activates OsbHLH148 transcriptional activity by interfering with the association of OsJAZ12 with OsbHLH148.

OsWRKY76 directly activates *OsDREB1E* expression in response to drought stress

OsDREB1E was activated in *OsWRKY76*-knockout mutants (*w76-1* and *w76-2*) under normal conditions, but the activity showed repression under drought stress (Figure 3G). There were several W-box elements (TTGACT/C, WRKY recognition sites) and E-box elements (CANNTG, bHLH recognition sites) in the *OsDREB1E* promoter region using the PlantCARE database (Figure 6A). Therefore, we investigated whether OsWRKY76 and OsbHLH148 bound to the *OsDREB1E* promoter to confer drought tolerance in rice. We performed a yeast one-hybrid assay, which revealed direct binding of OsWRKY76 and OsbHLH148 to the *OsDREB1E* promoter (Figure 6B). To further verify that OsWRKY76 bound to the *OsDREB1E* promoter, we performed an

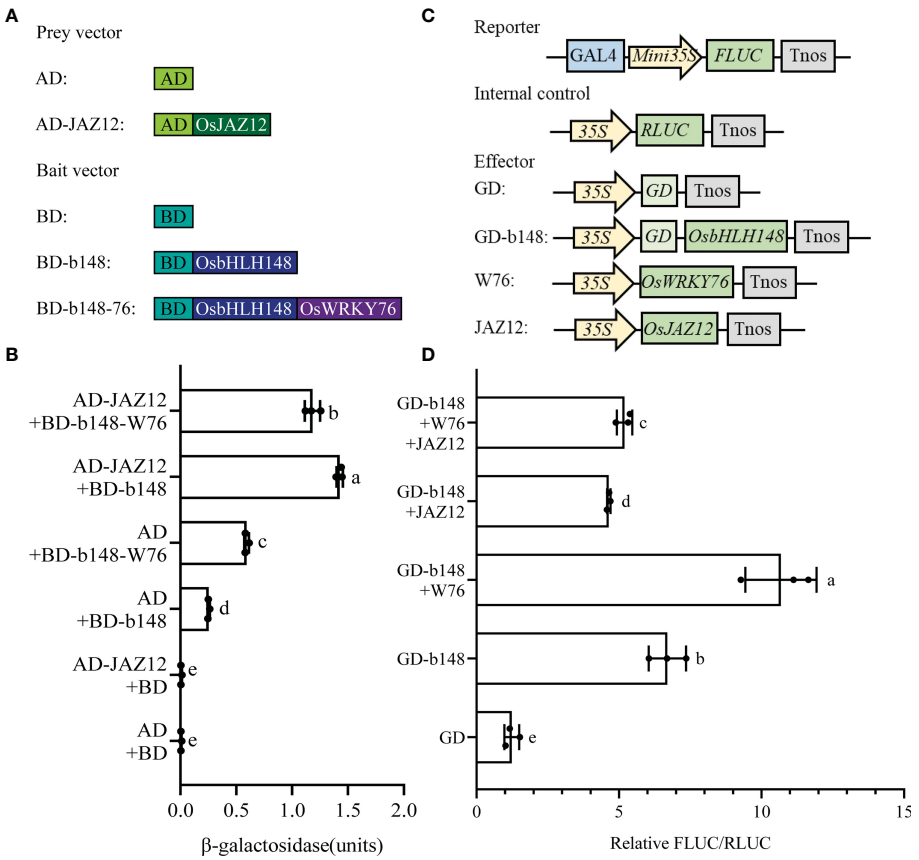


FIGURE 5
OsWRKY76 competes with OsJAZ12 to bind OsbHLH148. **(A)** In the yeast three-hybrid assay, prey vector (AD or AD-JAZ12) and bait vector (BD, BD-b148, or BD-b148-W76) construction. **(B)** Yeast three-hybrid assay. Yeast strain Y190 cells were co-transformed with a prey vector (AD or AD-JAZ12) and bait vector (BD, BD-b148, or BD-b148-W76). The positive transformants were grown on SD/-Trp-Leu-Met dropout plates, and β-galactosidase activity levels were detected. **(C)** In the Gal4-dependent chimeric transactivation assay, vector construction of the OsbHLH148 transcriptional activity assay. **(D)** Relative FLUC/RLUC of the OsbHLH148 transcriptional activity assay in rice protoplasts by co-transformation of different effector vectors (OsWRKY76 and OsJAZ12 proteins) using the Gal4-dependent chimeric transactivation assay (n = 3; $P < 0.05$; one-way ANOVA).

10.3389/fpls.2023.1168723

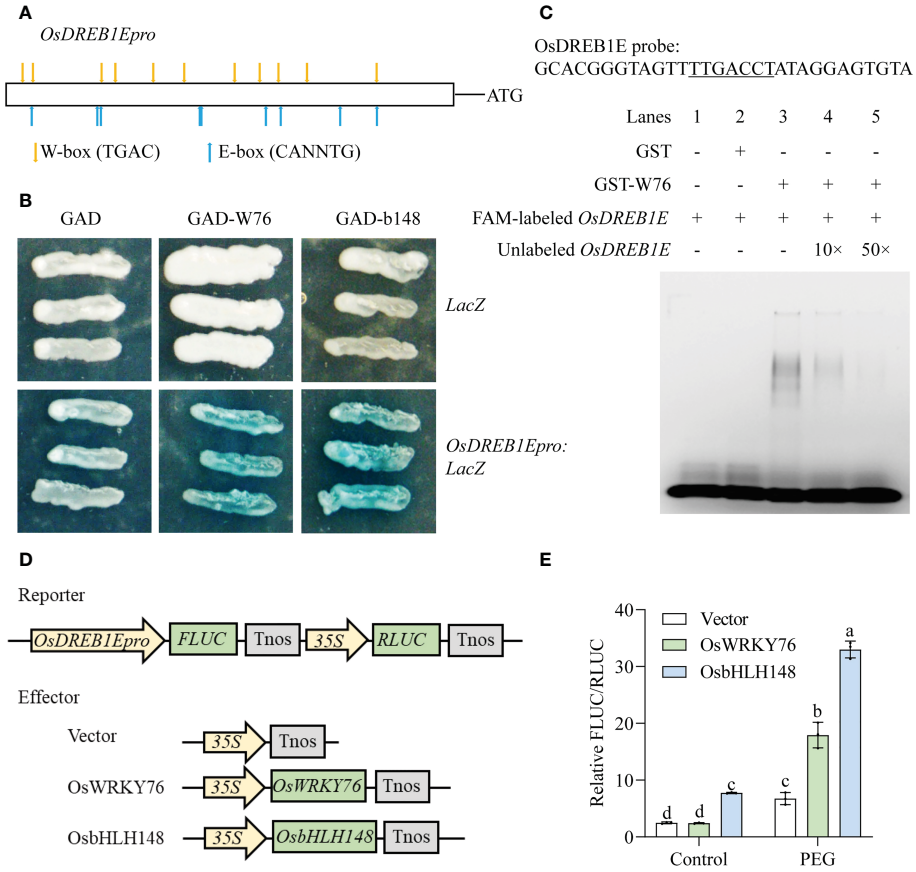


FIGURE 6
OsWRKY76 and OsbHLH148 directly regulate *OsDREB1E* expression. **(A)** Schematic of the *OsDREB1E* promoter showing the W-box and E-box elements. **(B)** Yeast one-hybrid assay. The GAL4-Activation Domain (GAD), OsWRKY76 fused with GAD (GAD-W76), or OsbHLH148 fused with the GAD (GAD-b148) constructs were separately co-transformed with the *LacZ* reporter gene driven by the *OsDREB1E* promoter (*OsDREB1Epro* : LacZ) into the yeast strain EGY48. The positive transformants were identified using SD/-Trp-Ura dropout plates containing X-Gluc for blue color development. **(C)** Oligonucleotides of the probe of the *OsDREB1E* promoter (*OsDREB1E* probe) used in the electrophoretic mobility shift assay (EMSA). The W-box elements are labeled with an underline. EMSA binding of OsWRKY76 with the *OsDREB1E* promoter containing the W-box element. The 6-FAM 5′ end-labeled *OsDREB1E* probe is shown in lanes 1–5. The 6-FAM 5′ end-labeled *OsDREB1E* probe was incubated with the glutathione S-transferase (GST)-OsWRKY76 protein (lane 3) and GST protein (lane 2), and the *OsDREB1E* probe alone (lane 1) served as the negative control. Unlabeled *OsDREB1E* probe competitors were used in 10 or 50 molar excesses (lanes 4 and 5). **(D)** Vector construction of the *OsDREB1E* promoter activity assay. The *OsDREB1E* promoter was cloned into the double vector pGreenII 0800-LUC as the reporter vector. The full-length CDSs of *OsWRKY76* and *OsbHLH148* were cloned into pCAMBIA1300 to serve as the effector vector. **(E)** OsWRKY76 and OsbHLH148 activated *OsDREB1E* promoter activity using a dual-luciferase assay (relative FLUC/RLUC) (n = 3; $P < 0.05$; one-way ANOVA).

EMSA. Strong mobility shift bands in the *OsDREB1E* probe containing the W-box element (Figure 6C) were detected for the GST-OsWRKY76 protein (lane 3) but not for the GST protein (lane 2) or the *OsDREB1E* probe alone (lane 1) (Figure 6C). Strong mobility shift bands were reduced when increasing amounts (10× and 50×) of the unlabeled *OsDREB1E* competitor probe were added (lanes 3–5) (Figure 6C). Thus, EMSA showed that OsWRKY76 bound directly to the *OsDREB1E* promoter containing the W-box element *in vitro*.

To investigate whether OsWRKY76 and OsbHLH148 regulated the transcription of *OsDREB1E*, we conducted dual-luciferase assays in rice protoplasts. The *OsDREB1E* promoter was fused with the *FLUC* reporter gene, and *OsWRKY76* or *OsbHLH148*, driven by 35S, was the effector (Figure 6D). There was no significant difference in the relative FLUC/RLUC activity of co-transfection with the *35S:OsWRKY76* vector and with the empty vector under normal conditions (Figure 6E). When the transformed protoplasts were treated with PEG treatment for 20 min, the transcription of *OsDREB1E* was strongly activated by OsWRKY76 (Figure 6E). Under normal conditions and PEG treatment, the relative FLUC/RLUC activity co-transfected with *35S:OsbHLH148* was significantly higher than that of the empty vector, indicating that OsbHLH148 elevated *OsDREB1E* promoter activity in rice protoplasts (Figure 6E). These results revealed that OsWRKY76 and OsbHLH148 directly activated the transcription of *OsDREB1E* under drought stress.

Discussion

As global climate change continues to cause water scarcity, drought is emerging as a prevalent and important stress factor for crop production worldwide. The latest FAO data have shown that

drought has cost the world $29 billion in crop losses over the past decade (https://www.fao.org/, accessed 24 May 2022). Rice serves as a staple crop for more than half of the world's population (Seck et al., 2012). The identification of drought-tolerance genes can speed up the development of drought-tolerant rice varieties. A few WRKY TFs conferring drought tolerance in rice, including OsWRKY11, OsWRKY30, OsWRKY47, and OsWRKY87, have been identified (Shen et al., 2012; Raineri et al., 2015; Lee et al., 2018; Yan et al., 2021). In this study, *OsWRKY76* was regulated by drought stress, and its knockout weakened drought tolerance at the seedling stage (Figures 1 and 2).

Under drought stress, plants regulate adaptive and physiological responses through the metabolism of plant hormones and their signaling pathways. JA is a key phytohormone that regulates plant drought stress adaptation. In pepper (*Capsicum annuum* L.), CaCIPK3 increases drought and MeJA tolerance by enhancing the expression of JA-related genes (Ma et al., 2021). In *Arabidopsis*, JASMONIC ACID OXIDASES (JAO1–4) catalyze the specific oxidation of JA to 12OH-JA for attenuating JA-Ile formation and the JA signaling pathway (Smirnova et al., 2017). *JAO2* mutants possess higher JA-Ile signaling and drought survival compared with wild-type plants, which is further enhanced by JAO3 and JAO4 deficiency (Marquis et al., 2022). *AtNOG1-1* or *AtNOG1-2* overexpression in rice positively regulates the expression of genes related to the JA signaling pathway and stomata regulation to prevent water loss (Pant et al., 2022). In sea buckthorn (*Hippophae rhamnoides* L.), HrTCP20 confers drought tolerance by mediating the JA signaling pathway (Yao et al., 2022). MeSPL9 weakens drought tolerance by regulating protectant metabolite contents and JA signaling in *cassava* (Li et al., 2022). In this study, *OsWRKY76* knockout decreased sensitivity to exogenous MeJA in seed germination and seedling development (Figures 3A–E). JAZ proteins suppress various TF activities and negatively regulate the JA signaling pathway (Ke et al., 2015). Our research showed that *OsJAZ12* was significantly induced by drought stress, and its expression was significantly higher in *OsWRKY76*-knockout mutants than in wild-type ZH11 under drought stress (Figure 3F). And then, JAZ12 protein dramatically suppressed activities of various TF participating in the JA signaling pathway. Based on these findings, we suggest that OsWRKY76 positively regulates drought stress in a JA-dependent signaling pathway.

Under normal conditions, JAZ proteins interacted with bHLH148 and suppressed its activity, causing an inhibition state of JA signaling in rice (Seo et al., 2011; Ke et al., 2015). When rice plants suffer from drought stress, JA levels are elevated, and JA promotes the interaction of JAZ proteins with COI1 of the SCF^{COI1} complex and leads to JAZ protein degradation, which releases bHLH148 and activates bHLH148 activity (Mosblech et al., 2011; Seo et al., 2011; Wasternack and Song, 2017). Our data showed that OsWRKY76 interacted with OsJAZ proteins and weakened the interaction between OsbHLH148 and OsJAZ12 in yeast cells (Figures 4 and 5B). The OsJAZ12 protein repressed the transactivation activity of OsbHLH148, and this repression was partly restored by OsWRKY76 (Figure 5D). *OsJAZ12* expression was notably higher in *OsWRKY76*-knockout mutants than in wild-type ZH11 under drought treatment (Figure 3F). Based on the results, we propose that OsWRKY76 plays an essential role in OsbHLH148-mediated JA signaling. However, OsWRKY76 is upstream of OsbHLH148 in drought stress, lacking genetic evidence for the double mutants of OsWRKY76 and OsbHLH148. In future work, we should analyze the double mutants of OsWRKY76 and OsbHLH148 phenotypes of drought stress by compared with single gene mutants, which could further help to understand their relationships.

Induced stress responses allow plants to survive under a wider range of environmental conditions (VanWallendael et al., 2019). The extreme environment triggers overall and rapid reprogramming events in cells (Wu et al., 2021). Transcription of most *DREB* genes in various plant species exhibits relatively low basal expression levels but is rapidly induced by different environmental stressors (Agarwal et al., 2017). In rice, *OsDREB1E* could be significantly induced and positively regulate tolerance to drought stress (Chen et al., 2008). Here, *OsDREB1E* expression was lower in *OsWRKY76*-knockout mutants than in wild-type ZH11 under drought stress, but it was upregulated under normal growth conditions (Figure 4G). OsWRKY76 bound directly to the *OsDREB1E* promoter and activated *OsDREB1E* expression in response to drought stress (Figure 6). Similarly, SEUSS is transcriptional co-repressors that downregulates gene expression during flower development in *Arabidopsis thaliana* (Grigorova et al., 2011). Interestingly, SEUSS promotes the expression of auxin-related genes and positively regulates warm temperature-mediated hypocotyl growth (Huai et al., 2018). Moreover, OsMADS57 could suppress *OsWRKY94* activity under normal temperatures but activates its transcription in response to cold stress (Chen et al., 2018). Therefore, OsWRKY76 activated *OsDREB1E* transcription under drought stress instead of under normal growth conditions, which avoids incurring costly fitness trade-offs and may act as a molecular link between drought tolerance and plant growth. Moreover, OsWRKY76 responds to multiple biotic and abiotic stresses (Yokotani et al., 2013). OsWRKY76 positively regulates cold stress by enhancing *OsDREB1B* transcription (Zhang et al., 2022). Thus, OsWRKY76 is not only a positive regulator of cold tolerance in rice, but also it confers the drought tolerance of rice at the seedling stage. OsWRKY76 may be involved in multiple resistance of rice, but their mechanisms may be different.

Conclusions

In the present study, our findings support a model in which OsWRKY76 acts as a key regulator in drought stress and jasmonate signaling in rice (Figure 7). Under normal growth conditions, OsWRKY76 interacted with OsJAZ proteins and weakened the interaction between OsbHLH148 and OsJAZ12. Furthermore, the OsJAZ12 protein repressed the transactivation activity of OsbHLH148, and this repression was partly restored by OsWRKY76. Under drought stress, JA-Ile levels were elevated,

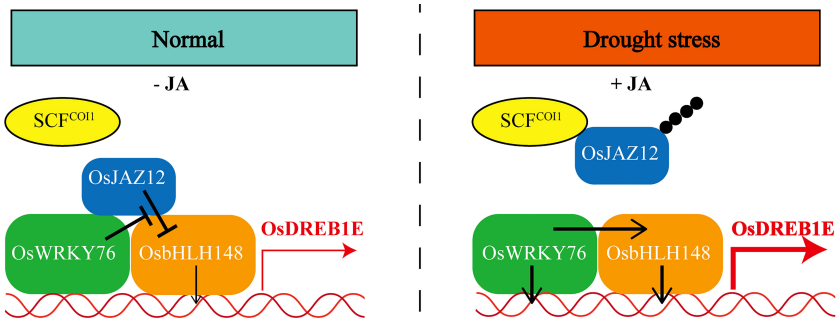


FIGURE 7
A model illustrating that OsWRKY76 positively regulates drought stress by OsbHLH148-mediated jasmonate signaling in rice.

leading to the degradation of OsJAZ12 and the activation of *OsWRKY76* and *OsbHLH148* expressions. OsWRKY76 and OsbHLH148 directly activated the transcription of *OsDREB1E* and positively regulated drought tolerance.

Data availability statement

The original contributions presented in the study are included in the article/Supplementary Material. Further inquiries can be directed to the corresponding authors.

Author contributions

TW, XD and MZ designed the study. MZ performed experiments, data analysis, and wrote the manuscript. RZ, KH, ZW and BG assisted in performing part of the experiments. KH, SH, ZL and WJ assisted in analyzing the data XD and TW supervised the project and modified the manuscript. All authors contributed to the article and approved the submitted version.

Funding

This research was supported by Science and Technology Development Plan of Jilin Province of China (20210302008NC) and National Natural Science Foundation of China (32101664).

Acknowledgments

We thank LetPub (Accdon LLC) for his help in polishing the English text. The content of the manuscript has previously appeared online in a preprint.

Conflict of interest

The authors declare that the research was conducted in the absence of any commercial or financial relationships that could be construed as a potential conflict of interest.

Publisher's note

All claims expressed in this article are solely those of the authors and do not necessarily represent those of their affiliated organizations, or those of the publisher, the editors and the reviewers. Any product that may be evaluated in this article, or claim that may be made by its manufacturer, is not guaranteed or endorsed by the publisher.

Supplementary material

The Supplementary Material for this article can be found online at: https://www.frontiersin.org/articles/10.3389/fpls.2023.1168723/full#supplementary-material

References

Agarwal, P. K., Gupta, K., Lopato, S., and Agarwal, P. (2017). Dehydration responsive element binding transcription factors and their applications for the engineering of stress tolerance. *J. Exp. Bot.* 68 (9), 2135–2148. doi: 10.1093/jxb/erx118

Bang, S. W., Lee, D. K., Jung, H., Chung, P. J., Kim, Y. S., Choi, Y. D., et al. (2019). Overexpression of OsTF1L, a rice HD-zip transcription factor, promotes lignin biosynthesis and stomatal closure that improves drought tolerance. *Plant Biotechnol. J.* 17 (1), 118–131. doi: 10.1111/pbi.12951

Chen, J. Q., Meng, X. P., Zhang, Y., Xia, M., and Wang, X. P. (2008). Over-expression of OsDREB genes lead to enhanced drought tolerance in rice. *Biotechnol. Lett.* 30 (12), 2191–2198. doi: 10.1007/s10529-008-9811-5

Chen, L., Zhao, Y., Xu, S., Zhang, Z., Xu, Y., Zhang, J., et al. (2018). OsMADS57 together with OsTB1 coordinates transcription of its target OsWRKY94 and D14 to switch its organogenesis to defense for cold adaptation in rice. *New Phytol.* 218 (1), 219–231. doi: 10.1111/nph.14977

Fernández-Calvo, P., Chini, A., Fernández-Barbero, G., Chico, J. M., Gimenez-Ibanez, S., Geerinck, J., et al. (2011). The arabidopsis bHLH transcription factors MYC3 and MYC4 are targets of JAZ repressors and act additively with MYC2 in the activation of jasmonate responses. *Plant Cell* 23 (2), 701–715. doi: 10.1105/tpc.110.080788

Fu, J., Wu, H., Ma, S., Xiang, D., Liu, R., and Xiong, L. (2017). OsJAZ1 attenuates drought resistance by regulating JA and ABA signaling in rice. *Front. Plant Sci.* 8. doi: 10.3389/fpls.2017.02108

Gao, J., Yan, S., Yu, H., Zhan, M., Guan, K., Wang, Y., et al. (2019). Sweet sorghum (Sorghum bicolor l.) SbSTOP1 activates the transcription of a β-1,3-glucanase gene to reduce callose deposition under Al toxicity: A novel pathway for Al tolerance in plants. *Biosci. Biotechnol. Biochem.* 83 (3), 446–455. doi: 10.1080/09168451.2018.1540290

Grigorova, B., Mara, C., Hollender, C., Sijacic, P., Chen, X., and Liu, Z. (2011). LEUNIG and SEUSS co-repressors regulate miR172 expression in arabidopsis flowers. *Development* 138 (12), 2451–2456. doi: 10.1242/dev.058362

Gu, X., Gao, S., Li, J., Song, P., Zhang, Q., Guo, J., et al. (2021). The bHLH transcription factor regulated gene OsWIH2 is a positive regulator of drought tolerance in rice. *Plant Physiol. Biochem.* 169, 269–279. doi: 10.1016/j.plaphy.2021.11.031

Gupta, A., Rico-Medina, A., and Caño-Delgado, A. I. (2020). The physiology of plant responses to drought. *Science* 368 (6488), 266–269. doi: 10.1126/science.aaz7614

Hu, H., and Xiong, L. (2014). Genetic engineering and breeding of drought-resistant crops. *Annu. Rev. Plant Biol.* 65, 715–741. doi: 10.1146/annurev-arplant-050213-040000

Huai, J., Zhang, X., Li, J., Ma, T., Zha, P., Jing, Y., et al. (2018). SEUSS and PIF4 coordinately regulate light and temperature signaling pathways to control plant growth. *Mol. Plant* 11 (7), 928–942. doi: 10.1016/j.molp.2018.04.005

Huang, H., Liu, B., Liu, L., and Song, S. (2017). Jasmonate action in plant growth and development. *J. Exp. Bot.* 68 (6), 1349–1359. doi: 10.1093/jxb/erw495

Huang, K., Wu, T., Ma, Z., Li, Z., Chen, H., Zhang, M., et al. (2021). Rice transcription factor OsWRKY55 is involved in the drought response and regulation of plant growth. *Int. J. Mol. Sci.* 22 (9), 4337. doi: 10.3390/ijms22094337

Ke, J., Ma, H., Gu, X., Thelen, A., Brunzelle, J. S., Li, J., et al. (2015). Structural basis for recognition of diverse transcriptional repressors by the TOPLESS family of corepressors. *Sci. Adv.* 1 (6), e1500107. doi: 10.1126/sciadv.1500107

Lee, H., Cha, J., Choi, C., Choi, N., Ji, H. S., Park, S. R., et al. (2018). Rice WRKY11 plays a role in pathogen defense and drought tolerance. *Rice (N Y)* 11 (1), 5. doi: 10.1186/s12284-018-0199-0

Li, S., Cheng, Z., Li, Z., Dong, S., Yu, X., Zhao, P., et al. (2022). MeSPL9 attenuates drought resistance by regulating JA signaling and protectant metabolite contents in cassava. *Theor. Appl. Genet.* 135 (3), 817–832. doi: 10.1007/s00122-021-04000-z

Li, X., Yu, B., Wu, Q., Min, Q., Zeng, R., Xie, Z., et al. (2021). OsMADS23 phosphorylated by SAPK9 confers drought and salt tolerance by regulating ABA biosynthesis in rice. *PLoS Genet.* 17 (8), e1009699. doi: 10.1371/journal.pgen.1009699

Lim, C., Kang, K., Shim, Y., Yoo, S. C., and Paek, N. C. (2022). Inactivating transcription factor OsWRKY5 enhances drought tolerance through abscisic acid signaling pathways. *Plant Physiol.* 188 (4), 1900–1916. doi: 10.1093/plphys/kiab492

Lin, R., Ding, L., Casola, C., Ripoll, D. R., Feschotte, C., and Wang, H. (2007). Transposase-derived transcription factors regulate light signaling in arabidopsis. *Science* 318 (5854), 1302–1305. doi: 10.1126/science.1146281

Lorenzo, O., Chico, J. M., Sánchez-Serrano, J. J., and Solano, R. (2004). JASMONATE-INSENSITIVE1 encodes a MYC transcription factor essential to discriminate between different jasmonate-regulated defense responses in arabidopsis. *Plant Cell* 16 (7), 1938–1950. doi: 10.1105/tpc.022319

Ma, X., Li, Y., Gai, W. X., Li, C., and Gong, Z. H. (2021). The CaCIPK3 gene positively regulates drought tolerance in pepper. *Hortic. Res.* 8 (1), 216. doi: 10.1038/s41438-021-00651-7

Mao, D., Xin, Y., Tan, Y., Hu, X., Bai, J., Liu, Z. Y., et al. (2019). Natural variation in the HAN1 gene confers chilling tolerance in rice and allowed adaptation to a temperate climate. *Proc. Natl. Acad. Sci. U.S.A.* 116 (9), 3494–3501. doi: 10.1073/pnas.1819769116

Marquis, V., Smirnova, E., Graindorge, S., Delcros, P., Villette, C., Zumsteg, J., et al. (2022). Broad-spectrum stress tolerance conferred by suppressing jasmonate signaling attenuation in arabidopsis JASMONIC ACID OXIDASE mutants. *Plant J.* 109 (4), 856–872. doi: 10.1111/tpj.15598

Marquis, V., Smirnova, E., Poirier, L., Zumsteg, J., Schweizer, F., Reymond, P., et al. (2020). Stress- and pathway-specific impacts of impaired jasmonoyl-isoleucine (JA-ile) catabolism on defense signalling and biotic stress resistance. *Plant Cell Environ.* 43 (6), 1558–1570. doi: 10.1111/pce.13753

Mosblech, A., Thurow, C., Gatz, C., Feussner, I., and Heilmann, I. (2011). Jasmonic acid perception by COI1 involves inositol polyphosphates in arabidopsis thaliana. *Plant J.* 65 (6), 949–957. doi: 10.1111/j.1365-313X.2011.04480.x

Pant, B. D., Lee, S., Lee, H. K., Krom, N., Pant, P., Jang, Y., et al. (2022). Overexpression of arabidopsis nucleolar GTP-binding 1 (NOG1) proteins confers drought tolerance in rice. *Plant Physiol* 189 (2), 988–1004. doi: 10.1093/plphys/kiac078

Pauwels, L., Barbero, G. F., Geerinck, J., Tilleman, S., Grunewald, W., Pérez, A. C., et al. (2010). NINJA connects the co-repressor TOPLESS to jasmonate signalling. *Nature* 464 (7289), 788–791. doi: 10.1038/nature08854

Raineri, J., Wang, S., Peleg, Z., Blumwald, E., and Chan, R. L. (2015). The rice transcription factor OsWRKY47 is a positive regulator of the response to water deficit stress. *Plant Mol. Biol.* 88 (4-5), 401–413. doi: 10.1007/s11103-015-0329-7

Rodrigues, J., Inzé, D., Nelissen, H., and Saibo, N. J. M. (2019). Source-sink regulation in crops under water deficit. *Trends Plant Sci.* 24 (7), 652–663. doi: 10.1016/j.tplants.2019.04.005

Schweizer, F., Fernández-Calvo, P., Zander, M., Diez-Diaz, M., Fonseca, S., Glauser, G., et al. (2013). Arabidopsis basic helix-loop-helix transcription factors MYC2, MYC3, and MYC4 regulate glucosinolate biosynthesis, insect performance, and feeding behavior. *Plant Cell* 25 (8), 3117–3132. doi: 10.1105/tpc.113.115139

Seck, P. A., Diagne, A., Mohanty, S., and Wopereis, M. (2012). Crops that feed the world 7: Rice. *Food Secur.* 4 (1), 7–24. doi: 10.1007/s12571-012-0168-1

Seo, J. S., Joo, J., Kim, M. J., Kim, Y. K., Nahm, B. H., Song, S. I., et al. (2011). OsbHLH148, a basic helix-loop-helix protein, interacts with OsJAZ proteins in a jasmonate signaling pathway leading to drought tolerance in rice. *Plant J.* 65 (6), 907–921. doi: 10.1111/j.1365-313X.2010.04477.x

Shen, H., Liu, C., Zhang, Y., Meng, X., Zhou, X., Chu, C., et al. (2012). OsWRKY30 is activated by MAP kinases to confer drought tolerance in rice. *Plant Mol. Biol.* 80 (3), 241–253. doi: 10.1007/s11103-012-9941-y

Sinclair, T. R. (2011). Challenges in breeding for yield increase for drought. *Trends Plant Sci.* 16 (6), 289–293. doi: 10.1016/j.tplants.2011.02.008

Smirnova, E., Marquis, V., Poirier, L., Aubert, Y., Zumsteg, J., Ménard, R., et al. (2017). Jasmonic acid oxidase 2 hydroxylates jasmonic acid and represses basal defense and resistance responses against botrytis cinerea infection. *Mol. Plant* 10 (9), 1159–1173. doi: 10.1016/j.molp.2017.07.010

VanWallendael, A., Soltani, A., Emery, N. C., Peixoto, M. M., Olsen, J., and Lowry, D. B. (2019). A molecular view of plant local adaptation: Incorporating stress-response networks. *Annu. Rev. Plant Biol.* 70, 559–583. doi: 10.1146/annurev-arplant-050718-100114

Wang, Y., Mostafa, S., Zeng, W., and Jin, B. (2021). Function and mechanism of jasmonic acid in plant responses to abiotic and biotic stresses. *Int. J. Mol. Sci.* 22 (16), 8568. doi: 10.3390/ijms22168568

Wang, F., Niu, H., Xin, D., Long, Y., Wang, G., Liu, Z., et al. (2021). OsIAA18, an Aux/IAA transcription factor gene, is involved in salt and drought tolerance in rice. *Front. Plant Sci.* 12, 8568. doi: 10.3389/fpls.2021.738660

Wang, S. C., Tiwari, S. B., Hagen, G., and Guilfoyle, T. J. (2005). AUXIN RESPONSE FACTOR7 restores the expression of auxin-responsive genes in mutant arabidopsis leaf mesophyll protoplasts. *Plant Cell* 17 (7), 1979–1993. doi: 10.1105/tpc.105.031096

Wasternack, C., and Hause, B. (2013). Jasmonates: biosynthesis, perception, signal transduction and action in plant stress response, growth and development. an update to the 2007 review in annals of botany. *Ann. Bot.* 111 (6), 1021–1058. doi: 10.1093/aob/mct067

Wasternack, C., and Song, S. (2017). Jasmonates: biosynthesis, metabolism, and signaling by proteins activating and repressing transcription. *J. Exp. Bot.* 68 (6), 1303–1321. doi: 10.1093/jxb/erw443

Wu, T. Y., Goh, H., Azodi, C. B., Krishnamoorthi, S., Liu, M. J., and Urano, D. (2021). Evolutionarily conserved hierarchical gene regulatory networks for plant salt stress response. *Nat. Plants* 7 (6), 787–799. doi: 10.1038/s41477-021-00929-7

Yan, L., Baoxiang, W., Jingfang, L., Zhiguang, S., Ming, C., Yungao, X., et al. (2021). A novel SAPK10-WRKY87-ABF1 biological pathway synergistically enhance abiotic stress tolerance in transgenic rice (Oryza sativa). *Plant Physiol. Biochem.* 168, 252–262. doi: 10.1016/j.plaphy.2021.10.006

Yao, Y., Dong, L., Fu, X., Zhao, L., Wei, J., Cao, J., et al. (2022). HrTCP20 dramatically enhance drought tolerance of sea buckthorn (Hippophae rhamnoides l). by mediating the JA signaling pathway. *Plant Physiol. Biochem.* 174, 51–62. doi: 10.1016/j.plaphy.2022.01.026

Yokotani, N., Sato, Y., Tanabe, S., Chujo, T., Shimizu, T., Okada, K., et al. (2013). WRKY76 is a rice transcriptional repressor playing opposite roles in blast disease resistance and cold stress tolerance. *J. Exp. Bot.* 64 (16), 5085–5097. doi: 10.1093/jxb/ert298

Yu, L., Chen, X., Wang, Z., Wang, S., Wang, Y., Zhu, Q., et al. (2013). Arabidopsis enhanced drought tolerance1/HOMEODOMAIN GLABROUS11 confers drought tolerance in transgenic rice without yield penalty. *Plant Physiol.* 162 (3), 1378–1391. doi: 10.1104/pp.113.217596

Zhang, M., Zhao, R., Huang, K., Huang, S., Wang, H., Wei, Z., et al. (2022). The OsWRKY63-OsWRKY76-OsDREB1B module regulates chilling tolerance in rice. *Plant J.* 112 (2), 383–398. doi: 10.1111/tpj.15950

Zhou, H., Zhang, F., Zhai, F., Su, Y., Zhou, Y., Ge, Z., et al. (2022). Rice GLUTATHIONE PEROXIDASE1-mediated oxidation of bZIP68 positively regulates ABA-independent osmotic stress signaling. *Mol. Plant* 15 (4), 651–670. doi: 10.1016/j.molp.2021.11.006

Zhu, Z., An, F., Feng, Y., Li, P., Xue, L. A., M., Jiang, Z., et al. (2011). Derepression of ethylene-stabilized transcription factors (EIN3/EIL1) mediates jasmonate and ethylene signaling synergy in arabidopsis. *Proc. Natl. Acad. Sci. U.S.A.* 108 (30), 12539–12544. doi: 10.1073/pnas.1103959108

frontiers | Frontiers in Plant Science

TYPE Original Research
PUBLISHED 14 April 2023
DOI 10.3389/fpls.2023.1118548

Check for updates

OPEN ACCESS

EDITED BY
Meng Jiang,
Zhejiang University, China

REVIEWED BY
Rui-Qing Li,
Anhui Agricultural University, China
Xu Ning,
Guizhou University, China

*CORRESPONDENCE
Ming Zhong
mingzhong@syau.edu.cn
Hai Xu
chinaxuhai@163.com

†These authors have contributed equally to this work and share first authorship

SPECIALTY SECTION
This article was submitted to Plant Abiotic Stress, a section of the journal Frontiers in Plant Science

RECEIVED 07 December 2022
ACCEPTED 20 March 2023
PUBLISHED 14 April 2023

CITATION
Xu J, Yang C, Ji S, Ma H, Lin J, Li H, Chen S, Xu H and Zhong M (2023) Heterologous expression of *MirMAN* enhances root development and salt tolerance in *Arabidopsis*. *Front. Plant Sci.* 14:1118548. doi: 10.3389/fpls.2023.1118548

COPYRIGHT
© 2023 Xu, Yang, Ji, Ma, Lin, Li, Chen, Xu and Zhong. This is an open-access article distributed under the terms of the Creative Commons Attribution License (CC BY). The use, distribution or reproduction in other forums is permitted, provided the original author(s) and the copyright owner(s) are credited and that the original publication in this journal is cited, in accordance with accepted academic practice. No use, distribution or reproduction is permitted which does not comply with these terms.

Heterologous expression of *MirMAN* enhances root development and salt tolerance in *Arabidopsis*

Juanjuan Xu[1†], Caiyu Yang[1†], Shangyao Ji[1], Hui Ma[1], Jingwei Lin[1], Hui Li[1], Shuisen Chen[1], Hai Xu[2*] and Ming Zhong[1*]

[1]Key Laboratory of Agricultural Biotechnology of Liaoning Province, College of Bioscience and Biotechnology, Shenyang Agricultural University, Shenyang, Liaoning, China, [2]Collaborative Innovation Center for Genetic Improvement and High Quality and Efficiency Production of Northeast Japonica Rice in China, Rice Research Institute, Shenyang Agricultural University, Shenyang, Liaoning, China

Introduction: β-Mannanase is a plant cell wall remodeling enzyme involved in the breakdown of hemicellulose and plays an important role in growth by hydrolyzing the mannan-like polysaccharide, but its function in adaptation to salt stress has been less studied.

Methods: Based on cloned the *mannanase (MAN)* gene from *Mirabilis jalapa* L., the study was carried out by heterologously expressing the gene in *Arabidopsis thaliana*, and then observing the plant phenotypes and measuring relevant physiological and biochemical indicators under 150 mM salt treatment.

Results and discussion: The results indicate that MirMAN is a protein with a glycohydrolase-specific structural domain located in the cell wall. We first found that MirMAN reduced the susceptibility of transgenic *Arabidopsis thaliana* to high salt stress and increased the survival rate of plants by 38%. This was corroborated by the following significant changes, including the reduction in reactive oxygen species (ROS) levels, increase in antioxidant enzyme activity, accumulation of soluble sugars and increase of the expression level of RD29 in transgenic plants. We also found thatthe heterologous expression of *MirMAN* promoted root growth mainly by elongating the primary roots and increasing the density of lateral roots. Meanwhile, the expression of *ARF7, ARF19, LBD16* and *LBD29* was up-regulated in the transgenic plants, and the concentration of IAA in the roots was increased. Those results indicate that *MirMAN* is involved in the initiation of lateral root primordia in transgenic plants through the *IAA-ARF* signalling pathway. In conclusion, MirMAN improves plant salt tolerance not only by regulating ROS homeostasis, but also by promoting the development of lateral roots. Reflecting the potential of the *MirMAN* to promote root plastic development in adaptation to salt stress adversity.

KEYWORDS

***mannanase*, salt stress, antioxidant enzyme system, transgenic Arabidopsis, *Mirabilis jalapa* L**

1 Introduction

Soil salinity is one of the major issues limiting plant growth and agricultural production, affecting an estimated 50% of arable land in China by 2050 (Jiang et al., 2019; Lu et al., 2019). High salinity reduces water absorption and ultimately leads to osmotic stress in the plant cell. Moreover, root uptake of large amounts of Na^+ and Cl^- can harm metabolic processes and reduce photosynthetic efficiency (Oka et al., 2013). Oxidative stress, mediated by reactive oxygen species (ROS), is typically accompanied by osmotic stress and ionic toxicity. The effective control of the oxidative damage induced by osmotic and toxic is still critical for plant tolerance to stress.

The root is the first plant organ to encounter salt stress and sense the salt signal. Root activity and biomass are the main indicators to assess the tolerance of plants to stress due to directly affecting plant growth (Li et al., 2018). Root cells respond to adverse environments and boost endogenous defense mechanisms, involving the enhanced processes of synthesis of compatible osmolytes, antioxidants, hormones, transporters, and regulatory proteins. The upregulated expression gene, the response to dehydration 29A (*AtRD29A*), regarded as an indicator of stress tolerance, performs a protective and regulatory mechanism in plants (Jiang et al., 2019). These physiological processes further influence root system conformation *via* distinct mechanisms, including control of cell cycle progression, cell size and shape, and cell wall biosynthesis (Zelm et al., 2020).

Root cell proliferation, elongation, and differentiation all involve cell wall remodeling. As we know, the hemicellulose of the cell wall consists of many different polysaccharides that play a significant role in the highly dynamic changes of the cell wall (Cosgrove, 2005; Mohnen, 2008; Moreira and Filho, 2008). Mannans are major components of polysaccharides present within the plant cell wall and endosperm and are highly difficult to degrade (Jin et al., 2019). The enzymatic cleavage of mannans is achieved by several glycoside hydrolase (GH) enzymes, which act on concert to deconstruct the β-1,4-mannan backbone, ultimately releasing D-mannose and/or mannan oligosaccharides (Wang et al., 2013; Malgas et al., 2015), including mannan endo-1,4-β-mannosidase (EC 3.2.1.25) and 1,4-β-D-mannanase (EC 3.2.1.78), commonly named β-mannanase (MAN) (Sak-Ubol et al., 2016). According to the Carbohydrate-Active enZYmes (CAZY) database, MAN belongs to the glycoside hydrolase family 5 (GH5), a multigene family (Guillon et al., 2012). Previous studies have shown that endo-β-1,4-mannanases regulates a variety of plant growth and developmental processes including embryogenesis, leaf formation, stem elongation, shoot branching, fruit development, pollen development, and lateral root emergence (Nonogaki et al., 2000; Peters and Tomos, 2000; Buckeridge, 2010; Konozy et al., 2012; Yan et al., 2012; Wang et al., 2013; Carrillo-Barral et al., 2018; Yamamoto, 2019; Zang et al., 2019).

PtrMAN6 in poplar is specifically expressed in xylem duct cells and catalyzes hydrolysis for the production of mannan oligosaccharides (Zhao et al., 2013). It confirms that MAN coordinates xylem cell expansion and secondary cell wall deposition. It has been determined that *AtMAN3* gene plays an important role in the regulation of heavy metal Cd tolerance in *Arabidopsis* (Chen et al., 2015). Notably, *MAN2/6* gene expression significantly increased in *Carex rigescens* following salt treatment from transcriptome data and then may have contributed to salt tolerance in *C. rigescens* (Zhang et al., 2020). In plants, MAN participates in a large number of developmental processes. Nevertheless, its function in abiotic stress tolerance remains unknown.

Mirabilis jalapa L., a kind of ornamental plant, has a strong tolerance to petroleum hydrocarbon-contaminated soil and the ability to promote the degradation of pollutant organic molecules (Peng et al., 2009). In this study, we successfully isolated the β-mannanases gene (*MirMAN*); *MirMAN* encodes a protein of 411 amino acids that contains a domain showing 68.13% sequence homology to the glycosyl hydrolase motif with *Spinacia oleracea* (XP_021852790.1), but its exact biological function has not yet been characterized. Complete loss of *MirMAN* function in plants suggests that *MirMAN* may be important for cell wall development and plant-related defense systems following salt stress. Accordingly, we generated *Arabidopsis* plants by heterologous expression of *MirMAN* and compared phenotypic features and responses to salt stress with wild-type plants. Then, we identified the role of *MirMAN* in responding to salt stress with an evaluation of the antioxidant status, soluble sugar accumulation, and lipid peroxidation, as well as an analysis of the expression levels of stress resistance-related genes. These results provide important new insights into the function of *MirMAN* gene in plant stress tolerance.

2 Materials and methods

2.1 Total RNA extraction and PCR amplification of *MirMAN* gene

M. jalapa RNA was extracted from plants grown with petroleum contamination for 45 days using the RNAprep Pure Plant Total RNA Extraction Kit (TianGen, Beijing, China) following the manufacturer's instructions. After detection by 1% gel electrophoresis, the total RNA was first treated to remove the genomic DNA and then transferred into the first strand of cDNA using the PrimeScript RT reagent kit with gDNA Eraser (TaKaRa, Dalian, China) according to the manufacturer's instructions. The first strand of synthesized cDNA was used as a template. The 2× PCR mix (TaKaRa, Dalian, China) was used to perform the PCR (Supplementary Table 1). The amplified product was recovered, directly ligated to the pMD-19T vector using the TA cloning method according to the operating instruction of pMD™ 19-T Vector Cloning Kit (TaKaRa, Dalian, China), and then transformed into TOP 10 competent cells. The positive clones, identified by bacterial liquid PCR using the sequencing primers M13 (M13F: TGTAAAACGACGGCCAGT, M13R: CAGGAAACAGCTATGACC) in the pMD-19T vector, were sent to Biobios (Shanghai, China) for sequencing.

2.2 *MirMAN* gene bioinformatics analysis

The molecular mass and isoelectric point of *MirMAN* were performed with ExPASy (http://web.expasy.org). The sequences of *MAN* in *Arabidopsis thaliana*, *L. esculentum*, and *Brachypodium*

distachyon were obtained from the National Center for Biotechnology Information (NCBI) database (https://blast.ncbi.nlm.nih.gov/Blast). The sequence secondary and tertiary structures were predicted using SOPMA (https://npsa-prabi.ibcp.fr/cgi-bin/npsa_automat.pl?page=/NPSA/npsa_sopma.html) and SWISSMODEL (https://www.swissmodel.expasy.org/interactive/DTDUCp/models/), respectively. The sequence was analyzed for potential nuclear localization signals using cNLS Mapper (http://nls-mapper.iab.keio.ac.jp/cgi-bin/NLS_Mapper_form.cgi), transmembrane regions using TMHMM (Services- DTU Health Tech), and signal peptides using seqNLS (http://mleg.cse.sc.edu/seqNLS/). The predicted amino acid sequences of *MirMAN* and homologous genes were compared using DNAMAN, and a molecular phylogenetic tree was constructed using the neighbor-joining method in MEGA ver. 7.0.

2.3 Subcellular localization of *MirMAN:* GFP

Primer 5.0 software was used to design the primers pCAMBIA1303-*MirMAN*-F: GAAGATCTAAAGAAAGAAAAAATGAAAATAAAT and pCAMBIA1303-*MirMAN*-R: CGGACTAGTTCACCTCCTTAACTTTCTAATAATCCTA. With the use of the double-enzyme (*Bgl*II and *Bam*HI) digestion method, the target gene was inserted into the plant overexpression vector pCAMBIA1303 to construct the pCAMBIA1303-*MirMAN :* GFP vector. The recombinant plasmid and PAD62 plasmid were transformed into competent *Agrobacterium tumefaciens* GV3101 cells, which were injected into tobacco leaves. Plants were grown in the dark for 1 day and then transferred to long-day conditions (16-h light/8-h dark) for 2 days. The leaf epidermal cells were incubated in 10% sucrose solution for 10 min to induce plasmolysis. The pCAMBIA1303-35S-*MirMAN :* GFP protein localization was observed under a laser confocal microscope (Leica, TCSSP8, Wetzlar, Germany).

2.4 Genetic transformation and identification of *MirMAN* overexpression transgenic lines

Agrobacterium LBA4404 containing the recombinant pCAMBIA1303-*MirMAN* overexpression vector was transfected into *Arabidopsis* Col-0 inflorescences, and the infected mature seeds (T0) were collected and cultured on 0.5× Murashige and Skoog (MS) (containing 20 mg/L of hygromycin) solid medium to screen for positive transformants. The *Arabidopsis* seedlings of various lines capable of rooting on the hygromycin-containing medium were identified by leaf PCR with a 2× PCR mix (Aidlab, Beijing, China) and the detection primers. A total of 33 transgenic lines with positive PCR results were selected for subsequent experiments. PCR conditions were 35 cycles of amplification (98°C for 10 s, 55°C for 5 s, and 72°C for 30 s). The total RNA was isolated from the transgenic *Arabidopsis* lines OE#1-33 and wild-type *Arabidopsis* using the RNA plant Plus reagent (TianGen, Beijing, China) based on the manufacturer's instructions. The quantitative PCR (qPCR) was carried out using a FastKing RT Kit with gDNase (KR116, TianGen, Beijing, China) and SYBR Green qPCR Mix (Monad, Suzhou, China) according to the manufacturer's protocols. qPCR was performed using Monad Selected q225MX (Monad Biotech Co., Ltd., Suzhou, China) real-time detection system. We used the reference gene *AtACTIN2* as endogenous controls for *Arabidopsis* (Supplementary Table 1). Three replicate reactions were routinely performed per sample.

2.5 Western blotting assays

For the Western blotting test of the *Arabidopsis* leaves, the protein content was measured using the method of Bradford (1976). Proteins were separated according to molecular weight by sodium dodecyl sulfate–polyacrylamide gel electrophoresis (SDS-PAGE) on a 10%–14% gradient gel and then transferred to an immobilon-P polyvinylidene difluoride (PVDF) membrane (Solarbio, Beijing, China). Proteins were conventionally detected with the MirMAN antibody (custom-made by GenScript, Piscataway, NJ, USA). Further, an anti-rabbit horseradish peroxidase (HRP) antibody was used as a secondary antibody. The blots were incubated with ECL Western Blotting Substrate (Solarbio, Beijing, China) and imaged using a Bio-Rad image analyzer (Bio-Rad, Hercules, CA, USA).

2.6 Morphological characterization of plant

Surface-sterilized seeds were plated on 0.5× MS medium with 1% sucrose and 1% agar (pH 5.7), and the plates were incubated in the dark at 4°C for 3 days. Then, plants were grown in the artificial growing room at a temperature of 22°C, 16-h light and 8-h dark (60% humidity and 120 μmol m^{-2} s^{-1} during a 16-h daily light period). We conducted digital images of root system morphology using a desktop scanner and determined the root length and the number of tips, forks, and crossings by using WinRHIZO. The seedlings were grown on 0.5× MS medium for 4 days, and then the agar plates were rotated 90°, causing the gravistimulus for 48 h. Data were compiled from three independent experiments with each line. Methods for the determination of IAA contents in the seedlings by mass spectrometry were described (Jia et al., 2020).

2.7 Salt stress treatment and physiological index determination of transgenic plants

For salt stress treatment, wild-type (WT) *Arabidopsis* and transgenic lines were planted in the same black plastic pots in the soil, and the plants were grown in a greenhouse. The 3-week-old seedlings in soil were irrigated with water and 150 mM of NaCl solution every 3 days and sampled at 0, 3, 5, and 7 days. Soil-grown *Arabidopsis* plants that were 24 days old were continuously watered with or without 150 mM of NaCl for 7 days, followed by an analysis of the survival rate after recovery for 1 week.

Catalase (CAT) activity was assayed on the basis of its ability to decompose H_2O_2 and measured at 240 nm. Superoxide dismutase (SOD) activity was determined by measuring its ability to inhibit the reduction of nitro blue tetrazolium chloride (NBT). Peroxidase (POD) activity was measured as the oxidation of guaiacol in the presence of H_2O_2, during which tetraguaiacol was formed. Lipid peroxidation in the plants was measured by the thiobarbituric acid-reacting substance and was expressed in terms of malondialdehyde (MDA) content. Diaminobenzidine (DAB) and NBT staining were used to confirm the detection of O_2^- and H_2O_2, respectively. Glutathione (GSH) levels were measured according to the instructions supplied with the GSH Assay Kit (Suzhou Comin Biotechnology, Suzhou, China). Total soluble sugar was assayed by the anthrone method, which is widely used for the determination of soluble sugars. In brief, approximately 2 mL of the anthrone chemical reagent was added to 1 mL of the sample and then measured at 630 nm, and total soluble sugar content was calculated. Endo-β-mannanase activity was measured by a spectrophotometric method (Determination of activity β-mannanase as feed additives—Spectrophotometric method, GB/T 36861-2018, China). Briefly, the reducing oligosaccharides and monosaccharides can react with the 3,5-dinitrosalicylic acid reagent in a boiling water bath to yield a color change indicative of mannose hydrolysis. Each measurement was repeated at least three times, with data collection repeated at least three times.

2.8 Statistical analysis

All the data were presented as averaged values of three independent replicates. Statistical analyses of the data were carried out using Student's *t*-tests, and multiple comparisons of means were analyzed using Tukey's test. Differences were considered statistically significant at $p< 0.05$.

3 Results

3.1 Cloning and characterization of *MirMAN* in *Mirabilis jalapa*

The coding sequence of *MirMAN* was predicted from transcriptome sequencing results (data not published). The open reading frame (ORF) sequence of *MirMAN* is 1,233 bp long and contains 411 amino acids, with a predicted molecular weight of 47.08 kDa and an isoelectric point of 7.16 (pI 7.16). The calculated instability coefficient and hydrophobicity are 38.81, and −0.46, respectively, which are indicative of stable hydrophilic protein. Multiple sequence comparisons showed that MirMAN was 46.96%, 45.85%, 43.99%, 42.65%, and 42.31% consistent with LeMAN1, AtMAN7, LeMAN4, AtMAN3, and AtMAN1, respectively (Figure 1). In the secondary structure of MirMAN, α-helix accounted for 38.2%, β-sheets for 10.7%, extension chain for 20.9%, and random structures for 30.17%. Computational analysis predicted that *MirMAN* folds in a typical (β/α)8-TIM barrel structure, with multiple β-sheets forming a hydrophobic domain (Supplementary Figure 2).

3.2 Subcellular localization of MirMAN protein

The marker for plasma membrane (PM), PAD62-mcherry, was co-expressed with pCAMBIA1303-35S-MirMAN-GFP by *Agrobacterium*-mediated transient expression in *Nicotiana benthamiana* leaves. After 16 h of agroinfiltration, we observed fluorescence in the green channel with a confocal laser scanning microscope and compared its position. Red PAD62 fluoresced in membrane epithelial cells (Figure 2A). pCAMBIA1303-35S-MirMAN-GFP green fluorescence was clearly distributed in a dotted pattern in the cell (Figure 2A). To investigate whether these signals were outside or inside the membrane, 30% sucrose was added to induce plasmolysis of *N. benthamiana* leaf cells, and images were acquired using a confocal microscope. Upon plasmolysis, the pCAMBIA1303-35S-MirMAN-GFP signal remained predominantly associated with the cell wall, although the PAD62-labeled PM retracted from the cell wall (Figure 2B).

3.3 Generation of transgenic *Arabidopsis* lines

The *MirMAN* ORF sequence was conducted into a plant binary vector control of the constitutive CaMV 35S promoter and transformed into *Arabidopsis* Columbia-0 (Col-0) plants. Thirty-three independent transgenic *Arabidopsis* lines were generated, their identity from 33 lines had already been confirmed by PCR analysis, and these lines were designated OE#1–33 (Figure 3A). Expression of MirMAN protein in the transgenic lines was demonstrated by Western blotting. Figure 3B shows the result of Western blotting after polyclonal MirMAN antibody detection. As shown in Figure 3B, a clear band was observed at approximately 47 kDa and was specifically precipitated by the antibody, but not in the control group. These results indicate that MirMAN has been successfully integrated into the *Arabidopsis* genome. Therefore, T3 mutants (#20, #26, and #33) were selected for further analysis. We identified *MirMAN* gene expression levels in T3 generation transgenic lines under normal conditions (Supplementary Figure 1).

3.4 Effects of root system architecture in *MirMAN* heterologous-expressing *Arabidopsis*

Compared to WT *Arabidopsis*, transgenic *Arabidopsis* lines #20/26/33 display an increased total number of lateral roots and primary root lengths in the 0.5× MS medium (Figure 4). Indeed, we noticed that the OE#20/26/33 lines with numerous lateral roots were up to 3.5–4-fold. To assess this possibility, we used gravitropic stimulation to synchronize lateral root primordia initiation in WT and OE#20/26/33 seedlings (Figure 5A). The period of the seedlings' lateral root primordia emergence was defined as eight time periods, and their temporal developmental axis is shown in Figure 5B. We observed that transgenic *Arabidopsis* #20/26/33 lines display increased lateral root density and lateral root primordia per developmental stage III–VIII (Figure 5C). To better understand the relationship between IAA

10.3389/fpls.2023.1118548

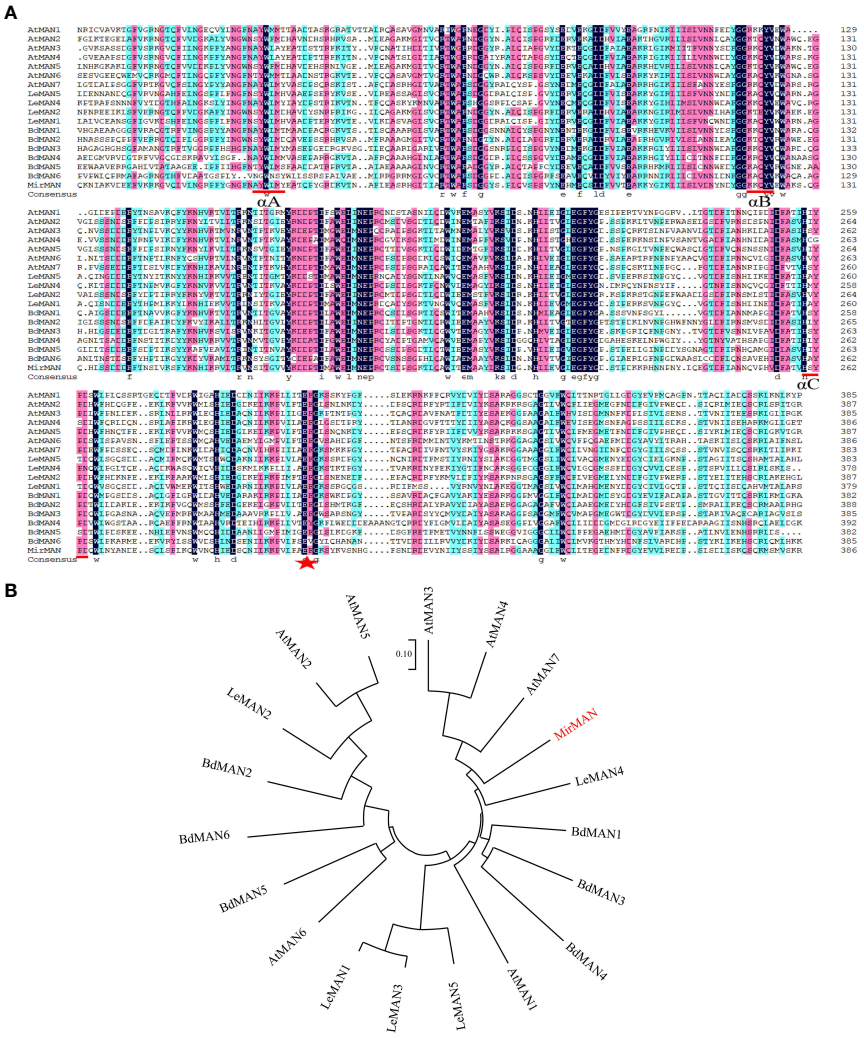


FIGURE 1
Alignment of sequences and phylogenetic tree of MirMAN proteins. **(A)** Alignment of sequences of MirMAN proteins and homologs from others species. Blue inverted triangles indicate signal peptide sites, red lines indicate the MAN conserved sequence, and red star indicates the catalytic glutamate residue structural motif. Multiple sequence comparisons showed that MirMAN was 46.96%, 45.85%, 43.99%, 42.65%, 42.31%, 41.79%, 39.72%, 39.15%, 39.08%, 35.71%, 35.03%, 34.98%, 34.57%, 34.41%, 33.64%, 31.98%, 31.57%, and 29.13%, consistent with LeMAN1, AtMAN7, LeMAN4, AtMAN3, AtMAN1, AtMAN4, LeMAN5, BdMAN1, LeMAN3, AtMAN6, BdMAN5, BdMAN2, AtMAN5, AtMAN2, BdMAN3, LeMAN2, BdMAN4 and AtMAN6, respectively. **(B)** Phylogenetic tree of MirMAN proteins from *Mirabilis jalapa* and other species. At, *Arabidopsis thaliana*; Bd, *Brachypodium distachyon*; Le, *Lycopersicon esculentum*.

content and the numerous lateral roots, transgenic *Arabidopsis* lines' IAA content was tested. IAA content was more accumulated in transgenic *Arabidopsis* line #26 (Figure 5D). We focused on the expression of root development-related genes, which was upregulated by 3–10-fold in transgenic lines compared to that of control plants, including *LBD16* (lateral organ boundaries domain), *LBD29*, *ARF7* (auxin response factor), and *ARF19* (Figure 5E).

3.5 Salt tolerance analysis of *MirMAN* heterologous-expressing transgenic *Arabidopsis*

In the comparison of phenotypic differences between the WT and the OE#26 plants under salt stress, the treatment of WT *Arabidopsis* with 150 mM of NaCl strongly inhibited root growth, and OE#26 showed less growth inhibition when treated with 150 mM of NaCl in soil (Figure 6). To determine salt tolerance in soil, we treated 24-day-old soil-grown plants with 150 mM of NaCl for additional 7 days, followed by recovery for 1 week. Most of the leaves of WT *Arabidopsis* gradually turned yellow, shrunk in size, and wilted, but the wilting symptoms of OE#26 plants were significantly slower than those of the control (Figure 6A). In addition, after rehydration, 61% of OE#26 plants and only 23.0% of control plants resumed their growth (Figure 6B). Salt stress significantly inhibited root and shoot fresh weight in WT and transgenic *Arabidopsis*. Specifically, the OE#26 plants showed a significantly higher root fresh weight, shoot fresh weight, and root/shoot ratio than those in WT plants under salt stress ($p \leq 0.05$) (Figures 6C, D). While WT plants responded to salt stress by

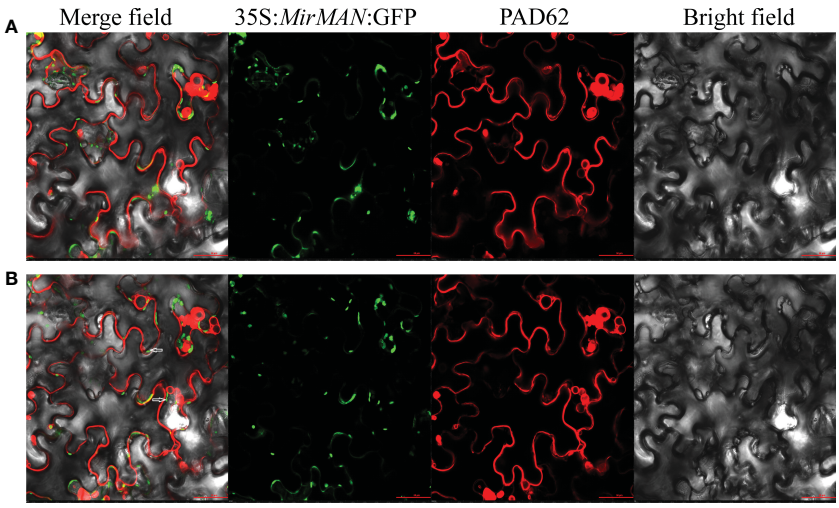


FIGURE 2
Subcellular localization of MirMAN. **(A)** Subcellular localization of 35S:*MirMAN:* GFP in tobacco cells. **(B)** Subcellular localization of 35S:*MirMAN:* GFP following 30% sucrose treatment. Bar = 50 μm. After plasmolysis, GFP signal observed in the cell wall is indicated by white arrows.

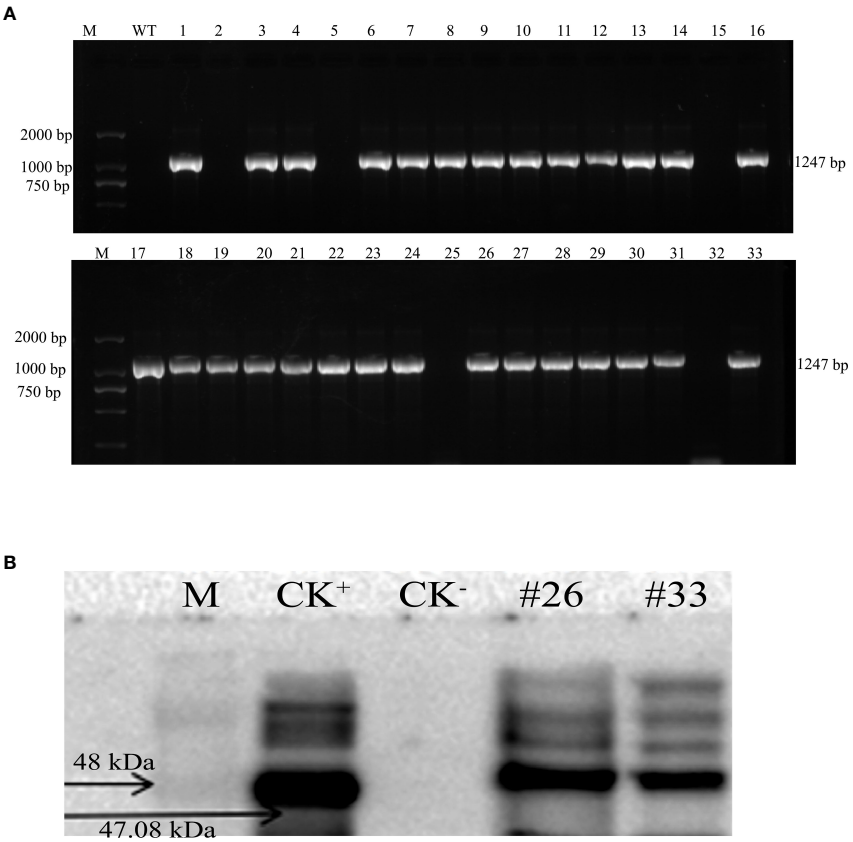


FIGURE 3
Characterization of recombinant *MirMAN* gene in *Arabidopsis*. **(A)** Cloning of *MirMAN* gene and PCR identification of T2 transgenic *Arabidopsis*. **(B)** The specific antibody was used for Western blotting. **(A)** M: DL marker 2,000; WT: wild type (negative control); the others are the 33 transgenic lines. **(B)** M: marker; CK^+, positive control; CK^-, negative control; the others are the transgenic lines.

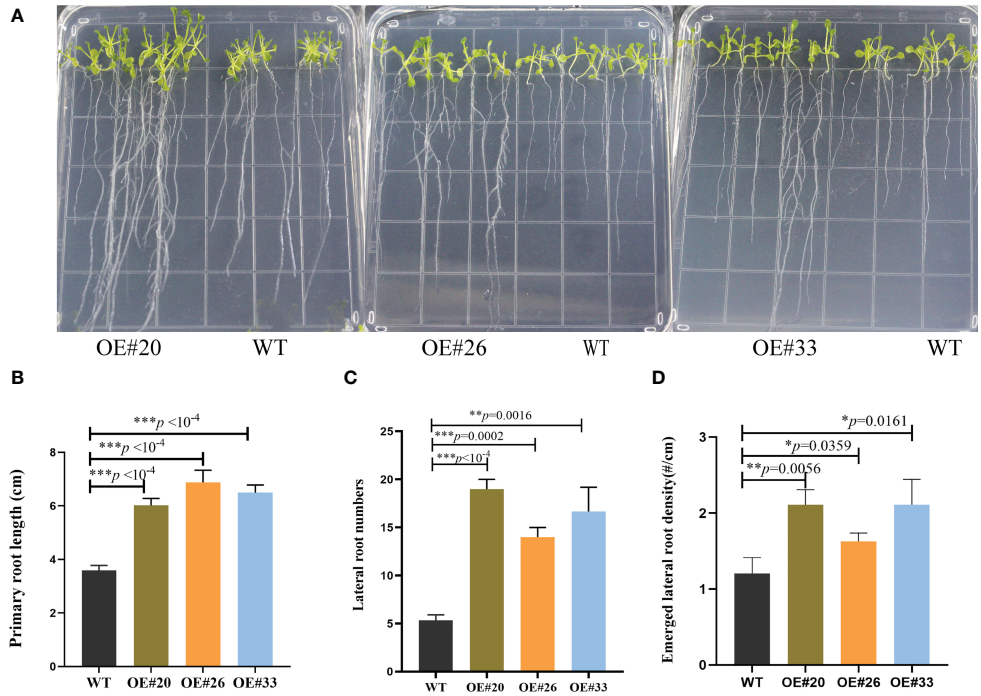


FIGURE 4
MirMAN regulation of root development on transgenic *Arabidopsis* plants. **(A)** The phenotypic root observation of wild type (WT) and *MirMAN-OE* lines. **(B)** Length of the primary root. **(C)** Number of lateral roots. **(D)** Density of lateral root primordia. The seedlings were cultured for 12 days. Data are means ± SD (n = 10). *p< 0.05, **p< 0.01, ***p< 0.001, independent-samples t-test.

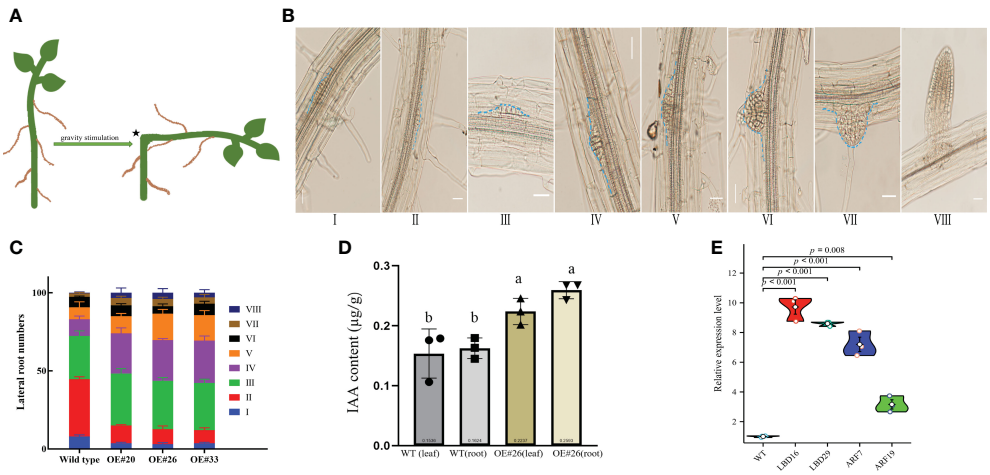


FIGURE 5
Comparison of lateral root density of wild type (WT) and OE lines *Arabidopsis* plants at various developmental stages. **(A)** Diagram showing a classic approach that was used to induce lateral root initiation and formation. Bending the horizontally placed primary root tip 90° and allowing the root tip to grow in the direction of gravity can induce the initiation and formation of lateral roots at the convex side of the bending site, as indicated by an asterisk. **(B)** Lateral root formation at different developmental stages detected from a root of single plant. **(C)** Measurements of the percentage of lateral root formation of WT and OE lines *Arabidopsis* at various developmental stages (n = 100). Measurements were carried out after gravity stimulation for 48 h. **(D)** IAA content in WT and OE#26 seedlings. **(E)** Expression level of *LED16*, *LBD29*, *ARF7*, and *ARF19* genes. At least three independent biological replicates were carried out, and consistent results were obtained. Results from one representative experiment are shown. Ten-day-old seedlings were used for analysis. Data shown represent average and SD (n = 100). Letters indicate the results for comparisons across groups using Tukey's *post hoc* tests.

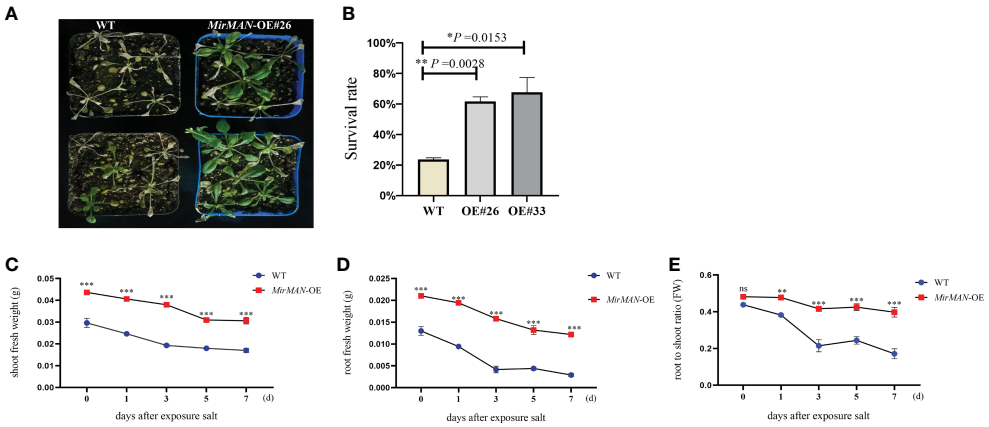


FIGURE 6
Effect of salt stress on *MirMAN*-overexpressed *Arabidopsis* plants. **(A)** Plants were grown on soil for 3 weeks and then exposed to 150 mM NaCl stress. **(B)** Survival rate under 150 mM NaCl stress. **(C)** Shoot fresh weight of plants. **(D)** Root fresh weight of plants. **(E)** Root-to-shoot ratio. n = 5. Error bars indicate ± SD. Student's t-tests were used to compare the measurements of OE lines with those from wild type (WT). *p< 0.05, **p< 0.01, ***p< 0.001. ns represents no significance at p > 0.05.

decreasing their root-to-shoot ratio, the ratio in transgenic *Arabidopsis* remained unchanged (Figure 6E).

3.6 *MirMAN* heterologous expression improves free radical scavenging activity and antioxidant status

We next tested the physiological alterations in WT and OE#20/26 plants under salt stress conditions. We also measured the H_2O_2 and O_2^- characteristics by chemical staining and analyzed the H_2O_2 and O_2^- contents of WT and OE#26 plants after salt treatment. We found that WT plants accumulated more H_2O_2 and O_2^- than OE#26 plants (Figures 7A, B). Upon NaCl treatment, the average MDA content in WT plants was 4.49 times higher than in MirMAN heterologous expression plants (Figure 7C). The OE#20/26 plants increased the levels of GSH compared to the values of the WT *Arabidopsis* during the normal conditions (Figure 7D). Upon salt treatment, the values of GSH and GSH/GSSH in both the OE lines and WT plants increased significantly, with the OE lines exhibiting significantly higher levels than WT *Arabidopsis* (Figures 7D, F). The opposite was true for oxidized GSH (GSSG) concentrations, whose levels were 25.64 and 24.67 significantly lower for the OE lines compared to the WT (52.09), respectively (Figure 7E). In addition, GSH/GSSG values in the OE lines under salt stress increased to a greater extent compared to those in the WT *Arabidopsis* (Figure 7F). The total soluble sugar content in the OE#20/26 plants was 1.6 times that in the WT plants (Figure 8A). Under control conditions, total mannanase activity in both OE lines had significant increases compared to that in the WT plants (Figure 8B), showing that increased *MirMAN* overexpression resulted in more mannanase production. Moreover, salt stress increased the

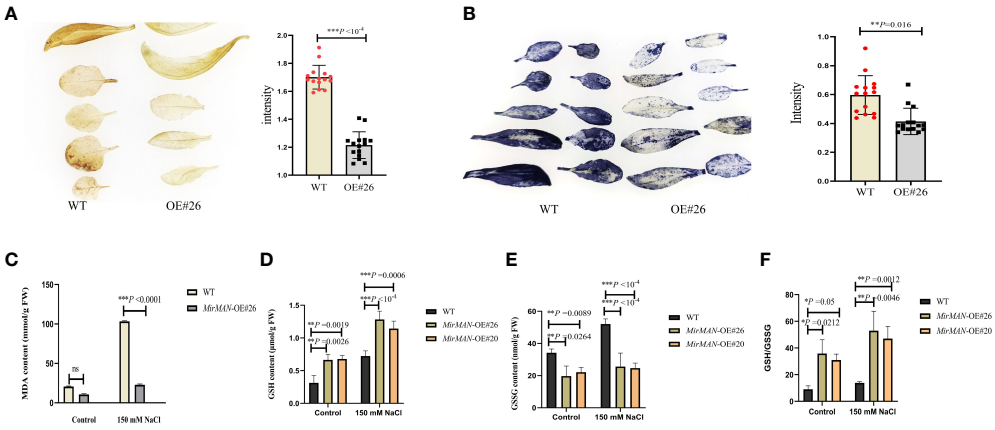


FIGURE 7
Evaluation of salt resistance in WT and OE lines *Arabidopsis* plants. **(A)** H_2O_2 contents. **(B)** O_2^- contents. **(C)** MDA contents. **(D)** GSH contents. **(E)** GSSG contents. **(F)** GSH/GSSG. MDA, malondialdehyde; GSH, glutathione; GSSG, oxidized glutathione; WT, wild type. Error bars indicate ± SD. Student's t-tests were used to compare the measurements of OE lines with those from WT. *p< 0.05, **p< 0.01, *** p< 0.001. ns represents no significance at p > 0.05.

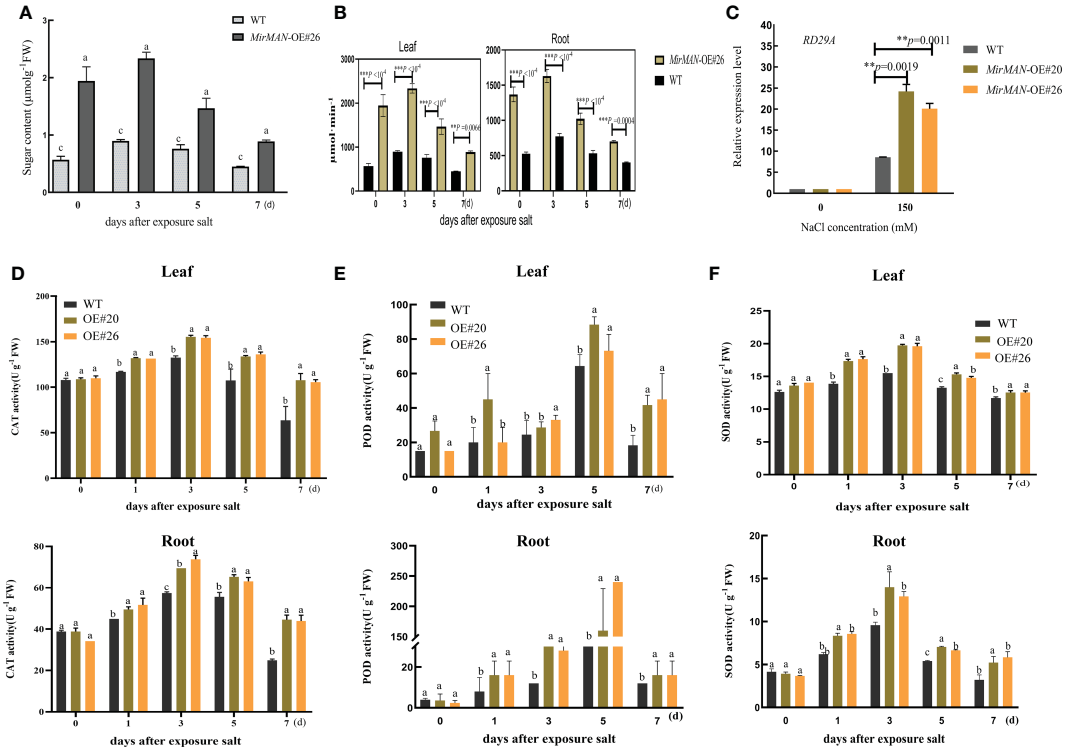


FIGURE 8
Salt resistance analysis of WT and transgenic lines of *Arabidopsis* plants. **(A)** Soluble sugar contents. **(B)** Endo-β-mannanase activity. **(C)** *RD29A* gene expressions after salt experiment. **(D)** CAT activity. **(E)** POD activity. **(F)** SOD activity. SOD, superoxide dismutase; POD, peroxidase; CAT, catalase; WT, wild type. Error bars indicate ± SD. Student's *t*-tests were used to compare the measurements of OE lines with those from WT. $^{**}p < 0.01$, $^{***}P < 0.001$. Letters indicate the results for comparisons across group using Tukey's *post hoc* test.

transcript levels of *RD29A* in transgenic plants by at least twice compared to those in WT plants (Figure 8C). Furthermore, our data show that *MirMAN* substantially increases CAT, POD, and SOD activities (Figures 8D–F).

4 Discussion

Although the orthologues of *MAN* genes have been identified in many plant species, such as *L. esculentum*, *B. distachyon*, and *Brassica rapa*, the influence of *MirMAN* on the regulation of growth remains almost unknown (Nonogaki et al., 2000; Iglesias-Fernández et al., 2011; González-Calle et al., 2015; Carrillo-Barral et al., 2018). Here, *MirMAN* was cloned from *M. jalapa* L., and its function of improving the growth and salt tolerance of plants was analyzed in *Arabidopsis*.

4.1 Characteristic and subcellular localization analyses of *MirMAN*

Sequence and phylogenetic analyses showed that *MirMAN* is homologous to *AtMAN7*, but its function has not been fully resolved (Figure 1). Here, we demonstrated that the heterologous expression of *MirMAN* can substantially alter relevant root development without abiotic stress in *Arabidopsis*. Like other MANs, *MirMAN* has a putative signal peptide and an active site with the expected conserved amino acids. The *MirMAN* is composed of a sole GH5 catalytic module without any attached carbohydrate-binding module (CBM). Judging from the subcellular distribution of *MirMAN :* GFP protein fluorescence signal in *Nicotiana tabacum* cells, *MirMAN* was localized to the cell wall (Figure 2). The subcellular localization of *MirMAN* on the cell wall might play an important role in cell-wall loosening, as many cell expansion requires primary cell-wall loosening and incorporation of newly synthesized cell-wall material.

4.2 Effects of heterologous expression of *MirMAN* on plant growth in *Arabidopsis*

Heterologous expression of *MirMAN* gene in *Arabidopsis* enhances plant growth. The effect of 35S: *MirMAN* transgenic plants on leaf development was particularly striking in rosette leaves. In *MirMAN* transgenic plants, the rosette leaves were large and elongated with increases in the compactness of the branches and leaves of the plants (Supplementary Figure 3). *MirMAN* causes a series of metabolic changes in transgenic plants, among which the increased cell growth rate is one of them. Moreover, the heterologous expression of *MirMAN* obviously changed root system architecture in transgenic plants, including longer primary roots and more numbers of lateral roots (Figures 4, 5). This

indicates that *MirMAN* ultimately affects lateral root formation at different developmental stages. Lateral roots are important not only for determining plants' root system phenotypes in soil but also for absorbing water and nutrients (Lucob-Agustin et al., 2020). Several studies have set to demonstrate cell wall composition and extensibility mediated by cell wall modification enzymes necessary for root cell elongation, thereby controlling root elongation and, consequently, root development (Tabuchi and Matsumoto, 2001; Ma et al., 2004). In our study, the number of lateral roots of transgenic plants increased, which may enable them to store more water. Transgenic plants showed an enhanced survival capacity compared with the control plants in salt treatment.

Exogenous application of auxin or improved endogenous auxin synthesis leads to a significant increase in the number of lateral roots (Laskowski et al., 1995). In these experimental results, the increase of lateral roots of overexpression *MirMAN* is closely related to the increase of endogenous auxin (Figure 5D). It is speculated that there may mechanisms, as follows: 1) the increase of auxin concentration promoted the early arrival of auxin oscillation peak. After detection of the initial signal auxin, rhizosphere meristem cells rapidly select lateral root cells, accelerate lateral root primordium development, and further develop lateral root organs. 2) When the lateral root primordium breaks through the epidermis, the cell wall is more likely to change; that is, cells are more likely to detach and form new cells, thereby speeding up the overall lateral root development. 3) The polysaccharide composition of the cell wall changed. Mannanase cleaves mannan or mannan oligosaccharide, and its products mannan oligosaccharide and mannose are speculated to be involved in upstream signal control hormone signal, which may have a positive development feedback mechanism, but the relationship between them needs to be further proved.

Like other *MAN*s, C has putative glutamate catalytic residues for breaking the mannosidic bond (http://smart.embl-heidelberg.de/). Typical MAN proteins are composed of three helices: αA, αB, and αC (Figure 1). *MirMAN* is mainly predicted to control the extensibility of the cell wall by causing crosslinking or cleaving of cell wall polysaccharides and thus promote cell wall loosening and therefore growth. We speculated that *MirMAN* promotes hydrolysis of hemicellulose by endo-β-1,4-mannanases, thereby enhancing cell wall expansion. Endo-β-mannanase hydrolyzes mannan oligosaccharide or mannans to produce mannose and/or mannan oligosaccharide (Wang et al., 2013). The research found that galactoglucomannan oligosaccharide (GGMO) treatment, while promoting the primary root elongation and stimulating the emergence of lateral roots, influences *Zea mays* L. growth development (Kollárová et al., 2018). Previous studies have focused on the downstream effects of lateral root formation during root development, as glucose acts upstream of the BR signal transduction pathway to regulate the lateral root process by dose-dependently. Similarly, glucose also acts on the fiber elongation in cotton directly by BR signal transduction (Gupta et al., 2015; Li et al., 2022).

4.3 Heterologous expression *MirMAN* most likely leads to salt tolerance in *Arabidopsis*

Salt stress is dramatically imposing severe constraints on plant adaptation, crop productivity, and quality. The search for molecule regulation of plant stress responses and plant development remains a key priority in the fight against abiotic stress resistance. As plants are exposed to abiotic stresses, most of the root system architectures (RSAs) altered according to the environment contribute to tolerance and recovery, which involves gene expression of root cell wall remodeling (Motte and Beeckman, 2019; Zhang et al., 2019). Overexpression of *MirMAN* causes suitable root phenotypes in transgenic plants within salt stress, including main root elongation and promoting lateral root density (Supplementary Figure 4), which positively regulates the salt stress resistance. This positive effect may have partially offset the growth inhibition induced by salt stress in transgenic *Arabidopsis*.

Adversity can cause the overproduction of ROS and thereby affects oxidative stress, endoplasmic reticulum (ER) stress, and consequent damage to proteins and subcellular organelles in plants (Mittler et al., 2011). Several cellular mechanisms have been shown to counterbalance the production of ROS, including enzymatic and non-enzymatic pathways. In plants undergoing salt stress responses, antioxidant enzyme activities are important for suppressing ROS-induced oxidative stress. At 150 mM NaCl-treated groups, H_2O_2 and O_2^- were overproduced in wild-type plants (Figures 7A, B). Considering SOD, CAT, and ascorbate peroxidase (APX) activity data in transgenic lines of *Arabidopsis* (Figures 8D–F), it is concluded that both antioxidant enzymes successfully eliminate the excess of H_2O_2 and O_2^-, avoiding the oxidative stress damage caused by salt stress. By contrast, the heterologous expression in *MirMAN* plants shows a lower MDA content than in wild-type plants (Figure 7C). Similarly, glutathione is an endogenous antioxidant that exists in either reduced (GSH) or oxidized (GSSG) form that protects various cellular structures from oxidative damage. Under salt stress, the GSH levels of both WT and *MirMAN* transgenic lines of *Arabidopsis* were significantly upregulated, but the GSH level of OE#26 was more significant (Figure 7D), indicating that there are more GSH in the OE#26 against more oxidative stress. Also, in the transgenic plants, more glutathione was used for the reduction reaction, and less glutathione was produced by oxidation (Figure 7E). Glutathione accumulated in higher concentrations in *MirMAN* transgenic lines, which in turn helped plants to withstand oxidative stress mediated by the H_2O_2 and O_2^- during episodes of salt stress. These results suggest that overexpression of *MirMAN* plants reduces the accumulation of oxidative H_2O_2 and O_2^- by enhancing antioxidant defenses to oxidative stress. The *MirMAN* transgenic *Arabidopsis* lines have optimized an antioxidant defense system to increase salt tolerance. Soluble sugar fraction levels in these lines are significantly increased compared with wild-type levels (Figure 8A). Plants can use metabolites to reduce the osmotic potential of plants, which

prevents the imbalance of ROS production and ensures water balance for the normal growth of plants under salt stress. The metabolites are bioactive molecules that play a key role in stress, but they are also osmotic regulators of many intracellular processes including preventing membrane fusion and stabilizing enzymes and other intracellular components to cope with salt stress. The relationship between these metabolites interacting with salt tolerance needs further studies (Ismail and Horie, 2017; Liu et al., 2021).

Moreover, we believe that the proposed root development strategy could also substantially improve their performance in salt stress and recovery efficiency. Studies showed that the BR signal transduction component *BES1* directly affects the expression of cell wall remodeling genes *XTH19* and *XTH23* as a positive regulator of salt stress, which promoted the development of lateral roots and thus improved the salt adaptability (Xu et al., 2020). Mannose acts as a signal molecule to regulate plant growth and development (Richterová-Kučerová et al., 2012). It suggests that these sugar molecules can specifically integrate various responses to endogenous and environmental signals to modulate root development in *Arabidopsis* (Valifard et al., 2021). Plant abiotic stress resistance is improved by the application of the small molecule sugar and interferes with the transcriptional dynamics of downstream signal transduction, indicating that it plays an important role in stress-related pathways. Most of the underlying molecular mechanisms remain unclear (Liu et al., 2021). Understanding how the *MirMAN* hydrolysate perceives, integrates, and responds to environmental signals is critical for improving plant resistance to stress and will be the focus of our future research efforts.

The experiment aimed to study the response mechanism of *MirMAN* to salt stress. Little is known about the physiological functions of these enzymes *in planta*. Although the causal relationship between hydrolysis products of mannanase and lateral root development is yet to be established by designing further experiments, this provides us a new insight into the accumulation of endo-β-mannanase in plants, which causes a change in plant growth and development under salt stress. It also provides further intriguing evidence suggesting that the cell wall remodeling gene may have widespread and as yet largely unrecognized functions in plant growth, development, and plant stress tolerance. At present, we cannot distinguish between direct effects (e.g., specific binding to a receptor) and indirect effects (e.g., hydrolysate). Nevertheless, elucidation of the mechanistic basis of these effects is likely to provide new insights into the factors that govern plant growth and stress tolerance.

In summary, we successfully isolated *MirMAN* gene from *M. jalapa* and defined its location and function (Figure 9). The heterologous expression of *MirMAN* enhanced *Arabidopsis* growth and development and improved the resistance of transgenic *Arabidopsis* to salt stress by increasing soluble sugar contents and enhancing antioxidant defenses. *MirMAN* plays an important role in plants by enhancing root growth. It can be a candidate gene for plant molecular breeding and provide valuable insights into the physiological significance of *MAN* in plant abiotic stress.

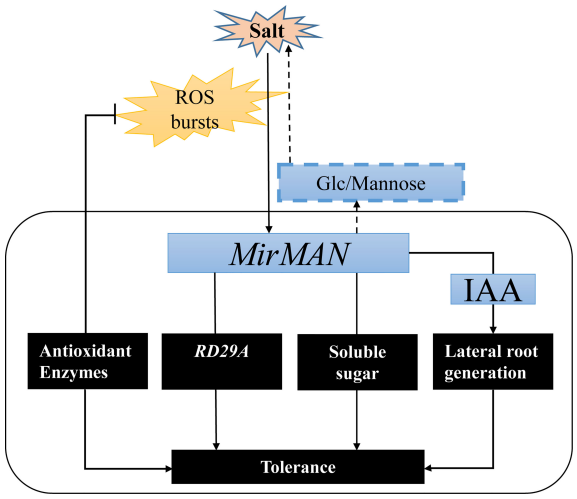


FIGURE 9
A hypothetical model showing the roles of MirMAN in regulating salt tolerance. MirMAN affects the expression of its downstream stress genes such as *RD29A*, mediating plant tolerance during development and salt stress. MirMAN can hydrolyze mannans and increase soluble sugar content to alleviate osmotic stress. It can also regulate plant tolerance by causing changes in the antioxidant enzyme system.

Data availability statement

The original contributions presented in the study are included in the article/Supplementary Materials, further inquiries can be directed to the corresponding author/s.

Author contributions

MZ and HX were responsible for the study design. JX, CY, SC and HL drafted the manuscript. JX, CY and SJ performed the experiments. SJ, CY, HM and JL performed the statistical analyses. All authors contributed to the article and approved the submitted version.

Funding

This work was supported by the Special funds of "Collaborative Innovation Center for Genetic Improvement and High Quality and Efficiency Production of Northeast Japonica Rice In China (2022)" (Grant No. KF2022-07).

Acknowledgments

We thank the team of researcher Lu Xiaochun from Liaoning Province Key Laboratory of Crop Molecular Improvement and Sorghum Institute of Liaoning Academy of Agricultural Sciences for kindly helping us with *Arabidopsis* cultivation.

Conflict of interest

The authors declare that the research was conducted in the absence of any commercial or financial relationships that could be construed as a potential conflict of interest.

Publisher's note

All claims expressed in this article are solely those of the authors and do not necessarily represent those of their affiliated organizations, or those of the publisher, the editors and the reviewers. Any product that may be evaluated in this article, or claim that may be made by its manufacturer, is not guaranteed or endorsed by the publisher.

Supplementary material

The Supplementary Material for this article can be found online at: https://www.frontiersin.org/articles/10.3389/fpls.2023.1118548/full#supplementary-material

References

Bradford, M. M. (1976). A rapid and sensitive method for the quantitation of microgram quantities of protein utilizing the principle of protein-dye binding. *Anal. Biochem.* 72, 248–254. doi: 10.1016/0003-2697(76)90527-3

Buckeridge, M. S. (2010). Seed cell wall storage polysaccharides: Models to understand cell wall biosynthesis and degradation. *Plant Physiol.* 154, 1017–1023. doi: 10.1104/pp.110.158642

Carrillo-Barral, N., Matilla, A. J., Rodríguez-Gacio, M., del, C., and Iglesias-Fernández, R. (2018). Mannans and endo-β-mannanase transcripts are located in different seed compartments during brassicaceae germination. *Planta* 247, 649–661. doi: 10.1007/s00425-017-2815-4

Chen, J., Yang, L., Gu, J., Bai, X., Ren, Y., Fan, T., et al. (2015). MAN3 gene regulates cadmium tolerance through the glutathione-dependent pathway in *Arabidopsis thaliana*. *New Phytol.* 205, 570–582. doi: 10.1111/nph.13101

Cosgrove, D. J. (2005). Growth of the plant cell wall. *Nat. Rev. Mol. Cell Biol.* 6, 850–861. doi: 10.1038/nrm1746

González-Calle, V., Barrero-Sicilia, C., Carbonero, P., and Iglesias-Fernández, R. (2015). Mannans and endo-β-mannanases (MAN) in brachypodium distachyon: Expression profiling and possible role of the *BdMAN* genes during coleorhiza-limited seed germination. *J. Exp. Bot.* 66, 3753–3764. doi: 10.1093/jxb/erv168

Guillon, F., Larré, C., Petipas, F., Berger, A., Moussawi, J., Rogniaux, H., et al. (2012). A comprehensive overview of grain development in *Brachypodium distachyon* variety Bd21. *J. Exp. Bot.* 63, 739–755. doi: 10.1093/jxb/err298

Gupta, A., Singh, M., and Laxmi, A. (2015). Interaction between glucose and brassinosteroid during the regulation of lateral root development in *arabidopsis*. *Plant Physiol.* 168, 307–320. doi: 10.1104/pp.114.256313

Iglesias-Fernández, R., Rodríguez-Gacio, M. C., Barrero-Sicilia, C., Carbonero, P., and Matilla, A. (2011). Three endo-β-mannanase genes expressed in the micropylar endosperm and in the radicle influence germination of *Arabidopsis thaliana* seeds. *Planta* 233, 25–36. doi: 10.1007/s00425-010-1257-z

Ismail, A. M., and Horie, T. (2017). Genomics, physiology, and molecular breeding approaches for improving salt tolerance. *Annu. Rev. Plant Biol.* 68, 405–434. doi: 10.1146/annurev-arplant-042916-040936

Jia, M., Li, Q., Hua, J., Liu, J., Zhou, W., Qu, B., et al. (2020). Phytohormones regulate both "Fish scale" galls and cones on picea koraiensis. *Front. Plant Sci.* 11. doi: 10.3389/fpls.2020.580155

Jiang, Z., Zhou, X., Tao, M., Yuan, F., Liu, L., Wu, F., et al. (2019). Plant cell-surface GIPC sphingolipids sense salt to trigger Ca^{2+} influx. *Nature* 572, 341–346. doi: 10.1038/s41586-019-1449-z

Jin, M., Guo, X., Zhang, R., Qu, W., Gao, B., and Zeng, R. (2019). Diversities and potential biogeochemical impacts of mangrove soil viruses. *Microbiome* 7, 1–15. doi: 10.1186/s40168-019-0675-9

Kollárová, K., Kamenická, V., Vatehová, Z., and Lišková, D. (2018). Impact of galactoglucomannan oligosaccharides and cd stress on maize root growth parameters, morphology, and structure. *J. Plant Physiol.* 222, 59–66. doi: 10.1016/j.jplph.2017.12.017

Konozy, E. H. E., Causse, M., and Faurobert, M. (2012). Cell wall glycosidase activities and protein content variations during fruit development and ripening in three texture contrasted tomato cultivars. *Saudi J. Biol. Sci.* 19, 277–283. doi: 10.1016/j.sjbs.2012.04.006

Laskowski, M. J., Williams, M. E., Nusbaum, H. C., Sussex, I. M., Biology, P., and Hall, K. (1995). Formation of lateral root meristems is a two-stage process. *Development* 3310, 3303–3310. doi: 10.1242/dev.121.10.3303

Li, X., Chen, R., Chu, Y., Huang, J., Jin, L., Wang, G., et al. (2018). Overexpression of RCc3 improves root system architecture and enhances salt tolerance in rice. *Plant Physiol. Biochem.* 130, 566–576. doi: 10.1016/j.plaphy.2018.08.008

Li, X., Liu, W., Ren, Z., Wang, X., Liu, J., Yang, Z., et al. (2022). Glucose regulates cotton fiber elongation by interacting with brassinosteroid. *J. Exp. Bot* 73 (3), 711–726. doi: 10.1093/jxb/erab451

Liu, L., Wu, X., Sun, W., Yu, X., Demura, T., Li, D., et al. (2021). Galactinol synthase confers salt-stress tolerance by regulating the synthesis of galactinol and raffinose family oligosaccharides in poplar. *Ind. Crops Prod.* 165, 113432. doi: 10.1016/j.indcrop.2021.113432

Lu, P., Magwanga, R. O., Kirungu, J. N., Hu, Y., Dong, Q., Cai, X., et al. (2019). Overexpression of cotton a DTX/MATE gene enhances drought, salt, and cold stress tolerance in transgenic *arabidopsis*. *Front. Plant Sci.* 10. doi: 10.3389/fpls.2019.00299

Lucob-Agustin, N., Kawai, T., Takahashi-Nosaka, M., Kano-Nakata, M., Wainaina, C. M., Hasegawa, T., et al. (2020). WEG1, which encodes a cell wall hydroxyproline-rich glycoprotein, is essential for parental root elongation controlling lateral root formation in rice. *Physiol. Plant* 169 (2), 214–227. doi: 10.1111/ppl.13063

Ma, J. F., Shen, R., Nagao, S., and Tanimoto, E. (2004). Aluminum targets elongating cells by reducing cell wall extensibility in wheat roots. *Plant Cell Physiol.* 45, 583–589. doi: 10.1093/pcp/pch060

Malgas, S., van Dyk, J. S., and Pletschke, B. I. (2015). A review of the enzymatic hydrolysis of mannans and synergistic interactions between β-mannanase, β-mannosidase and α-galactosidase. *World J. Microbiol. Biotechnol.* 31, 1167–1175. doi: 10.1007/s11274-015-1878-2

Mittler, R., Vanderauwera, S., Suzuki, N., Miller, G., Tognetti, V. B., Vandepoele, K., et al. (2011). ROS signaling: The new wave? *Trends Plant Sci.* 16, 300–309. doi: 10.1016/j.tplants.2011.03.007

Mohnen, D. (2008). Pectin structure and biosynthesis. *Curr. Opin. Plant Biol.* 11, 266–277. doi: 10.1016/j.pbi.2008.03.006

Moreira, L. R. S., and Filho, E. X. F. (2008). An overview of mannan structure and mannan-degrading enzyme systems. *Appl. Microbiol. Biotechnol.* 79, 165–178. doi: 10.1007/s00253-008-1423-4

Motte, H., and Beeckman, T. (2019). The evolution of root branching: Increasing the level of plasticity. *J. Exp. Bot.* 70 (3), 785–793. doi: 10.1093/jxb/ery409

Nonogaki, H., Gee, O. H., and Bradford, K. J. (2000). A germination-specific endo-β-mannanase gene is expressed in the micropylar endosperm cap of tomato seeds. *Plant Physiol.* 123, 1235–1245. doi: 10.1104/pp.123.4.1235

Oka, Y., Butnaru, M., Von Buchholtz, L., Ryba, N. J. P., and Zuker, C. S. (2013). High salt recruits aversive taste pathways. *Nature* 494, 472–475. doi: 10.1038/nature11905

Peng, S., Zhou, Q., Cai, Z., and Zhang, Z. (2009). Phytoremediation of petroleum contaminated soils by mirabilis jalapa l. in a greenhouse plot experiment. *J. Hazard Mater.* 168, 1490–1496. doi: 10.1016/j.jhazmat.2009.03.036

Peters, W. S., and Tomos, A. D. (2000). The mechanic state of "inner tissue" in the growing zone of sunflower hypocotyls and the regulation of its growth rate following excision. *Plant Physiol.* 123, 605–612. doi: 10.1104/pp.123.2.605

Richterová-Kučerová, D., Kollárová, K., Zelko, I., Vatehová, Z., and Lišková, D. (2012). How do galactoglucomannan oligosaccharides regulate cell growth in epidermal and cortical tissues of mung bean seedlings? *Plant Physiol. Biochem.* 57, 154–158. doi: 10.1016/j.plaphy.2012.05.014

Sak-Ubol, S., Namvijitr, P., Pechsrichuang, P., Haltrich, D., Nguyen, T. H., Mathiesen, G., et al. (2016). Secretory production of a beta-mannanase and a chitosanase using a lactobacillus plantarum expression system. *Microb. Cell Fact* 15, 1–12. doi: 10.1186/s12934-016-0481-z

Tabuchi, A., and Matsumoto, H. (2001). Changes in cell-wall properties of wheat (Triticum aestivum) roots during aluminum-induced growth inhibition. *Physiol. Plant* 112, 353–358. doi: 10.1034/j.1399-3054.2001.1120308.x

Valifard, M., Le Hir, R., Müller, J., Scheuring, D., Neuhaus, H. E., and Pommerrenig, B. (2021). Vacuolar fructose transporter *SWEET17* is critical for root development and drought tolerance. *Plant Physiol.* 187 (4), 2716–2730. doi: 10.1093/plphys/kiab436

Wang, Y., Vilaplana, F., Brumer, H., and Aspeborg, H. (2013). Enzymatic characterization of a glycoside hydrolase family 5 subfamily 7 (GH5-7) mannanase from *Arabidopsis thaliana*. *Planta* 239, 653–665. doi: 10.1007/s00425-013-2005-y

Xu, P., Fang, S., Chen, H., and Cai, W. (2020). The brassinosteroid-responsive xyloglucan endotransglucosylase/hydrolase 19 (XTH19) and XTH23 genes are involved in lateral root development under salt stress in *Arabidopsis*. *Plant J.* 104 (1), 59–75. doi: 10.1111/tpj.14905

Yamamoto, Y. (2019). Aluminum toxicity in plant cells: Mechanisms of cell death and inhibition of cell elongation. *Soil Sci. Plant Nutr.* 65, 41–55. doi: 10.1080/00380768.2018.1553484

Yan, M., Zhang, Y., Guo, W., and Wang, X. (2012). Soybean endo-β-Mannanase GmMAN1 is not associated with leaf abscission, but might be involved in the response to wounding. *PloS One* 7, 1–9. doi: 10.1371/journal.pone.0049197

Zhao, Y, Song, D, Sun, J, and Li, L. (2013). Populus endo-beta-mannanase PtrMAN6 plays a role in coordinating cell wall remodeling with suppression of secondary wall thickening through generation of oligosaccharide signals. *Plant J.* 74 (3), 473-485. doi: 10.1111/tpj.12137

Zang, H., Xie, S., Zhu, B., Yang, X., Gu, C., Hu, B., et al. (2019). Mannan oligosaccharides trigger multiple defence responses in rice and tobacco as a novel danger-associated molecular pattern. *Mol. Plant Pathol.* 20, 1067–1079. doi: 10.1111/mpp.12811

Zelm, E., Zhang, Y., and Testerink, C. (2020). Salt tolerance mechanisms of plants. *Annu. Rev. Plant Biol.* 71, 403–433. doi: 10.1146/annurev-arplant-050718-100005

Zhang, T., Tang, H., Vavylonis, D., and Cosgrove, D. J. (2019). Disentangling loosening from softening: Insights into primary cell wall structure. *Plant J.* 100, 1101–1117. doi: 10.1111/tpj.14519

Zhang, K, Cui, H, Li, M, Xu, Y, Cao, S, Long, R, et al (2020). Comparative time-course transcriptome analysis in contrasting Carex rigescens genotypes in response to high environmental salinity. *Ecotoxicol Environ Saf.* 194, 110435. doi: 10.1016/j.ecoenv.2020.110435

frontiers | Frontiers in Plant Science

TYPE Original Research
PUBLISHED 08 May 2023
DOI 10.3389/fpls.2023.1189020

Check for updates

OPEN ACCESS

EDITED BY
Xinyang Wu,
China Jiliang University, China

REVIEWED BY
Guang-Long Wang,
Huaiyin Institute of Technology, China
Si Ma,
China Agricultural University, China

*CORRESPONDENCE
Hongjian Wan
wanhongjian@sina.com
Jiaqiu Zheng
nky8236@163.com

RECEIVED 18 March 2023
ACCEPTED 12 April 2023
PUBLISHED 08 May 2023

CITATION
Pang X, Chen J, Xu Y, Liu J, Zhong Y, Wang L, Zheng J and Wan H (2023) Genome-wide characterization of ascorbate peroxidase gene family in pepper (*Capsicum annuum* L.) in response to multiple abiotic stresses.
Front. Plant Sci. 14:1189020.
doi: 10.3389/fpls.2023.1189020

COPYRIGHT
© 2023 Pang, Chen, Xu, Liu, Zhong, Wang, Zheng and Wan. This is an open-access article distributed under the terms of the Creative Commons Attribution License (CC BY). The use, distribution or reproduction in other forums is permitted, provided the original author(s) and the copyright owner(s) are credited and that the original publication in this journal is cited, in accordance with accepted academic practice. No use, distribution or reproduction is permitted which does not comply with these terms.

Genome-wide characterization of ascorbate peroxidase gene family in pepper (*Capsicum annuum* L.) in response to multiple abiotic stresses

Xin Pang[1], Jun Chen[1], Yang Xu[2], Jia Liu[3], Yangmin Zhong[4], Linlin Wang[4], Jiaqiu Zheng[5]* and Hongjian Wan[2]*

[1]Suzhou Polytechnic Institute of Agriculture, Suzhou, China, [2]State Key Laboratory for Managing Biotic and Chemical Threats to the Quality and Safety of Agro-Products, Institute of Vegetables, Zhejiang Academy of Agricultural Sciences, Hangzhou, China, [3]Wulanchabu Academy of Agricultural and Husbandry Sciences, Wulanchabu, China, [4]Institute of Crops, Lishui Academy of Agricultural and Forestry Sciences, Lishui, China, [5]Jiangsu Coastal Area Institute of Agricultural Sciences, Yancheng, China

Pepper is widely grown all over the world, so it faces many abiotic stresses, such as drought, high temperature, low temperature, salt damage, and so on. Stresses causing the accumulation of reactive oxidative species (ROS) in plants are removed by antioxidant defense systems, and ascorbate peroxidase (APX) is an important antioxidant enzyme. Therefore, the present study performed genome-wide identification of the *APX* gene family in pepper. We identified nine members of the *APX* gene family in the pepper genome according to the APX proteins' conserved domain in *Arabidopsis thaliana*. The physicochemical property analysis showed that *CaAPX3* had the longest protein sequence and the largest molecular weight of all genes, while *CaAPX9* had the shortest protein sequence and the smallest MW. The gene structure analysis showed that *CaAPXs* were composed of seven to 10 introns. The *CaAPX* genes were divided into four groups. The *APX* genes of groups I and IV were localized in the peroxisomes and chloroplasts, respectively; the group II genes were localized in the chloroplasts and mitochondria; and the group III genes were located in the cytoplasm and extracell. The conservative motif analysis showed that all *APX* genes in the pepper had motif 2, motif 3, and motif 5. The *APX* gene family members were distributed on five chromosomes (Chr. 2, 4, 6, 8, and 9). The *cis*-acting element analysis showed that most *CaAPX* genes contain a variety of *cis*-elements related to plant hormones and abiotic stress. RNA-seq expression analysis showed that the expression patterns of nine *APXs* were different in vegetative and reproductive organs at different growth and development stages. In addition, the qRT-PCR analysis of the *CaAPX* genes revealed significant differential expression in response to high temperature, low temperature, and salinity stresses in leaf tissue. In conclusion, our study identified the *APX* gene family members in the pepper and predicted the functions of this gene family, which would provide resources for further functional characterization of *CaAPX* genes.

KEYWORDS

pepper, ascorbate peroxidase, bioinformatics analysis, gene expression, phylogenetic relationship

Introduction

Plants will be subjected to various environmental stresses during their growth and development, comprising both abiotic stresses such as drought, freezing, high temperature, heavy metal, and salinity and biotic stresses such as viruses and fungi (Bhat et al., 2019; Raza et al., 2020). Environmental stress can directly or indirectly destroy the reactive oxygen species (ROS) balance in plants, causing a series of stress responses in crops. ROS has dual functions: on the one hand, an appropriate amount of ROS is necessary for organisms to participate in the regulation of signal networks as signaling molecules. On the other hand, excessive reactive oxygen species will cause certain damage to the cell membrane and organelles of crops, and when they exceed a certain limit, they will affect the growth and development of individual plants and even lead to their death, which must be removed as soon as possible (Davletova et al., 2005; Foyer and Shigeoka, 2011). Therefore, the balance between the production and removal of reactive oxygen species in cells is very important. Plants maintain the dynamic balance of reactive oxygen species through enzymatic or nonenzymatic mechanisms and form a complete antioxidant system in the process of evolution (Shigeoka et al., 2002; Maruta et al., 2016).

The clearance mechanism includes the enzymatic scavenging system, such as ascorbate peroxidase (APX), catalase (CAT), glutathione peroxidase (GPX), superoxide dismutase (SOD), and other antioxidant enzymes (Faize et al., 2011). APX is a very effective H_2O_2 scavenger and has the highest affinity for H_2O_2 among all H_2O_2 metabolic enzymes (Huang et al., 2017). Plant APX belongs to the type I heme peroxidase and copper oxidase families and can reduce H_2O_2 to O_2 and H_2O using ASA as an electron donor through the ascorbic acid (ASA)-glutathione (GSH) cycle (Asada, 1999).

Ascorbate peroxidase (APX) is a protease encoded by members of a multi-gene family. According to the subcellular localization of their proteins, they can be divided into four categories: cytoplasmic APX, peroxidase APX, chloroplast APX, and mitochondrial APX (Shigeru et al., 2002; Apel and Hirt, 2004). Eight members of the *AtAPX* gene family have been identified in *Arabidopsis thaliana*, including three in the cytoplasm (*APX1*, *APX2*, and *APX6*), three in the peroxidase (*APX3*, *APX4*, and *APX5*), and two in the chloroplast (*sAPX* both in the mitochondrial and chloroplast, *tAPX* in the thylakoid membrane) (Panchuk et al., 2002; Chew et al., 2003; Mittler et al., 2004; Narendra et al., 2006). The *APX* gene family of rice has eight genes, including two cytoplasmic isoforms (*OsAPx1* and *OsAPx2*), two peroxidase isoforms (*OsAPx3* and *OsAPx4*), two mitochondrial isoforms (*OsAPx5* and *OsAPx6*), and two in the chloroplast (*OsAPx7* and *OsAPx8*) (Teixeira et al., 2004; Teixeira et al., 2006; Hong et al., 2007; Ribeiro et al., 2017). Tomato has seven genes encoding APX isoforms: three cytoplasmic isoforms, two peroxidase isoforms, and two chloroplast isoforms (Najami et al., 2008). Recently, as more and more plant genomes have been sequenced, genome-wide identification and functional analysis of *APX* have been accomplished, such as upland cotton (Gossypium hirsutum Linn.) (Tao et al., 2018), sorghum (*Sorghum bicolor* L.) (Akbudak et al., 2018), maize (Qu et al., 2020), kiwifruit (*Actinidia chinensis*) (Liao et al., 2020), and so on.

The *APX* gene plays an important role in the growth and development of different plants and their response to environmental stress. The expression of *AtAPX1* was significantly upregulated in various biological and abiotic stress responses (Zimmermann et al., 2004). APX2 plays an important role in regulating heat stress response at different stages of plant development (Schramm et al., 2006; Frank et al., 2009). Overexpression of the *AtAPX3* gene in tobacco increased the protective effect of transgenic plants against oxidative stress (Wang et al., 1999). *APX6* modulates the ROS signal cross-talk with hormone signals to properly execute the germination program in *Arabidopsis*, and the apx6 mutant exhibited a high level of ROS and reduced germination (Chen et al., 2014). Loss of function in *OsAPX2* showed semi-dwarf seedlings, yellow–green leaves, leaf lesion mimics, and seed sterility (Zhang et al., 2013). Transgenic plants overexpressing the *SbpAPX* gene showed enhanced salt and drought stress tolerance compared to wild-type plants (Singh et al., 2014). Another study found that *BcAPX* genes were overexpressed in transgenic *Arabidopsis*, and the expression of APX and the APX activity in transgenic lines were higher than in nontransgenic (NT) plants under high temperatures (Chiang et al., 2015).

Pepper is an important solanaceous vegetable and is widely cultivated and eaten both as a vegetable and as a spice. However, pepper is particularly vulnerable to a number of biotic and abiotic stresses in production, such as pathogens, drought, and cold temperatures, which can easily cause a production drop. The *APX* gene, as an important class of antioxidant enzymes, has rarely been reported. In this study, *APX* gene family members were identified from the pepper genome database, and the physicochemical properties of *APX* gene members were analyzed by the bioinformatics method. The expression of *APX* gene members in different tissues was analyzed by downloading the RNA-seq data, and the gene expression under abiotic stress was analyzed by the qRT-PCR technique. This study provided the scientific basis for further exploring the molecular mechanism of *APX* gene family members in pepper under abiotic stress.

Materials and methods

Identification of the *APX* gene family in pepper

All of the pepper genome sequence data were downloaded from the Solanaceae Genomics Network (http://solgenomics.net/). The local database of the pepper genome sequences was constructed by the Bioedit7.0 software. In order to retrieve all the members of the APX family in pepper, two methods were employed, including the BLASTP algorithm and the Hidden Markov model (HMM). First, for BLASTP, we used 31 APX amino acid sequences from *Arabidopsis thaliana*, rice, tomato, and potato as an inquiry with the *e*-value set to $1e^{-10}$. The amino acid sequences of 23 APXs were retrieved from the PLAZA 4.0 (https://bioinformatics.psb.ugent.be/plaza/versions/) and Phytozome (https://phytozome.jgi.doe.gov/pz/portal.html). We then used the HMM profile of the APX domain (Pfam: PF00141), which was from the Pfam database (http://

pfam.xfam.org), as a query to detect this local pepper database. Finally, nine *CaAPX* genes were identified by merging the two methods in the pepper genome.

Characterization of *APX* gene family in pepper

Physicochemical properties of APX proteins, such as protein length, molecular weight, and isoelectric point were checked using the ExPASy server (www.expasy.org). The subcellular localization of the CaAPX proteins was predicted using the online Euk-mPLoc 2.0 (http://www.csbio.sjtu.edu.cn/bioinf/euk-multi-2/) (Chou and Shen, 2010). For the analysis of the structural feature, the Gene Structure Display Server (GSDS) (http://gsds.cbi.pku.edu.cn) online tool was adopted by comparing the CDS and genomic sequences of each *APX* gene (Hu et al., 2014). Conserved motif analyses of the *CaAPX* genes were then performed using the MEME tool (http://meme-suite.org/tools/meme), identifying a maximum of 10 motifs with a motif width range of 6 to 50 (Bailey et al., 2006). The chromosomal location of the *CaAPX* genes was determined from the SGN database. The map diagram showing the location of *APX* genes on chromosomes was drawn by implementing MapDraw V2.1 software.

Multiple sequence alignment and phylogenetic analysis

To determine the evolutionary relationship of the *APX* gene family, a phylogenetic tree was carried out among *A. thaliana*, *Oryza sativa*, *Solanum lycopersicum*, *Solanum tuberosum*, and *Capsicum annuum* protein sequences. The sequence alignment was constructed using Clustal X (version 1.8) and a neighbor-joining method with 1,000 bootstrap replicates in MEGA 7.0 software (Kumar et al., 2016). Any gaps or missing data in the sequence treatment were applied to partial deletion, and then branch lengths were assigned *via* the pairwise calculations of genetic distances.

Cis-element analysis in the *CaAPX* gene promoters

The 1-kb sequence upstream of the start code from each of the *CaAPX* genes was obtained from the SGN database. The *cis*-elements in the promoter regions of the individual gene were examined using the means of the PlantCARE server (http://bioinformatics.psb.ugent.be/webtools/plantcare/html/) (Lescot et al., 2002). The cis-element analysis figure was made by TBtools (Chen et al., 2020).

Expression analysis of *CaAPX* genes in diverse tissues

In this study, RNA-seq data from the NCBI database (http://pepperhub.hzau.edu.cn/) were used to investigate expression patterns of putative *CaAPX* genes in different tissues of cultivated pepper (Zunla-1). Different tissues in cultivated pepper included root, stem, leaf, bud, flower, and F-Dev1-9. The heatmap was formed using Multi Experiment Viewer (MeV) software (Howe et al., 2010).

Plant materials and stress treatments

This study's samples used for stress treatment were collected from a typical cultivated variety, D50. The pepper plants were cultivated in a chamber under 14-h light (28°C to 30°C) and 10-h dark (18°C to 20°C) period conditions.

Seedlings at the six true leaf stages were used for all experiments. For cold treatment, seedlings were subjected to 4°C for 1, 3, 6, and 12 h. For heat shock treatment, seedlings were subjected to 42°C for 0.5, 1, 3, and 6 h. Plants were subjected to 26°C for control. For salt stress treatment, seedlings were subjected to 300 mM NaCl. Plants were subjected to sterile water for control. Three biological replicates for each treatment were carried out in the experiments. All of the samples were immediately frozen in liquid nitrogen and stored at −80°C for further experimentation.

RNA isolation and quantitative real-time PCR analysis

The transcription profiles of *APX* genes in pepper were performed through qRT-PCR analysis. All primers used in the experiment were designed by the Primer 5.0 software and listed in Supplementary Table S1.

The total RNA isolation and cDNA synthesis was performed using Trizol (Tiangen, Beijing, China) and DNase I (Transgen, Beijing, China) according to manufacturer instructions. In total, 1 µg of each of the treated RNA samples was reverse transcribed using PrimeScriptTM RT reagent Kit for qPCR (Transgen, Beijing, China). A 20-µl qRT-PCR reaction mixture, which contained 10 µl of SYBR Green I, 1 µl of forward primer, 1 µl of reverse primer, 1 µl of diluted cDNA, and 7 µl of sterile distilled H_2O, was prepared. The mixture was subjected to the following program: 35 cycles of 3 min at 95°C, 30 s at 58°C, and 20 s at 72°C (ABI Real-Time PCR System, USA). GAPDH was used as an internal control (Cheng et al., 2017), and the fold change in gene expression was calculated using the $2^{-\Delta\Delta CT}$ method. Each qRT-PCR reaction was carried out using three biological and technical replicates.

Results

Identification of the *APX* gene family in the pepper genome

In the present study, a total of nine *APX* genes were recognized and designated as *CaAPX1* to *CaAPX9*, respectively, based on BLASTP examinations against the pepper genome employing 31 APX proteins (eight AtAPX proteins, eight OsAPX proteins, seven SlAPX proteins, and eight StAPXs) as inquiries (Table 1). The

10.3389/fpls.2023.1189020

comprehensive information of the nine *CaAPX* genes (e.g., molecular weights (MW), isoelectric points (p*I*), numbers of exons/introns, and subcellular localization) is shown in Table 1. CaAPX amino acid residue lengths ranged from 245 aa (CaAPX9) to 353 aa (CaAPX3), MW ranged from 27.0 (CaAPX9) to 38.8 kDa (CaAPX3), and p*I* ranged from 5.43 (CaAPX6) to 9.49 (CaAPX4). The number of exons ranged from eight to 11, with two genes comprising eight exons, three genes comprising nine exons, two genes comprising 10 exons, and two genes consisting of 11 exons (Table 1). The subcellular localization results predicted that five APX (CaAPX1, CaAPX5, CaAPX6, CaAPX8, and CaAPX9) proteins are located in the peroxisome, three proteins (CaAPX2, CaAPX3, and CaAPX4) are located in chloroplast, two proteins (CaAPX3 and CaAPX4) are also located in the mitochondrion, and only one protein (CaAPX7) is located in the cytoplasm and extracell (Table 1).

Phylogenetic analysis of *APX* genes

The 40 genes from five species (*Arabidopsis thaliana*, rice, tomato, potato, and pepper) were clustered into six groups (I–VI) (Figure 1). The nine *CaAPX* belonged to five groups in the phylogenetic tree, with the exception of group III. Group III only has one gene, *StAPX3*, including the lowest genes among the six groups. Group VI consisted of 13 genes, including the most genes among the six groups, which contained *AtAPX1* and *AtAPX2*; *OsAPX1* and *OsAPX2*; *SlAPX1*, *SlAPX2*, and *SlAPX3*; *StAPX4*, *StAPX5*, and *StAPX7*; and *CaAPX5*, *CaAPX6*, and *CaAPX9*. Groups IV, V, and VI exhibited five species of *APX* genes, while group I had *CaAPX* and *AtAPX*, group II had *CaAPX*, *StAPX*, and *AtAPX*, and group III only had *StAPX*.

This study also found nine pairs of orthologous genes between the various species: *CaAPX2* and *AtAPX4*; *CaAPX7* and *StAPX6*; *StAPX8* and *SlAPX6*; *CaAPX4* and *SlAPX7*; *StAPX1* and *SlAPX4*; *StAPX2* and *SlAPX4*; *StAPX7* and *SlAPX3*; *StAPX4* and *SlAPX2*; and *StAPX5* and *SlAPX1*, respectively. There are six pairs of the nine orthologous genes between the tomato and potato, and it may be noticed that *StAPXs* have a stronger phylogenetic link with the *SlAPXs*. There were also three pairs of paralogous genes discovered only in rice.

Gene structures and motif analysis of *CaAPX* genes

The gene structure of the *CaAPX* genes was guided to obtain insight into the evolution of the *APX* family genes. Moreover, the phylogenetic relationships of the APX proteins in pepper were identified using MEGA 7.0 software. It was to see whether the exon–intron distribution pattern and the phylogenetic tree were in compliance with each other. The results showed that the number of exons ranged from eight to 11, and the number of introns varied from seven to 10, as detailed in Figure 2. Group I includes seven to nine introns. Groups III and IV only have one gene, including nine and 10 introns, respectively. While *CaAPX3* and *CaAPX4* showed different exon–intron structures in group II.

The presence of conserved motifs was also identified in nine *CaAPX* genes using MEME. The conserved motif of the *CaAPX* genes explored 64 motifs that varied from three to nine. The motif distributed in the same group is highly similar. Group I includes eight to nine, and group II contains six to eight (Figure 2). Motifs 2, 3, and 5 were present in all CaAPX proteins, indicating that these motifs were conserved motifs and functional domains of the APX protein family in pepper. Motif 8 was only discovered in group I, and motif 9 was only present in group II. Overall, as shown in Figure 2, the closely related genes of *CaAPX* shared a similar pattern of motif distribution.

Chromosomal distributions of the *CaAPX* genes

The results showed that the *CaAPX* genes were distributed unevenly on five chromosomes, including chromosomes 2, 4, 6, 8,

TABLE 1 General information about the nine *CaAPX* genes.

Gene	Gene accession No.	Chromosome location	Length of protein (AA)	Predicted size (kDa)	Isoelectric point (p*I*)	No. of exons/introns	Subcellular localization
CaAPX1	**Capana02g002557**	**ch02:147290511.147293908**	**310**	**34.3**	**6.72**	**10/9**	**Peroxisome**
CaAPX2	**Capana04g000971**	**ch04:23506178.23513063**	**346**	**37.7**	**8.27**	**11/10**	**Chloroplast**
CaAPX3	**Capana04g002111**	**ch04:170729674.170735490**	**353**	**38.8**	**7.12**	**11/10**	**Chloroplast, mitochondrion**
CaAPX4	**Capana06g001732**	**ch06:48644312.48651554**	**304**	**32.9**	**9.49**	**8/7**	**Chloroplast, mitochondrion**
CaAPX5	**Capana06g002525**	**ch06:171804392.171807190**	**250**	**27.4**	**5.93**	**9/8**	**Peroxisome**
CaAPX6	**Capana06g002561**	**ch06:176301253.176303953**	**250**	**27.5**	**5.43**	**9/8**	**Peroxisome**
CaAPX7	**Capana08g000304**	**ch08:34207895.34214385**	**310**	**35.5**	**8.13**	**10/9**	**Cytoplasm, extracell**
CaAPX8	**Capana08g002729**	**ch08:151484880.151492967**	**287**	**31.6**	**7.10**	**9/8**	**Peroxisome**
CaAPX9	**Capana09g001881**	**ch09:213803706.213807771**	**245**	**27.0**	**6.00**	**8/7**	**Peroxisome**

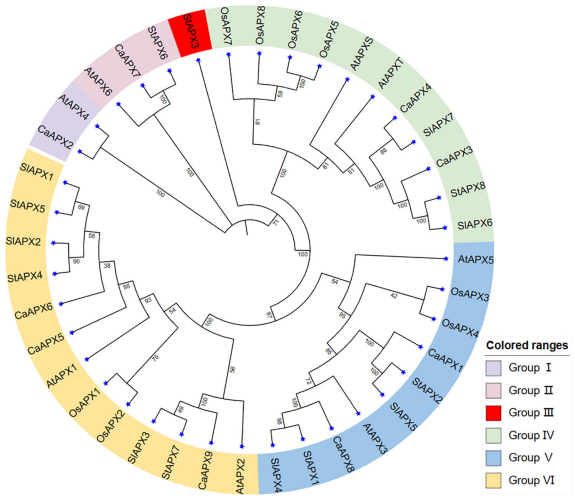


FIGURE 1
Phylogenetic relationships of *APX* gene family members in five species, including rice, tomato, potato, pepper, and *Arabidopsis thaliana*.

and 9. The other chromosomes did not carry the *APX* genes (Figure 3). A maximum of three genes (*CaAPX4*–*CaAPX6*) were localized on chromosome 6, which was followed by chromosome 4 (*CaAPX2* and *CaAPX3*) and chromosome 8 (*CaAPX7* and *CaAPX8*) with two genes. The remaining chromosomes (chromosomes 2 and 9) only consisted of one gene.

Cis-element in the promoters of *CaAPX* genes

To gain the gene functions and regulations of the *CaAPX* genes, *cis*-elements in *CaAPX* promoter regions were analyzed by searching a 1,000-bp upstream region from each individual *CaAPX* gene's transcriptional activation site against the PlantCARE database. The results depicted that five major classes of *cis*-elements were present in the promoter region of all *APX* genes: light response; process-specific; environment-specific; plant tissue, and binding site, as shown in Figure 4. Among all of the genes except *CaAPX3*, 15 light response elements were found. The results that four phytohormone-correlated (ABA, MeJA, GA, auxin) responsive elements comprising CGTCA-motif, TGACG-motif, p-box, ABRE, and TGA-element were documented. The *cis*-acting regulatory elements involved in environment-specific such as drought (MBS), anoxia (ARE, GC-motif), and low-temperature responsive element (LTR) among all of the genes were found in the promoter region of the *APX* genes of pepper. In addition, four tissue-specific *cis*-elements and five binding site *cis*-elements were also identified.

Expression profiles of *CaAPX* genes in different tissues

The tissue-specific expression profiles of *CaAPX* genes were investigated at various developmental stages of the pepper cultivar Zunla, as illustrated in Figure 5. Results of the study revealed that *CaAPX8* exhibits higher expression levels among all tissues except F-Dev5, implicating the vital roles for pepper, whereas four genes (*CaAPX1*, *CaAPX2*, *CaAPX3*, and *CaAPX4*) showed lower expression in all of the tissues. *CaAPX7* expressed higher values in ripe fruit (F-Dev7, F-Dev8, and F-Dev9), suggesting its participation in fruit development. Among those genes, it was observed that *CaAPX5* had the highest expression levels during the bud stage. The rest of the genes (*CaAPX6* and *CaAPX9*) with the higher expression level displayed tissue specificity in the root and F-Dev9.

Expression pattern of *CaAPX* genes in response to different abiotic stresses

In this study, to further investigate the expression patterns of nine *CaAPX* genes differentially expressed under abiotic stresses, we performed qRT-PCR analysis on the cultivated variety, D50, under cold (4°C), heat (42°C), and NaCl (300 mM) treatment conditions (Figure 6). Under cold treatment, *CaAPX1*, *CaAPX4*, *CaAPX5*, and

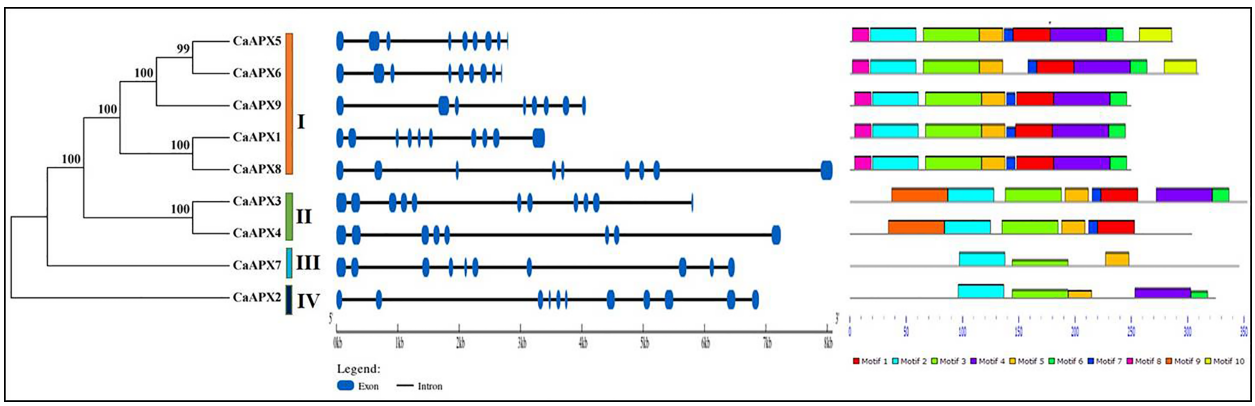


FIGURE 2
Phylogenetic analysis, gene structures, and conservation motifs of *APX* genes in pepper.

10.3389/fpls.2023.1189020

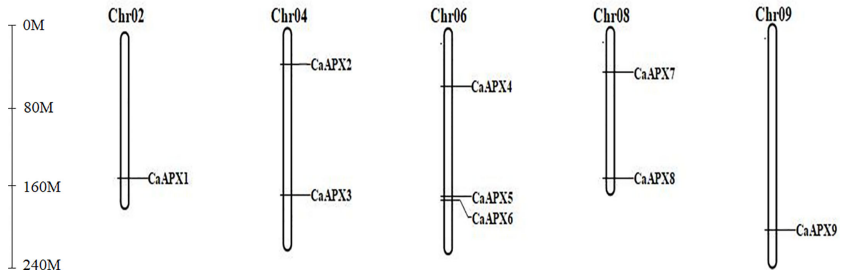


FIGURE 3
Chromosomal localization of *CaAPX* genes. Nine *CaAPX* genes were distributed unevenly on five chromosomes (Chr02, Chr04, Chr06, Chr08, and Chr09).

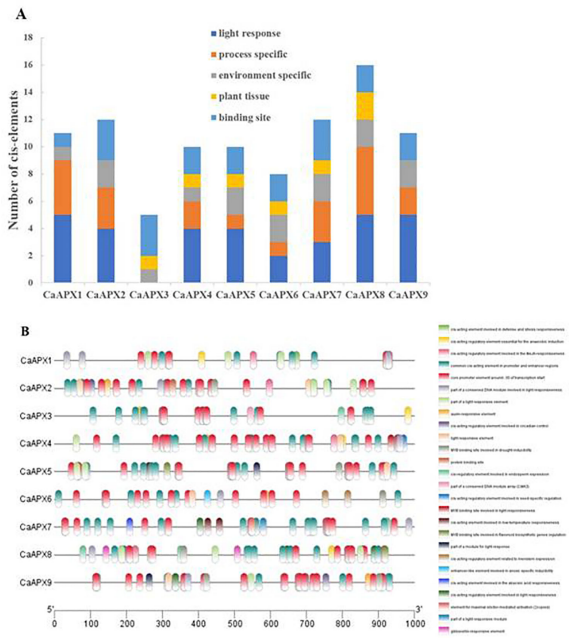


FIGURE 4
Predicted *cis*-elements in the promoter regions of *CaAPX* genes. **(A)** Number of different *cis*-elements. **(B)** The elements identified are in different colored boxes.

CaAPX9 were upregulated in response to cold stress at 1, 3, 6, and 12 h as compared to CK, while *CaAPX2* showed continuous downregulation at all treatment points. *CaAPX1* was upregulated (5.81-fold) at 1 h, *CaAPX5* was upregulated (22.45-fold) at 3 h, and *CaAPX9* was upregulated (18.13- and 7.62-fold) at 1 and 3 h, respectively, compared to CK. Under heat treatment, *CaAPX9* showed a continuous upregulation response as compared to CK and showed maximum expression (21.80-fold) at 6 h, while *CaAPX1* was downregulated at all treatment points. *CaAPX4* was upregulated (5.04-, 23.13-, and 13.43-fold) at 0.5, 4.5, and 6 h, *CaAPX5* was upregulated (3.24-, 7.81-, and 2.38-fold) at 0.5, 4.5, and 6 h, and *CaAPX6* was upregulated (5.58-fold) at 0.5 h, respectively, compared to CK. Under NaCl treatment, most of the genes were downregulated, especially *CaAPX1*, *CaAPX2*, *CaAPX3*, *CaAPX4*, and *CaAPX6*, which were continuously downregulated at all treatment points, except *CaAPX7*, which showed a slightly higher expression at 1 h.

Discussion

APX is one of the key enzymes for active oxygen removal in plants, playing an important role in plant growth and development as well as stress response. With the development of sequenced genomes, *APX* gene families have been found in many plants, such

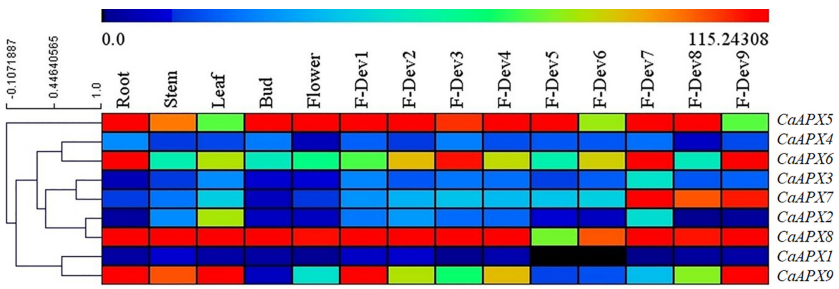


FIGURE 5
Expression profiles of *CaAPX* genes on RNA-seq in different pepper tissues. The one to nine stages of fruit development are presented in five early stages of color breaking (0–1-, 1–3-, 3–4-, and 4–5-cm-long fruit, and mature-green fruit), the color breaking stage (fruit began to turn red), and three late stages of color breaking (3, 5, and 7 days after color breaking), respectively.

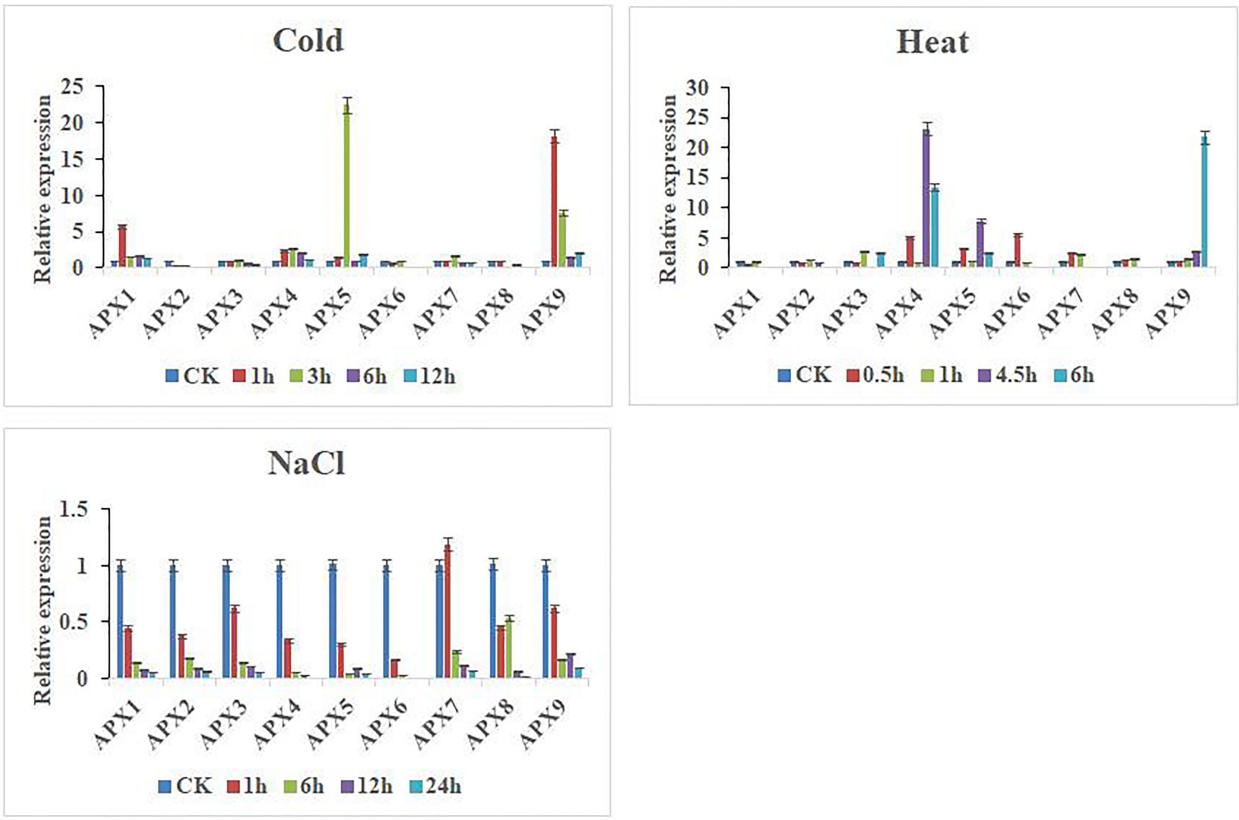


FIGURE 6
Expression of *CaAPX* genes under cold, heat, and salt stress.

as *Arabidopsis* (Panchuk et al., 2002), rice (Teixeira et al., 2004), upland cotton (Tao et al., 2018), tomato (Najami et al., 2008), and so on. According to the subcellular localization, APX can be divided into cytoplasmic APX, peroxisome APX, chloroplast APX, and mitochondrial APX, but the localization and quantity of APXs in cells are different in different species. Previous studies have shown that different types of *APX* genes have different functions. For example, chloroplast APX is mainly used to protect the photosynthetic system, while mitochondrial APX plays a positive role in removing hydrogen peroxide generated by fatty acid β oxidation (Renu et al., 2011; Andreia et al., 2014), the cytoplasmic *OsAPX2* gene plays an important role in maintaining H_2O_2 homeostasis (Wu et al., 2018), silened peroxisome *OsAPX4* can lead to premature aging of rice (Guan et al., 2010). In this work, nine *APX* genes were found in the pepper genome and divided into four subfamilies. The results of the phylogenetic tree showed that five genes of subfamily I were located in the peroxisome, two genes of subfamily II were located in chloroplasts/mitochondria, one gene of subfamily III was located in cytoplasm and extracell, and one member of subfamily IV was only located in chloroplasts, indicating that the close relatives may have had the same subcellular localization results (Figure 2). *CaAPX3* and *CaAPX4* of subfamily II were all located in two chloroplast/mitochondrial organelles, as well as in previous studies of *PtrAPX1* and *PtrAPX5* in *Populus trichocarpa* (Leng et al., 2021). *CaAPX* genes located in peroxisome all contain eight different conserved motifs and have eight to ten exon regions. Rice is a monocotyledonous plant, while *Arabidopsis thaliana*, tomato, potato, and pepper belong to the dicotyledonous family. Therefore, the phylogenetic tree of *Arabidopsis thaliana*, rice, tomato, potato, and pepper was constructed, and it was found that the *APX* gene of pepper is further related to the homologous evolution of rice.

The promoter *cis*-acting element plays an important role in regulating plant biological processes, such as participating in exogenous hormone induction and abiotic stress response (Yang et al., 2019). In this study, it was found that *CaAPX* genes contain hormone-induced related and stress regulatory elements, such as CGTCA-motif, TGACG-motif, TGA-element, ABRE, CGTCA-motif, TCA-element, ARE, MBS, and LTR, through the 1,000-bp upstream ATG sequence analysis of the *CaAPX* family members. Every *CaAPX* gene contains at least one process-specific and one environment-specific class, except *CaAPX3*, which has no hormone-induced *cis*-element, suggesting that *CaAPXs* play an important role in plant hormone and abiotic stress responses.

More and more evidence suggested that *APX* genes may exhibit different expression profiles in different organs/tissues and stress environments. Therefore, the tissue-specific expression of *CaAPX* genes was displayed in eight diverse developmental tissues using RNA-seq data (Figure 5), and these results are consistent with previous reports. For example, *AtAPX1* is involved in many biological processes (Pnueli et al., 2003; Davletova et al., 2005)

and is constitutionally higher expressed in plant roots, stems, leaves, and many other tissues (Zimmermann et al., 2004). The expression of *AtAPX6* was very high at the seed postmaturity stage (Chen et al., 2014). Maize *APXb1* is highly expressed in roots, shoots, and immature leaves, and *APXb2* is abundantly expressed in leaves and reproductive organs (Qu et al., 2020). In our study, *CaAPX8* and *CaAPX5* presented higher expressions in most tissue, suggesting two genes involved in many biological processes. The expression levels of *CaAPX1*, *CaAPX2*, *CaAPX3*, and *CaAPX4* exhibited very low levels during the most normal growth and development of pepper. These results indicate that the four genes may play a small role in the normal growth and development of plants. *CaAPX7* expression in pepper increased significantly with fruit maturation. These results suggest that *APX7* may play a key role in fruit development.

In this study, qRT-PCR was used to appraise the expression patterns of *CaAPXs* under low temperature, high temperature, and salt stress (Figure 6). Under the three abiotic stresses, the expression patterns of *CaAPXs* were different, *CaAPX5* and *CaAPX9* showed upregulated expression under low temperature, and *CaAPX4* and *CaAPX9* showed higher expression under high temperature, indicating that *CaAPXs* may play an important role in the abiotic stress response of pepper, which was consistent with previous research results (Sharma and Dubey, 2005; Koussevitzky et al., 2008). However, the expression levels of some genes showed a downregulated expression under stress. For example, under salt stress, the expression levels of all the *CaAPXs* except *CaAPX7* at 1 h were downregulated at all times. It is speculated that the expression of these genes was inhibited after stress and that ROS is cleared by other genes or by other means. In addition, the expression patterns of individual genes were different under different stresses. The expression level of *CaAPX1* was significantly upregulated in low-temperature stress but downregulated in high-temperature stress, suggesting that *CaAPX* genes played different functions under different stresses. The result agreed with earlier discoveries; for example, *cAPX* expression of *Spinacia oleracea* was upregulated under strong light and ultraviolet light, but the transcription level did not change under drought and salt stress. The transcription levels of *mAPX*, *sAPX*, and *tAPX* did not change after ABA, drought, strong light, and salt treatment (Yoshimura et al., 2000). The results of qRT-PCR showed that *APX* genes were induced to express under high temperatures, and *CaAPX5* and *CaAPX9* showed significantly upregulated expression every time. By constructing a phylogenetic tree, we found that *CaAPX5*, *CaAPX9*, and *AtAPX2* are clustered into a cluster that is close in evolutionary relationship. Studies have shown that *AtAPX2* plays a very important regulatory role in the process of heat stress response at different developmental stages of plants (Shi et al., 2001; Frank et al., 2009). These discoveries offered compelling evidence that *APX* genes play a well-maintained role in defending diverse plant species against abiotic stresses. In the future, we could validate the function of *CaAPX* genes using overexpression and the CRISPR/Cas system and provide a basis study for breeding pepper.

Data availability statement

The original contributions presented in the study are included in the article/Supplementary Material. Further inquiries can be directed to the corresponding authors.

Author contributions

Conceived and designed the experiments: XP and HW. Performed the experiments: JC, YX, JL, and YZ. Analyzed the data: XP, YX, LW, and JZ. Wrote the paper: XP, YX, and HW. All authors contributed to the article and approved the submitted version.

Funding

This research was funded by the National Natural Science Foundation of China (32100302, 31960601, 32060446, 32260769), Young and middle-aged academic leaders of the "Qing Lan Project" in universities of Jiangsu Province (2022), Technology Cultivation Project of Suzhou Polytechnic Institute of Agriculture (PY2005), Jiangsu Provincial Natural Science Foundation of China (BK20211113), Natural Science Foundation of Inner Mongolia Autonomous Region of China (2021MS03106, 2021MS03071), Zhejiang Provincial Natural Science Foundation of China (LQ23C020004), and Basic Research Project of Ulanqab, Inner Mongolia Autonomous Region of China (2021JC202).

Conflict of interest

The authors declare that the research was conducted in the absence of any commercial or financial relationships that could be construed as a potential conflict of interest.

Publisher's note

All claims expressed in this article are solely those of the authors and do not necessarily represent those of their affiliated organizations, or those of the publisher, the editors and the reviewers. Any product that may be evaluated in this article, or claim that may be made by its manufacturer, is not guaranteed or endorsed by the publisher.

Supplementary material

The Supplementary Material for this article can be found online at: https://www.frontiersin.org/articles/10.3389/fpls.2023.1189020/full#supplementary-material

References

Akbudak, M. A., Filiz, E., Vatansever, R., and Kontbay, K. (2018). Genome-wide identification and expression profiling of ascorbate peroxidase (APX) and glutathione peroxidase (GPX) genes under drought stress in sorghum (Sorghum bicolor l.). *J. Plant Growth Regul.* 37 (3), 925–936. doi: 10.1007/s00344-018-9788-9

Andréia, C., Aurenivia, B., Fabricio, E. L. C., Claudia, M. B. A., Gisele, P., Mariana, S., et al. (2014). The knockdown of chloroplastic ascorbate peroxidases reveals its regulatory role in the photosynthesis and protection under photo-oxidative stress in rice. *Plant Sci.* 214, 74–87. doi: 10.1016/j.plantsci.2013.10.001

Apel, K., and Hirt, H. (2004). Reactive oxygen species: metabolism, oxidative stress, and signal transduction. *Annu. Rev. Plant Biol.* 55, 373–399. doi: 10.1146/annurev.arplant.55.031903.141701

Asada, K. (1999). The water-water cycle in chloroplasts: scavenging of active oxygens and dissipation of excess photons. *Annu. Rev. Plant Physiol. Plant Mol. Biol.* 50 (1), 601–639. doi: 10.1146/annurev.arplant.50.1.601

Bailey, T. L., Williams, N., Misleh, C., and Li, W. W. (2006). MEME: discovering and analyzing DNA and protein sequence motifs. *Nucleic Acids Res.* 34, W369–W373. doi: 10.1093/nar/gkl198

Bhat, J. A., Shivaraj, S., Singh, P., Navadagi, D. B., Tripathi, D. K., Dash, P. K., et al. (2019). Role of silicon in mitigation of heavy metal stresses in crop plants. *Plants.* 8, 71. doi: 10.3390/plants8030071

Chen, C. J., Chen, H., Zhang, Y., Thomas, H. R., Frank, M. H., and He, Y. H. (2020). TBtools: an integrative toolkit developed for interactive analyses of big biological data. *Mol. Plant* 13 (8), 1194–1202. doi: 10.1016/j.molp.2020.06.009

Chen, C., Letnik, I., Hacham, Y., Dobrev, P., Ben-Daniel, B. H., Vanková, R., et al. (2014). ASCORBATE PEROXIDASE6 protects arabidopsis desiccating and germinating seeds from stress and mediates cross talk between reactive oxygen species, abscisic acid, and auxin. *Plant Physiol.* 166 (1), 370–383. doi: 10.1104/pp.114.245324

Cheng, Y., Pang, X., Wan, H. J., Ahammed, G. J., Yu, J., Yao, Z., et al. (2017). Identification of optimal reference genes for normalization of qPCR analysis during pepper fruit development. *Front. Plant Sci.* 8. doi: 10.3389/fpls.2017.01128

Chew, O., Whelan, J., and Millar, A. H. (2003). Molecular definition of the ascorbate-glutathione cycle in arabidopsis mitochondria reveals dual targeting of antioxidant defenses in plants. *J. Biol. Chem.* 278 (47), 46869–46877. doi: 10.1074/jbc.M307525200

Chiang, C. M., Chien, H. L., Chen, L. O., Hsiung, T. C., Chiang, M. C., and Chen, S. P. (2015). Overexpression of the genes coding ascorbate peroxidase from brassica campestris enhances heat tolerance in transgenic arabidopsis thaliana. *Biol. Plant* 59 (2), 305–315. doi: 10.1007/s10535-015-0489-y

Chou, K. C., and Shen, H. B. (2010). A new method for predicting the subcellular localization of eukaryotic proteins with both single and multiple sites: euk-mPLoc 2.0. *PloS One* 5 (4), e9931. doi: 10.1371/journal.pone.0009931

Davletova, S., Rizhsky., L., Liang, H., Shengqiang, Z., Oliver, D. J., Coutu, J., et al. (2005). Cytosolic ascorbate peroxidase 1 is a central component of the reactive oxygen gene network of arabidopsis. *Plant Cell.* 17 (1), 268–281. doi: 10.1105/tpc.104.026971

Faize, M., Burgos, L., Faize, L., Piqueras, A., Nicolas, E., Barba-Espin, G., et al. (2011). Involvement of cytosolic ascorbate peroxidase and Cu/Zn superoxide dismutase for improved tolerance against drought stress. *J. Exp. Bot.* 62 (8), 2599–2613. doi: 10.1093/jxb/erq432

Foyer, C. H., and Shigeoka, S. (2011). Understanding oxidative stress and antioxidant functions to enhance photosynthesis. *Plant Physiol.* 155 (1), 93–100. doi: 10.1104/pp.110.166181

Frank, G., Pressman, E., Ophir, R., Althan, L., Shaked, R., Freedman, M., et al. (2009). Transcriptional profiling of maturing tomato (Solanum lycopersicum l.) microspores reveals the involvement of heat shock proteins, ROS scavengers, hormones, and sugars in the heat stress response. *J. Exp. Bot.* 60 (13), 3891–3908. doi: 10.1093/jxb/erp234

Guan, Q. J., Xia, D. X., and Liu, S. K. (2010). OsAPX4 gene response to several environmental stresses in rice *(Oryza sativa* l.). *Afr J. Biotechnol.* 9 (36), 5908–5913. doi: 10.5897/AJB10.037

Hong, C. Y., Hsu, Y. T., Tsai, Y. C., and Kao, C. H. (2007). Expression of ASCORBATE PEROXIDASE 8 in roots of rice (Oryza sativa l.) seedlings in response to NaCl. *J. Exp. Bot.* 58, 3273–3283. doi: 10.1093/jxb/erm174

Howe, E., Holton, K., Nair, S., Schlauch, D., Sinha, R., and Quackenbush, J. (2010). *Mev: multiexperiment viewer in biomedical informatics for cancer research.* Ed. M. F. Ochs (New York, NY: Springer US), 267–277.

Hu, B., Jin, J., Guo, A. Y., Zhang, H., Luo, J., and Gao, G. (2014). GSDS 2.0: an upgraded gene feature visualization server. *Bioinformatics.* 31 (8), 1296–1297. doi: 10.1093/bioinformatics/btu817

Huang, L. P., Jia, J., Zhao, X. X., Zhang, M. Y., Huang, X. X., Ji, E., et al. (2017). The ascorbate peroxidase APX1 is a direct target of a zinc finger transcription factor ZFP36 and a late embryogenesis abundant protein OsLEA5 interacts with ZFP36 to co-regulate OsAPX1 in seed germination in rice. *Biochem. Bioph Res. Co.* 495 (1), 339–345. doi: 10.1016/j.bbrc.2017.10.128

Koussevitzky, S., Suzuki, N., Huntington, S., Armijo, L., Sha, W., Cortes, D., et al. (2008). Ascorbate peroxidase 1 plays a key role in the response of arabidopsis thaliana to stress combination. *J. Biol. Chem.* 283 (49), 34197–34203. doi: 10.1074/jbc.M806337200

Kumar, S., Stecher, G., and Tamura, K. (2016). MEGA7: molecular evolutionary genetics analysis version 7.0 for bigger datasets. *Mol. Biol. Evol.* 33 (7), 1870–1874. doi: 10.1093/molbev/msw054

Leng, X., Wang, H. Z., Zhang, S., Qu, C. P., Yang, C. P., Xu, Z., et al. (2021). Identification and characterization of the APX gene family and its expression pattern under phytohormone treatment and abiotic stress in *Populus trichocarpa*. *Genes.* 12 (3), 334. doi: 10.3390/genes12030334

Lescot, M., Déhais, P., Thijs, G., Marchal, K., Moreau, Y., Van de Peer, Y., et al. (2002). PlantCARE, a database of plant cis-acting regulatory elements and a portal to tools for in silico analysis of promoter sequences. *Nucleic Acids Res.* 30 (1), 325–327. doi: 10.1093/nar/30.1.325

Liao, G. L., Liu, Q., Li, Y. Q., Zhong, M., Huang, C. H., Jia, D. F., et al. (2020). Identification and expression profiling analysis of ascorbate peroxidase gene family in actinidia chinensis (Hongyang). *J. Plant Res.* 133, 715–726. doi: 10.1007/s10265-020-01206-y

Maruta, T., Sawa, Y., Shigeoka, S., and Ishikawa, T. (2016). Diversity and evolution of ascorbate peroxidase functions in chloroplasts: more than just a classical antioxidant enzyme? *Plant Cell Physiol.* 57 (7), 1377–1386. doi: 10.1093/PCP/PCV203

Mittler, R., Vanderauwera, S., Gollery, M., and Van Breusegem, F. (2004). Reactive oxygen gene network of plants. *Trends Plant Sci.* 9 (10), 490–498. doi: 10.1016/j.tplants.2004.08.009

Najami, N., Janda, T., Barriah, W., Kayam, G., Tal, M., Micha, G., et al. (2008). Ascorbate peroxidase gene family in tomato: its identification and characterization. *Mol. Genet. Genomics* 279, 171–182. doi: 10.1007/s00438-007-0305-2

Narendra, S., Venkataramani, S., Shen, G. X., Wang, J., Pasapula, V., Lin, Y., et al. (2006). The arabidopsis ascorbate peroxidase 3 is a peroxisomal membrane-bound antioxidant enzyme and is dispensable for arabidopsis growth and development. *J. Exp. Bot.* 57, 3033–3042. doi: 10.1093/jxb/erl060

Panchuk, I. I., Volkov, R. A., and Schöffl, F. (2002). Heat stress- and heat shock transcription factor-dependent expression and activity of ascorbate peroxidase in arabidopsis. *Plant Physiol.* 129, 838–853. doi: 10.1104/pp.001362

Pnueli, L., Liang, H., Rozenberg, M., and Mittler, R. (2003). Growth suppression, altered stomatal responses, and augmented induction of heat shock proteins in cytosolic ascorbate peroxidase (Apx1)-deficient arabidopsis plants. *Plant J.* 34 (2), 187–203. doi: 10.1046/j.1365-313x.2003.01715.x

Qu, C. X., Wang, L., Zhao, Y. W., and Liu, C. (2020). Molecular evolution of maize ascorbate peroxidase genes and their functional divergence. *Genes.* 11 (10), 1204. doi: 10.3390/genes11101204

Raza, A., Ashraf, F., Zou, X., Zhang, X., and Tosif, H. (2020). "Plant adaptation and tolerance to environmental stresses: mechanisms and perspectives," in *Plant ecophysiology and adaptation under climate change: mechanisms and perspectives I* (Singapore: Springer), 117–145.

Renu, K. C., Anjana, J., and Vimal, K. S. (2011). Chloroplasts and mitochondria have multiple heat tolerant isozymes of SOD and APX in leaf and inflorescence in chenopodium album. *Biochem. Biophys. Res. Commun.* 412 (4), 522–525. doi: 10.1016/j.bbrc.2011.06.179

Ribeiro, C. W., Korbes, A. P., Garighan, J. A., Jardim-Messeder, D., Carvalho, F. E. L., and Sousa, R. H. V. (2017). Rice peroxisomal ascorbate peroxidase knockdown affects ROS signaling and triggers early leaf senescence. *Plant Sci.* 263, 55–65. doi: 10.1016/j.plantsci.2017.07.009

Schramm, F., Ganguli, A., Kiehlmann, E., Englich, G., Walch, D., and von Koskull-Döring, P. (2006). The heat stress transcription factor HsfA2 serves as a regulatory amplifier of a subset of genes in the heat stress response in *Arabidopsis*. *Plant Mol. Biol.* 60 (5), 759–772. doi: 10.1007/s11103-005-5750-x

Sharma, P., and Dubey, R. S. (2005). Modulation of nitrate reductase activity in rice seedlings under aluminium toxicity and water stress: role of osmolytes as enzyme protectant. *J. Plant Physiol.* 162 (8), 854–864. doi: 10.1016/j.jplph.2004.09.011

Shi, W. M., Muramoto, Y., Ueda, A., and Takabe, T. (2001). Cloning of peroxisomal ascorbate peroxidase gene from barley and enhanced thermotolerance by overexpressing in arabidopsis thaliana. *Gene.* 273 (1), 23–27. doi: 10.1016/S0378-1119(01)00566-2

Shigeoka, S., Ishikawa, T., Tamoi, M., Miyagawa, Y., Takeda, T., Yabuta, Y., et al. (2002). Regulation and function of ascorbate peroxidase isoenzymes. *J Exp Bot* 53 (3772), 1305–1319. doi: 10.1093/jxb/53.372.1305

Shigeru, S., Takahiro, I., Masahiro, T., Yoshiko, M., Toru, T., Yukinori, Y., et al. (2002). Regulation and function of ascorbate peroxidase isoenzymes. *J. Exp. Bot.* 53 (372), 1305–1319. doi: 10.1093/jxb/53.372.1305

Singh, N., Mishra, A., and Jha, B. (2014). Over-expression of the peroxisomal ascorbate peroxidase (SbpAPX) gene cloned from halophyte salicornia brachiata

confers salt and drought stress tolerance in transgenic tobacco. *Mar. Biotechnol.* 16 (3), 321–332. doi: 10.1007/s10126-013-9548-6

Tao, C. C., Jin, X., Zhu, L. P., Xie, Q. L., Wang, X. C., and Li, H. B. (2018). Genome-wide investigation and expression profiling of APX gene family in gossypium hirsutum provide new insights in redox homeostasis maintenance during different fiber development stages. *Mol. Genet. Genomics* 293, 685–697. doi: 10.1007/s00438-017-1413-2

Teixeira, F. K., Menezes-Benavente, L., Galvão, V. C., Margis, R., and Margis-Pinheiro, M. (2006). Rice ascorbate peroxidase gene family encodes functionally diverse isoforms localized in different subcellular compartments. *Planta.* 224, 300–314. doi: 10.1007/s00425-005-0214-8

Teixeira, F. K., Menezes-Benavente, L., Margis, R., and Margis-Pinheiro, M. (2004). Analysis of the molecular evolutionary history of the ascorbate peroxidase gene family: inferences from the rice genome. *J. Mol. Evol.* 59 (6), 761–770. doi: 10.1007/s00239-004-2666-z

Wang, J., Zhang, H., and Allen, R. D. (1999). Overexpression of an arabidopsis peroxisomal ascorbate peroxidase gene in tobacco increases protection against oxidative stress. *Plant Cell Physiol.* 40 (7), 725–732. doi: 10.1093/oxfordjournals.pcp.a029599

Wu, B. M., Li, L., Qiu, T. H., Zhang, X., and Cui, S. X. (2018). Cytosolic APX2 is a pleiotropic protein involved in H2O2 homeostasis, chloroplast protection, plant architecture and fertility maintenance. *Plant Cell Rep.* 37 (6), 833–848. doi: 10.1007/s00299-018-2272-y

Yang, Y. X., Ahammed, G. J., Wan, C. P., Liu, H. J., Chen, R. R., and Zhou, Y. (2019). Comprehensive analysis of TIFY transcription factors and their expression profiles under jasmonic acid and abiotic stresses in watermelon. *Int. J. Genomics* 2314 (436), 1–13. doi: 10.1155/2019/6813086

Yoshimura, K., Yabuta, Y., Ishikawa, T., and Shigeoka, S. (2000). Expression of spinach ascorbate peroxidase isoenzymes in response to oxidative stresses. *Plant Physiol.* 123 (1), 223–234. doi: 10.1104/pp.123.1.223

Zhang, Z. G., Zhang, Q., Wu, J. X., Zheng, X., Zheng, S., Sun, X. H., et al. (2013). Gene knockout study reveals that cytosolic ascorbate peroxidase 2(OsAPX2) plays a critical role in growth and reproduction in rice under drought, salt and cold stresses. *PloS One* 8 (2), e57472. doi: 10.1371/journal.pone.0057472

Zimmermann, P., Hirsch-Hoffmann, M., Hennig, L., and Gruissem, W. (2004). GENEVESTIGATOR. arabidopsis microarray database and analysis toolbox. *Plant Physiol.* 136 (1), 2621–2632. doi: 10.1104/pp.104.046367

frontiers | Frontiers in Plant Science

TYPE Original Research
PUBLISHED 31 May 2023
DOI 10.3389/fpls.2023.1197781

Check for updates

OPEN ACCESS

EDITED BY
Meng Jiang,
Zhejiang University, China

REVIEWED BY
Muhammad Azhar Hussain,
Hainan University, China
Muhammad Waseem,
Hainan University, China
Ali Raza,
Fujian Agriculture and Forestry University, China
Muhammad Zulfiqar Ahmad,
Gomal University, Pakistan

*CORRESPONDENCE
Jian Wang
wangjian@zaas.ac.cn

†These authors have contributed equally to this work

RECEIVED 31 March 2023
ACCEPTED 02 May 2023
PUBLISHED 31 May 2023

CITATION
Yang S, Chen J, Ding Y, Huang Q, Chen G, Ulhassan Z, Wei J and Wang J (2023) Genome-wide investigation and expression profiling of *LOR* gene family in rapeseed under salinity and ABA stress.
Front. Plant Sci. 14:1197781.
doi: 10.3389/fpls.2023.1197781

COPYRIGHT
© 2023 Yang, Chen, Ding, Huang, Chen, Ulhassan, Wei and Wang. This is an open-access article distributed under the terms of the Creative Commons Attribution License (CC BY). The use, distribution or reproduction in other forums is permitted, provided the original author(s) and the copyright owner(s) are credited and that the original publication in this journal is cited, in accordance with accepted academic practice. No use, distribution or reproduction is permitted which does not comply with these terms.

Genome-wide investigation and expression profiling of *LOR* gene family in rapeseed under salinity and ABA stress

Su Yang[1,2†], Jialuo Chen[1†], Yonghe Ding[1], Qian Huang[2], Guangna Chen[1], Zaid Ulhassan[2], Ji'an Wei[3] and Jian Wang[4*]

[1]Key Laboratory of Specialty Agri-products Quality and Hazard Controlling Technology of Zhejiang Province, College of Life Sciences, China Jiliang University, Hangzhou, Zhejiang, China, [2]Institute of Crop Science and Zhejiang Key Laboratory of Crop Germplasm, Zhejiang University, Hangzhou, China, [3]Mizuda Group Co., Ltd., Huzhou, Zhejiang, China, [4]Institute of Vegetables, Zhejiang Academy of Agricultural Sciences, Hangzhou, China

The *Brassica napus* (*B. napus*) *LOR* (*Lurp-One-Related*) gene family is a little-known gene family characterized by a conserved LOR domain in the proteins. Limited research in *Arabidopsis* showed that *LOR* family members played important roles in *Hyaloperonospora parasitica* (*Hpa*) defense. Nevertheless, there is a paucity of research investigating the role of the *LOR* gene family towards their responses to abiotic stresses and hormone treatments. This study encompassed a comprehensive survey of 56 *LOR* genes in *B. napus*, which is a prominent oilseed crop that holds substantial economic significance in China, Europe, and North America. Additionally, the study evaluated the expression profiles of these genes in response to salinity and ABA stress. Phylogenetic analysis showed that 56 *BnLORs* could be divided into 3 subgroups (8 clades) with uneven distribution on 19 chromosomes. 37 out of 56 *BnLOR* members have experienced segmental duplication and 5 of them have undergone tandem repeats events with strong evidence of purifying selection. Cis-regulatory elements (CREs) analysis indicated that *BnLORs* involved in process such as light response, hormone response, low temperature response, heat stress response, and dehydration response. The expression pattern of *BnLOR* family members revealed tissue specificity. RNA-Seq and qRT-PCR were used to validate *BnLOR* gene expression under temperature, salinity and ABA stress, revealing that most *BnLORs* showed inducibility. This study enhanced our comprehension of the *B. napus LOR* gene family and could provide valuable information for identifying and selecting genes for stress resistant breeding.

KEYWORDS

***Brassica napus*, *LOR* gene family, phylogenetic tree, expression profiles, abiotic stress**

Introduction

Abiotic stress can reduce plant growth and development *via* inhibiting cell division and elongation, reducing leaf expansion, and slowing down metabolic processes (Suzuki et al., 2014). Consequently, plants may exhibit stunted growth and a decrease in biomass. Among them, salt stress could lead to osmotic stress, ion toxicity and nutrient imbalance (Raza et al., 2022; Sheteiwy et al., 2022). Abscisic acid (ABA) treatment could lead to the inhibition of growth, stomatal closure, and senescence (Waadt et al., 2022). Salt stress and ABA are known to have significant effects on rapeseed (*Brassica napus*). Salt stress induces oxidative stress and disrupts ion homeostasis in rapeseed, resulting in reduced growth, photosynthesis, and yield (Shu et al., 2018). ABA plays a crucial role in mediating the response of rapeseed to salt stress, by regulating stomatal closure, antioxidant defense, and osmotic adjustment (Zhu and Assmann, 2017). Salt stress and ABA also modulate the expression of stress-related genes, including those involved in ion transport, osmotic regulation, and stress signaling pathways in rapeseed (Raza et al., 2023). Furthermore, salt stress and ABA have been shown to interact with other signaling molecules, such as calcium and reactive oxygen species (ROS), to modulate the physiological and molecular responses of rapeseed to stress (Raza et al., 2023).

The *LOR* (*Lurp-One-Related*) gene family is widely presented in various organisms, including plants, fungi, bacteria, and certain archaea. *LOR* family members are characterized by a conserved LOR domain in the protein (Knoth and Eulgem, 2008). Members of this gene family typically exhibit a 12-stranded β-barrel structure that encompasses a central C-terminal α-helix, similar to the C-terminal domain observed in Tubby proteins (Bateman et al., 2009). β-barrel and α-helix are structural motifs commonly found in proteins that play important roles in gene structure organization. β-barrel structures are characterized by a cylindrical shape formed by β-strands arranged in a closed loop, while α-helices refer to α-helices located at the C-terminus of a protein. These structural elements are involved in protein-protein interactions, protein stability, and protein-DNA interactions, influencing gene expression, transcriptional regulation, and chromatin organization (Yin et al., 2017). The *LOR* gene family was initially named after the first member discovered in *Arabidopsis thaliana*, *LURP1* (*Late up-regulated in response to Hyaloperonospora parasitica*). *LURP1* belongs to the LURP cluster and plays a pivotal role in plant defense against pathogenic bacteria. Knoth and Eulgem (2008) demonstrated that *LURP1* is indispensable in the defense response against *Hyaloperonospora parasitica* (*Hpa*) in *Arabidopsis*. Moreover, the promoter of *AtLURP1* contain a W box and two TGA boxes, which could mediate gene expression in response to *Hpa* and salicylic acid (SA) (Knoth and Eulgem, 2008). Later Caillaud et al. (2016) proved that *AtLURP1* could respond to SA and function as a marker gene of SA triggered immunity. Gupta and Senthil-Kumar (2017) conducted a global transcriptome profiling of *Arabidopsis* investigating their response to *Pseudomonas syringae* infection during drought recovery stage. They found that the transcription level of *AtLURP1* was up-regulated in response to pathogen infection, but down-regulated during drought stress or at the time of drought recovery. Lee et al. (2017) found that *AtLURP1* was the target gene of NAC4 transcription factor (TF) and could negatively regulate cell death caused by plant pathogen infection. *AtLURP1* also participated in plant defense against the widespread pest *Myzus persicae* (Bricchi et al., 2012). Apart from *AtLURP1*, *AtLOR1* is another gene that has been extensively studied. Baig (2018) reported that *AtLOR1* displayed constitutive expression and played a significant role in basal defense against *Hpa*. These findings highlight the potential important roles of *LOR* gene family in plant in response to environmental stimuli. However, apart from the *AtLURP1* and *AtLOR1*, the expression pattern and biological function of other members are still unknown.

Brassica napus (*B. napus*, AACC, 2n=4x=38), also called rapeseed, is a prominent oilseed crop that holds substantial economic significance in China, Europe, and North America, with extensive applications as oilseeds, vegetable, biofuel, and fodder (Yang et al., 2022). As a representative species of Brassicaceae, *B. napus* was originated from the spontaneous hybridization between *Brassica rapa* (*B. rapa*, AA, 2n=2x=20) and *Brassica oleracea* (*B. oleracea*, CC, 2n=2x=18) at nearly 7500 years ago, followed by allopolyploidization (Yang et al., 2016; Yang et al., 2018; Yang et al., 2020). With the continuous development of sequencing technology, the reference genomes of Darmor-bzh (winter ecotype), Zhongshuang 11 and NY7 (semi-winter ecotype) had been successfully sequenced and assembled (Chalhoub et al., 2014; Sun et al., 2017; Zou et al., 2019), but no systematic analysis and function prediction about the *LOR* gene family in *B. napus* had been reported yet. A comprehensive investigation of the *BnLOR* gene family could shed light on the evolutionary mechanisms of allopolyploidization between *B. rapa* and *B. oleracea* and provide a theoretical foundation for future studies on the roles of *BnLOR* genes.

In this study, 56 *LOR* family members were identified in the *B. napus* reference genome. The phylogenetic relationship, chromosomal distributions, protein conserved motifs, gene structures, whole genome duplication (WGD) events, synteny relationship, and putative cis-regulatory elements (CREs) in promoter regions were systematically analyzed. Besides, the expression pattern of *BnLORs* in different tissue as well as under salt stress and ABA treatment was analyzed. Results showed that most *BnLOR* genes could be induced by salt stress and ABA treatment, suggesting their potential function on salinity and ABA stress responsiveness. These results could provide useful information for further investigation about the function and molecular mechanisms of *BnLOR* genes towards abiotic salinity and ABA stress.

Materials and methods

Sequence extraction and domain identification

The reference genome and protein sequences of *B. napus* were downloaded from http://yanglab.hzau.edu.cn/BnIR/ while the reference genome of *B. rapa, B. oleracea* and *Arabidopsis* was

obtained from http://plants.ensembl.org/index.html. The Hidden Markov Model (HMM) file of the *LOR* domain was acquired from Pfam protein family database (http://pfam.xfam.org/) (El-Gebali et al., 2019). *LOR* genes were searched from *B. napus* reference genome using HMMER 3.3 (Potter et al., 2018). The preliminarily identified *LOR* family members from *B. napus* (*BnLOR*) were validated by blasting with *LOR* gene family from *A. thaliana* as queries and all candidate genes were further validated at CDD (https://www.ncbi.nlm.nih.gov/cdd/), Pfam and SMART (http://smart.embl.de/) to verify the existence of LOR domain. The length of the *BnLOR* protein sequences as well as the molecular weight (Mw) and the isoelectric points (pI) were predicted by the pI/Mw tool in ExPASy (http://www.expasy.ch/tools/pi_tool.html). Besides, the subcellular location of *BnLOR* genes were predicted by the Cell-PLoc web-server (http://www.csbio.sjtu.edu.cn/bioinf/Cell-PLoc/).

Multiple sequence alignment and phylogenetic analysis

To identify the evolutionary relationship among *LOR* gene family from different species, the protein sequences of *LORs* from *Arabidopsis*, *B. rapa*, *B. oleracea*, and *B. napus* were aligned by the Clustal W algorithm with default parameters (Larkin et al., 2007). The ALN file was converted into MEGA 6.0 to build a neighbor-joining (NJ) phylogenetic tree with following parameters: Poisson model, and pairwise deletion for the reliability of interior branches (Tamura et al., 2013). The phylogenetic tree was modified and displayed using the iTol tool (https://itol.embl.de/).

Gene structures and protein conserved motifs analysis

The gene structures and protein conserved motifs of the *BnLOR* family members were analyzed in this study. The exon-intron structures of each *BnLOR* gene were extracted using gene structure view (advanced) in TBtools (Chen et al., 2020), which provided a graphical representation of the gene structures. The conserved motifs within the BnLOR protein sequences were identified using the Multiple Em for Motif Elicitation program (MEME, https://meme-suite.org/meme/) with default parameters set for maximum number of motifs, distribution of motif occurrences, and optimum motif width (Bailey et al., 2009). The identified exon-intron structures and conserved motifs were then visualized by TBtools (Chen et al., 2020).

Gene distribution and WGD visualization

The chromosomal positions and relative distances of the *BnLOR* family members were drafted using TBtools (Chen et al., 2020). The WGD landscape within *B. napus* was generated by MCScanX (Wang et al., 2012). To confirm WGD events, the shorter aligned sequence was required to cover over 70% of the longer sequence and the similarity of the aligned regions had to be over 70% (Gu et al., 2002; Yang et al., 2008). WGD events includes segmental duplication and tandem repeats. Tandem repeats are defined as two genes located in the same chromosomal fragment with a length of less than 100 kb (Wang et al., 2010b). Segmental duplications refer to two genes experienced polyploidization followed by chromosome rearrangements (Yu et al., 2005). The synteny map was created using Circos (Krzywinski et al., 2009). Additionally, the MCScanX was used to show the collinearity relationship between *B. napus*, *B. rapa* and *B. oleracea*. Finally, the KaKs_Calculator 2.0 program was utilized to calculate the non-synonymous (ka) and synonymous (ks) substitutions of each duplicated *LOR* gene (Wang et al., 2010a).

CREs prediction in the promoter regions

The promoter sequence (about 2000 bp upstream of the translation start codon) of *BnLOR* family members were extracted from the *B. napus* reference genome. PlantCARE program (http://bioinformatics.psb.ugent.be/webtools/plantcare/html/) was used to predict the putative CRE responsive to transcription binding sites, hormone treatments, biotic and abiotic stresses. PlantRegMap program (http://plantregmap.gao-lab.org/) was used to predict the potential TFs using *B. napus* as the target species (Jin et al., 2017).

Orthologous gene clusters among multiple species

To identify orthologous gene clusters among multiple species, the reference genomes of eight commonly studied species including *Arabidopsis*, *B. oleracea*, *B. rapa*, *B. napus*, *Glycine max* (*G. max*), *Oryza sativa* (*O. sativa*), *Triticum aestivum* (*T. aestivum*) and *Zea mays* (*Z. mays*) were analyzed using the Ortho Venn 2.0 tool (https://orthovenn2.bioinfotoolkits.net/home). The e-value threshold and the inflation value were set at 1e-5 and 1.5, respectively. The protein sequences of *LORs* in these species were uploaded, analyzed, and visualized. (Wang et al., 2022; Wang et al., 2023).

Gene expression patterns analysis

To determine the gene expression pattern of *BnLOR* gene family, transcriptome file of various tissues including blossomy pistil, flower, leaf, ovule, pericarp, pistil, root, silique, sepal, stamen, stem, and wilting pistil were obtained from a previous study by Sun et al. (2017) under the project ID of PRJNA394926 in the NCBI. Moreover, transcriptome data of *B. napus* under dehydration, salt stress, ABA treatment and cold stress conditions were obtained from Zhang et al. (2019) under the project ID of CRA001775. Differential expression analysis of *BnLOR* genes was performed

using the DSEeq2 R package and the heatmaps were created by TBtools software (Chen et al., 2020).

Comparative modeling of BnLOR proteins

Homology modeling was used to create the three-dimensional (3D) structures of BnLOR proteins from their amino acid sequences. The amino acid sequences of BnLORs were submitted to SWISS-MODEL program (https://swissmodel.expasy.org/) for model generating. The quality of the models was assessed using ERRAT and PROCHECK tests through SAVES program (https://saves.mbi.ucla.edu/). The resulting 3D structures of BnLOR proteins were visualized using the Pymol software (Karnes and Shaikh, 2021).

Plant materials and treatments

One leading cultivar of *B. napus* (ZD622) was chosen in this research to validate the relative expression levels of *BnLORs* under salinity and ABA stress (Ma et al., 2022). Mature and healthy seeds of ZD622 underwent sterilization by submersion in 1% NaClO for 15 minutes. The seeds were thoroughly rinsed with distilled water before being germinated in a petri dish for 24 hours with a damp filter paper placed underneath. After germination, the seedlings were transferred to a 12 cm^2 growth box containing full-strength Hoagland's solution, along with a sponge placed inside. Germinated plants were shifted to growth chamber with 16-hr photoperiod, 24/16 day/night temperature, 300 µmol/m^2/s light intensity and 60% to 70% humidity. After one week, uniformly developed seedlings were subjected to salt stress (200 mM) and ABA treatment (25 µM). Leaf samples were immediately frozen using liquid nitrogen and stored in a -80°C refrigerator in preparation for RNA isolation at 0 h, 4 h, and 24 h after treatment. Each sample had at least three replicates.

qRT-PCR validation

The MiniBEST Plant RNA Extraction Kit (Takara, Japan) was employed to isolate total RNA from leaf samples. The PrimeScriptTM RT reagent Kit (Takara, Japan) was used to carry out reverse transcription reactions with 1 µg RNA. The synthesized cDNAs were used as templates for qRT-PCR by employing the SuperReal PreMix Plus/SYBR Green (Tiangen, China) on a Bio-Rad CFX96 (BIO RAD, USA). The qRT-PCR conditions were elucidated in our recently published research (Wang et al., 2022). *B. napus actin-7* was used as the internal control gene. All qRT-PCR primers used were listed in Table S1. The relative expression levels were calculated using the $2^{-\Delta\Delta Ct}$ method with three replicates each (Livak and Schmittgen, 2001). Statistical analysis of the data was performed using the SPSS 20.0 statistical package (SPSS, Chicago, IL, USA). One-way variance analysis (ANOVA) was conducted followed by Duncan's multiple range test ($p < 0.05$) to determine significant differences. Figures were generated using GraphPad Prism 7.0 (Yang et al., 2022).

Results

Systematic identification and classification of *BnLORs*

According to the HMM file (PF04525) of *LOR* gene family, 72 candidate *BnLOR* genes were identified through model search of the *B. napus* reference genome. After filtering out the redundant genes and alternative splicing, the existence of LOR domain in candidate genes was further verified by CDD, Pfam and SMART program. As a result, 56 *LOR* genes in *B. napus* with complete open reading frame and LOR domain were identified. Their details, along with their encoded proteins, were listed in Tables S2, S3. The predicted length of BnLOR proteins range from 90 amino acids (BnLOR15/48) to 257 amino acids (BnLOR17) (Tables S2, S3). The MWs of BnLOR proteins ranged from 10.49 kDa (BnLOR48) to 29.28 kDa (BnLOR17), suggesting structural variance and functional diversity among members of this gene family (Table S2). The pIs of 15 BnLOR proteins were less than 7, indicating that they were acidic proteins (Table S2). The rest 41 proteins were alkalinity proteins with pIs higher than 7 (Table S2). The largely variance of pIs indicated the possibility of the proteins existing in different parts of cells. The grand average of hydropathicity (GRAVY) prediction results showed that all proteins were hydrophilic (Table S2). The instability index of 25 proteins were lower than 40, indicating that these proteins were relatively stable, while the rest 31 proteins were relatively unstable (Table S2). The aliphatic index of 56 BnLOR proteins fluctuated from 71.48 (BnLOR11) to 100.88 (BnLOR28). Aliphatic index is positively correlated with the thermal stability of protein, suggesting that the thermal stability of the BnLOR proteins was largely variant. Besides, the prediction of subcellular localization of BnLOR proteins exhibited significant variation. Among the 56 identified BnLOR proteins, 25 were exclusively localized in a single compartment such as nucleus, cytoplasm, or chloroplast, while the remaining 31 proteins were found in at least two different subcellular locations. Notably, chloroplast was the most frequent localization site for BnLOR proteins (75.00%), followed by nucleus (48.21%), cytoplasm (33.93%), cell membrane (14.29%), mitochondrion (14.29%), peroxisome (12.50%), cell wall (10.71%), and vacuole (3.57%).

Phylogenetic analysis of Brassicaceae species

The phylogenetic tree among *B. napus* (56 *BnLORs*), model plants *Arabidopsis* (20 *AtLORs*), ancestral species *B. rapa* (33 *BrLORs*) and *B. oleracea* (30 *BoLORs*) was constructed by NJ method. According to its topological structures, *BnLORs* could be divided into three subgroups (Figure 1). Subgroup I was the largest group with 27 *BnLOR* genes and could be further divided into four clades (Clade A to D) (Figure 1). Subgroup II (Clade E) was the smallest group with only 3 *BnLOR* genes (Figure 1). Subgroup III had 26 *BnLOR* genes and could be further divided into three clades (Clade F to H) (Figure 1). Clade A, C and H were relatively large, each contains 10 or more family members. Clade D and E had only

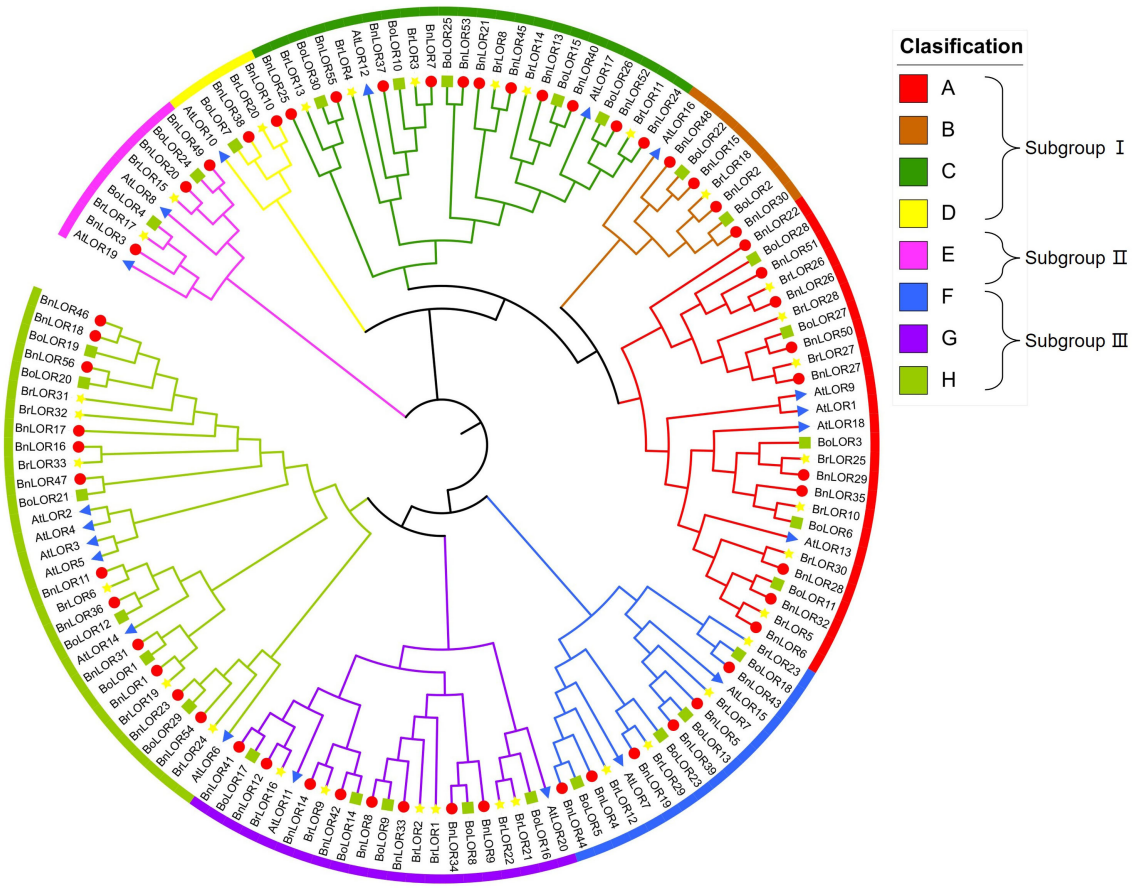


FIGURE 1
A neighbor-joining (NJ) phylogenetic tree of 142 LOR proteins from *B. napus*, *B. oleracea*, *B.rapa*, and *A. thaliana*. Overall, 56 BnORs (red circle), 33 BrLORs (yellow star), 30 BoLORs (green box), and 20 AtLORs (blue triangle) were grouped into 3 subgroups (8 clades) based on domain and 1000 bootstrap values.

2 or 3 members each while Clade B, F and G had 4 to 8 family members, respectively. Both Subgroup I and III had plenty of members and branches, indicating that the structures and function of these two subgroups were relatively diverse. Each clade had *LOR* family members from four species (*B. napus*, *Arabidopsis*, *B. rapa* and *B. oleracea*), indicating that the phylogenic relationship among these four species were relatively close (Figure 1). At the end of the phylogenetic tree branch, there were 46 homologous gene pairs, among which 22 were Bn-Bo homologous gene pairs, 17 were Bn-Br homologous gene pairs and 2 were Br-Bo homologous gene pairs (Figure 1). Bn-Bo and Bn-Br homologous gene pairs could be found in every clade, but their distribution rates were inconsistent. It is noticed that all homologous gene pairs in Clade B, C, D and F belonged to Bn-Bo or Bn-Br homologous gene pairs (Figure 1).

Gene structures and protein conserved motif analysis

The reference genome sequences of *BnLOR*s were submitted to GSDS server to display their gene structures. Results showed that the exon-intron composition from Clade A to Clade D was similar (Figure 2). Each of them owned 3 exons separated by 2 introns apart from *BnLOR48/15/53*, which had one intro inside two exons (Figure 2). Meanwhile, the motif structures from Clade E to H were also similar (Figure 2). Most of them contained two exons and one intron with a few exceptions (Figure 2). *BnLOR3* and *BnLOR54* had three exons separated by two introns; *BnLOR47/16/17* only had one exon; *BnLOR20* had two exons and two introns (Figure 2). Among all the 56 *BnLORs*, 19 *BnLOR* family members had no upstream or downstream non-coding regions regulating the transcription of coding regions (Figure 2).

The reference protein sequences of BnLORs were uploaded to MEME Suite to identify their conserved motif. As a result, the MEME program identified 15 conserved motifs ($p<0.05$) with the length varied from 11 to 36 amino acids (Figure 2; Supplementary Figure S1; Table S4). The range of conserved motifs in BnLOR proteins was from 4 to 52 (Figure 2). Most of the BnLOR proteins contained motif 3 while only 4 proteins (BnLOR31/1/11/36) contained motif 14 (Figure 2). It was noticed that the motif structures of these BnLOR proteins showed high similarities. Most proteins had motif 1 at the head and motif 2 at the tail (Figure 2). Besides, BnLOR proteins on the same clade or adjacent

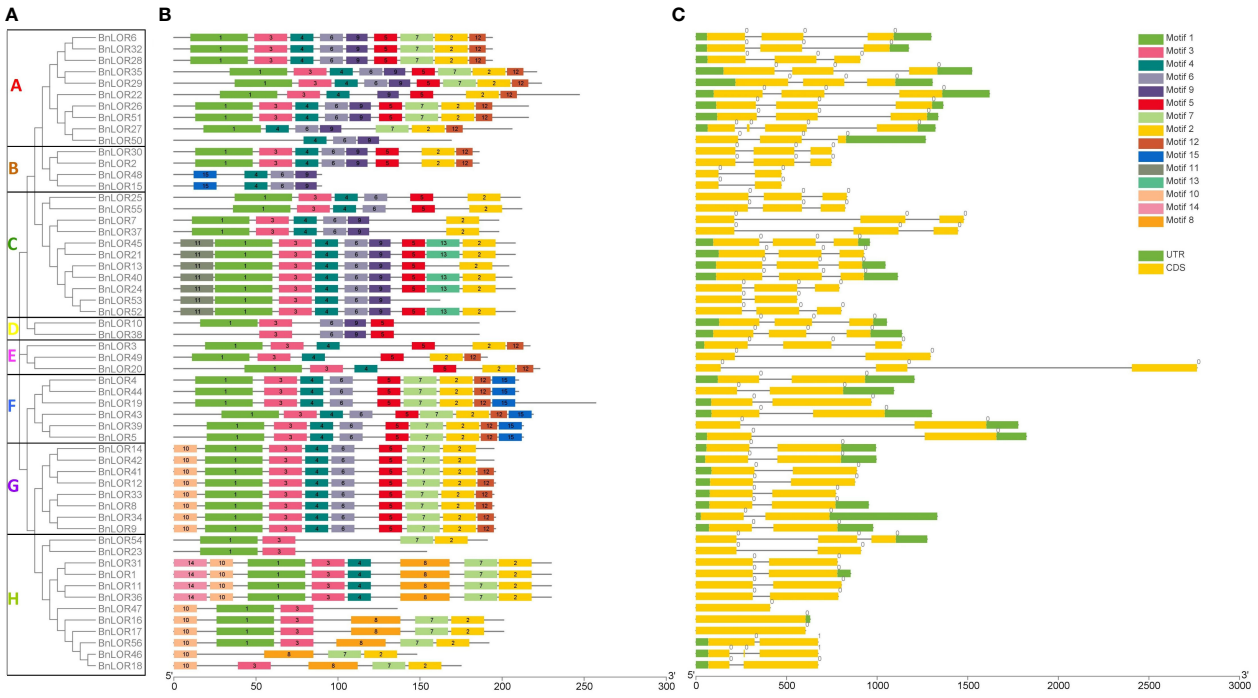


FIGURE 2
The gene structures and motif analysis of *LOR* family in *B. napus*. **(A)** Based on phylogenetic relationship and domain identification, the *BnLORs* were grouped into eight clades. **(B)** Conserved motif compositions identified in BnLOR proteins. 15 Different color boxes denote different motifs. **(C)** Gene structures of *BnLORs*. The yellow rectangle represents CDS or exons, and the grey line represents introns. Different numbers indicate the phase of introns.

clade had similar motif structures. For example, all proteins in Clade A have the same motif composition except for BnLOR50 (Figure 2). Each protein in Clade F shared the same motif composition (Figure 2). In Clade G, every protein had the same motif distribution except BnLOR14 and 42, which lacked motif 12 (Figure 2). Most proteins from Clade A to G had motif 6 (Figure 2). At the same time, we also noticed that the distribution of motifs in BnLOR proteins showed specificity. For instance, motif 11 only existed in Clade C while motif 10 only existed in Clade G and H (Figure 2). Motif 15 only appeared in Clade F while motif 13 only appeared in Clade C (Figure 2). Motif 14 only existed in Clade H and there was no motif 12 in Clade C or H (Figure 2).

Gene distribution and WGD visualization

The position of 56 *BnLOR* gene were retrieved from the *B. napus* reference genome and their position was visualized and mapped on chromosomes with TBtools (Chen et al., 2020). To facilitate identification, these genes were named as *BnLOR1* to *BnLOR56* based on their chromosomal location (Figure 3). Our analysis revealed that the distribution of *BnLORs* across the A and C genomes of *B. napus* was uneven, with 29 genes located on the A genome and 27 genes located on the C genome (Figure 3). Notably, chromosomes A3 and C3 exhibited the highest number of *BnLOR* genes, with 7 and 8 genes, respectively (Figure 3). There were 4 genes on chromosome C6 and C8 and 3 genes on chromosome A6, A7, A9, C4 (Figure 3). Two genes were located on chromosome A1, A2, A4, A5, C1, C5 and C9, one *BnLOR* gene was located on chromosome A10 and C7 while no *BnLOR* gene was found on chromosome A8 and C2 (Figure 3). For random chromosomes, there were 0 to 3 *BnLOR* genes, respectively (Figure 3).

WGD has been widely recognized as a crucial impetus underlying the evolution of species, providing the foundation for morphological and physiological changes in plants. WGD events include tandem repeats and segmental duplication. *B. napus* was originated from the spontaneous hybridization between *B. rapa* and *B. oleracea* followed by allopolyploidization, leading to the prevalence of paralogous genes with multiple copies in rapeseed. Thus, in this study, we aimed to gain insights into the expansion of *BnLOR* genes by analyzing the WGD. As a result, 42 pairs of gene duplication events occurred in 28 *BnLOR* family members on 19 chromosomes (Figure 4; Table 1). Among them, there were five tandem repeats (*BnLOR9/8*, *BnLOR16/17*, *BnLOR17/18*, *BnLOR26/27*, *BnLOR50/51*) (Table 1). The other 37 were all segmental duplication (Table 1). Our findings suggest that *BnLOR* genes have undergone a considerable number of duplication events throughout the evolutionary process, thereby contributing to the rapid expansion of the *BnLOR* gene family.

To elucidate the phylogenetic relationship among *LOR* family members, we employed MCScanX to conduct collinearity analysis across *B. napus*, *B. rapa*, and *B. oleracea* genomes. Our analysis identified 148 sets of collinearity relationships, including 78 pairs of collinear genes between *B. napus* and *B. rapa* and 70 pairs of collinear genes between *B. napus* and *B. oleracea* (Figure 5 and Table S5). The collinear genes on each chromosome were

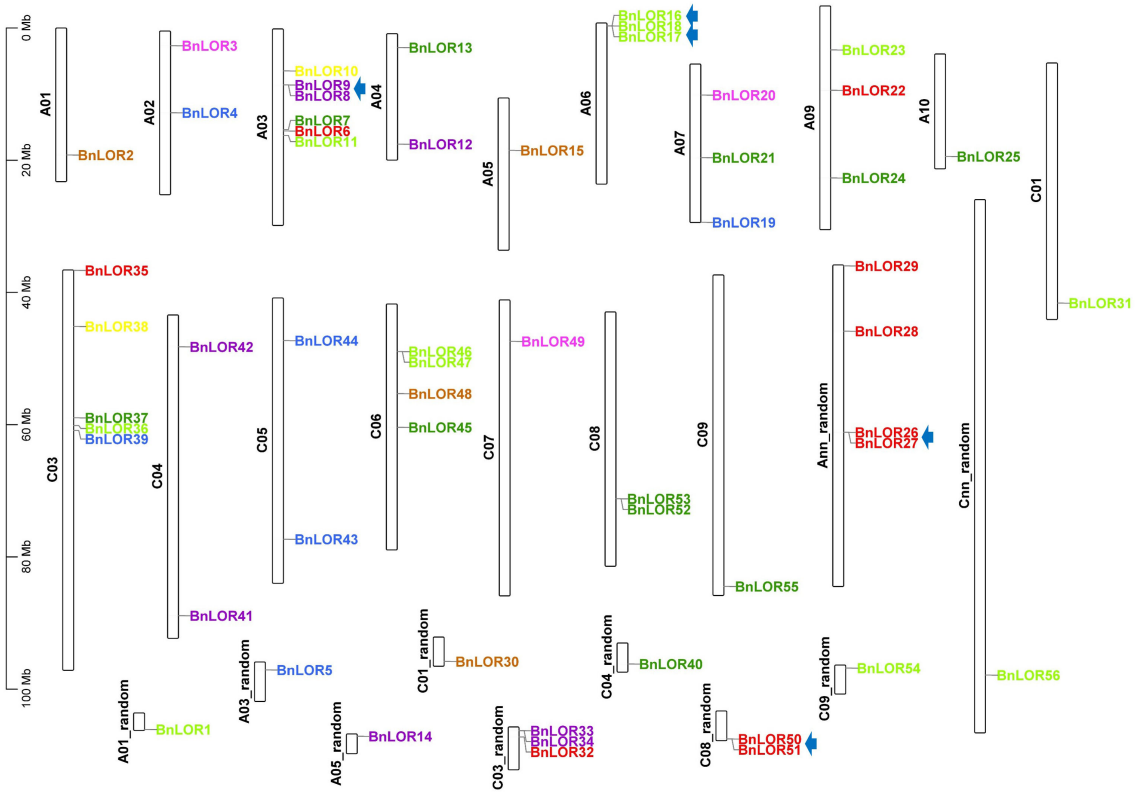


FIGURE 3
The distribution of *LOR* genes on *B. napus* chromosomes. The tandem repeats are highlighted with arrow. Different color of genes is accordance with their group distribution in Figure 1.

distributed on two to several chromosomes. For example, the collinear genes of *B. napus* on Chromosome A2 were located on Chromosome A2, A7 of *B. rapa* and on Chromosome C2 and C8 of *B. oleracea* (Figure 5). Notably, chromosomes A3 and C3 exhibited the largest number of collinear gene pairs.

To further explore the diversity of duplicated gene pairs during evolution, we calculated the Ka/Ks value. Except for one gene (*BnLOR15*) that could not be calculated in *B. napus*, the Ka/Ks value of all the segmental duplications and tandem repeats of *BnLOR* genes were less than 1, indicating that *BnLOR* genes were under the pressure of purifying selection during the evolutionary process of *B. napus* (Table 1).

Putative CREs analysis of *BnLOR* genes

After uploading the promoter sequence of *BnLORs* onto PlantCARE web server, a total of 1333 CREs with annotations were discovered. Nearly half (41.34%) of the CREs were associated with light responsiveness, such as AE-box, Box 4, ATCT-motif, GATA-motif, G-Box, GT1-motif, ACE, MRE, GA-motif, TCT-motif, I-box, AT1-motif, etc. 32.11% of them were involved in hormone responsiveness, such as ABRE, P-box, CGTCA-motif, TCA-element, TGA-element, TATC-box and TGACG-motif. Among them, ABRE was an ABA responsive CRE. 49 out of the 56 *BnLOR* promoters had ABRE element, indicating that most of *BnLORs* might be inducted by ABA treatment. 18.38% of the CREs were related to stress responsiveness, such as LTR, ARE, TC-rich repeats, GC-motif, MBS, and WUN-motif. About 80% of the CREs in *BnLOR* promoter regions were associated with anaerobic induction, implying that *BnLOR* gene family might confer the ability to survive under inundation stress or high-altitude environments. CREs related to circadian control were also detected in the *BnLOR* promoter regions, suggesting that this gene family might be regulated by light induction and circadian rhythms. Besides, CREs involved in metabolic regulation and meristem expression were also discovered.

This study focused on CREs in response to hormone treatments such as auxin responsive elements (TGA element and AuxRR core), ethylene responsive element (ERE), gibberellin (GA) responsive elements (GARE motif and TATC box), SA responsive elements (SARE), ABA responsive elements (ABRE) and methyl jasmonate (MeJA) related motif (TGACG motif and CGTCA motif) (Song et al., 2020). Besides, CREs associated with abiotic stress were also our focus, such as low temperature responsive element (LTR), heat stress responsive element (HSE), anaerobic induced elements (ARE), drought-induced elements (MBS), etc. (Song et al., 2020). Results showed that ABA and MeJA responsive CREs were the most abundant in the promoter regions of *BnLOR* genes, with 135 and 154 elements respectively, followed by auxin (47), GA (41) and SA (38) responsive elements (Figure 6A; Table S6). Among the stress responsive elements, the anaerobic induced elements were the most

10.3389/fpls.2023.1197781

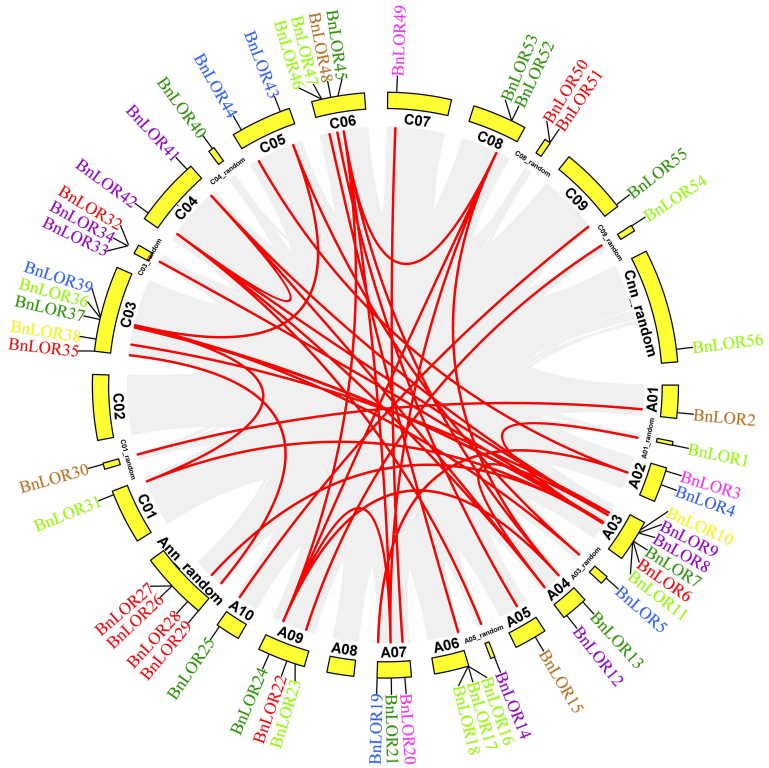


FIGURE 4
Chromosome locations and inter-chromosomal associations of *BnLOR* genes. Grey lines in the background display all syntenic blocks in the *B. napus* genome and the red lines display syntenic *BnLOR* gene pairs. Different color of genes is accordance with their group distribution in Figure 1.

TABLE 1 Duplication events and synonymous distances among *BnLOR* genes.

Duplicated pair gene 1	Duplicated pair gene 2	Duplication type	Ka	Ks	Ka/Ks
BnLOR9	*BnLOR8*	Tandem	0.017736	0.136061	0.130353
BnLOR16	*BnLOR17*	Tandem	0.045226	0.266653	0.169606
BnLOR17	*BnLOR18*	Tandem	0.018573	0.179015	0.103751
BnLOR26	*BnLOR27*	Tandem	0.190260	0.278870	0.682254
BnLOR50	*BnLOR51*	Tandem	0.266700	0.307243	0.868040
BnLOR1	*BnLOR11*	Segmental	0.093685	0.239040	0.391921
BnLOR2	*BnLOR30*	Segmental	0.009330	0.032285	0.288978
BnLOR4	*BnLOR19*	Segmental	0.029892	0.228597	0.130763
BnLOR4	*BnLOR44*	Segmental	0.000000	0.046943	0.000000
BnLOR5	*BnLOR39*	Segmental	0.008200	0.034449	0.238020
BnLOR5	*BnLOR43*	Segmental	0.045767	0.403696	0.113370
BnLOR6	*BnLOR28*	Segmental	0.033739	0.508172	0.066393
BnLOR6	*BnLOR32*	Segmental	0.011087	0.082728	0.134013
BnLOR7	*BnLOR37*	Segmental	0.019095	0.069477	0.274839
BnLOR9	*BnLOR12*	Segmental	0.061166	0.314890	0.194245

(Continued)

TABLE 1 Continued

Duplicated pair gene 1	Duplicated pair gene 2	Duplication type	Ka	Ks	Ka/Ks
BnLOR9	*BnLOR41*	Segmental	0.063458	0.316422	0.200548
BnLOR9	*BnLOR42*	Segmental	0.069552	0.316620	0.219671
BnLOR10	*BnLOR38*	Segmental	0.019352	0.091542	0.211400
BnLOR11	*BnLOR31*	Segmental	0.084275	0.233776	0.360493
BnLOR11	*BnLOR36*	Segmental	0.011344	0.019346	0.586397
BnLOR12	*BnLOR41*	Segmental	0.006527	0.032350	0.201747
BnLOR12	*BnLOR42*	Segmental	0.055164	0.321388	0.171642
BnLOR13	*BnLOR24*	Segmental	0.037097	0.332348	0.111621
BnLOR13	*BnLOR45*	Segmental	0.066963	0.280798	0.238474
BnLOR13	*BnLOR53*	Segmental	0.142818	0.431167	0.331236
BnLOR14	*BnLOR42*	Segmental	0.015318	0.033155	0.462012
BnLOR15	*BnLOR48*	Segmental	0.000000	0.000000	–
BnLOR16	*BnLOR46*	Segmental	0.043742	0.144445	0.302828
BnLOR20	*BnLOR49*	Segmental	0.064871	0.093163	0.696315
BnLOR21	*BnLOR24*	Segmental	0.057629	0.337448	0.170780
BnLOR21	*BnLOR45*	Segmental	0.006112	0.063614	0.096080
BnLOR21	*BnLOR52*	Segmental	0.061982	0.338534	0.183088
BnLOR23	*BnLOR54*	Segmental	0.019632	0.030384	0.646128
BnLOR24	*BnLOR45*	Segmental	0.056515	0.308642	0.183107
BnLOR24	*BnLOR53*	Segmental	0.133876	0.176046	0.760461
BnLOR25	*BnLOR55*	Segmental	0.008403	0.069173	0.121484
BnLOR29	*BnLOR35*	Segmental	0.017840	0.283483	0.062932
BnLOR31	*BnLOR36*	Segmental	0.092670	0.242993	0.381371
BnLOR33	*BnLOR34*	Tandem	0.017742	0.126616	0.140129
BnLOR39	*BnLOR43*	Segmental	0.041390	0.369240	0.112094
BnLOR42	*BnLOR41*	Segmental	0.059784	0.298567	0.200235
BnLOR45	*BnLOR52*	Segmental	0.059761	0.339080	0.176245

(123). Moreover, a relatively high number of low-temperature responsive elements, defense responsive elements and stress responsive elements were also detected, with 40, 39 and 37 CREs respectively. Generally speaking, *BnLOR* genes should be able to respond to various abiotic stresses and hormone treatments. However, we noticed that some genes contained very limited CREs such as *BnLOR17/14/31*, indicating that their expression might weakly or couldn't respond to abiotic stresses and hormone treatments.

To further understand the regulation network of *BnLORs*, the putative TFs regulating *BnLOR* family members were also predicted. As a result, 56 *BnLORs* were regulated by 347 TFs (Figure 6B; Table S7). Except for *BnLOR56* which couldn't be retrieved, the rest 55 *BnLOR* genes were regulated by 1 (*BnLOR38*) to 15 (*BnLOR49*) TFs. Among the 347 TFs, NAC had the largest amount (31), followed by C2H2 (30), Dof (25), ERF (25), AP2 (19), B3(18), bHLH (17) and MIKC_MADS (17). These eight types of TFs occupied more than 50% of the total numbers (Figure 6B; Table S7). Most of these TFs are related to abiotic stresses and hormone treatments. For instance, The NAC Transcription factor family is unique to plants and plays a crucial role in plant growth and development as well as biotic and abiotic stress resistance (Wu et al., 2020). Dof proteins are involved in various biological processes, including but not limited to endosperm development, plant defense, seed germination, gibberellin response and auxin response (Yu et al., 2019). AP2/ERF proteins play vital roles in regulating plant growth and development and various abiotic stress response (Wu et al., 2021). It has noticed that *BnLORs* were mainly regulated by these TFs, further supporting the prediction that *BnLORs* perform crucial functions in the regulation of abiotic stresses and hormone treatments.

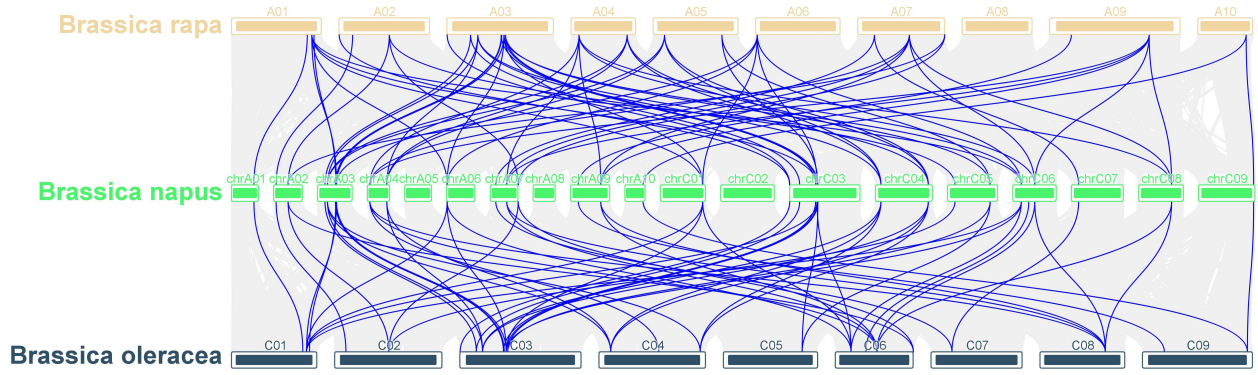


FIGURE 5
Collinearity analysis of *LOR* gene family in *B. napus*, *B. rapa* and *B. oleracea*. The grey lines in the background indicate the collinearity blocks within *B. napus*, *B. rapa* and *B. oleracea*, whereas the blue lines indicate the syntenic *LOR* gene pairs.

Orthologous clusters comparisons among multiple species

To deepen our understanding about the evolutionary history and the orthologous relationship among *LOR* genes, orthologous gene clusters in different species were compared and annotated. The quantity of orthologous proteins in each cluster exhibited variability, with the number ranging from 5 to 37 (Figure 7; Table S8). Twenty-nine orthologous proteins in *B. oleracea* and 28 orthologous proteins in *B. rapa* were predicted to have similar conserved domains to BnLOR proteins. Only 6 orthologous proteins were discovered in *O. sativa*, showing a large difference, this might be due to their early evolutionary differentiation. For the other six species (*Arabidopsis*, *B. oleracea*, *B. rapa*, *G. max*, *T. aestivum* and *Z. mays*), the number of orthologous proteins ranged from 8 (*Z. mays*) to 14 (*Arabidopsis*). Ten BnLORs proteins only had orthologous proteins in *B. oleracea* while another 10 BnLOR proteins only had orthologous proteins in *B. rapa*. The orthologous proteins of BnLOR5 could only be found in *G. max*. None of the BnLORs had orthologous proteins in every species. BnLOR49 had orthologous proteins in up to 6 species except *B. rapa*. Additionally, BnLOR4/29/44 proteins had orthologous proteins in 5 different kinds of species. Two orthologous clusters, comprising a total of 31 proteins, were found to be overlapping in each species (Figure 7; Table S8). Furthermore, 9 singleton proteins (BnLOR8/18/22/23/30/45/46/50/56) didn't have any orthologous proteins in any of the studied species.

Expression profiling of *BnLORs* in different tissues

The expression profiles of 56 *BnLOR* genes among 12 distinct tissues including blossomy pistil, flower, leaf, ovule, pericarp, pistil, root, silique, sepal, stamen, stem, wilting pistil were obtained by Sun et al. (2017) under the project ID of PRJNA394926. Results indicated that some members of the *BnLOR* gene family exhibited closely resembling expression patterns across diverse tissues of *B. napus* (Figure 8A; Table S9). For example, *BnLOR28/29/35* had high expression levels in almost every tissue while *BnLOR4/5/33/39/43* had relatively high expression levels in each tissue. However, the expression levels of *BnLOR1/16/18/22/46/54/56* were relatively low in every tissue. *BnLOR22* were found not expressed in any tissue. These 8 genes with low relative expression levels were all belonged to Clade H, suggesting that genes in this clade might be pseudogenes or act in response to biotic/abiotic stresses or hormone treatments. Certain genes in the *BnLOR* family displayed tissue-specific expression patterns. For instance, *BnLOR13/21/40/45* were mainly expressed in stamen. These four genes also had a small amount of expression in blossomy pistil, wilting pistil and flower, but they didn't express in other tissues, suggesting that these genes might have a potential association with reproductive growth. *BnLOR6* and *BnLO32* were also highly expressed in reproductive organs, but their distribution was different. Both of them were largely expressed in stamen and flower, followed by wilting pistil and blossomy pistil. *BnLOR10* and *BnLOR12* had high expression levels in ovule and moderate expression levels in other tissues. *BnLOR14* and *BnLOR42* demonstrated elevated expression levels in blossomy pistil with moderate expression levels in other tissues, indicating that these two genes might involve in plant reproductive growth, but might regulate reproductive growth through different pathways. *BnLOR19* was highly expressed in pericarp, suggesting that it might take part in the vegetative growth. The remaining genes were slightly expressed in different tissues.

Expression profiling of *BnLORs* under temperature, salinity, and ABA stress

To examine the initial changes in gene expression, we obtained the transcriptional profile of *B. napus* under temperature, salinity and ABA stress under the project ID of CRA001775 (Zhang et al., 2019). The stress treatments consisted of drought stress, salt stress (200 mM), ABA treatment (25 μM), and low temperature stress (4 °C). The differentially expressed genes (DEGs) with a false rate less than 0.5 and an absolute

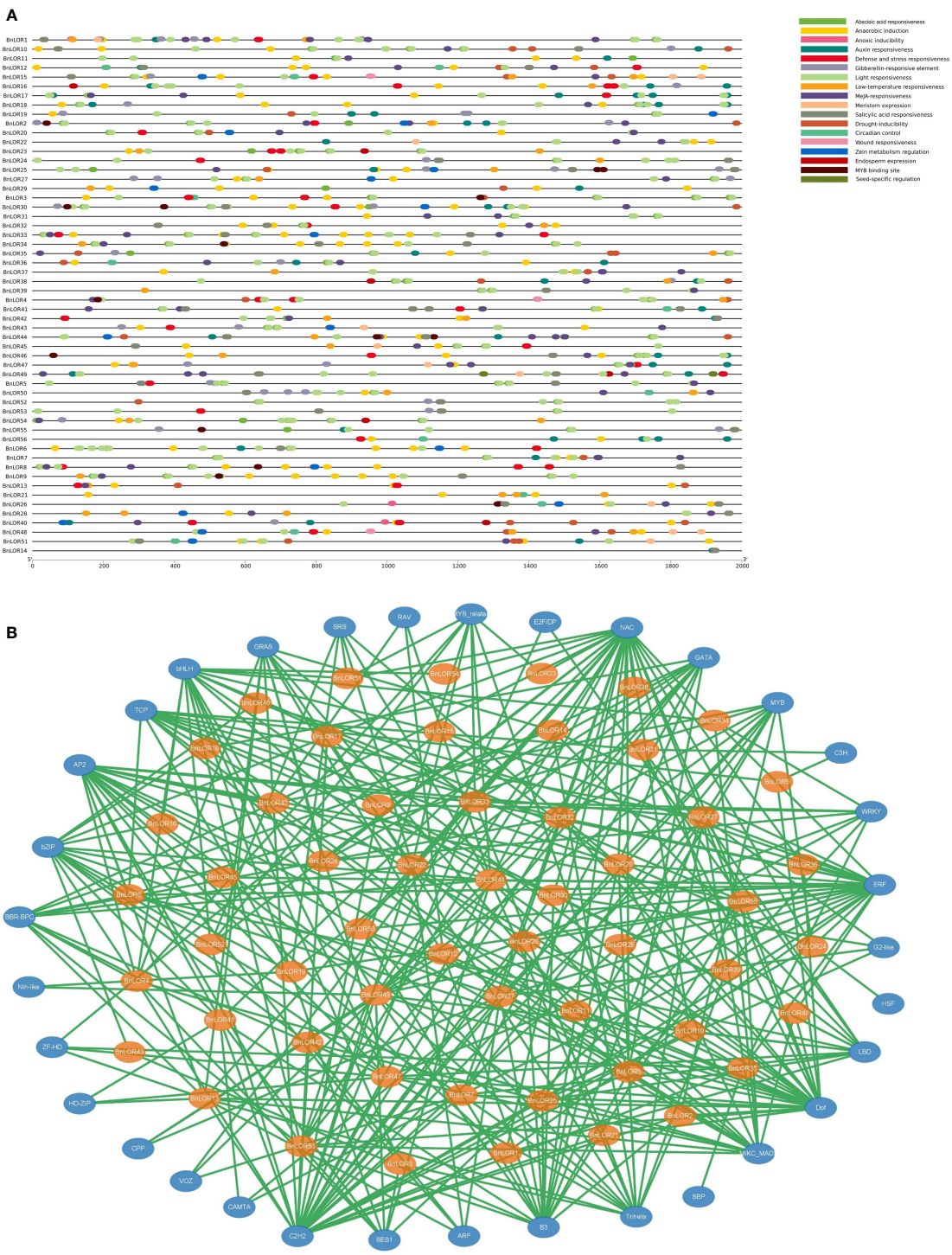


FIGURE 6
Analysis of cis-regulatory elements (CREs) in the *BnLORs* promoter regions and the predicted transcription factors (TFs) that regulate *BnLORs*. **(A)** CREs in the *BnLORs* promoter regions. Different CREs with functional similarity is denoted by similar colors. **(B)** Putative TFs that regulate *BnLORs*. The orange ovals indicate the *BnLORs*, and the yellow ovals indicate the predicted TFs. The green lines indicate the regulation relationship between TFs and *BnLOR* genes.

fold change over 2 were chosen and displayed in Figure 8B. In general, the relative expression levels of most *BnLOR* gene at 4 h was higher than that at 24 h under salt stress, ABA treatment and cold stress while and the situation was similar under dehydration stress, indicating that the response speed of mRNA was very fast in *BnLOR* gene family (Figure 8B; Table S10). The relative expression levels of *BnLOR5/29/33/35/39/42/43* genes showed a significant up-regulation while *BnLOR1/6/13/16/21/22/32/40/45/50/54* were significantly down-regulated under four different treatments. Among them, *BnLOR33* exhibited significant upregulation in response to cold stress,

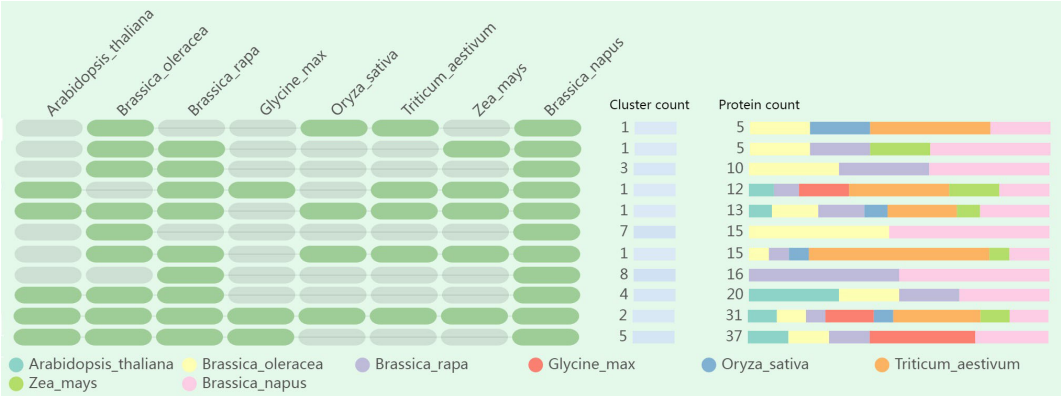


FIGURE 7
Comparative analysis of orthologous gene clusters among eight species (*Arabidopsis thaliana*, *Brassica oleracea*, *Brassica rapa*, *Glycine max*, *Oryza sativa*, *Triticum aestivum* and *Zea mays*). Green ovals on the left represent the presence of orthologous genes while grey ovals represent the absence of orthologous genes. Different colors bars on the right indicate the number and ratio of orthologous proteins in eight species.

indicating its potential significance in facilitating adaptation to such stress. For the remaining 19 *BnLOR* genes, their relative expression levels varied under different stress. Almost all of these 19 genes could increase their expression levels under cold stress, but the degree was different, and the relative expression levels at 4 h were larger than 24 h. Meanwhile, the expression of *BnLOR4/8/9/14/34/41* was partially up regulated at 4 h and decreased at 24 h under dehydration stress. Several other genes demonstrated slight up or down regulation in response to dehydration, salt stress, and ABA treatment.

To further verify the expression pattern under salinity and ABA stress, twelve *BnLOR* family members were chosen at random for qRT-PCR analysis. The relative expression levels of these genes had altered in varying degrees under salt stress or ABA treatment, indicating that these genes were capable of being induced by salinity and ABA stress (Figure 8C; Table S10). Under salt stress, the relative expression levels of *BnLOR4/29/39/44/51* increased dramatically at 4 h and went down a little bit at 24 h, but still showed an overall upward trend. The remaining seven genes increased at the initial stage of salt stress but decreased dramatically compared to control after 24 h, indicating an exceptionally swift response under salt stress. Under ABA treatment, the relative expression levels of *BnLOR4/39/44/51* exhibited an upward trend, with a larger increase observed at 4 h compared to 24 h. Conversely, the relative expression levels of *BnLOR3* and *BnLOR28* decreased at both 4 h and 24 h after treatment. The relative expression levels of the remaining six genes increased at the initial stage and then decreased over time, as depicted in Figure 8C and Table S10. Overall, the expression pattern trends of qRT-PCR and transcriptome file were relatively consistent, but there were some differences in the specific values.

Comparative modeling of BnLOR proteins

To deepen our understanding about the structures of BnLOR proteins, homology modeling was carried out to predict the 3D structures of BnLOR proteins. The predicted models were generated based on reported templates and optimized to maximize alignment coverage, percentage identity, global model quality estimate (GMQE), and overall quality factor. Models were considered reliable if the sequence identity between the template and the BnLOR protein was greater than 30%. Results showed that the 3D structures of 31 BnLOR proteins could be predicted by SWISS-MOLDEL (Figure 9; Table S11). The LOR protein family was discovered to exhibit structural similarities to the mammalian PLSCR (Phospholipid scramlase) protein family (Baig, 2018). X-ray crystallography technique was employed to determine the 3D structures of AtLOR1 and found that this protein comprised a 12-stranded β-barrel structure that encompassed a central C-terminal α-helix (Bateman et al., 2009). According to this structural model, sequence conservation was found to be mainly located within the secondary structures and β-hairpin turns between strands 2 to 3 and 4 to 5 (Bateman et al., 2009). All 31 proteins shared the same template 2q4m.1.A. The tertiary structures of the BnLOR proteins were relatively similar and complex with a few exceptions. For the 31 BnLOR proteins with predicted 3D structures, BnLOR15/48/50/53 were significantly different from the other 27 members, with no central C-terminal α-helix and less than 12 stranded β-barrels. Among these four genes, the expression pattern of *BnLOR15/48/53* couldn't be detected by RNA-seq, indicating that they were either low expressive genes or pseudogene. The relative expression level of *BnLOR50* could be induced by abiotic stress suggests that it may be involved in facilitating adaptation to such stress.

Discussion

With the availability of reference genomes for numerous plant species, many gene families have been identified, yet the *LOR* gene family remains relatively unknown. In this research, the *LOR* gene family in *B. napus* was identified by investigating its phylogenetic relationship, chromosomal locations, protein conserved motifs, gene structures, WGD events, synteny relationship, putative CREs in

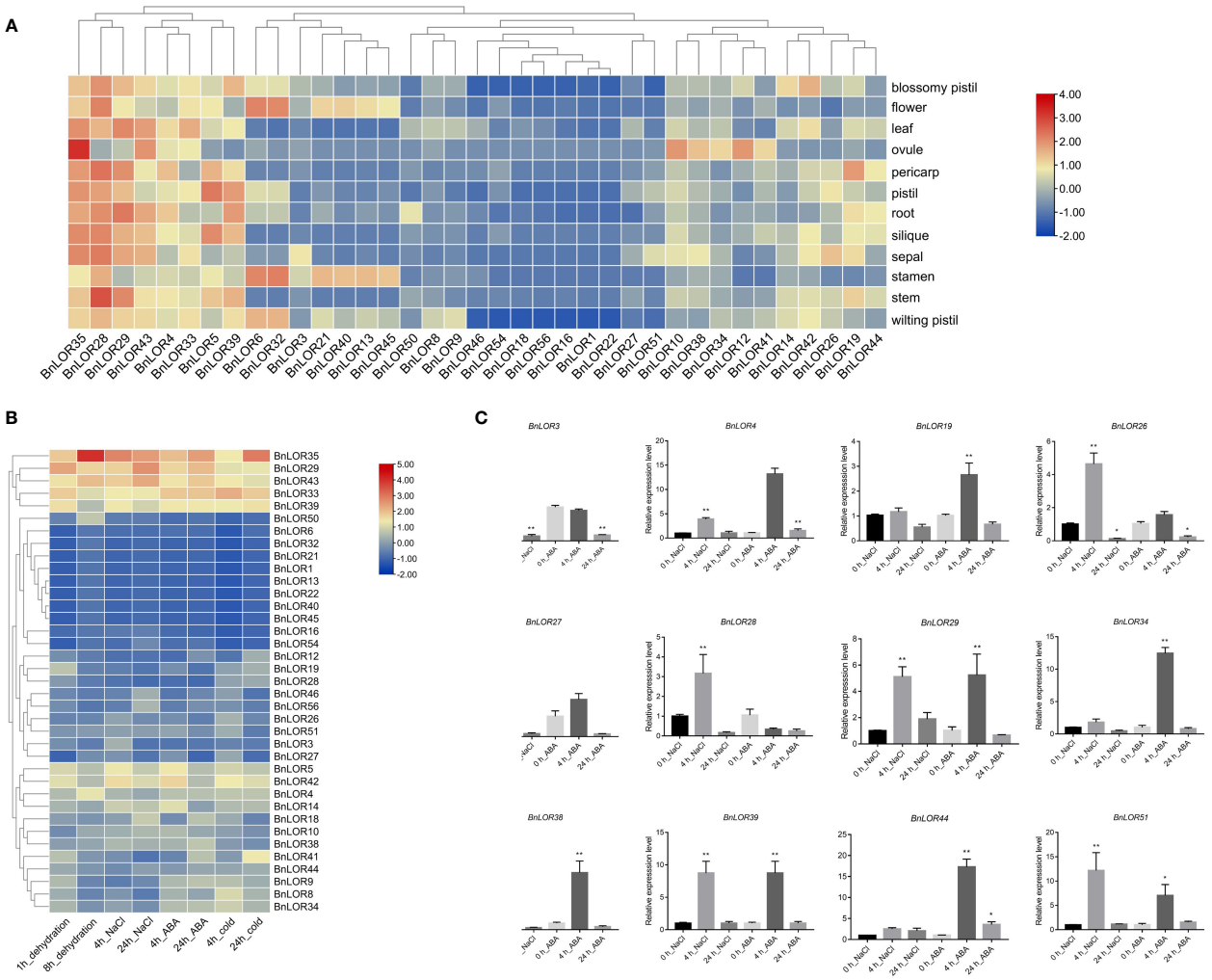


FIGURE 8
Expression profile of *BnLOR* genes under normal condition and abiotic stress. **(A)** Expression analysis of *BnLOR* genes in different tissues (blossomy pistil, flower, leaf, ovule, pericarp, pistil, root, silique, sepal, stamen, stem, wilting pistil) under normal condition. Data were transformed with a $\log_2$ (TPM+1) transformation. Red square means the gene is up-regulated while blue square means the gene is down-regulated. **(B)** The expression levels of differentially expressed genes in *B. napus* (ZS11) under dehydration, salt stress, ABA treatment and cold stress. Data were transformed with a $\log_2$ (TPM+1) transformation. Red color means the gene is up-regulated while blue color means the gene is down-regulated. **(C)** Relative expression levels of 12 randomly selected *BnLOR* genes in response to salt stress and ABA treatment in *B. napus* (ZD622). Mean ± SE of three replicates represent the significant difference with LSD test. * and ** indicate significance at the 5% and 1% level, respectively.

promoter regions, expression profiles, and responses to temperature, salinity and ABA stress. The *LOR* gene family, been discovered in plants, fungi, eubacteria, and some archaea, is distinguished by its conserved LOR domain. Our phylogenetic analysis revealed that *BnLORs*, *BoLORs*, *BrLORs*, and *AtLORs* could be divided into three subgroups and these three subgroups can be further divided into eight clades (Clade A to H) (Figure 1). Notably, the *BnLOR* family comprises a relatively large number of family members (56), which is approximately three times that of *Arabidopsis* (20), *Solanum lycopersicum* (17), and *Solanum tuberosum* (16). Basically, plants with larger genome sizes tend to possess a greater number of gene family members (Wang et al., 2020). *B. napus* was derived from the spontaneous hybridization between *B. rapa* and *B. oleracea* followed by allopolyploidization (Chalhoub et al., 2014). It has not only experienced genome wide triplication events specific to *Brassica* species, but also experienced allopolyploidization, resulting in a larger genome size and larger gene family members. Additionally, due to homoeologous recombination and chromosomal structural variation between the A and C genomes of *B. napus* during the domestication process, a small number of genes were lost or gained (Chalhoub et al., 2014). Consequently, the number of *BnLORs* is not simply the sum of *BoLORs* and *BrLORs*. Previous studies found that *AtLURP1* and *AtLOR1* were both located in Clade A and demonstrated significant involvement in the resistance to *Hpa*, suggesting that genes in Clade A (*BnLOR6/32/28/35/29/27/50/26/51/22*) might be associated with plant defense.

During the process of evolution, multiple gene families underwent differential adaptation (Xu et al., 2012), with introns being a crucial component in the acquisition of new gene functions (Roy et al., 2003). Among the 56 *BnLOR* members, 27 contained two introns, 26 had one intron, and 3 had no introns (Figure 2). It is commonly believed that the presence of introns is more prevalent

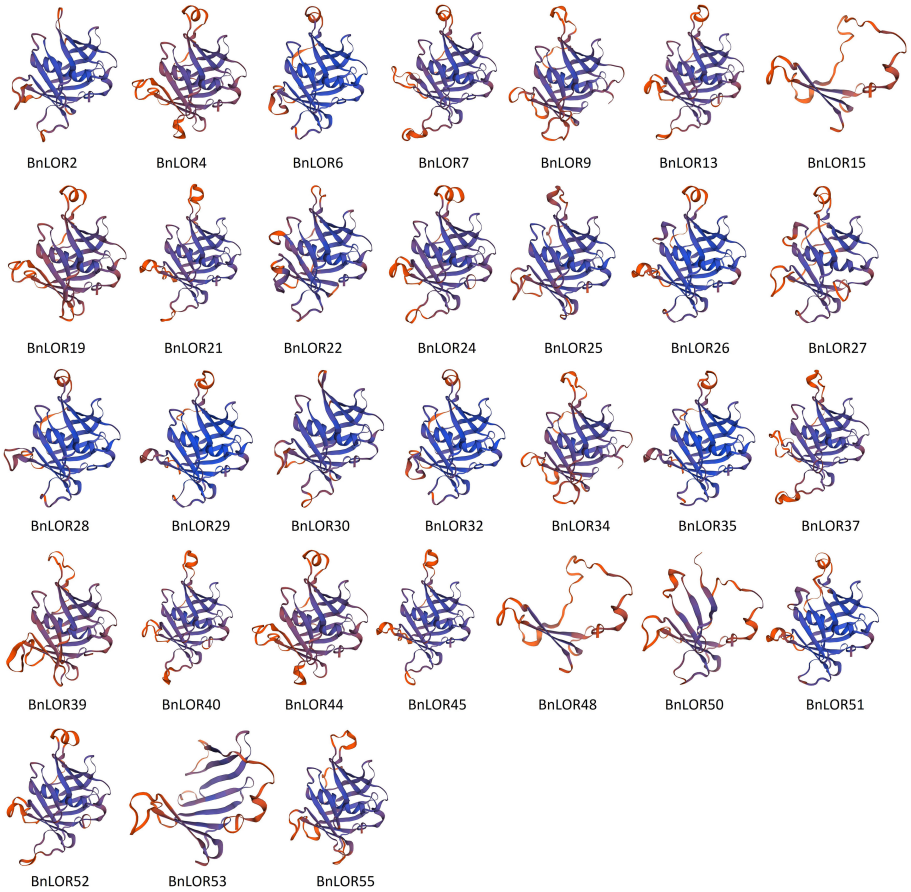


FIGURE 9
The homology modelling of the 3D structures of BnLOR proteins.

during the earlier stages of gene expansion, and gradually diminishing during the evolutionary process (Roy and Gilbert, 2006; Roy and Penny, 2007; Rose, 2019), as they play a crucial role in activating genes by providing compact gene structures with fewer introns, thereby facilitating timely responses to various stresses (Chung et al., 2006; Jeffares et al., 2008). Consistent with these findings, the majority of the *BnLOR* genes could be rapidly and significantly induced under salt stress and ABA treatment (Figures 8B, C, Table S10), indicating their important roles towards abiotic stresses and hormone treatments. With the help of MEME online tools, up to 15 putative conserved motifs were predicted within the BnLOR proteins (Figure 2). The majority of these proteins contained 6 to 9 conserved motifs, with motifs 1 to 6 being highly conservative and could be found in most BnLOR proteins (Figure 2). The other motifs had an obvious preference in certain subgroups or clades. The rest motifs demonstrated distinct preferences within specific subgroups or clades. For instance, motif 10 only existed in Clade G and H, while motif 11 and 13 were merely presented in Clade C. The functions of these conserved motifs in the BnLOR proteins were not well understood yet, but they might play a role in the interaction between LOR proteins and their substrates (Fang et al., 2021). Motifs 1 to 6 may be integral in determining essential molecular functions among *BnLOR* genes, while the preference for certain motifs may contribute to the structural foundation for the diversity in gene functions. Similarities in intron numbers and motif arrangements were observed within the same subgroups or clades, further supporting the phylogenetic relationship of the *BnLOR* gene family.

The syntenic relationship of *BnLORs*, *BrLORs*, *BoLORs*, and *AtLORs* family members were investigated in this research. A total of 78 collinear gene pairs between *B. napus* and *B. rapa* and 70 collinear gene pairs between *B. napus* and *B. oleracea* were discovered (Figure 5; Table S5). Chromosomes A3 and C3 showed the highest number of collinear gene pairs. We also identified 14 pairs of orthologous genes between *B. napus* and *Arabidopsis*, 28 pairs of orthologous genes between *B. napus* and *B. rapa*, and 29 pairs of orthologous genes between *B. napus* and *B. oleracea* (Table S8). Notably, one *AtLOR* gene showed two syntenic orthologous gene pairs (*AT1G80120-BnLOR4/44*), indicating that these two genes originated after the divergence of *Arabidopsis*. The remaining 12 orthologous gene pairs were one-to-one syntenic orthologs. The high conservation of collinearity among *LORs* in *B. napus*, *B. rapa*, and *B. oleracea* suggests that these genes have been evolutionarily conserved. Gene duplication is a crucial impetus for expanding gene families and evolving new functions, such as stress adaptation and disease resistance (Vision et al., 2000; Panchy et al., 2016). Previous studies have suggested that tandem repeats and segmental duplications are the primary patterns of gene family expansion, with segmental duplications occurring more frequently

due to the retention of duplicated chromosomal blocks in polyploidy plants followed by chromosome rearrangements (Yu et al., 2005; Kong et al., 2010). Our analysis showed that 56 *BnLOR* genes underwent 37 segmental duplications and five tandem repeat events under purifying selection, suggesting that *BnLOR* gene family had undergone gene expression during the evolutionary process.

CREs has been reported to play crucial roles in regulating the transcription of genes involved in environmental stress responses (Yamaguchi-Shinozaki and Shinozaki, 2005; Chen et al., 2016). Knoth et al. (2007) identified a region in the *AtLURP1* promoter that contained a key pathogen response element W box (a binding site for WRKY TFs). After binding with W box, *AtWRKY70* could regulate the expression of *AtLURP1* (Knoth et al., 2007). In this study, we analyzed the CREs presented in the promoter regions of *BnLOR* genes and classified them into three main categories including TF binding sites, hormone responsive elements, and stress responsive elements. CREs analysis revealed that *BnLORs* were mainly involved in light response, hormone response, and stress response processes. Specifically, we identified 123 anaerobic induction related CREs, 40 low temperature responsive elements, 39 defense responsive elements, and 37 stress responsive elements among the 56 *BnLOR* genes. These elements might contribute to the resistance of *B. napus* to various abiotic stresses, such as cold, heat, drought, and salt stress, and could explain the differential expression patterns and stress responses of duplicated genes. The presence of a wide range of CREs distributed throughout the promoter regions of *BnLOR* genes suggested that these genes might have complex expression profiles and played important roles in regulating stress resistance in rapeseed. These CREs provided valuable genetic information for breeding rapeseed varieties with improved stress resistance.

Transcription regulatory networks play a crucial role in the regulation of gene expression in plants. Among these networks, NAC, WRKY, MYB, and GATA transcription factors have been identified as important players in abiotic stress responses. NAC transcription factors are known to be involved in various plant developmental processes as well as responses to abiotic stress. They have been reported to regulate the expression of stress-responsive genes and play a role in enhancing plant tolerance to abiotic stresses such as drought, salinity, and temperature extremes (Nuruzzaman et al., 2013). WRKY transcription factors are another important group of regulators that are involved in plant responses to abiotic stress. In *B. napus*, WRKY transcription factors have been shown to play a role in response to abiotic stresses such as drought, cold, and salt stress (Jiang et al., 2016). MYB and GATA transcription factors have been implicated in the regulation of genes involved in abiotic stress responses, including drought and salt stress in *B. napus* (Hajiebrahimi et al., 2017; Zhu et al., 2020). These transcription factors have been implicated in the regulation of the majority of the *BnLOR* genes., showing consistency with the predicted function of *BnLORs* on abiotic stress resistance. However, the regulatory mechanisms involving NAC, WRKY, MYB, and GATA transcription factors in modulating *BnLOR* expression and its role in abiotic stress responses in *B. napus* are still being elucidated and represent a promising area of research.

The expression profile of *BnLORs* exhibited gene specificity, whereby *BnLOR35/28/29/43/4/33/5/39/6/32* exhibited relatively high expression levels across various tissues, suggesting their indispensable functions. Certain *BnLOR* genes may perform specialized functions in specific tissues, thereby potentially participating in the life cycle of *B. napus*. Conversely, other *BnLOR* genes displayed negligible or non-existent expression levels. Moreover, the expression levels of the same gene differed across diverse tissues, thus indicating tissue-specificity. Notably, the majority of the *BnLOR* members displayed low expression levels in 12 tissues under normal conditions, whereas their relative expression levels were significantly induced by abiotic stress.

Previous studies in *Arabidopsis* have reported the participation of *AtLURP1* and *AtLOR1* in biotic stress (Knoth and Eulgem, 2008; Coker et al., 2015; Lee et al., 2017; Baig, 2018). Nevertheless, it remains uncertain whether the *LOR* family in plants responds to abiotic stress or not. In this study, we investigated the transcriptional responses of 56 *B. napus LOR* genes under dehydration, salt stress, ABA treatment, and cold stress. Our findings revealed that *BnLOR5/29/33/35/39/42/43* exhibited significantly up-regulated expression levels, whereas *BnLOR1/6/13/16/21/22/32/40/45/50/54* displayed significant down-regulation under diverse stress conditions. These results implied that these genes may have pivotal roles in response to dehydration, salt stress, ABA treatment, and cold stress. Additionally, qRT-PCR was employed to validate the expression pattern of *BnLORs* under salinity and ABA stress. Results showed that the expression trends of qRT-PCR and transcriptome profile were relatively consistent, although differed in specific values. Therefore, these genes might serve as promising candidates for genetic engineering to enhance plant fitness in response to salt stress and ABA treatment.

To gain a better understanding of the interplay between BnLOR proteins, we generated 3D structures via homology modeling. Interestingly, all 31 predicted proteins shared the same template, 2q4m.1.A, which was derived from the ensemble refinement of the crystal structure of *At5g01750* from the DUF567 family in *Arabidopsis* (Table S11). Notably, the DUF567 family solely comprises uncharacterized proteins that are found in plants, fungi, eubacteria, and some archaea. In plants, DUF567 is extensively expanded, with *Arabidopsis* harboring 21 family members. Gene ontology analysis revealed that *At5g01750* is involved in protein domain-specific binding in the plasma membrane. Wang et al. (2022) reported that NBS-LRR proteins in *Lagenaria siceraria* can be classified into four groups, indicating that NBS-LRR proteins form a complex protein network to recognize multiple effectors. Similar results were also observed in Yer et al. (2018). Nonetheless, our study demonstrated that the tertiary structures of all predicted BnLOR proteins were remarkably consistent, sharing the same template. This finding implied that *BnLORs* might be functionally consistent, which was consistent with our observation that most *BnLORs* genes could respond to abiotic stresses and hormone treatments.

Conclusion

This study conducted a genome-wide survey of *B. napus LOR* gene family and analyzed their phylogenetic relationships, chromosomal distributions, protein conserved motifs, gene structures, WGD events, synteny relationship, putative CREs in promoter regions, expression profile and response to temperature, salinity and ABA stress through bioinformatics analysis and qRT-PCR. Results showed that there was a high degree of homology within *BnLOR* members. 56 *BnLOR* genes could be divided into 3 subgroups (8 clades) and have undergone 37 segmental duplication and 5 tandem repeats events with purifying selection. The *LORs* in *B. napus* had a high level of collinearity with that of *B. rapa* and *B. oleracea*, indicating they were quite conservative during the evolutionary process. The analysis of conserved domain, motif structures and WGD events of *BnLORs* were consistent with the phylogenetic analysis. *BnLOR* family genes had tissue specific expression patterns and most of them could be induced by salt stress and ABA treatment, suggesting their potential function on stress and hormone responsiveness. These results provided a reference for comprehensive understanding and utilization of *BnLOR* genes in *B. napus* in the future.

Data availability statement

The datasets presented in this study can be found in online repositories. The names of the repository/repositories and accession number(s) can be found in the article/Supplementary Material.

Author contributions

SY and YD analyzed the data. JC and QH grew the plants and conducted the qRT-PCR analysis. JWang drew the figures, SY and ZU edited the manuscript. GC, JWei, JC, and QH contributed regents/materials/analysis tool. SY and JWang conceived and designed the study, obtained funds, and critically revised the manuscript. All authors contributed to the article and approved the submitted version.

Funding

This research was supported by the National Natural Science Foundation of China (32200251) and the Science and Technology Department of Zhejiang Province (2021C02064-2).

Conflict of interest

Author JWei was employed by the Mizuda Group Co., Ltd.

The remaining authors declare that the research was conducted in the absence of any commercial or financial relationships that could be construed as a potential conflict of interest.

Publisher's note

All claims expressed in this article are solely those of the authors and do not necessarily represent those of their affiliated organizations, or those of the publisher, the editors and the reviewers. Any product that may be evaluated in this article, or claim that may be made by its manufacturer, is not guaranteed or endorsed by the publisher.

Supplementary material

The Supplementary Material for this article can be found online at: https://www.frontiersin.org/articles/10.3389/fpls.2023.1197781/full#supplementary-material

SUPPLEMENTARY FIGURE 1
The motif logos of 15 motifs among BnLOR family proteins.

References

Baig, A. (2018). Role of arabidopsis *LOR1* (*LURP*-one related one) in basal defense against *Hyaloperonospora arabidopsidis*. *Physiol. Mol. Plant Pathol.* 103, 71–77. doi: 10.1016/j.pmpp.2018.05.003

Bailey, T. L., Boden, M., Buske, F. A., Frith, M., Grant, C. E., Clementi, L., et al. (2009). MEME SUITE: tools for motif discovery and searching. *Nucleic Acids Res.* 37, 202–208. doi: 10.1093/nar/gkp335

Bateman, A., Finn, R. D., Sims, P. J., Wiedmer, T., Biegert, A., and Soding, J. (2009). Phospholipid scramblases and tubby-like proteins belong to a new superfamily of membrane tethered transcription factors. *Bioinformatics* 25, 159–162. doi: 10.1093/bioinformatics/btn595

Bricchi, I., Bertea, C. M., Occhipinti, A., Paponov, I. A., and Maffei, M. E. (2012). Dynamics of membrane potential variation and gene expression induced by spodoptera littoralis, myzus persicae, and *Pseudomonas syringae* in *Arabidopsis*. *PloS One* 7, e46673. doi: 10.1371/journal.pone.0046673

Caillaud, M. C., Asai, S., Rallapalli, G., Piquerez, S., Fabro, G., and Jones, J. D. G. (2016). A downy mildew effector attenuates salicylic acid-triggered immunity in *Arabidopsis* by interacting with the host mediator complex. *PloS Biol.* 14, e1002408. doi: 10.1371/journal.pbio.1002408

Chalhoub, B., Denoeud, F., Liu, S., Parkin, I. A. P., Tang, H., Wang, X., et al. (2014). Early allopolyploid evolution in the post-neolithic *Brassica napus* oilseed genome. *Science* 345, 950–953. doi: 10.1126/science.1253435

Chen, C., Chen, H., Zhang, Y., Thomas, H. R., Frank, M. H., He, Y., et al. (2020). TBtools: an integrative toolkit developed for interactive analyses of big biological data. *Mol. Plant* 13, 1194–1202. doi: 10.1016/j.molp.2020.06.009

Chen, H. Y., Hsieh, E. J., Cheng, M. C., Chen, C. Y., Hwang, S. Y., and Lin, T. P. (2016). ORA47 (octadecanoid-responsive AP2/ERF-domain transcription factor 47) regulates jasmonic acid and abscisic acid biosynthesis and signaling through binding to a novel cis-element. *New Phytol.* 211, 599–613. doi: 10.1111/nph.13914

Chung, B. Y., Simons, C., Firth, A. E., Brown, C. M., and Hellens, R. P. (2006). Effect of 5'UTR introns on gene expression in *Arabidopsis thaliana*. *BMC Genomics* 7, 120. doi: 10.1186/1471-2164-7-120

Coker, T. L. R., Cevik, V., Beynon, J. L., and Gifford, M. L. (2015). Spatial dissection of the *Arabidopsis thaliana* transcriptional response to downy mildew using fluorescence activated cell sorting. *Front. Plant Sci.* 6. doi: 10.3389/fpls.2015.00527

El-Gebali, S., Mistry, J., Bateman, A., Eddy, S. R., Luciani, A., Potter, S. C., et al. (2019). The pfam protein families database in 2019. *Nucleic Acids Res.* 47, 427–432. doi: 10.1093/nar/gky995

Fang, Y., Cao, D., Yang, H., Guo, W., Ouyang, W., Chen, H., et al. (2021). Genome-wide identification and characterization of soybean *GmLOR* gene family and expression analysis in response to abiotic stresses. *Int. J. Mol. Sci.* 22, 12515. doi: 10.3390/ijms222212515

Gu, Z., Cavalcanti, A., Chen, F. C., Bouman, P., and Li, W. H. (2002). Extent of gene duplication in the genomes of *Drosophila*, nematode, and yeast. *Mol. Biol. Evol.* 19, 256–262. doi: 10.1093/oxfordjournals.molbev.a004079

Gupta, A., and Senthil-Kumar, M. (2017). Transcriptome changes in *Arabidopsis thaliana* infected with *Pseudomonas syringae* during drought recovery. *Sci. Rep.* 7, 9124. doi: 10.1038/s41598-017-09135-y

Hajiebrahimi, A., Owji, H., and Hemmati, S. (2017). Genome-wide identification, functional prediction, and evolutionary analysis of the R2R3-MYB superfamily in *Brassica napus*. *Genome* 60 (10), 797–814. doi: 10.1139/gen-2017-0059

Jeffares, D. C., Penkett, C. J., and Bahler, J. (2008). Rapidly regulated genes are intron poor. *Trends Genet.* 24, 375–378. doi: 10.1016/j.tig.2008.05.006

Jiang, J., Ma, S., Ye, N., Jiang, M., Gao, J., and Zhang, J. (2016). WRKY transcription factors in plant responses to stresses. *J. Integr. Plant Biol.* 59 (2), 86. doi: 10.1111/jipb.12513

Jin, J., Tian, F., Yang, D. C., Meng, Y. Q., Kong, L., Luo, J., et al. (2017). PlantTFDB 4.0: toward a central hub for transcription factors and regulatory interactions in plants. *Nucleic Acids Res.* 45, 1040–1045. doi: 10.1093/nar/gkw982

Karnes, K., and Shaikh, K. (2021). Characterization and structure-function analysis of autophagy factor ATG7 from *Trypanosoma brucei* (TbATG7) as a potential drug target. *FASEB J.* 35, 03861. doi: 10.1096/fasebj.2021.35.S1.03861

Knoth, C., and Eulgem, T. (2008). The oomycete response gene *LURP1* is required for defense against *Hyaloperonospora parasitica* in *Arabidopsis thaliana*. *Plant J.* 55, 53–64. doi: 10.1111/j.1365-313X.2008.03486.x

Knoth, C., Ringler, J., Dangl, J. L., and Eulgem, T. (2007). *Arabidopsis* WRKY70 is required for full *RPP4*-mediated disease resistance and basal defense against *Hyaloperonospora parasitica*. *Mol. Plant Microbe Interact.* 20, 120–128. doi: 10.1094/MPMI-20-2-0120

Kong, H., Landherr, L. L., Frohlich, M. W., Leebens-Mack, J., and Depamphilis, C. W. (2010). Patterns of gene duplication in the plant *SKP1* gene family in angiosperms: evidence for multiple mechanisms of rapid gene birth. *Plant J.* 50, 873–885. doi: 10.1111/j.1365-313X.2007.03097.x

Krzywinski, M., Schein, J., Birol, I., Connors, J., Gascoyne, R., Horsman, D., et al. (2009). Circos: an information aesthetic for comparative genomics. *Genome Res.* 19, 1639–1645. doi: 10.1101/gr.092759.109

Larkin, M. A., Blackshields, G., Brown, N., Chenna, R., McGettigan, P. A., McWilliam, H., et al. (2007). Clustal W and clustal X version 2.0. *Bioinformatics* 23, 2947–2948. doi: 10.1093/bioinformatics/btm404

Lee, M. H., Jeon, H. S., Kim, H. G., and Park, O. K. (2017). An *Arabidopsis* NAC transcription factor NAC4 promotes pathogen-induced cell death under negative regulation by microRNA164. *New Phytol.* 214, 343–360. doi: 10.1111/nph.14371

Livak, K. J., and Schmittgen, T. D. (2001). Analysis of relative gene expression data using real-time quantitative PCR and the $2^{-\Delta\Delta CT}$ method. *Methods* 25, 402–408. doi: 10.1006/meth.2001.1262

Ma, J., Islam, F., Ayyaz, A., Fang, R., Hannan, F., Farooq, M. A., et al. (2022). Wood vinegar induces salinity tolerance by alleviating oxidative damages and protecting photosystem II in rapeseed cultivars. *Ind. Crop Prod.* 189, 115763. doi: 10.1016/j.indcrop.2022.115763

Nuruzzaman, M., Sharoni, A. M., and Kikuchi, S. (2013). Roles of NAC transcription factors in the regulation of biotic and abiotic stress responses in plants. *Front. Microbiol.* 4. doi: 10.3389/fmicb.2013.00248

Panchy, N., Lehti-Shiu, M., and Shiu, S. H. (2016). Evolution of gene duplication in plants. *Plant Physiol.* 171, 2294–2316. doi: 10.1104/pp.16.00523

Potter, S. C., Luciani, A., Eddy, S. R., Park, Y., Lopez, R., and Finn, R. D. (2018). HMMER web server: 2018 update. *Nucleic Acids Res.* 46, 200–204. doi: 10.1093/nar/gky448

Raza, A., Tabassum, J., Fakhar, A. Z., Sharif, R., Chen, H., Zhang, C., et al. (2022). Smart reprograming of plants against salinity stress using modern biotechnological tools. *Crit. Rev. Biotechnol.* 1–28. doi: 10.1080/07388551.2022.2093695

Raza, A., Charagh, S., Najafi-Kakavand, S., Abbas, S., Shoaib, Y., Anwar, S., et al. (2023). Role of phytohormones in regulating cold stress tolerance: physiological and molecular approaches for developing cold-smart crop plants. *Plant Stress.* 8, 100152. doi: 10.1016/j.stress.2023.100152

Rose, A. B. (2019). Introns as gene regulators: a brick on the accelerator. *Front. Genet.* 9. doi: 10.3389/fgene.2018.00672

Roy, S. W., Fedorov, A., and Gilbert, W. (2003). Large-Scale comparison of intron positions in mammalian genes shows intron loss but no gain. *P. Natl. Acad. Sci.* 100 (12), 7158–7162. doi: 10.1073/pnas.1232297100

Roy, S. W., and Gilbert, W. (2006). The evolution of spliceosomal introns: patterns, puzzles and progress. *Nat. Rev. Genet.* 7, 211–221. doi: 10.1038/nrg1807

Roy, S. W., and Penny, D. (2007). A very high fraction of unique intron positions in the intron-rich diatom *Thalassiosira pseudonana* indicates widespread intron gain. *Mol. Biol. Evol.* 24, 1447–1457. doi: 10.1093/molbev/msm048

Sheteiwy, M. S., Ulhassan, Z., Qi, W., Lu, H., AbdElgawad, H., Minkina, T., et al. (2022). Association of jasmonic acid priming with multiple defense mechanisms in wheat plants under high salt stress. *Front. Plant Sci.* 13. doi: 10.3389/fpls.2022.886862

Shu, K., Qi, Y., Chen, F., Meng, Y., Luo, X., Shuai, H., et al. (2018). Salt stress represses soybean seed germination by negatively regulating GA biosynthesis while positively mediating ABA biosynthesis. *Front. Plant Sci.* 9. doi: 10.3389/fpls.2017.01372

Song, C., Zhang, D., Zheng, L., Shen, Y., Zuo, X., Mai, J., et al. (2020). Genome-wide identification and expression profiling of the YUCCA gene family in *Malus domestica*. *Sci. Rep.* 10, 10866. doi: 10.1038/s41598-020-66483-y

Sun, F., Fan, G., Hu, Q., Zhou, Y., Guan, M., Tong, C., et al. (2017). The high-quality genome of *Brassica napus* cultivar 'ZS11' reveals the introgression history in semi-winter morphotype. *Plant J.* 92, 452–468. doi: 10.1111/tpj.13669

Suzuki, N., Rivero, R. M., Shulaev, V., Blumwald, E., and Mittler, R. (2014). Abiotic and biotic stress combinations. *New Phytol.* 203, 32–43. doi: 10.1111/nph.12797

Tamura, K., Stecher, G., Peterson, D., Filipski, A., and Kumar, S. (2013). MEGA6: molecular evolutionary genetics analysis version 6.0. *Mol. Biol. Evol.* 30, 2725–2729. doi: 10.1093/molbev/mst197

Vision, T. J., Brown, D. G., and Tanksley, S. D. (2000). The origins of genomic duplications in *Arabidopsis*. *Science* 290, 2114–2117. doi: 10.1126/science.290.5499.2114

Waadt, R., Seller, C. A., Hsu, P. K., Takahashi, Y., Munemasa, S., and Schroeder, J. I. (2022). Plant hormone regulation of abiotic stress responses. *Nat. Rev. Mol. Cell Biol.* 23, 680–694. doi: 10.1038/s41580-022-00479-6

Wang, L., Ding, X., Gao, Y., and Yang, S. (2020). Genome-wide identification and characterization of *GRAS* genes in soybean (*Glycine max*). *BMC Plant Biol.* 20, 415. doi: 10.1186/s12870-020-02636-5

Wang, L., Guo, K., Li, Y., Tu, Y., Hu, H., Wang, B., et al. (2010a). Expression profiling and integrative analysis of the *CESA/CSL* superfamily in rice. *BMC Plant Biol.* 10, 282. doi: 10.1186/1471-2229-10-282

Wang, D., Zhang, Y., Zhang, Z., Zhu, J., and Yu, J. (2010b). KaKs_Calculator 2.0: a toolkit incorporating gamma-series methods and sliding window strategies. *Genom. Proteom. Bioinf.* 8, 77–80. doi: 10.1016/S1672-0229(10)60008-3

Wang, Y., Tang, H., DeBarry, J. D., Tan, X., Li, J., Wang, X., et al. (2012). *MCScanX*: a toolkit for detection and evolutionary analysis of gene synteny and collinearity. *Nucleic Acids Res.* 40, e49. doi: 10.1093/nar/gkr1293

Wang, J., Yang, C., Wu, X., Wang, Y., Wang, B., Wu, X., et al. (2022). Genome-wide characterization of *NBS-LRR* family genes and expression analysis under powdery mildew stress in *Lagenaria siceraria*. *Physiol. Mol. Plant Pathol.* 118, 101798. doi: 10.1016/j.pmpp.2022.101798

Wang, J., Wang, Y., Wu, X., Wang, B., Lu, Z., Zhong, L., et al. (2023). Insight into the bZIP gene family in *Lagenaria siceraria*: genome and transcriptome analysis to understand gene diversification in cucurbitaceae and the roles of *LsbZIP* gene expression and function under cold stress. *Front. Plant Sci.* 13. doi: 10.3389/fpls.2022.1128007

Wu, X., Lai, Y., Lv, L., Ji, M., Han, K., Yan, D., et al. (2020). Fasciclin-like arabinogalactan gene family in *Nicotiana benthamiana*: genome-wide identification, classification and expression in response to pathogens. *BioMed. Central.* 20, 305. doi: 10.1186/s12870-020-02501-5

Wu, X., Lai, Y., Rao, S., Lv, L., Ji, M., Han, K., et al. (2021). Genome-wide identification reveals that *Nicotiana benthamiana* hypersensitive response (HR)-like lesion inducing protein 4 (NbHRLI4) mediates cell death and salicylic acid-dependent defense responses to turnip mosaic virus. *Front. Plant Sci.* 12. doi: 10.3389/fpls.2021.627315

Xu, G., Guo, C., Shan, H., and Kong, H. (2012). Divergence of duplicate genes in exon-intron structure. *Proc. Natl. Acad. Sci. U.S.A.* 109, 1187–1192. doi: 10.1073/pnas.1109047109

Yamaguchi-Shinozaki, K., and Shinozaki, K. (2005). Organization of cis-acting regulatory elements in osmotic- and cold-stress-responsive promoters. *Trends Plant Sci.* 10, 88–94. doi: 10.1016/j.tplants.2004.12.012

Yang, S., Chen, S., Geng, X. X., Yan, G., Li, Z. Y., Meng, J. L., et al. (2016). The first genetic map of a synthesised allohexaploid *Brassica* with a, b and c genomes based on simple sequence repeat markers. *Theor. Appl. Genet.* 129, 689–701. doi: 10.1007/s00122-015-2657-z

Yang, S., Chen, S., Zhang, K., Li, L., Yin, Y., and Gill, R. A. (2018). A high-density genetic map of an allohexaploid *Brassica* doubled haploid population reveals quantitative trait loci for pollen viability and fertility. *Front. Plant Sci.* 9, 1161. doi: 10.3389/fpls.2018.01161

Yang, S., Gill, R. A., Zaman, Q. U., Ulhassan, Z., and Zhou, W. (2020). Insights on SNP types, detection methods and their utilization in *Brassica* species: recent progress and future perspectives. *J. Biotechnol.* 324, 11–20. doi: 10.1016/j.jbiotec.2020.09.018

Yang, S., Zhang, K., Lu, C., Chen, G., Huang, Q., Ulhassan, Z., et al. (2022). Genetic variation and stability analysis of an artificially synthesized allohexaploid *Brassica* for breeding innovations. *Agronomy* 12, 2843. doi: 10.3390/agronomy12112843

Yang, S., Zhang, X., Yue, J. X., Tian, D., and Chen, J. Q. (2008). Recent duplications dominate NBS-encoding gene expansion in two woody species. *Mol. Genet. Genom.* 280, 187–198. doi: 10.1007/s00438-008-0355-0

Yer, E. N., Baloglu, M. C., and Ayan, S. (2018). Identification and expression profiling of all hsp family member genes under salinity stress in different poplar clones. *Gene* 678, 324–336. doi: 10.1016/j.gene.2018.08.049

Yin, Y., Morgunova, E., Jolma, A., Kaasinen, E., Sahu, B., Khund-Sayeed, S., et al. (2017). Impact of cytosine methylation on DNA binding specificities of human transcription factors. *Science* 356 (6337), eaaj2239. doi: 10.1126/science.aaj223

Yu, Y. H., Bian, L., Wan, Y. T., Jiao, Z. L., Yu, K. K., Zhang, G. H., et al. (2019). Grape (*Vitis vinifera*) VvDOF3 functions as a transcription activator and enhances powdery mildew resistance. *Plant Physiol. Biochem.* 143, 183–189. doi: 10.1016/j.plaphy.2019.09.010

Yu, J., Wang, J., Lin, W., Li, S., Li, H., Zhou, J., et al. (2005). The genomes of *Oryza sativa*: a history of duplications. *PloS Biol.* 3, e38. doi: 10.1371/journal.pbio.0030038

Zhang, Y., Ali, U., Zhang, G., Yu, L., Fang, S., Iqbal, S., et al. (2019). Transcriptome analysis reveals genes commonly responding to multiple abiotic stresses in rapeseed. *Mol. Breed.* 39, 158. doi: 10.1007/s11032-019-1052-x

Zhu, M., and Assmann, S. M. (2017). Metabolic signatures in response to abscisic acid (ABA) treatment in *Brassica napus* guard cells revealed by metabolomics. *Sci. Rep.* 7, 12875. doi: 10.1038/s41598-017-13166-w

Zhu, W., Guo, Y., Chen, Y., Wu, D., and Jiang, L. (2020). Genome-wide identification, phylogenetic and expression pattern analysis of GATA family genes in *Brassica napus*. *BMC Plant Biol.* 20, 543. doi: 10.21203/rs.3.rs-30607/v1

Zou, J., Mao, L., Qiu, J., Wang, M., Lei, J., Wu, D. Y., et al. (2019). Genome-wide selection footprints and deleterious variations in young Asian allotetraploid rapeseed. *Plant Biotechnol. J.* 17, 1998–2010. doi: 10.1111/pbi.13115

frontiers | Frontiers in Plant Science

TYPE Review
PUBLISHED 02 June 2023
DOI 10.3389/fpls.2023.1110622

Check for updates

OPEN ACCESS

EDITED BY
Meng Jiang,
Zhejiang University, China

REVIEWED BY
Muhammad Iqbal,
Jamia Hamdard University, India
Md. Kamrul Hasan,
Sylhet Agricultural University, Bangladesh
Rongbin Hu,
University of California, Riverside,
United States

*CORRESPONDENCE
Guoxin Shen
guoxin.shen@ttu.edu
Neelam Mishra
neelamiitkgp@gmail.com;
neelammishra@sjc.ac.in

RECEIVED 29 November 2022
ACCEPTED 15 May 2023
PUBLISHED 02 June 2023

CITATION
Mishra N, Jiang C, Chen L, Paul A, Chatterjee A and Shen G (2023) Achieving abiotic stress tolerance in plants through antioxidative defense mechanisms. *Front. Plant Sci.* 14:1110622. doi: 10.3389/fpls.2023.1110622

COPYRIGHT
© 2023 Mishra, Jiang, Chen, Paul, Chatterjee and Shen. This is an open-access article distributed under the terms of the Creative Commons Attribution License (CC BY). The use, distribution or reproduction in other forums is permitted, provided the original author(s) and the copyright owner(s) are credited and that the original publication in this journal is cited, in accordance with accepted academic practice. No use, distribution or reproduction is permitted which does not comply with these terms.

Achieving abiotic stress tolerance in plants through antioxidative defense mechanisms

Neelam Mishra[1]*, Chenkai Jiang[2], Lin Chen[2], Abhirup Paul[3], Archita Chatterjee[3] and Guoxin Shen[2]*

[1]Department of Botany, St. Joseph's University, Bangalore, KA, India, [2]Institute of Sericulture and Tea, Zhejiang Academy of Agricultural Sciences, Hangzhou, Zhejiang, China, [3]Independent Researcher, Bangalore, KA, India

Climate change has increased the overall impact of abiotic stress conditions such as drought, salinity, and extreme temperatures on plants. Abiotic stress adversely affects the growth, development, crop yield, and productivity of plants. When plants are subjected to various environmental stress conditions, the balance between the production of reactive oxygen species and its detoxification through antioxidant mechanisms is disturbed. The extent of disturbance depends on the severity, intensity, and duration of abiotic stress. The equilibrium between the production and elimination of reactive oxygen species is maintained due to both enzymatic and non-enzymatic antioxidative defense mechanisms. Non-enzymatic antioxidants include both lipid-soluble (α-tocopherol and β-carotene) and water-soluble (glutathione, ascorbate, etc.) antioxidants. Ascorbate peroxidase (APX), superoxide dismutase (SOD), catalase (CAT), and glutathione reductase (GR) are major enzymatic antioxidants that are essential for ROS homeostasis. In this review, we intend to discuss various antioxidative defense approaches used to improve abiotic stress tolerance in plants and the mechanism of action of the genes or enzymes involved.

KEYWORDS

abiotic stress, reactive oxygen species, enzymatic antioxidants, non-enzymatic antioxidants, stress signaling

Introduction

Abiotic stress, namely drought, temperature extremes (such as heat, chilling, and freezing), salinity, heavy metals, and UV radiation, can decrease plant growth and productivity by more than 50% (Khan et al., 2015; Minhas et al., 2017). Due to global warming and varying climatic conditions, abiotic stresses have become more severe and unpredictable. Furthermore, sustainable food production is also at risk due to the reduction in the availability of land for agriculture and the increasing global population (Dubey et al., 2020).

Abiotic stresses significantly limit plant productivity by disturbing cellular biochemistry and physiology via overproduction of reactive oxygen species (ROS) (Apel and Hirt, 2004). ROS are known to play a dual role in plant growth and development as both signaling molecules and harmful agents that can cause oxidative damage to plant tissues (Figure 1). Excessive ROS accumulation due to the absence of ROS redox homeostasis can have detrimental effects on plant genetic materials, such as DNA, RNA, and proteins, leading to mutations, chromosomal aberrations, and even cell death (Apel and Hirt, 2004; Nakano et al., 2006; Mittler et al., 2011; Hussain et al., 2020). ROS such as hydrogen peroxide (H_2O_2), superoxide radical ($O_2^{\bullet-}$), hydroxyl radical ($OH^{\bullet}$) and singlet oxygen ($^1O_2$), that are produced due to excitation or incomplete reduction of molecular oxygen are harmful byproducts of normal cellular metabolism in aerobic organisms (Mittler et al., 2011).

Plants have evolved various mechanisms to cope with oxidative stress, including the production of antioxidants and the activation of stress response pathways. Several transcription factors, including WRKY and NAC, have been identified as key regulators of ROS signaling and stress response pathways (Zhu, 2016; Zhang et al., 2017; Wang et al., 2021). Studies have also shown that epigenetic modifications, such as DNA methylation and histone acetylation, can modulate the expression of stress-responsive genes and enhance plant stress tolerance (Jaleel et al., 2007; Gill and Tuteja, 2010). Plants are endowed with a variety of enzymatic and non-enzymatic antioxidants that help them scavenge excess ROS and thereby play a crucial role in ROS homeostasis. Antioxidant enzymes in plants include superoxide dismutase (SOD), ascorbate peroxidase (APX), catalase (CAT), glutathione peroxidase (GPX), monodehydroascorbate reductase (MDHAR), dehydroascorbate reductase (DHAR), glutathione reductase (GR), and glutathione S-transferase (GST) (Mittler et al., 2011). Non-enzymatic antioxidants include glutathione, ascorbate, tocopherols, carotenoids, and flavonoids. Alternatively, excess generation of ROS can be prevented via manipulation of alternative oxidase (AOX) enzymes that can prevent the leakage of electrons to oxygen (Jaleel et al., 2007). In this review, we provide an overview of ROS regulation by enzymatic and non-enzymatic antioxidants. Furthermore, we discuss the improvement of abiotic stress tolerance through ROS regulation by means of antioxidants.

Non- enzymatic antioxidants

Non-enzymatic antioxidants consist of low-molecular-weight compounds that are further categorized into water-soluble antioxidants, such as ascorbic acid and glutathione, and lipophilic antioxidants, such as tocopherols and β-carotenes. Ascorbic acid is one of the most comprehensively studied antioxidants and is present in the majority of plant cell types, organelles, and apoplasts (Gill and Tuteja, 2010; Dumanović et al., 2021). Mitochondria are the major site for ascorbate (AsA) synthesis, and ascorbate is transported through a proton-electrochemical gradient or facilitated diffusion to other cellular compartments (Gill and Tuteja, 2010). AsA is involved in the regulation of growth, metabolism, and differentiation in plants, alongside being known to scavenge free radicals and prevent oxidative damage caused by abiotic stress. In the ascorbate–glutathione (AsA-GSH) cycle, two molecules of AsA are utilized by ascorbate peroxidase (APX) to reduce hydrogen peroxide to water, generating monodehydroascorbate (MDHA) (a radical with a short lifespan). MDHA can further disproportionate into dehydroascorbate (DHA) and AsA. Also, AsA provides membrane protection by directly scavenging free radicals of oxygen and regenerates tocopherol from tocopheroxyl radical. Enhanced tolerance to ozone, salt, and polyethylene glycol was observed in tobacco when the MDHAR gene of *Arabidopsis thaliana* was overexpressed in tobacco

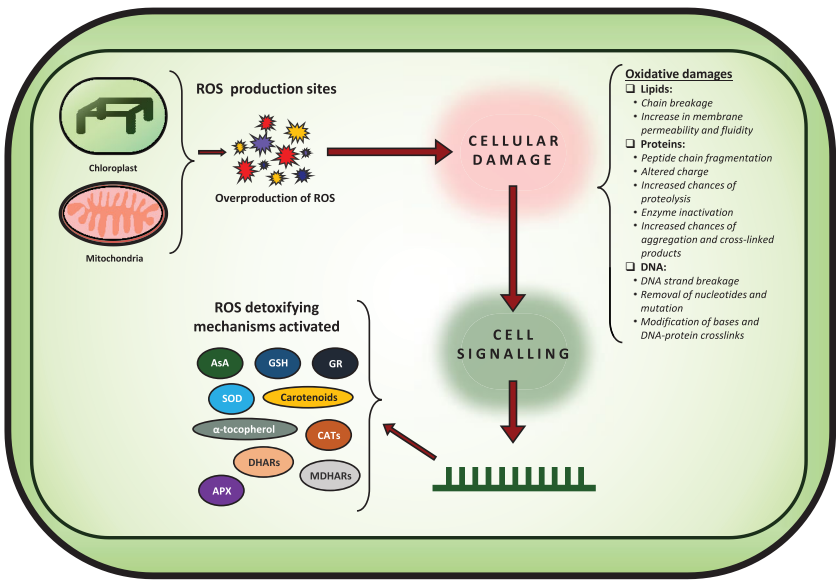


FIGURE 1
Figure showing how overproduction of ROS leads to various oxidative damages affecting the cellular machinery. Furthermore, the various ROS detoxifying mechanisms are shown as well.

(Dumanović et al., 2021). Increased AsA content was found in *Picea aspertata* seedlings when exposed to light and drought stress and in *Cassia auriculata* seedlings under UV-B stress (Eltayeb et al., 2007; Matos et al., 2022).

Tocopherols have a unique ability to quench singlet oxygen by a charge transfer mechanism. Out of all the four isomers (α, β, γ, and δ), the most biologically active is the α isomer. It is one of the most abundant antioxidants in the chloroplast membranes and is known to protect plants against photo-oxidative damage. The concentration of tocopherol increases under drought stress and high light stress, and it protects plants against oxidative damage. α-tocopherols are known to prevent the chain propagation step in lipid auto-oxidation and effectively scavenge and quench various ROS and lipid oxidation products, stabilize membranes, and regulate signal transduction (Peñuelas and Munné-Bosch, 2005; Agarwal, 2007; Pourcel et al., 2007; Shao et al., 2007; Yang et al., 2008; Bagheri et al., 2017; Kumar et al., 2020).

Glutathione, a tripeptide, occurs primarily as the reduced form (GSH), and its concentration is highest in chloroplasts (1-4 mM) in comparison to other organelles (Hajam et al., 2023). It has the ability to regenerate another powerful antioxidant, i.e., ascorbic acid via the AsA-GSH cycle (Hajam et al., 2023). Isoprenoids, such as carotenoids and tocopherols, play an important role in photoprotection as well as the response to cadmium stress (Nagajyoti et al., 2010; Nareshkumar et al., 2015). Carotenoids have the ability to delocalize unpaired electrons due to the presence of a conjugated double-bonded structure (Nareshkumar et al., 2015). They are responsible for quenching singlet oxygen without degradation and are known to chemically react with free radicals such as peroxyl ($ROO^{\bullet}$), hydroxyl ($^{\bullet}OH$), and superoxide radicals ($O_2^{\bullet-}$) (Bagheri et al., 2017). Another commonly occurring antioxidant, polyphenols, is known to possess free radical scavenging activity. Phenolic compounds react with peroxyl radicals and form phenoxy radical intermediates that are rather stable and unreactive (Bagheri et al., 2017). These function as terminators of free radical chains and as chelators of redox-active metal.

Enzymatic antioxidants

Superoxide dismutase (SOD) [EC 1.15.1.1]

Overview and types

SOD (EC 1.15.1.1) is a metalloenzyme and one of the most effective components of a plant cell's antioxidant defense system against ROS toxicity. It catalyzes the conversion of $O_2^{\bullet-}$ to O_2 and H_2O_2. Initially, SOD was isolated as a green Cu-protein from bovine blood and was thought to be involved in Cu storage (Mittler, 2002). SOD is divided into three isoenzymes based on the presence of metal cofactors (Cu/Zn/Mn/Fe) at the active site (Alscher et al., 2002). All oxygen-metabolizing cells, as well as all subcellular compartments (such as chloroplasts, mitochondria, nuclei, peroxisomes, cytoplasm, and apoplasts), are assumed to contain SODs (Fink and Scandalios, 2002; Mahanty et al., 2012). Based on their localization, structure, and functions in plants, SOD can be classified into three isoenzymes, namely Cu/Zn-SOD, Mn-SOD, and Fe-SOD (Corpas et al., 2006) (Figure 2; Table 1). Cu/Zn-SOD has been found in cytosol, chloroplasts, and peroxisomes. Mn-SOD is found primarily in mitochondria, but also in peroxisomes and apoplasts (Pan et al., 2006). Fe-SOD is found primarily in chloroplasts and to a lesser extent in peroxisomes and apoplasts. A fourth group of SOD isoenzyme, Ni (II/III) at the active site (Ni-SOD), has also been discovered (Mahanty et al., 2012). Nonetheless, all SOD isoforms (Cu/Zn-SOD, Mn-SOD, Fe-SOD) are nuclear-coded and are transported to their organellar locations via NH_2-terminal targeting sequences when necessary (Sharma et al., 2012). Further studies have revealed that Mn and Fe-SODs are found in both prokaryotes and eukaryotes, whereas Cu/Zn-SODs are primarily found in eukaryotes. Fe-SODs exist in homodimeric and tetrameric forms. They are resistant to KCN but not to H_2O_2. Similarly, Mn-SOD is homodimeric and homotetrameric, and it is resistant to both KCN and H_2O_2, whereas Cu/Zn-SOD is activated by both inhibitors (Gepstein and Glick, 2013). Furthermore, hormones such as abscisic acid and multifunctional signaling molecules such as melatonin regulate SOD activity via gene expression, like other antioxidant enzymes (Tuteja and Gill, 2013; Khan et al., 2020).

Response of SOD to abiotic stress

Abiotic stresses such as heat, cold, drought, salinity, and chemical contaminants are major factors limiting agricultural productivity around the world. As a result, understanding plant responses to these abiotic stresses has become a prerequisite for developing crop plants that can withstand abiotic stresses (Gepstein and Glick, 2013). Nonetheless, SODs are the first line of defense against abiotic stress because they are an important component of plant defense machinery. Due to stress, ROS and its reaction products increase, and dismutation of O_2 is catalyzed by SODs into hydrogen peroxide (H_2O_2) and oxygen (O_2). The impact of all SODs on the direct or indirect metabolism of various ROS has been confirmed (Mittler, 2006). Salinity is one of the most important abiotic stress factors that can affect the quality and yield of crops (Mittler, 2006). Although many plants have the ability to tolerate high salinity levels, most plants are susceptible to salt stress and show decreased photosynthetic activity or morphological disorders under such conditions (Sheokand et al., 2008; Szepesi et al., 2008; Zsigmond et al., 2012; Duque et al., 2013). Salinity causes an increase in ROS generation and alters the activity of ROS-scavenging enzymes. In certain plants, salt stress causes an increase in total SOD activity, while in others, no change or reduction in SOD activity was observed under abiotic stress. For example, under salt stress, increased numbers of leaves were seen in *Cicer arietinum*, *Beta vulgaris*, and *Brassica juncea* due to SOD activity, while a decrease in the number of leaves was observed in *Vigna unguiculata* (Hernandez et al., 2006; Sheokand et al., 2008; Kumar et al., 2013; Rasool et al., 2013). Furthermore, increased SOD activity under salt stress was reported in *Arabidopsis thaliana* and *Nicotiana tobacum* seedlings (Zsigmond et al., 2012; Lee et al., 2013). The significant differences in SOD activities in various plants under salt stress are evidence of its functioning at the inter-specific

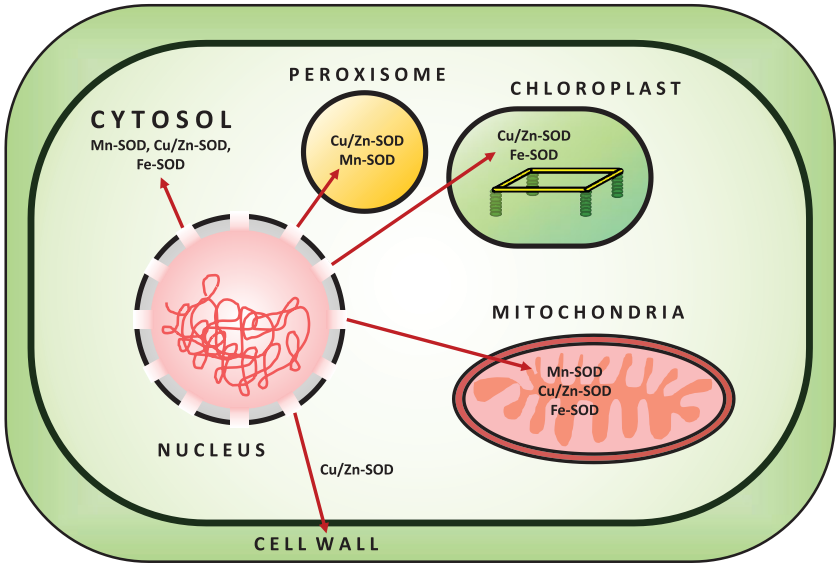


FIGURE 2
Localization of SOD enzymes in the Plant Cell.

or intra-specific level. The effect of Cu/Zn-SOD was increased in the salt-tolerant and sensitive cultivars of Oryza sativa in response to salinity (Mishra et al., 2013). While studying the long-term effects of salt stress in two salt-tolerant lines (Kharchia65, KRL19) and two salt-sensitive lines (HD2009, HD2687) of *Triticum aestivum*, higher levels of SOD activity were observed in Kharchia65 when compared to HD2687 (Sairam et al., 2005). These inconsistencies show that SOD activity is influenced by a variety of factors, including the type of plant species (tolerant or sensitive), the intensity and duration of stress, and the plant organ used for the assays. Mn-SOD activity is found substantially in the cytosolic fraction. On the other hand, Kharchia65 had enhanced Mn-SOD activity in both fractions, which increases with salt stress. The activity of cytosolic Mn-SOD was very low, implying that it plays a minor role in scavenging salinity-induced O_2 free-radical generation. Another isozyme, Cu/Zn-SOD, was found in all three cell compartments, with the chloroplast having the highest concentration, followed by mitochondria and cytosol. Salt stress enhanced Cu/Zn-SOD activity in both cytosolic and chloroplastic fractions in Kharchia65, but there was little or no increase in the enzyme's activity in mitochondria. Fe-SOD was predominantly active in the chloroplastic fraction. However, the enzyme was also found to be active in the cytosolic and mitochondrial fractions. Kharchia65 showed higher Fe-SOD and Cu/Zn-SOD activity than HD2687 under both normal and salt-stress conditions. In *Pisum sativum*, a salinity-induced increase in chloroplastic Fe-SOD was observed (Camejo et al., 2013).

Apart from salt stress, drought stress also causes a variety of physiological changes in plants, including a decrease in CO_2 fixation due to abscisic acid-mediated stomatal closure, which leads to a reduction in photosynthetic rate and/or morphological abnormalities, mostly lower organ growth (Anjum et al., 2011). Furthermore, an increase in ROS production is associated with lipid peroxidation and alterations in enzymatic and non-enzymatic antioxidants (Csiszar et al., 2007; Tari et al., 2008; Dinakar et al., 2012). It has been found that total SOD activity appears to increase in the leaves of *Olea europaea* and the shoots of *Oryza sativa* cultivars when exposed to water stress (Sharma and Dubey, 2005; Sen and Alikamanoglu, 2013). However, an increase in total SOD activity was followed by a decrease in the number of leaves of *Gossypium* sp. and two grass species (*Festuca arundinacea* and *Poa pratensis*). On the flip side, a significant reduction of SOD activity was noticed for the pea plant, under drought stress (Deeba et al., 2012; Doupis et al., 2013). SOD activity enhanced or remained

TABLE 1 Types of SOD, subcellular location and sensitivity.

SOD Isoenzymes	Structure	Species	Sensitivity	Subcellular localization
Cu/Zn-SOD	Homodimeric and Homotetrameric	*Pisum sativum, Zea mays, Spinacia oleracea, Avena sativa, Citrillus lanatus*	H_2O_2 and KCN	Cytosol, Chloroplast, Peroxisome Mitochondria
Mn-SOD	Homodimeric and Homotetrameric	*Vigna mungo, Zea mays, Pisum sativum, Spinacia oleracea, Nicotiana plumbaginifolia*	Not to H_2O_2 and KCN	Mitochondria Peroxisome Cytosol
Fe-SOD	Homodimeric and tetrameric	*Arabidopsis thaliana, Glycine max, Oryza sativa, Gingko biloba, Zea mays, Brassica campestris*	H_2O_2 but not to KCN	Cytosol Chloroplast Mitochondria

constant in *Triticum aestivum* during the early stages of drought but declined with chronic water stress (Deeba et al., 2012). Studies suggest that photosystem II can be protected by SOD from reactive O_2 induced by oxidative and water stress (Deeba et al., 2012). In a recent study, the Tibetan wild *Hordeum vulgare* genotypes XZ16 and XZ5 were found to have considerably elevated SOD activity throughout the anthesis period when subjected to drought stress (Ahmed et al., 2013).

Cold stress is another major abiotic stress that can cause functional abnormalities in chloroplasts or mitochondria, resulting in ROS overproduction (Latef, 2021). Earlier research demonstrated that plants produce a lot of H_2O_2 during cold stress, and higher antioxidant enzyme activity tends to correlate with higher tolerance (Huang and Guo, 2005a). Studies in tolerant rice, barley, and tobacco cultivar roots and shoots revealed a differential amount of SOD activity under cold stress (Huang and Guo, 2005a; Xu et al., 2010; Mutlu et al., 2013). In sensitive as well as tolerant cultivars of tobacco the roots exhibited a higher SOD and catalase activity as compared to peroxidase activity (Xu et al., 2010). While tobacco shoots exhibited a higher peroxidase activity in comparison to SOD and catalase activity (Xu et al., 2010). In paraquat-treated *Nicotiana plumbaginifolia*, increased mRNA levels for mitochondrial Mn-SOD, chloroplastic Fe-SOD, and cytosolic Cu/Zn-SOD were observed in the presence of light. However, only cytosolic Cu/Zn-SOD expression was observed in the dark (Mylona et al., 2007). Further, convincing evidence was found for the stimulation of genes and enzyme activity in *Zea mays* embryos in response to paraquat. Benzyl viologen-produced O_2 and $O_2^{\bullet}$ was found to increase the expression of mitochondrial Mn-SOD and cytoplasmic Cu/Zn-SOD genes (Mylona et al., 2007). O_3 (ozone) is a contaminant in the atmosphere that breaks down in the apoplast to produce primarily $O_2^{\bullet}$ and H_2O_2. Acute or chronic exposure of *Zea mays* seedlings resulted in increased transcript levels of mitochondrial Mn-SOD and cytosolic Cu/Zn-SODs in the leaves (Rossa et al., 2002). On the other hand, the transcript level of chloroplastic Cu/Zn-SOD was shown to be down-regulated. The blue light wavelength has been shown to induce SOD activity more effectively in *Gracilariopsis tenuifrons* than other wavelengths (Rossa et al., 2002). UV B (280-350 nm) irradiation increased SOD activity in *Cassia auriculata* seedlings (Agarwal, 2007). Expression of Mn-SOD enzyme was also increased in *Nicotiana tabacum* leaves when exposed to high light intensity. However, increased total SOD activity was observed in *Hordeum vulgare* catalase-deficient mutants RPr 79/4 after the plants were exposed to high intensities of light (Azevedo et al., 1998; Dat et al., 2003).

Genetic engineering of plant SOD

The activation of SOD in response to various environmental conditions, as discussed in the previous section, suggests that it is a significant component of the plant's defense system, and therefore, its genetic modification could lead to the development of stress-tolerant phenotypes. It was observed that *Oryza sativa* showed better resistance to methylmercury and drought stress when the *Pisum sativum* Mn-SOD gene was expressed in the chloroplasts (Wang et al., 2005). In another instance, overexpression of the Cu/Zn-SOD gene in *Nicotiana tabacum* plants was done to improve oxidative stress resistance, while tolerance to methyl viologen and pure cercosporin was achieved in sugar beet by transferring a *Lycopersicon esculentum* SOD gene (Tertivanidis et al., 2004; Wang et al., 2005). SOD genes have been shown to help plants eliminate ROS more efficiently under methyl viologen exposure or environmental stresses such as cold, ozone, water deficit, and salt stress (Wang et al., 2005). Nonetheless, there are several transgenic plants with SOD genes from different plants that did not show any improvement in stress tolerance (Tertivanidis et al., 2004; Sunkar et al., 2006). The differences in SOD isoenzymes, as well as the complexity of the ROS detoxification system, have been proposed as key variables for these instances (Kwon et al., 2002; Jia et al., 2009). When Mn-SOD was overexpressed in Arabidopsis, Mn-SOD, Cu/Zn-SOD, and Fe-SOD activity was higher in transgenic plants than wild-type plants, and the transgenic plants grew well and produced fewer lipid peroxidation products when treated with 150 mM NaCl (Mylona and Polidoros, 2010). The transcriptome of knockdown Arabidopsis plants with suppressed expression of chloroplastic Cu/Zn-SOD (CSD2) revealed the appearance of induced chloroplast and nuclear-encoded genes as a result of O_2 buildup under optimal conditions (Mylona and Polidoros, 2010). Mn-SOD gene from halophilic archaeon was extracted and transferred into *Oryza sativa* by agrobacterium-mediated transformation to explore new gene resources for increasing *Oryza sativa* tolerance to salt stress (Wang et al., 2004). The transformants (L1 and L2) showed some MnSOD expression and increased overall SOD activity, resulting in improved ROS removal efficiency under salt stress. The amounts of oxygen and hydrogen peroxide (H_2O_2) were dramatically reduced; they also had better levels of photosynthesis and lower levels of relative ion leakage and malondialdehyde (MDA) concentration than wild-type plants (Wang et al., 2004). In contrast to the reports discussed above, overexpression of cytosolic or chloroplastic SOD in some transgenics only provided moderate or minimal tolerance, owing to the type of overexpressed SOD and its subcellular localization (Wang et al., 2004). Cu/Zn-SOD and FeSOD inactivation by H_2O_2, their reaction end product, and the competing resistance of Mn-SOD to H_2O_2 may be relevant to their specific effects. In this scenario, antisense technology is now feasible and should be used in conjunction with any overexpression research.

Ascorbate peroxidase (APX) [EC 1.11.1.11]

Overview and types

Ascorbate peroxidase is a heme-containing peroxidase that catalyzes the oxidation of a wide spectrum of organic compounds in the presence of H_2O_2. APX is found in higher plants, chlorophytes, red algae, and members of the protist kingdom, and plays a crucial role in growth regulation (Wang et al., 2004; Chen et al., 2013). The peroxidase database contains APX and other peroxidase sequences from all kingdoms of life, as well as a set of bioinformatics tools for evaluating peroxidase sequences. Genomic and cDNA APX sequences have been discovered from a wide range

of plants, demonstrating that APX is found throughout the vegetal domain. In these organisms, small gene families encode this enzyme (Oliva et al., 2009; Chen et al., 2013). The different isoforms of APX are categorized based on subcellular localization in the cell (Figure 3). Membrane-bound isoforms are present in microbodies (including peroxisome and glyoxysome) and chloroplast thylakoids, while soluble isoforms are found in the cytosol, mitochondria, and chloroplast stroma. The subcellular localization of the isoenzyme is determined by the presence of organelle-specific targeting peptides and transmembrane domains in the N and C-terminal regions of the protein (Teixeira et al., 2004; Passardi et al., 2007).

Furthermore, the plant chloroplastic APX isoenzyme-encoding genes are divided into two groups in plants. The first group consists of single genes that encode two isoenzymes. Genes from spinach (*S. oleracea*), tobacco (*N. tabacum*), pumpkin (*Cucurbita* sp), and ice plant (*Mesembryanthemum crystallinum*) are included in this group. Individual genes code for distinct isoenzymes that are separately regulated in the second category. Arabidopsis, rice, and tomato genes are included in this group. In spinach, the mechanism of alternative splicing in chlAPX was investigated, and the results revealed that alternative splicing is critical for modulating the expression of stromal (sAPX) and thylakoid (tAPX) isoenzymes, and this regulation happens in a tissue-dependent manner. In certain plant species, ascorbate peroxidases have been partially identified. The APX family in spinach is composed of genes that code for one cytosolic, two chloroplastic (sAPX and tAPX membrane) isoenzymes, one microbody membrane-targeted isoenzyme, and an unknown putative cytosol-soluble isoenzyme (Teixeira et al., 2006). Four cDNAs belonging to potential cytosolic, peroxisomal, and chloroplastic (thylakoid and stromal) APX isoforms were identified and studied in Cowpea (D'Arcy-Lameta et al., 2006). Six APX-coding loci were discovered in *Eucalyptus grandis*, with prediction tools indicating their subcellular localization. Three out of six isoforms were predicted to be cytosolic, one as a putative peroxisomal protein, and two as chloroplast-associated proteins (Teixeira et al., 2005). Another study in tomato revealed seven members where three were cytosolic, two peroxisomal, and two chloroplastic members (Najami et al., 2008). Two chloroplastic, one thylakoid-bound, and one membrane-bound, whose product is targeted to both chloroplast stroma and mitochondria, were identified in the model plant *Arabidopsis thaliana*, with the intracellular localization of an additional member still being unknown (Najami et al., 2008). Two chloroplastic, one thylakoid-bound, and one membrane-bound APX, whose product is targeted to both chloroplast stroma and mitochondria, were identified in the model plant *Arabidopsis thaliana*, while the intracellular localization of an additional member is still unknown (Najami et al., 2008). The APX gene family of rice has a total of eight members, with two members each in cytosol, peroxisome, chloroplast, and mitochondria. In rice, a novel protein called APX-R (Ascorbate peroxidase-related) has recently been discovered to be functionally connected with APX (Lazzarotto et al., 2011). Further analysis revealed that the Apx-R gene corresponds to a new class of heme peroxidases (Lazzarotto et al., 2011).

In the absence of AsA, APX isoenzymes are labile, and thus, a high quantity of endogenous AsA is required for the antioxidant system to effectively protect plants from oxidative damage (Maruta et al., 2010). The APX activity is quickly lost under particular conditions when the concentration of AsA is less than 20 µM, making chlAPX the least stable isoform. Both cAPX and mAPX have half-inactivation times of one hour or more, whereas mAPX and chlAPX have half-inactivation times of less than 30 seconds (Anjum et al., 2016).

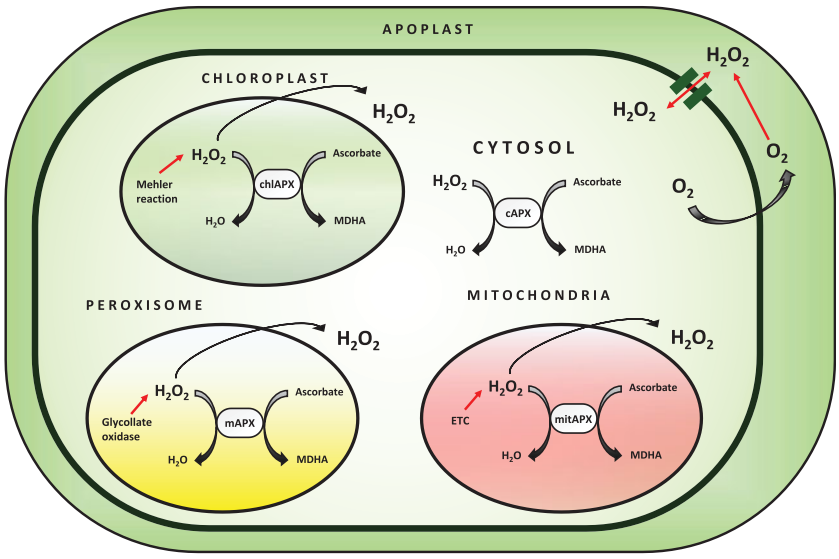


FIGURE 3
Subcellular localization of APX enzyme and detoxification of ROS.

Response of APX under different abiotic stresses

Drought stress, salt stress, high levels of light, high and low temperatures, pathogen attacks, H_2O_2, and abscisic acid all affect the expression of APX-producing genes (Teixeira et al., 2004; Passardi et al., 2007; Anjum et al., 2016). Furthermore, the transcriptional expression of APX genes varies depending on tissue and developmental stage (Teixeira et al., 2005). By restricting the amount of water available to the plant, salinity stress causes ion imbalances and physiological drought-like conditions. In such situations, APX provides varied levels of salt tolerance to affected plants. Salinity-induced oxidative damage is seen in cAPX mutants, but constitutive overexpression lines demonstrate increased resistance to 100 mM NaCl stress (Diaz-Vivancos et al., 2013). Tomato plants that overexpress pea cAPX are found to be more resistant to salinity stress (Wang et al., 2005). In transgenic Arabidopsis plants, overexpression of OsAPX2 exhibits higher tolerance to salt stress than OsAPX1. However, it is possible that the observed differences in tolerance are attributable to the positional influence of distinct transgenic lines. In transgenic tobacco, a cAPX from Arabidopsis displayed enhanced salt, drought, and PEG tolerance. Furthermore, in sensitive plants, salt stress causes lipid peroxidation and membrane damage, as well as low levels of antioxidant enzymes. Transgenic tobacco BY-2 cell lines with 50 and 75 percent decreased cAPX activity revealed higher ROS buildup. The study found that ascorbate peroxidase gene expression during stress resulted in salt and heat tolerance with no significant changes in levels of other ROS scavenging enzymes (Ishikawa et al., 2005; Wang et al., 2005; Nakano et al., 2006; Lu et al., 2007; Berwal et al., 2021).

Pea chloroplast APXs responded differently in saline conditions, with sAPX gradually increasing and tAPX gradually dropping, but a tAPX from *Solanum lycopersicum* introduced in tobacco gave enhanced resistance to salt and osmotic stress. Under salt stress, chlAPX activity increases, which protects against ROS generated in mitochondria and/or peroxisomes. Transgenic tobacco accumulating higher ascorbate was used to induce salt stress tolerance. Drought and salt conditions increased the expression of the APX gene in French bean seedlings (Eltelib et al., 2012; Nageshbabu and Jyothi, 2013). In Arabidopsis, overexpression of an APX from *Puccinellia tenuiflora*, a salinity-tolerant wild grass, boosted tolerance to 175 mM NaCl while also protecting against lipid peroxidation. Under salinity conditions, transcripts for mAPX from *Hordeum vulgare*, while a Populus peroxisomal APX in tobacco, conferred salt, drought, and MV stress resistance as well as larger roots (Li et al., 2009; Eltelib et al., 2012). Furthermore, APX mutants can upregulate other peroxidases to compensate for the loss of APX and give stress tolerance. This is validated by the expression of rice GPX in rice APX 1/2 mutants, as well as the upregulation of other enzymes (CAT and GP) in Arabidopsis APX3 knockout mutants that showed no indications of stress. When salicylic acid is administered topically, it stimulates APX and GR activity, resulting in increased salt tolerance in mung bean (Narendra et al., 2006; Bonifacio et al., 2011; Nazar et al., 2011; Guan et al., 2015; Husen et al., 2018). The response of all antioxidant enzymes to salt stress in Brazilian indica rice was studied at two developmental phases, and it was discovered that cAPX expression was up-regulated in 11-day-old seedlings but not in 6-week-old plants (Guan et al., 2015). This stress causes the production of ROS. The response of APX isozymes to this circumstance at different phases of plant growth is regulated. Under salinity stress, the normal salinity-resistant rice leaf basal region showed an increase in CAT and APX transcripts, whereas APX8 levels were slightly reduced. Under saline conditions, the expression of OsAPX2 did not change (Yamane et al., 2010). Another study found a similar drop in APX8 responsiveness when the other isoforms, APX2 and APX7, were strongly expressed during salt stress. In a different experiment, OsAPX8 demonstrated high expression in rice roots over a wide range of salt concentrations, from 150 to 300 mM, but OsAPX7 transcripts dropped dramatically at 300 mM. Age, cultivar, plant sections, and physiological conditions of plant growth all contribute to variances in APX gene expression (Teixeira et al., 2004; Hong et al., 2007; Passardi et al., 2007). Sweet potato plants with various levels of sensitivity to salt stress accumulated APX transcripts differently, with larger quantities in tolerant genotypes. APX plays a key function in plant drought resistance and recovery. Overexpressed P5CS gene in transgenic soybean and tobacco under drought stress elevate APX transcripts. In *Prunus* sp., APX and other Asc-GSH pathway enzymes were up-regulated during drought treatment and reduced throughout the recovery period (Sofo et al., 2005b; Teixeira et al., 2006; Zarei et al., 2012; Cruz et al., 2013). Studies have reported that glycine betaine (GB) increases APX under drought (Sofo et al., 2005b; Teixeira et al., 2006; Zarei et al., 2012; Cruz et al., 2013). Overexpression of cAPX (APX1) reduces drought symptoms, and transgenic tobacco plants outperformed non-transgenic plants. The relevance of this isoform in plant growth and development was also demonstrated by loss of function APX2 mutants, which were more vulnerable to drought than over-expression lines. Drought resistance was improved in over-expression lines of an mAPX from *Salicornia brachiata* relative to control plants (Zhang et al., 2013; Singh et al., 2014). cAPX is found to be important in drought stress tolerance in tobacco, with a primary benefit being membrane protection (Faize et al., 2011). Even under non-stressed conditions, APX activity is observed to be higher in tolerant cowpea plants. The sensitive cultivar up-regulates cAPX and mAPX in response to stress, whereas the tolerant cultivar up-regulates chlAPX (D'Arcy-Lameta et al., 2006). Various wheat genotypes have different levels of APX expression when there is a water crisis. cAPX1 was up-regulated in both genotypes, sAPX2 only in sensitive, and tAPX and cAPX2 only in tolerant cultivars (Secenji et al., 2009). After 15 days of drought stress in rice, the tAPX gene was down-regulated, while numerous other isoforms were upregulated. However, certain microsomal isoforms were only slightly or not at all altered (Rosa et al., 2010). This indicates that APXs are expressed differently in different species and under different conditions.

The temperatures that are either too low or too high have an adverse impact on plant physiology. Cold stress induces APX expression in tolerant maize lines, but not in sensitive ones (Caverzan et al., 2012). When compared to heat stress, low temperatures increase cAPX expression in potato tubers, implying that it plays a role in cold adaptation (Caverzan et al., 2012).

Tobacco plants with a higher level of tAPX were more resistant to freezing and light stress, whereas Arabidopsis plants with a lower level of tAPX were more resistant to heat stress (Miller et al., 2007; Wang et al., 2016). Rice plants with homologous overexpression of a cAPX were tolerant to colder temperatures at the booting stage than wild-type plants, owing to enhanced APX activity in spikelets (Sato et al., 2011). SOD and APX gene expression in potato chloroplasts was induced using an inducible promoter SWPA2 that works under oxidative stress. With a substantial difference from the control, the plants obtained were tolerant to higher temperatures and methyl viologen (MV) stressors (Tang et al., 2006). In a similar experiment with sweet potatoes, tolerance to cold and MV stressors was observed (Lim et al., 2007). Transgenic plants with tomato tAPX expressed in tobacco were more resistant to both temperature and light stressors, and their photosynthetic efficiency was higher than non-transformed plants (Sun et al., 2010). High temperature increases cAPX in sweet potato leaves, but cAPX, mAPX, and sAPX were all up-regulated in cucumber after an initial decline (Park et al., 2004; Song et al., 2005). A cAPX has been reported to decrease quickly after heat shock treatment, negating its positive role in this stress, whereas some studies claim that APX2 is increased under heat circumstances (Gao et al., 2010). In Arabidopsis cells, APX1 is known to be active largely in response to heat and drought stress (Koussevitzky et al., 2008). In Arabidopsis, a mAPX from barley was overexpressed to display heat stress tolerance (Smeets et al., 2008). As a result, different APX isoforms and antioxidative mechanisms at multiple subcellular sites can be used to breed plants that can withstand environmental stress.

Heavy metal ion pollution in the soil is a major problem that reduces crop productivity. Under cadmium and arsenic stress, APX expression was induced in the leaves of *Arabidopsis thaliana, Solanum nigrum, and Brassica juncea*, but it was reduced in the leaves of *Brassica napus* (Smeets et al., 2008; Khan et al., 2009; Markovska et al., 2009; Nouairi et al., 2009; Pinto et al., 2009; Ansari et al., 2015). Copper stress increased APX expression in leaves of *Elsholtzia splendens*, however it was variable in *Withania somnifera* depending on metal ion concentrations (Peng et al., 2006; Khatun et al., 2008). The expression of APX isoforms in *Nicotiana tabacum* and *Typha angustifolia* leaves was observed to remain constant with varying levels of cadmium stress, while chromium and lead stresses did not cause any changes in APX expression in Typha leaves (Bah et al., 2011). Cadmium stress caused APX expression to vary in *Zea mays* (Ekmekçi et al., 2008). Low concentrations of cadmium stimulated APX activity in cells of coffee plant, but higher concentrations had no effect after 24 hours, while nickel enhanced APX activity at two extreme concentrations (Gomes-Junior et al., 2006). In rice, aluminium exposure causes practically all APX isoforms to become active. Double mutants of cAPX1/2 had a higher tolerance to high concentrations of aluminium (Sharma and Dubey, 2007; Rosa et al., 2010). This heavy metal enhances cAPX activity in pea at higher concentrations for longer periods of time, whereas it decreases and becomes constant beyond it (Panda and Matsumoto, 2010). De-rooted bean plants with inadequate cAPX were susceptible to iron, as were tobacco plants with deficient cAPX (Caverzan et al., 2012). Copper and cadmium increased APX activity in transgenic tall fescue plants compared to control, but arsenic decreased it in both transgenic and control plants (Lee et al., 2007). In *Eichhornia crassipes* seedlings, lead stress boosted APX activity (Lee et al., 2007). Cadmium chloride boosted APX activity in salt tolerant and sensitive rice cultivars, with the former having a higher activity (Roychoudhury and Ghosh, 2013; Malar et al., 2014). A similar increase in APX activity was seen in *Vigna radiata* (Roychoudhury and Ghosh, 2013). Salt and lead stress doubled on *Vigna radiata* seedlings resulted in an increase in APX activity (Siddiqui, 2013). As a result, several scientific publications have shown that APXs play a significant role in protecting plants from heavy metal stress in soil (Siddiqui, 2013).

Catalases (CAT) [EC 1.11.1.6]

Overview

Catalases are tetrameric heme-containing enzymes that convert hydrogen peroxide to water and oxygen and are mostly found in peroxisomes (Srivalli et al., 2003). Catalase isozyme forms are found in many plants, including two in castor bean and six in Arabidopsis, and they can directly dismutate H_2O_2 or oxidize substrates such as methanol, ethanol, formaldehyde, and formic acid (Ben-Amor et al., 2005).

Plant catalases are divided into three groups based on their structures: class 1 catalases are found in photosynthetic tissues and are involved in the removal of H_2O_2 produced during photorespiration; class 2 catalases are found in vascular tissues and may play a role in lignification, though their exact biological role is unknown; and class 3 catalases are found in seeds and young plants, and their activity is linked to the removal of excess H_2O_2 produced during fatty acid degradation in the glyoxylate cycle in glyoxisomes (Ben-Amor et al., 2005). Catalases are the primary scavenging enzymes that may directly dismutate H_2O_2 and are required for ROS detoxification during stress (Ben-Amor et al., 2005). This is also related to the fact that during stress, peroxisomes proliferate, possibly aiding in the scavenging of H_2O_2 that diffuses from the cytosol (Ben-Amor et al., 2005). Increased catalase activity is thought to be an adaptive characteristic that could aid in overcoming tissue metabolic damage by lowering harmful levels of H_2O_2 (Mhamdi et al., 2010). In these organelles, a 200mM NaCl concentration resulted in a decrease in catalase activity (Srivalli et al., 2003). Increased catalytic activity in transgenic tobacco with sense cDNA of cotton catalase was shown to reduce photorespiratory loss, but antisense constructions reduced catalase specific activity, resulting in a commensurate increase in the CO_2 compensation point. In alfalfa nodule, tea, cotton, and tobacco, abiotic stress causes upregulation of the genes responsible for catalase expression (Sekmen et al., 2007; Upadhyaya et al., 2008; Vital et al., 2008; Mhamdi et al., 2010). Catalases of class II have mostly been examined in relation to disease progression and resistance. It has been discovered that they are a target for SA (salicylic acid), and transgenic potato plants expressing the tobacco Cat2Nt gene could result in constitutive expression of the endogenous potato Cat2St gene and increased resistance to *Phytophthora infestans* (Vital et al., 2008). In dry and arid areas, two of the most common and frequent abiotic stresses are drought

and salinity. Vegetation experiencing salt and drought stresses has evolved a range of physiological mechanisms to cope with harsh climatic circumstances (Zhang et al., 2008; Deeba et al., 2012). Abiotic stresses in semi-arid regions result in a loss of plant growth and productivity, which leads to several developmental, physiological, cellular, and molecular responses (Grover et al., 2011; Pinheiro and Chaves, 2011; Sobhanian et al., 2011). The majority of these responses are caused by photon intensity beyond the absorption capacity of stressed plants (Figure 3). Photorespiration is known to allow oxygenic photosynthesis by scavenging its most poisonous by-product, 2-phosphoglycolate, but it also causes substantial losses of freshly assimilated CO_2 from most land plants (Rahman et al., 2023). Many studies have focused on the importance of the CAT catalysis pathway under drought and salt stress because of the critical involvement of CAT in photorespiration. Indeed, the persistence of CAT activity in drought-stressed plants' leaves is likely responsible for the elimination of photorespiratory H_2O_2 generated when plants are subjected to higher levels of water deficit and salinity stresses. Photorespiration acts as an energy sink in these conditions, limiting photoinhibition and over-reduction of the photosynthetic electron transport chain (Bauwe et al., 2012). On this basis, photorespiration and the CAT pathway are no longer regarded as wasteful activities, but rather as critical and accessory components of photosynthesis and aspects of stress responses in green tissues for preventing ROS accumulation (De Pinto et al., 2013; Rahman et al., 2023). Drought stress and salt predispose the photosynthetic system to photoinhibition, leading to light-dependent inactivation of the principal photochemistry associated with photosystem II that often persists after rewatering (Deeba et al., 2012).

Indeed, decreased CO_2 transport to the chloroplast and metabolic restrictions influence photosynthesis, which is one of the primary activities affected by water deficiencies and high salt concentrations (Grover et al., 2011; Pinheiro and Chaves, 2011). Due to the concurrent or even earlier suppression of growth, total plant carbon uptake is further reduced. Water deficiency, either directly or indirectly resulting in lower growth, has a significant impact on leaf carbohydrate status and hormonal balance. Increased levels of reactive oxygen species (ROS) such as superoxide anion (O_2^-), hydrogen peroxide (H_2O_2), and hydroxyl radicals are commonly related to plant adaptation to drought and salinity. ROS are by-products of aerobic metabolism, and their generation is boosted by the disturbance of the electron transport system and oxidizing metabolic processes in chloroplasts, mitochondria, and microbodies during stressful situations (Grover et al., 2011; Voss et al., 2013; Ramakrishna and Gill, 2018; Rajput et al., 2021). ROS are effectively eliminated by non-enzymatic and enzymatic antioxidants in non-stressful conditions, but during drought and saline conditions, ROS production surpasses the ability of antioxidative systems to remove them, resulting in oxidative stress (Vanderauwera et al., 2012; Nawaz et al., 2021). Catalase (CAT) isoforms are iron porphyrin enzymes that act as an efficient ROS scavenging system to protect cells from the oxidative damage caused by these two stressors (Mittler et al., 2011). Based on previous research, an increase in CAT activity is often connected to the degree of dryness that plants experience (Grover et al., 2011; Mittler et al., 2011). The root length increases gradually in *Panicum sumatrense* under drought stress at all growth stages, whereas the chlorophyll pigments and plant height decrease (Vanderauwera et al., 2012). According to the researchers, compatible solutes such as proline, glycine betaine, and free amino acid increased in all drought treatments (Ajithkumar and Panneerselvam, 2014; Nawaz and Wang, 2020). Furthermore, stress treatment increased the activity of antioxidant enzymes such as superoxide dismutase (SOD), catalase, and peroxidases, enabling this species to exhibit strong drought-tolerance characteristics. Leaf CO_2 absorption rate and carboxylation efficiency characteristics decreased as the water deficit increased in another drought-tolerant species (*Jatropha curcas*). Leaf H_2O_2 level and lipid peroxidation were negatively and strongly linked with CAT activity in this species, indicating that drought-induced suppression of this enzyme could have a negative impact. Differences in antioxidant responses to drought in C3 and C4 plants are few, but they may be essential in understanding the metabolic antioxidant patterns of these two plant groups. Relative shoot growth rate, relative water content and osmotic potential, H_2O_2 content and nicotinamide adenine dinucleotide phosphate (NADPH) oxidase activity, CAT activity, CAT1 mRNA level, and lipid peroxidation were studied in *Cleome spinosa* (C3) and *Cleome gynandra* (C4) seedlings. Seedlings grown under control conditions consistently had higher antioxidant enzymes (excluding SOD) in *Cleoma spinosa* than in *Cleoma gynandra* (Ajithkumar and Panneerselvam, 2014). CAT activity was linked with CAT1 gene expression in *Cleoma spinosa*, but not with CAT1 gene expression in *Cleoma gynandra* for 10 days. Drought stress increased the levels and activity of the CAT enzyme in both species. The findings revealed that the antioxidant defense system in *Cleoma spinosa* was unable to limit the increased ROS generation under stress. The antioxidant system in *Cleoma gynandra*, on the other hand, was able to cope with ROS generation under drought stress, despite its induction being lower than in *Cleoma spinosa*. Ford et al. investigated the quantitative changes in protein abundance of three Australian bread wheat cultivars (*Triticum aestivum* L.) in response to drought stress using a series of multiplexed experiments (Uzilday et al., 2012). The three cultivars, namely Kukri (drought-intolerant), Excalibur (drought-tolerant), and RAC875 (drought-tolerant), were produced in the glasshouse with cyclic drought treatment that replicated field conditions. The proteome modifications in the three cultivars at different times during the water shortage period represented their physiological responses to drought. An increase in CAT and SOD isoforms, as well as a decrease in proteins involved in photosynthesis and the Calvin cycle, were seen in all three cultivars, indicating an increase in oxidative stress metabolism and ROS scavenging capacity, as well as ROS avoidance.

Using a transgenic wheat line, researchers evaluated the response of photosynthesis to drought, heat stress, and their combination in the same species (Ford et al., 2011). According to the study, all stresses reduced photosynthesis, but their combination amplified the negative impacts. For instance, drought stress was found to reduce the transpiration rate, stomatal conductance, and intercellular CO_2 concentration. On the other hand, heat stress boosted these photosynthetic characteristics, but it also decreased

antioxidant enzyme activity, and hence, the antioxidative defense system. Given the difficulty of examining biochemical and molecular responses in the field, where a variety of factors other than dryness play a crucial role, scientific work on CAT in tree species is uncommon. Olive plants were found to up-regulate the enzymatic antioxidant system under water deficient conditions (Wang et al., 2010). This reaction protects the cellular machinery and reduces ROS-induced cellular damage. In fact, CAT activity increased significantly in plant leaves subjected to drought stress. The significant increase in CAT activity found in leaves may protect chloroplasts, which are the principal generators and targets of ROS action and present persistent electron fluxes under stress conditions (Sofo et al., 2005a). Under drought conditions, the efficiency of autochthonous plant growth-promoting rhizobacteria (*Bacillus megaterium* (Bm), *Enterobacter* sp., *Bacillus thuringiensis*, and *Bacillus* spp.) was investigated in *Lavandula dentata* and *Salvia officinalis* (Foyer and Shigeoka, 2011). In these two plant species, each bacterium used various ways to ameliorate water constraint and drought stress, including CAT up-regulation. It was found that plant characteristics, such as a low shoot/root ratio and a high stomatal conductance, are essential determinants limiting bacterial effectiveness in increasing nutritional, physiological, and metabolic plant activities (Armada et al., 2014). Salinity in agricultural land is a serious concern worldwide, which puts severe constraints on crop growth and productivity in many places (Zhang et al., 2008; Tanou et al., 2012; Armada et al., 2014). High salinity causes water deficit and ion toxicity in many plant species, and their sensitivity to salt stress varies. Compatible solutes, such as proline, trehalose, and glycine betaine, are deposited at millimolar concentrations in transgenic plants under salt stress, acting as osmoprotectors in physiological responses and allowing the plants to better withstand soil salinity (Chen and Murata, 2011; Vanderauwera et al., 2011). Low levels of GB, administered exogenously, or created by transgenes for the production of suitable solutes, can also trigger the expression of stress-responsive genes, such as those responsible for scavenging reactive oxygen species (Vanderauwera et al., 2011). Furthermore, significant efforts have been made to investigate how genes react to salt stress in many organisms. The effects of NaCl on H_2O_2 content and CAT activity were investigated in various plants, including a single-celled alga (*Chlorella* sp.), an aquatic macrophyte (*Najas graminea*), and a mangrove plant (*Suaeda maritima*), which have a high tolerance to NaCl. When exposed to high levels of NaCl, all the examined plants produced considerable amounts of H_2O_2, and CAT activity rose dramatically in response to the NaCl treatment (Nounjan et al., 2012). Interestingly, the same investigators discovered that cultivating the plants in a high-salinity environment led to the generation of novel CAT isoforms. A gene encoding a small GTPase (MfARL1) from a subtracted cDNA library in *Medicago falcate* was identified to better understand the role of certain essential genes in the response to salt stress (Mallik et al., 2011).

Under salt stress, transgenic seedlings that constitutively express MfARL1 showed a higher survival rate. Salt stress significantly reduced chlorophyll concentration in wild-type plants, but not in transgenic plants. During these saline conditions, transgenic plants accumulated less H_2O_2 and showed less oxidative damage than their wild-type counterparts, which can be attributed to higher CAT activity. Peroxisomal CAT activity was found to be higher in tomato leaves and roots treated with various degrees of salt stress compared to controls, although CAT activity in pure leaf peroxisomes did not increase in response to salinity in other species such as peas (Wang et al., 2013). AtWNK8, mostly expressed in the primary root, hypocotyl, stamen, and pistil, appears to play a crucial role in salt and osmotic stress tolerance (Yang and Guo, 2018). Indeed, mutants overexpressing the WNK8 gene are more resistant to salt and osmotic stressors than the wild type (Yang and Guo, 2018). CAT activity in WNK8 mutants is higher than in wild-type plants under NaCl and sorbitol stress. This study provides evidence that the improved resistance of WNK8 mutants to salt stress is due to increased endogenous activities of CAT and GPX in association with increased proline synthesis and accumulation. Some plant pretreatments have been identified as effective ways to stimulate plant defenses against salt stress. For instance, the effects of two exogenous osmoprotectants (proline and trehalose) on a salt-sensitive rice variety reveal that salt stress caused growth reduction, an increase in the Na^+/K^+ ratio, an increase in proline level, and up-regulation of proline synthesis genes (pyrroline-5-carboxylate synthetase, P5CS) (Chen and Murata, 2011). Exogenous osmoprotectants did not appear to ameliorate growth inhibition during salt stress, but they appeared to have a significant favorable effect during the recovery period, with a larger percentage of growth recovery. The scientists discovered that an increase in CAT activity was linked to a considerable decrease in H_2O_2, especially in proline-treated plants. Administering proline to tree species (different wild almond species) can reduce the negative impacts of abiotic stresses like salinity, allowing leaves to better withstand oxidative stress by functioning as an effective H_2O_2 scavenger (Zhang et al., 2013). Furthermore, salt stress has been shown to cause considerable alterations in CAT activity in a variety of wild almond species (Sorkheh et al., 2012a). One study investigated the effects of H_2O_2 leaf spraying pretreatment on plant growth, and it was found that spraying H_2O_2 boosted antioxidant enzyme activity, with CAT being the most sensitive (Sorkheh et al., 2012b). Considering the protective effect of CAT, increased CAT activity appears to be linked to gene expression regulation, and decreased oxidative damage was identified in plants with higher CAT activity.

Glutathione reductase (GR) [EC 1.8.1.7]

Overview

Glutathione Reductase (GR or GSR) is a flavoprotein oxidoreductase that helps catalyze the reduction of glutathione disulfide (GSSG) to its reduced sulfhydryl form (GSH) using NADPH as a reductant. The reduced GSH formed is then utilized for the regeneration of ascorbic acid (AsA) using monodehydroascorbate (MDHA) and dehydroascorbic acid (DHA), thereby converting GSH to GSSG (Figure 4). GR has been shown to play a pivotal role in the plant defense against reactive oxygen metabolites generated by various abiotic stress conditions to which the plant is exposed (Gondim et al., 2012; Das and

Roychoudhury, 2014; Aftab and Hakeem, 2022). Studies have described glutathione reductase as "a boon in disguise for abiotic stress defense operations". GR efficiently maintains a relatively high cellular GSH/GSSG ratio by catalyzing the formation of a disulfide bond in glutathione disulfide (Gondim et al., 2012; Aftab and Hakeem, 2022). This enzyme is predominantly localized in the stroma of the chloroplast, but its isomers can also be found in mitochondria, cytosol, and peroxisomes (Gill et al., 2013). The enzyme is a homodimer of flavin adenine dinucleotide (FAD) having a molecular mass ranging from 100 to 150 kDa (Figure 5). An active site is located between the FAD binding domain and NADPH binding domain where the GSSG is bound (Ahmad et al., 2010). There is an additional interface region on each of the monomers of FAD that not only helps the GSSG to be bound between the subunits but also brings the FAD domains of each subunit in close proximity with the opposite catalytic site (Ahmad et al., 2010). It has been observed that in the absence of thiols, glutathione reductase has a tendency to form tetramers. However, GSH formed helps to maintain GR in its homodimeric configuration (Ahmad et al., 2010; Yousuf et al., 2012).

Catalytic activity of GR and response to abiotic stress

Glutathione reductase undergoes redox interconversion reactions (GSSG to GSH and GSH to GSSG) which depend on the availability of the required substrate (Rao and Reddy, 2008). For every mole of GSSG reduced to GSH, GR requires one mole of NADPH. The enzyme acts like a ping-pong mechanism where a hydride is transferred to FAD as the NADPH binds and it leaves before the di-glutathione binds (Rao and Reddy, 2008). The catalytic mechanism of GR has two phases. The first phase involves the reduction of the flavin moiety by NADPH. GR splits the 2 electrons provided by the reductant NADPH and donates the electrons to each of the two sulfur atoms of GSSG, one at a time. The second phase involves oxidation where the resulting dithiol reacts with GSSG and is reduced to 2 GSH at the active site of the enzyme (Rao and Reddy, 2008; Yousuf et al., 2012). The complete reaction can be represented as:

$$GSSG + NADPH \rightarrow 2GSH + NADP^{+} (\text{by GR})$$

GR helps to regulate the GSH/GSSG ratio and supplies GSH to guaiacol peroxidase (GPX) and dehydroascorbate reductase (DHAR). GPX helps to remove H_2O_2 by combining GSH with H_2O_2 to form H_2O and GSSG while DHAR reduces DHA using the GSH to form AA and GSSG (Dumanović et al., 2021).

$$H_2O_2 + GSH \rightarrow H_2O + GSSG \text{ (by GPX)}$$

$$DHA + GSH \rightarrow AA + GSSG \text{ (by DHAR)}$$

GR catalyses the last rate limiting step of the Halliwell-Asada (AsA-GSH) pathway and is therefore linked with detoxification of ROS and abiotic stress tolerance in plants (Rao and Reddy, 2008; Hasanuzzaman et al., 2010; Hasanuzzaman et al., 2012). The maintenance of AsA and GSH reduced pools inside the cells is vital for ROS scavenging pathways and performing normal physiological activities. By converting GSSG to GSH, GR helps to maintain this equilibrium and thereby provide stress tolerance in plants (Rao and Reddy, 2008). Additionally, increased GR activity levels help increase the $NADP^{+}$/NADPH ratio. Thus, the availability of $NADP^{+}$ to accept electrons from the photosynthetic ETC is ensured, thereby minimizing the formation of ROS species (Mallik et al., 2011). A diagrammatic representation of abiotic stress control by GR is shown in Figure 6. Therefore, an implication of GR in transgenic plants can greatly reduce the ROS induced oxidative stress on the plant and enhance better plant development (Table 2).

Response to drought stress and salinity

Shortages of water and high temperatures that lead to drought-like conditions have serious implications for the cellular machinery of a plant. Drought stress leads to impaired stomatal conductivity, slower rates of electron transport through the membrane transport chain,

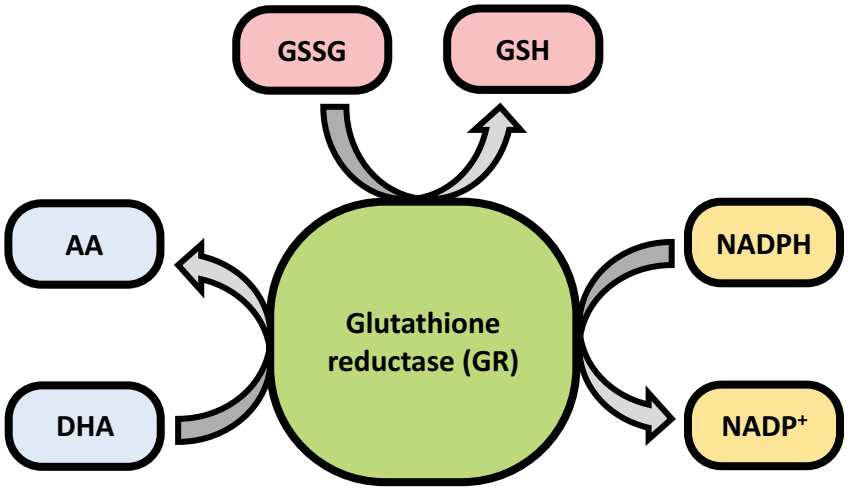


FIGURE 4
Diagram showing the role of glutathione reductase (GR).

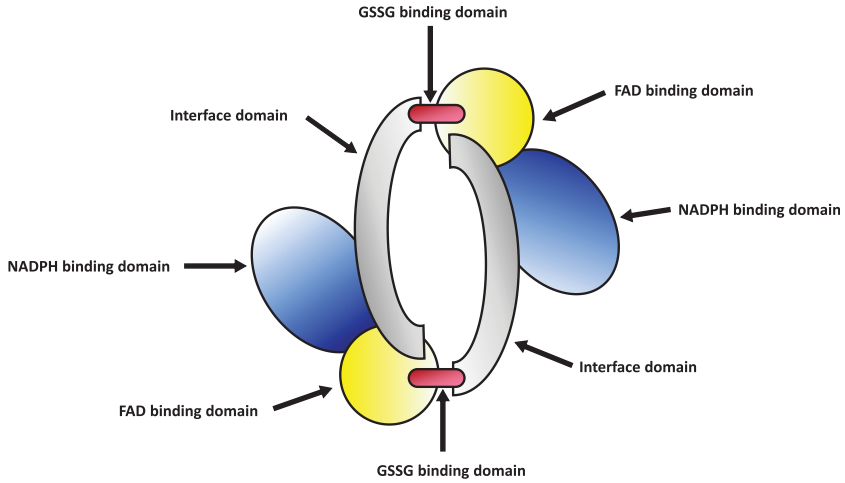


FIGURE 5
Structure of glutathione reductase homodimer.

impaired CO_2 diffusion levels, and reduced rates of photosynthesis. All these effects result in significant levels of ROS that cause extensive oxidative damage. Prolonged exposure to drought stress ultimately leads to reduced growth, resulting in lower crop yields (Grover et al., 2011). Several studies have shown an increase in GR activity when plants are exposed to drought stress (Hasanuzzaman et al., 2017). Water scarcity in *Ctenanthe setosa* results in a characteristic leaf-rolling adaptive response accompanied by increased GSH levels and decreased GSSG levels (Bian and Jiang, 2009; Saruhan et al., 2009). High GSH levels are known to be correlated with water content regulation in leaves (Jiang and Zhang, 2002). Studies have confirmed the effects of elevated GSH levels on drought stress tolerance and the reduction of damages induced by ROS (Bian and Jiang, 2009). GR helps to reduce GSSG to GSH in the presence of NADPH and maintains the reduced GSH pool inside the cell, thereby playing a significant role in stress tolerance. Numerous studies have confirmed the elevated levels of GR activity during drought stress in plants, including barley, maize, wheat, and rice (Kocsy et al., 2002; Chen et al., 2004; Chinnusamy et al., 2005; Selote and Chopra, 2006). A primary effect of drought stress is osmotic stress leading to a sudden change in the solute concentration around the cell and a rapid efflux of water from inside the cell. Kocsy et al. observed that osmotic stress resulted in an increase in GSH levels in wheat seedlings and GR activity in maize (Sumithra et al., 2006). With water scarcity, salinity levels also increase. Saline conditions result in osmotic inhibition and ionic toxicity, affecting normal physiological functions (Demiral and Turkan, 2005; Huang and Guo, 2005b). An increase in GR activity during salinity stress was reported in pea, cantaloupe, soybean, rice, tomato, *Arabidopsis thaliana*, and wheat (Szalai et al., 2009; Repetto et al., 2012; Hasanuzzaman et al., 2013). These results provide conclusive evidence that GR plays a key role during drought and salt stress in plants.

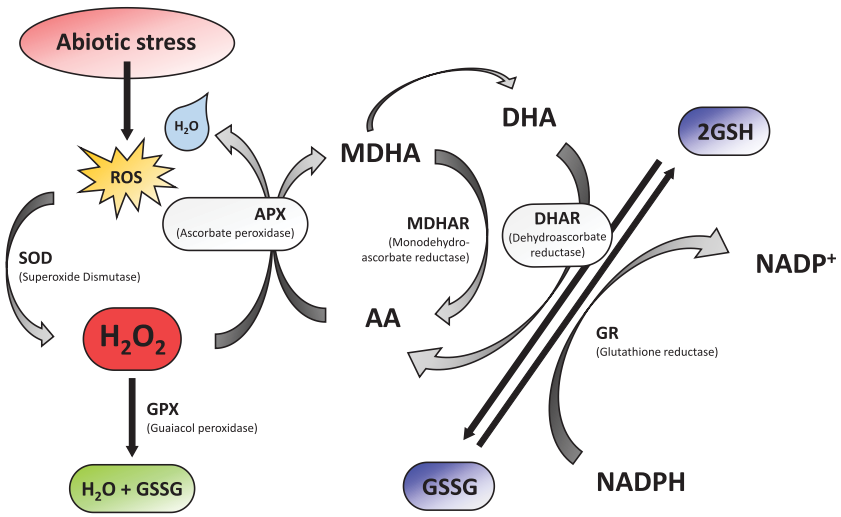


FIGURE 6
Diagram showing control of abiotic stress in plant GR.

TABLE 2 List of a few transgenic approaches implied for improved GR activity in plants.

Sl. No.	Transgenic plant	GR source	Response	Reference
1.	*Nicotiana tabacum* cv Samsun	*Escherichia coli* (gor)	Increase in GR activity by 2-10 folds	(Foyer et al., 1991)
2.	*Nicotiana tabacum* cv SR1	*Escherichia coli* (gor)	Increase in GR activity by 3 folds	(Aono et al., 1993)
3.	*Nicotiana tabacum* cv Samsun	*Pisum sativum* (gor1)	Increase in GR activity by 4.5 folds increase in overall GSH level	(Kornyeyev et al., 2001)
4.	Poplar hybrid (*Populus tremula x Populus alba*)	*Escherichia coli* (gor)	Chloroplasts were reported to show 1000 times higher GR activity; 2-10 times higher GR activity in cytosol; Transgenic plants with increased GR showed resistance to methyl viologen (MV)	(Sairam et al., 1998)
5.	*Brassica juncea*	*Escherichia coli* (gor)	A 2-fold increase of GR activity was noticed in cytosol while chloroplast showed 50 fold increase	(Hasanuzzaman et al., 2017)
6.	*Gossypium hirsutum* cv coker 312	*Arabidopsis thaliana* (GR)	Increased GR activity; Improved photochemical light utilization and decreased cold stress induced photo inhibition of PS II.	(Grover et al., 2011)

Response to extreme temperatures

Extremes of temperature, both high and low, are major factors that contribute to poor crop yield and overall plant development. Higher temperatures result in overproduction of ROS, which leads to increased lipid peroxidation, inactivation of the oxygen evolving complex, membrane damage, and DNA damage (Nahar et al., 2015). Similarly, extreme low temperatures also lead to overproduction of ROS due to membrane fluidity degradation, impaired photosynthetic activity, and improper ROS detoxification (Zhang et al., 2008). This highlights the importance of the GSH pools and GSH redox state as vital components in plant thermotolerance. In some maize varieties, GR activity was reported to increase greatly under high temperature (HT) stress treatment (Sumithra et al., 2006). Elevated levels of GSH in wheat at high temperatures suggest the role of GR in thermotolerance (Nahar et al., 2015a). Similar findings were reported in maize and *Vigna radiata* (Payton et al., 2011). Elevated GSH levels in mustard seedlings suggest efficient eradication of H_2O_2, thereby confirming increased GR activity (Kuk et al., 2003). High levels of GSH and GR activity were also reported in apple during the reproductive stages, further suggesting their enhanced roles in thermotolerance (Kuk et al., 2003). Low ambient temperature limits the activity of enzymes in the Calvin Cycle, disrupting the sulfhydryl groups and reducing CO_2 assimilation (Zitka et al., 2013). Restricted carbon metabolism in the Calvin Cycle leads to insufficient supplies of electron acceptors and overproduction of ROS (Voss et al., 2013). Several studies have shown a positive correlation between cold stress and increased GR activity, including French bean seedlings, rice, and eastern white pine (Peuke and Rennenberg, 2005a; Hasanuzzaman and Fujita, 2013).

Response to heavy metal toxicity

Heavy metals are required for various plant processes and development, but excess heavy metal concentration can lead to toxicity (Peuke and Rennenberg, 2005a). Rapid industrialization has increased heavy metal concentrations in the environment beyond natural sources, disrupting normal physiological growth and generating ROS and oxidative damage (Peuke and Rennenberg, 2005b). To reduce damage and restore normalcy, plants activate various anti-oxidative defense responses, including phytoremediation (Jablonkai, 2022). GSH protects the plant cellular machinery against ROS-oxidative damage in three potential ways: 1) direct quenching of ROS; 2) conjugation of heavy metals and xenobiotic agents to GST; and 3) acting as a precursor for the synthesis of phytochelatins (PCs). By maintaining high levels of PCs, plants can withstand heavy metal stress. GR plays a key role in plant tolerance against heavy metals. GSH is a pivotal factor in the rate-limiting step for phytochelatin formation. The phytochelatins produced form complexes with various heavy metal ions and are sequestered to the vacuole for degradation, thereby limiting oxidative damage (Nahar et al., 2016). Reduced GSH levels are constantly monitored by GR and play a key role in heavy metal stress tolerance. Elevated levels of GR have been reported in Cd-induced stress, and its role in detoxification of ROS via the AsA-GSH cycle has been reported in plants such as radish, soybean, sugarcane, and *Arabidopsis thaliana*.

Conclusion

Abiotic stresses pose a great challenge for plant growth and development by causing physiological, morphological, and biochemical changes in plant cells. The most common manifestation of abiotic stress is the production of ROS. ROS is both a harmful and beneficial molecule. At low or moderate concentrations, it mediates signal transduction that assists in maintaining cellular homeostasis and facilitates plant acclimatization to stresses. However, its overproduction causes significant damage to plant cells, such as lipid peroxidation, DNA damage, etc. The mechanism for maintaining equilibrium between ROS generation and their quenching involves the production of both enzymatic and non-enzymatic antioxidants. In the last two decades, significant progress has been made in effective ROS scavenging through genetic engineering approaches towards the

development of stress-resilient crops. Furthermore, there is a pressing need to identify the genes and understand their mechanisms in the regulation of ROS signaling pathways. Knowledge about the genes and their mechanism of action will definitely help enhance abiotic stress resistance under real agricultural field conditions.

Author contributions

NM and GS provided the fundings. NM and CJ wrote the article. LC and AP gathered the data. AC polished the article.

Funding

This work was supported by grants of the Key Scientific and Technological Grant of Zhejiang for Breeding New Agricultural Varieties (2021C02072-5), Key Research and Development Program of Zhejiang Province (2021C02002) and the International cooperation project of ZAAS (20230012).

Conflict of interest

The authors declare that the research was conducted in the absence of any commercial or financial relationships that could be construed as a potential conflict of interest.

Publisher's note

All claims expressed in this article are solely those of the authors and do not necessarily represent those of their affiliated organizations, or those of the publisher, the editors and the reviewers. Any product that may be evaluated in this article, or claim that may be made by its manufacturer, is not guaranteed or endorsed by the publisher.

References

Aftab, T., and Hakeem, K. R. (2022). *Antioxidant defense in plants: molecular basis of regulation* (Singapore: Springer).

Agarwal, S. (2007). Increased antioxidant activity in cassia seedlings under UV-b radiation. *Biol. Plant* 51, 157–160. doi: 10.1007/s10535-007-0030-z

Ahmad, P., Jaleel, C. A., Salem, M. A., Nabi, G., and Sharma, S. (2010). Roles of enzymatic and nonenzymatic antioxidants in plants during abiotic stress. *Crit. Rev. Biotechnol.* 30 (3), 161–175. doi: 10.3109/07388550903524243

Ahmed, I. M., Cao, F., Zhang, M., Chen, X., Zhang, G., Wu, F., et al (2013). Difference in yield and physiological features in response to drought and salinity combined stress during anthesis in Tibetan wild and cultivated barleys. *PloS One* 8 (10), e77869. doi: 10.1371/journal.pone.0077869

Ajithkumar, I. P., and Panneerselvam, R. (2014). ROS scavenging system, osmotic maintenance, pigment and growth status of panicum sumatrense roth. under drought stress. *Cell Biochem. Biophys.* 68, 587–595. doi: 10.1007/s12013-013-9746-x

Alscher, R. G., Erturk, N., and Heath, L. S. (2002). Role of superoxide dismutases (SODs) in controlling oxidative stress in plants. *J. Exp. Bot.* 53, 1331–1341. doi: 10.1093/jexbot/53.372.1331

Anjum, N. A., Sharma, P., Gill, S. S., Hasanuzzaman, M., Khan, E. A., Kachhap, K., et al. (2016). Catalase and ascorbate peroxidase–representative H2O2-detoxifying heme enzymes in plants. *Environ. Sci. pollut. Res.* 23, 19002–19029. doi: 10.1007/s11356-016-7309-6

Anjum, S. A., Xie, X., Wang, L. C., Saleem, M. F., Man, C., and Lei, W. (2011). Morphological, physiological and biochemical responses of plants to drought stress. *Afr. J. Agric. Res.* 6 (9), 2026–2032. doi: 10.5897/AJAR10.027

Ansari, M. K. A., Zia, M. H., Ahmad, A., Aref, I. M., Fatma, T., Iqbal, M., et al. (2015). Status of antioxidant defense system for detoxification of arsenic in brassica juncea (L.). *Ecoprint: Int. J. Ecol.* 22, 7–19. doi: 10.3126/eco.v22i0.15466

Aono, M., Kubo, A., Saji, H., Natori, T., Tanaka, K., and Kondo, N. (1993). Enhanced tolerance to photooxidative stress of transgenic nicotiana tabacum with high chloroplastic glutathione reductase activity. *Plant Cell Physiol.* 34, 129–135. doi: 10.1093/oxfordjournals.pcp.a078386

Apel, K., and Hirt, H. (2004). Reactive oxygen species: metabolism, oxidative stress, and signal transduction. *Annu. Rev. Plant Biol.* 55, 373–399. doi: 10.1146/annurev.arplant.55.031903.141701

Armada, E., Roldán, A., and Azcon, R. (2014). Differential activity of autochthonous bacteria in controlling drought stress in native lavandula and salvia plants species under drought conditions in natural arid soil. *Microb. Ecol.* 67, 410–420. doi: 10.1007/s00248-013-0326-9

Azevedo, R. A., Alas, R. M., Smith, R. J., and Lea, P. J. (1998). Response of antioxidant enzymes to transfer from elevated carbon dioxide to air and ozone fumigation, in the leaves and roots of wild-type and a catalase deficient mutant of barley. *Physiol. Plant* 104, 280–292. doi: 10.1034/j.1399-3054.1998.1040217.x

Bagheri, R., Ahmad, J., Bashir, H., Iqbal, M., and Qureshi, M. I.. (2017). Changes in rubisco, cysteine-rich proteins and antioxidant system of spinach (Spinacia oleracea l.) due to sulphur deficiency, cadmium stress and their combination. *Protoplasma* 254, 1031–1043. doi: 10.1007/s00709-016-1012-9

Bah, A. M., Dai, H., Zhao, J., Sun, H., Cao, F., Zhang, G., et al. (2011). Effects of cadmium, chromium and lead on growth, metal uptake and antioxidative capacity in typha angustifolia. *Biol. Trace Elem. Res.* 142, 77–92. doi: 10.1007/s12011-010-8746-6

Bauwe, H., Hagemann, M., Kern, R., and Timm, S. (2012). Photorespiration has a dual origin and manifold links to central metabolism. *Curr. Opin. Plant Biol.* 15, 269–275. doi: 10.1016/j.pbi.2012.01.008

Ben-Amor, N., Hamed, K. B., Debez, A., Grignon, C., and Abdelly, C. (2005). Physiological and antioxidant response of the perennial halophytes crithmum maritimum to salinity. *Plant Sci.* 168, 889–899. doi: 10.1016/j.plantsci.2004.11.002

Berwal, M. K., Kumar, R., Prakash, K., Rai, G. K., and Hebbar, K. B. (2021). "Antioxidant defense system in plants against abiotic stress," in *Abiotic stress tolerance mechanisms in plants*. Eds. G. K. Rai, R. R. Kumar and S. Bagati (CRC Press), 175–202.

Bian, S., and Jiang, Y. (2009). Reactive oxygen species, antioxidant enzyme activities and gene expression patterns in leaves and roots of Kentucky bluegrass in response to drought stress and recovery. *Scientia Hortic.* 120 (2), 264–270. doi: 10.1016/j.scienta.2008.10.014

Bonifacio, A., Martins, M. O., Ribeiro, C. W., Fontenele, A. V., Carvalho, F. E., Margis-Pinheiro, M., et al. (2011). Role of peroxidases in the compensation of cytosolic ascorbate peroxidase knockdown in rice plants under abiotic stress. *Plant Cell Environ.* 34, 1705–1722. doi: 10.1111/j.1365-3040.2011.02366.x

Camejo, D., del C. Romero-Puertas, M., Rodríguez-Serrano, M., Sandalio, L. M., Lázaro, J. J., Jiménez, A., et al. (2013). Salinity-induced changes in s-nitrosylation of pea mitochondrial proteins. *J. Proteomics* 79, 87–99. doi: 10.1016/J.JPROT.2012.12.003

Caverzan, A., Passaia, G., Rosa, S. B., Ribeiro, C. W., Lazzarotto, F., and Margis-Pinheiro, M. (2012). Plant responses to stresses: role of ascorbate peroxidase in the antioxidant protection. *Genet. Mol. Biol.* 35, 1011–1019. doi: 10.1590/S1415-47572012000600016

Chen, K. M., Gong, H. J., Chen, G. C., Wang, S. M., and Zhang, C. L. (2004). Gradual drought under field conditions influences the glutathione metabolism, redox balance and energy supply in spring wheat. *J. Plant Growth Regul.* 23, 20–28. doi: 10.1007/s00344-003-0053-4

Chen, T. H., and Murata, N. (2011). Glycinebetaine protects plants against abiotic stress: mechanisms and biotechnological applications. *Plant Cell Environ.* 34, 1–20. doi: 10.1111/j.1365-3040.2010.02232.x

Chen, Z., Pan, Y. H., An, L. Y., Yang, W. J., Xu, L. G., and Zhu, C. (2013). Heterologous expression of a halophilic archaeon manganese superoxide dismutase enhances salt tolerance in transgenic rice. *Russian J. Plant Physiol.* 60, 359–366. doi: 10.1134/S1021443713030059

Chinnusamy, V., Jagendorf, A., and Zhu, J. K. (2005). Understanding and improving salt tolerance in plants. *Crop Sci.* 45, 437–448. doi: 10.2135/cropsci2005.0437

Corpas, F. J., Fernández-Ocaña, A., Carreras, A., Valderrama, R., Luque, F., Esteban, F. J., et al. (2006). The expression of different superoxide dismutase forms is

cell-type dependent in olive (Olea europaea l.) leaves. *Plant Cell Physiol.* 47, 984–994. doi: 10.1093/pcp/pcj071

Cruz, F. J. R., Castro, G. L. S., Júnior, D. D. S., and Pinheiro, H. A. (2013). Exogenous glycine betaine modulates ascorbate peroxidase and catalase activities and prevent lipid peroxidation in mild water stressed carapa guianensis plants. *Photosynthetica* 51, 102–108. doi: 10.1007/s11099-013-0004-7

Csiszar, J., Lantos, E., Tari, I., Madosa, E., Wodala, B., Vashegyi, A., et al. (2007). Antioxidant enzyme activities in allium species and their cultivars under water stress. *Plant Soil Environ.* 53, 517–523. doi: 10.17221/2192-PSE

D'Arcy-Lameta, A., Ferrari-Iliou, R., Contour-Ansel, D., Pham-Thi, A. T., and Zuily-Fodil, Y. (2006). Isolation and characterization of four ascorbate peroxidase cDNAs responsive to water deficit in cowpea leaves. *Ann. Bot.* 97, 133–140. doi: 10.1093/aob/mcj010

Das, K., and Roychoudhury, A. (2014). Reactive oxygen species (ROS) and response of antioxidants as ROS-scavengers during environmental stress in plants. *Front. Environ. Sci.* 2. doi: 10.3389/fenvs.2014.00053

Dat, J. F., Pellinen, R., Beeckman, T., Van De Cotte, B., Langebartels, C., Kangasjarvi, J., et al. (2003). Changes in hydrogen peroxide homeostasis trigger an active cell death process in tobacco. *Plant J.* 33, 621–632. doi: 10.1046/j.1365-313X.2003.01655.x

Deeba, F., Pandey, A. K., Ranjan, S., Mishra, A., Singh, R., Sharma, Y. K., et al. (2012). Physiological and proteomic responses of cotton (Gossypium herbaceum l.) to drought stress. *Plant Physiol. Biochem.* 53, 6–18. doi: 10.1016/j.plaphy.2012.01.002

Demiral, T., and Turkan, I. (2005). Comparative lipid peroxidation, antioxidant defense systems and proline content in roots of two rice cultivars differing in salt tolerance. *Environ. Exp. Bot.* 53, 247–257. doi: 10.1016/j.envexpbot.2004.03.017

De Pinto, M. C., Locato, V., Sgobba, A., Romero-Puertas, M. D. C., Gadaleta, C., Delledonne, M., et al. (2013). S-nitrosylation of ascorbate peroxidase is part of programmed cell death signaling in tobacco bright yellow-2 cells. *Plant Physiol.* 163, 1766–1775. doi: 10.1104/pp.113.222703

Diaz-Vivancos, P., Faize, M., Barba-Espin, G., Faize, L., Petri, C., Hernández, J. A., et al. (2013). Ectopic expression of cytosolic superoxide dismutase and ascorbate peroxidase leads to salt stress tolerance in transgenic plums. *Plant Biotech. J.* 11, 976–985. doi: 10.1111/pbi.12090

Dinakar, C., Djilianov, D., and Bartels, D. (2012). Photosynthesis in desiccation tolerant plants: energy metabolism and antioxidative stress defense. *Plant Sci.* 182, 29–41. doi: 10.1016/j.plantsci.2011.01.018

Doupis, G., Bertaki, M., Psarras, G., Kasapakis, I., and Chartzoulakis, K. (2013). Water relations, physiological behavior and antioxidant defence mechanism of olive plants subjected to different irrigation regimes. *Sci. Horticult.* 153, 150–156. doi: 10.1016/j.scienta.2013.02.010

Dubey, P. K., Singh, G. S., and Abhilash, P. C. (2020). *Agriculture in a changing climate. adaptive agricultural practices: building resilience in a changing climate* (Cham: Springer), 1–10.

Dumanović, J., Nepovimova, E., Natić, M., Kuča, K., and Jaćević, V. (2021). The significance of reactive oxygen species and antioxidant defense system in plants: a concise overview. *Front. Plant Sci.* 11. doi: 10.3389/fpls.2020.552969

Duque, A. S., de Almeida, A. M., da Silva, A. B., da Silva, J. M., Farinha, A. P., Santos, D., et al. (2013). "Abiotic stress responses in plants: unraveling the complexity of genes and networks to survive," in *Abiotic stress: plant responses and applications in agriculture*. Eds. K. Vahdati and C. Leslіepp (In Tech), 49_101.

Ekmekçi, Y., Tanyolac, D., and Ayhan, B. (2008). Effects of cadmium on antioxidant enzyme and photosynthetic activities in leaves of two maize cultivars. *J. Plant Physiol.* 165, 600–611. doi: 10.1016/j.jplph.2007.01.017

Eltayeb, A. E., Kawano, N., Badawi, G. H., Kaminaka, H., Sanekata, T., Shibahara, T., et al. (2007). Overexpression of monodehydroascorbate reductase in transgenic tobacco confers enhanced tolerance to ozone, salt and polyethylene glycol stresses. *Planta* 225, 1255–1264. doi: 10.1007/s00425-006-0417-7

Eltelib, H. A., Fujikawa, Y., and Esaka, M. (2012). Overexpression of the acerola (Malpighia glabra) monodehydroascorbate reductase gene in transgenic tobacco plants results in increased ascorbate levels and enhanced tolerance to salt stress. *S. Afr. J. Bot.* 78, 295–301. doi: 10.1016/j.sajb.2011.08.005

Faize, M., Burgos, L., Faize, L., Piqueras, A., Nicolas, E., Barba-Espin, G., et al. (2011). Involvement of cytosolic ascorbate peroxidase and Cu/Zn-superoxide dismutase for improved tolerance against drought stress. *J. Exp. Bot.* 62, 2599–2613. doi: 10.1093/jxb/erq432

Fink, R. C., and Scandalios, J. G. (2002). Molecular evolution and structurefunction relationships of the superoxide dismutase gene families in angiosperms and their relationship to other eukaryotic and prokaryotic superoxide dismutases. *Arch. Biochem. Biophys.* 399, 19–36. doi: 10.1006/abbi.2001.2739

Ford, K. L., Cassin, A., and Bacic, A. (2011). Quantitative proteomic analysis of wheat cultivars with differing drought stress tolerance. *Front. Plant Sci.* 2. doi: 10.3389/fpls.2011.00044

Foyer, C. H., Lelandais, M., Galap, C., and Kunert, K. J. (1991). Effects of elevated cytosolic glutathione reductase activity on the cellular glutathione pool and photosynthesis in leaves under normal and stress conditions. *Plant Physiol. ogy* 97, 863–872. doi: 10.1104/pp.97.3.863

Foyer, C. H., and Shigeoka, S. (2011). Understanding oxidative stress and antioxidant functions to enhance photosynthesis. *Plant Physiol.* 155, 93–100. doi: 10.1104/pp.110.166181

Gao, Y., Guo, Y. K., Lin, S. H., Fang, Y. Y., and Bai, J. G. (2010). Hydrogen peroxide pretreatment alters the activity of antioxidant enzymes and protects chloroplast ultrastructure in heat-stressed cucumber leaves. *Scientia Hortic.* 126 (1), 20–26. doi: 10.1016/j.scienta.2010.06.006

Gepstein, S. H., and Glick, B. R. (2013). Strategies to ameliorate abiotic stress-induced plant senescence. *Plant Mol. Biol.* 82, 623–633. doi: 10.1007/s11103-013-0038-z

Gill, S. S., Anjum, N. A., Hasanuzzaman, M., Gill, R., Trivedi, D. K., Ahmad, I., et al. (2013). Glutathione and glutathione reductase: a boon in disguise for plant abiotic stress defense operations. *Plant Physiol. Biochem.* 70, 204–212. doi: 10.1016/j.plaphy.2013.05.032

Gill, S. S., and Tuteja, N. (2010). Reactive oxygen species and antioxidant machinery in abiotic stress tolerance in crop plants. *Plant Physiol. Biochem.* 48, 909–930. doi: 10.1016/j.plaphy.2010.08.016

Gomes-Junior, R. A., Moldes, C. A., Delite, F. S., Gratão, P. L., and Mazzafera, P. (2006). Nickel elicits a fast antioxidant response in coffea arabica cells. *Plant Physiol. Biochem.* 44, 420–429. doi: 10.1016/j.plaphy.2006.06.002

Gondim, F. A., Gomes-Filho, E., Costa, J. H., Mendes Alencar, N. L., and Prisco, J. T. (2012). Catalase plays a key role in salt stress acclimation induced by hydrogen peroxide pretreatment in maize. *Plant Physiol. Biochem.* 56, 62–71. doi: 10.1016/j.plaphy.2012.04.012

Grover, A., Singh, A., and Blumwald, E. (2011). "Transgenic strategies toward the development of salt-tolerant plants," in *Agricultural salinity assessment and management, 2nd ed*. Eds. W. W. Wallender and K. K. Tanji (Reston, VA, USA: American Society of Civil Engineers), 235–274.19.

Guan, Q., Wang, Z., Wang, X., Takano, T., and Liu, S. (2015). A peroxisomal APX from puccinellia tenuiflora improves the abiotic stress tolerance of transgenic arabidopsis thaliana through decreasing of H2O2 accumulation. *J. Plant Physiol.* 175, 183–191. doi: 10.1016/j.jplph.2014.10.020

Hajam, Y. A., Lone, R., and Kumar, R. (2023). "Role of plant phenolics against reactive oxygen species (ROS) induced oxidative stress and biochemical alterations," in *Plant phenolics in abiotic stress management*. Eds. R. Lone, S. Khan and A. Mohammed Al-Sadi (Singapore: Springer). doi: 10.1007/978-981-19-6426-8_7

Hasanuzzaman, M., and Fujita, M. (2013). Exogenous sodium nitroprusside alleviates arsenic-induced oxidative stress in wheat (Triticum aestivum l.) seedlings by enhancing antioxidant defense and glyoxalase system. *Ecotoxicology* 22, 584–596. doi: 10.1007/s10646-013-1050-4

Hasanuzzaman, M., Hossain, M. A., and Fujita, M. (2010). Physiological and biochemical mechanisms of nitric oxide induced abiotic stress tolerance in plants. *Am. J. Plant Physiol.* 5. doi: 10.3923/ajpp.2010.295.324

Hasanuzzaman, M., Hossain, M., Silva, J. T., and Fujita, M. (2012). "Plant response and tolerance to abiotic oxidative stress: antioxidant defense is a key factor," in *Crop stress and its management: perspectives and strategies*. Eds. B. Venkateswarlu, A. K. Shanker, C. Shanker and M. Maheswari (Netherlands: Springer), 261e315.

Hasanuzzaman, M., Nahar, K., Alam, M., Roychowdhury, R., and Fujita, M. (2013). Physiological, biochemical, and molecular mechanisms of heat stress tolerance in plants. *Int. J. Mol. Sci.* 14, 9643–9684. doi: 10.3390/ijms14059643

Hasanuzzaman, M., Nahar, K., Anee, T. I., and Fujita, M. (2017). Glutathione in plants: biosynthesis and physiological role in environmental stress tolerance. *Physiol. Mol. Biol. Plants* 23 (2), 249–268. doi: 10.1007/s12298-017-0422-2

Hernandez, J. A., del Rıo, L. A., and Sevilla, F. (2006). Salt stress-induced changes in superoxide dismutase isozymes in leaves and mesophyll protoplasts from vigna unguiculata (L.) walp. *New Phytology* 126, 37–44. doi: 10.1111/j.1469-8137.1994.tb07527.x

Hong, C. Y., Hsu, Y. T., Tsai, Y. C., and Kao, C. H. (2007). Expression of ascorbate peroxidase 8 in roots of rice (Oryza sativa l.) seedlings in response to NaCl. *J. Exp. Bot.* 58, 3273–3283. doi: 10.1093/jxb/erm174

Huang, M., and Guo, Z. (2005a). Responses of antioxidative system to chilling in two rice cultivars differing in sensitivity. *Biol. Plant* 49, 81–84. doi: 10.1007/s00000-005-1084-3

Huang, M., and Guo, Z. (2005b). Responses of antioxidative system to chilling stress in two rice cultivars differing in sensitivity. *Biol. Plant* 49, 81–84. doi: 10.1007/s00000-005-1084-3

Husen, A., Iqbal, M., Sohrab, S. S., and Ansari, M. K. A. (2018). Salicylic acid alleviates salinity-caused damage to foliar functions, plant growth and antioxidant system in Ethiopian mustard (Brassica carinata a. br.). *Agric. Food Secur* 7, 44. doi: 10.1186/s40066-018-0194-0

Hussain, A., Tanveer, M., Brestic, M., Fatma, M., Iqbal, N., and Hashem, A. (2020). Reactive oxygen species and abiotic stress tolerance in plants. *Plant Cell Rep.* 39 (3), 281–292.

Ishikawa, T., Morimoto, Y., Madhusudhan, R., Sawa, Y., Shibata, H., Yabuta, Y., et al. (2005). Acclimation to diverse environmental stresses caused by a suppression of cytosolic ascorbate peroxidase in tobacco BY-2 cells. *Plant Cell Physiol.* 46, 1264–1271. doi: 10.1093/pcp/pci135

Jablonkai, I. (2022). "Molecular defense mechanisms in plants to tolerate toxic action of heavy metal environmental pollution," in *Plant defense mechanisms, June* (IntechOpen). doi: 10.5772/intechopen.102330

Jaleel, C. A., Manivannan, P., Kishorekumar, A., Sankar, B., et al. (2007). Alterations in osmoregulation, antioxidant enzymes and indole alkaloid levels in catharanthus roseus exposed to water deficit. *Colloids Surf B: Biointerfaces* 59, 150–157. doi: 10.1016/j.colsurfb.2007.05.001

Jia, X., Wang, W. X., Ren, L., Chen, Q. J., Mendu, V., Willcut, B., et al. (2009). Differential and dynamic regulation of miR398 in response to ABA and salt stress in populus tremula and arabidopsis thaliana. *Plant Mol. Biol.* 71, 51–59. doi: 10.1007/s11103-009-9508-8

Jiang, M., and Zhang, J. (2002). Water stress-induced abscisic acid accumulation triggers the increased generation of reactive oxygen species and up-regulates the activities of antioxidant enzymes in maize leaves. *J. Exp. Bot.* 53, 2401–2410. doi: 10.1093/jxb/erf090

Khan, I., Ahmad, A., and Iqbal, M. (2009). Modulation of antioxidant defense system for arsenic detoxification in Indian mustard. *Ecotoxic. Environ. Saf.* 72, 626–634. doi: 10.1016/j.ecoenv.2007.11.016

Khan, M. I., Fatma, M., Per, T. S., Anjum, N. A., and Khan, N. A. (2015). Salicylic acid-induced abiotic stress tolerance and underlying mechanisms in plants. *Front. Plant Sci.* 6, 462. doi: 10.3389/fpls.2015.00462

Khan, A., Numan, M., Khan, A. L., Lee, I.-J., Imran, M., Asaf, S., et al. (2020). Melatonin: awakening the defense mechanisms during plant oxidative stress. *Plants* 9 (4), 407. doi: 10.3390/plants9040407

Khatun, S., Babar, M., Hahn, E., and Paek, K. (2008). Copper toxicity in withania somnifera : growth and antioxidant enzymes responses of *in vitro* grown plants. *J. Environ. Exp. Bot.* 64, 279–285. doi: 10.1016/j.envexpbot.2008.02.004

Kocsy, G., Szalai, G., and Galiba, G. (2002). Induction of glutathione synthesis and glutathione reductase activity by abiotic stresses in maize and wheat. *Sci. World J.* 2, 1726–1732. doi: 10.1100/tsw.2002.812

Kornyeyev, D., Logan, B. A., Payton, P., Allen, R. D., and Holaday, A. S. (2001). Enhanced photochemical light utilization and decreased chilling induced photoinhibition of photosystem II in cotton over expressing genes encoding chloroplast targeted antioxidant enzymes. *Physiol. Plant* 113, 323–331. doi: 10.1034/j.1399-3054.2001.1130304.x

Koussevitzky, S., Suzuki, N., Huntington, S., Armijo, L., Sha, W., Cortes, D., et al. (2008). Ascorbate peroxidase 1 plays a key role in the response of arabidopsis thaliana to stress combination. *J. Biol. Chem.* 283, 34197–34203. doi: 10.1074/jbc.M806337200

Kuk, Y. I., Shin, J. S., Burgos, N. R., Hwang, T. E., Han, O., Cho, B. H., et al. (2003). Antioxidative enzymes offer protection from chilling damage in rice plants. *Crop Sci.* 43, 2109–2117. doi: 10.2135/cropsci2003.2109

Kumar, N., Singh, H., and Sharma, S. K. (2020). "Antioxidants: responses and importance in plant defense system," in *Sustainable agriculture in the era of climate change*. Eds. R. Roychowdhury, S. Choudhury, M. Hasanuzzaman and S. Srivastava (Cham: Springer), 251–264.

Kumar, D., Yusuf, M. A., Singh, P., Sardar, M., and Sarin, N. B. (2013). Modulation of antioxidant machinery in α-tocopherol-enriched transgenic brassica juncea plants tolerant to abiotic stress conditions. *Protoplasma* 250, 1079–1089. doi: 10.1007/s00709-013-0484-0

Kwon, S., Jeong, Y., Lee, H., Kim, J., Cho, K., Allen, R., et al. (2002). Enhanced tolerances of transgenic tobacco plants expressing both superoxide dismutase and ascorbate peroxidase in chloroplasts against methyl viologen mediated oxidative stress. *Plant Cell Environ.* 25, 873–882. doi: 10.1046/j.1365-3040.2002.00870.x

A. A. H. A. Latef (Ed.) (2021). *Organic solutes, oxidative stress, and antioxidant enzymes under abiotic stressors. 1st ed* (CRC Press). doi: 10.1201/9781003022879

Lazzarotto, F., Teixeira, F. K., Rosa, S. B., Dunand, C., Fernandes, C. L., de Vasconcelos Fontenele, A., et al. (2011). Ascorbate peroxidaserelated (APx-r) is a new heme-containing protein functionally associated with ascorbate peroxidase but evolutionarily divergent. *New Phytol.* 191, 234–250. doi: 10.1111/j.1469-8137.2011.03659.x

Lee, Y. P., Ahmad, R., Lee, H. S., Kwak, S. S., Shafqat, M. N., and Kwon, S. Y. (2013). Improved tolerance of Cu/Zn superoxide dismutase and ascorbate peroxidase expressing transgenic tobacco seeds and seedlings against multiple abiotic stresses. *Int. J. Agric. Biol.* 15, 725–730.

Lee, S. H., Ahsan, N., Lee, K. W., Kim, D. H., Lee, D. G., Kwak, S. S., et al. (2007). Simultaneous overexpression of both CuZn superoxide dismutase and ascorbate peroxidase in transgenic tall fescue plants confers increased tolerance to a wide range of abiotic stresses. *J. Plant Physiol.* 164, 1626–1638. doi: 10.1016/j.jplph.2007.01.003

Li, Y. J., Hai, R. L., Du, X. H., Jiang, X. N., and Lu, H. (2009). Overexpression of a populus peroxisomal ascorbate peroxidase (PpAPX) gene in tobacco plants enhances stress tolerance. *Plant Breed.* 128, 404–410. doi: 10.1111/j.1439-0523.2008.01593.x

Lim, S., Kim, Y. H., Kim, S. H., Kwon, S. Y., Lee, H. S., Kim, J. S., et al. (2007). Enhanced tolerance of transgenic sweetpotato plants that express both CuZnSOD and APX in chloroplasts to methyl viologen-mediated oxidative stress and chilling. *Mol. Breed.* 19, 227–239. doi: 10.1007/s11032-006-9051-0

Lu, Z., Liu, D., and Liu, S. (2007). Two rice cytosolic ascorbate peroxidases differentially improve salt tolerance in transgenic arabidopsis. *Plant Cell Rep.* 26, 1909–1917. doi: 10.1007/s00299-007-0395-7

Mahanty, S., Kaul, T., Pandey, P., Reddy, R. A., Mallikarjuna, G., Reddy, C. S., et al. (2012). Biochemical and molecular analyses of copper_zinc superoxide dismutase from a C4 pennisetum glaucum reveals an adaptive role in response to oxidative stress. *Gene* 505, 309–317. doi: 10.1016/j.gene.2012.06.001

Malar, S., Vikram, S. S., Favas, P. J. C., and Perumal, V. (2014). Lead heavy metal toxicity induced changes on growth and antioxidative enzymes level in water hyacinths [Eichhornia crassipes (Mart.)]. *Bot. Stud.* 55, 54. doi: 10.1186/s40529-014-0054-

Mallik, S., Nayak, M., Sahu, B. B., Panigrahi, A. K., and Shaw, B. P. (2011). Response of antioxidant enzymes to high NaCl concentration in different salt-tolerant plants. *Biol. Plant* 55, 191–195. doi: 10.1007/s10535-011-0029-3

Markovska, Y. K., Gorinova, N. I., Nedkovska, M. P., and Miteva, K. M. (2009). Cadmium-induced oxidative damage and antioxidant responses in brassica juncea plants. *Biol. Plant* 53, 151–154. doi: 10.1007/s10535-009-0023-1

Maruta, T., Tanouchi, A., Tamoi, M., Yabuta, Y., Yoshimura, K., Ishikawa, T., et al. (2010). Arabidopsis chloroplastic ascorbate peroxidase isoenzymes play a dual role in photoprotection and gene regulation under photooxidative stress. *Plant Cell Physiol.* 51 (2), 190–200. doi: 10.1093/pcp/pcp177

Matos, I. F., Morales, L. M. M., Santana, D. B., Silva, G. M. C., Gomes, M. M. A., Ayub, R. A., et al. (2022). Ascorbate synthesis as an alternative electron source for mitochondrial respiration: possible implications for the plant performance. *Front. Plant Sci.* 13. doi: 10.3389/fpls.2022.987077

Mhamdi, A., Queval, G., Chaouch, S., Vanderauwera, S., Van Breusegem, F., and Noctor, G. (2010). Catalase function in plants: a focus on arabidopsis mutants as stress-mimic models. *J. Exp. Bot.* 61 (15), 4197–4220. doi: 10.1093/jxb/erq282

Miller, G., Suzuki, N., Rizhsky, L., Hegie, A., Koussevitzky, S., and Mittler, R. (2007). Double mutants deficient in cytosolic and thylakoid ascorbate peroxidase reveal a complex mode of interaction between reactive oxygen species, plant development, and response to abiotic stresses. *Plant Physiol.* 144, 1777–1785. doi: 10.1104/pp.107.101436

Minhas, P. S., Rane, J., and Pasala, R. K. (2017). "Abiotic stresses in agriculture: an overview," in *Abiotic stress management for resilient agriculture* (Singapore: Springer), 3–8.

Mishra, P., Bhoomika, K., and Dubey, R. S. (2013). Differential responses of antioxidative defense system to prolonged salinity stress in salttolerant and salt-sensitive indica rice (Oryza sativa l.) seedlings. *Protoplasma* 250, 3–19. doi: 10.1007/s00709-011-0365-3

Mittler, R. (2002). Oxidative stress, antioxidants and stress tolerance. *Trends Plant Sci.* 7, 405–410. doi: 10.1016/S1360-1385(02)02312-9

Mittler, R. (2006). Abiotic stress, the field environment and stress combination. *Trends Plant Sci.* 11, 15–19. doi: 10.1016/j.tplants.2005.11.002

Mittler, R., Vanderauwera, S., Suzuki, N., Miller, G., Tognetti, V. B., Vandepoele, K., et al. (2011). ROS signaling: the new wave? *Trends Plant Sci.* 16, 300–309. doi: 10.1016/j.tplants.2011.03.007

Mutlu, S., Karadagoglu, O., Atici, O., and Nalbantoglu, B. (2013). Protective role of salicylic acid applied before cold stress on antioxidative system and protein patterns in barley apoplast. *Biol. Plantarum* 57, 507–513. doi: 10.1007/s10535-013-0322-4

Mylona, P. V., and Polidoros, A. N. (2010). "ROS regulation of antioxidant genes," in *Reactive oxygen species and antioxidants in higher plants*. Ed. S. D. Gupta (Science Publishers), 101–127.

Mylona, P. V., Polidoros, A. N., and Scandalios, J. G. (2007). Antioxidant gene responses to ROS-generating xenobiotics in developing and germinated scutella of maize. *J. Exp. Bot.* 58, 1301–1312. doi: 10.1093/jxb/erl292

Nagajyoti, P. C., Lee, K. D., and Sreekanth, T. V. M. (2010). Heavy metals, occurrence and toxicity for plants: a review. *Environ. Chem. Lett.* 8, 199–216. doi: 10.1007/s10311-010-0297-8

Nageshbabu, R., and Jyothi, M. N. (2013). Profile of small interfering RNAs from french bean phaseolus vulgaris under abiotic stress conditions. *Int. J. Pharm. Bio. Sci.* 4, 176–185.

Nahar, K., Hasanuzzaman, M., Alam, M. M., and Fujita, M. (2015). Glutathione-induced drought stress tolerance in mung bean: coordinated roles of the antioxidant defence and methylglyoxal detoxification systems. *AoB Plants*. doi: 10.1093/aobpla/plv069

Nahar, K., Rahman, M., Hasanuzzaman, M., Alam, M. M., Rahman, A., Suzuki, T., et al. (2016). Physiological and biochemical mechanisms of spermine-induced cadmium stress tolerance in mung bean (Vigna radiata l.) seedlings. *Environ. Sci. pollut. Res. Int.* 23 (21), 21206–21218. doi: 10.1007/s11356-016-7295-8

Najami, N., Janda, T., Barriah, W., Kayam, G., Tal, M., Guy, M., et al. (2008). Ascorbate peroxidase gene family in tomato: its identification and characterization. *Mol. Genet. Genomics* 279, 171–182. doi: 10.1007/s00438-007-0305-2

Nakano, T., Suzuki, K., and Fujimura, T. (2006). Shinkei-kasokuka (SK) genes encode previously unknown zinc finger proteins involved in oxidative stress response in yeast. *J. Biol. Chem.* 281 (39), 28389–28397.

Narendra, S., Venkataramani, S., Shen, G., Wang, J., Pasapula, V., Lin, Y., et al. (2006). The arabidopsis ascorbate peroxidase 3 is a peroxisomal membranebound antioxidant enzyme and is dispensable for arabidopsis growth and development. *J. Exp. Bot.* 57, 3033–3042. doi: 10.1093/jxb/erl060

Nareshkumar, A., Veeranagamallaiah, G., Pandurangaiah, M., Kiranmai, K., Amaranathareddy, V., Lokesh, U., et al. (2015). Pb-Stress induced oxidative stress caused alterations in antioxidant efficacy in two groundnut (Arachis hypogaea l.) cultivars. *Agric. Sci.* 6, 1283–1297. doi: 10.4236/as.2015.610123

Nawaz, M., Anjum, S. A., Ashraf, U., Azeem, F., and Wang, Z. (2021). "Antioxidant defense system and reactive oxygen species (ROS) interplay in plants under drought condition," in *Handbook of climate change management*. Eds. J. M. Luetz and D. Ayal (SpringerCham), 93–117. doi: 10.1007/978-3-030-57281-5_121

Nawaz, M., and Wang, Z. (2020). Abscisic acid and glycine betaine mediated tolerance mechanisms under drought stress and recovery in axonopus compressus: a new insight. *Sci. Rep.* 10, 6942. doi: 10.1038/s41598-020-63447-0

Nazar, R., Iqbal, N., Syeed, S., and Khan, N. A. (2011). Salicylic acid alleviates decreases in photosynthesis under salt stress by enhancing nitrogen and sulfur assimilation and antioxidant metabolism differentially in two mungbean cultivars. *J. Plant Physiol.* 168, 807–815. doi: 10.1016/j.jplph.2010.11.001

Nouairi, I., Ammar, W. B., Youssef, N. B., Miled, D. D. B., Ghorbal, M. H., and Zarrouk, M. (2009). Antioxidant defense system in leaves of Indian mustard (Brassica juncea) and rape (Brassica napus) under cadmium stress. *Acta Physiol. Plant* 31, 237–247. doi: 10.1007/s11738-008-0224-9

Nounjan, N., Nghia, P. T., and Theerakulpisut, P. (2012). Exogenous proline and trehalose promote recovery of rice seedlings from salt-stress and differentially modulate antioxidant enzymes and expression of related genes. *J. Plant Physiol.* 169, 596–604. doi: 10.1016/j.jplph.2012.01.004

Oliva, M., Theiler, G., Zamocky, M., Koua, D., Margis-Pinheiro, M., Passardi, F., et al. (2009). PeroxiBase: a powerful tool to collect and analyse peroxidase sequences from viridiplantae. *J. Exp. Bot.* 60, 453–459. doi: 10.1093/jxb/ern317

Pan, Y., Wu, L. J., and Yu, Z. L. (2006). Effect of salt and drought stress on antioxidant enzymes activities and SOD isoenzymes of liquorice (Glycyrrhiza uralensis fisch). *Plant Growth Regul.* 49, 157–165. doi: 10.1007/s10725-006-9101-y

Panda, S. K., and Matsumoto, H. (2010). Changes in antioxidant gene expression and induction of oxidative stress in pea (Pisum sativum l.) under Al stress. *Biometals* 23, 753–762. doi: 10.1007/s10534-010-9342-0

Park, S. Y., Ryu, S. H., Jang, I. C., Kwon, S. Y., Kim, J. G., and Kwak, S. S. (2004). Molecular cloning of a cytosolic ascorbate peroxidase cDNA from cell cultures of sweetpotato and its expression in response to stress. *Mol. Genet. Genomics* 271, 339–346. doi: 10.1007/s00438-004-0986-8

Passardi, F., Bakalovic, N., Teixeira, F. K., Margis-Pinheiro, M., Penel, C., and Dunand, C. (2007). Prokaryotic origins of the nonanimal peroxidase superfamily and organelle-mediated transmission to eukaryotes. *Genomics* 89, 567–579. doi: 10.1016/j.ygeno.2007.01.006

Payton, P., Webb, R., Kornyeyev, D., Allen, R., and Holaday, A. S. (2011). Protecting cotton photosynthesis during moderate chilling at high light intensity by increasing chloroplastic antioxidant enzyme activity. *J. Exp. Bot.* 52, 2345–2354. doi: 10.1093/jexbot/52.365.2345

Peng, H. Y., Yang, X. E., Yang, M. J., and Tian, S. K. (2006). Responses of antioxidant enzyme system to copper toxicity and copper detoxification in the leaves of elsholtzia splendens. *J. Plant Nutr.* 29, 1619–1635. doi: 10.1080/01904160600851478

Peñuelas, J., and Munné-Bosch, S. (2005). Isoprenoids: an evolutionary pool for photoprotection. *Trends Plant Sci.* 10, 166–169. doi: 10.1016/j.tplants.2005.02.005

Peuke, A. D., and Rennenberg, H. (2005a). Phytoremediation with transgenic trees. *Z Naturforsch.* 60, 199–207.

Peuke, A. D., and Rennenberg, H. (2005b). Phytoremediation: molecular biology, requirements for application, environmental protection, public attention and feasibility. *EMBO Rep.* 6, 497–501. doi: 10.1038/sj.embor.7400445

Pinheiro, C., and Chaves, M. M. (2011). Photosynthesis and drought: can we make metabolic connections from available data? *J. Exp. Bot.* 62, 869–882. doi: 10.1093/jxb/erq340

Pinto, A. P., Alves, A. S., Candeias, A. J., Cardoso, A. I., de Varennes, A., Martins, L. L., et al. (2009). Cadmium accumulation and antioxidative defenses in brassica juncea l. czern, nicotiana tabacum l. and solanum nigrum l. *Int. J. Environ. Anal. Chem.* 89, 661–676. doi: 10.1080/03067310902962585

Pourcel, L., Routaboul, J. M., Cheynier, V., Lepiniec, L., and Debeaujon, I. (2007). Flavonoid oxidation in plants: from biochemical properties to physiological functions. *Trends Plant Sci.* 12, 29–36. doi: 10.1016/j.tplants.2006.11.006

Rahman, S., Iqbal, M., and Husen, A. (2023). "Medicinal plants and abiotic stress: an overview," in *Medicinal plants*. Eds. A. Husen and M. Iqbal (Singapore: Springer). doi: 10.1007/978-981-19-5611-9_1

Rajput, V. D., Singh, R. K., Verma, K. K., Sharma, L., Quiroz-Figueroa, F. R., Meena, M., et al. (2021). Recent developments in enzymatic antioxidant defence mechanism in plants with special reference to abiotic stress. *Biology* 10 (4), 267. doi: 10.3390/biology10040267

Ramakrishna, A., and Gill, S. S. (2018). Metabolic adaptations in plants during abiotic stress. *CRC Press Boca Raton*, 442.

Rao, A. S. V. C., and Reddy, A. R. (2008). "Glutathione reductase: a putative redox regulatory system in plant cells," in *Sulfur assimilation and abiotic stress in plants*. Eds. N. A. Khan, S. Singh and S. Umar (Berlin: Springer). doi: 10.1007/978-3-540-76326-0_6

Rasool, S., Ahmad, A., Siddiqi, T. O., and Ahmad, P. (2013). Changes in growth, lipid peroxidation and some key antioxidant enzymes in chickpea genotypes under salt stress. *Acta Physiologia Plantarum* 35, 1039–1050. doi: 10.1007/s11738-012-1142-4

Repetto, M., Semprine, J., and Boveris, A. (2012). "Lipid peroxidation: chemical mechanism, biological implications and analytical determination," in *Lipid peroxidation*. Ed. A. Catala (Rijeka, Croatia: InTech), 3–30.

Rosa, S. B., Caverzan, A., Teixeira, F. K., Lazzarotto, F., Silveira, J. A., Ferreira-Silva, S. L., et al. (2010). Cytosolic APX knockdown indicates an ambiguous redox response in rice. *Phytochemistry* 71, 548–558. doi: 10.1016/j.phytochem.2010.01.003

Rossa, M. M., de Oliveira, M. C., Okamoto, O. K., Lopes, P. F., and Colepicolo, P. (2002). Effect of visible light on superoxide dismutase (SOD) activity in the red alga *Gracilariopsis tenuifrons* (Gracilariales, rhodophyta). *J. Appl. Phycology* 14, 151–157. doi: 10.1023/A:1019985722808

Roychoudhury, A., and Ghosh, S. (2013). Physiological and biochemical responses of mungbean (Vigna radiata l. wilczek) to varying concentrations of cadmium chloride or sodium chloride. *Unique J. Pharm. Biol. Sci.* 1, 11–21.

Sairam, R. K., Shukla, D. S., and Saxena, D. C. (1998). Stress-induced injury and antioxidant enzymes in relation to drought tolerance in wheat genotypes. *Biol. Plant* 40, 357–364. doi: 10.1023/A:1001009812864

Sairam, R. K., Srivastava, G. C., Agarwal, S., and Meena, R. C. (2005). Differences in antioxidant activity in response to salinity stress in tolerant and susceptible wheat genotypes. *Biol. Plantarum* 49, 85–91. doi: 10.1007/s10535-005-5091-2

Saruhan, N., Terzi, R., Saglam, A., and Kadioglu, A. (2009). The relationship between leaf rolling and ascorbate-glutathione cycle enzymes in apoplastic and symplastic areas of ctenanthe setosa subjected to drought stress. *Biol. Res.* 42, 315–326. doi: 10.4067/S0716-97602009000300006

Sato, Y., Masuta, Y., and Saito, K. (2011). Enhanced chilling tolerance at the booting stage in rice by transgenic overexpression of the ascorbate peroxidase gene, OsAPXa. *Plant Cell Rep.* 30, 399–406. doi: 10.1007/s00299-010-0985-7

Secenji, M., Hideg, É., Bebes, A., and Györgyey, J. (2009). Trans ˇ criptional differences in gene families of the ascorbate-glutathione cycle in wheat during mild water deficit. *Plant Cell Rep.* 29, 37–50. doi: 10.1007/s00299-009-0796-x

Sekmen, A. H., Türkan, I., and Takio, S. (2007). Differential responses of antioxidative enzymes and lipid peroxidation to salt stress in salt-tolerant plantago maritima and salt-sensitive plantago media. *Physiol. Plant* 131, 399–411. doi: 10.1111/j.1399-3054.2007.00970.x

Selote, D. S., and Chopra, R. K. (2006). Drought acclimation confers oxidative stress tolerance by inducing co-ordinated antioxidant defense at cellular and subcellular level in leaves of wheat seedlings. *Physiol. Plant* 127, 494–450. doi: 10.1111/j.1399-3054.2006.00678.x

Sen, A., and Alikamanoglu, S. (2013). Antioxidant enzyme activities, malondialdehyde, and total phenolic content of PEG-induced hyperhydric leaves in sugar beet tissue culture. *In Vitro Cell. Dev. Biology-Plant* 49, 396–404. doi: 10.1007/s11627-013-9511-2

Shao, H. B., Chu, L. Y., Wu, G., Zhang, J. H., Lu, Z. H., and Hu, Y. C. (2007). Changes of some anti-oxidative physiological indices under soil water deficits among 10 wheat (Triticum aestivum) genotypes at tillering stage. *Biointerfaces* 59, 113–119. doi: 10.1016/j.colsurfb.2006.09.004

Sharma, P., and Dubey, R. S. (2005). Drought induces oxidative stress and enhances the activities of antioxidant enzymes in growing rice seedlings. *Plant Growth Regul.* 46, 209–221. doi: 10.1007/s10725-005-0002-2

Sharma, P., and Dubey, R. S. (2007). Involvement of oxidative stress and role of antioxidative defense system in growing rice seedlings exposed to toxic concentrations of aluminum. *Plant Cell Rep.* 26, 2027–2038. doi: 10.1007/s00299-007-0416-6

Sharma, P., Jha, A. B., Dubey, R. S., and Pessarakli, M. (2012). Reactive oxygen species, oxidative damage, and antioxidative defense mechanism in plants under stressful conditions. *J. Bot.*, 1–26. doi: 10.1155/2012/217037

Sheokand, S., Kumari, A., and Sawhney, V. (2008). Effect of nitric oxide and putrescine on antioxidative responses under NaCl stress in chickpea plants. *Physiol. Mol. Biol. Plants* 14, 355–362. doi: 10.1007/s12298-008-0034-y

Siddiqui, Z. S. (2013). Effects of double stress on antioxidant enzyme activity in vigna radiata (L.) wilczek. *Acta Bot. Croatica* 72, 145–156. doi: 10.2478/v10184-012-0011-y

Singh, N., Mishra, A., and Jha, B. (2014). Ectopic over-expression of peroxisomal ascorbate peroxidase (SbpAPX) gene confers salt stress tolerance in transgenic peanut (Arachis hypogaea). *Gene* 547, 119–125. doi: 10.1016/j.gene.2014.06.037

Smeets, K., Ruytinx, J., Semane, B., Van Belleghem, F., Remans, T., Van Sanden, S., et al. (2008). Cadmium-induced transcriptional and enzymatic alterations related to oxidative stress. *Environ. Exp. Bot.* 63, 1–8. doi: 10.1016/j.envexpbot.2007.10.028

Sobhanian, H., Aghaei, K., and Komatsu, S. (2011). Changes in the plant proteome resulting from salt stress: toward the creation of salt-tolerant crops? *J. Proteomics* 74, 1323–1337. doi: 10.1016/j.jprot.2011.03.018

Sofo, A., Dichio, B., Xiloyannis, C., and Masia, A. (2005a). Antioxidant defences in olive tree during drought stress: changes in activity of some antioxidant enzymes. *Funct. Plant Biol.* 32, 45–53. doi: 10.1071/FP04003

Sofo, A., Tuzio, A. C., Dichio, B., and Xiloyannis, C. (2005b). Influence of water deficit and rewatering on the components of the ascorbate – glutathione cycle in four interspecific prunus hybrids. *Plant Sci.* 169, 403–412. doi: 10.1016/j.plantsci.2005.04.004

Song, X. S., Hu, W. H., Mao, W. H., Ogweno, J. O., Zhou, Y. H., and Yu, J. Q. (2005). Response of ascorbate peroxidase isoenzymes and ascorbate regeneration system to abiotic stresses in cucumis sativus l. *Plant Physiol. Biochem.* 43, 1082–1088. doi: 10.1016/j.plaphy.2005.11.003

Sorkheh, K., Shiran, B., Khodambashi, M., Rouhi, V., Mosavei, S., and Sofo, A. (2012a). Exogenous proline alleviates the effects of H2O2-induced oxidative stress in

wild almond species (Prunus spp.). *Russ. J. Plant Physiol.* 59, 788–798. doi: 10.1134/S1021443712060167

Sorkheh, K., Shiran, B., Rouhi, V., Khodambashi, M., and Sofo, A. (2012b). Salt stress induction of some key antioxidant enzymes and metabolites in eight Iranian wild almond species. *Acta Physiol. Plant* 34, 203–213. doi: 10.1007/s11738-011-0819-4

Srivalli, B., Chinnusamy, V., and Khanna-Chopra, R. (2003). Antioxidant defense in response to abiotic stresses in plants. *J. Plant Biol.* 30, 121–139.

Sumithra, K., Jutur, P. P., Dalton, C. B., and Reddy, A. R. (2006). Salinity-induced changes in two cultivars of vigna radiata: responses of antioxidative and proline metabolism. *Plant Growth Regul.* 50, 11–22. doi: 10.1007/s10725-006-9121-7

Sun, W. H., Duan, M., Shu, D. F., Yang, S., and Meng, Q. W. (2010). Overexpression of StAPX in tobacco improves seed germination and increases early seedling tolerance to salinity and osmotic stresses. *Plant Cell Rep.* 29, 917–926. doi: 10.1007/s00299-010-0878-9

Sunkar, R., Kapoor, A., and Zhu, J. K. (2006). Post-transcriptional induction of two Cu/Zn superoxide dismutase genes in arabidopsis is mediated by down-regulation of miR398 and important for oxidative stress tolerance. *Plant Cell* 18, 2051–2065. doi: 10.1105/tpc.106.041673

Szalai, G., Kellos, T., Galiba, G., and Kocsy, G. (2009). Glutathione as an antioxidant and regulatory molecule in plantsunder abiotic stress conditions. *Plant Growth Regul.* 28, 66–80. doi: 10.1007/s00344-008-9075-2

Szepesi, A., Poor, P., Gémes, K., Horvath, E., and Tari, I. (2008). Influence of exogenous salicylic acid on antioxidant enzyme activities in the roots of salt stressed tomato plants. *Acta Biologica Szegediensis* 52, 199–200.

Tang, L., Kwon, S. Y., Kim, S. H., Kim, J. S., Choi, J. S., Cho, K. Y., et al. (2006). Enhanced tolerance of transgenic potato plants expressing both superoxide dismutase and ascorbate peroxidase in chloroplasts against oxidative stress and high temperature. *Plant Cell Rep.* 25, 1380–1386. doi: 10.1007/s00299-006-0199-1

Tanou, G., Filippou, P., Belghazi, M., Job, D., Diamantidis, G., Fotopoulos, V., et al. (2012). Oxidative and nitrosative-based signaling and associated post-translational modifications orchestrate the acclimation of citrus plants to salinity stress. *Plant J.* 72, 585–599. doi: 10.1111/j.1365-313X.2012.05100.x

Tari, I., Camen, D., Coradini, G., Csiszar, J., Fediuc, E., Gémes, K., et al. (2008). Changes in chlorophyll fluorescence parameters and oxidative stress responses of bush bean genotypes for selecting contrasting acclimation strategies under water stress. *Acta Biologica Hungarica* 59, 335–345. doi: 10.1556/ABiol.59.2008.3.7

Teixeira, F. K., Menezes-Benavente, L., Galvão, V. C., Margis, R., and Margis-Pinheiro, M. (2006). Rice ascorbate peroxidase gene family encodes functionally diverse isoforms localized in different subcellular compartments. *Planta* 224, 300–314. doi: 10.1007/s00425-005-0214-8

Teixeira, F. K., Menezes-Benavente, L., Galvão, V. C., and MargisPinheiro, M. (2005). Multigene families encode enzymes of antioxidant metabolism in eucalyptus grandis l. *Genet. Mol. Biol.* 28, 529–538. doi: 10.1590/S1415-47572005000400007

Teixeira, F. K., Menezes-Benavente, L., Margis, R., and Margis Pinheiro, M. (2004). Analysis of the molecular evolutionary history of the ascorbate peroxidase gene family: inferences from the rice genome. *J. Mol. Evol.* 59, 761–770. doi: 10.1007/s00239-004-2666-z

Tertivanidis, K., Goudoula, C., Vasilikiotis, C., Hassiotou, E., Perl-Treves, R., and Tsaftaris, A. (2004). Superoxide dismutase transgenes in sugar beets confer resistance to oxidative agents and the fungus c. beticola. *Transgenic Res.* 13, 225–233. doi: 10.1023/B:TRAG.0000034610.35724.04

Tuteja, N., and Gill, S. S. (2013). *Crop improvement under adverse conditions. 1st edn* (New York: Springer).

Upadhyaya, H., Panda, S. K., and Dutta, B. K. (2008). Variation of physiological and antioxidative responses in tea cultivars subjected to elevated water stress followed by rehydration recovery. *Acta Physiol. Plant* 30, 457–468. doi: 10.1007/s11738-008-0143-9

Uzilday, B., Turkan, I., Sekmen, A. H., Ozgur, R., and Karakaya, H. C. (2012). Comparison of ROS formation and antioxidant enzymes in cleome gynandra (C4) and cleome spinosa (C3) under drought stress. *Plant Sci.* 182, 59–70. doi: 10.1016/j.plantsci.2011.03.015

Vanderauwera, S., Suzuki, N., Miller, G., van de Cotte, B., Morsa, S., Ravanat, J. L., et al. (2011). Extranuclear protection of chromosomal DNA from oxidative stress. *Proc. Natl. Acad. Sci. U.S.A.* 108, 1711–1716. doi: 10.1073/pnas.1018359108

Vanderauwera, S., Vandenbroucke, K., Inzé, A., van de Cotte, B., Mühlenbock, P., de Rycke, R., et al. (2012). AtWRKY15 perturbation abolishes the mitochondrial stress response that steers osmotic stress tolerance in arabidopsis. *Proc. Natl. Acad. Sci. U.S.A.* 109, 20113–20118. doi: 10.1073/pnas.1217516109

Vital, S. A., Fowler, R. W., Virgen, A., Gossett, D. R., Banks, S. W., and Rodriguez, J. (2008). Opposing roles for superoxide and nitric oxide in the NaCl stress-induced upregulation of antioxidant enzyme activity in cotton callus tissue. *Environ. Exp. Bot.* 62, 60–68. doi: 10.1016/j.envexpbot.2007.07.006

Voss, I., Suni, B., Scheibe, R., and Raghavendra, S. (2013). Emerging concept for the role of photorespiration as an important part of abiotic stress response. *Plant Biol.* 15, 713–722. doi: 10.1111/j.1438-8677.2012.00710.x

Wang, G. P., Hui, Z., Li, F., Zhao, M. R., Zhang, J., and Wang, W. (2010). Improvement of heat and drought photosynthetic tolerance in wheat by overaccumulation of glycinebetaine. *Plant Biotechnol. Rep.* 4, 213–222. doi: 10.1007/s11816-010-0139-y

Wang, X., Li, Q. T., Chen, H. W., Zhang, W. K., Ma, B., and Wu, W. R. (2021). Epigenetic regulation and gene expression changes associated with maize response to abiotic stress. *Plant Cell Environ.* 44 (1), 201–212.

Wang, X., Shan, X., Wu, Y., Su, S., Li, S., Liu, H., et al. (2016). iTRAQ-based quantitative proteomic analysis reveals new metabolic pathways responding to chilling stress in maize seedlings. *J. Proteomics* 146, 14–24. doi: 10.1016/j.jprot.2016.06.007

Wang, F. Z., Wang, Q. B., Know, S. Y., Kwak, S. S., and Su, W. (2005). A. enhanced drought tolerance of transgenic rice plants expressing a pea manganese superoxide dismutase. *J. Plant Physiol.* 162, 465–472. doi: 10.1016/j.jplph.2004.09.009

Wang, Y., Wisniewski, M., Meilan, R., Cui, M., Webb, R., and Fuchigami, L. (2005). Overexpression of cytosolic ascorbate peroxidase in tomato confers tolerance to chilling and salt stress. *J. Am. Soc Hortic. Sci.* 130, 167–173. doi: 10.21273/JASHS.130.2.167

Wang, T. Z., Xia, X. Z., Zhao, M. G., Tian, Q. Y., and Zhang, W. H. (2013). Expression of a medicago falcata small GTPase gene, MfARL1 enhanced tolerance to salt stress in arabidopsis thaliana. *Plant Physiol. Biochem.* 63, 227–235. doi: 10.1016/j.plaphy.2012.12.004

Wang, Y., Ying, Y., Chen, J., and Wang, X. (2004). Transgenic arabidopsis overexpressing Mn-SOD enhanced salt-tolerance. *Plant Sci.* 167 (4), 671–677. doi: 10.1016/j.plantsci.2004.03.03

Xu, S. C., Li, Y. P., Hu, J., Guan, Y. J., Ma, W. G., Zheng, Y. Y., et al. (2010). Responses of antioxidant enzymes to chilling stress in tobacco seedlings. *Agric. Sci. China* 9, 1594–1601. doi: 10.1016/S1671-2927(09)60256-X

Yamane, K., Mitsuya, S., Taniguchi, M., and Miyake, H. (2010). Transcription profiles of genes encoding catalase and ascorbate peroxidase in the rice leaf tissues under salinity. *Plant Prod. Sci.* 13, 164–168. doi: 10.1626/pps.13.164

Yang, Y., and Guo, Y. (2018). Unraveling salt stress signaling in plants. *J. Integr. Plant Biol.* 60 (9), 796–804. doi: 10.1111/jipb.12689

Yang, Y., Han, C., Liu, Q., Lin, B., and Wang, J. (2008). Effect of drought and low light on growth and enzymatic antioxidant system of picea asperata seedlings. *Acta Physiol. Plant* 30, 433–440. doi: 10.1007/s11738-008-0140-z

Yousuf, P. Y., Hakeem, K. U. R., Chandna, R., and Ahmad, P. (2012). "Role of glutathione reductase in plant abiotic stress," in *Abiotic stress responses in plants*, vol. pp. Eds. P. Ahmad and M. N. V. Prasad (Springer), 149e158.

Zarei, S., Ehsanpour, A. A., and Abbaspour, J. (2012). The role of over-expression of P5CS gene on proline, catalase, ascorbate peroxidase activity and lipid peroxidation of transgenic tobacco (*Nicotiana tabacum* l.) plant under *in vitro* drought stress. *J. Cell Mol. Res.* 4, 43–49. doi: 10.22067/jcmr.v4i1.18249

Zhang, J., Chen, S., Li, Y., Di, B., Zhang, J., and Liu, Y. (2008). Effect of high temperature and excessive light on glutathione content in apple peel. *Front. Agric. China* 2, 97–102. doi: 10.1007/s11703-008-0002-x

Zhang, B., Liu, K., Zheng, Y., Wang, Y., Wang, J., and Liao, H. (2013). Disruption of AtWNK8 enhances tolerance of arabidopsis to salt and osmotic stresses via modulating proline content and activities of catalase and peroxidase. *Int. J. Mol. Sci.* 14, 7032–7047. doi: 10.3390/ijms14047032

Zhang, Y., Yang, J., Lu, S., Cai, J., and Guo, Z. (2008). Overexpressing SgNCED1 in tobacco increases aba level, antioxidant enzyme activities, and stress tolerance. *J. Plant Growth Regul.* 27, 151–158. doi: 10.1007/s00344-008-9041-z

Zhang, Z., Zhang, Q., Wu, J., Zheng, X., Zheng, S., and Sun, X. (2013). Gene knockout study reveals that cytosolic ascorbate peroxidase 2 (osapx2) plays a critical role in growth and reproduction in rice under drought, salt and cold stresses. *PloS One* 8, e57472. doi: 10.1371/journal.pone.0057472

Zhang, L., Zhao, G., Jia, J., Liu, X., and Kong, X. (2017). Molecular characterization of the catalase gene family and its response to abiotic stress in grape (Vitis vinifera l.). *PloS One* 12 (11), e0188346.

Zhu, J. K. (2016). Abiotic stress signaling and responses in plants. *Cell* 167 (2), 313–324. doi: 10.1016/j.cell.2016.08.029

Zitka, O., Krystofova, O., Hynek, D., Sobrova, P., Kaiser, J., Sochor, J., et al. (2013). "Metal transporters in plants," in *Metal transporters in plants*. Eds. D. K. Gupta, F. J. Corpas and J. M. Palma (New York: Springer), 19–41.

Zsigmond, L., Szepesi, A., Tari, I., Rigo, G., Kiraly, A., and Szabados, L. (2012). Overexpression of the mitochondrial PPR40 gene improves salt tolerance in arabidopsis. *Plant Sci.* 182, 87–93. doi: 10.1016/j.plantsci.2011.07.008

frontiers | Frontiers in Plant Science

TYPE Perspective
PUBLISHED 15 June 2023
DOI 10.3389/fpls.2023.1167376

Check for updates

OPEN ACCESS

EDITED BY
Xinyang Wu,
China Jiliang University, China

REVIEWED BY
Zakaria Hossain Prodhan,
Neijiang Normal University, China
Long Wang,
Zhejiang University, China

*CORRESPONDENCE
Matthew Alan Jones
Matt.Jones@glasgow.ac.uk

RECEIVED 16 February 2023
ACCEPTED 02 June 2023
PUBLISHED 15 June 2023

CITATION
Trovato M, Brini F, Mseddi K, Rhizopoulou S and Jones MA (2023) A holistic and sustainable approach linked to drought tolerance of Mediterranean crops. *Front. Plant Sci.* 14:1167376. doi: 10.3389/fpls.2023.1167376

COPYRIGHT
© 2023 Trovato, Brini, Mseddi, Rhizopoulou and Jones. This is an open-access article distributed under the terms of the Creative Commons Attribution License (CC BY). The use, distribution or reproduction in other forums is permitted, provided the original author(s) and the copyright owner(s) are credited and that the original publication in this journal is cited, in accordance with accepted academic practice. No use, distribution or reproduction is permitted which does not comply with these terms.

A holistic and sustainable approach linked to drought tolerance of Mediterranean crops

Maurizio Trovato[1], Faiçal Brini[2], Khalil Mseddi[3], Sophia Rhizopoulou[4] and Matthew Alan Jones[5]*

[1]Department of Biology and Biotechnologies, Sapienza University of Rome, Rome, Italy, [2]Biotechnology and Plant Improvement Laboratory, Centre of Biotechnology of Sfax (CBS), Sfax, Tunisia, [3]Faculty of Sciences of Sfax, University of Sfax, Sfax, Tunisia, [4]Department of Biology, National and Kapodistrian University of Athens, Athens, Greece, [5]School of Molecular Biosciences, University of Glasgow, Glasgow, United Kingdom

The rapid increase in average temperatures and the progressive reduction in rainfalls caused by climate change is reducing crop yields worldwide, particularly in regions with hot and semi-arid climates such as the Mediterranean area. In natural conditions, plants respond to environmental drought stress with diverse morphological, physiological, and biochemical adaptations in an attempt to escape, avoid, or tolerate drought stress. Among these adaptations to stress, the accumulation of abscisic acid (ABA) is of pivotal importance. Many biotechnological approaches to improve stress tolerance by increasing the exogenous or endogenous content of ABA have proved to be effective. In most cases the resultant drought tolerance is associated with low productivity incompatible with the requirements of modern agriculture. The on-going climate crisis has provoked the search for strategies to increase crop yield under warmer conditions. Several biotechnological strategies, such as the genetic improvement of crops or the generation of transgenic plants for genes involved in drought tolerance, have been attempted with unsatisfactory results suggesting the need for new approaches. Among these, the genetic modification of transcription factors or regulators of signaling cascades provide a promising alternative. To reconcile drought tolerance with crop yield, we propose mutagenesis of genes controlling key signaling components downstream of ABA accumulation in local landraces to modulate responses. We also discuss the advantages of tackling this challenge with a holistic approach involving different knowledge and perspectives, and the problem of distributing the selected lines at subsidized prices to guarantee their use by small family farms.

KEYWORDS

global warming, drought tolerance, crop yield, ABA, genome editing, wild plants

Introduction

The combined effects of climatic change, overpopulation and unregulated urbanization are reducing water availability in large areas of the world, leading to severe crop losses. The impact of global warming varies across geographic regions, with issues especially prevalent in regions with hot and semi-arid climates such as some Mediterranean countries, where the average temperatures are expected to increase by 20% by the end of the 21st century, with dramatic effects on crop yields and the socio-economic conditions of these regions (Hilmi et al., 2022). The Middle East and North Africa (MENA) region is ranked as the driest region in the world (The World Bank, 2018), with only 1.4% of the world's available fresh water (Roudi-Fahimi et al., 2000). In this context, climate change in Mediterranean MENA regions is expected to proceed faster and with more negative economic effects due to the combination of low rainfall, overpopulation, and agricultural economies based on small family farms (Borghesi and Ticci, 2019). Tunisia, for example, experienced five major drought events in the last decade, reducing yields by up to 50% (World Food Programme, 2011) and leading to spikes in wheat imports. Furthermore, according to the World Bank (The World Bank, 2021) the average temperature is expected to increase by 2°C by 2030, with an estimated loss of cereal production of 30%.

The negative economic effects caused by climate change are particularly severe in countries where agriculture significantly contributes to Gross Domestic Product (GDP) and employment. Since primary food production is the most critical node of the food supply chain, the reduction in crop yield caused by climate change can cause dramatic effects on subsequent nodes of the chain leading to food shortages, higher food prices, loss of employment and political instability. As noted by the FAO report "The State of Food and Agriculture 2021" (FAO, 2021) small-family farms of low-income regions are particularly vulnerable to stresses reducing primary crop production and personal income. This situation can lead to increased poverty and migration, further weakening the economic structure and contributing to poltical instability. Furthermore, climate change-induced crop yield reduction can indirectly affect human health, leading to food insecurity, malnutrition and, in turn, acute and chronic diseases with high social and economic costs.

The traditional strategy to cope with this problem relies upon crop breeding, which has led to some promising improvement and the identification of numerous SNPs (Single Nucleotide Polymorphisms), and QTLs (Quantitative Trait Loci) associated with drought resistance or productivity (Hussain et al., 2017; Tahmasebi et al., 2017). Unfortunately breeding programs are slow, expensive, and laborious and are falling behind the fast pace of global warming. Due to a widespread belief of the scientific community that engineering single genes involved in stress response would have generated drought-tolerant crops, several transgenic plants overexpressing these genes have been created as a popular alternative to breeding programs (Brini et al., 2007a; Brini et al., 2007b; Carraro and Di Iorio, 2022). Although several studies have reported the successful generation of transgenic crops more tolerant to environmental stresses, in most of the cases they did not provide information on productivity, and in some cases even reported a reduction in some yield indicators, such as plant height and number of seeds, especially under unstressed conditions (Mansour and Ali, 2017; Forlani et al., 2019). Proline accumulation, for example, is commonly associated with stress tolerance (Trovato et al., 2008) and several papers report increased drought or salt tolerance in plants overexpressing proline biosynthesis genes (Per et al., 2017). However, commercially-available crops overexpressing proline synthesis genes are not known to date, and a work specifically designed to evaluate the effect of proline on yield did not find convincing evidence that proline can improve seed production under stress (Mattioli et al., 2020).

Considering the complexity of the environmental stresses a plant can be exposed to in Africa, any attempt to improve plant tolerance by modifying single genes may be overly simplistic. Drought stress, in particular, is particularly complex and variable, in terms of intensity, duration and timing of action, and is known to induce the expression of many genes and signaling pathways (Lawlor, 2012). Accordingly, a multi-gene transformation strategy achieved by genetic modification of transcription factors or regulators of signaling cascades seems more promising than targeting single genes for improving drought resistance (Fang and Xiong, 2015). In line with these considerations, HB4®, the only drought-tolerant wheat approved for growth, consumption and commercialization in some countries relies on the stress-inducible expression of the homeo-domain-leucine zipper (HD-zip) transcription factor (TF) HaHB4 from sunflower (*Helianthus annuus*), which can bind to promoters containing the cognate recognition element to regulate the expression of numerous downstream genes (Bergau, 2019). Overall, despite the urge to develop better-adapted crops to a changing climate, the relatively modest results achieved so far leave room to develop novel and more sustainable strategies to produce productive crops under drought conditions and affordable for smallholder farmers in Africa. To be effective, these strategies should identify drought-resistant genes in local landraces, carry out random mutagenesis with TILLING or CRISPR/Cas9, and co-select lines with drought tolerance and good productivity. Finally, actions should be taken to guarantee small farmers free or subsidized distribution of the selected lines.

Defining how plants cope with environmental stresses

It is worthwhile to look at the multiple strategies developed by plant species to survive drought stress. Drought is a complex trait encoded by many genes, the majority of which contribute only a minor genetic contribution. The effects of drought on plants may be different depending on drought duration and intensity, on the developmental phase that stress is perceived by the plants, and on the type of drought stress. Although drought is generally defined as a prolonged period of water deficit, usually because of rainfall

absence, its effects overlap those caused by water shortage, occurring when transpiration exceeds water uptake, but also under conditions of salinity or osmotic stress (Bray, 1997). Because of this coincidence, it is common practice to simulate drought in laboratory conditions using high PEG (Polyethylene glycol) concentrations in liquid or solid media. The results achieved in the laboratory, however, are seldom confirmed in field conditions which makes it difficult to apply these advances in the field.

In natural conditions, plants respond to environmental drought stress with diverse morphological, physiological, and biochemical adaptations (Bohnert et al., 1995), trying to escape, avoid, or tolerate drought stress (Figure 1). Drought escape is typically obtained through early flowering (Rhizopoulou and Pantazi, 2015), which allows the plant to quickly set a few seeds and survive by accelerating the life cycle (Dolferus, 2014). A good example of drought escape is found in resurrection plants, such as *Craterostigma plantagineum* or *Selaginella lepidophylla*, which can survive for months without water, but flower and set seeds in a few days when occasional rains fall (Scott, 2000). Drought avoidance tries to reduce water loss by preventing excessive transpiration with morpho-physiological adaptations such as covering the leaves with wax cuticles or transforming leaves into thorns. Some halophyte plants, such as the wild crop *Trifolium fragigera*, provide examples of drought avoidance that can attain by removing salt excess by secretion or compartmentalization into vacuoles (Jēkabsone et al., 2022). In addition, some wild plant species, e.g. caper (*Capparis spinosa*) and carob (*Ceratonia siliqua*), possess ecophysiological strategies to cope with water shortage and exhibit growth and productivity during and after the dry summer period in the Mediterranean region (Rhizopoulou, 1990; Rhizopoulou and Davies, 1991; Rhizopoulou, 2004; Rhizopoulou and Kapolas, 2015). Drought tolerance, on the contrary, attempts to permit plant life even in the absence of sufficient water supply, usually by accumulating compatible osmolytes or enhancing the antioxidant plant's capacity (Bartels and Sunkar, 2005), or by delaying flowering and slowing down metabolism until favorable conditions return (Syed et al., 2015). Some members of the halophyte family, such as *Thellungiella* or *Salicornia*, capable of accumulating high cellular levels of compatible osmolytes, are good examples of drought-tolerant plants (Mishra and Tanna, 2017). Most of the mechanisms evolved to improve drought tolerance in wild plants are associated with strong reductions in seed yield, which is limited to offspring survival and is much lower than under favorable environmental conditions (Figure 1). Thus, while it is important to study the mechanisms underlying drought tolerance of these plants to identify the relevant genes involved, we must be cautious in mimicking their strategies not to risk limiting productivity.

ABA is involved in drought tolerance, which is often associated with low productivity

Many phytohormones, such as abscisic acid (ABA), auxin, cytokinins, gibberellins, ethylene, and jasmonic acid, as well many compatible osmolytes like proline, γ-aminobutyric acid (GABA), and sugars accumulate after stress and are thought to contribute to tolerance, but ABA, universally considered as the stress hormone, seems to play a pivotal role in stress tolerance. Irrespective of the type of drought a plant experiences, the ultimate consequence of the stress is cell dehydration, and, soon after, ABA accumulation, which, in turn, triggers diverse signaling pathways to activate downstream adaptive responses, such as stomatal closure, improved hydraulic conductivity, improved photosynthetic activity, organized soil microbial communities, activation of transcriptional and post-transcriptional gene expression, metabolic alterations, root elongation, and stimulation of antioxidant capacity (Todaka et al., 2019). The strict correlation between ABA accumulation and water deficiency strongly suggests that this phytohormone can play a key role in establishing drought tolerance in plants (Yoshida et al., 2014; Puértolas et al., 2017). Indeed, several studies have reported increased drought tolerance in plants treated with exogenous ABA (Ali et al., 2020) or synthetic ABA analogs (Zhou et al., 2019), as well as in transgenic plants expressing genes involved in ABA signaling (Fujii and Zhu, 2009).

Despite this promise, ABA-induced drought tolerance is often associated with low levels of crop productivity. Since negative or ambiguous results are usually not published, this concept is underestimated but only indirectly supported by the lack of transgenic lines or working protocols currently available in the market or used by farmers. A few examples of drought-tolerant plants with no yield gain, though, can be found here and there in the scientific literature, as in He et al. (2019), who reported improved drought tolerance but no yield benefit in soybean plants treated with exogenous ABA. Given our fundamental understanding of ABA signaling, it is likely that ABA-induced stomatal closure limits water loss by evapotranspiration, but also carbon dioxide entry, reducing carbon assimilation and photosynthesis efficiency (Lamaoui et al., 2018). The problem of reconciling drought tolerance with crop yield, especially in field conditions, holds true for transgenic plants transformed with other stress-related genes or treated with other exogenous substances, such as proline, sugars, and plant hormones, and remains the biggest challenge to tackle.

Alternative approaches to reconcile drought tolerance with crop yield

Considering the number of physiological traits contributing to yield under drought stress and potentially modulated by ABA signaling (e.g. relative water content, water-use efficiency, transpiration efficiency, crop growth and partitioning rate, root traits, osmolyte accumulation), the targeted mutagenesis of ABA signaling modulators followed by co-selection of high-yielding and drought-tolerant lines seems a promising strategy. Instead of focusing on drought tolerance in the vegetative phase (by measuring indicators not necessarily correlated with grain yields, such as leaf water potential or osmotic adjustment), variability in genes involved in drought tolerance should be generated and analyzed at the reproductive phase to select the lines most

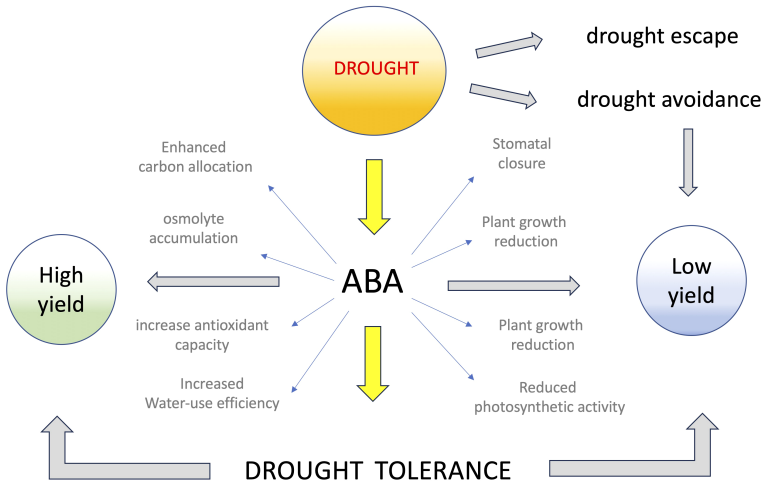


FIGURE 1
Main mechanisms of drought resistance and effects of ABA on crop yield. Plants try to escape, avoid or tolerate drought stress through various morphological, physiological, and biochemical adaptations, including accumulation of ABA, which triggers different signaling pathways leading to drought tolerance and, often, low productivity. ABA-induced drought tolerance, however, can be associated with high productivity, possibly due to improved water use efficiency, carbon allocation, and osmolytes accumulation.

productive under drought conditions. To optimize crop productivity, high-performance lines should be selected in both drought and well-hydrated conditions to avoid the frequently reported problem of plants performing well under stress but poorly without stress. A more comprehensive approach to mutant selection will be vital, including molecular biology, botany, ecophysiology, and crop breeding expertise.

Genome editing of ABA signaling in durum wheat

Under optimal growing conditions, the levels of productivity of modern crops are not comparable with that of their wild relatives, although a few species perform better in drought conditions and could serve as a reservoir of genetic and phenotypic diversity (Kiani et al., 2015; Rafique et al., 2017; Mammadov et al., 2018). A good example is the wild emmer wheat (*Triticum dicoccoides*), a naturally drought-tolerant species that can set fertile seeds even in desert environments (Khan et al., 2022). By comparing the most high-yielding, drought-tolerant wild species, with phenomic and genome-wide techniques, we could discover common traits and genes associated with productivity to be used for genetic improvement. As a proof-of-concept, we chose to generate mutations leading to constitutive ABA activation and drought tolerance, to select lines with the best possible yield under suitable drought conditions.

We think that genes involved in drought-related signaling pathways are better suited to cope with the complexity of dehydration stress. Indeed, drought and water stress have profound effects on plant life and elicit correspondingly complex physiological responses, many of which are induced by ABA accumulation. In a transcriptome analysis of *Arabidopsis* plants subjected to moderate dehydration stress, for example, Urano et al. (2017) found upregulation of 5271 genes and downregulation of 6303 genes. Most of these genes were found to code for proteins indirectly involved in drought tolerance, such as genes for osmolyte biosynthesis and catabolism, antioxidant genes, sugars, chaperones, heat shock proteins, and late embryogenesis abundant (LEA) proteins. A second class of genes was found to encode proteins involved in stress signaling, such as protein kinases, protein phosphatases, transcription factors, and proteins involved in protein degradation (Urano et al., 2017). In response to drought, ABA levels quickly increase in vegetative tissues leading to the activation of PYRABACTIN RESISTANCE1 (PYL)/PYR1-LIKE (PYR) ABA receptors and inhibition of group A PP2C phosphatase. In turn, PP2C inhibition allows autophosphorylation and activation of the SUCROSE NONFERMENTING 1-RELATED SUBFAMILY2 (SnRK2) kinase and subsequent phosphorylation of multiple downstream targets (Figure 2; Yoshida et al., 2014). As expected, ABA-mediated responses to drought are complex and involve hundreds of genes. Microarray analysis of *sal1* mutant, a phosphatase involved in retrograde signaling and constitutive activation of ABA signaling in *Arabidopsis* (Wilson et al., 2009), for example, revealed altered expression of more than 1800 genes, including heat shock proteins, transcription factors, aquaporins, light-inducible proteins, stress signaling kinases, stress-inducible proteins and antioxidant enzymes (Wilson et al., 2009). In addition, SAL1 has been shown to alter the circadian system (Litthauer et al., 2018), affecting the recently discovered relationships between stress response and the circadian clock and potentially allowing a better modulation of the plant's response to the actual drought levels.

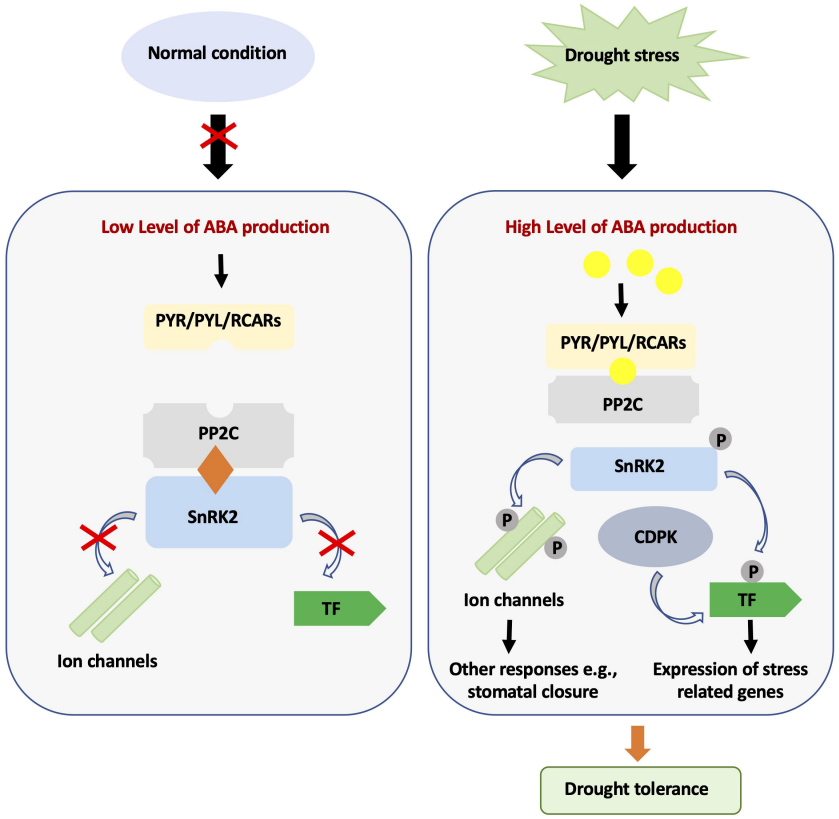


FIGURE 2
ABA-mediated signaling pathway during normal and drought stress conditions. Under normal conditions, ABA content is low, and SnRK2 protein kinase activity is inhibited by PP2C phosphatases. Under drought stress, the cellular ABA level increases, and ABA then binds to PYR/PYL/RCARs, which in turn bind and inactivate PP2Cs. The SnRK2s autoactivate when they dissociate from PP2Cs. Activated SnRK2s phosphorylate downstream targets and trigger ABA-induced physiological and molecular responses.

To select drought-tolerant, well-productive wheat varieties, ABA signaling mutants should be first identified for drought tolerance and then selected for productivity under drought conditions. The use of CRISPR/Cas mutagenesis is key to accelerating genetic improvement, especially for cereal crops, which have large and polyploid genomes, and long generation times. Importantly, the use of imprecise non-homologous end-joining (NHEJ) recombination by CRISPR/Cas9, and the possibility to introduce multiple gRNAs in the plant genome is expected to widen the genetic variability with beneficial effects in the process of selection (Jaganathan et al., 2018). Last but not least, CRISPR/Cas9 is gaining increasing popularity in crop research and is socially more accepted than transgenic plants, although full acceptance by public regulatory organizations is still awaited.

Development of sustainable solutions for African farmers

Maintaining high crop yields in drought conditions can be achieved or supported in many ways, such as using sophisticated irrigation methods guided by artificial intelligence (AI), drones, and satellite systems, desalting seawater, or using automated shelters and fertilizations. However, all these methods require technological skills and high economic and energy costs that are difficult for small rural farmers to bear. The introduction of new crop varieties capable of good yields in arid climates, combined with good practices of conservation agriculture, on the contrary, may be a practical solution suitable for small family farms, provided the lines are distributed for free or at low cost. The generation of high-yielding drought-resistant plants adapted to increasingly hotter and drier climates is a long and expensive process in itself that needs to be reconciled with economic and environmental sustainability and adapted to specific local conditions. This objective is particularly significant for countries where agriculture is based on many small family farms. Provided the proof-of-concept is successful, it will be pivotal to search for local wild crops or landraces to edit the genomes of varieties most suited to local conditions. Accordingly, a close collaboration between molecular biologists, botanists, ecophysiologists, and policy-makers is required for the effective development of highly productive crops resistant to specific local conditions and freely available to local stakeholders.

Another potential problem is the number of registered patents on CRISPR/Cas9 technology which could translate into royalties or

commissions at unsustainable costs for small farmers. From a scientific point of view, the identification of genetic determinants capable of good yields under drought conditions is a complex task that justifies the use of multiple strategies, including CRISPR/Cas9. Once the genes and signaling pathways involved in drought tolerance are known, it will be possible to improve crop yield with less problematic tools, such as precision breeding or TILLING. From a socio-economic point of view, on the other hand, it is desirable that governments and policymakers can tackle the long-standing problem of the intellectual and commercial protection of patents. Faced with possible humanitarian crises, such as world hunger, global warming, and the COVID pandemic, has already happened that humanitarian organizations or sovereign governments have stepped in to cover the costs associated with patent-holding companies to address these issues. Given the context, such an eventuality could well occur for many countries in North Africa and the sub-Saharan belt to prevent the spread of socio-political instability. Research and educational use of these technologies are already possible, and some academic subjects are pushing for complete liberalization. Wageningen University and Research in the Netherlands, one of the major patent holders of CRISPR technology, has recently announced that it will allow non-profit organizations to freely use its CRISPR/Cas9 gene-editing technology for non-commercial applications in food and agriculture (Nature Editorial, 2021). Overall, this perspective highlights the potentiality of targeting ABA signaling genes through CRISPR/Cas9 mutagenesis, which seems a promising strategy to select high-yielding, drought-tolerant crops, provided collaborative efforts and equitable access to genetic resources is guaranteed.

Data availability statement

The original contributions presented in the study are included in the article/supplementary material. Further inquiries can be directed to the corresponding author.

Author contributions

All authors listed have made a substantial, direct, and intellectual contribution to the work and approved it for publication.

Funding

This work was partially funded by the CIVIS grant "Seed funding for joint projects with CIVIS' African partner universities" N° 0000000025 to MT, and by the UKRI (BB/S005404/1) to MJ.

Acknowledgments

We thank Karim El Bahnsawy, Sofia Papadopoulos, Foteini Kolyva, Dimitrios Gkikas, and Franco Vegliani for their participation and support of the CIVIS project.

Conflict of interest

The authors declare that the research was conducted in the absence of any commercial or financial relationships that could be construed as a potential conflict of interest.

Publisher's note

All claims expressed in this article are solely those of the authors and do not necessarily represent those of their affiliated organizations, or those of the publisher, the editors and the reviewers. Any product that may be evaluated in this article, or claim that may be made by its manufacturer, is not guaranteed or endorsed by the publisher.

References

Ali, S., Hayat, K., Iqbal, A., and Xie, L. (2020). Implications of abscisic acid in the drought stress tolerance of plants. *Agronomy* 10 (9), 1323. doi: 10.3390/agronomy10091323

Bartels, D., and Sunkar, R. (2005). Drought and salt tolerance in plants. *Crit. Rev. Plant Sci.* 24 (1), 23–58. doi: 10.1080/07352680590910410

Bergau, J. (2019). "Verdeca introduces HB4® drought tolerant soybeans to growers at argentina's expoagro," in *Arcadia Biosciences*. Available at: https://www.businesswire.com https://www.businesswire.com/news/home/20190326005300/en/Verdeca-Introduces-HB4%C2%AE-Drought-Tolerant-Soybeans-Growers.

Bohnert, H. J., Nelson, D. E., and Jensen, R. G. (1995). Adaptations to environmental stresses. *Plant Cell* 7 (7), 1099–1111. doi: 10.1105/tpc.7.7.1099

Borghesi, S., and Ticci, E. (2019) Climate change in the MENA region: environmental risks, socioeconomic effects and policy challenges for the future. *IEMed. Mediterranean Yearbook 2019*. Available at: https://www.iemed.org/wp-content/uploads/2021/01/Climate-Change-in-the-MENA-Region.pdf (Accessed 5/2 2023).

Bray, E. A. (1997). Plant responses to water deficit. *Trends Plant Sci.* 2 (2), 48–54. doi: 10.1016/S1360-1385(97)82562-9

Brini, F., Hanin, M., Lumbreras, V., Amara, I., Khoudi, H., Hassairi, A., et al. (2007a). Overexpression of wheat dehydrin DHN-5 enhances tolerance to salt and osmotic stress in *Arabidopsis thaliana*. *Plant Cell Rep.* 26 (11), 2017–2026. doi: 10.1007/s00299-007-0412-x

Brini, F., Hanin, M., Mezghani, I., Berkowitz, G. A., and Masmoudi, K. (2007b). Overexpression of wheat Na+/H+ antiporter TNHX1 and h+-pyrophosphatase TVP1 improve salt- and drought-stress tolerance in *Arabidopsis thaliana* plants. *J. Exp. Bot.* 58 (2), 301–308. doi: 10.1093/jxb/erl251

Carraro, E., and Di Iorio, A. (2022). Eligible strategies of drought response to improve drought resistance in woody crops: a mini-review. *Plant Biotechnol. Rep.* 16 (3), 265–282. doi: 10.1007/s11816-021-00733-x

Dolferus, R. (2014). To grow or not to grow: a stressful decision for plants. *Plant Sci.* 229, 247–261. doi: 10.1016/j.plantsci.2014.10.002

Fang, Y., and Xiong, L. (2015). General mechanisms of drought response and their application in drought resistance improvement in plants. *Cell. Mol. Life Sci.* 72 (4), 673–689. doi: 10.1007/s00018-014-1767-0

FAO (2021). "The state of food and agriculture 2021," in *Making agrifood systems more resilient to shocks and stresses* (Rome: FAO). doi: 10.4060/cb4476en

Forlani, G., Trovato, M., Funck, D., and Signorelli, S. (2019). "Regulation of proline accumulation and its molecular and physiological functions in stress defence," in *Osmoprotectant-mediated abiotic stress tolerance in plants: recent advances and future perspectives*. Eds. M. A. Hossain, V. Kumar, D. Burritt, M. Fujita and P. Mäkelä (Switzerland: Springer Nature), 73–97.

Fujii, H., and Zhu, J.-K. (2009). *Arabidopsis* mutant deficient in 3 abscisic acid-activated protein kinases reveals critical roles in growth, reproduction, and stress. *Proc. Natl. Acad. Sci.* 106 (20), 8380–8385. doi: 10.1073/pnas.0903144106

He, J., Jin, Y., Palta, J. A., Liu, H.-Y., Chen, Z., and Li, F.-M. (2019). Exogenous ABA induces osmotic adjustment, improves leaf water relations and water use efficiency, but not yield in soybean under water stress. *Agronomy* 9 (7), 395. doi: 10.3390/agronomy9070395

Hilmi, N., Ali, E., Carnicer Cols, J., Cramer, W., Georgopoulou, E., Le Cozannet, G., et al. (2022). "IPCC AR6 WGII cross-chapter paper 4: Mediterranean region," in *EGU general assembly 2022* (Vienna, Austria). doi: 10.5194/egusphere-egu22-10590

Hussain, W., Baenziger, P. S., Belamkar, V., Guttieri, M. J., Venegas, J. P., Easterly, A., et al. (2017). Genotyping-by-Sequencing derived high-density linkage map and its application to QTL mapping of flag leaf traits in bread wheat. *Sci. Rep.* 7 (1), 16394. doi: 10.1038/s41598-017-16006-z

Jaganathan, D., Ramasamy, K., Sellamuthu, G., Jayabalan, S., and Venkataraman, G. (2018). CRISPR for crop improvement: an update review. *Front. Plant Sci.* 9. doi: 10.3389/fpls.2018.00985

Jēkabsone, A., Andersone-Ozola, U., Karlsons, A., Romanovs, M., and Ievinsh, G. (2022). Effect of salinity on growth, ion accumulation and mineral nutrition of different accessions of a crop wild relative legume species, trifolium fragiferum. *Plants* 11 (6), 797. doi: 10.3390/plants11060797

Khan, A., Ali, A., Ullah, Z., Ali, I., Kaushik, P., Alyemeni, M. N., et al. (2022). Exploiting the drought tolerance of wild *Elymus* species for bread wheat improvement. *Front. Plant Sci.* 13. doi: 10.3389/fpls.2022.982844

Kiani, R., Arzani, A., and Habibi, F. (2015). Physiology of salinity tolerance in *Aegilops cylindrica*. *Acta Physiologiae Plantarum* 37 (7), 135. doi: 10.1007/s11738-015-1881-0

Lamaoui, M., Jemo, M., Datla, R., and Bekkaoui, F. (2018). Heat and drought stresses in crops and approaches for their mitigation. *Front. Chem.* 6. doi: 10.3389/fchem.2018.00026

Lawlor, D. W. (2012). Genetic engineering to improve plant performance under drought: physiological evaluation of achievements, limitations, and possibilities. *J. Exp. Bot.* 64 (1), 83–108. doi: 10.1093/jxb/ers326

Litthauer, S., Chan, K. X., and Jones, M. A. (2018). 3′-phosphoadenosine 5′-phosphate accumulation delays the circadian system. *Plant Physiol.* 176 (4), 3120–3135. doi: 10.1104/pp.17.01611

Mammadov, J., Buyyarapu, R., Guttikonda, S. K., Parliament, K., Abdurakhmonov, I. Y., and Kumpatla, S. P. (2018). Wild relatives of maize, rice, cotton, and soybean: treasure troves for tolerance to biotic and abiotic stresses. *Front. Plant Sci.* 9. doi: 10.3389/fpls.2018.00886

Mansour, M. M. F., and Ali, E. F. (2017). Evaluation of proline functions in saline conditions. *Phytochemistry* 140, 52–68. doi: 10.1016/j.phytochem.2017.04.016

Mattioli, R., Palombi, N., Funck, D., and Trovato, M. (2020). Proline accumulation in pollen grains as potential target for improved yield stability under salt stress. *Front. Plant Sci.* 11. doi: 10.3389/fpls.2020.582877

Mishra, A., and Tanna, B. (2017). Halophytes: potential resources for salt stress tolerance genes and promoters. *Front. Plant Sci.* 8. doi: 10.3389/fpls.2017.00829

Nature Editorial (2021). License CRISPR patents for free to share gene editing globally. *Nature* 597, 152. doi: 10.1038/d41586-021-02420-x

Per, T. S., Khan, N. A., Reddy, P. S., Masood, A., Hasanuzzaman, M., Khan, M. I. R., et al. (2017). Approaches in modulating proline metabolism in plants for salt and drought stress tolerance: phytohormones, mineral nutrients and transgenics. *Plant Physiol. Biochem.* 115, 126–140. doi: 10.1016/j.plaphy.2017.03.018

Puértolas, J., Larsen, E. K., Davies, W. J., and Dodd, I. C. (2017). Applying 'drought'to potted plants by maintaining suboptimal soil moisture improves plant water relations. *J. Exp. Bot.* 68 (9), 2413–2424. doi: 10.1093/jxb/erx116

Rafique, K., Rauf, C. A., Gul, A., Bux, H., Memon, R. A., Ali, A., et al. (2017). Evaluation of d-genome synthetic hexaploid wheats and advanced derivatives for powdery mildew resistance. *Pakistan J. Bot.* 49 (2), 735–743.

Rhizopoulou, S. (1990). Physiological responses of *Capparis spinosa* l. @ to drought. *J. Plant Physiol.* 136 (3), 341–348. doi: 10.1016/S0176-1617(11)80060-X

Rhizopoulou, S. (2004). Aspects of cell wall extensibility in *Ceratonia siliqua* l. *Flora - Morphology Distribution Funct. Ecol. Plants* 199 (4), 327–333. doi: 10.1078/0367-2530-00160

Rhizopoulou, S., and Davies, W. J. (1991). Influence of soil drying on root development, water relations and leaf growth of *Ceratonia siliqua* l. *Oecologia* 88 (1), 41–47. doi: 10.1007/BF00328401

Rhizopoulou, S., and Kapolas, G. (2015). *In situ* study of deep roots of *Capparis spinosa* l. during the dry season: evidence from a natural "rhizotron" in the ancient catacombs of milos island (Greece). *J. Arid Environments* 119, 27–30. doi: 10.1016/j.jaridenv.2015.03.010

Rhizopoulou, S., and Pantazi, H. (2015). Constraints on floral water status of successively blossoming Mediterranean plants under natural conditions. *Acta Botanica Gallica* 162 (1), 97–102. doi: 10.1080/12538078.2014.991753

Roudi-Fahimi, F., Creel, L., and De Souza, R. M. (2000) *). Finding the balance: population and water scarcity in the middle East and north Africa*. Available at: https://www.prb.org/resources/finding-the-balance-population-and-water-scarcity-in-the-middle-east-and-north-africa/ (Accessed 10/1 2023).

Scott, P. (2000). Resurrection plants and the secrets of eternal leaf. *Ann. Bot.* 85 (2), 159–166. doi: 10.1006/anbo.1999.1006

Syed, N. H., Prince, S. J., Mutava, R. N., Patil, G., Li, S., Chen, W., et al. (2015). Core clock, SUB1, and ABAR genes mediate flooding and drought responses via alternative splicing in soybean. *J. Exp. Bot.* 66 (22), 7129–7149. doi: 10.1093/jxb/erv407

Tahmasebi, S., Heidari, B., Pakniyat, H., and McIntyre, C. L. (2017). Mapping QTLs associated with agronomic and physiological traits under terminal drought and heat stress conditions in wheat (*Triticum aestivum* l.). *Genome* 60 (1), 26–45. doi: 10.1139/gen-2016-0017

The World Bank (2018) *Beyond scarcity: water security in the middlle est and north Africa*. Available at: http://hdl.handle.net/10986/27659 (Accessed 10/1 2023).

The World Bank (2021) *Climate risk profile: tunisia (2021)*. Available at: https://climateknowledgeportal.worldbank.org/sites/default/files/2021-02/15727WB_TunisiaCountryProfile-WEB.pdf (Accessed 10/1 2023).

Todaka, D., Takahashi, F., Yamaguchi-Shinozaki, K., and Shinozaki, K. (2019). "Chapter three - ABA-responsive gene expression in response to drought stress: cellular regulation and long-distance signaling," in *Advances in botanical research*. Eds. M. Seo and A. Marion-Poll (United Kingdom: Academic Pres), 83–113.

Trovato, M., Mattioli, R., and Costantino, P. (2008). Multiple roles of proline in plant stress tolerance and development. *Rendiconti Lincei-Scienze Fisiche E Naturali* 19 (4), 325–346. doi: 10.1007/s12210-008-0022-8

Urano, K., Maruyama, K., Jikumaru, Y., Kamiya, Y., Yamaguchi-Shinozaki, K., and Shinozaki, K. (2017). Analysis of plant hormone profiles in response to moderate dehydration stress. *Plant J.* 90 (1), 17–36. doi: 10.1111/tpj.13460

Wilson, P. B., Estavillo, G. M., Field, K. J., Pornsiriwong, W., Carroll, A. J., Howell, K. A., et al. (2009). The nucleotidase/phosphatase SAL1 is a negative regulator of drought tolerance in *Arabidopsis*. *Plant J.* 58 (2), 299–317. doi: 10.1111/j.1365-313X.2008.03780.x

World Food Programme (2011) *Secondary data analysis of the food security situation in Tunisia*. Available at: https://www.wfp.org/content/tunisia-secondary-data-analysis-food-security-situation-april-2011 (Accessed 25/1 2023).

Yoshida, T., Mogami, J., and Yamaguchi-Shinozaki, K. (2014). ABA-dependent and ABA-independent signaling in response to osmotic stress in plants. *Curr. Opin. Plant Biol.* 21, 133–139. doi: 10.1016/j.pbi.2014.07.009

Zhou, Y., He, R., Guo, Y., Liu, K., Huang, G., Peng, C., et al. (2019). A novel ABA functional analogue B2 enhances drought tolerance in wheat. *Sci. Rep.* 9 (1), 2887. doi: 10.1038/s41598-019-39013-8

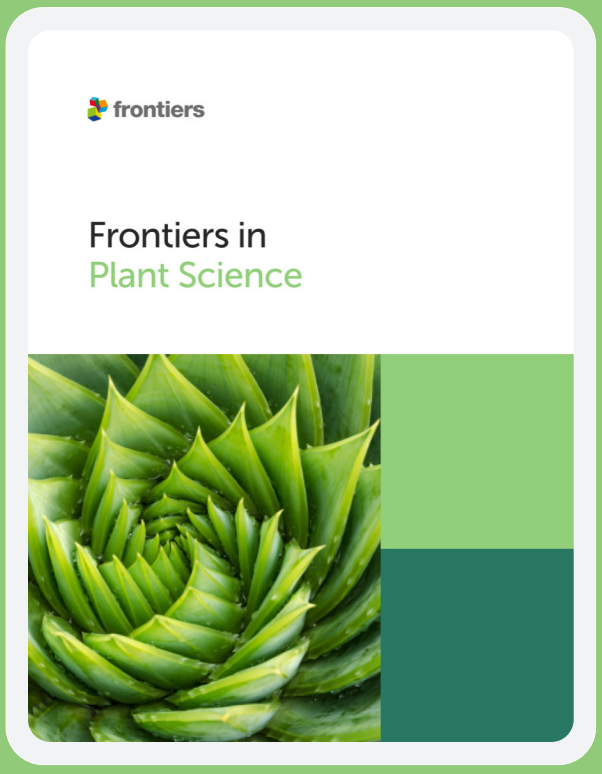
Frontiers in
Plant Science

Cultivates the science of plant biology and its applications

The most cited plant science journal, which advances our understanding of plant biology for sustainable food security, functional ecosystems and human health.

Discover the latest Research Topics

See more →



Frontiers

Avenue du Tribunal-Fédéral 34
1005 Lausanne, Switzerland
frontiersin.org

Contact us

+41 (0)21 510 17 00
frontiersin.org/about/contact